Phytochemical Analysis of Rhododendron Species

by

Abhinandan Shrestha

a Thesis submitted in partial fulfillment
of the requirements for the degree of

Doctor of Philosophy
in Chemistry

Approved Dissertation Committee

Prof. Dr. Nikolai Kuhnert

Prof. of Chemistry, Jacobs University Bremen

Prof. Dr. Matthias S. Ullrich

Prof. of Microbiology, Jacobs University Bremen

Prof. Dr. Dirk Albach

Prof. of Plant Biodiversity, University of Oldenburg

Prof. Dr. Klaudia Brix

Prof. of Cell Biology, Jacobs University Bremen

Date of Defense: 24th May 2016

Statutory Declaration
(on Authorship of a Dissertation)

I, Abhinandan Shrestha hereby declare that I have written this PhD thesis independently, unless where clearly stated otherwise. I have used only the sources, the data and the support that I have clearly mentioned. This PhD thesis has not been submitted for conferral of degree elsewhere.

I confirm that no rights of third parties will be infringed by the publication of this thesis.

Bremen, May 31, 2016

Signature _____

Dedicated to my parents,

Meera Shrestha & Gyan Prakash Shrestha

Acknowledgement

I would like to thank Prof. Dr. Nikolai Kuhnert for providing me the opportunity to research on Rhododendron, which is the national flower of Nepal. I am grateful not only for my PhD research, but also my Bachelors research. Through his guidance, encouragement and motivation, I was able to develop both personally and professionally in the field of analytical chemistry.

The Rhododendron project also included Prof. Dr. Matthias S. Ullrich, Prof. Dr. Klaudia Brix and Prof. Dr. Dirk Albach, who were supportive of my results, gave me new ideas and suggestions through different scientific perspectives during numerous project meetings. I would also like to thank them for reviewing my thesis.

I am indebted to Dr. Hartwig Schepker for providing the Rhododendron plant material including the huge database of information, which included their subgenus, gene bank number and origin of samples. Due to the timely arrival of the samples, it was possible to perform the necessary experiments within the time frame.

I enjoyed working with my colleagues in the Rhododendron project, Dr. Ahmed Rezk, Jennifer Nolzen and Inamullah Hakeem Said. They were helpful in making me understand the different studies being conducted on Rhododendron and were available whenever required. I appreciate their efforts and hard work for this project.

I would like to thank my students whom I got to supervise during my PhD studies, Lucas Lansing, Naika Thielen, Victoria von Glasenapp and Rachelle Smith. Their efforts helped me significantly in analyzing the enormous amount of data efficiently. It was a wonderful experience for me to introduce the field of analytical chemistry to them.

Dr. Anne Grimbs and Dr. Sergio Grimbs assisted the Rhododendron project with their expertise in bioinformatics, graphics and statistical analysis and by combining the large amount of data generated from all studies. I am grateful for all their help. Dr. Javier González had helped me with the Gaussian software and scripting during his short stay in our group. Thank you!

I would like to thank the entire Kuhnert group, including current and former members for all their help during my PhD stay. It was the most comfortable environment to carry out my PhD research, along with many fun group activities like paintball, BBQ, Kohlfahrt and Freimarkt. In addition, I would like to thank Anja Müller for her excellent technical assistance in the lab.

I would like to individually thank all of my colleagues, Dr. Mohamed Elsadig Karar for helping me in many aspects of my thesis like compound assignment, neutral losses, proof-reading and sharing his funny outlook on life, Dr. Farnoosh Dairpoosh for supervising me during my undergraduate research and inspiring me to make protocols, Dr. Rakesh Jaiswal for his helpful suggestions in polyphenol assignment, Dr. Sagar Anil Deshpande for his positive attitude and liquid nitrogen and acetone experiment, Dr. Marius-Febi Matei for scientific suggestions, Dr. Hande Karaköse for supervising me during Bachelors and also guiding me and answering all my questions during my PhD, Dr. Agnieszka Golon-Duda for scientific, instrumental and lunch time discussions, Borislav Milev for his help with RStudio and XCMS, Maria Alexandra Patras for sharing her broad knowledge of chemistry, Beatrix Tetzlaff for her help with Refworks, Rohan Shah for instrumental discussions and bringing delicious sweets from India, Inamullah Hakeem Said for his fruitful discussions, Seung-Hun Lee for scientific discussions, his impeccable standards of proof-reading and his enthusiasm to offer me coffee, Diana Sirbu for her delicious cakes and meals and her dynamic energy, Anastasiia Shevchuk for her help in organizing group events, Roberto Megías Pérez for bringing sweets and chorizo from Spain, Britta Behrends for keeping the lab organized and registering all chemicals to the database, Dr. Ghada Yassin for analyzing some samples with the ion mobility mass spectrometer, Dr. Roy D'Souza for helping with mass spectrometry software (MZ mine), Audrey Bergounhou for her positive and effervescent energy and lunch time discussions, Paweł Andruszkiewicz for bringing sweets from Poland, Maria Bikaki for various philosophy discussions, Joanna Dabrowska and Adam Lalewicz for scientific discussions and Polish gifts. In addition, I would like to thank Dr. Hany Nour, Dr. Nadim Hourani, Dr. Foad Tehrani, Dr. Maribel Alarcon Flores, Dr. Mohamed Rafi, Prof. Dr. Lalith Jayasinghe, Dr. Mubo Adeola Sonibare, Sabur Badmos, Nickolet Ncube, Irem Altun, Selin Gencer, Jonathan, Maria Ines and the complete Chemistry Faculty at Jacobs University. Also, I would like to thank the Chemistry Society of Jacobs University for bringing together students in the field of Chemistry and organizing amazing Chemistry parties.

For financial support, I would like to thank Jacobs University & Rhododendron Stiftung for providing me the necessary means for my research. I would like to thank Zoltan Czentnar from Bruker Daltonics for his help with scripting and Bruker software related issues. Due to his scripts, it was possible to make data tables by just a few clicks instead of writing them down manually.

During my Master studies in the Erasmus EMQAL program, I got to experience life in Spain and Poland. And I am grateful to my professors (Prof. Isabel Cavaco, Prof. Miguel Esteban, Prof. Ramon Companyó, Dr. *hab. inz.* Andrzej Wasik and Prof. Dr. *hab. inz.* Bogdan Zygmunt) for helping me explore the field of analytical chemistry in depth.

My parents, Meera Shrestha and Gyan Prakash Shrestha have provided me everything since my childhood. Their immense support and sacrifices have resulted in all that I have achieved in my life. They have always been enthusiastic about my studies and have given me enough freedom to fulfill my dreams. I am grateful to have you both by my side.

I would like to thank my sister Ayushma Shrestha Bansode along with Kapil Bansode and Aashvath Bansode for finding time for me and supporting me despite being very far away. In addition, I would like to thank my other sister Radha Lama, who has helped and supported me during all these years.

Monita Dhaubanjar, thank you for being by my side during all times. You helped me transform all the hours spent analyzing chromatograms and looking at numbers and data tables into this thesis. I am indebted for your support and I hope to support you the same way. Thank you for your patience and persistence.

I would also like to thank all members of my extended family, who are distributed over the globe. During my PhD, I got to spend some quality time with my relatives in London (Shrestha, Khadka and Sangani family), who gave me an insight of my family history and supported me with positive energy when I needed it the most.

I am thankful to Sweccha Joshi and Prabal Subedi, who both started the journey into the field of chemistry with me since 2007 and simultaneously did their Bachelors, Masters and PhD studies with me, with whom I could easily share my PhD stories. Science was enjoyable because of you. Thank you for being there for me. I wish you good luck for writing your respective thesis!

My host family has been a part of my life since I started my Bachelor studies in 2007. They have always been there to support me and have presented me with traditional German sweets even while I was away from Germany. Thank you for being my wonderful host family, Ronald Michaelis and Birgit Michaelis, along with Mareike and Katina.

A big thank you to the Nawatzki family (Shashank Bajimaya, Anuraag Raj Shakya, Anup Sherchan, Arpan Rijal, Eugenia Rosca, Samip Dhoj Raut, Remun Koirala, Papul Koirala, Nikhil Ratna Shakya and Tenzin Tenpa) with whom I spent most of my time after work. Thank you for the relaxing times, football discussions, musical sessions and the delicious cuisines.

I picked up volleyball as my hobby during my PhD studies, which really helped during the time of writing my thesis. So, I would like to thank Dr. Pratik Raj Singh, Sidhant Bom, Jayanta Gauchan, Asman Tamang, Sushil KC and the entire volleyball team on-campus and off-campus for the competitive games in a fun environment.

I would also like to thank the Nepalese community on campus for their support and organizing cultural events on campus so that I didn't feel homesick too often. Finally, I would like to thank Jacobs University for offering me the resources to complete my Bachelor and PhD studies and providing me the opportunity to meet fascinating people.

Publications

- Abhinandan Shrestha, Ahmed Rezk, Inamullah Hakeem Said, Jennifer Nolzen, Victoria von Glasenapp, Rachelle Smith, Matthias S. Ullrich, and Nikolai Kuhnert*, "Distinguishing the polyphenolic and antibacterial profile of the leaves, fruits and flowers of *Rhododendron ambiguum* and *Rhododendron cinnabarinum* using high performance liquid chromatography coupled with ion trap and time of flight mass spectrometry", 2016, *submitted*.
- Abhinandan Shrestha, Inamullah Hakeem Said, Naika Thielen, Lucas Lansing, Hartwig Schepker and Nikolai Kuhnert*, "Determination of hydroxycinnamic acids present in *Rhododendron* species", 2016, *in preparation*
- Anne Grimbs, Abhinandan Shrestha, Ahmed Sayed Deyab Rezk, Jennifer Nolzen, Sergio Grimbs, Inamullah Hakeem Said, Hartwig Schepker, Marc-Thorsten Hütt, Dirk Carl Albach, Klaudia Brix, Nikolai Kuhnert, Matthias S. Ullrich*, "Bioactivity in *Rhododendron*: A systemic analysis of antimicrobial and cytotoxic activities and their phylogenetic and phytochemical origins", 2016, *in preparation*

Poster Presentations

- Abhinandan Shrestha, Inamullah Hakeem Said, Ahmed Rezk, Naika Thielen, Lucas Lansing, Victoria von Glasenapp, Rachelle Smith, Matthias S. Ullrich, Nikolai Kuhnert*. LC-MS analysis of *Rhododendron* species. Bremen Life Sciences Meeting. 2015. Jacobs University Bremen. Bremen, Germany.
- Abhinandan Shrestha, Inamullah Hakeem Said, Ahmed Rezk, Matthias S. Ullrich, Nikolai Kuhnert*. Identification and characterization of polyphenols found in different species of the genus *Rhododendron* by using tandem and time of flight mass spectrometry. 7th ISANH World Congress on Polyphenols Applications. 2013. Bonn, Germany.
- Abhinandan Shrestha, Inamullah Hakeem Said, Nikolai Kuhnert*. Identification and characterization of polyphenols found in *Rhododendron* species. Retreat-MOLIFE center (Jacobs University). 2013. Bad Bevensen, Germany.

Table of Contents

Abbreviations 12
Abstract 14
1. Introduction 15
1.1. Rhododendron Park Bremen (Germany) & Rhododendron Project 15
1.2. The genus *Rhododendron* 16
1.3. Traditional uses of *Rhododendron* species 16
1.4. Pharmacological studies of *Rhododendron* species 17
1.5. Toxicological studies of *Rhododendron* species 19
1.6. Phytochemical studies of *Rhododendron* species 20
1.7. Polyphenols 21
1.8. Polyphenols – Biosynthesis 32
1.9. Polyphenols – Bioavailability 34
1.10. Polyphenols – Analysis 35
1.11. Plant metabolomics and Chemotaxonomy 39
2. Motivation for the Project 40
3. Materials and Methods 42
3.1. Liquid Chromatography-Tandem Mass Spectrometry (LC-Ion Trap-MS) 42
3.2. Liquid Chromatography-Time of Flight Mass Spectrometry (LC-TOF-MS) 42
3.3. SPE 43
3.4. Preparative High Performance Liquid Chromatography (Prep-HPLC) 43
3.5. NMR 43
3.6. Chemicals 43
3.7. Extraction 44
3.8. Bruker Software 44
3.9. XCMS, RStudio and Metaboanalyst 44
3.10. Rhododendron Samples 45
4. Data Analysis 51
4.1. Scripting in Bruker Data Analysis 51
4.2. Methods in Bruker Data Analysis 51
4.3. Library 51
4.4. AutoMS(n) and Identify functions in Bruker Data Analysis 52
5. Neutral Losses 53
6. Data Interpretation 58

7. Hydroxycinnamic acid derivatives 60
7.1. Chlorogenic acids 60
7.2. Caffeic acid derivatives 66
7.3. *p*-Coumaric acid derivatives 68
7.4. Dihydrocoumaric acid derivatives 70
7.5. Ferulic acid derivatives 70
8. Hydroxybenzoic acid derivatives 73
8.1. Gallic acid derivatives 73
8.2. Protocatechuic acid derivatives 78
8.3. Salicylic acid derivatives 80
8.4. Vanillic acid derivatives 82
8.5. Methyl gallate derivatives 85
9. Flavan-3-ols 87
9.1. (Epi)catechin derivatives 87
10. Flavanones 103
10.1. Naringenin and its derivatives 103
10.2. Taxifolin and its derivatives 105
11. Flavonols 109
11.1. Myricetin and its derivatives 109
11.2. Quercetin and its derivatives 113
11.3. Kaempferol and its derivatives 121
11.4. Laricitrin and its derivatives 125
11.5. Isorhamnetin and its derivatives 127
12. Derivatives 129
12.1. Quinic acid derivatives 129
12.2. Hydroxycinnamic acid derivatives 129
12.3. Hydroxybenzoic acid derivatives 130
12.4. Flavan-3-ol derivatives 131
12.5. Flavonol derivatives 132
12.6. Other derivatives 132
13. Polyphenol distribution in *Rhododendron* 133
14. Anti-bacterial, Cytotoxic and Genetic studies 160
14.1. Anti-bacterial studies 160
14.2. Cytotoxic studies 160

14.3. Genetic studies 161
15. Metabolomic and Statistical Studies 163
15.1. Box Plots for Subgenera 164
15.2. Box Plots for Isomers 181
15.3. Marker Compounds 187
15.4. Correlation, Principal Component Analysis and Hierarchical Cluster Analysis 194
16. Comparison of the polyphenolic profile and anti-bacterial activity of the leaves, fruits and flowers of *Rhododendron ambiguum* and *Rhododendron cinnabarinum* 207
17. Additional Studies 222
17.1. Frost studies on *Rhododendron* leaves 222
17.2. Activity guided fractionation by Preparative HPLC of *Rhododendron ambiguum* leaf extracts 224
18. Discussion 229
19. Conclusion 232
20. Reference 235
21. Appendix 254
21.1. Phylogenetic tree and intensity of compounds 254
21.2. Standards 260
21.3. Compound Structures 263
21.4. Fragmentation Pattern of identified compounds 284
21.5. Fragmentation Pattern of derivatives 313
21.6. Additional Information on CD 319

Abbreviations

AcNPV: *Autographa californica nuclear* polyhedrosis Virus

CA: Caffeic Acid

CID: Collision Induced Dissociation

CO_2: Carbon dioxide

CoA: Acetyl Coenzyme A

Da: Daltons

DAD: Diode Array Detector

ECD: Electron Capture Detection

EIC: Extract Ion Chromatogram

ESI: Electro Spray Ionization

FA: Ferulic Acid

FID: Flame Ionization Detector

Glc: Glucopyranoside (Hexoside)

Glu: Glucuronide

H: Hydrogen

H_2O: Water

HIV: Human Immunodeficiency Virus

HPLC: High Performance Liquid Chromatography

HRF: Heterocyclic Ring Fission

HSV-1: Herpes Simplex Virus type-1

HSV-2: Herpes Simplex Virus type-2

IEC6: Intestinal Epithelial Cells

ITS: Internal Transcribed Spacer

M: Molecular ion

M_r: Molecular Weight

MS: Mass Spectrometry

MTT: 3-(4,5-dimethylthiazol-2-yl)-2,5-diphenyltetrazolium bromide

NMR: Nuclear Magnetic Resonance

PA: Proanthocyanidin

PAL: Phenyl Alanine Lyase

p-CouA: *p*-Coumaric Acid

QA: Quinic Acid

QM: Quinone Methide fission

RDA: Retro Diels Alder reaction

Rha: Rhamnoside

RP: Reversed Phase

PDA: Photodiode array

SPE: Solid Phase Extraction

Thr: Threonate

TIC: Total Ion Chromatogram

TOF: Time Of Flight

t_R: Retention Time

UV-Vis: Ultra Violet – Visible

Xyl: Xyloside (Pentoside)

Abstract

This research was successful in creating a polyphenolic profile of the leaves of 100 *Rhododendron* species, which belong to the six subgenera: *Azaleastrum*, *Hymenanthes*, *Rhododendron*, *Pentanthera*, *Tsutsusi* and *Mumeazalea*. The polyphenolic profile of the fruits and flowers of a few *Rhododendron* species was also studied. This was achieved by using the technique of liquid chromatography coupled to mass spectrometry. Compounds were identified based on their retention time, UV absorption, fragmentation pattern and high resolution mass data. A few authentic standards were used for comparison purposes.

The leaves of *Rhododendron* species were determined to be a good source of polyphenolic secondary metabolites with a total of 348 polyphenols identified. Out of the 348 identified compounds, 221 compounds were novel in *Rhododendron* species and 7 compounds were novel in nature. The most abundant compounds included quercetin derivatives, protocatechuic acid-*O*-hexoside, catechin, epicatechin, procyanidin A and B dimers, kaempferol-*O*-rhamnoside, *p*-coumaric acid-*O*-hexoside, 3-*O*-caffeoylquinic acid and 5-*O*-caffeoylquinic acid.

The actual function of secondary metabolites in *Rhododendron* species is mostly unknown. From the identified secondary metabolites in *Rhododendron* species, a few marker compounds were identified for some individual *Rhododendron* species and also for the six subgenera. The use of polyphenolic secondary metabolites as chemotaxonomic markers needs to be assessed.

Multivariate statistical analysis was carried out to investigate whether phytochemistry, phylogeny and biological activity showed any correlation. The relative quantities of polyphenolic compounds were compared using box plots. Some compounds were found in higher intensity in certain subgenus. Some isomers of these compounds were found to be relatively more abundant than others. PCA plots and hierarchical clustering plot were generated using LC-TOF-MS data and it was determined that the genetically similar *Rhododendron* species produces a diverse variety of secondary metabolites. The number of compounds present in *Rhododendron* species was found to have no correlation to the ploidy level or their anti-bacterial activity against *Bacillus subtilis*.

1. Introduction

1.1. Rhododendron Park Bremen (Germany) & Rhododendron Project

The Rhododendron Park is located in Deliusweg 40, Bremen, Germany. It covers a total of 46 hectares and is cultivating more than 1000 varieties of *Rhododendron* species. It has an open park as well as a botanical garden. The botanical garden was created in 1905 by businessman Ernst Franz Schütte. However, the park was created in 1933 with the help of German Rhododendron Society and was later opened to public from 1937.

With the availability of a wide variety of *Rhododendron* species in the Rhododendron Park, the Rhododendron Project was initiated with the vision to combine the different fields of research in order to investigate the *Rhododendron* species in detail from different perspectives. The project has been divided into the following three parts:

a. Genetic Research (Jennifer Nolzen under the supervision of Prof. Dr. Dirk Albach): The phylogenetic studies were conducted on *Rhododendron* species using different gene markers such as *trn*K, *trn*L-F, and ITS. The markers were used to create a maximum likelihood tree, which was used to compare the different subgenera of *Rhododendron* species.

b. Microbiology and Cell Biology Research (Dr. Ahmed Rezk under the supervision of Prof. Dr. Matthias S. Ullrich and Prof. Dr. Klaudia Brix): The extracts of *Rhododendron* species were tested against different bacterial strains to test for anti-microbial activity. The same extracts were also tested against HaCaT (skin) cells and intestinal epithelial cells to test for cytotoxic effects.

c. Chemical Research (Abhinandan Shrestha under the supervision of Prof. Dr. Nikolai Kuhnert): The extracts of *Rhododendron* species were analyzed for the secondary metabolites present in them to generate a phytochemical profile. Some species were also selected for activity guided fractionation to identify the compounds producing anti-microbial effects.

1.2. The genus *Rhododendron*

The genus *Rhododendron L.* belongs to the Ericaceae family of flowering plants. It is one of the largest and diverse genera of vascular plants that are distributed mostly in the Northern hemisphere. The genus consists of more than 1000 species, which are divided further into 8 subgenera, namely *Rhododendron*, *Hymenanthes*, *Pentanthera*, *Tsutsusi*, *Azaleastrum*, *Candidastrum*, *Mumeazalea* and *Therorhodion*.[1, 2] They are mostly found in the Himalayan region (Bhutan, China, India, Myanmar, Nepal, Sri Lanka and Thailand), South-East Asia and Malesia.[3, 4] A minority of species are found in Europe and North America and only two species in North-East Australia.[5]

The *Rhododendron* species vary in size and shape, ranging from shrubs to trees.[5] They are mostly evergreen and can grow in diverse climatic conditions.[6] A few species are known to be deciduous. There is also variation in the size and shape of the entire margined leaves, ranging from linear to orbicular. The colorful flowers are found in a raceme or corymb cluster and are used for decorative purposes. The fruits are found as capsule-shaped while the seeds are found as flattened or spindle-shaped to ellipsoid.[5]

1.3. Traditional uses of *Rhododendron* species

Rhododendron species have been traditionally used in the treatment of different ailments and disorders.[5, 6] In China, *Rhododendron* species have been used for treating arthritis, asthma and bronchitis.[5, 7-11] *Rhododendron brachycarpum* has been employed in Korea for treating diabetes, headache, arthritis and hypertension.[5, 12] The flowers and leaves of *Rhododendron anthopogon* and *Rhododendron anthopogonoides* have been used in Tibetan herbalism to treat inflammation and skin and lung ailments.[5, 13, 14] In Nepal, *Rhododendron lepidotum*, *Rhododendron anthopogon* and *Rhododendron campanulatum* are used to treat different ailments.[5, 15, 16] The Ayurvedic medical system in India have used 12 *Rhododendron* species (*Rhododendron abroberum*, *Rhododendron lepidotum*, *Rhododendron campanulatum*) for treating altitude sickness, diarrhea, dyspepsia, nose bleeding and headaches.[5, 17, 18]

Rhododendron hirsutum and *Rhododendron ferrugineum* flowers have been used in Austria for the treatment of cardio-vascular, gastro-intestinal, urinary and respiratory tract ailments.[5, 19] In Germany, *Rhododendron ferrugineum* leaves have been employed to treat rheumatism, muscle pain, hypertension and metabolic disease.[5, 20, 21] *Rhododendron kotschyi* has been used in Romania to treat cough, rheumatism and lung ailments.[5] In Turkey, *Rhododendron ponticum* and *Rhododendron luteum* have been employed for the treatment of rheumatism, inflammation and fungal infections.[5, 22-24]

The Native Americans have used *Rhododendron calendulaceum*, *Rhododendron maximum* and *Rhododendron albiflorum* to treat rheumatism, women's ailments, sore throats common cold, gastro-intestinal disorders and swelling.[5, 25] *Rhododendron groenlandicum* has been used in Northern Canada against diabetes.[5, 26, 27]

Besides traditionally being used to treat human illnesses, *Rhododendron* species have also been used as psychoactive ritual incense[28] (*Rhododendron tomentosum*, *Rhododendron aureum*, *Rhododendron lepidotum* and *Rhododendron caucasicum*) in Asia and Europe, narcotic (*Rhododendron viscosum*) in North America, diaphoretic (*Rhododendron caucasicum*) in Caucasus, to preserve fruits (*Rhododendron albiflorum*) by Native Americans and as an insect repellent (*Rhododendron tomentosum*) in Siberia.[5]

1.4. Pharmacological studies of *Rhododendron* species

Different parts of *Rhododendron* species have been tested in numerous studies to find out the beneficial effects on human health. From these studies, it has been observed that some *Rhododendron* species have anti-inflammatory activity[24], analgesic activity[29, 30], anti-microbial activity[31, 32], anti-fungal activity[33], anti-protozoal activity[34], anti-viral activity[35-39], immuno-modulatory activity[40, 41], anti-oxidant activity[42, 43], anti-diabetic activity[12, 27, 44], anti-spasmodic activity[30], hepato-protective activity[45], cardio-protective activity[46], tyrosinase (pigmentation enzyme of mammalian skin and hair) inhibitory activity[47] and acetylcholinestherase (enzyme that prevents acetyl-choline breakdown, which is used to treat Alzheimer's disease) inhibitory activity[48].[5] The list of *Rhododendron* species

that have displayed such activities are shown in Table 1.1. Most of the pharmacological activity of *Rhododendron* species has been linked to their flavonoid composition.[5, 24, 29]

In anti-microbial studies, some *Rhododendron* species were found to be active against *Escherichia coli*, *Staphylococcus aureus*, *Enterococcus fecalis* and *Bacillus subtilis*.[2, 5, 31, 32] In anti-protozoal studies, a few *Rhododendron* species were observed to be active against *Leishmania donovani* and *Plasmodium falciparum*.[34] From anti-viral studies, it was determined that some *Rhododendron* species were active against herpes simplex virus type-1 (HSV-1)[38, 39] and type-2 (HSV-1)[35], HIV[37] and *Autographa californica nuclear* polyhedrosis virus (AcNPV)[36].[5]

Table 1.1: Pharmacological activities of *Rhododendron* species

Biological Activity	**Species**
Anti-inflammatory activity	*Rhododendron arboretum* *Rhododendron ponticum* *Rhododendron spinuliferum* *Rhododendron dauricum* *Rhododendron anthopogon* *Rhododendron aureum* *Rhododendron mucronulatum*
Analgesic activity	*Rhododendron micranthum* *Rhododendron ponticum* *Rhododendron collettianum* *Rhododendron arboretum*
Anti-microbial activity	*Rhododendron setosum* *Rhododendron lepidotum* *Rhododendron anthopogon* *Rhododendron arboretum* *Rhododendron brachycarpum* *Rhododendron luteum*
Anti-fungal activity	*Rhododendron tomentosum*
Anti-protozoal activity	*Rhododendron luteum* *Rhododendron ponticum* *Rhododendron simrnowii* *Rhododendron ungenii*

Biological Activity	Species
Anti-viral activity	*Rhododendron dauricum* (Anti-HIV) *Rhododendron simsii* (Anti-HSV-2) *Rhododendron caucasicum* (Anti-AcNPV) *Rhododendron ungernii* (Anti-HSV-1) *Rhododendron ferrugineum* (Anti-HSV-1)
Immunomodulatory activity	*Rhododendron spiciferum*
Anti-oxidant activity	*Rhododendron simsii* *Rhododendron dauricum* *Rhododendron yedoense* var. *poukhanense* *Rhododendron griffithianum* *Rhododendron lepidotum* *Rhododendron virgatum*
Anti-diabetic activity	*Rhododendron arboretum* *Rhododendron tomentosum* *Rhododendron groenlandicum* *Rhododendron brachycarpum* *Rhododendron schlippenbachii*
Anti-spasmodic activity	*Rhododendron collettianum*
Tyrosinase inhibitory activity	*Rhododendron collettianum*
Hepatoprotective activity	*Rhododendron arboreum*
Cardioprotective activity	*Rhododendron arboreum*
Acetylcholinestherase inhibitory activity	*Rhododendron ponticum* *Rhododendron luteum*

1.5. Toxicological studies of *Rhododendron* species

Rhododendron species have been known to be toxic mostly due to the presence of grayanotoxins (Figure 1.1), which belong to the terpenoid class of compounds.[5, 6] In India, *Rhododendron arboretum*, *Rhododendron campanulatum* and *Rhododendron cinnabarinum* have been known to be poisonous to humans or livestock. The *Rhododendron* species have also been used as an insecticide in India (*Rhododendron thomsonii*) and additionally as fish poison in India (*Rhododendron barbatum* and *Rhododendron falconeri*), Siberia (*Rhododendron aureum*) and Caucasus (*Rhododendron caucasicum*).[5]

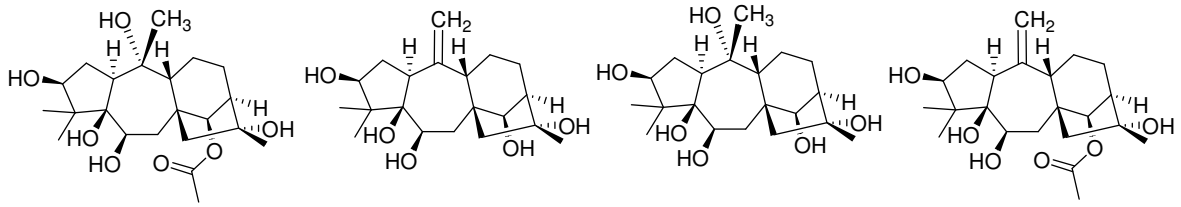

Figure 1.1 Grayanotoxins found in *Rhododendron* species

Some *Rhododendron* species have been used to produce honey. They are sometimes referred to as "toxic honey" or "mad honey".[49] In Turkey, *Rhododendron ponticum* and *Rhododendron luteum* growing in the Black Sea region is the major source of honey.[5, 49] Besides Turkey, *Rhododendron* honey is also produced in Nepal, Japan, Brazil and a few regions of Europe and North America.[49] The honey poisoning at lower doses can cause bradycardia, dizziness, hypotension and gastro-intestinal discomfort. At higher doses, it can case seizures, consciousness disorder and blockage of the atria and ventricles of the heart.[5, 50, 51] Intoxications caused by *Rhododendron* honey have been reported in Turkey, Austria and Nepal.[5]

Rhododendron poisoning in animals (sheep, lamps, goats, kangaroos and cattle) were observed after ingestion of the *Rhododendron* plants.[5, 52-54] The effects of this poisoning include spasm, bloating, diarrhea, salivation, loss of energy and lactating potential and even death.[5, 55] A few *Rhododendron* species (*Rhododendron anthopogon*, *Rhododendron brachycarpum* and *Rhododendron metternichii* var. *pentamerum*) were tested against mice, which resulted in minor liver lesions and increased respiratory, locomotive and stimulant activity.[5, 56, 57]

Rhododendron ferrugineum was observed to have cytotoxic activity against human promyelocytic leukemia HL-60 cells.[5, 58] *Rhododendron brachycarpum* was found to be cytotoxic against human cancer cell lines (A549, AGS, Hep3B and MCF7).[5, 59] *Rhododendron mucronatum* displayed cytotoxic activity against HaCaT keratinocyte cell line.[5, 60]

1.6. Phytochemical studies of *Rhododendron* species

There have been some phytochemical studies on the secondary metabolites of *Rhododendron* species. They are known to be a good source of flavonoids and terpenoids.[5, 61] They are also known to consist of essential oils, iridoids, steroids, coumarins, β-diketones, chromones,

chromanes and chromenes and other phenol derivatives.[6, 61] Diterpenoids, triterpenoids and sesquiterpenoids are the types of terpenoids identified in *Rhododendron* species. The flavonoids identified in *Rhododendron* species belonged to the group of chromones, flavones, flavanones, flavonols, flavan-3-ols, dihydrochalcones and proanthocyanidins.[6, 61] However, there has been limited number of studies in the polyphenolic profile of *Rhododendron* species.

1.7. Polyphenols

Polyphenols are secondary metabolites produced by plants that facilitate the growth of plants and also help in their defense mechanism against pests and herbivores. The structure of polyphenols consists of a single or multiple aromatic rings and hydroxyl groups. The diversely structured polyphenols are responsible for different characteristics such as color and flavor of the plant parts (roots, leaves, fruits, flowers). They are divided into four major categories, namely phenolic acids, flavonoids, lignans and stilbenes as shown in Figure 1.2.[62] The extensive studies on polyphenols have resulted in the identification of over 8000 phenolic structures from natural sources, of which more than 4000 are flavonoids.[63] In plants, the polyphenols are usually found as glycosides with different associated sugar moieties, which may be acylated.[62]

Polyphenols are a major part of the human diet in the form of fruits (apples, strawberries, grapes and peaches), beverages (tea, coffee, juices, wine, cider and beer), vegetables, leguminous plants, chocolate and cereals. They are known to contribute to beneficial effects towards human health.[62] The anti-oxidant effect of polyphenols was considered to be responsible for this effect; however recent studies have indicated that anti-oxidant effect is grossly overestimated and should be marginalized in the search of other mechanisms of action.[62, 64] They are also known to have anti-mutagenic, anti-carcinogenic, anti-microbial and metal-chelating properties.[62] In addition, they have protective effects against wounds, skin diseases, cardiovascular diseases, drug toxicity and UV radiations.[65]

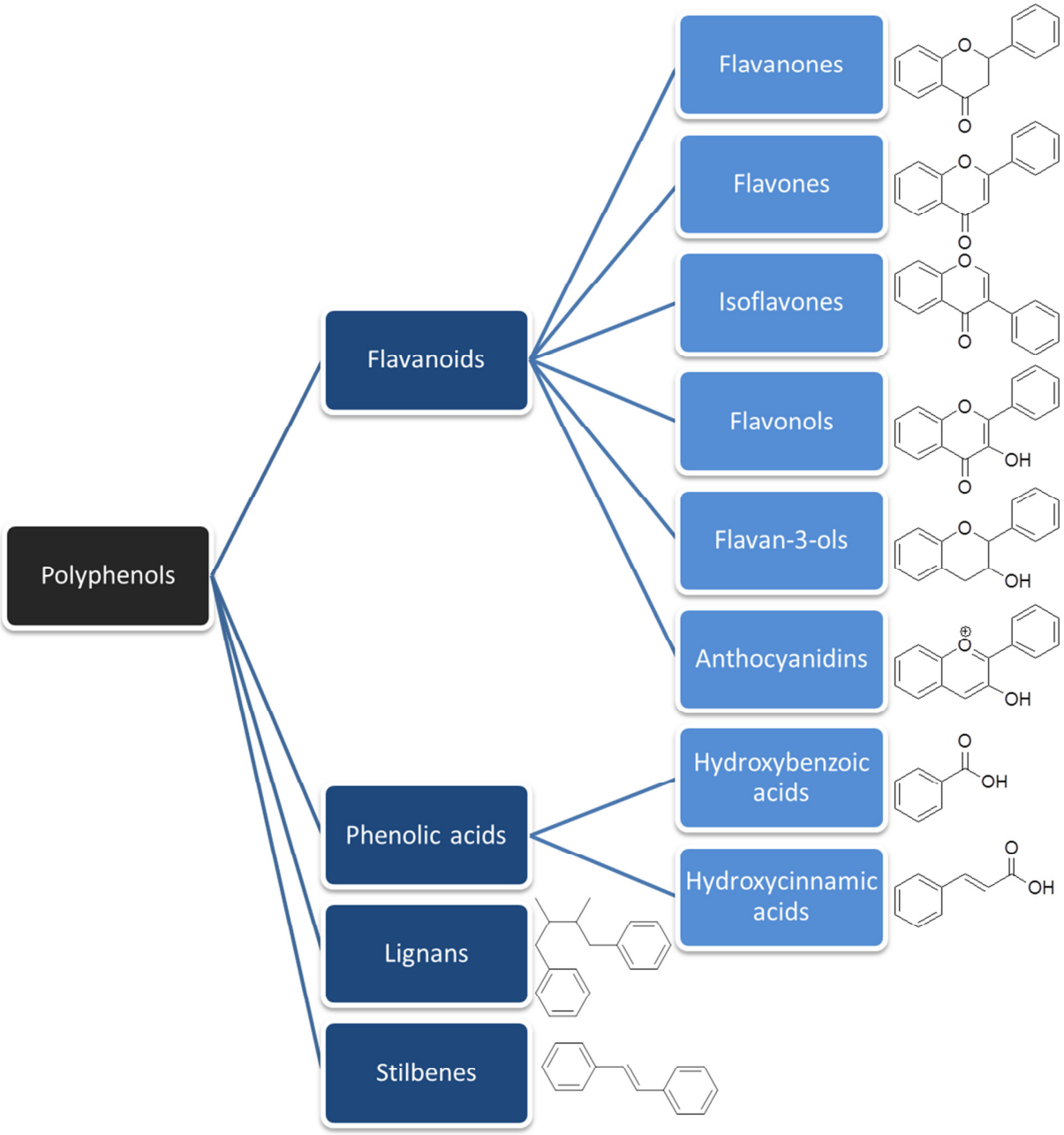

Figure 1.2: Classification of polyphenols and their basic structures

1.7.1. Phenolic acids

Phenolic acids are aromatic acids found in plants, which consist of a phenol ring and a carboxylic functional group. They are divided into two groups: hydroxybenzoic acid derivatives and hydroxycinnamic acid derivatives, which have backbone structures of C1-C6 and C3-C6 respectively.

Hydroxybenzoic acids

Hydroxybenzoic acid derivatives include acids such as gallic acid, ellagic acid, protocatechuic acid, vanillic acid, salicylic acid and syringic acid. They are found in fruits (strawberries, raspberries and blackberries), vegetables (onion and radish), beverages (tea, juice, wine, stout, ale and lager) and cereals. They are usually found in the free or esterified or glycosylated form. There have been extensive studies conducted for gallic acid and ellagic acid and they are known to be a part of hydrolysable tannins. Gallic acid, found in black tea is also known to be esterified to condensed or derived tannins and quinic acid.[62, 66]

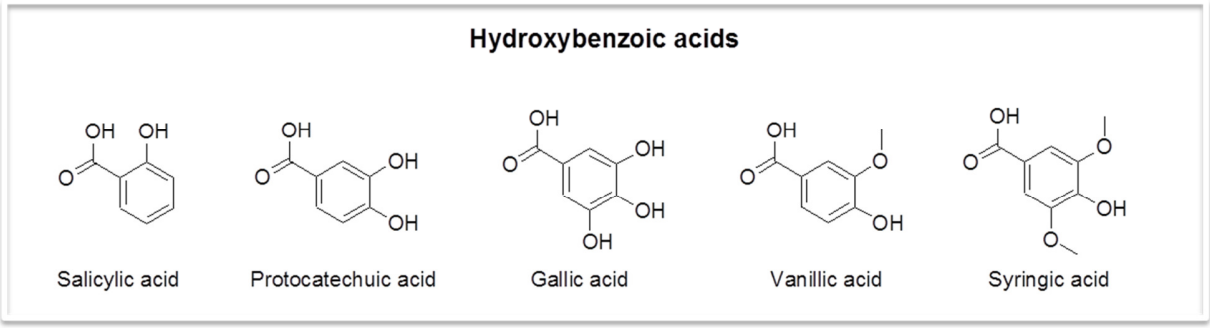

Figure 1.3: Hydroxybenzoic acids

Hydroxycinnamic acids

Hydroxycinnamic acid derivatives include acids such as caffeic, ferulic, sinapic and *p*-coumaric acids. They are found in fruits (kiwi, cherries, plums and apples), beverages (coffee and beer) and cereals. They are usually found in glycosylated form or esterified form with quinic acid, shikimic acid and tartaric acid, however their free form is found only in processed foods. Caffeic acid is abundantly found in fruits and coffee, while ferulic acid is found mostly in cereals such as wheat, rice, oat and maize. The hydroxycinnamic acids (caffeic, ferulic, and *p*-coumaric acid) form esters with quinic acid, which are commonly referred to as chlorogenic acids. Coffee is a rich source of chlorogenic acids with concentrations ranging from 70-350 mg per 200 mL cup.[62] There has been a considerable amount of research conducted on hydroxycinnamic acids, which have displayed beneficial properties such as anti-oxidant, anti-mutagenic, anti-inflammatory, anti-diabetic and anti-carcinogenic activities.[67]

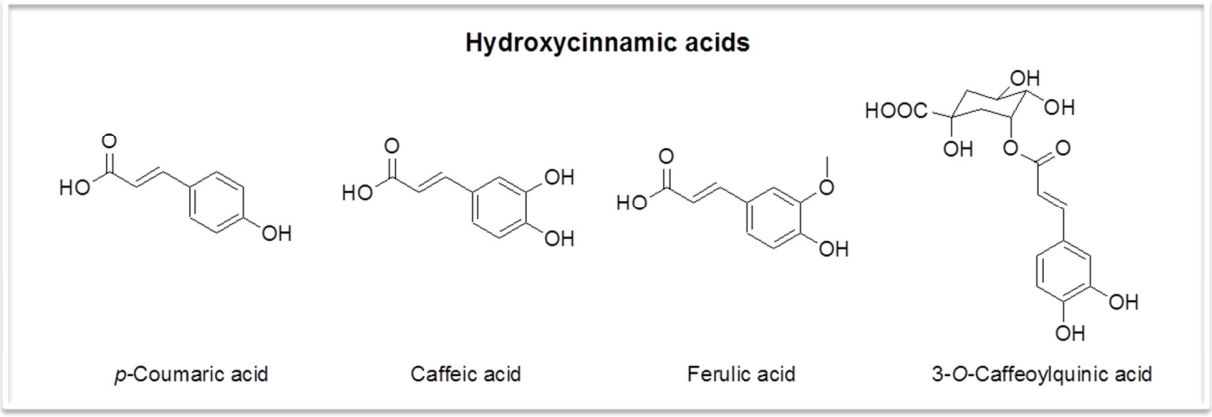

Figure 1.4: Hydroxycinnamic acids

1.7.2. Flavonoids

Flavonoids are compounds found in plants with a backbone structure of C6-C3-C6 in which both C6 units (Ring A and Ring B) are phenolic in nature. The variations in the chromane ring (Ring C) and hydroxylation patterns leads to further classification of flavonoids into sub-groups such as flavonols, flavones, flavanones, isoflavones, flavan-3-ols and anthocyanidins. In most of the flavonoid structures, Ring B is attached to Ring C via the C2 position. However, in some flavonoids such as isoflavones and neoflavonoids, Ring B is attached to Ring C via the C3 and C4 position respectively. Another exception is chalcones, which lack Ring C in their structures.[62]

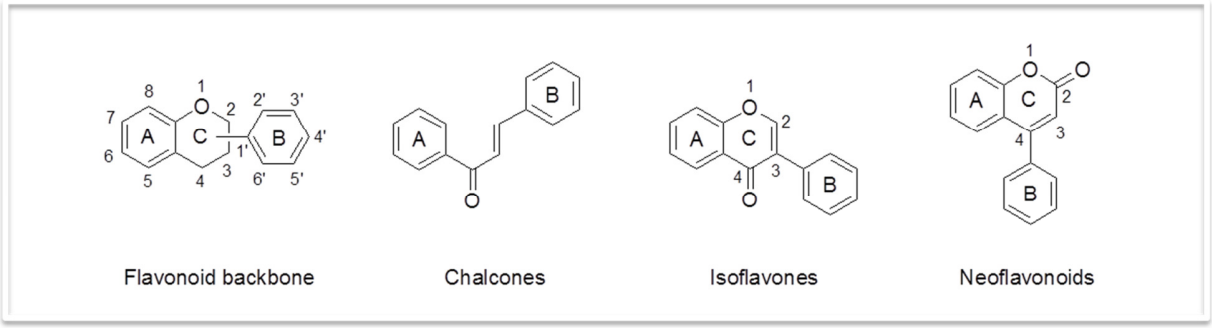

Figure 1.5: Backbone structures of flavonoids

Flavonols

Flavonols such as quercetin and kaempferol derivatives are commonly found in plants, and in human diet they are found in fruits (blueberries), vegetables (broccoli and onions) and beverages

(tea and wine). Myricetin, laricitrin, azaleatin and fisetin are other examples of flavonols. They are generally found in the glycosylated form. Glucose or rhamnose are the most common sugar units attached to them followed by galactose, arabinose, xylose and glucuronic acid. The biosynthesis of flavonols is stimulated by light and thus they are present in higher quantities in outer aerial tissues (leaves and fruit skin).[62] Quercetin has been extensively researched upon and is known to have anti-oxidant and anti-inflammatory effects *in vitro* and *in vivo*. However, some *in vitro* studies have shown its toxic effects, most probably due to the formation of quinones (after oxidation), which reacts with glutathione or protein sulfhydryl groups and consequently impairs enzyme functions.[68] Kaempferol is known to have anti-oxidant and anti-cancer properties[69] and myricetin is known to have anti-diabetic properties.[70]

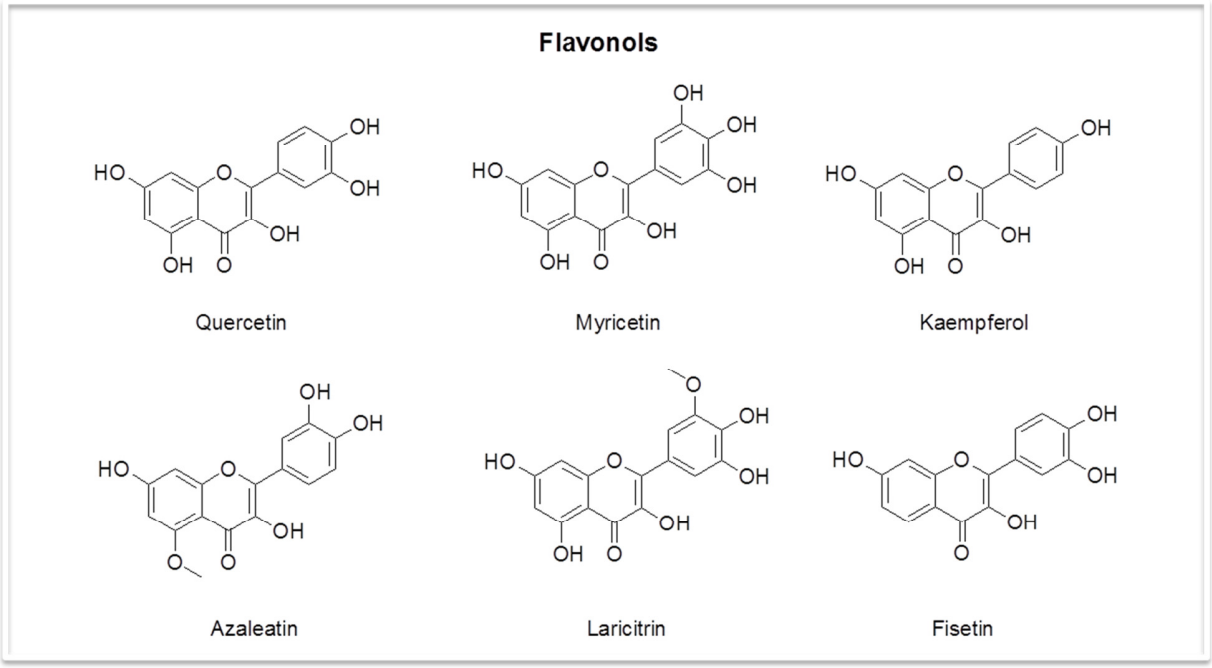

Figure 1.6: Flavonols [71]

Flavones

Flavones are usually found in fruits, vegetables (celery and parsley) and cereals (wheat and millet). The most common flavones identified are the glycosylated derivatives of apigenin and luteolin. The skin of citrus fruits is a major source of polymethoxylated flavones (tangeretin, nobiletin and sinensetin), which are hydrophobic in nature.[62] Apigenin is known to have anti-

cancer properties[72] and luteolin is known to have anti-inflammatory and neuro-protective properties.[73]

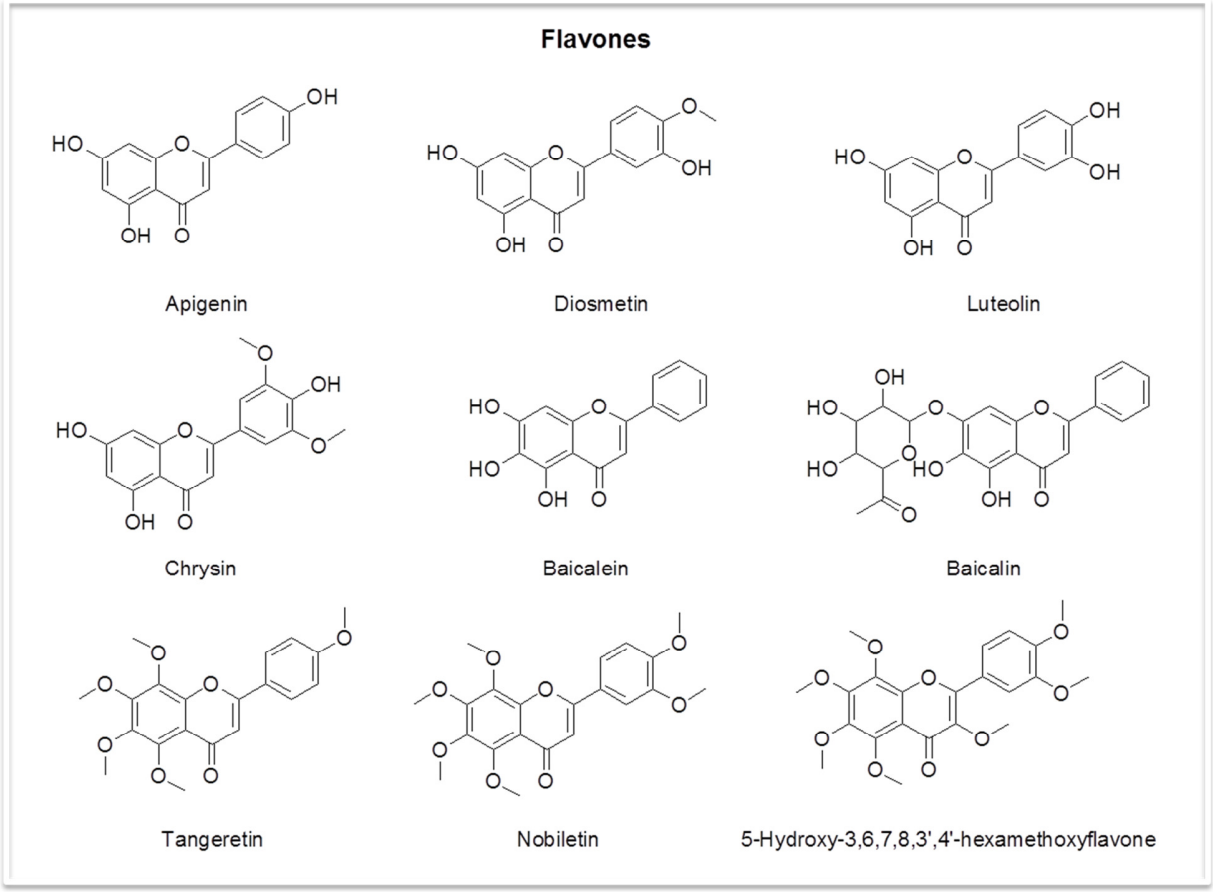

Figure 1.7: Flavones [71]

Flavanones

Flavanones are found prevalently in citrus fruits and relatively smaller amounts in tomatoes and aromatic plants (mint). Naringenin, hesperetin and eriodictyol are found in their free form and glycosylated form in grapefruits, oranges and lemons respectively. The glycosylated derivatives can influence the taste of the fruits.[62] Many different substituted derivatives have been identified for flavanones. For example, taxifolin, which is a compound found in citrus fruits and is further classified as a flavanonol as it consists of an additional hydroxyl group in Ring C.[63] Naringenin is known to have anti-cancer and anti-atherogenic properties[74], hesperetin and eriodictyol are known to have anti-inflammatory and anti-atherogenic properties.[75, 76]

Taxifolin is known to have anti-inflammatory, anti-cancer, anti-microbial and metal-chelating (it chelates to Cadmium and thus reduces its toxicity) properties.[77]

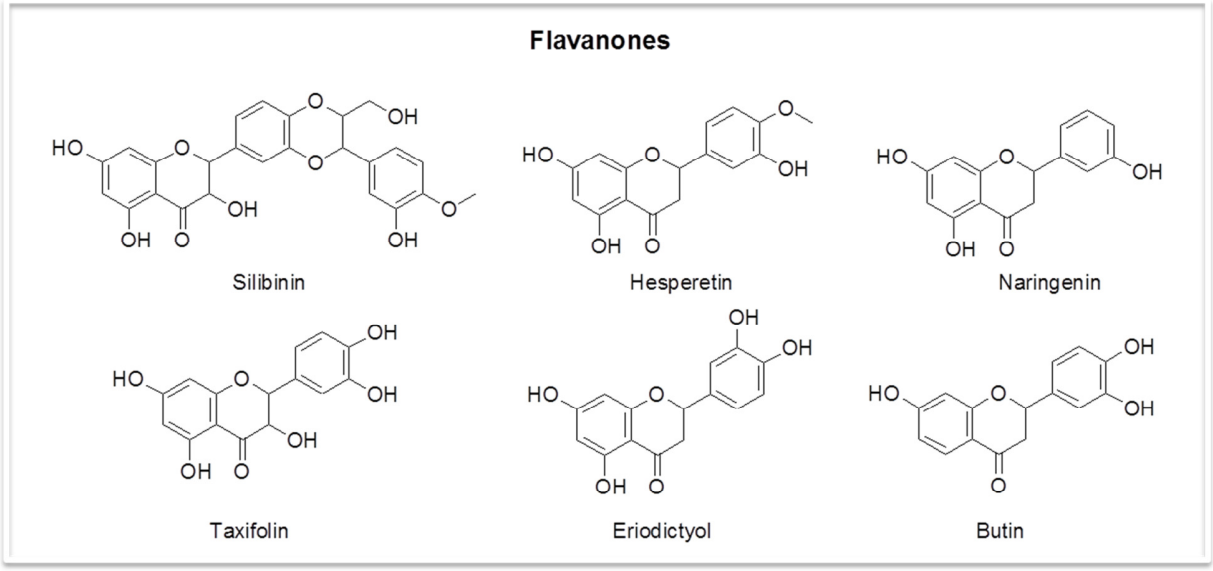

Figure 1.8: Flavanones [71]

Isoflavones

Isoflavones are found mostly in leguminous plants. The structure of isoflavones are similar to estrogen, hence they are classified as phytoestrogens. The amount of isoflavones in soybean is around 580-3800 mg/kg fresh weight. In soybean, genistein and daidzein are found in relatively large quantities, while glycitein, biochanin A and formononetin are found in relatively small quantities. They are found in free form and glycosylated form (which may consist of additional acetyl or malonyl units). The glycosylated derivatives consisting of malonyl group are responsible for a bitter taste.[62, 63]

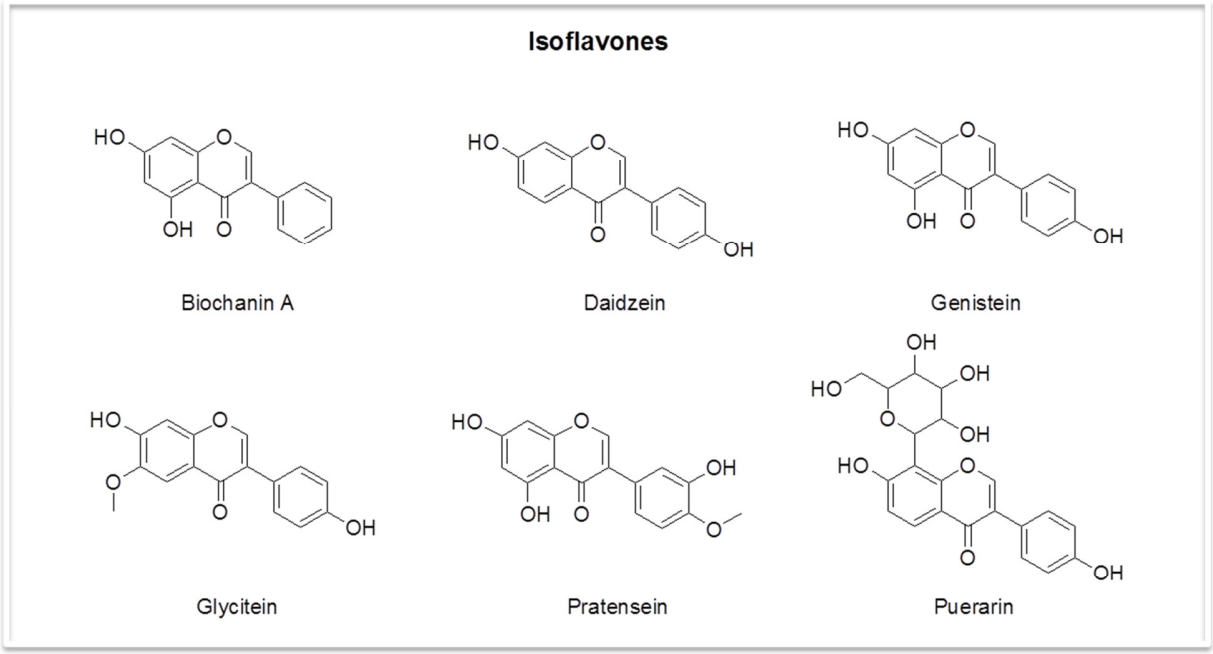

Figure 1.9: Isoflavones [71]

Flavan-3-ols and Proanthocyanidins

Flavan-3-ols are found in plants in the form of monomers and polymers, which are commonly known as catechins and proanthocyanidins respectively. In human diet, they are found in fruits (apricots, grapes, apples, peaches and pears), beverages (tea, beer, cider and wine) and chocolate. They are usually found in the aglycone form. Catechin and epicatechin are mainly present in fruits, while galloylated catechin derivatives such as gallocatechin and epigallocatechin are present in tea, grapes and leguminous plants. Green tea is known to have more catechins (up to 200 mg per cup), while black tea is known to have more theaflavins and thearubigins due to fermentation.[62]

Proanthocyanidins, also known as condensed tannins are produced from the oligomerization, dimerization and polymerization of flavan-3-ol units such as afzelechin, epiafzelechin, catechin, epicatechin, gallocatechin and epigallocatechin.[6] The B-type proanthocyanidins are linked together via C4-C8 or C4-C6 bonds and the A-type proanthocyanidins are linked together via C2-*O*-C7 or C2-*O*-C5 bonds.[63] The dimers and trimers of catechins are the most abundant proanthocyanidins found in nature. Proanthocyanidins react with salivary proteins to form

complexes that are responsible for the bitter taste of chocolate and astringent taste of fruits and beverages.[62] They have been reported to have anti-oxidant, anti-diabetic, anti-inflammatory and anti-mutagenic and cardio-protective properties.[6]

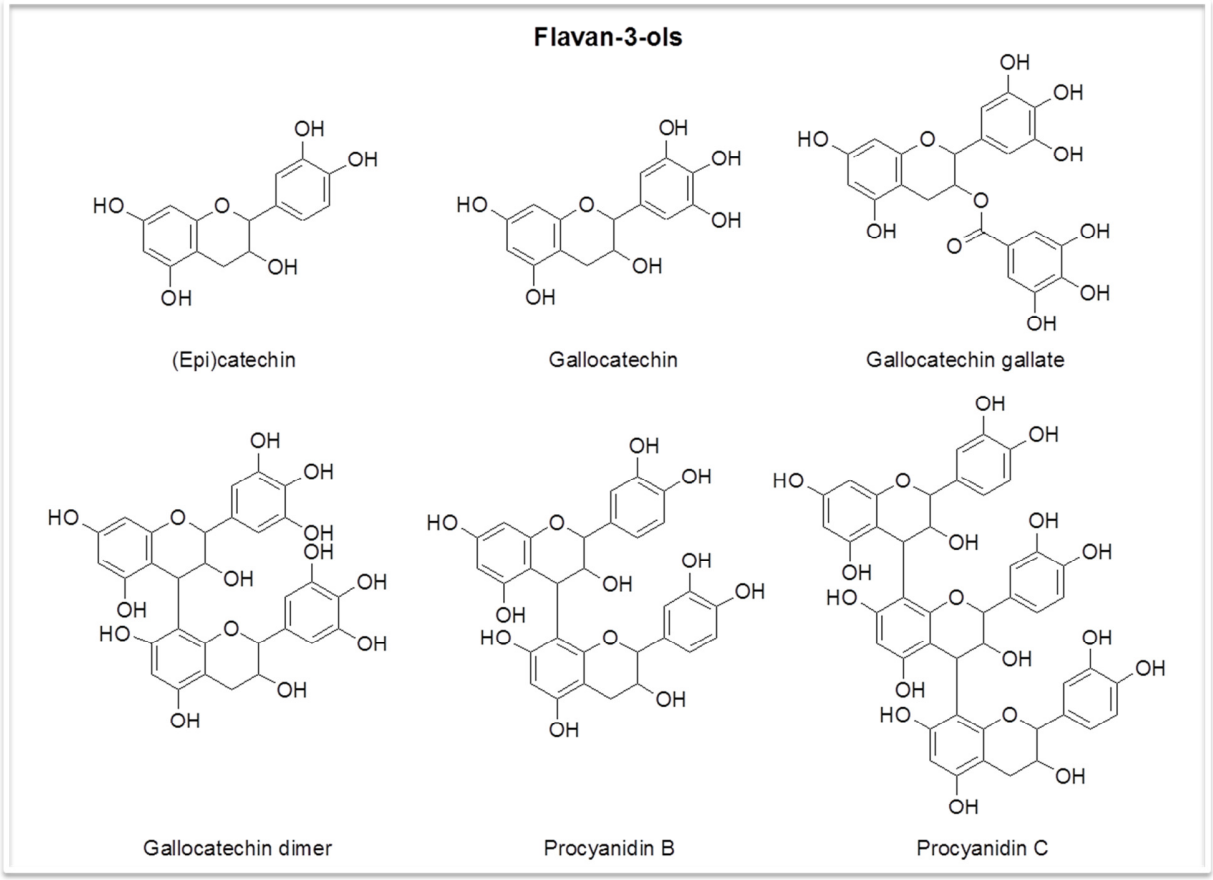

Figure 1.10: Flavan-3-ols and Proanthocyanidins [71]

Anthocyanidins

Anthocyanidins are fundamental parts of different color (blue, purple and red) pigments found in flowers, fruits and vegetables. They are also found in a substantial amount in wines (~200-300 mg/L). The aglycone form of anthocyanidins is unstable and thus they are generally glycosylated or esterified with organic and phenolic acids. The glycosylated anthocyanidins are known as anthocyanins. They are known to form complexes with other flavonoid groups, which results in copigmentation. The most abundant anthocyanins are cyanidin, delphinidin and pelargonidin. The color of anthocyanidins is dependent on hydroxylation, glycosylation and methylation patterns

and pH conditions. They are known to be stable in acidic conditions.[62, 63] Anthocyanidins are known to have anti-oxidant, anti-inflammatory and anti-cancer properties.[78]

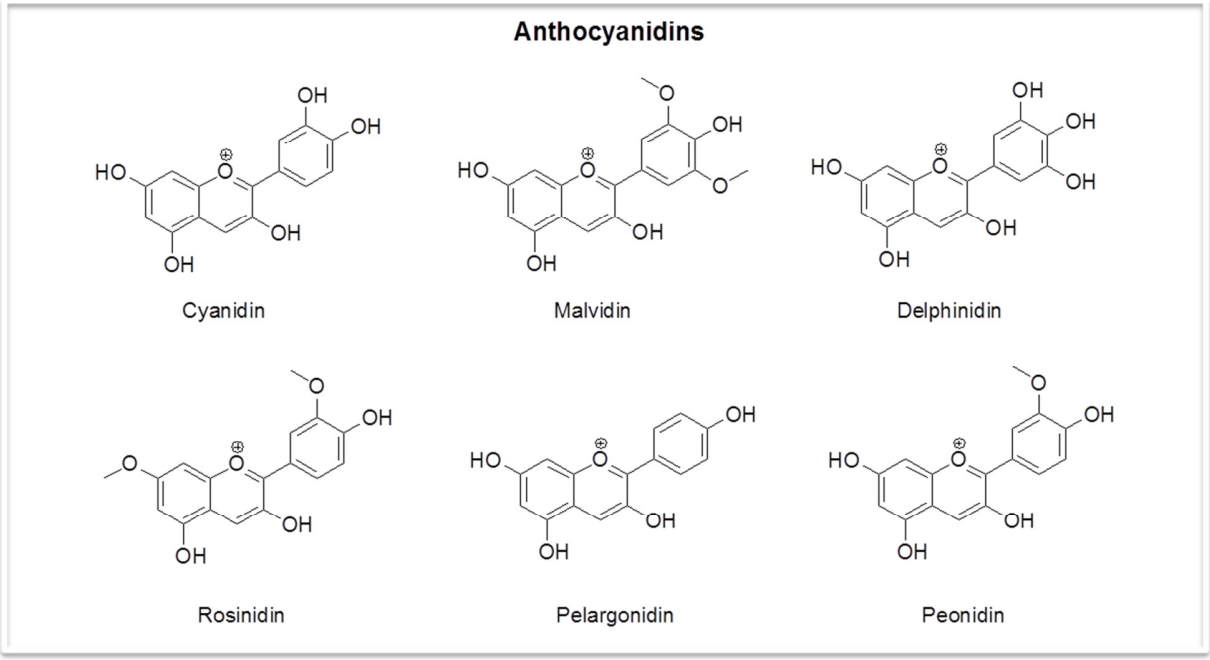

Figure 1.11: Anthocyanidins [71]

1.7.3. Lignans

Lignans consist of two phenylpropane units and are known to have protective effects in plants. The major source of lignans in human diet is oleaginous seeds (linseed), which contains a high amount of secoisolariciresinol and low amount of matairesinol. Lignans are also found in small quantities in some fruits (prunes and pears), vegetables (asparagus, carrots and garlic), leguminous plants (lentils) and cereals.[62] They are known to have anti-cancer and chemo-protective properties and have been used in treatments for cancer, lymphoma and leukemia.[79]

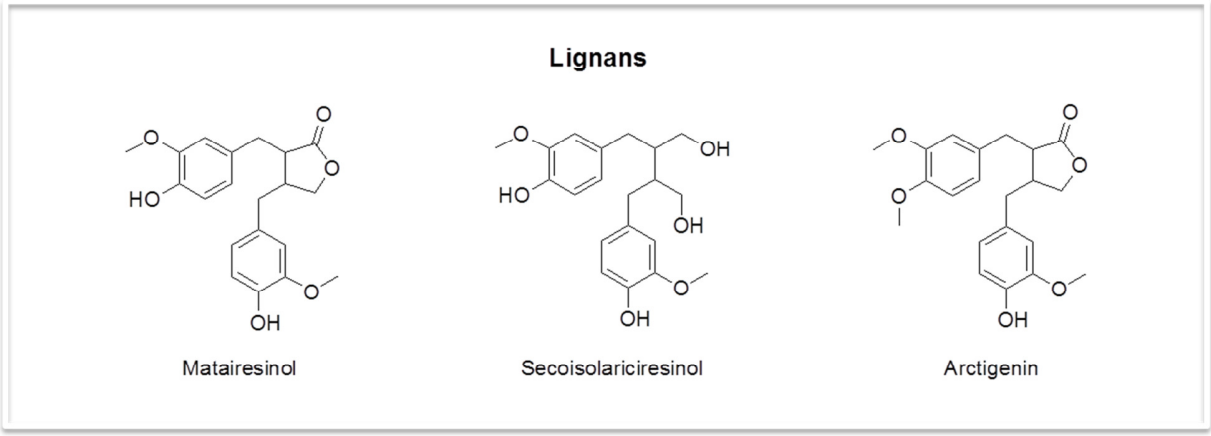

Figure 1.12: Lignans [71]

1.7.4. Stilbenes

Stilbenes (C6-C2-C6) such as resveratrol, piceid and viniferin are found in small quantities in Vitaceae plant family, which includes grapes. They aid in the defense mechanism of such plants. Resveratrol is known to have anti-carcinogenic and coronary-protective properties; however the effect is insignificant due to its low concentration in a normal dietary intake.[62, 80, 81]

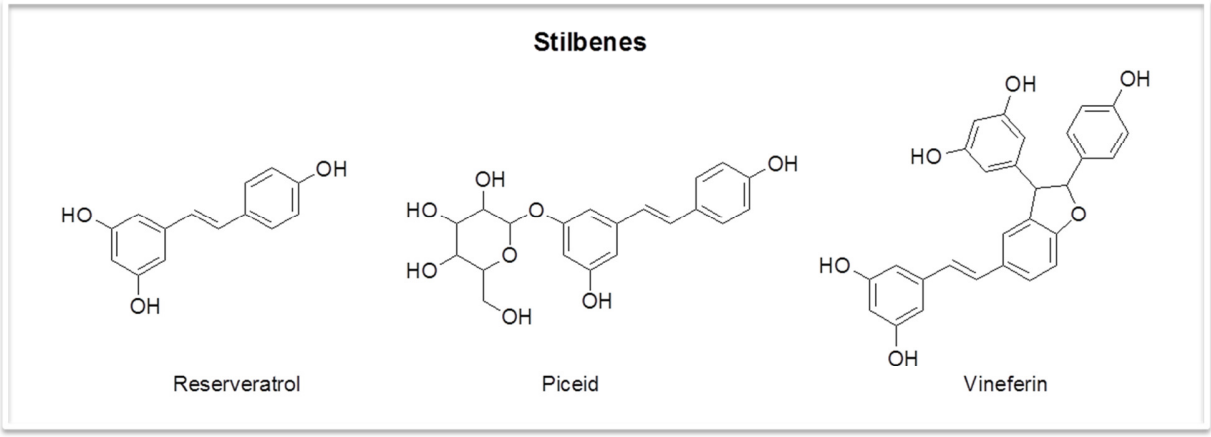

Figure 1.13: Stilbenes [71]

1.8. Polyphenols – Biosynthesis

The biosynthesis of polyphenols occurs inside the plant through different pathways such as shikimate, mevalonic acid, pentose phosphate and phenylpropanoid pathways. The shikimate pathway is known to produce phenylalanine, gallic acid and cinnamic acid as metabolites. The three units of malonyl-CoA are considered to generate Ring A, while phenylalanine is considered to generate Ring B and chromane ring of the flavonoids. The transformation of phenylalanine to cinnamate is catalyzed by phenylalanine ammonia lyase. The cinnamate produces *p*-coumaroyl-CoA, which subsequently reacts with three malonyl-CoA molecules to produce naringenin chalcone through a condensation reaction. Naringenin chalcone is the first flavonoid structure generated in the biosynthetic pathway, which reacts with different enzymes to generate different types of flavonoids. The enzyme glucosyltransferase is responsible for the glucosylation of flavonoids. The study of polyphenol biosynthesis can aid in the field of designer food production (polyphenol-rich food for healthy diets).[63]

The speculated biosynthetic pathway of flavonoids is shown in Figure 1.14.[82-85]

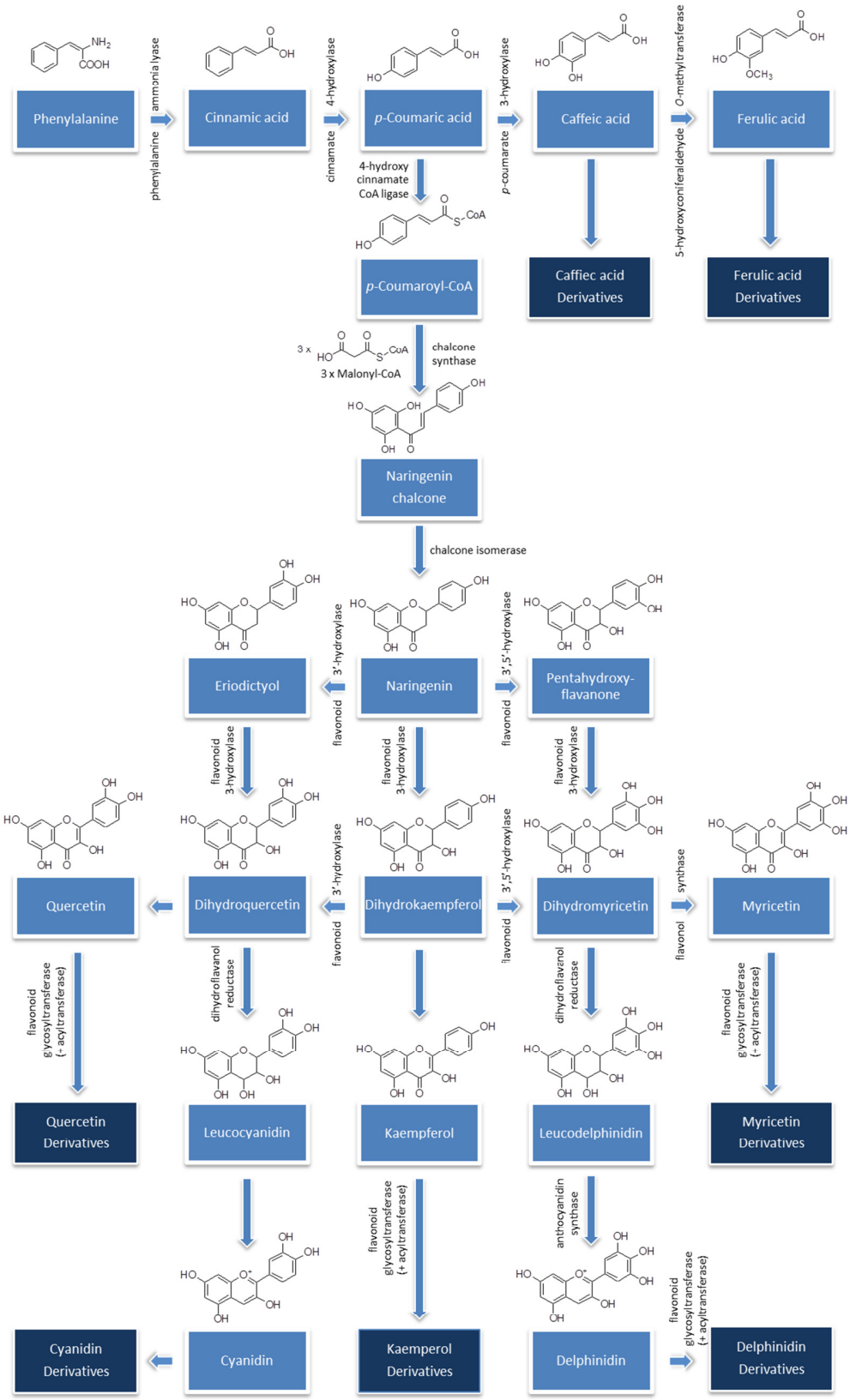

Figure 1.14: Presumed biosynthetic pathway of flavonoids [82-85]

1.9. Polyphenols – Bioavailability

Polyphenols have demonstrated many beneficial health effects in different studies. However, an important aspect to consider is bioavailability, since the compounds need to be absorbed by the human body in order to generate any desired effect on human health.

The bioavailability studies of polyphenols mainly involve the interaction of polyphenols with the stomach, intestines (duodenum), colon and the micro-flora present in them. The polyphenols suffer from poor absorption, high metabolism and swift elimination in the human body. The small intestine can readily absorb aglycones. But, food polyphenols are found in the form of esters, polymers or glycosides, which cannot be absorbed by the intestine.[62]

It is speculated that the flavonoids and their glycosides pass through into the duodenum from the stomach unscathed. The intestinal enzymes and micro-flora interact with the polyphenols after they enter the duodenum. The intestinal enzymes are responsible for the hydrolysis of food polyphenols. The micro-flora present in the duodenum and colon are responsible for breaking down the aglycones (glycosides) into different aromatic acids. The resulting products from these processes are easily absorbed by the intestine.[62]

During absorption, the polyphenols undergo conjugation through sulfation, methylation or glucuronidation in the small intestine and liver. The effectiveness of the conjugation process results in the aglycones being found in low amounts or being completely absent in blood. The elimination of polyphenols from the human body occurs mainly through urine and bile.[62]

From numerous studies, it was observed that gallic acid, flavanones and isoflavones are the most readily absorbed polyphenols. The absorption rate of quercetin glucosides, catechins and flavanones was quite good. However, the absorption rate of anthocyanins, esters of hydroxycinnamates (chlorogenic acids), proanthocyanidins and galloylated catechins was relatively poor. Further research is required to comprehensively study the polyphenol bioavailability in humans.[62]

1.10. Polyphenols – Analysis

Polyphenols are present in a vast diversity in plants with different structures and properties. Even though there has been rapid development of new technologies, the analysis of polyphenols along with their extraction, isolation and characterization still remains a challenge.[63]

A homogenous mixture of the representative samples must be used for the analysis. The sample must be carefully transported and preserved prior to the analysis in order to prevent the loss of compounds. The samples are pre-treated before extraction usually by drying, freezing of lyophilizing in order to prevent compound degradation and moisture-enhanced enzymatic activities. The samples should not be treated with high-temperature or excessive light exposure.[63]

Depending upon the type of samples, different extraction methods such as liquid-liquid or solid-liquid extraction are employed. The polyphenols are quite hydrophilic in nature and are generally extracted using a mixture of water and organic solvents such as methanol, ethanol, acetonitrile and acetone. Since polyphenols are more stable at low pH conditions, a weak acid or a small concentration of strong acid may be used for extractions. Sometimes, due to lack of authentic standards and to perform quantification studies and structural studies (glycosylation patterns), the polyphenols are deliberately hydrolyzed to aglycones using a strong acid or hydrolyzing enzymes such as β-glucosidase.[63]

The total phenolic content can be measured using spectrophotometric methods; however they are unable to analyze individual compounds in the mixture and may also have interferences from other non-phenolic compounds. The most commonly used method for analyzing polyphenols is a reversed phase high performance liquid chromatography combined with a diode array detector and/or mass spectrometer. Other methods that have been used for polyphenol studies are capillary electrophoresis (coupled with UV detector and/or mass spectrometer) and gas chromatography (coupled with FID, ECD and/or mass spectrometer).[63]

HPLC is a powerful technique used to separate and characterize the polyphenolic compounds as it can simultaneously separate compounds from an extracted mixture. The most commonly used

column is the RP C18 column, however other columns such as diphenyl columns have also been used.[65, 86] The columns are generally 100-250 mm in length and have 3.9-4.6 mm internal diameter and particle size of 3-10 µm. The columns are usually used at ambient temperatures and maintaining the column temperature helps in generating reproducible retention time of compounds. Two-dimensional LC is achieved by using two columns serially and has been used to analyze complex samples like beer and wine. The major development in this technology was UPLC, which uses a reduced particle size of 2.5 µm. The reduction in particle size enabled higher efficiency of separation as higher flow rates of solvents could be used to achieve better separation of peaks in a reduced time and with better sensitivity.[86]

Isocratic and gradient elution methods have been used for the analyses of polyphenols. Simple isocratic methods are used to analyze free phenolic acids while complex gradient methods are used to analyze polyphenols with diverse chemical structures and polarity. In gradient methods, a binary solvent system is used with an aqueous phase (water) and an organic phase. Methanol and acetonitrile are the most common organic solvents used as the organic phase. The aqueous phase is generally acidified with weak acids such as formic, phosphoric or acetic acid in order to prevent the ionization of analytes in the HPLC system and enhance the peak resolution and retention time reproducibility.[86]

The widely used detectors for polyphenols are ultraviolet/visible, photodiode array and ultraviolet/fluorescence detectors. They can also be detected using a mass spectrometer, nuclear magnetic resonance, electrochemical coulometric array, electroarray and chemical reaction detectors. Due to the presence of conjugated double bonds and aromatic bonds, polyphenols exhibit absorption in the UV or UV/VIS range. The benzoic acid derivatives have maximum absorption in the range of 200-290 nm while the cinnamic acid derivatives have maximum absorption in the range of 270-360 nm due to additional conjugation. The flavonoids usually have first and second maxima in the range of 240-280 nm (A-ring) and 300-550 nm (C-ring) respectively. Thus, taking into account all the absorption ranges, a UV detector at 280 nm is mostly used to identify polyphenols and if available, a combination of 254 and 280 nm, or 280 and 320 nm is used.[86]

For mass spectrometers used for polyphenolic studies, the most universally used ionization method is the electrospray ionization followed by atmospheric pressure chemical ionization. [HPLC] The tandem mass spectrometer is used to generate characteristic fragment ions of compounds by employing collision-induced dissociation. It is observed that similar building units produce similar fragment ions, which is used to identify new derivatives of specific polyphenolic groups. With the help of the pre-cursor ion and the fragment ions, the neutral losses can be studied and with the combined information the structure of the compound can be tentatively assigned. In the case of polyphenols, the fragment ions and neutral losses provide information on the aglycone part and glycone (glycosyl) part respectively. The fragmentation sequence can also provide information on the aglycone-glycone bonds and interglycosidic bonds. The use of a tandem mass spectra library composed of fragmentation data of standards can aid in identifying the compounds. To identify the vast variety of compounds found in nature, scientists have been trying to construct a virtual mass spectra library by developing algorithms for the prediction of fragment ions and their intensities. However, the algorithms have so far not been successful in simulating peak intensities similar to the experimental values.[86, 87]

The time of flight mass spectrometer is used to determine the high resolution molecular weight of the compounds. The resolution is high enough to detect many elemental mass defects (difference between the mass of the individual nucleons (neutrons and protons) and the mass of the combined nucleus). The molecular weight is used to generate the molecular formulas of compounds, which are influenced by the parameters chosen in the software (number of carbons, hydrogen, oxygen, nitrogen atoms). The molecular formulas are filtered through various chemical rules, isotopic patterns and elemental ratios to determine the best possible fit to the respective polyphenolic peak. Specific target libraries (metabolites, pesticides, drugs) can be used to aid identification of compounds. The mass spectra can be visualized using *van Krevelen* plots, *Kendrik* plots and principal component analysis plots to investigate complex samples. Due to the complexity and diversity of chromatograms, further software functions are required to handle the processing of the large amount of data generated.[87, 88]

In this study, the combination of RP-HPLC-DAD-ESI-MS was used to study the polyphenols and characterize them based on their specific retention time, UV absorption, fragmentation pattern and high resolution mass data.

1.11. Plant metabolomics and Chemotaxonomy

Plants produce a wide variety of metabolites that serve different functions important for their survival. The metabolites are divided into two groups, namely primary metabolites and secondary metabolites. The primary metabolites are responsible for the physiological functions such as growth and reproduction. The secondary metabolites are apparently responsible for signal mechanisms that promote pollination and defense mechanisms against microbes, herbivores and viruses.[89] The scientific study of plant metabolites is known as plant metabolomics.

Plants produce different types of secondary metabolites as a result of exposure to different environmental factors. The secondary metabolite distribution is dependent on the age of the plant, the part of the plant, geographical location and ecological habitat of the plant.[89, 90]

Chemotaxonomy is established on the assumption that organisms can be biologically classified according to the similarities and dissimilarities of specific compounds present in them. The use of plant secondary metabolites in the field of chemotaxonomy has received mixed reviews.[89, 90]

Individual or specific classes of secondary plant metabolites have been used to aid the field of chemotaxonomy. Marker compounds have been identified for individual plant species such as morphine in *Papaver somniforum* and, sinapoyl quinic acids in *Coffea canephora*, stevioside in *Stevia rebaudiana*.[90-92] Some classes of compounds have been found to be exclusive for certain plant families such as tropane and steroidal alkaloids in Solanaceae and quinolizidine alkaloids in Fabaceae.[89]

In this study, a large variety of polyphenols, which belong to different groups were studied in the *Rhododendron* leaf extracts in order to determine if marker compounds could be identified for a specific *Rhododendron* species or a specific subgenus. The question whether polyphenolic secondary metabolites serve as useful chemotaxonomic markers should be addressed.

2. Motivation for the Project

The Rhododendron Project was a collaborative project between the Rhododendron Park Bremen, University of Oldenburg and Jacobs University Bremen. The main objective of this project was to determine the relationship between the phylogenetic, phytochemical, anti-bacterial and cytotoxic properties of *Rhododendron* species. In the phytochemical analysis, the main aim was to identify the polyphenols and other novel secondary metabolites present in the species. Liquid chromatography coupled to the ion trap and micro-TOF were the techniques used for the identification of the compounds. In this study, 100 *Rhododendron* species were analyzed, which belonged to one of the following six subgenera: *Azaleastrum*, *Hymenanthes*, *Rhododendron*, *Pentanthera*, *Tsutsusi* and *Mumeazalea*.

An additional objective of the project was to determine the biologically active compounds by activity based fractionation. The crude extracts of *Rhododendron* species were tested against Gram-positive bacteria (*Bacillus subtilis*) using the agar diffusion assay. An inhibition zone of more than 0.4 cm was considered to be active against the bacteria. The species *Rhododendron ambiguum* was one of the highly active species with an inhibition zone of 1.0 cm. Preparative-HPLC was used to isolate the bioactive compounds present in the crude extract of *Rhododendron ambiguum*. LC-MS and NMR were used to identify the bioactive compounds.

The objective of the genetic study was to generate a phylogenetic tree of *Rhododendron* species, which belong to different subgenera with the help of three genetic markers, namely *trn*K, *trn*L-F, and ITS. The phytochemical profile would be compared from different *Rhododendron* species in order to determine if the genetically similar *Rhododendron* species produced similar secondary metabolites.

A few hypotheses of the Rhododendron project, which were tested within this thesis, are given below:

- *Rhododendron* species have significantly high anti-bacterial activity and low cytotoxicity.
- The natural products from *Rhododendron* species will provide lead structures for potential antibiotics.
- Bioinformatics is a useful tool for differentiating *Rhododendron* species based on their secondary metabolite profile.
- Bioinformatics is useful for predicting the anti-bacterial activity of *Rhododendron* species.
- Phylogenetically similar *Rhododendron* species have a similar secondary metabolite profile.
- *Rhododendron* species or their subgenera have marker compounds that aid in their chemotaxonomy.
- The total number of compounds present in *Rhododendron* leaf extracts is dependent on the polyploidy level.
- The total number of compounds present in *Rhododendron* leaf extracts influences the anti-bacterial activity.
- A specific subgenus of *Rhododendron* species produces high number of compounds compared to others.
- Some compounds are present in a higher relative quantity in certain subgenus of *Rhododendron* species.
- Frost influences the secondary metabolite profile of *Rhododendron* species.
- Different plant organs produce different phytochemical profiles with altering bioactivity.

3. Materials and Methods

3.1. Liquid Chromatography-Tandem Mass Spectrometry (LC-Ion Trap-MS)

The LC equipment (Agilent 1100 series, Bremen, Germany) consisted of a binary pump, an auto-sampler with 100 µL loop and a diode array detector with a light-pipe flow cell. The detector can record at 254, 280 and 320 nm and scan from the range of 200-600 nm. The 5 µm diphenyl column having 250 x 3 mm inner diameter (Varian, Darmstadt, Germany) was used for separation. This was connected to the ion-trap mass spectrometer equipped with an electrospray ionization source (Bruker Daltonics HCT Ultra, Bremen, Germany). It was operated in full-scan mode and auto-MS^n mode was used to acquire the fragments. Tandem mass spectra were achieved by using a ramping of the collision energy.[93]

Water/formic acid (1000:0.05 v/v) and methanol were used as solvent A and B respectively. The flow rate of the solvents was adjusted to 0.5 mL/min. A linear gradient was used from 10% B to 80% B in 70 min and a further 10 min was assigned for the gradient to equilibrate from 80% B to 10% B for the next run.[93]

3.2. Liquid Chromatography-Time of Flight Mass Spectrometry (LC-TOF-MS)

The LC equipment (Agilent 1200 series, Bremen, Germany) consisted of a binary pump, an auto-sampler with 100 µL loop and a UV-Vis detector with a light-pipe flow cell. The UV detector was used at 280 nm to measure the polyphenols. The 5 µm Diphenyl column having 250 x 3 mm inner diameter (Varian, Darmstadt, Germany) was used for separation. This was connected to the microTOF mass spectrometer (Bruker Daltonics, Bremen, Germany) equipped with an electrospray ionization source. The internal calibration was achieved by using 0.1 M sodium formate solution at 30 µL/min, which was injected through the six-port valve. The calibration was achieved by using the enhanced quadratic mode.[93]

Water/formic acid (1000:0.05 v/v) and methanol were used as solvent A and B respectively. The flow rate of the solvents was adjusted to 0.5 mL/min. A linear gradient was used from 10% B to 80% B in 70 min and a further 10 min was assigned for the gradient to equilibrate from 80% B to 10% B for the next run.[93]

3.3. SPE

The C18 ec SPE cartridges were purchased from Macherey-Nagel. The stationary phase consisted of octadecyl-modificed silica (endcapped). The size of the cartridges varied from 6 – 15 mL and the amount of silica varied from 1000 – 2000 mg.

3.4. Preparative High Performance Liquid Chromatography (Prep-HPLC)

The Preparative LC equipment (Varian Prep Star Model 218, USA) consisted of two pumps, a six port manual injector with 500 µL loop. The VP 250/10 NUCLEODUR Sphinx RP (5µm) fitted with an 8 mm guard column (Macherey-Nagel, Germany) was used for separation. It was connected to the UV-Vis detector (Varian Pro Star, USA) followed by the fraction collector (Varian Pro Star Model 701, USA). The UV detector was used at 280 nm to measure polyphenols.

Water/formic acid (1000:0.05 v/v) and acetonitrile were used as solvent A and B respectively. The flow rate of the solvents was adjusted to 4 mL/min. A linear gradient was used from 10% B to 80% B in 40 min followed by an isocratic at 80% B until 50 min and a further 15 min was assigned for the gradient to equilibrate from 80% B to 10% B for the next run. The method development is discussed in the results.

3.5. NMR

A 400 MHz NMR (Oxford, United Kingdom) machine was used to determine the structure of the compounds separated by using Prep-HPLC. The magnets have an extremely low B0 drift and outstanding field homogeneity and provide high resolution and non-spinning line shape.

3.6. Chemicals

The chemicals (analytical grade) were purchased from Carl ROTH (Karlsruhe, Germany).

3.7. Extraction

The *Rhododendron* leaves were freeze dried using liquid nitrogen. A mortar and pestle was used to crush the dried brittle leaves. The leaves were then powdered using a grinder and stored at -80°C until further use. 2 g of the powdered leaves were dissolved in 10 mL of aqueous methanol (80%) and left in the fridge at 0°C for 24 h. The mixture was then sonicated for 15 min and centrifuged at 4400 RPM for 10 min. The aliquot was then separated and stored at -23°C until further analyses.[2]

3.8. Bruker Software

Bruker Data Analysis was the software used extensively for analyzing the data produced by LC-MS. The data generated by the ion trap MS and TOF MS were both analyzed using Bruker software. The total and extracted ion chromatograms and tandem mass spectra present in this thesis are all generated from this software. The Smart Formula function was used to generate molecular formula for compounds using high resolution data. It was also used to convert the ".d" files to ".mzxml" files, which could be analyzed using other software such as XCMS and MZMine. The Bruker Library Editor was used to prepare the Polyphenol library, which was compared with the *Rhododendron* species for identification and assignment of compounds and their derivatives. Bruker Profile Analysis was used to perform PCA analysis on the *Rhododendron* data generated by LC-TOF-MS. The Bruker Data Analysis Method Editor as the name suggests was used to edit methods and scripts used for a group of samples. Automation Engine was used to process a group of samples with the same method.

3.9. XCMS, RStudio and Metaboanalyst

The converted ".mzxml" files were combined into a big ".csv" file, which included peaks grouped together based on their *m/z* value and retention time. This conversion was performed using the XCMS package for R or RStudio, which are conventionally used for statistical analysis. RStudio was also used for generating box plots for some compounds. The ".csv" file with compounds was analyzed using Metaboanalyst, which is free online software available at http://www.metaboanalyst.ca. It was used for PCA analysis and to generate hierarchical clustering of *Rhododendron* species.[94-96]

3.10. Rhododendron Samples

The *Rhododendron* plant material, along with their detailed information was obtained from Rhododendron Park, Bremen, Germany. The plant species were verified according to the German Gene bank Rhododendron Database, which is provided by the Bundessortenamt (www.bundessortenamt.de/rhodo). The herbarium number for most species is provided by University of Oldenburg. The samples included *Rhododendron* species from six subgenera, namely *Rhododendron*, *Hymenanthes*, *Tsutsusi*, *Azaleastrum*, *Mumeazalea* and *Pentanthera*. The *Rhododendron* species were assigned an internal lab number in order to simplify the reference number used during experiments.

The *Rhododendron* species obtained from the Rhododendron Park, their gene bank number, herbarium number, lab number and subgenus are given in Table 3.1. Not all species were analyzed with LC-MS.

Table 3.1: *Rhododendron* samples from Rhododendron Park (Bremen)

Lab No.	Gene bank No.	Herbarium No.	Species Name	Subgenus
1	100.467_A_LE	OLD00698	*Rhododendron macabeanum*, WATT EX BALF. F. (1920)	*Hymenanthes*
2	100.463_A_LE	OLD00676	*Rhododendron arboreum* ssp. *arboreum*	*Hymenanthes*
3	100.007_A_LE	OLD00801	*Rhododendron ambiguum*, HEMSL. (1911)	*Rhododendron*
4	100.750_A_LE	OLD00783	*Rhododendron maddenii* ssp. *maddenii*	*Rhododendron*
5	100.403_A_LE	OLD00894	*Rhododendron mucronatum* var. *ripense*, (Makino) E.H. Wilson (1921)	*Tsutsusi*
6	100.426_A_LE	OLD00778	*Rhododendron tomentosum*, HARMAJA (1990)	*Rhododendron*
7	100.799_A_LE	OLD00723	*Rhododendron wasonii*, HEMSL. & E.H. WILSON (1910)	*Hymenanthes*
8	100.368_A_LE	OLD00785	*Rhododendron micranthum*, TURCZ. (1937)	*Rhododendron*
9	100.353_A_LE	OLD00771	*Rhododendron hippophaeoides* var. *hippophaeoides*	*Rhododendron*
10	100.370_A_LE	OLD00756	*Rhododendron minus*, MICHX. (1792)	*Rhododendron*
11	100.891_A_LE	OLD00692	*Rhododendron decorum* ssp. *diaprepes*, (BALF.F. & W.W. SM.) T.L. MING (1984)	*Hymenanthes*
12	100.812_A_LE	OLD00679	*Rhododendron argyrophyllum* ssp. *nankingense*, (COWAN) D.F. CHAMB. (1979)	*Hymenanthes*
13	100.393_A_LE	OLD00714	*Rhododendron ponticum*, L. (1762)	*Hymenanthes*

Lab No.	Gene bank No.	Herbarium No.	Species Name	Subgenus
14	100404_B_LE	OLD00768	*Rhododendron rubiginosum*, FRANCH. (1974)	*Rhododendron*
15	100322_B_LE	OLD00757	*Rhododendron cinnabarinum*, HOOK. (1849)	*Rhododendron*
16	100016_B_LE	OLD00683	*Rhododendron auriculatum*, HEMSL. (1899)	*Hymenanthes*
17	100784_B_LE	OLD00686	*Rhododendron campanulatum* ssp. *aeruginosum*, (HOOK.F.) D.F. CHAMB. (1979)	*Hymenanthes*
18	100470_B_LE	OLD00670	*Rhododendron hongkongense*, HUTCH. (1930)	*Azaleastrum*
19	100468_B_LE	OLD00754	*Rhododendron leucaspis*, TAGG (1929)	*Rhododendron*
20	100345_B_LE	OLD00788	*Rhododendron ferrugineum*, L. (1753)	*Rhododendron*
21	100420_B_LE	OLD00704	*Rhododendron strigillosum*, FRANCH. (1886)	*Hymenanthes*
22	100491_B_LE	OLD00728	*Rhododendron thomsonii* ssp. *lopsangianum*	*Hymenanthes*
23	100349_B_LE	OLD00691	*Rhododendron galactinum*, BALF. F. EX TAGG (1926)	*Hymenanthes*
24	100794_B_LE	OLD00702	*Rhododendron annae*, FRANCH. (1898)	*Hymenanthes*
25	100374_B_LE	OLD00787	*Rhododendron moupinense*, FRANCH. (1886)	*Rhododendron*
26	100496_B_LE	OLD00708	*Rhododendron elliottii*, WATT EX BRANDIS (1906)	*Hymenanthes*
27	100483_B_LE	OLD00701	*Rhododendron griersonianum*, BALF. F. & FORREST (1919)	*Hymenanthes*
28	100338_B_LE	OLD00712	*Rhododendron degronianum* ssp. *yakushimanum*, (NAKAI) H. HARA (1986)	*Hymenanthes*
29	100417_C_LE	OLD00715	*Rhododendron smirnowii*, TRAUTV. (1885)	*Hymenanthes*
30	100329_C_LE	OLD00809	*Rhododendron davidsonianum*, REHDER & E.H. WILSON (1913)	*Rhododendron*
31	101054_C_LE	OLD00776	*Rhododendron tapetiforme*, BALF.F. & KINGDON-WARD	*Rhododendron*
32	100384_C_LE	OLD00774	*Rhododendron russatum*, BALF.F. & FORREST (1919)	*Rhododendron*
33	100803_C_LE	OLD00818	*Rhododendron trichanthum*, REHDER (1934)	*Rhododendron*
34	100882_C_LE	OLD00790	*Rhododendron ledebourii*, POJARK. (1952)	*Rhododendron*
35	100377_C_LE	OLD00772	*Rhododendron nitidulum* var. *omeiense*, M.N. PHILIPSON & PHILIPSON (1975)	*Rhododendron*
36	100392_C_LE	OLD00773	*Rhododendron polycladum*, FRANCH. (1886)	*Rhododendron*
37	100449_C_LE	OLD00822	*Rhododendron yunnanense*, FRANCH. (1886)	*Rhododendron*
38	100343_C_LE	OLD00770	*Rhododendron fastigiatum*, FRANCH. (1886)	*Rhododendron*
39	100362_C_LE	OLD00811	*Rhododendron lutescens*, FRANCH. (1886)	*Rhododendron*

Lab No.	Gene bank No.	Herbarium No.	Species Name	Subgenus
40	100886_D_LE	OLD00673	*Rhododendron moulmainense*, HOOK.F. (1856)	*Azaleastrum*
41	100464_D_LE	OLD00797	*Rhododendron spinuliferum*, FRANCH. (1974)	*Rhododendron*
42	100326_D_LE	OLD00807	*Rhododendron concinnum*, HEMSL. (1889)	*Rhododendron*
43	100441_D_LE	OLD00730	*Rhododendron williamsianum*, REHDER & E.H. WILSON (1913)	*Hymenanthes*
44	100484_D_LE	OLD00761	*Rhododendron genestierianum*, FORREST (1920)	*Rhododendron*
45	100412_D_LE	OLD00716	*Rhododendron selense* ssp. *jucundum*, (BALF.F. & W.W. SM.) D.F. CHAMB. (1978)	*Hymenanthes*
46	100498_D_LE	OLD00814	*Rhododendron rigidum*, FRANCH. (1886)	*Rhododendron*
47	100477_D_LE	OLD00796	*Rhododendron scabrifolium* var. *spiciferum*, (FRANCH) CULLEN (1978)	*Rhododendron*
48	100495_D_LE	OLD00813	*Rhododendron polylepis*, FRANCH. (1886)	*Rhododendron*
49	100906_D_LE	-	*Rhododendron anthopogon* ssp.*hypenanthum*, Annapurna Form	*Rhododendron*
50	100474_D_LE	OLD00799	*Rhododendron xanthostephanum*, MERRILL (1941)	*Rhododendron*
51	100439_D_LE	OLD00688	*Rhododendron wardii* var. *puralbum*, (BALF.F. & W.W. SM.) D.F. CHAMB. (1978)	*Hymenanthes*
52	100880_E_LE	OLD00700	*Rhododendron protistum*, BALF.F. & FORREST (1920)	*Hymenanthes*
53	100874_E_LE	OLD00689	*Rhododendron coriaceum*, FRANCH. (1898)	*Hymenanthes*
54	100748_E_LE	OLD00758	*Rhododendron keysii*, NUTT. (1853)	*Rhododendron*
55	100003_E_LE	OLD00717	*Rhododendron adenogynum*, DIELS (1912)	*Hymenanthes*
56	100887_E_LE	OLD00678	*Rhododendron adenopodum*, FRANCH. (1895)	*Hymenanthes*
57	100821_E_LE	OLD00719	*Rhododendron alutaceum* var. *iodes*, (BALF.F. & FORR.) D.C. CHAMB. (1982)	*Hymenanthes*
58	100830_E_LE	OLD00718	*Rhododendron aganniphum* var. *flavorufum*, (BALF.F. & FORREST) D.F. CHAMB. (1978)	*Hymenanthes*
59	100456_E_LE	OLD00735	*Rhododendron austrinum*, (SMALL) REHDER (1917)	*Pentanthera*
60	100824_E_LE	OLD00720	*Rhododendron beesianum*, DIELS (1912)	*Hymenanthes*
61	100848_E_LE	OLD00766	*Rhododendron bracteatum*, REHD.& WILS. (1913)	*Rhododendron*
62	100791_E_LE	OLD00721	*Rhododendron bureavii*, FRANCH. (1887)	*Hymenanthes*
63	100457_E_LE	OLD00703	*Rhododendron longesquamatum*, C.K. SCHNEID. (1909)	*Hymenanthes*

Lab No.	Gene bank No.	Herbarium No.	Species Name	Subgenus
64	100363_E_LE	OLD00738	*Rhododendron luteum*, SWEET (1830)	*Pentanthera*
65	100431_E_LE	OLD00745	*Rhododendron vaseyi*, GRAY (1879)	*Pentanthera*
66	100408_E_LE	OLD00750	*Rhododendron schlippenbachii*, MAXIM. (1870)	*Pentanthera*
67	100005_E_LE	OLD00746	*Rhododendron albrechtii*, (LINDL.) MAXIM. (1871)	*Pentanthera*
68	101044_E_LE	OLD00732	*Rhododendron arborescens*, (PURSH) TORREY (1824)	*Pentanthera*
69	100012_E_LE	OLD00733	*Rhododendron atlanticum*, (ASHE) REHDER (1921)	*Pentanthera*
70	101046_E_LE	OLD00742	*Rhododendron prunifolium*, (SMALL) MILLAIS (1917)	*Pentanthera*
71	100391_E_LE	OLD00740	*Rhododendron periclymenoides*, (MICHAUX) SHINNERS (1962)	*Pentanthera*
72	101045_E_LE	OLD00737	*Rhododendron cumberlandense*, E.L. BRAUN (1941)	*Pentanthera*
73	100250_E_LE	OLD00736	*Rhododendron calendulaceum*, (MICHX.) TORR. (1824)	*Pentanthera*
74	100380_E_LE	OLD00739	*Rhododendron occidentale*, (TORR. & A. GRAY) A. GRAY (1876)	*Pentanthera*
75	100015_E_LE	OLD00709	*Rhododendron aureum*, GEORGI (1775)	*Hymenanthes*
76	2006/232	OLD00751	*Rhododendron anthopogon* ssp. *anthopogon*	*Rhododendron*
77	without Gene bank-No.**	OLD00802	*Rhododendron ambiguum*, Hemsl. (1911)	*Rhododendron*
78	100009_F_LE	OLD00803	*Rhododendron amesiae*, Rehder & E.H. Wilson (1913)	*Rhododendron*
79	100654_F_LE	OLD00805	*Rhododendron augustinii* ssp. *chasmanthum*, Cullen (1978)	*Rhododendron*
80	without Gene bank-No. 2008/375_F_LE	OLD00808	*Rhododendron concinnum*, Hemsl. (1898) Pseudoyanthinum Grp.	*Rhododendron*
81	without Gene bank-No.**	OLD00789	*Rhododendron hirsutum*, L.	*Rhododendron*
82	101358_F_LE	OLD00810	*Rhododendron keiskei*, Miq. (1866)	*Rhododendron*
83	100471_F_LE	OLD00812	*Rhododendron pleistanthum*, Balf.f. ex Wilding (1923)	*Rhododendron*
84	100796_F_LE	OLD00675	*Rhododendron purdomii*, Rehder & E.H. Wilson (1913)	*Hymenanthes*
85	100889_F_LE	OLD00681	*Rhododendron ririei*, Hemsl. & E.H. Wilson (1910)	*Hymenanthes*
86	100422_F_LE	OLD00896	*Rhododendron tashiroi*, Maxim. (1887)	*Tsutsusi*
87	100424_F_LE	OLD00817	*Rhododendron tatsienense*, Franch. (1895)	*Rhododendron*

Lab No.	Gene bank No.	Herbarium No.	Species Name	Subgenus
88	without Gene bank-No. xxxx/1470_F_LE	OLD00819	*Rhododendron triflorum*, Hook. F. (1849)	*Rhododendron*
89	without Gene bank-No. xxxx/1266_F_LE	OLD00748	*Rhododendron pilosum*, Craven (2011)	*Pentanthera*
90	without Gene bank-No.**	OLD00747	*Rhododendron multiflorum* var. *purpureum*, (Makino) Craven (2011)	*Pentanthera*
91	100904_G_LE	OLD00889	*Rhododendron dilatatum*, MIQ. (1863)	*Tsutsusi*
92	101066_G_LE	OLD00722	*Rhododendron faberi*, Hemsl. (1889)	*Hymenanthes*
93	100018_G_LE	OLD00697	*Rhododendron balangense*, FANG (1983)	*Hymenanthes*
94	100466_G_LE	OLD00677	*Rhododendron arboreum* ssp. *delavayi*, (FRANCH.) D.F. CHAMB. (1979)	*Hymenanthes*
95	100856_G_LE	OLD00682	*Rhododendron thayerianum*, REHDER & E.H. WILSON (1913)	*Hymenanthes*
96	100390_G_LE	OLD00671	*Rhododendron ovatum*, (LINDL.) MAXIM. (1870)	*Azaleastrum*
97	100357_G_LE	OLD00893	*Rhododendron kaempferi*, PLANCH. (1854)	*Tsutsusi*
98	101118_G_LE	-	*Rhododendron campanulatum*, D. DON (1821)	*Hymenanthes*
99	100376_G_LE	OLD00791	*Rhododendron mucronulatum*, TURCZ. (1837)	*Rhododendron*
100	without Gene bank-no 2010/384_G_LE	OLD00775	*Rhododendron setosum*	*Rhododendron*
101	100397_G_LE	OLD00741	*Rhododendron prinophyllum*, (SMALL) MILLAIS (1917)	*Pentanthera*
102	100872_G_LE	OLD00895	*Rhododendron oldhamii*, MAXIM. (1870)	*Tsutsusi*
103	without Gene bank-no 2002/1084_G_LE	OLD00784	*Rhododendron scopulorum*	*Rhododendron*
104	101115_G_LE	OLD00744	*Rhododendron canadense*, (L.) Torr. (1814)	*Pentanthera*
105	100795_G_LE	OLD00726	*Rhododendron sherriffii*, COWAN (1937)	*Hymenanthes*
106	1999/259	OLD00707	*Rhododendron neriiflorum*, FRANCH. (1886)	*Hymenanthes*
107	100315_G_LE	OLD00687	*Rhododendron campylocarpum* ssp. *caloxanthum*, (BALF.F. & FARR.) D.F. CHAMB. (1978) Telopeum Grp.	*Hymenanthes*
108	101047_G_LE	OLD00777	*Rhododendron neoglandulosum*, HARMAJA (1990)	*Rhododendron*
109	100249_G_LE	OLD00711	*Rhododendron brachycarpum* ssp. *fauriei*, (FRANCH.) D.F. CHAMB. (1979)	*Hymenanthes*
110	100248_G_LE	OLD00710	*Rhododendron brachycarpum*, D.Don ex G. Don (1834) ssp. brachycarpum	*Hymenanthes*

Lab No.	Gene bank No.	Herbarium No.	Species Name	Subgenus
111	100860_G_LE	OLD00724	*Rhododendron wasonii*, HEMSL. & E.H. WILSON (1910) Rhododactylum Grp.	*Hymenanthes*
112	100473_G_LE	OLD00690	*Rhododendron falconeri* ssp. *eximium*, (NUTT.) D.F. CHAMB. (1979)	*Hymenanthes*
113	100881_G_LE	OLD00792	*Rhododendron sichotense*, POJARK. (1952)	*Rhododendron*
114	without number	OLD00795	*Rhododendron racemosum*, FRANCH. (1886)	*Rhododendron*
115	100394_G_LE	OLD00693	*Rhododendron praevernum*, HUTCH. (1920)	*Hymenanthes*
116	100489_G_LE	OLD00725	*Rhododendron hylaeum*, BALF. F. & FARRER (1922)	*Hymenanthes*
117	101052_G_LE	OLD00798	*Rhododendron auritum*, TAGG (1931)	*Rhododendron*
118	100884_G_LE	OLD00699	*Rhododendron montroseanum*, DAVIDIAN (1979)	*Hymenanthes*
119	100650_G_LE	OLD00892	*Rhododendron eriocarpum*, (HAYATA) NAKAI (1922)	*Tsutsusi*
120	100837_G_LE	OLD00713	*Rhododendron macrophyllum*, D. DON EX G. DON (1834)	*Hymenanthes*
121	100355_G_LE	OLD00680	*Rhododendron insigne*, HEMSL. & E.H. WILSON (1910)	*Hymenanthes*
122	101048_H_LE	-	*Rhododendron myrtifolium*, SCHOTT & KOTSCHY (1851)	*Rhododendron*
123	100436_J_LE	OLD00891	*Rhododendron wadanum*, MAKINO (1917)	*Tsutsusi*
124	100781_J_LE	OLD00731	*Rhododendron semibarbatum*, Maxim. (1870)	*Mumeazalea*

4. Data Analysis

The data analysis for all the *Rhododendron* species was a challenging task. Each species had two sets of data, namely LC-Ion Trap-MS and LC-TOF-MS data. Bruker Data Analysis was the main software used for data analysis. The use of different functions like scripting, methods, using a compound library was explored in order to efficiently analyze the data in a consistent way. Selected authentic standards were run so that they could be compared in terms of retention time and fragmentation pattern with the analyzed compounds.

4.1. Scripting in Bruker Data Analysis

The field of scripting in Bruker Data Analysis software was explored. The programming commands were studied and the most useful command was

"val = Analysis.Chromatograms.Add(daEIC, daAllMS, "n", daNegative"

where n was the *m/z* value of the desired compound. This command was used to make the extracted ion chromatogram of the required *m/z* value. A script was generated with a list of *m/z* values of compounds reported in literature. This script could be used independently for the generation of the EIC of the interested compounds. It could also be saved in a method and run after the method has been loaded.

4.2. Methods in Bruker Data Analysis

All the parameters required for the LC-MS data analysis such as mass precision, internal calibration values, AutoMS(n) limits, scripts could be saved in a method and loaded for each analysis. This saved time by eliminating the need to enter the parameters every time when a new set of data was loaded. It also eliminated the possibility of human error.

4.3. Library

There were many compounds which were identified in more than one *Rhododendron* species. To make this identification more efficient a library was generated using the LC-MS^n data of identified compounds in the *Rhododendron* species. The MS^n spectra were saved in a user-defined library called "Polyphenols" using the Identify → Add to Library function. Using the

Bruker Compass Library Editor, the MS^1 spectra were cleaned up by removing all the unwanted peaks with the exception of the precursor ion peak. The structures of these compounds were created using ChemDraw and saved as ".mol" files. The structures could be incorporated with the MS^n data by using Compound → Import Structure. The visual advantage of using structures was that when the compounds were identified in the spectra, they had a corresponding structure to the match. The personal library was created using 80 identified compounds. The main advantage of using the library is that it reduces the time required to identify known compounds and it also produces matches for new derivatives of these compounds. This library can be used not only to identify compounds in *Rhododendron* species, but also in other plant samples.

4.4. AutoMS(n) and Identify functions in Bruker Data Analysis

The AutoMS(n) function is used to create compound spectra for each peak in the chromatogram. The parameters can be changed according to the desired result. The *Rhododendron* species were analyzed in both polarities (positive and negative) using the LC-Ion Trap-MS data. In order to generate compound spectra only in negative mode from this data, the following parameters were used for AutoMS(n) mode:

Intensity threshold positive: 1000000000

Intensity threshold negative: 1000

Maximum number of compounds: 1000

Retention time window [min]: 0.5

The Identify function is used to match the spectra generated by the AutoMS(n) function with the spectra present in the library. This function can be used to match the spectra by the MS^n fragmentation and retention time. However, a lot of compounds were present as isomers. To identify the isomers, the retention time was disregarded. This was achieved by using retention time matching of 70 min, which included the complete run time of the LC-MS^n analysis. When a match occurs, this function copies the library spectra along with the compound structure below the spectra generated in the data. In the case of new derivatives, the identify function identifies the fragments based on the library data. The high resolution data of these compounds can be used to identify their molecular formula, which can be searched in the scifinder database for possible matches. In this way, the compounds can be identified in the *Rhododendron* species.

5. Neutral Losses

Plants produce a variety of secondary metabolites. These compounds are derivatives of a certain classes of compounds. To identify and assign the derivative, their retention time, molecular formula from high resolution data and fragmentation are studied. Characteristic fragmentation patterns are observed for a specific group of compounds. In fragmentation, besides the pattern, the other important parameter is the neutral loss. The Ion Trap mass spectrometer can only detect charged ions, while neutral fragments are discarded into the waste and cannot be detected. This can be circumvented using software where the neutral losses can be calculated by the difference between the pre-cursor ion and the fragment ions. A constant neutral loss chromatogram can also be generated using Bruker software for specific neural losses. In Figure 5.1, a constant neutral loss chromatogram of 162 Da is shown for *Rhododendron davidsonianum*. The peaks in the chromatogram represent fragment ions generated from precursor ions with a loss of 162 Da, which can be generally attributed to a loss of hexoside or a caffeoyl moiety.

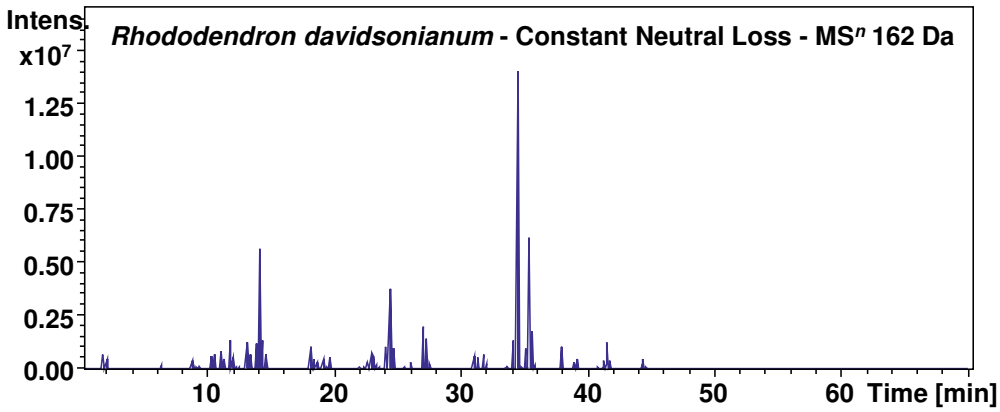

Figure 5.1: Constant neutral loss chromatogram of 162 Da in *Rhododendron davidsonianum*

Some common neutral losses are observed for specific functional groups or substituents. For example, a neutral loss of 44 Da (CO_2) is observed for the carboxyl functional group. This is observed usually for hydroxycinnamic and hydroxybenzoic acids, which carry a carboxylic acid.

Glycosides are compounds commonly found in plants. In glycosides, a sugar moiety is connected to a functional group via a glycosidic linkage. Pentose, hexose and rhamnose are the most common sugar molecules found attached to groups like flavonoids (quercetin, myricetin, kaempferol), phenolic acids (vanillic acid, *p*-coumaric acid) and other groups. The neutral loss observed for attached groups are 18 Da (H_2O) less than the original molecular weight due to the linkage formed by the loss of a water molecule. For example, a neutral loss of 162 Da ($C_6H_{10}O_5$) is observed for hexoside, which is originally 180 Da ($C_6H_{12}O_6$) as a hexose. Similarly, a neutral loss of 132 Da ($C_5H_8O_4$) and 146 Da ($C_6H_{10}O_4$) are observed for pentoside and rhamnoside respectively.

Similarly, different classes of compounds can be attached to each other. The neutral loss is observed similarly as that of sugars, with 18 Da (H_2O) less than the original molecular weight. A good example would be the class of chlorogenic acids consisting of caffeoylquinic acids, coumaroylquinic acids and ferruloylquinic acids. In caffeoyl quinic acids, quinic acid is attached to caffeic acid. In this case, a neutral loss of 162 Da ($C_9H_6O_3$) is observed for the caffeoyl group, which is originally 180 Da ($C_9H_8O_4$) as caffeic acid. In coumaroylquinic acids, quinic acid is attached to coumaric acid. In this case, a neutral loss of 146 Da ($C_9H_6O_2$) is observed for the coumaroyl group, which is originally 164 Da ($C_9H_8O_3$) as coumaric acid. In ferruloylquinic acids, quinic acid is attached to ferulic acid. In this case, a neutral loss of 174 Da ($C_7H_{10}O_5$) is observed for the quinoyl group, which is originally 192 Da ($C_7H_{12}O_6$) as quinic acid.

Neutral losses can be also useful to assign derivatives having more than one sugar moiety attached to it. For example, quercetin-*O*-pentoside-*O*-hexoside consists of a pentoside and a hexoside. The most common linkage is the 3-*O*-glycosidic bond, followed by 7-*O*-glycosidic bond. However with the presence of multiple sugar moieties they can be either connected via 3-*O*-glycosidic bond or 7-*O*-glycosidic bond or connected only with one with the presence of interglycosidic linkage between the sugar moieties. In previous studies in our group, it has been observed that the sugar moiety attached via the 7-*O*-glycosidic bond is lost before the one attached via the 3-*O*-glycosidic bond. Also, the connection of the sugar moieties to the hydryoxyl groups at position 5 of the A-ring or positions 3, 4 and 5 of the B-ring is usually uncommon.

The fragmentation of quercetin-*O*-pentoside-*O*-hexoside can follow two different paths depending upon the linkage of the sugar moieties to quercetin. If the sugar moieties are connected to each other, fragmentation occurs with the loss of 294 Da ($C_{11}H_{18}O_9$) in one step, which is a combination of 132 Da ($C_5H_8O_4$) pentoside and 162 Da ($C_6H_{10}O_5$) hexoside.

If the sugar moieties are not connected to each other and are attached to quercetin through two different glycosidic bonds, then the fragmentation occurs in two steps. If the neutral loss of 132 Da ($C_5H_8O_4$) is observed in the first step followed by 162 Da ($C_6H_{10}O_5$) in the second step, then the pentoside and hexoside are connected via 7-*O*-glycosidic bond and 3-*O*-glycosidic bond respectively and vice versa.

An extensive library of neutral losses will help in assigning novel compounds found in different samples. A small list of neutral losses has been compiled in Table 5.1. An additional list in Table 5.2 consists of neutral loss combinations.

Table 5.1: Common neutral losses

Neutral loss (Da)	**Group**	**Molecular Formula**
15	methyl	CH_3
42	acetyl group	C_2H_2O
44	carbon dioxide	CO_2
56	propanoyl	C_3H_4O
72	oxaloyl	C_2O_3
86	maloyl	$C_3H_2O_3$
98	fumaroyl	$C_4H_2O_3$
100	succinoyl	$C_4H_4O_3$
104	benzoyl	C_7H_4O
108	benzyl alcohol	C_7H_8O
110	benzenediol	$C_6H_6O_2$
114	glutaryl	$C_5H_6O_3$
118	threonate (Thr)	$C_4H_6O_4$
120	hydroxybenzoyl	$C_7H_4O_2$
132	pentose (Xyl)	$C_5H_8O_4$

Neutral loss (Da)	Group	Molecular Formula
132	tartaroyl	$C_4H_4O_5$
136	dihydroxy-phenyl-ethanol	$C_8H_8O_2$
136	protocatechuoyl	$C_7H_4O_3$
146	coumaroyl	$C_9H_6O_2$
146	rhamnose (Rha)	$C_6H_{10}O_4$
152	galloyl	$C_7H_4O_4$
156	shikimoyl	$C_7H_8O_4$
162	hexose (Glc)	$C_6H_{10}O_5$
162	caffeoyl	$C_9H_6O_3$
166	methyl-gallate	$C_8H_6O_4$
166	oleuropeoyl	$C_{10}H_{14}O_2$
174	quinoyl	$C_7H_{10}O_5$
176	glucuronide (Glu)	$C_6H_8O_6$
176	feruloyl	$C_{10}H_8O_3$
178	trihydroxycinnamate	$C_9H_6O_4$
180	dimethylgallate	$C_9H_8O_4$
194	trimethoxybenzoate	$C_{10}H_{10}O_4$
206	sinapoyl	$C_{11}H_{10}O_4$

Table 5.2: Common combinations of neutral losses

Neutral loss (Da)	Combination	Molecular Formula
174	acetyl + pentose	$C_7H_{10}O_5$
188	acetyl + rhamnose	$C_8H_{12}O_5$
194	acetyl + gallose	$C_9H_6O_5$
248	maloyl + hexose	$C_9H_{12}O_8$
204	acetyl + hexose	$C_8H_{12}O_6$
246	diacetyl + hexose	$C_{10}H_{14}O_7$
264	pentose + pentose	$C_{10}H_{16}O_8$
266	benzoyl + hexose	$C_{13}H_{14}O_6$
278	rhamnose + pentose	$C_{11}H_{18}O_8$
282	hydroxybenzoyl + hexose	$C_{13}H_{14}O_7$
284	galloyl + pentose	$C_{12}H_{12}O_8$

Neutral loss (Da)	Combination	Molecular Formula
292	rhamnose + rhamnose	$C_{12}H_{20}O_8$
292	coumaroyl + rhamnose	$C_{15}H_{16}O_6$
294	pentose + hexose	$C_{11}H_{18}O_9$
298	galloyl + rhamnose	$C_{13}H_{14}O_8$
308	rutinoside (rhamnose + hexose)	$C_{12}H_{20}O_9$
308	coumaroyl + hexose	$C_{15}H_{16}O_7$
314	galloyl + hexose	$C_{13}H_{14}O_9$
322	rhamnose + glucuronoide	$C_{12}H_{18}O_{10}$
322	feruloyl + rhamnose	$C_{16}H_{18}O_7$
324	hexose + hexose	$C_{12}H_{20}O_{10}$
324	trihydroxycinnamate + rhamnose	$C_{15}H_{16}O_8$
338	feruloyl + hexose	$C_{16}H_{18}O_8$
368	sinapoyl + hexose	$C_{17}H_{20}O_9$

6. Data Interpretation

The following chapters deal with the identification of polyphenolic compounds in the *Rhododendron* leaf extracts using the LC-Ion Trap-MS and LC-TOF-MS data. The chapters are divided by the different classes of polyphenols identified (hydroxycinnamic acid derivatives, hydroxybenzoic acid derivatives, flavan-3-ols, flavanones and flavonols). The different classes are further sub-divided into derivatives from a specific group for example derivatives of caffeic acid, *p*-coumaric acid and ferulic acid in the case of hydroxycinnamic acid derivatives. The chapters are not classified based on individual *Rhododendron* species due to the large number of data set in terms of samples and identified compounds.

The extracts are injected into the LC-MS system where the diphenyl column and the binary solvent gradient system of water (0.005% formic acid) and methanol are responsible for eluting compounds at different solvent concentrations, which generates different retention times for compounds. The compounds are then injected into the MS system. All the data discussed here have been analyzed in the negative mode in the MS system. In an Ion Trap mass spectrometer, the pre-cursor ions of compounds are fragmented into daughter ions and neutral losses. The neutral losses are useful to identify the substituents attached to an aglycon. The daughter ions can be further fragmented depending upon the experimental conditions. The first, second and third step of fragmentation are called MS^2, MS^3 and MS^4 respectively. The fragmentation is characteristic to the compounds and can be used for the complete or partial identification of the compound structure. The authentic standards are used for comparing the retention time and the fragmentation of aglycone part of the derivatives. In a TOF mass spectrometer, the high resolution molecular weight of the compounds can be calculated by using their detected time of flight at a set kinetic energy. The molecular weight is accurate up to 4 digits after the decimal (Bruker micro-TOF system) and is used to generate the molecular formula of the compounds using the Bruker software.

In the chapters, each compound discussed consists of its name (3-*O*-*p*-coumaroylquinic acid), its unique identification number in bold and inside brackets (**1**), molecular formula obtained by TOF-MS ($C_{16}H_{18}O_8$), the mass to charge ratio or *m/z* ratio observed in Ion Trap-MS for the molecular ion after a loss of hydrogen $[M-H]^-$ (*m/z* 337) and retention time (t_R 18.0 min). The fragmentation of the compounds is discussed in MS^2, MS^3 and MS^4 mode, wherever applicable. The major fragment ion of the pre-cursor ion is represented by the base peak, while the other fragments are represented by secondary peaks. The *m/z* values of peaks along with the moieties lost during fragmentation are described within rectangular brackets. For example, in the base peak of compound **1**, *m/z* 191 $[M-H-coumaroyl]^-$ was observed, which is formed after a loss of hydrogen and coumaroyl group.

The extract ion chromatogram of some *m/z* values are shown for selected compounds in randomly chosen *Rhododendron* leaf extracts. The compounds are labelled in the extract ion chromatograms using their unique identification number. The tandem MS spectra are shown for these selected compounds and their compound structures are shown besides it. The proposed fragmentation schemes are also shown for some compounds.

The additional information including literature references, the experimental and theoretical molecular weight of compounds, the error observed, the fragmentation and relative intensity of ions along with the name, unique identification number, molecular formula and retention time are mentioned in the Appendix section (Fragmentation pattern of identified compounds and Fragmentation pattern of derivatives). The structures of all the identified compounds can also be found in the Appendix section (Compound Structures).

7. Hydroxycinnamic acid derivatives

7.1. Chlorogenic acids

The chlorogenic acid isomers were previously identified by our Group with the help of fragmentation data, retention time and UV spectra. The hydroxycinnamic acids of selected *Rhododendron* species have been used in a manuscript to be submitted soon.

7.1.1. Characterization of coumaroylquinic acids (M_r 338)

Five isomers of coumaroylquinic acid (**1**-**5**) with $C_{16}H_{18}O_8$ and *m/z* 337 were identified. They were assigned as 3-*O*-*p*-coumaroylquinic acid (**1**) at t_R 18.0 min, *cis*-3-*O*-*p*-coumaroylquinic acid (**2**) at t_R 19.4 min, 5-*O*-*p*-coumaroylquinic acid (**3**) at t_R 24.6 min, 4-*O*-*p*-coumaroylquinic acid (**4**) at t_R 26.6 min and *cis*-5-*O*-*p*-coumaroylquinic acid (**5**) at t_R 28.4 min. Compounds **1** and **2** produced a base peak of *m/z* 163 [*p*-CouA-H]$^-$, which further fragmented to *m/z* 119 [*p*-CouA-H-CO_2]$^-$. Compounds **3** and **5** produced a base peak of *m/z* 191 [M-H-coumaroyl]$^-$. Compound **4** produced a base peak of *m/z* 173 [M-H-coumaroyl-H_2O]$^-$. The EIC of *m/z* 337 in *Rhododendron micranthum* in negative mode is shown in Figure 7.1, along with the MS^n spectra of compounds **1** and **3** in Figure 7.2 and Figure 7.3 respectively. The proposed fragmentation of compound **3** is shown in Figure 7.4. The EIC of *m/z* 337 in *Rhododendron trigillosum* in negative mode is shown in Figure 7.5, along with the MS^n spectra of compound **4** in Figure 7.6.

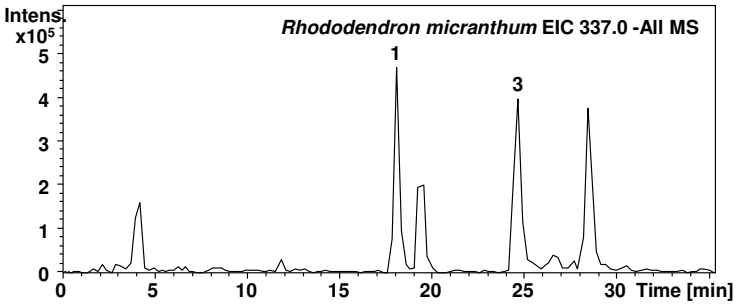

Figure 7.1: EIC of *m/z* 337 in *Rhododendron micranthum* in negative mode

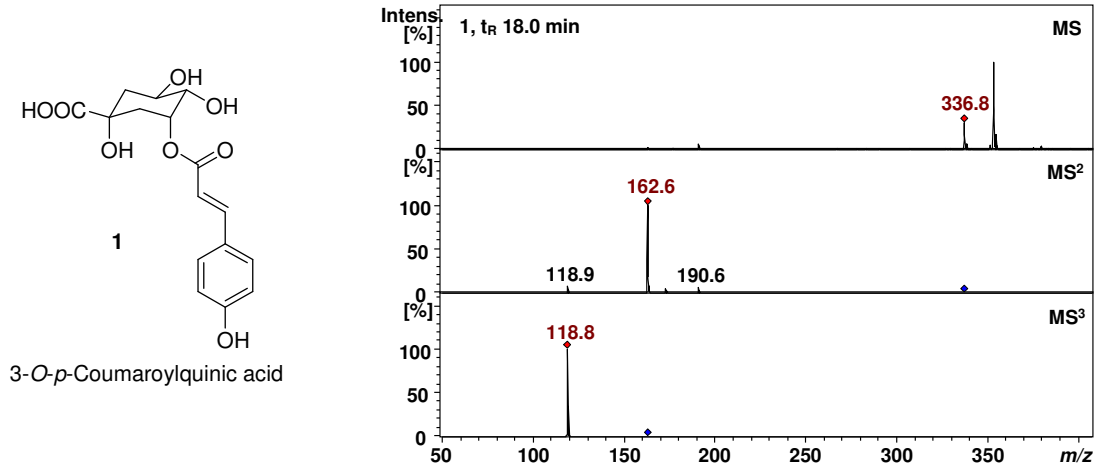

Figure 7.2: MS^n spectra of 3-*O*-*p*-coumaroylquinic acid

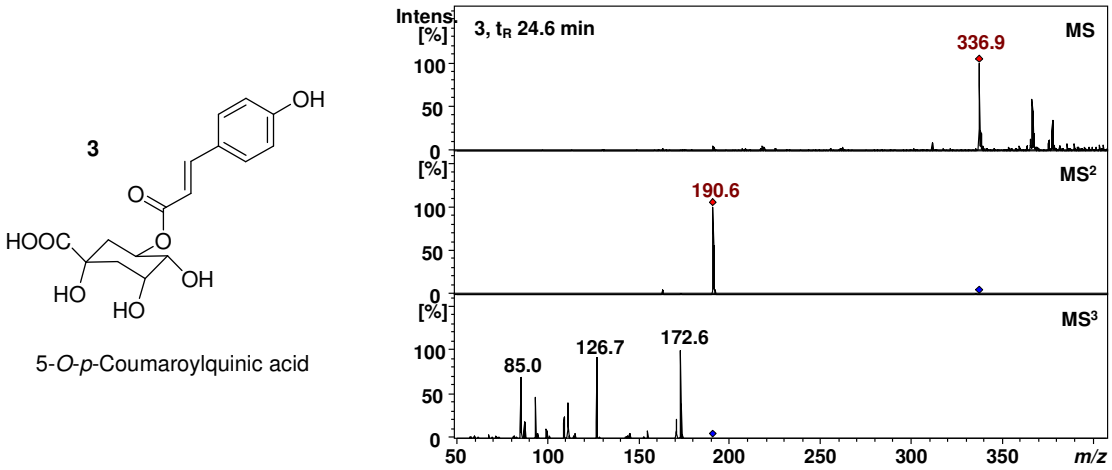

Figure 7.3: MS^n spectra of 5-*O*-*p*-coumaroylquinic acid

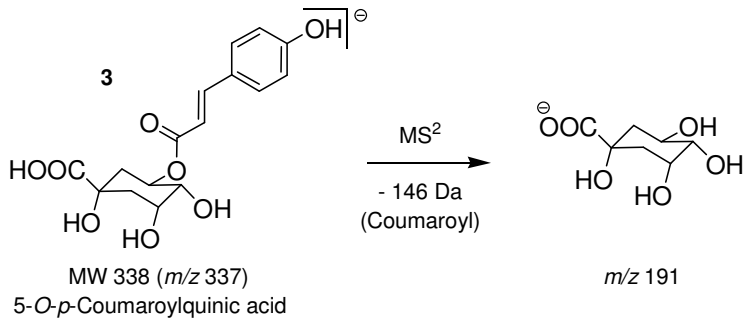

Figure 7.4: Proposed fragmentation of 5-*O*-*p*-coumaroylquinic acid

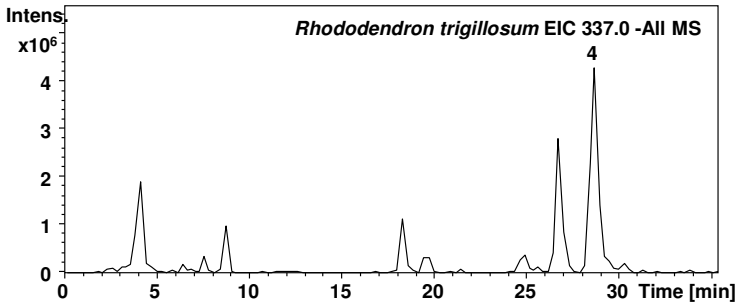

Figure 7.5: EIC of *m/z* 337 in *Rhododendron trigillosum* in negative mode

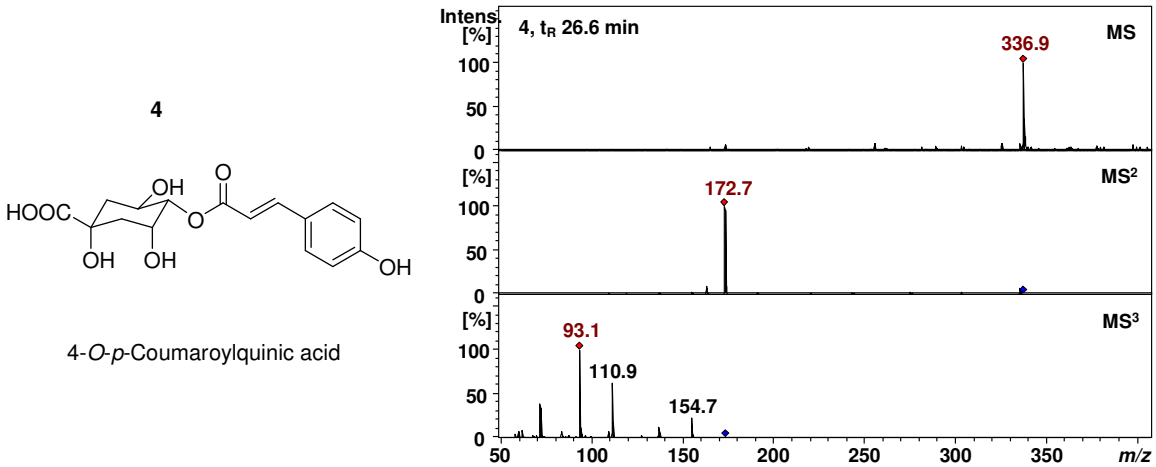

Figure 7.6: MS^n spectra of 4-*O*-*p*-coumaroylquinic acid

7.1.2. Characterization of caffeoylquinic acids (M_r 354)

Six isomers of caffeoylquinic acid (**6-11**) with *m/z* 353 and molecular formula of $C_{16}H_{18}O_9$ were identified. They were assigned as 3-*O*-caffeoylquinic acid (**6**) at t_R 13.0 min, *cis*-3-*O*-caffeoylquinic acid (**7**) at t_R 14.0 min, 5-*O*-caffeoylquinic acid (**8**) at t_R 18.2 min, *cis*-4-*O*-caffeoylquinic acid (**9**) at t_R 20.6 min, 4-*O*-caffeoylquinic acid (**10**) at t_R 23.0 min, and *cis*-5-*O*-caffeoylquinic acid (**11**) at t_R 24.1 min. All of the caffeoylquinic acids with the exception of compounds **9** and **10** produced a base peak of *m/z* 191 $[QA-H]^-$. Compounds **9** and **10** produced a base peak of *m/z* 173 $[QA-H-H_2O]^-$. Compounds **6**, **7**, **9** and **10** also consisted of the secondary peak of *m/z* 179 $[CA-H]^-$. The EIC of *m/z* 353 in *Rhododendron hippophaeoides* in negative mode is shown in Figure 7.7, along with the MS^n spectra of compounds **6**, **8** and **10** in Figure 7.8, Figure 7.9 and Figure 7.11 respectively. The proposed fragmentation of compound **8** is shown in Figure 7.10.

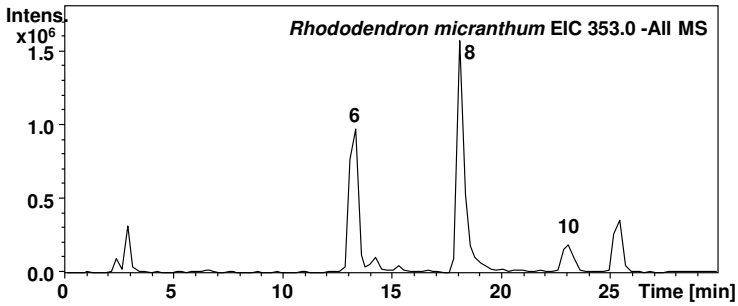

Figure 7.7: EIC of *m/z* 353 in *Rhododendron hippophaeoides* in negative mode

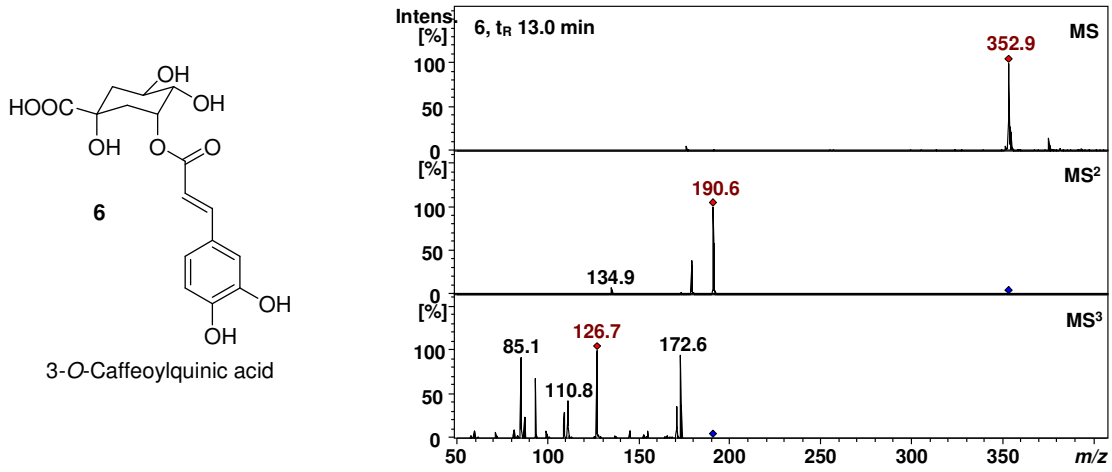

Figure 7.8: MS^n spectra of 3-*O*-caffeoylquinic acid

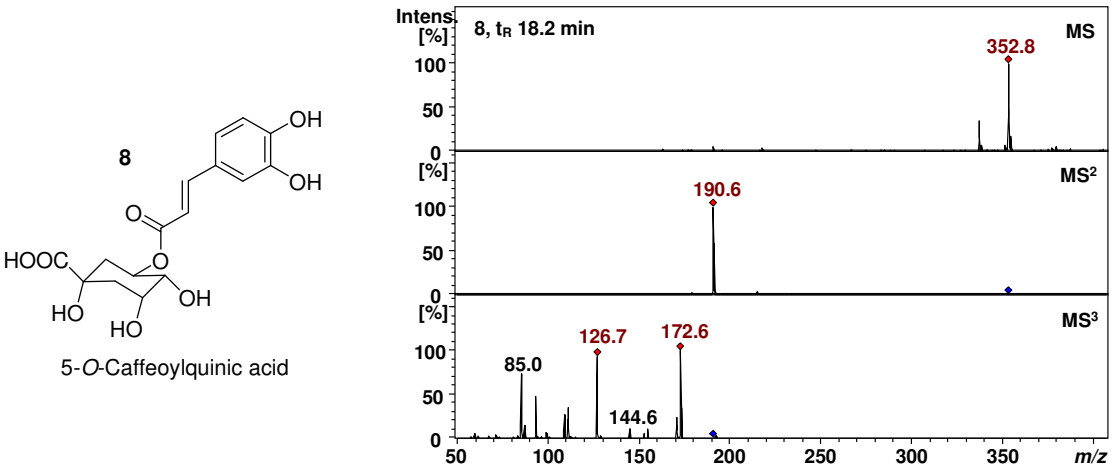

Figure 7.9: MS^n spectra of 5-*O*-caffeoylquinic acid

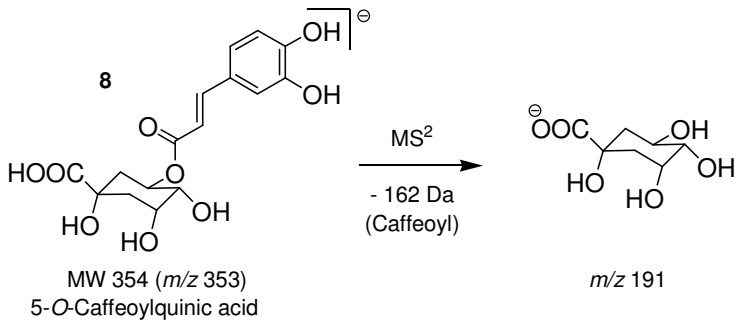

Figure 7.10: Proposed fragmentation of 5-*O*-caffeoylquinic acid

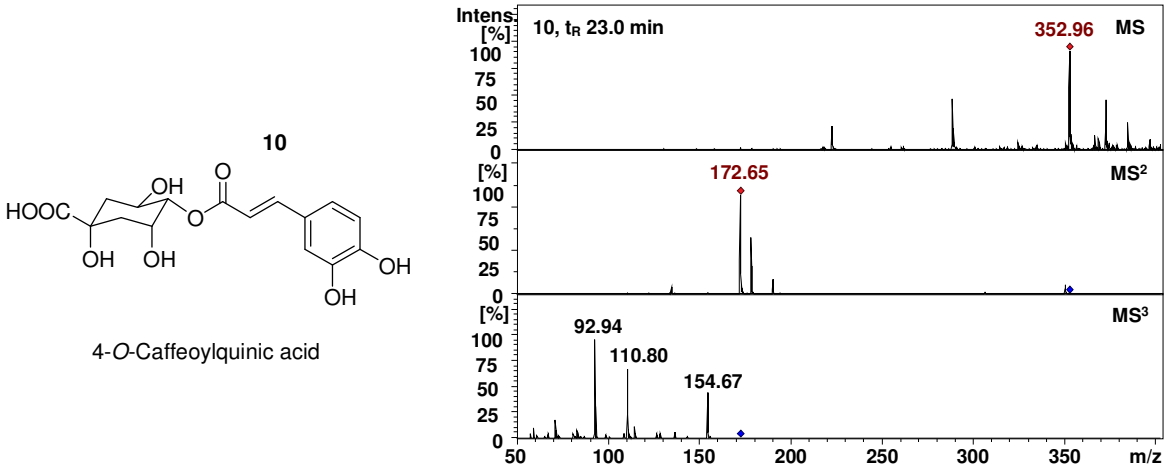

Figure 7.11: MS^n spectra of 4-*O*-caffeoylquinic acid

7.1.3. Characterization of feruloylquinic acids (M_r 368)

Three isomers of feruloylquinic acid (**12**-**14**) with $C_{17}H_{20}O_9$ and *m/z* 367 were identified. They were assigned as 3-*O*-feruloylquinic acid (**12**) at t_R 21.7 min, 5-*O*-feruloylquinic acid (**13**) at t_R 27.5 min and 4-*O*-feruloylquinic acid (**14**) at t_R 31.6 min. Compound **12** produced a base peak of *m/z* 193 $[FA-H]^-$, which fragmented into *m/z* 134 $[FA-H-CH_3-CO_2]^-$. Compound **13** produced a base peak of *m/z* 191 $[QA-H]^-$, which fragmented into *m/z* 127 and 173 $[QA-H-H_2O]^-$. Compound **14** produced a base peak of *m/z* 173 $[QA-H-H_2O]^-$ and secondary peak of *m/z* 193. In MS^3, it further fragmented to give a base peak of *m/z* 93 and secondary peaks of *m/z* 111 and 155. The EIC of *m/z* 367 in *Rhododendron hippophaeoides* in negative mode is shown in Figure 7.12, along with the MS^n spectra of compound **12** in Figure 7.13.

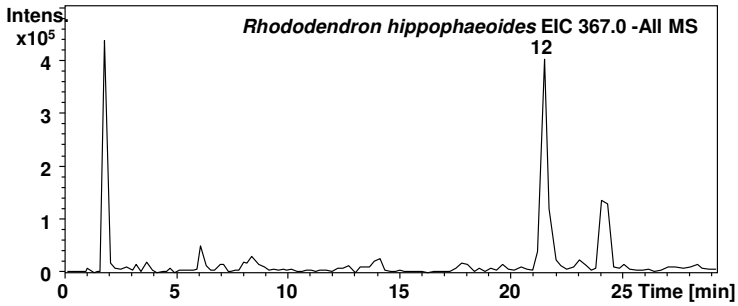

Figure 7.12: EIC of *m/z* 367 in *Rhododendron hippophaeoides* in negative mode

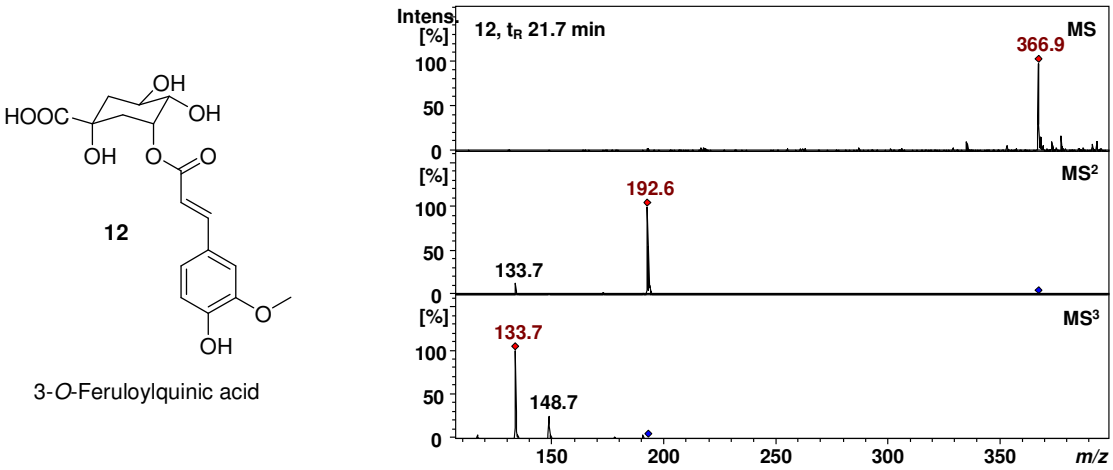

Figure 7.13: MS^n spectra of 3-*O*-feruloylquinic acid

7.1.4. Characterization of hydroxydihydro-caffeoylquinic acids (M_r 372)

Five isomers of hydroxydihydro-caffeoylquinic acid (**15**-**19**) with $C_{16}H_{20}O_{10}$ and *m/z* 371 were identified. A peak at t_R 5.9 min was assigned as 3-*O*-hydroxydihydro-caffeoylquinic acid (**15**). It produced an MS^2 base peak of *m/z* 353 and secondary peak of *m/z* 233. In MS^3, it produced a base peak of *m/z* 191 and secondary peaks of *m/z* 179 and 173. Two peaks at t_R 5.4 and 7.0 min were assigned as 5-*O*-hydroxydihydro-caffeoylquinic acid (**16**-**17**). They produced an MS^2 base peak of *m/z* 191 and secondary peak of *m/z* 233. Two peaks at t_R 9.8 and 10.8 min were assigned as 4-*O*-hydroxydihydro-caffeoylquinic acid (**18**-**19**). They produced an MS^2 base peak of *m/z* 173 and secondary peaks of *m/z* 191 and 233. In MS^3, they produced a base peak of *m/z* 93.

7.2. Caffeic acid derivatives

The caffeic acid derivatives were identified based on their characteristic fragmentation peaks. The caffeic acid aglycon can be identified in MS^n by comparison with an authentic standard. In negative mode, caffeic acid at *m/z* 179 (after a loss of hydrogen) fragments to give *m/z* 135 (after a loss of hydrogen and carbon dioxide).

7.2.1. Characterization of caffeoylthreonates (M_r 298)

Two isomers of caffeoylthreonates (**20**-**21**) at t_R 15.5 and 23.7 min were assigned to the peaks with $C_{13}H_{14}O_8$ and *m/z* 297. The compounds produced an MS^2 base and secondary peak of *m/z* 135 $[M-H-Thr-CO_2]^-$ and 179 $[M-H-Thr]^-$ respectively.

7.2.2. Characterization of teucrol (M_r 316)

A peak at t_R 51.0 min with *m/z* 315 and $C_{17}H_{16}O_6$ was speculated to be teucrol (**22**). Teucrol produced MS^2 and MS^3 base peaks of *m/z* 179 and 135 respectively. The neutral loss of 136 Da could be attributed to dihydroxy-phenyl-ethanol.

7.2.3. Characterization of caffeoylshikimic acid (M_r 336)

A peak at t_R 24.6 min with *m/z* 335 and $C_{16}H_{16}O_8$ was assigned as caffeoylshikimic acid (**23**). It produced MS^2 and MS^3 base peaks of *m/z* 179 $[M-H-shikimoyl]^-$ and 135 $[M-H-shikimoyl-CO_2]^-$ respectively.

7.2.4. Characterization of caffeic acid-*O*-hexoside (M_r 342)

Eight isomers of caffeic acid-*O*-hexoside (**24**-**31**) at t_R 8.1, 9.2, 10.9, 12.5, 13.9, 15.1, 17.6 and 19.2 min were assigned to the peaks with $C_{15}H_{18}O_9$ and *m/z* 341. Compounds **24**, **25** and **29** produced a base peak of *m/z* 135 $[M-H-Glc-CO_2]^-$, which further fragmented to *m/z* 107 $[M-H-Glc-CO_2-CO]^-$ and a secondary peak of *m/z* 179 $[M-H-Glc]^-$. Compounds **26**, **27**, **28**, **30** and **31** produced a base peak of *m/z* 179 $[M-H-Glc]^-$, which fragmented into *m/z* 135 $[M-H-Glc-CO_2]^-$. The EIC of *m/z* 341 in *Rhododendron campylocarpum* ssp. *caloxanthum* in negative mode is shown in Figure 7.14, along with the MS^n spectra of compound **26** in Figure 7.15. The proposed fragmentation of compounds **24**-**31** is shown in Figure 7.16.

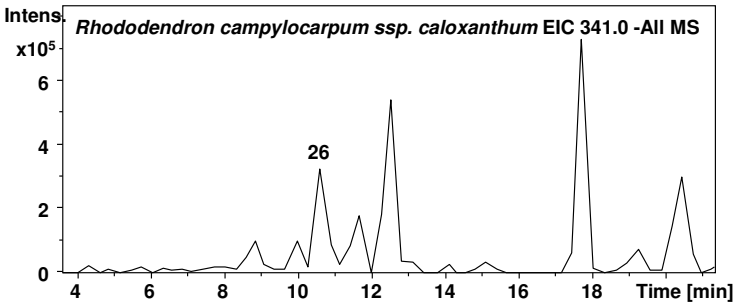

Figure 7.14: EIC of *m/z* 341 in *Rhododendron campylocarpum* ssp. *caloxanthum* in negative mode

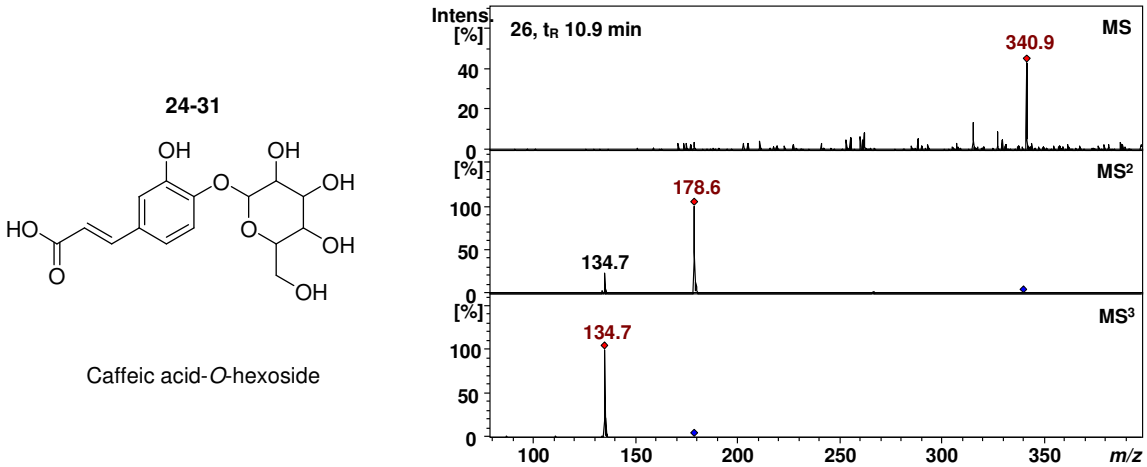

Figure 7.15: MS^n spectra of caffeic acid-*O*-hexoside

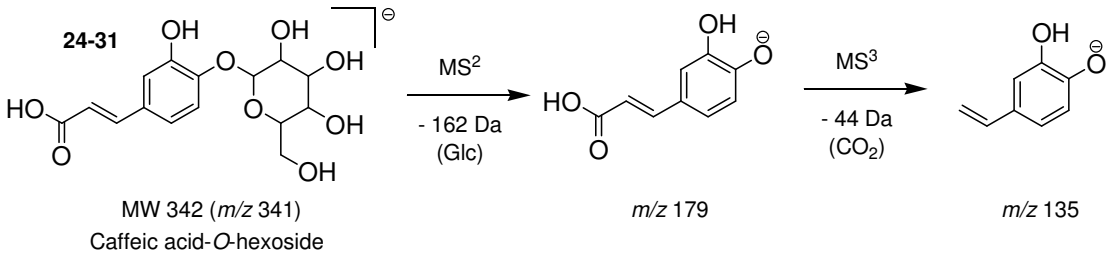

Figure 7.16: Proposed fragmentation of caffeic acid-*O*-hexoside

7.2.5. Characterization of teucrol-*O*-hexoside (M_r 478)

A peak at t_R 42.0 min with *m/z* 477 and $C_{23}H_{26}O_{11}$ was speculated to be teucrol-*O*-hexoside, which is an isomer plantainoside (**32**). It produced MS^2, MS^3 and MS^4 base peaks of *m/z* 315 $[M-H-Glc]^-$, 179 and 135 respectively. The neutral loss of 136 Da could be attributed to dihydroxy-phenyl-ethanol.

7.3. *p*-Coumaric acid derivatives

The *p*-coumaric acid derivatives were identified based on their characteristic fragmentation peaks. The *p*-coumaric acid aglycon can be identified in MS^n by comparison with an authentic standard. In negative mode, *p*-coumaric acid at *m/z* 163 (after a loss of hydrogen) fragments to give *m/z* 119 (after a loss of hydrogen and carbon dioxide).

7.3.1. Characterization of *p*-coumaric acid-*O*-shikimate (M_r 320)

A peak at t_R 42.0 min with *m/z* 319 and $C_{16}H_{16}O_7$ was assigned as *p*-coumaric acid-*O*-shikimate (**33**). It produced MS^2 and MS^3 base peaks of *m/z* 163 $[M-H-shikimoyl]^-$ and 119 $[M-H-shikimoyl-CO_2]^-$ respectively.

7.3.2. Characterization of *p*-coumaric acid-*O*-hexoside (M_r 326)

Four isomers of *p*-coumaric-*O*-hexoside (**34**-**37**) were assigned to the peaks at t_R 15.7, 16.5, 24.1 and 26.2 min with $C_{15}H_{18}O_8$ and *m/z* 325. The compounds produced MS^2 and MS^3 base peaks of *m/z* 163 $[M-H-Glc]^-$ and 119 $[M-H-Glc-CO_2]^-$ respectively. The EIC of *m/z* 325 in *Rhododendron thayerianum* in negative mode is shown in Figure 7.17, along with the MS^n spectra of compound **34** in Figure 7.18. The proposed fragmentation of compounds **34**-**37** is shown in Figure 7.19.

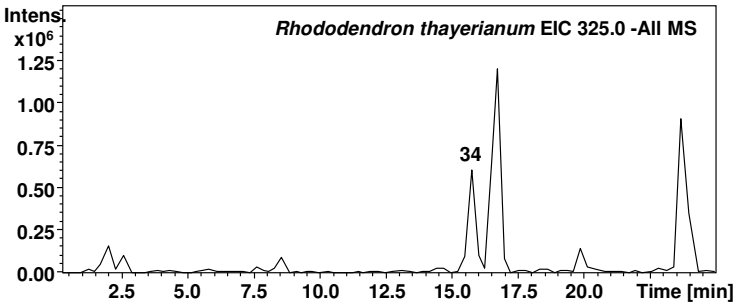

Figure 7.17: EIC of *m/z* 325 in *Rhododendron thayerianum* in negative mode

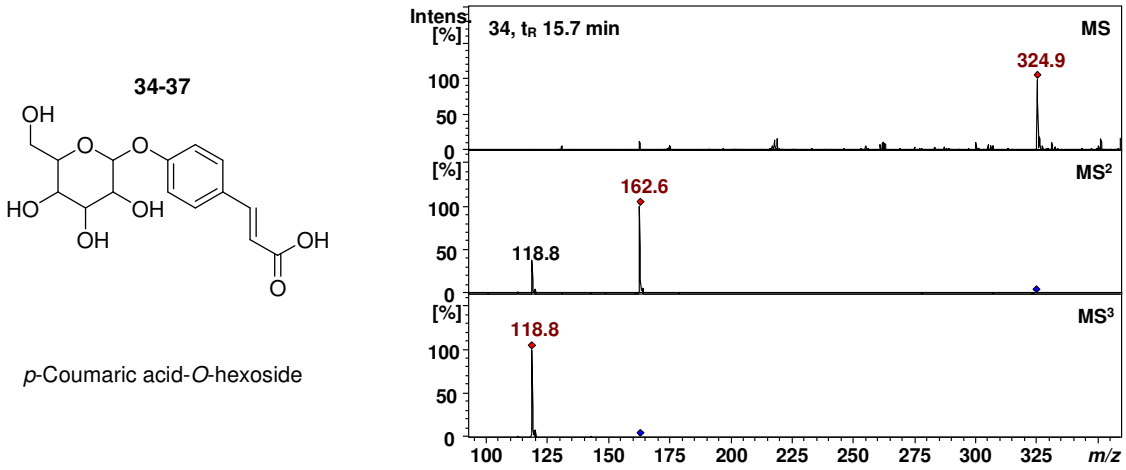

Figure 7.18: MS^n spectra of *p*-coumaric acid-*O*-hexoside

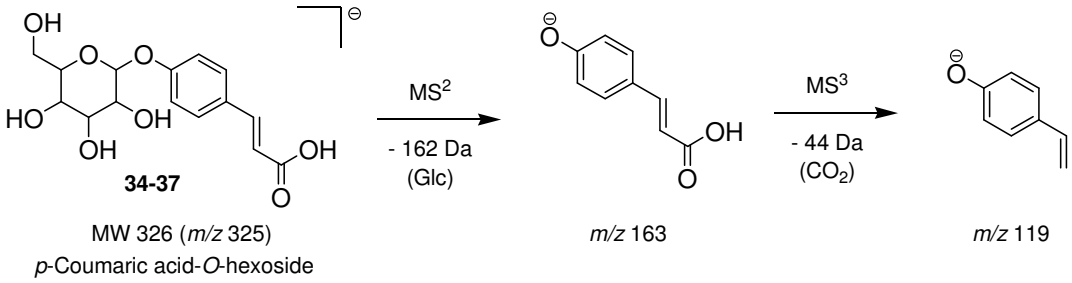

Figure 7.19: Proposed fragmentation of *p*-coumaric acid-*O*-hexoside

7.3.3. Characterization of *p*-coumaric acid-*O*-glucosyl ester (M_r 326)

Two isomers of *p*-coumaric acid-*O*-glucosyl ester (**38** and **39**) were assigned to the peaks at t_R 17.5 and 18.7 min with $C_{15}H_{18}O_8$ and *m/z* 325. The compounds produced MS^2 and MS^3 base peaks of *m/z* 163 $[M\text{-}H\text{-}Glc]^-$ and 119 $[M\text{-}H\text{-}Glc\text{-}CO_2]^-$ respectively. In MS^2 fragmentation, they also produced secondary peaks of *m/z* 265 $[M\text{-}H\text{-}60\ Da]^-$, 235 $[M\text{-}H\text{-}90\ Da]^-$ and 205 $[M\text{-}H\text{-}120\ Da]^-$.

7.3.4. Characterization of *p*-coumaric acid-*O*-hexoside-*O*-pentoside (M_r 458)

Two isomers of *p*-coumaric acid-*O*-hexoside-*O*-pentoside (**40**-**41**) were assigned to the peaks at t_R 17.6 and 19.2 min with $C_{20}H_{26}O_{12}$ and *m/z* 457. Both the compounds produced a base peak of *m/z* 163 $[M\text{-}H\text{-}Glc\text{-}Xyl]^-$, which fragmented into *m/z* 119 $[M\text{-}H\text{-}Glc\text{-}Xyl\text{-}CO_2]^-$. The neutral loss of 294 Da could be attributed to hexose and pentose. The absence of intermediate fragment ions explained that the hexose and pentose were interconnected.

7.3.5. Characterization of Everlastoside M (M_r 482)

A peak at t_R 27.0 min with *m/z* 481 and $C_{22}H_{26}O_{12}$ was speculated to be an isomer of Everlastoside M (**42**) with MS^2, MS^3 and MS^4 base peaks of *m/z* 367, 163 and 119 respectively.

7.3.6. Characterization of *p*-coumaric acid-*O*-dihexoside (M_r 488)

Two isomers of *p*-coumaric acid-*O*-dihexoside (**43**-**44**) were assigned to the peaks at t_R 14.4 and 20.0 min with $C_{21}H_{28}O_{13}$ and *m/z* 487. They produced a base peak of *m/z* 163 $[M-H-Glc-Glc]^-$, which fragmented into *m/z* 119 $[M-H-Glc-Glc-CO_2]^-$ and secondary peak of *m/z* 325 $[M-H-Glc]^-$.

7.4. Dihydrocoumaric acid derivatives

The dihydrocoumaric acid derivatives were identified based on their characteristic fragmentation peaks. In negative mode, the aglycon of dihydrocoumaric acid at *m/z* 165 (after a loss of hydrogen) fragments to give *m/z* 121 (after a loss of hydrogen and carbon dioxide).

7.4.1. Characterization of dihydrocoumaric acid-*O*-hexoside (M_r 328)

Two isomers of dihydrocoumaric acid-*O*-hexoside (**45**-**46**) were assigned to the peaks at t_R 15.5 and 20.4 min with $C_{15}H_{20}O_8$ and *m/z* 327. Both compounds produced an MS^2 base peak of *m/z* 165 $[M-H-Glc]^-$ and MS^3 base peak of *m/z* 121 $[M-H-Glc-CO_2]^-$.

7.5. Ferulic acid derivatives

The ferulic acid derivatives were identified based on their characteristic fragmentation peaks. The ferulic acid aglycon can be identified in MS^n by comparison with an authentic standard. In negative mode, ferulic acid at *m/z* 193 (after a loss of hydrogen) fragments to give *m/z* 149 (after a loss of hydrogen and carbon dioxide) and 134 (after a loss of hydrogen, carbon dioxide and a methyl group).

7.5.1. Characterization of ferulic acid-*O*-hexoside (M_r 356)

Three isomers of ferulic acid-*O*-hexoside (**47**-**49**) at t_R 19.0, 21.2 and 28.9 min were assigned to the peaks with $C_{16}H_{20}O_9$ and *m/z* 355. All the isomers produced an MS^2 and MS^3 base peak of *m/z* 193 $[M-H-Glc]^-$ and *m/z* 149 $[M-H-Glc-CO_2]^-$ respectively with the exception of compound

43, which produced *m/z* 134 [M-H-Glc-CO_2-CH_3]$^-$. The EIC of *m/z* 355 in *Rhododendron macabeanum* in negative mode is shown in Figure 7.20, along with the MS^n spectra of compound **47** in Figure 7.21. The proposed fragmentation of compounds **47**-**49** is shown in Figure 7.22.

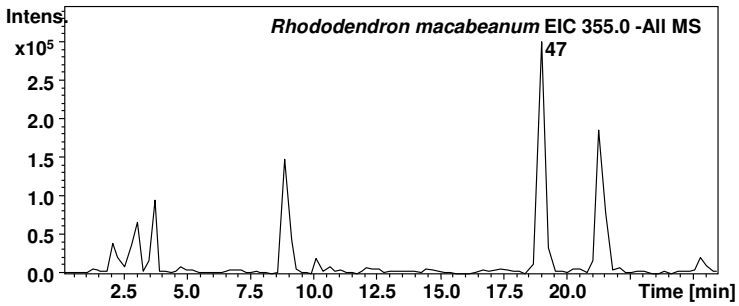

Figure 7.20: EIC of *m/z* 355 in *Rhododendron macabeanum* in negative mode

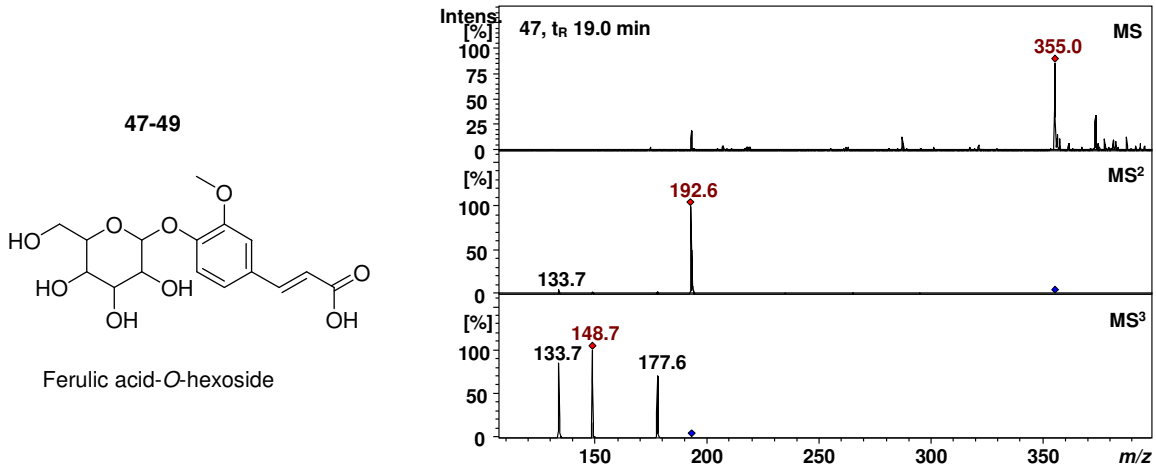

Figure 7.21: MS^n spectra of ferulic acid-*O*-hexoside

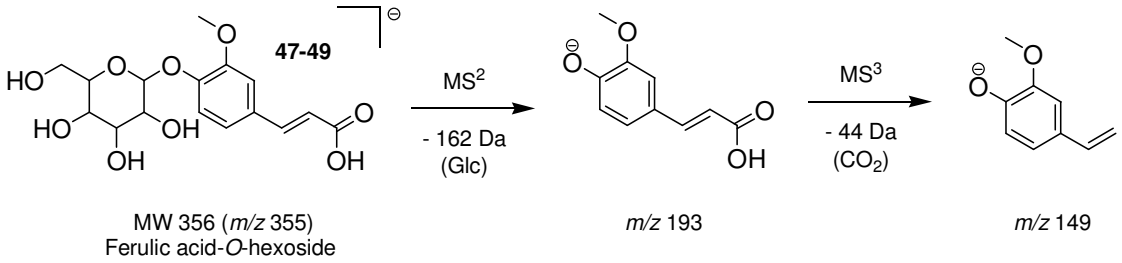

Figure 7.22: Proposed fragmentation of ferulic acid-*O*-hexoside

7.5.2. Characterization of ferulic acid-*O*-glucosyl ester (M_r 356)

A peak at t_R 20.4 min with *m/z* 355 and $C_{16}H_{20}O_9$ was assigned as ferulic acid-*O*-glucosyl ester (**50**). The peak produced MS^2 and MS^3 base peaks of *m/z* 193 $[M-H-Glc]^-$ and 134 $[M-H-Glc-CO_2-CH_3]^-$ respectively. In MS^2 fragmentation, it also produced secondary peaks of *m/z* 295 $[M-H-60\ Da]^-$, 265 $[M-H-90\ Da]^-$ and 235 $[M-H-120\ Da]^-$. And in MS^3 fragmentation, it produced a secondary peak of *m/z* 149 $[M-H-Glc-CO_2]^-$.

7.5.3. Characterization of ferulic acid-*O*-dihexoside (M_r 518)

A peak at t_R 17.2 min with *m/z* 517 and $C_{22}H_{30}O_{14}$ was assigned as ferulic acid-*O*-dihexoside (**51**). The compound produced an MS^2 and MS^3 base peak of *m/z* 193 $[M-H-Glc-Glc]^-$ and *m/z* 149 $[M-H-Glc-Glc-CO_2]^-$ respectively. The neutral loss of 324 Da could be attributed to two hexoses. The absence of intermediate fragment ions explained that the two hexoses were interconnected.

8. Hydroxybenzoic acid derivatives

8.1. Gallic acid derivatives

The gallic acid derivatives were identified based on their characteristic fragmentation peaks. The gallic acid aglycon can be identified in MS^n by comparison with an authentic standard. In negative mode, gallic acid at *m/z* 169 (after a loss of hydrogen) fragments to give *m/z* 125 (after a loss of hydrogen and carbon dioxide).

8.1.1. Characterization of gallic acid-*O*-pentoside (M_r 302)

A peak at t_R 6.6 min with *m/z* 301 and $C_{12}H_{14}O_9$ was assigned as gallic acid-*O*-pentoside (**52**). It produced MS^2 and MS^3 base peaks of *m/z* 169 $[M-H-Xyl]^-$ and 125 $[M-H-Xyl-CO_2]^-$ respectively.

8.1.2. Characterization of gallic shikimic acid (Mr 326)

Two isomers of galloyl shikimic acid (**53**-**54**) were identified at t_R 8.9 and 9.6 min with $C_{14}H_{14}O_9$ and *m/z* 325. Both the peaks produced a base peak of *m/z* 169 $[M-H-shikimoyl]^-$, which fragmented to *m/z* 125 $[M-H-shikimoyl-CO_2]^-$.

8.1.3. Characterization of gallic acid-*O*-hexoside (M_r 332)

Two isomers of gallic acid-*O*-hexoside (**55**-**56**) were identified at t_R 4.6 and 7.9 min with $C_{13}H_{16}O_{10}$ and *m/z* 331. Both the peaks produced a base peak of *m/z* 169 $[M-H-Glc]^-$, which fragmented to *m/z* 125 $[M-H-Glc-CO_2]^-$. The EIC of *m/z* 331 in *Rhododendron strigillosum* in negative mode is shown in Figure 8.1, along with the MS^n spectra of compound **55** in Figure 8.2. The proposed fragmentation of compounds **55**-**56** is shown in Figure 8.3.

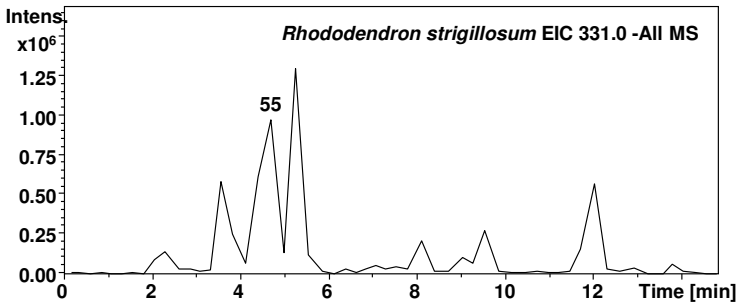

Figure 8.1: EIC of *m/z* 331 in *Rhododendron strigillosum* in negative mode

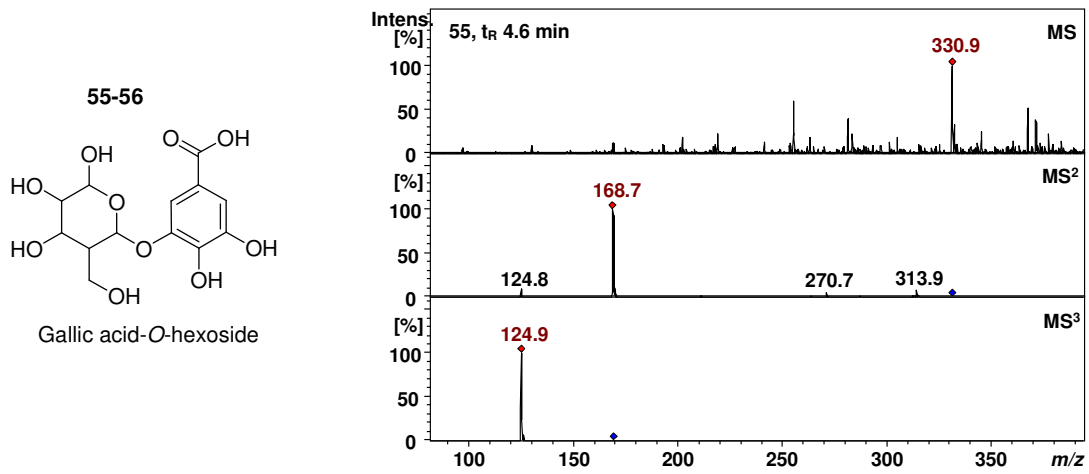

Figure 8.2: MS^n spectra of gallic acid-*O*-hexoside

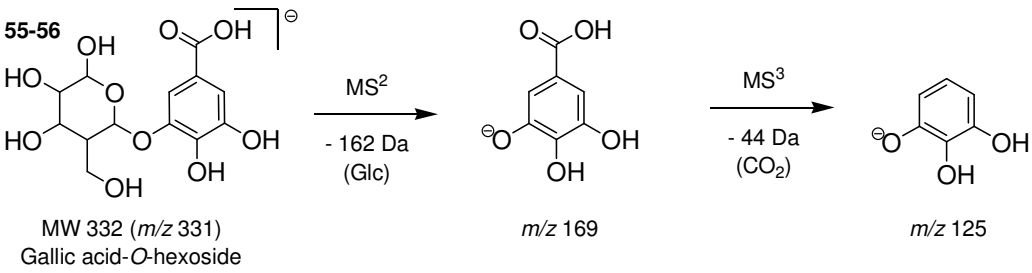

Figure 8.3: Proposed fragmentation of gallic acid-*O*-hexoside

8.1.4. Characterization of gallic acid-*O*-glucosyl ester (M_r 332)

A peak at t_R 3.7 min with *m/z* 331 and $C_{13}H_{16}O_{10}$ was assigned as gallic acid-*O*-glucosyl ester (**57**). The peak produced MS^2 and MS^3 base peaks of *m/z* 169 $[M-H-Glc]^-$ and 125 $[M-H-Glc-CO_2]^-$ respectively. In MS^2 fragmentation, it also produced secondary peaks of *m/z* 271 $[M-H-60\ Da]^-$, 241 $[M-H-90\ Da]^-$ and 211 $[M-H-120\ Da]^-$.

8.1.5. Characterization of galloyl quinic acid (M_r 344)

Three isomers of galloyl quinic acid (**58-60**) were identified at t_R 4.3, 5.8 and 9.6 min with $C_{14}H_{16}O_{10}$ and *m/z* 343. Both the peaks produced the fragments of *m/z* 169 $[M-H-quinoyl]^-$ and *m/z* 125 $[M-H-quinoyl-CO_2]^-$. The compounds **53** and **54** also produced the peak of *m/z* 191 $[M-H-galloyl]^-$.

8.1.6. Characterization of gallic acid-*O*-acetyl-hexoside (M_r 374)

A peak at t_R 13.9 min with *m/z* 373 and $C_{15}H_{18}O_{11}$ was assigned as gallic acid-*O*-acetyl-hexoside (**61**). It produced MS^2 and MS^3 base peaks of *m/z* 169 $[M\text{-}H\text{-acetyl-Glc}]^-$ and 125 $[M\text{-}H\text{-acetyl-Glc-}CO_2]^-$ respectively.

8.1.7. Characterization of benzyl-6'-*O*-galloyl-β-D-hexoside (M_r 422)

A peak at t_R 32.1 min with *m/z* 421 and $C_{20}H_{22}O_{10}$ was assigned as benzyl-6'-*O*-galloyl-β-D-hexoside (**62**). It produced MS^2 peaks of *m/z* 313 and base peak of 169, which fragmented into *m/z* 125 in MS^3. The neutral loss of 252 Da was assumed to be the loss of a benzyl group attached to a hexose.

8.1.8. Characterization of galloyl arbutin (M_r 424)

Two isomers of galloyl arbutin (**63**-**64**) were identified at t_R 11.7 and 17.7 min with $C_{19}H_{20}O_{11}$ and *m/z* 423. It produced MS^2, MS^3 and MS^4 base peaks of *m/z* 313, 169 and 125 respectively. The neutral loss of 254 Da was assumed to be the loss of a benzenediol group attached to a hexose.

8.1.9. Characterization of 6-galloyl-1-*O*-(phloroglucinol)-hexoside (M_r 440)

A peak at t_R 15.0 min with *m/z* 439 and $C_{19}H_{20}O_{12}$ was assigned as 6-galloyl-1-*O*-(phloroglucinol)-hexoside (**65**). It produced MS^2, MS^3 and MS^4 base peaks of *m/z* 313, 169 and 125 respectively. The neutral loss of 270 Da was assumed to be the loss of a benzenetriol group attached to a hexose.

8.1.10. Characterization of gallic acid-3-*O*-hexoside-4-*O*-pentoside (M_r 464)

A peak at t_R 7.9 min with *m/z* 463 and $C_{18}H_{24}O_{14}$ was assigned as gallic acid-3-*O*-hexoside-4-*O*-pentoside (**66**). It produced MS^2, MS^3 and MS^4 base peaks of *m/z* 301 $[M\text{-}H\text{-Glc}]^-$, 169 $[M\text{-}H\text{-Glc-Xyl}]^-$ and 125 $[M\text{-}H\text{-Glc-Xyl-}CO_2]^-$ respectively.

8.1.11. Characterization of *p*-hydroxyphenethyl alcohol-1-*O*-β-D-(6"-*O*-galloyl)-hexoside (M_r 468)

A peak at t_R 22.3 min with *m/z* 467 and $C_{21}H_{24}O_{12}$ was assigned as *p*-hydroxyphenethyl alcohol-1-*O*-β-D-(6"-*O*-galloyl)-hexoside (**67**). It produced MS^2, MS^3 and MS^4 base peaks of *m/z* 313, 169 and 125 respectively. The neutral loss of 298 Da was assumed to be the loss of a dihydroxyphenyethanol group attached to a hexose.

8.1.12. Characterization of gallic acid-*O*-galloyl-rhamnoside (M_r 468)

A peak at t_R 36.6 min with *m/z* 467 and $C_{20}H_{20}O_{13}$ was assigned as gallic acid-*O*-galloyl-rhamnoside (**68**). It produced MS^2, MS^3 and MS^4 base peaks of *m/z* 423, 313 and 169 respectively. The neutral loss of 298 Da was attributed to the loss of galloyl-rhamnose.

8.1.13. Characterization of gallic acid-*O*-rutinoside (M_r 478)

A peak at t_R 6.6 min with *m/z* 477 and $C_{19}H_{26}O_{14}$ was assigned as gallic acid-*O*-rutinoside (**69**). It produced MS^2 and MS^3 base peaks of *m/z* 169 $[M-H-Glc-Rha]^-$ and 125 $[M-H-Glc-Rha-CO_2]^-$ respectively.

8.1.14. Characterization of gallic acid-*O*-coumaroyl-hexoside (M_r 478)

Three isomers of gallic acid-*O*-coumaroyl-hexoside (**70-72**) were identified at t_R 31.0, 32.6 and 35.9 min with $C_{22}H_{22}O_{12}$ and *m/z* 477. The peaks produced MS^2, MS^3 and MS^4 base peaks of *m/z* 313, 169 and 125 respectively. The neutral loss of 308 Da was attributed to the loss of a coumaroyl group attached to a hexose.

8.1.15. Characterization of querglanin (M_r 480)

A peak at t_R 31.9 min with *m/z* 479 and $C_{23}H_{28}O_{11}$ was tentatively assigned as querglanin (**73**). It produced MS^2 and MS^3 base peaks of *m/z* 169 and 125 respectively.

8.1.16. Characterization of galloyl-*O*-vanilloyl-*O*-hexoside (M_r 482)

Two isomers of galloyl-*O*-vanilloyl-*O*-hexoside were identified at t_R 27.1 and 30.1 min with *m/z* 481 and $C_{21}H_{22}O_{13}$ (**74-75**). The compound **74** produced MS^2, MS^3 and MS^4 base peaks of *m/z* 313, 169 and 125 respectively. The neutral loss of 312 Da was attributed to vanilloyl group

attached to a hexose. The compound **75** produced MS^2, MS^3 and MS^4 base peaks of *m/z* 437, 313 and 169 respectively and a secondary MS^4 base peak of *m/z* 125.

8.1.17. Characterization of gallic acid-3-*O*-(6'-*O*-galloyl)-β-D-hexoside (M_r 484)

A peak at t_R 22.5 min with *m/z* 483 and $C_{20}H_{20}O_{14}$ was assigned as gallic acid-3-*O*-(6'-*O*-galloyl)-β-D-hexoside (**76**). It produced MS^2, MS^3 and MS^4 base peaks of *m/z* 439 $[M-H-CO_2]^-$, 287 $[M-H-CO_2\text{-galloyl}]^-$ and 125 $[M-H-CO_2\text{-galloyl-}CO_2]^-$ respectively.

8.1.18. Characterization of gallic acid-*O*-dihexoside (M_r 494)

Three isomers of gallic acid-*O*-dihexoside (**77-79**) were identified at t_R 3.2, 5.2 and 6.7 min with $C_{19}H_{26}O_{15}$ and *m/z* 493. The compounds **77** and **78** produced MS^2, MS^3 and MS^4 base peaks of *m/z* 331 $[M-H-Glc]^-$, 169 $[M-H-Glc-Glc]^-$ and 125 $[M-H-Glc-Glc-CO_2]^-$ respectively. The presence of an intermediate fragment of *m/z* 331 suggested the absence of interglycosidic linkage. Compound **79** on the other hand produced MS^2 and MS^3 base peaks of *m/z* 169 $[M-H-Glc-Glc]^-$ and 125 $[M-H-Glc-Glc-CO_2]^-$ respectively and the absence of an intermediate fragment suggested the presence of interglycosidic linkage.

8.1.19. Characterization of gallic acid-*O*-feruloyl-hexoside (M_r 508)

A peak at t_R 36.2 min with *m/z* 507 and $C_{23}H_{24}O_{13}$ was speculated to be gallic acid-*O*-feruloyl-hexoside (**80**). It produced MS^2, MS^3 and MS^4 base peaks of *m/z* 331 $[M-H-\text{feruloyl}]^-$, 169 $[M-H-\text{feruloyl-Glc}]^-$ and 125 $[M-H-\text{feruloyl-Glc-}CO_2]^-$ respectively.

8.1.20. Characterization of Hyemaloside B or Guavinoside A (M_r 544)

A peak at t_R 30.9 min with *m/z* 543 and $C_{26}H_{24}O_{13}$ was tentatively assigned as an isomer of Hyemaloside B or Guavinoside A (**81**). It produced MS^2 and MS^3 base peaks of 169 and 125 respectively.

8.1.21. Characterization of galloylalbiflorin (M_r 632)

A peak at t_R 42.8 min with *m/z* 631 and $C_{30}H_{32}O_{15}$ was tentatively assigned as galloylalbiflorin (**82**). It produced MS^2, MS^3 and MS^4 base peaks of *m/z* 479, 169 and 125 respectively.

8.2. Protocatechuic acid derivatives

The protocatechuic acid derivatives were identified based on their characteristic fragmentation peaks. The protocatechuic acid aglycon can be identified in MS^n by comparison with an authentic standard. In negative mode, protocatechuic acid at *m/z* 153 (after a loss of hydrogen) fragments to give *m/z* 109 (after a loss of hydrogen and carbon dioxide).

8.2.1. Characterization of protocatechuic acid-*O*-pentoside (M_r 286)

A peak at t_R 15.1 min with *m/z* 285 and $C_{12}H_{14}O_8$ was assigned as protocatechuic acid-*O*-pentoside (**83**). It produced MS^2 and MS^3 base peaks of *m/z* 153 $[M-H-Xyl]^-$ and 109 $[M-H-Xyl-CO_2]^-$ respectively.

8.2.2. Characterization of protocatechuic acid-*O*-hexoside (M_r 316)

Two isomers of protocatechuic acid-*O*-hexoside (**84**-**85**) were identified at t_R 5.9 and 10.5 min with $C_{13}H_{16}O_9$ and *m/z* 315. Both the peaks produced a base peak of *m/z* 153 $[M-H-Glc]^-$, which fragmented to *m/z* 109 $[M-H-Glc-CO_2]^-$. The EIC of *m/z* 315 in *Rhododendron maddenii* in negative mode is shown in Figure 8.4, along with the MS^n spectra of compound **84** in Figure 8.5. The proposed fragmentation of compounds **84**-**85** is shown in Figure 8.6.

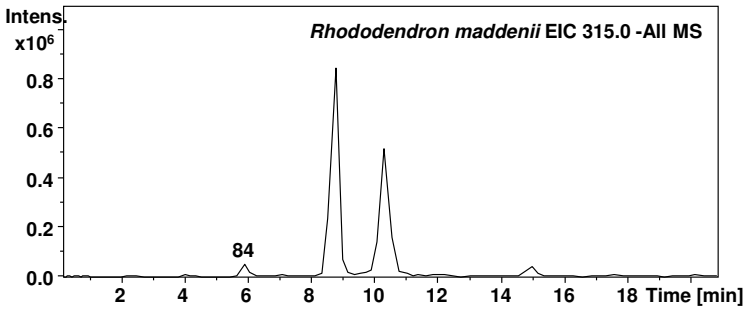

Figure 8.4: EIC of *m/z* 315 in *Rhododendron maddenii* in negative mode

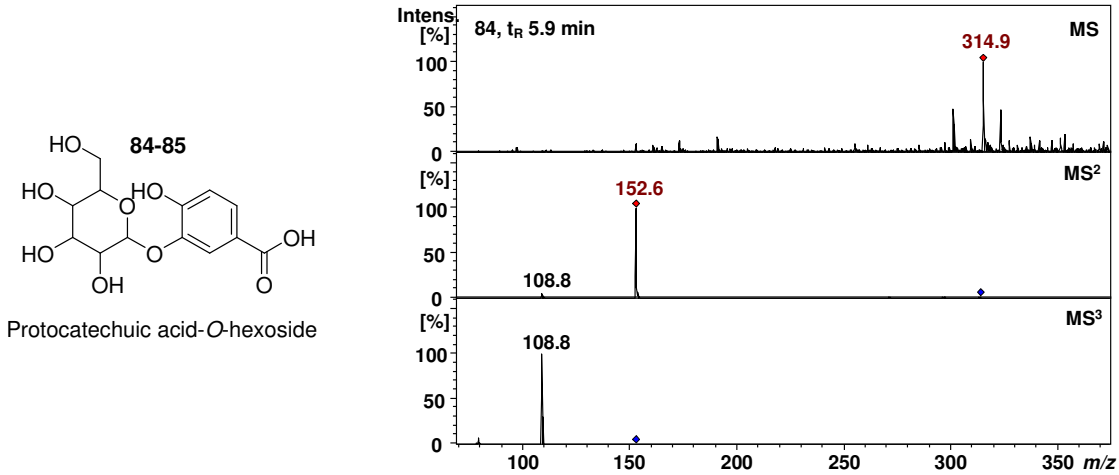

Figure 8.5: MS^n spectra of protocatechuic acid-*O*-hexoside

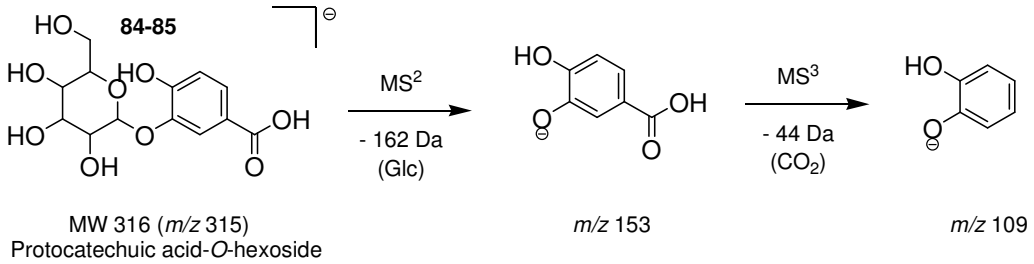

Figure 8.6: Proposed fragmentation of protocatechuic acid-*O*-hexoside

8.2.3. Characterization of protocatechuic acid-*O*-benzoyl-hexoside (M_r 420)

A peak at t_R 51.8 min with *m/z* 419 and $C_{20}H_{20}O_{10}$ was tentatively assigned as protocatechuic acid-*O*-benzoyl-hexoside (**86**). It produced MS^2 and MS^3 base peaks of *m/z* 153 [M-H-benzoyl-Glc]$^-$ and 109 [M-H-benzoyl-Glc-CO_2]$^-$ respectively. The absence of an intermediate fragment suggested the presence of linkage between the benzoyl group and hexose.

8.2.4. Characterization of protocatechuic acid-*O*-feruloyl-hexoside (M_r 492)

A peak at t_R 51.1 min with *m/z* 491 and $C_{23}H_{24}O_{12}$ was speculated to be protocatechuic acid-*O*-feruloyl-hexoside (**87**). It produced MS^2, MS^3 and MS^4 base peaks of *m/z* 315 [M-H-feruloyl]$^-$, 153 [M-H-feruloyl-Glc]$^-$ and 109 [M-H-feruloyl-Glc-CO_2]$^-$ respectively. The presence of an intermediate fragment of *m/z* 315 suggested the absence of linkage between the feruloyl group and hexose.

8.3. Salicylic acid derivatives

The salicylic acid derivatives were identified based on their characteristic fragmentation peaks. The salicylic acid aglycon can be identified in MS^n by comparison with an authentic standard. In negative mode, salicylic acid at *m/z* 137 (after a loss of hydrogen) fragments to give *m/z* 93 (after a loss of hydrogen and carbon dioxide).

8.3.1. Characterization of salicylic acid-*O*-hexoside (M_r 300)

Two isomers of salicylic acid-*O*-hexoside (**88**-**89**) were identified at t_R 6.3 and 13.0 min with $C_{13}H_{16}O_8$ and *m/z* 299. The compounds produced a base peak of *m/z* 137 $[M-H-Glc]^-$, which fragmented to *m/z* 93 $[M-H-Glc-CO_2]^-$. The EIC of *m/z* 299 in *Rhododendron macabeanum* in negative mode is shown in Figure 8.7, along with the MS^n spectra of compound **88** in Figure 8.8. The proposed fragmentation of compounds **88**-**89** is shown in Figure 8.9.

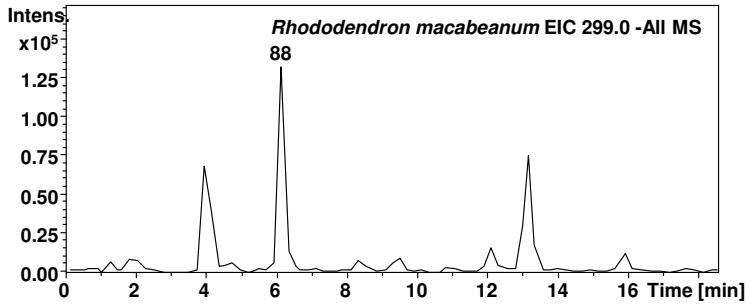

Figure 8.7: EIC of *m/z* 299 in *Rhododendron macabeanum* in negative mode

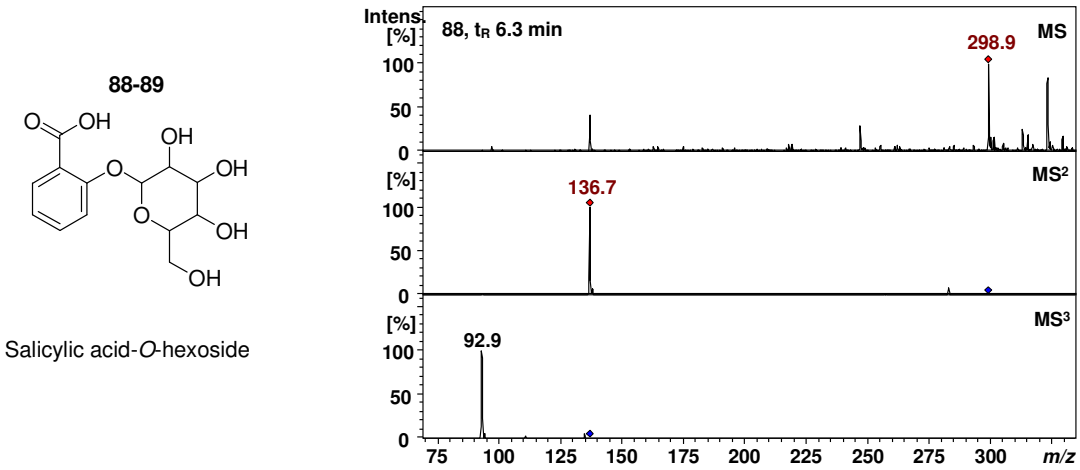

Figure 8.8: MS^n spectra of salicylic acid-*O*-hexoside

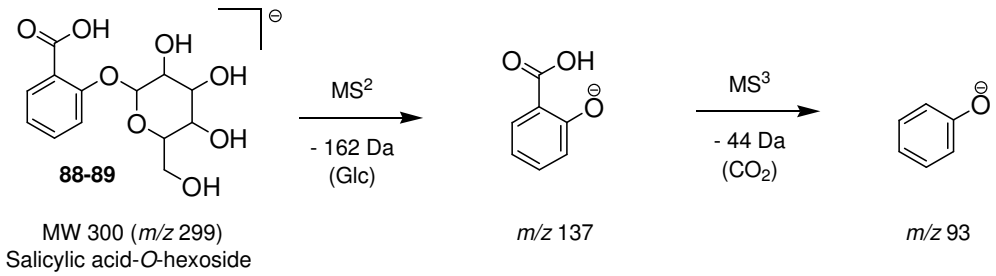

Figure 8.9: Proposed fragmentation of salicylic acid-*O*-hexoside

8.3.2. Characterization of salicylic acid-*O*-glucosyl ester (M_r 300)

A peak at t_R 8.5 min with *m/z* 299 and $C_{13}H_{16}O_8$ was assigned as salicylic acid-*O*-glucosyl ester (**90**). The peak produced MS^2 and MS^3 base peaks of *m/z* 137 $[M-H-Glc]^-$ and 93 $[M-H-Glc-CO_2]^-$ respectively. In MS^2 fragmentation, it also produced secondary peaks of *m/z* 239 $[M-H-60\ Da]^-$, 209 $[M-H-90\ Da]^-$ and 179 $[M-H-120\ Da]^-$.

8.3.3. Characterization of salicyloylsalicin (M_r 406)

A peak at t_R 36.6 min with *m/z* 405 and $C_{20}H_{22}O_9$ was assigned as salicyloylsalicin (**91**). It produced MS^2, MS^3 and MS^4 base peaks of *m/z* 281, 137 and 93 respectively. The neutral loss of 268 Da was attributed to the loss of a hydroxybenzyl alcohol group attached to a hexose.

8.3.4. Characterization of salicylic acid-*O*-coumaroyl-hexoside (M_r 446)

Two peaks at t_R 42.4 and 46.2 min with *m/z* 445 and $C_{22}H_{22}O_{10}$ were tentatively assigned as salicylic acid-*O*-coumaroyl-hexoside (**92-93**). The compounds produced MS^2, MS^3 and MS^4 base peaks of *m/z* 281, 137 and 93 respectively. The neutral loss of 308 Da was attributed to the loss of a coumaroyl group attached to a hexose.

8.3.5. Characterization of salicylic acid-*O*-dihexoside (M_r 462)

A peak at t_R 7.0 min with *m/z* 461 and $C_{19}H_{26}O_{13}$ was assigned as salicylic acid-*O*-dihexoside (**94**). It produced MS^2 and MS^3 base peaks of *m/z* 137 $[M-H-Glc-Glc]^-$ and 93 $[M-H-Glc-Glc-CO_2]^-$ respectively and the absence of an intermediate fragment suggested the presence of interglycosidic linkage.

8.4. Vanillic acid derivatives

The vanillic acid derivatives were identified based on their characteristic fragmentation peaks. The vanillic acid aglycon can be identified in MS^n by comparison with an authentic standard. In negative mode, vanillic acid at *m/z* 167 (after a loss of hydrogen) fragments to give *m/z* 152 (hydrogen and methyl group), 149 (after a loss of hydrogen and water) and 123 (after a loss of hydrogen and carbon dioxide).

8.4.1. Characterization of vanillic acid-*O*-hexoside (M_r 330)

Four isomers of vanillic acid-*O*-hexoside (**95-98**) were identified at t_R 7.7, 10.2, 11.7 and 13.9 min with $C_{14}H_{18}O_9$ and *m/z* 329. The compounds produced an MS^2 base peak of *m/z* 167 $[M-H-Glc]^-$. Compounds **95** and **98** produced an MS^3 base peak of *m/z* 123 $[M-H-Glc-CO_2]^-$, while compounds **96** and **97** produced an MS^3 base peak of *m/z* 152 $[M-H-Glc-CH_3]^-$ and 149 $[M-H-Glc-H_2O]^-$ respectively. The EIC of *m/z* 329 in *Rhododendron minus* in negative mode is shown in Figure 8.10, along with the MS^n spectra of compound **98** in Figure 8.11. The proposed fragmentation of compounds **95-98** is shown in Figure 8.12.

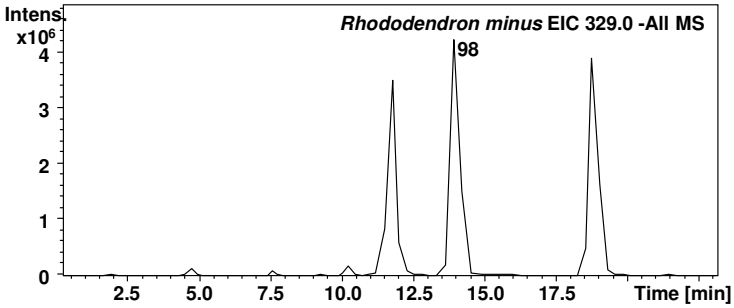

Figure 8.10: EIC of *m/z* 329 in *Rhododendron minus* in negative mode

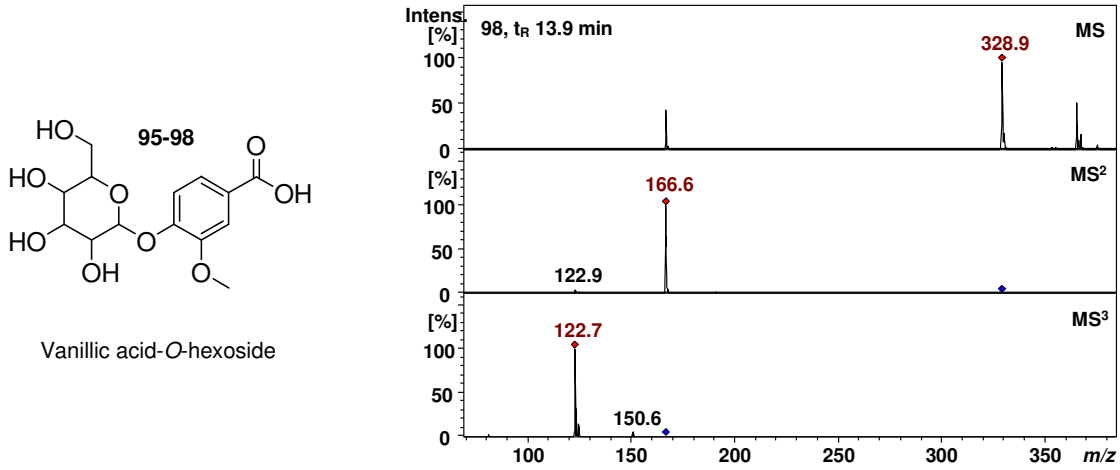

Figure 8.11: MS^n spectra of vanillic acid-*O*-hexoside

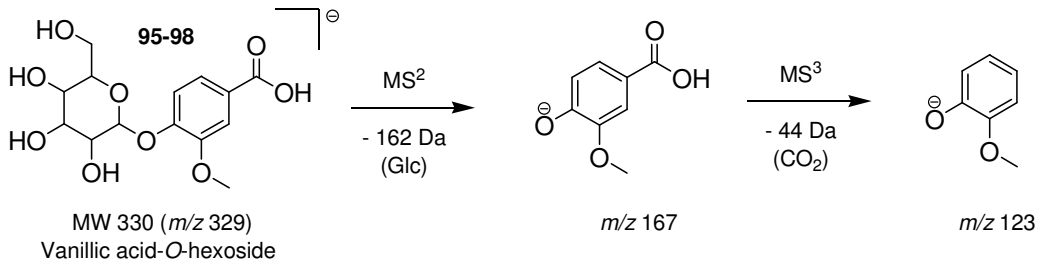

Figure 8.12: Proposed fragmentation of vanillic acid-*O*-hexoside

8.4.2. Characterization of Amburoside B (M_r 436)

A peak at t_R 36.3 min with *m/z* 435 and $C_{21}H_{24}O_{10}$ was assigned as Amburoside B (**99**). It produced MS^2, MS^3 and MS^4 base peaks of *m/z* 273, 167 and 123 respectively. The neutral loss of 268 Da was attributed to the loss of a hydroxybenzyl alcohol group attached to a hexose.

8.4.3. Characterization of vanillic acid-*O*-hydroxybenzoyl-hexoside (M_r 450)

Two isomers of vanillic acid-*O*-hydroxybenzoyl-hexoside (**100**-**101**) were identified at t_R 17.5 and 40.8 min with $C_{21}H_{22}O_{11}$ and *m/z* 449. Compound **100** produced MS^2, MS^3 and MS^4 base peaks of *m/z* 329, 301 and 167 respectively and the presence of an intermediate fragment at *m/z* 329 $[M\text{-}H\text{-hydroxybenzoyl}]^-$ suggested the absence of linkage between the hydroxybenzoyl group and hexose. Compound **101** produced MS^2 and MS^3 base peaks of *m/z* 167 and 123 respectively and the absence of an intermediate fragment suggested the presence of linkage between the hydroxybenzoyl group and hexose.

8.4.4. Characterization of vanillic acid-*O*-hexoside-*O*-pentoside (M_r 462)

Two isomers of vanillic acid-*O*-hexoside-*O*-pentoside or 6-*O*-[5-*O*-(4-hydroxy, 3-methoxybenzoyl)]-β-apiofuranosyl]-α/β-glucopyranoside (**102**-**103**) were identified at t_R 14.9 and 19.1 min with $C_{19}H_{26}O_{13}$ and *m/z* 461. Both the isomers produced MS^2 and MS^3 base peaks of *m/z* 167 $[M-H-Glc-Xyl]^-$ and 123 $[M-H-Glc-Xyl-CO_2]^-$. The absence of an intermediate fragment suggested the presence of linkage between the hexose and pentose.

8.4.5. Characterization of vanillic acid-*O*-rutinoside (M_r 476)

Two isomers of vanillic acid-*O*-rutinoside (**104**-**105**) were identified at t_R 12.5 and 18.9 min with $C_{20}H_{28}O_{13}$ and *m/z* 475. Both the isomers produced MS^2 and MS^3 base peaks of *m/z* 167 $[M-H-Glc-Rha]^-$ and 123 $[M-H-Glc-Rha-CO_2]^-$. The absence of an intermediate fragment suggested the presence of linkage between the hexose and rhamnose.

8.4.6. Characterization of vanillic acid-*O*-coumaroyl-hexoside (M_r 476)

A peak at t_R 47.8 min with *m/z* 475 and $C_{23}H_{24}O_{11}$ was assigned as vanillic acid-*O*-coumaroyl-hexoside (**106**). It produced MS^2, MS^3 and MS^4 base peaks of *m/z* 311, 167 and 123 respectively. The neutral loss of 308 Da was assumed to be the loss of a coumaroyl group attached to a hexose.

8.4.7. Characterization of vanillic acid-*O*-dihexoside (M_r 492)

Three isomers of vanillic acid-*O*-dihexoside (**107**-**109**) were identified at t_R 4.6, 5.3 and 8.5 min with $C_{20}H_{28}O_{14}$ and *m/z* 491. The compounds **107** and **108** produced MS^2, MS^3 and MS^4 base peaks of *m/z* 329 $[M-H-Glc]^-$, 167 $[M-H-Glc-Glc]^-$ and 123 $[M-H-Glc-Glc-CO_2]^-$ respectively. The presence of an intermediate fragment of *m/z* 329 suggested the absence of interglycosidic linkage. Compound **109** on the other hand produced MS^2 and MS^3 base peaks of *m/z* 167 $[M-H-Glc-Glc]^-$ and 123 $[M-H-Glc-Glc-CO_2]^-$ respectively and the absence of an intermediate fragment suggested the presence of interglycosidic linkage.

8.4.8. Characterization of Litseaefoloside A (M_r 494)

A peak at t_R 47.0 min with *m/z* 493 and $C_{23}H_{26}O_{12}$ was assigned as Litseaefoloside A (**110**). It produced an MS^2 base peak of *m/z* 167, which fragmented into 152 and 123 in MS^3.

8.5. Methyl gallate derivatives

The methyl gallate derivatives were identified based on their characteristic fragmentation peaks. The methyl gallate aglycon can be identified in MS^n by comparison with an authentic standard. In negative mode, methyl gallate at *m/z* 183 (after a loss of hydrogen) fragments to give *m/z* 168 (after a loss of hydrogen and a methyl group) and 124 (after a loss of hydrogen, a methyl group and carbon dioxide).

8.5.1. Characterization of methyl gallate-*O*-hexoside (M_r 346)

Three isomers of methyl gallate-*O*-hexoside (**111**-**113**) were identified at t_R 7.4, 8.5 and 11.8 min with $C_{14}H_{18}O_{10}$ and *m/z* 345. It produced MS^2, MS^3 and MS^4 base peaks of *m/z* 183 $[M\text{-}H\text{-}Glc]^-$, 168 $[M\text{-}H\text{-}Glc\text{-}CH_3]^-$ and 124 $[M\text{-}H\text{-}Glc\text{-}CH_3\text{-}CO_2]^-$ respectively. The EIC of *m/z* 337 in *Rhododendron moulmainense* in negative mode is shown in Figure 8.13, along with the MS^n spectra of compound **111** in Figure 8.14.

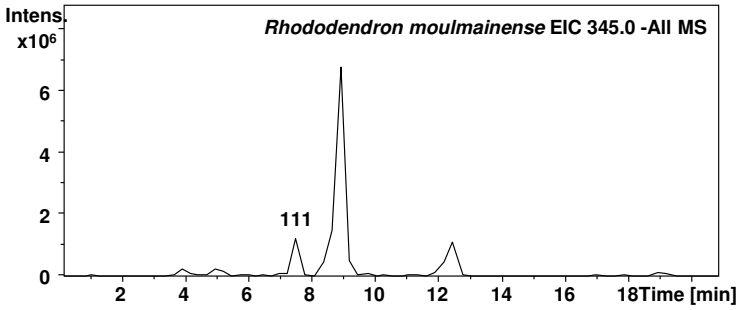

Figure 8.13: EIC of *m/z* 345 in *Rhododendron moulmainense* in negative mode

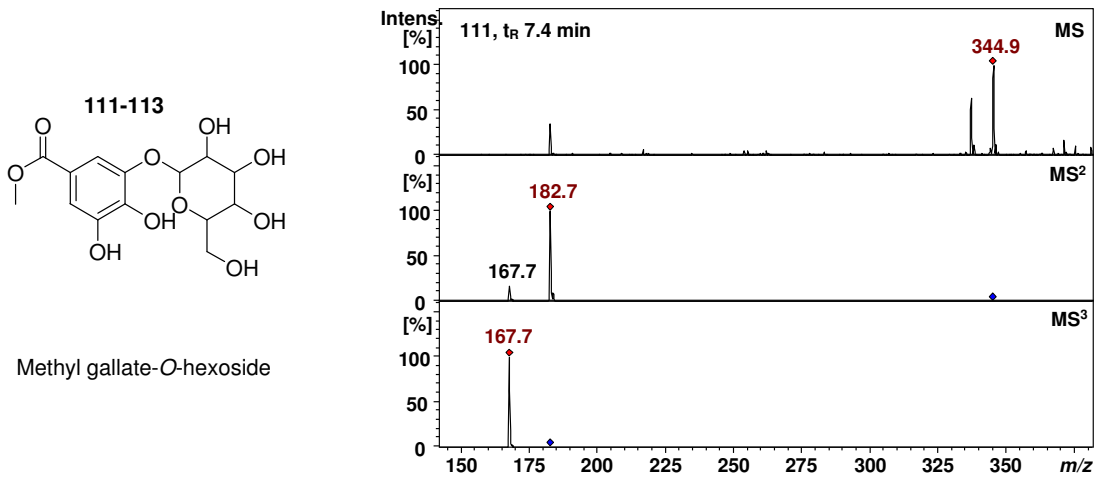

Figure 8.14: MS^n spectra of methyl-gallate-*O*-hexoside

8.5.2. Characterization of methyl gallate-*O*-coumaroyl-hexoside (M_r 492)

A peak at t_R 42.1 min with *m/z* 491 and $C_{23}H_{24}O_{12}$ was tentatively assigned as methyl gallate-*O*-coumaroyl-hexoside (**114**). It produced MS^2, MS^3 and MS^4 base peaks of *m/z* 327, 183 and 168 respectively. The neutral loss of 308 Da was attributed to the loss of a coumaroyl group attached to a hexose.

8.5.3. Characterization of methyl gallate-*O*-dihexoside (M_r 508)

A peak at t_R 8.0 min with *m/z* 507 and $C_{20}H_{28}O_{15}$ was assigned as methyl gallate-*O*-dihexoside (**115**). It produced MS^2, MS^3 and MS^4 base peaks of *m/z* 345 $[M-H-Glc]^-$, 183 $[M-H-Glc-Glc]^-$ and 168 $[M-H-Glc-Glc-CH_3]^-$ respectively. The presence of an intermediate fragment of *m/z* 345 suggested the absence of interglycosidic linkage.

9. Flavan-3-ols

The fragmentation of flavan-3-ols involves three fragmentation pathways, namely Retro Diels Alder (RDA) reaction, Heterocyclic Ring Fission (HRF) and Quinone Methide (QM) fission. RDA reaction as the name suggests is the opposite reaction of a Diels Alder reaction, which is the reaction between a conjugated diene and an alkene (commonly referred as dienophile) that produces a cyclohexene product. In RDA, the cyclohexene ring of flavan-3-ols separates into a conjugated diene and alkene. HRF on the other hand is the breakage of the heterocyclic ring in flavan-3-ols. In QM fission, the breakage of flavan-3-ols forms a quinone methide, which is a conjugated fragment consisting of cyclohexadiene with a carbonyl group and an exocyclic methylene group.[97] In addition, a characteristic loss of 44 Da (C_2H_4O) is observed for flavan-3-ols consisting of (epi)catechin units.

9.1. (Epi)catechin derivatives

The flavan-3-ols identified in *Rhododendron* species were the derivatives of (epi)catechin units. With the available MS data, it was not possible to distinguish between catechin and (epi)catechin units in the fragmentation of their derivatives as they produced the same fragments.

9.1.1. Characterization of catechin and epicatechin (M_r 290)

Two peaks at t_R 16.0 and 23.0 min with *m/z* 289 and $C_{15}H_{14}O_6$ were identified as catechin (**116**) and epicatechin (**117**) respectively. They were assigned by comparing the retention time to standards. The peaks were compared with the retention time, fragmentation and UV data of commercially available standards. Both peaks produced an MS^2 base peak of *m/z* 245 and secondary peaks of *m/z* 205 and 179. This fragmentation occurred due to RDA and QM. The *m/z* 245 peak further fragmented in MS^3 to give a base peak of 203 and secondary peaks of *m/z* 227, 187 and 161. The EIC of *m/z* 289 in *Rhododendron moulmainense* in negative mode is shown in Figure 9.1, along with the MS^n spectra of compounds **116** and **117** in Figure 9.2 and Figure 9.3 respectively. The proposed fragmentation of compounds **116-117** is shown in Figure 9.4.

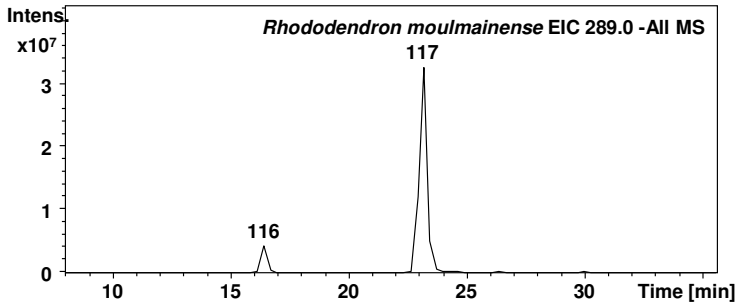

Figure 9.1: EIC of *m/z* 289 in *Rhododendron moulmainense* in negative mode

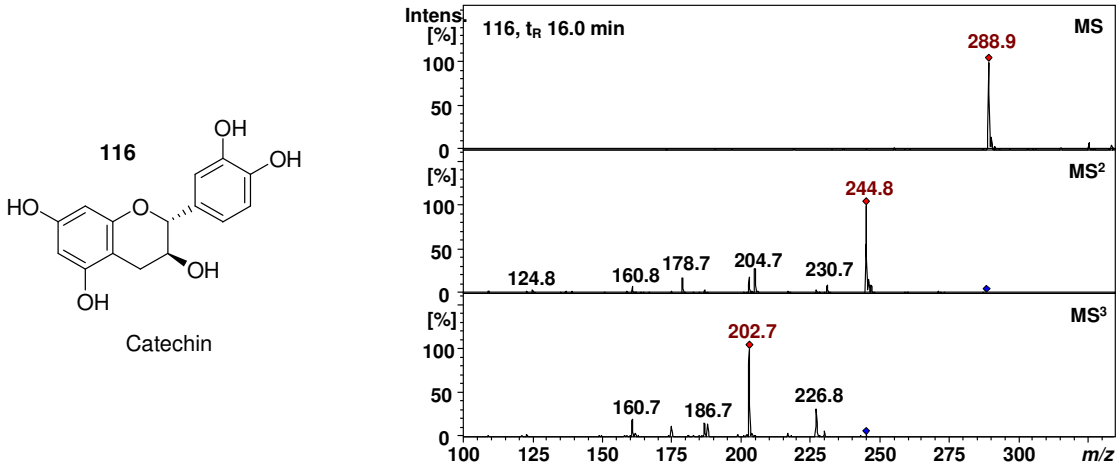

Figure 9.2: MS^n spectra of catechin

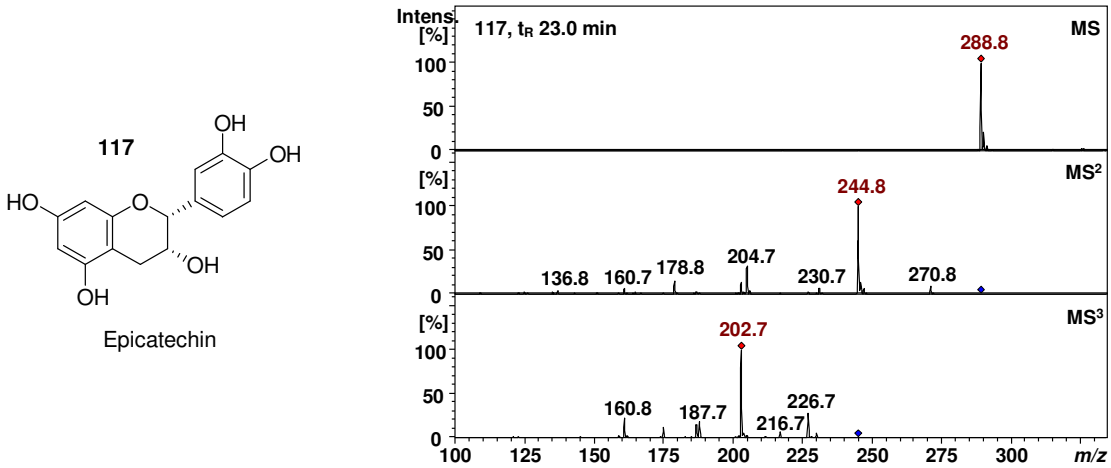

Figure 9.3: MS^n spectra of epicatechin

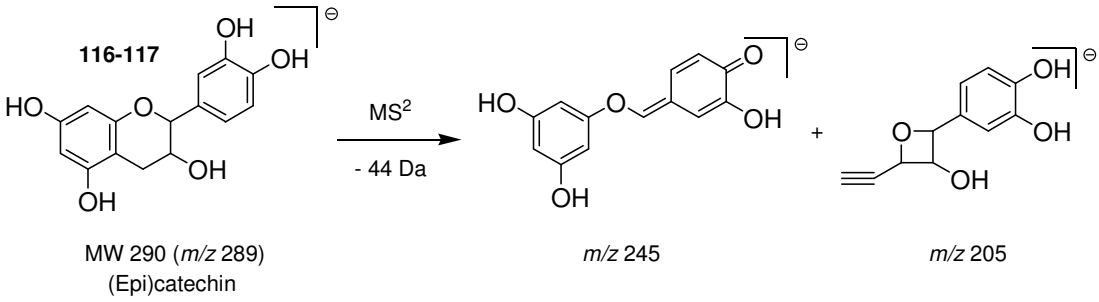

Figure 9.4: Proposed fragmentation of (epi)catechin

9.1.2. Characterization of gallocatechin and epigallocatechin (M_r 306)

Two peaks at t_R 8.5 and 15.4 min with *m/z* 305 and $C_{15}H_{14}O_7$ were identified as gallocatechin (**118**) and epigallocatechin (**119**) respectively. The peaks were compared with the retention time, fragmentation and UV data of authentic standards. Both peaks produced an MS^2 base peak of *m/z* 179 and secondary peaks of *m/z* 221 and 261. This fragmentation occurred due to RDA and QM. The *m/z* 179 peak further fragmented in MS^3 to give a base peak of 164 and secondary peaks of *m/z* 151 and 135. The EIC of *m/z* 305 in *Rhododendron minus* in negative mode is shown in Figure 9.5, along with the MS^n spectra of compounds **118** and **119** in Figure 9.6 and Figure 9.7 respectively.

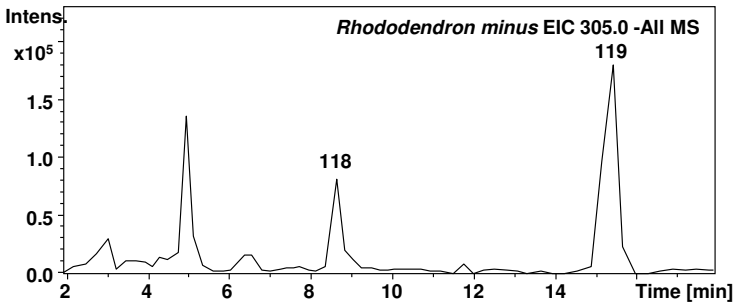

Figure 9.5: EIC of *m/z* 305 in *Rhododendron minus* in negative mode

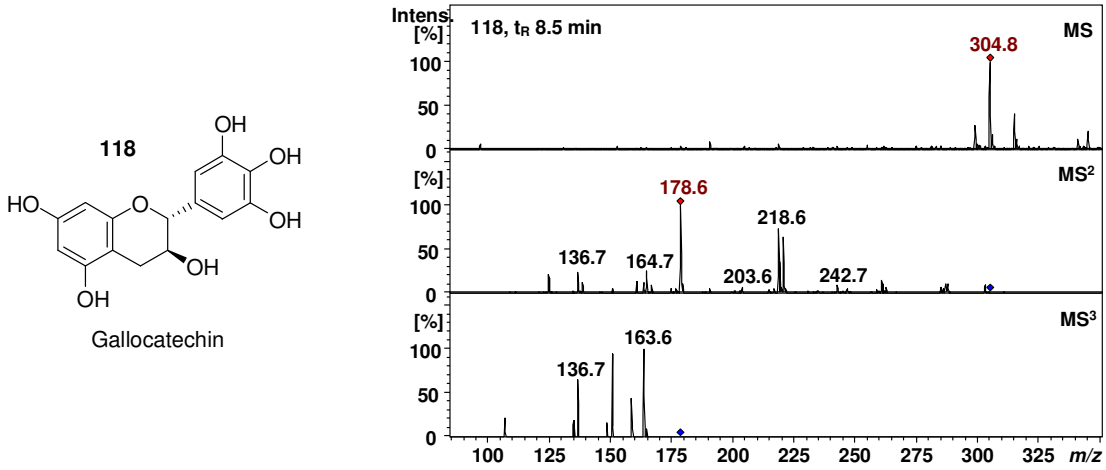

Figure 9.6: MS^n spectra of gallocatechin

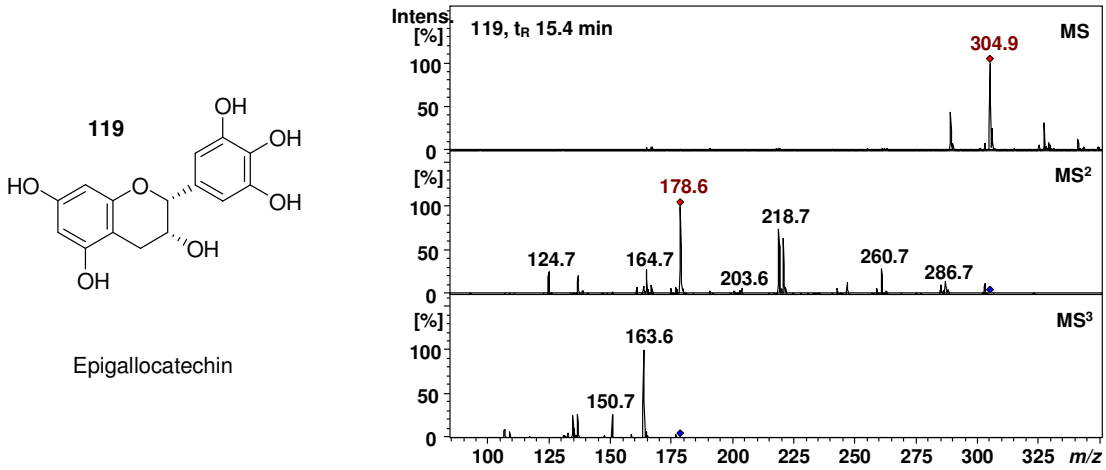

Figure 9.7: MS^n spectra of epigallocatechin

9.1.3. Characterization of (epi)catechin-*O*-hydroxybenzoate (M_r 410)

A peak at t_R 35.8 min with *m/z* 409 and $C_{22}H_{18}O_8$ was assigned as (epi)catechin-*O*-hydroxybenzoate (**120**). The peak produced an MS^2 base peak of *m/z* 289, which fragmented into *m/z* 245 and 205 in MS^3 after RDA and QM.

9.1.4. Characterization of (epi)catechin-*O*-rhamnoside (M_r 436)

A peak at t_R 22.5 min with *m/z* 435 and $C_{21}H_{24}O_{10}$ was assigned as (epi)catechin-*O*-rhamnoside (**121**). The peak produced an MS^2 base peak of *m/z* 289, which fragmented into *m/z* 245 and 205 in MS^3 after RDA and QM.

9.1.5. Characterization of Malaferin B (Mr 436)

A peak at t_R 40.1 min with *m/z* 435 and $C_{24}H_{20}O_8$ was assigned as Malaferin B, which is an isomer of (epi)catechin-*O*-coumarate (**122**). The peak produced an MS^2 base peak of *m/z* 289, which fragmented into *m/z* 245 and 205 in MS^3 after RDA and QM.

9.1.6. Characterization of (epi)catechin gallate (M_r 442)

Four isomers of (epi)catechin gallate (**123**-**126**) were identified at t_R 28.1, 29.6, 31.8 and 36.8 min with $C_{22}H_{18}O_{10}$ and *m/z* 441. The peaks produced an MS^2 base peak of *m/z* 289, which fragmented into *m/z* 245 and 205 in MS^3 after RDA and QM.

9.1.7. Characterization of (epi)catechin-*O*-hexoside (M_r 452)

A peak at t_R 10.5 min with *m/z* 451 and $C_{21}H_{24}O_{11}$ was assigned as (epi)catechin-*O*-hexoside (**127**). The peak produced an MS^2 base peak of *m/z* 289, which fragmented into *m/z* 245 and 205 in MS^3 after RDA and QM.

9.1.8. Characterization of (epi)catechin-*O*-methyl-gallate (M_r 456)

A peak at t_R 34.4 min with *m/z* 455 and $C_{23}H_{20}O_{10}$ was tentatively assigned as (epi)catechin-*O*-methyl-gallate (**128**). The peak produced an MS^2 base peak of *m/z* 289, which fragmented into *m/z* 245 and 205 in MS^3 after RDA and QM.

9.1.9. Characterization of (epi)gallocatechin gallate (M_r 458)

Three peaks were identified with *m/z* 457 and $C_{22}H_{18}O_{11}$. One peak at t_R 22.7 min (**130**) was identified as epigallocatechin gallate. It was confirmed by comparing it with the fragmentation and retention time of an authentic standard. Two peaks at t_R 19.8 and 26.6 min (**129** and **131**) were assigned as isomers of (epi)gallocatechin gallate. Compound **129** produced an MS^2 base peak of *m/z* 305 $[M\text{-}H\text{-galloyl}]^-$, which further fragmented into *m/z* 179 due to RDA. Compound **130** and **131** produced MS^2 and MS^3 base peaks of *m/z* 169 and 125, which are similar to the fragments of gallic acid. They also produced a secondary fragment of *m/z* 305 in MS^2.

9.1.10. Characterization of Malaferin C (M_r 466)

A peak at t_R 41.2 min with *m/z* 465 and $C_{25}H_{22}O_9$ was assigned as malaferin C (**132**). The peak produced an MS^2 base peak of *m/z* 289, which fragmented into *m/z* 245 and 205 in MS^3 after RDA and QM.

9.1.11. Characterization of (epi)catechin-*O*-dimethyl-gallate (M_r 470)

A peak at t_R 38.9 min with *m/z* 469 and $C_{24}H_{22}O_{10}$ was assigned as (epi)catechin-*O*-dimethyl-gallate (**133**). The peak produced an MS^2 base peak of *m/z* 289, which fragmented into *m/z* 245 and 205 in MS^3 after RDA and QM.

9.1.12. Characterization of (epi)catechin-*O*-trimethoxybenzoate (M_r 484)

Two peaks at t_R 29.5 and 32.9 min with *m/z* 483 were tentatively assigned as (epi)catechin-*O*-trimethoxybenzoate (**134-135**). Both peaks produced an MS^2 base peak of *m/z* 289, which fragmented into *m/z* 245 and 205 in MS^3 after RDA and QM.

Proanthocyanidins

The oligomerization, dimerization and polymerization of flavan-3-ol units such as catechin, epicatechin, gallocatechin and epigallocatechin results in the formation of condensed tannins, which are known as proanthocyanidins. Dimerization proceeds via oxidation of the A-ring followed by the nucleophilic attack of a catechin onto the electrophilic quinone methide. Several regioisomers and stereoisomers can be formed. The A-type proanthocyanidins are connected by C2-*O*-C7 or C2-*O*-C5 bonds and the B-type proanthocyanidins are connected by C4-C8 or C4-C6 bonds.

9.1.13. Characterization of (epi)catechin-(4,8/2,6)-(epi)catechin [A-type procyanidin dimer] (M_r 576)

Nine isomers of (epi)catechin-(4,8/2,6)-(epi)catechin or A-type dimer of (epi)catechin were identified at t_R 5.5, 8.7, 10.1, 12.0, 14.0, 18.1, 27.2, 32.4 and 34.8 min with *m/z* 575 and $C_{30}H_{24}O_{12}$. Compounds **136-140**, **143** and **144** produced an MS^2 base peak of *m/z* 423 and secondary MS^2 peaks of *m/z* 449 and 407. Compound **141** produced an MS^2 base peak of *m/z* 407 and secondary MS^2 peaks of *m/z* 449 and 423. Compound **142** produced an MS^2 base peak of *m/z*

449 and secondary MS^2 peaks of *m/z* 423 and 407. The fragment *m/z* 449 was formed by HRF while fragments *m/z* 423 and 407 were formed by RDA.

9.1.14. Characterization of (epi)catechin-(epi)catechin [B-type procyanidin dimer] (M_r 578)

Six isomers of (epi)catechin-(epi)catechin (**145-150**) or (epi)catechin dimer or commonly known as procyanidin B were identified at t_R 13.4, 14.3, 18.6, 20.3, 23.1 and 32.8 min with *m/z* 577 and $C_{30}H_{26}O_{12}$. Although 16 dimers of (epi)catechin are theoretically viable, only 8 are naturally occurring as only 3-4 trans stereochemistry is found in nature.[6] Compounds **145** and **147** produced an MS^2 base peak of *m/z* 407 and secondary MS^2 peaks of *m/z* 451, 425 and 289. The fragment *m/z* 407 further fragmented into *m/z* 285 in MS^3. Compound **146** produced an MS^2 base peak of *m/z* 425 and secondary MS^2 peaks of *m/z* 451, 407 and 289. The fragment *m/z* 407 further fragmented into *m/z* 285 in MS^3. Compounds **148** and **150** produced MS^2, MS^3 and MS^4 base peaks of 425, 407, and 285 respectively. They also produced secondary peaks of *m/z* 451, 407 and 289 in MS^2. All the isomers produced similar fragment ions. The fragment *m/z* 451 was formed by HRF, fragments *m/z* 425 and 407 were formed by RDA and fragments *m/z* 289 and 285 were formed by QM fission. Compounds **145** and **148** at t_R 13.4 and 20.3 min were assigned as procyanidin B1 and B2 respectively by comparing it with the fragmentation and retention time of a reference standard. The EIC of *m/z* 577 in *Rhododendron wasonii* in negative mode is shown in Figure 9.8, along with the MS^n spectra of compound **145** in Figure 9.9. The proposed fragmentation of compounds **145-150** is shown in Figure 9.10.

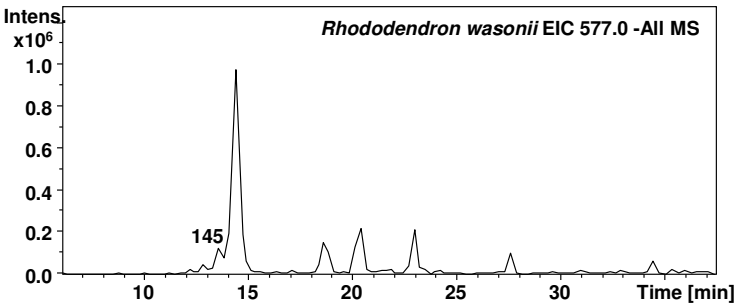

Figure 9.8: EIC of *m/z* 577 in *Rhododendron wasonii* in negative mode

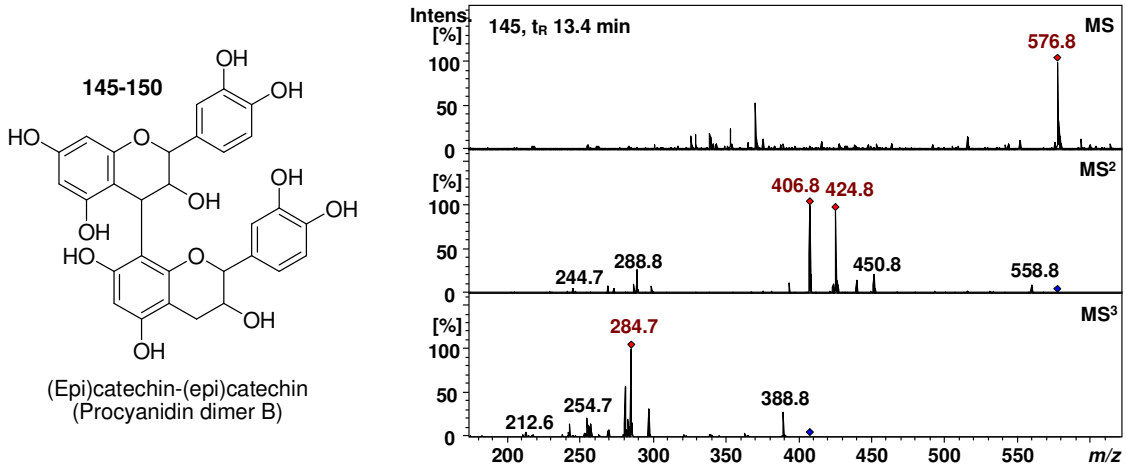

Figure 9.9: MS^n spectra of procyanidin B

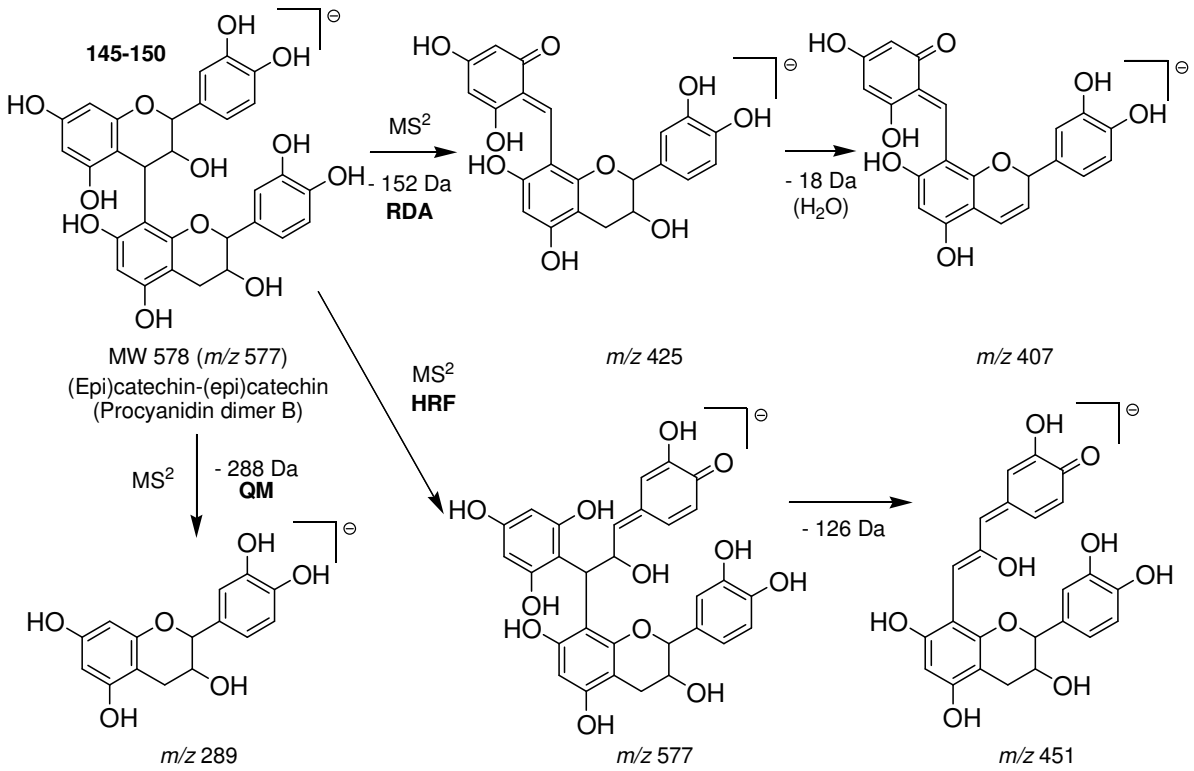

Figure 9.10: Proposed fragmentation of procyanidin B

9.1.15. Characterization of Gambiriin A or D (M_r 580)

A peak at t_R 19.2 min with *m/z* 579 and $C_{30}H_{28}O_{12}$ was assigned as Gambiriin A or D (**151**). The peak produced an MS^2 base peak of *m/z* 289, which fragmented into *m/z* 245 and 205 in MS^3 after RDA and QM.

9.1.16. Characterization of (epi)gallocatechin-(epi)catechin (M_r 594)

Eight isomers of (epi)gallocatechin-(epi)catechin (**152**-**159**) were identified at t_R 7.7, 9.7, 10.5, 12.6, 13.7, 15.2, 16.5 and 18.2 min with *m/z* 593 and $C_{30}H_{26}O_{13}$. Compounds **152**, **153**, **155**, **156** and **159** produced MS^2, MS^3 and MS^4 base peaks of 425, 407, and 285 respectively. They also produced secondary peaks of *m/z* 407 and 289 in MS^2. Compound **154** produced an MS^2 base peak of *m/z* 423 and secondary MS^2 peaks of *m/z* 467, 441 and 305. The fragment *m/z* 423 further fragmented into *m/z* 283 and 297 in MS^3. Compounds **157** and **158** produced an MS^2 base peak of *m/z* 423 and secondary MS^2 peaks of *m/z* 575, 441 and 305. The fragment *m/z* 423 further fragmented into *m/z* 297 and 283 in MS^3. The fragment m/z 575 was formed by the loss of water, *m/z* 467 was formed by HRF, fragments *m/z* 425, 423 and 407 were formed by RDA and fragments *m/z* 305, 289 and 285 were formed by QM fission. The RDA fragmentation of the top unit was compared to that of the base unit. The top unit produced a fragment ion with a larger π-π hyperconjugated system, which is more favorable than the fragment from the base unit energetically. With this argument, compounds **152**, **153**, **155**, **156** and **159** produced a secondary peak of *m/z* 289, which suggests that (epi)catechin was the base unit and (epi)gallocatechin was the top unit. Similarly, compounds **154**, **157** and **158** produced a secondary peak of *m/z* 305, which suggests that (epi)gallocatechin was the base unit and (epi)catechin was the top unit.

9.1.17. Characterization of (epi)gallocatechin-(epi)gallocatechin (M_r 610)

Four isomers of (epi)gallocatechin-(epi)gallocatechin (**160**-**164**) were identified at t_R 4.5, 6.5, 7.5, 10.2 and 13.1 min with *m/z* 609 and $C_{30}H_{26}O_{14}$. All the compound peaks produced an MS^2 base peak of *m/z* 423 and secondary peaks of *m/z* 441 and 305. The fragment *m/z* 423 produced a base peak of either *m/z* 283 or 297 in MS^3 and secondary peak of *m/z* 255. The fragments *m/z* 441 and 423 were formed by RDA and the fragment *m/z* 305 was formed by QM fission. Since all the compounds produced a secondary peak of *m/z* 305, it implied that (epi)gallocatechin was the top and base unit.

9.1.18. Characterization of (epi)catechin-*O*-dihexoside (M_r 614)

Three peaks at t_R 9.6, 11.8 and 13.2 min with *m/z* 613 and $C_{27}H_{34}O_{16}$ were assigned as (epi)catechin-*O*-dihexoside or (epi)catechin-3-*O*-hexoside-7-*O*-hexoside (**165**-**167**). It produced

MS^2, MS^3 and MS^4 base peaks of *m/z* 451 $[M-H-Glc]^-$, 289 $[M-H-Glc-Glc]^-$ and 245 respectively. The presence of an intermediate fragment of *m/z* 451 suggested the absence of interglycosidic linkage.

9.1.19. Characterization of 3-*O*-galloyl(epi)catechin-(4,8/2,6)-(epi)catechin (M_r 728)

A peak at t_R 36.6 min with *m/z* 727 and $C_{37}H_{28}O_{16}$ was assigned as 3-*O*-galloyl(epi)catechin-(4,8/2,6)-(epi)catechin (**168**). It produced an MS^2 base peak of *m/z* 575 and secondary peak of *m/z* 423. The fragment *m/z* 575 produced a base peak of *m/z* 449 in MS^3 and secondary peak of *m/z* 289. The fragment *m/z* 449 was formed by HRF, fragments *m/z* 575 and 423 were formed by RDA and fragment *m/z* 289 was formed by QM fission.

9.1.20. Characterization of 3-*O*-galloyl(epi)catechin-(4,8/2,6)-(epi)catechin and (epi)catechin-(4,8′)-3′-*O*-galloyl-(epi)catechin (M_r 730)

Three peaks at t_R 20.3, 23.6 and 27.9 min with *m/z* 729 and $C_{37}H_{30}O_{16}$ were assigned as gallates of dimeric (epi)catechin (**169**-**171**). Compounds **169** and **171** at t_R 20.3 and 27.9 min produced an MS^2 base peak of *m/z* 577 and secondary peak of *m/z* 559. The fragment *m/z* 577 produced a base peak of *m/z* 407 in MS^3 and secondary peaks of *m/z* 407, 451, 425 and 289. Compound **170** at t_R 23.6 min produced an MS^2 base peak of *m/z* 407 and secondary peaks of *m/z* 577, 559, 451, 441 and 289. The fragment *m/z* 407 produced a base peak of *m/z* 285 in MS^3. The fragment *m/z* 577 was formed by the loss of gallic acid, the fragment *m/z* 451 was formed by HRF, fragments *m/z* 559, 441 and 425 were formed by RDA and fragments *m/z* 289 and 285 were formed by QM fission. The galloyl residue is either attached to the C3 of the top unit or the base unit. If it is attached to the base unit, the loss of gallic acid is favored over the RDA fragmentation of the top unit with *m/z* 425. Since the fragment *m/z* 425 was not found in compound **170**, it was determined that the galloyl group was connected to the base unit and thus it was named (epi)catechin-(4,8′)-3′-*O*-galloyl-(epi)catechin. The fragment *m/z* 425 was found in compounds **169** and **171**, so it was determined that the galloyl group was connected to the top unit and it was named 3-*O*-galloyl(epi)catechin-(4,8)-(epi)catechin.

9.1.21. Characterization of (epi)gallocatechin-(4,8′)-3′-*O*-galloyl-(epi)catechin (M_r 746)

A peak at t_R 20.6 min with *m/z* 745 with $C_{37}H_{30}O_{17}$ was assigned as (epi)gallocatechin-(4,8′)-3′-*O*-galloyl-(epi)catechin (**172**). It produced an MS^2 base peak of *m/z* 407 and secondary peaks of *m/z* 727, 593, 441 and 289. The fragment *m/z* 407 produced a base peak of *m/z* 285 in MS^3. The fragment *m/z* 593 was formed by the loss of a galloyl group, the fragment *m/z* 451 was formed by HRF, fragment *m/z* 441 was formed by RDA and fragments *m/z* 289 and 285 were formed by QM fission. The presence of the fragment *m/z* 289 implied that the base unit is (epi)catechin and top unit is (epi)gallocatechin. The presence of fragment *m/z* 407 as the base peak implied that the galloyl group was connected to the base unit.

9.1.22. Characterization of (epi)gallocatechin-(4,8)-3′-*O*-galloyl(epi)gallocatechin (M_r 762)

Two peaks at t_R 13.7 and 25.7 min with *m/z* 761 with $C_{37}H_{30}O_{18}$ were assigned as (epi)gallocatechin-(4,8)-3′-*O*-galloyl(epi)gallocatechin (**173**-**174**). Both compounds produced an MS^2 base peak of *m/z* 423 and secondary peaks of *m/z* 609, 575 and 305. The fragment *m/z* 423 produced a base peak of *m/z* 283 in MS^3. The fragment *m/z* 609 was formed by the loss of a galloyl group, the fragment *m/z* 575 was formed by HRF, fragment *m/z* 423 was formed by RDA and fragments *m/z* 305 and 283 were formed by QM fission. The fragment *m/z* 305 implied the presence of (epi)gallocatechin-(4,8)-(epi)gallocatechin. The presence of fragment *m/z* 423 as the base peak implied that the galloyl group was connected to the base unit.

9.1.23. Characterization of A-type procyanidin trimer (M_r 864)

Four peaks at t_R 22.6, 23.2, 26.7 and 33.7 min with *m/z* 863 with $C_{45}H_{36}O_{18}$ were assigned as A-type (epi)catechin trimers (**175**-**178**). Compounds **175** and **176** produced an MS^2 base peak of *m/z* 711 and secondary peaks of *m/z* 693, 559, 541, 451, 411 and 289. The fragment *m/z* 711 produced a base peak of *m/z* 693 in MS^3 and secondary peaks of *m/z* 559, 541 and 407. The fragments *m/z* 451 and 411 were formed by HRF, fragments *m/z* 711 and 693 were formed by RDA and fragment *m/z* 289 was formed by QM fission. The presence of fragments *m/z* 451, 411 and 289 implied that the top and middle units were connected via an A-type linkage. Thus,

compounds **175** and **176** were assigned as (epi)catechin-(4,8′/2,7′)-(epi)catechin-(4′,8″)-(epi)catechin.

Compound **177** produced an MS^2 base peak of *m/z* 575 and secondary peaks of *m/z* 711, 693, and 559. The fragment *m/z* 575 produced a base peak of *m/z* 449 in MS^3 and secondary peaks of *m/z* 539 and 289. Compound **178** produced an MS^2 base peak of *m/z* 693 and secondary peaks of *m/z* 575 and 449. The fragment *m/z* 693 produced a base peak of *m/z* 657 in MS^3 and secondary peaks of *m/z* 541, 449 and 403. The fragment *m/z* 449 was formed by HRF, fragments *m/z* 711 and 693 were formed by RDA and fragments *m/z* 575 and 289 were formed by QM fission. The presence of fragment *m/z* 575 implied that the bottom and middle units were connected via an A-type linkage. Thus, compounds **177** and **178** were assigned as (epi)catechin-(4,8′)-(epi)catechin-(4′,8″/2′,7″)-(epi)catechin.

9.1.24. Characterization of B-type procyanidin trimer (M_r 866)

Seven peaks at t_R 5.6, 14.9, 15.6, 16.6, 19.2, 22.2 and 25.6 min with *m/z* 865 with $C_{45}H_{38}O_{18}$ were assigned as (epi)catechin trimers or procyanidin C (**179**-**185**). The seven compounds had similar fragmentation. Compounds **179**, **181**, **182**, **183** and **185** produced an MS^2 base peak of *m/z* 695 and secondary peaks of *m/z* 577, 575, 543, 451, 425, 407 and 287. The fragment *m/z* 695 produced a base peak of either *m/z* 243 or 543 in MS^3 and secondary peaks of *m/z* 525, 451, 405 and 289. Compound **180** produced an MS^2 base peak of *m/z* 745 and secondary peaks of *m/z* 695, 577, 575, 451 and 407. Compound **184** produced an MS^2 base peak of *m/z* 711 and secondary peaks of *m/z* 695, 577, 575, 543, 451, 425, 407 and 287. The fragment *m/z* 711 produced a base peak of *m/z* 693 in MS^3 and secondary peaks of *m/z* 559, 541, 407 and 285. The fragment *m/z* 695 was formed by RDA and fragments *m/z* 577 and 575 were formed by QM fission. The EIC of *m/z* 865 in *Rhododendron neriiflorum* in negative mode is shown in Figure 9.11, along with the MS^n spectra of compound **180** in Figure 9.12.

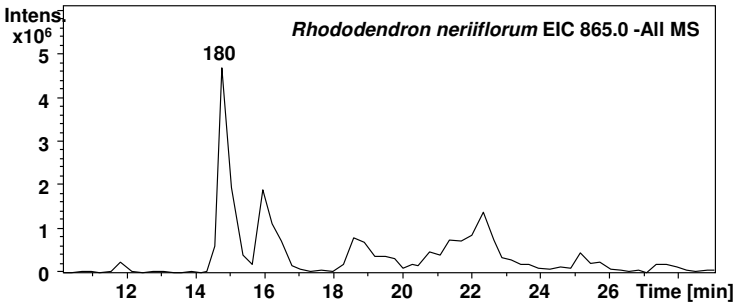

Figure 9.11: EIC of *m/z* 865 in *Rhododendron neriiflorum* in negative mode

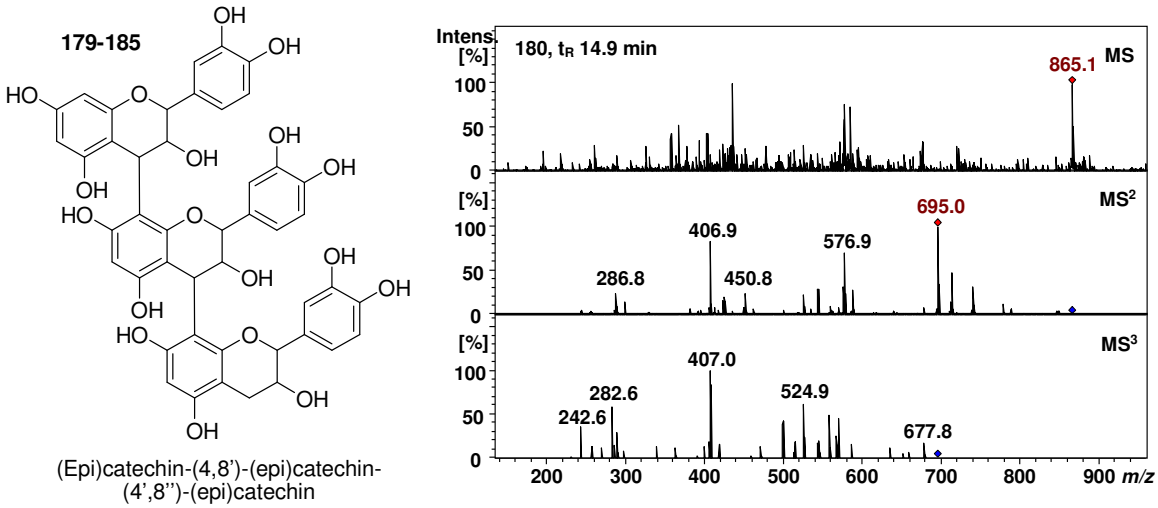

Figure 9.12: MS^n spectra of procyanidin C

9.1.25. Characterization of (epi)gallocatechin-(4,8′)-(epi)catechin-(4′,8′′)-(epi)catechin and (epi)catechin-(4,8′)-(epi)gallocatechin-(4′,8′′)-(epi)catechin (M_r 882)

Three peaks at t_R 11.1, 12.1 and 13.2 min with *m/z* 881 with $C_{45}H_{38}O_{19}$ were assigned as trimeric B-type proanthocyanidins with one unit of (epi)gallocatechin and two units of (epi)catechin (**186-188**). Compounds **186** and **188** produced an MS^2 base peak of *m/z* 695 and secondary peaks of *m/z* 755, 577, 451, 407 and 303. The fragment *m/z* 695 produced a base peak of either *m/z* 243 and 543 in MS^3 and secondary peaks of *m/z* 525, 451 and 289. The fragment *m/z* 695 was formed by RDA and fragments *m/z* 577 and 303 were formed by QM fission. The presence of fragments *m/z* 303 and 577 implied that the top unit was (epi)gallocatechin and base and middle units were (epi)catechin. Thus, compounds **186** and **188** at t_R 11.1 and 13.2 min were assigned as (epi)gallocatechin-(4,8′)-(epi)catechin-(4′,8′′)-(epi)catechin.

Compound **187** produced an MS^2 base peak of *m/z* 711 and secondary peaks of *m/z* 695, 593, 543, 425, 407 and 289. The fragment *m/z* 711 produced a base peak of *m/z* 543 in MS^3 and secondary peaks of *m/z* 525, 407 and 289. The fragment *m/z* 711 was formed by RDA and fragments *m/z* 593 and 289 were formed by QM fission. The presence of fragments *m/z* 289 and 593 implied that the base unit was (epi)catechin, the middle unit was (epi)gallocatechin and top unit was (epi)catechin. Thus, compound **187** at t_R 12.1 min was assigned as (epi)catechin-(4,8′)-(epi)gallocatechin-(4′,8″)-(epi)catechin.

9.1.26. Characterization of (epi)gallocatechin-(4,8′/2,7′)-(epi)gallocatechin-(4′,8″)-(epi)catechin (M_r 896)

One peak at t_R 15.9 min with *m/z* 895 with $C_{45}H_{36}O_{20}$ was assigned as trimeric A-type proanthocyanidins with one unit of (epi)catechin and two units of (epi)gallocatechin (**189**). It produced an MS^2 base peak of *m/z* 727 and secondary peaks of *m/z* 709, 575, 467, 427 and 289. The fragment *m/z* 727 produced a base peak of *m/z* 575 in MS^3 and secondary peaks of *m/z* 525 and 407. The fragments *m/z* 467 and 427 were formed by HRF, the fragments *m/z* 727, 709 and 575 were formed by RDA and fragment *m/z* 289 was formed by QM fission. The presence of fragments *m/z* 289, 427 and 467 implied that the base unit was (epi)catechin and top and middle units were (epi)gallocatechin connected by an A-type linkage. Thus, compound **189** was assigned as (epi)gallocatechin-(4,8′/2,7′)-(epi)gallocatechin-(4′,8″)-(epi)catechin.

9.1.27. Characterization of (epi)gallocatechin-(4,8′)-(epi)gallocatechin-(4′,8″)-(epi)catechin (M_r 898)

One peak at t_R 9.1 min with *m/z* 897 with $C_{45}H_{38}O_{20}$ was assigned as trimeric B-type proanthocyanidin with one unit of (epi)catechin and two units of (epi)gallocatechin (**190**). It produced an MS^2 base peak of *m/z* 711 and secondary peaks of *m/z* 771, 543, 467, 423, 407 and 289. The fragment *m/z* 711 produced a base peak of *m/z* 283 in MS^3 and secondary peaks of *m/z* 297 and 243. The fragments *m/z* 467 was formed by HRF, the fragments *m/z* 711 and 543 were formed by RDA and fragment *m/z* 289 was formed by QM fission. The presence of fragments *m/z* 289 and 467 implied that the bottom unit was (epi)catechin and middle unit was

(epi)gallocatechin. Thus, compound **190** was assigned as (epi)gallocatechin-(4,8′)-(epi)gallocatechin-(4′,8″)-(epi)catechin.

9.1.28. Characterization of B-type procyanidin trimer gallate (M_r 1018)

Two doubly charged peaks at t_R 13.1 and 18.3 min with *m/z* 508 with $C_{52}H_{42}O_{22}$ were assigned as gallates of trimeric B-type proanthocyanidins with three units of (epi)catechin (**191**-**192**). Compound **191** produced an MS^2 base peak of *m/z* 695 and secondary peaks of *m/z* 727, 577, 303 and 289. The fragment *m/z* 695 produced a base peak of *m/z* 525 in MS^3 and secondary peaks of *m/z* 451, 289 and 243. Compound **192** produced an MS^2 base peak of *m/z* 423 and secondary peaks of *m/z* 727, 695, 303 and 289. The fragment *m/z* 423 produced a base peak of *m/z* 243 in MS^3 and secondary peak of *m/z* 289. The compounds produced different fragmentation than the compounds identified by our group previously.

9.1.29. Characterization of A-type procyanidin tetramer (M_r 1152)

Four doubly charged peaks at t_R 12.9, 19.5, 24.5 and 25.9 min with *m/z* 575 with $C_{60}H_{48}O_{24}$ were assigned as tetrameric A-type proanthocyanidins with four units of (epi)catechin (**193**-**196**). Compound **193** produced an MS^2 base peak of *m/z* 863 and secondary peaks of *m/z* 711, 499, 490, 451, 289 and 245. The fragment *m/z* 863 produced a base peak of *m/z* 411 in MS^3 and secondary peaks of *m/z* 711, 693, 573, 559, 451 and 289. Compounds **194** and **195** produced an MS^2 base peak of *m/z* 861 and secondary peaks of *m/z* 739, 451, 411, 289 and 245. The fragment *m/z* 861 produced a base peak of *m/z* 411 in MS^3 and secondary peaks of *m/z* 691, 449 and 287. Compound **196** produced an MS^2 base peak of *m/z* 863 and secondary peaks of *m/z* 739, 693, 491, 451, 423, 407, 289 and 245. The fragment *m/z* 863 produced a base peak of *m/z* 575 in MS^3 and secondary peaks of *m/z* 449, 287 and 245. The fragment ions *m/z* 863 and 575 correspond to the loss of one and two units of (epi)catechin respectively.

9.1.30. Characterization of B-type procyanidin tetramer (M_r 1154)

Six doubly charged peaks at t_R 17.7, 21.3, 22.2, 24.5, 26.2 and 30.5 min with *m/z* 576 with $C_{60}H_{50}O_{24}$ were assigned as tetrameric B-type proanthocyanidins with four units of (epi)catechin (**197**-**202**). All the six compounds consisted of similar fragmentation peaks with a few differences. Compound **197** produced an MS^2 base peak of *m/z* 865 and secondary peaks of *m/z*

739, 693, 491, 451, 407, 289 and 287. The fragment *m/z* 865 produced a base peak of *m/z* 695 in MS^3 and secondary peaks of *m/z* 543, 451 and 245. Compounds **198**, **199** and **201** produced an MS^2 base peak of *m/z* 863 and secondary peaks of *m/z* 739, 693, 491, 451, 407, 289, 287 and 245. The fragment *m/z* 863 produced a base peak of either *m/z* 575 or 695 in MS^3 and secondary peak of *m/z* 449. Compound **200** produced an MS^2 base peak of *m/z* 407 and secondary peaks of *m/z* 863, 739, 693, 491, 451, 425, 289, 287 and 245. The fragment *m/z* 407 produced a base peak of *m/z* 285 in MS^3 and secondary peak of *m/z* 243. Compound **202** produced an MS^2 base peak of *m/z* 863 and secondary peaks of *m/z* 739, 693, 491, 451, 425, 407, 289, 287 and 243. The fragment *m/z* 863 produced a base peak of *m/z* 413 in MS^3 and secondary peaks of *m/z* 693, 575 and 287. The fragment ions *m/z* 865, 863 and 575 correspond to the loss of one and two units of (epi)catechin respectively.

10. Flavanones

The only flavanones and flavanone derivatives found in *Rhododendron* species were naringenin and taxifolin and their derivatives.

10.1. Naringenin and its derivatives

Naringenin derivatives were identified based on their characteristic fragmentation peaks. The aglycon of naringenin can be identified in MS^n by comparison with an authentic standard. In negative mode, naringenin at *m/z* 271 (after a loss of hydrogen) fragments to give *m/z* 151 and 107.

10.1.1. Characterization of naringenin (M_r 272)

A peak at t_R 47.9 min with *m/z* 271 and $C_{15}H_{12}O_5$ was assigned as naringenin (**203**). It produced MS^2 base peak of *m/z* 151 and secondary peak of *m/z* 177. The fragment *m/z* 151 produced a base peak of *m/z* 107 in MS^3. The EIC of *m/z* 271 in *Rhododendron ambiguum* in negative mode is shown in Figure 10.1, along with the MS^n spectra of compound **203** in Figure 10.2.

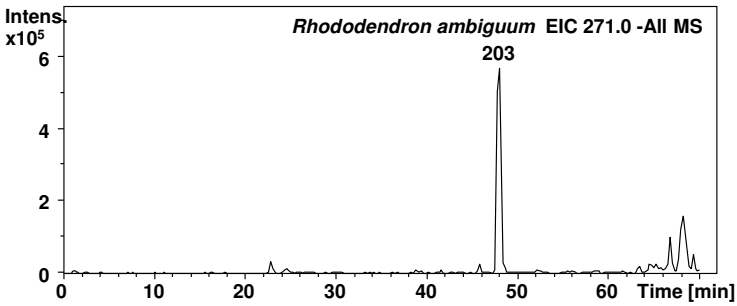

Figure 10.1: EIC of *m/z* 271 in *Rhododendron ambiguum* in negative mode

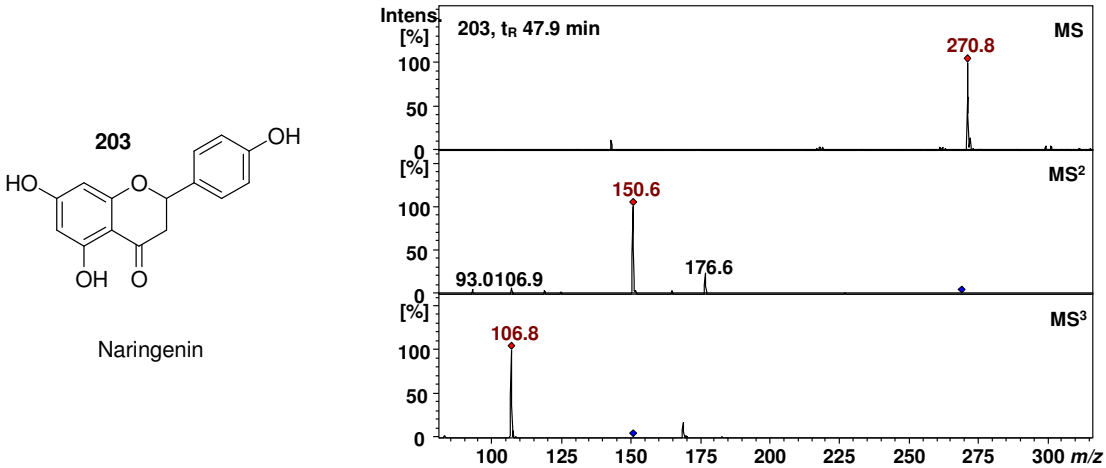

Figure 10.2: MS^n spectra of naringenin

10.1.2. Characterization of naringenin-*O*-hexoside (M_r 434)

A peak at t_R 38.3 min with *m/z* 433 and $C_{21}H_{22}O_{10}$ was assigned as naringenin-*O*-hexoside (**204**). It produced MS^2 MS^3 and MS^4 base peaks of *m/z* 271 $[M-H-Glc]^-$, 151 and 107 respectively. The EIC of *m/z* 433 in *Rhododendron alutaceum* in negative mode is shown in Figure 10.3, along with the MS^n spectra of compound **204** in Figure 10.4. The proposed fragmentation of compound **204** is shown in Figure 10.5.

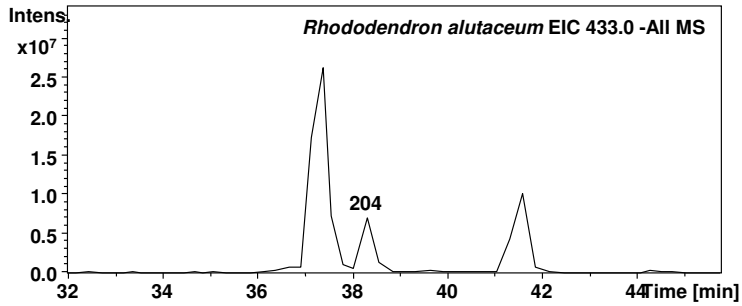

Figure 10.3: EIC of *m/z* 433 in *Rhododendron alutaceum* in negative mode

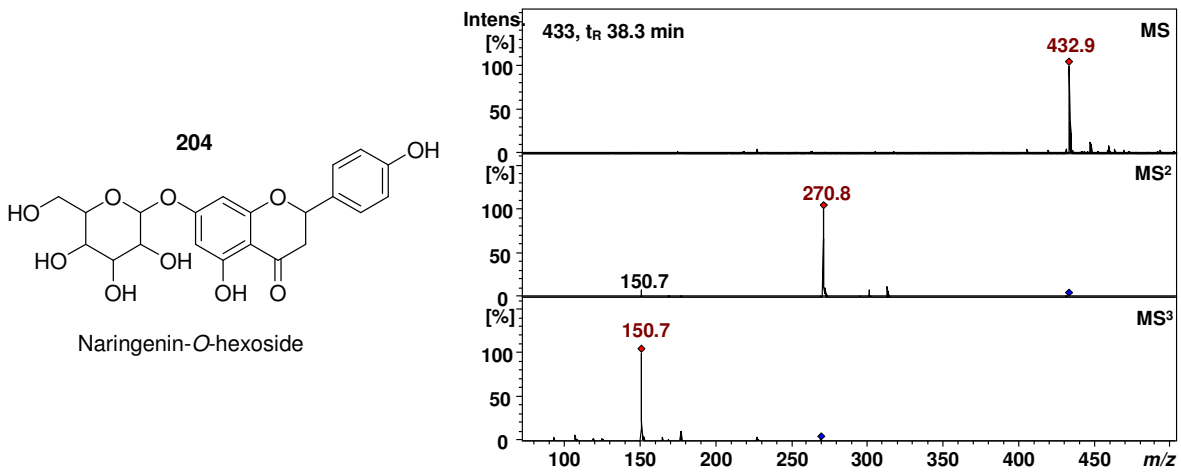

Figure 10.4: MS^n spectra of naringenin-*O*-hexoside

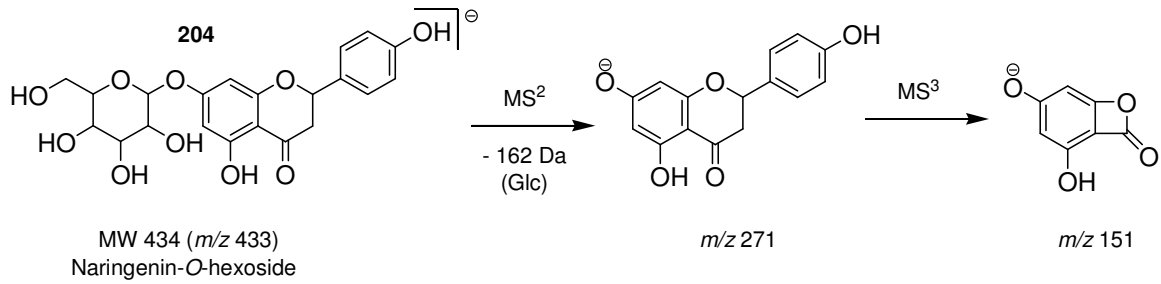

Figure 10.5: Proposed fragmentation of naringenin-*O*-hexoside

10.1.3. Characterization of naringenin-*O*-hexoside-*O*-pentoside (M_r 566)

A peak at t_R 38 min with *m/z* 565 and $C_{26}H_{30}O_{14}$ was assigned as naringenin-*O*-hexoside-*O*-pentoside (**205**), which is an isomer of naringenin-*O*-hexoside-*O*-pentoside. It produced MS^2 base peak of 271, which fragmented into *m/z* 151 in MS^3. The absence of an intermediate fragment suggested the presence of linkage between the hexose and pentose.

10.2. Taxifolin and its derivatives

Taxifolin derivatives were identified based on their characteristic fragmentation peaks. The aglycon of taxifolin can be identified in MS^n by comparison with an authentic standard. In negative mode, taxifolin at *m/z* 303 (after a loss of hydrogen) fragments to give *m/z* 285, 241 and 175. The fragment *m/z* 285 was found to be present in a higher intensity usually compared to *m/z* 303, which can be explained by the loss of water being favorable under these MS conditions.

10.2.1. Characterization of taxifolin (M_r 304)

A peak at t_R 29.1 min with *m/z* 303 and $C_{15}H_{12}O_7$ was assigned as taxifolin (**206**). It produced an MS^2 base peak of *m/z* 285 $[M-H-H_2O]^-$ and secondary peaks of *m/z* 177 and 125. The fragment *m/z* 285 further fragmented to give an MS^3 base peak of *m/z* 241.

10.2.2. Characterization of taxifolin-*O*-pentoside (M_r 436)

Five isomers of taxifolin-*O*-pentoside (**207**-**211**) were identified at t_R 27.8, 31.1, 32.4, 33.6 and 35.5 min with $C_{20}H_{20}O_{11}$ and *m/z* 435. The three isomers produced an MS^2 base peak of either *m/z* 303 $[M-H-Xyl]^-$ or 285 $[M-H-Xyl-H_2O]^-$, which further fragmented to give an MS^3 base peak of *m/z* 241 and secondary peak of *m/z* 175.

10.2.3. Characterization of taxifolin-*O*-rhamnoside (M_r 450)

Three isomers of taxifolin-*O*-rhamnoside (**212**-**214**) were identified at t_R 36.2, 36.6 and 37.4 min $C_{21}H_{22}O_{11}$ and *m/z* 449. It produced MS^2 and MS^3 base peaks of *m/z* 285 $[M-H-Rha-H_2O]^-$ and 241 respectively and a secondary peak of *m/z* 303 $[M-H-Rha]^-$ in MS^2.

10.2.4. Characterization of taxifolin-*O*-hexoside (M_r 466)

Seven isomers of taxifolin-*O*-hexoside (**215**-**221**) were identified at t_R 15.1, 19.3, 22.8, 24.8, 26.2, 27.9 and 30.0 min with $C_{21}H_{22}O_{12}$ and *m/z* 465. The compounds produced similar fragments. Compounds **215** and **216** produced MS^2, MS^3 and MS^4 base peaks of *m/z* 303 $[M-H-Glc]^-$, 285 $[M-H-Glc-H_2O]^-$ and 241 respectively and a secondary peak of *m/z* 175 in MS^4. Compounds **217**, **218**, **219** and **220** produced an MS^2 base peak of *m/z* 285 $[M-H-Glc-H_2O]^-$ and a secondary peak of *m/z* 303 $[M-H-Glc]^-$. In MS^3, *m/z* 285 further fragmented to give a base peak of *m/z* 241 and a secondary peak of *m/z* 175. Compound **221** produced an MS^2 base peak of *m/z* 303 $[M-H-Glc]^-$ and secondary peak of *m/z* 285 $[M-H-Glc-H_2O]^-$. It further fragmented in MS^3 to give a base peak of *m/z* 151. The EIC of *m/z* 465 in *Rhododendron tapetiforme* in negative mode is shown in Figure 10.6, along with the MS^n spectra of compound **219** in Figure 10.7. The proposed fragmentation of compounds **215**-**221** is shown in Figure 10.8.

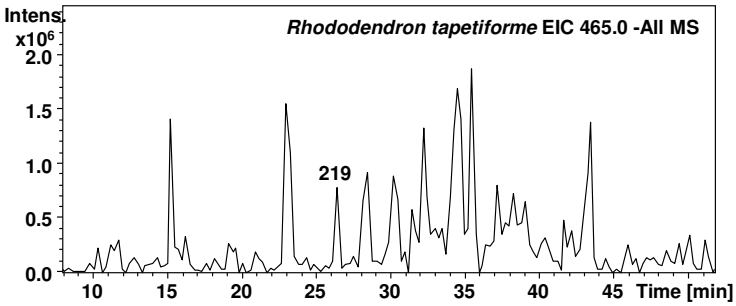

Figure 10.6: EIC of *m/z* 465 in *Rhododendron tapetiforme* in negative mode

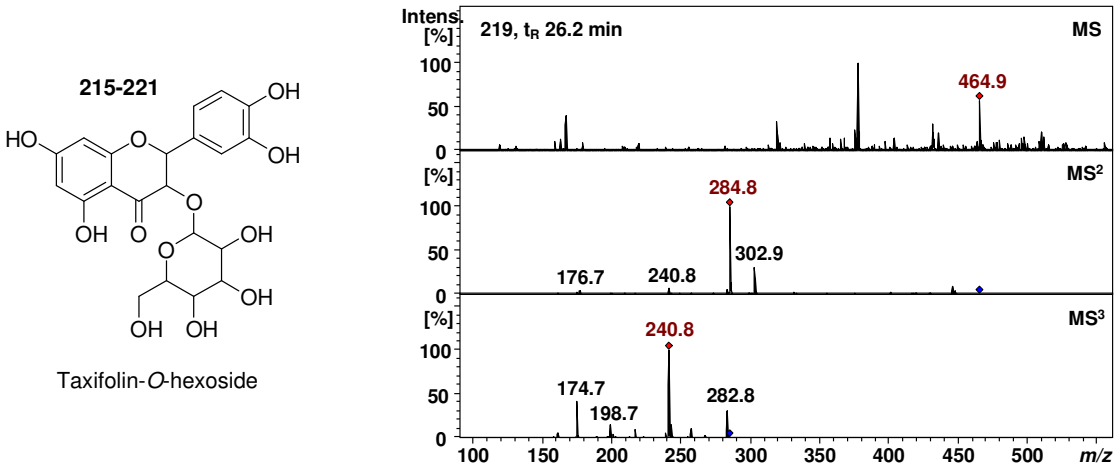

Figure 10.7: MS^n spectra of taxifolin-*O*-hexoside

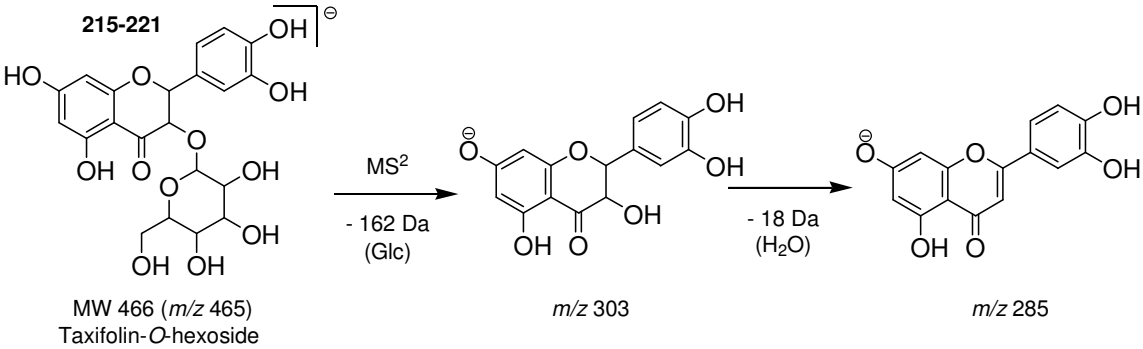

Figure 10.8: Proposed fragmentation of taxifolin-*O*-hexoside

10.2.5. Characterization of taxifolin-*O*-acetyl-rhamnoside (M_r 492)

Two isomers of taxifolin-*O*-acetyl-rhamnoside (**222**-**223**) were identified at t_R 39.9 and 45.0 min with $C_{23}H_{24}O_{12}$ and *m/z* 491. The compounds produced an MS^2 base peak of *m/z* 285 $[M\text{-}H\text{-acetyl-Rha-}H_2O]^-$ and a secondary peak of *m/z* 303 $[M\text{-}H\text{-acetyl-Rha}]^-$. In MS^3, *m/z* 285 further

fragmented to give a base peak of *m/z* 241. The absence of an intermediate peak implied that the acetyl group was connected to the rhamnoside.

10.2.6. Characterization of taxifolin-*O*-acetyl-hexoside (M_r 508)

Two isomers of taxifolin-*O*-acetyl-hexoside (**224**-**225**) were identified at t_R 46.7 and 48.1 min with $C_{23}H_{24}O_{13}$ and *m/z* 507. Both compounds produced an MS^2 base peak of *m/z* 285 $[M-H-acetyl-Glc-H_2O]^-$ and a secondary peak of *m/z* 303 $[M-H-acetyl-Glc]^-$. In MS^3, *m/z* 285 further fragmented to give a base peak of *m/z* 241 and secondary peaks of *m/z* 175 and 151. The absence of an intermediate peak implied that the acetyl group was connected to the hexoside.

10.2.7. Characterization of taxifolin-*O*-pentoside-*O*-hexoside (M_r 598)

A peak at t_R 17.7 min with *m/z* 597 and $C_{26}H_{30}O_{16}$ was assigned as taxifolin-*O*-pentoside-*O*-hexoside (**226**). It produced MS^2, MS^3 and MS^4 base peaks of *m/z* 435 $[M-H-Glc]^-$, 285 $[M-H-Glc-Xyl-H_2O]^-$ and 241 respectively and a secondary peak of *m/z* 303 $[M-H-Glc-Xyl]^-$. The presence of an intermediate peak *m/z* 435 implied that there was no linkage between pentoside and hexoside.

10.2.8. Characterization of taxifolin-*O*-rhamnoside-*O*-hexoside (M_r 612)

Two isomers of taxifolin-*O*-rhamnoside-*O*-hexoside (**227**-**228**) were identified at t_R 20.1 and 32.8 min with $C_{27}H_{32}O_{16}$ and *m/z* 611. Both compounds produced MS^2, MS^3 and MS^4 base peaks of *m/z* 449 $[M-H-Glc]^-$, 285 $[M-H-Glc-Rha-H_2O]^-$ and 241 respectively and a secondary peak of *m/z* 303 $[M-H-Glc-Rha]^-$. The presence of an intermediate fragment *m/z* 449 implied that there was no linkage between rhamnoside and hexoside.

11. Flavonols

The flavonols and their derivatives were identified with their characteristic fragmentation patterns. According to previous studies, the 7-*O*-glycosylated flavonoid elutes before the 3-*O*-glycosylated flavonoid. Also, if flavonoids have both 3-*O*-glycosulated and 7-*O*-glycosylated bonds, then the 7-*O*-glycosylated bond is fragmented before the 3-*O*-glycosulated bond.

11.1. Myricetin and its derivatives

Myricetin derivatives were identified based on their characteristic fragmentation peaks. The aglycon of myricetin can be identified in MS^n by comparison with an authentic standard. In negative mode, myricetin at *m/z* 317 (after a loss of hydrogen) fragments to give *m/z* 316, 271, 179 and 151.

11.1.1. Characterization of myricetin (M_r 318)

A peak at t_R 38.9 min with *m/z* 317 and $C_{15}H_{10}O_8$ was assigned as myricetin (**229**). It produced the characteristic MS^2 base peak of *m/z* 179, which produced a base peak of *m/z* 151 in MS^3.

11.1.2. Characterization of myricetin-*O*-pentoside (M_r 450)

Three isomers of myricetin-*O*-pentoside (**230**-**232**) were identified at t_R 32.1, 37.8 and 39.1 min with $C_{20}H_{18}O_{12}$ and *m/z* 449. The compounds produced an MS^2 base peak of either *m/z* 317 $[M-H-Xyl]^-$ or 316, which produced fragments of *m/z* 271, 179 and 151.

11.1.3. Characterization of myricetin-*O*-rhamnoside (M_r 464)

A peak at t_R 33.0 min with *m/z* 463 and $C_{21}H_{20}O_{12}$ was assigned as myricetin-*O*-rhamnoside (**233**). It produced the characteristic MS^2 base peak of either *m/z* 317 $[M-H-Rha]^-$ or 316, which produced a base peak of *m/z* 271 and secondary peaks of *m/z* 179 and 151 in MS^3.

11.1.4. Characterization of myricetin-*O*-hexoside (M_r 480)

Three isomers of myricetin-*O*-hexoside (**234**-**236**) were identified at t_R 30.8, 31.2 and 35.3 min with $C_{21}H_{20}O_{13}$ and *m/z* 479. The compounds produced an MS^2 base peak of either *m/z* 317 $[M-H-Glc]^-$ or 316, which produced fragments of *m/z* 271, 179 and 151. The EIC of *m/z* 479 in

Rhododendron decorum in negative mode is shown in Figure 11.1, along with the MS^n spectra of compound **234** in Figure 11.2. The proposed fragmentation of compounds **234**-**236** is shown in Figure 11.3.

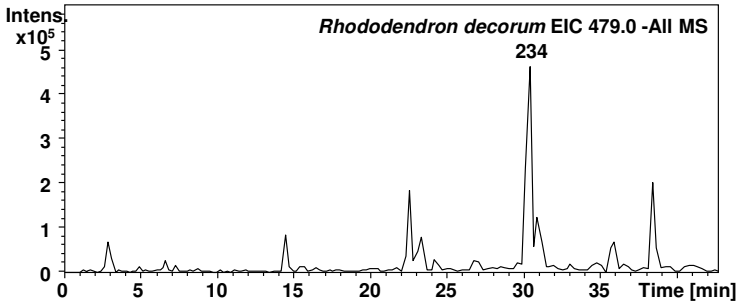

Figure 11.1: EIC of *m/z* 479 in *Rhododendron decorum* in negative mode

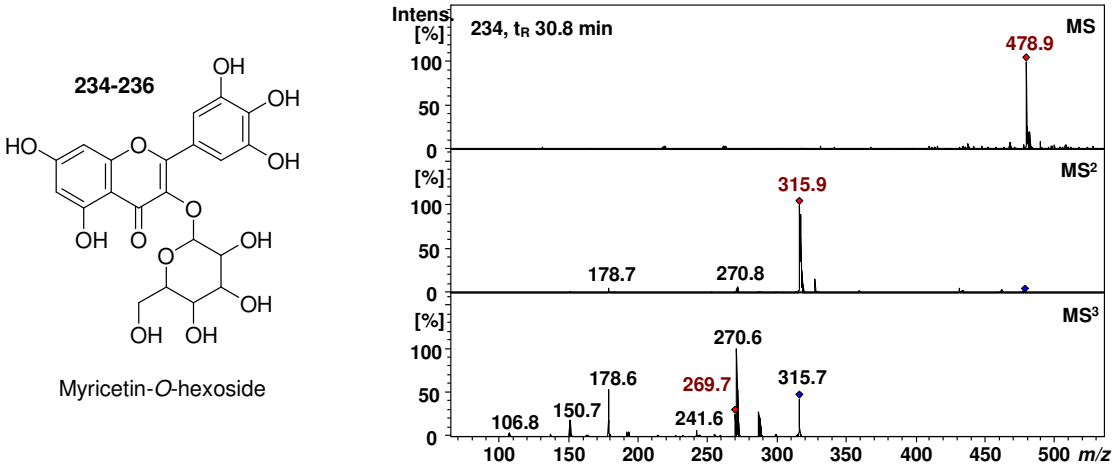

Figure 11.2: MS^n spectra of myricetin-*O*-hexoside

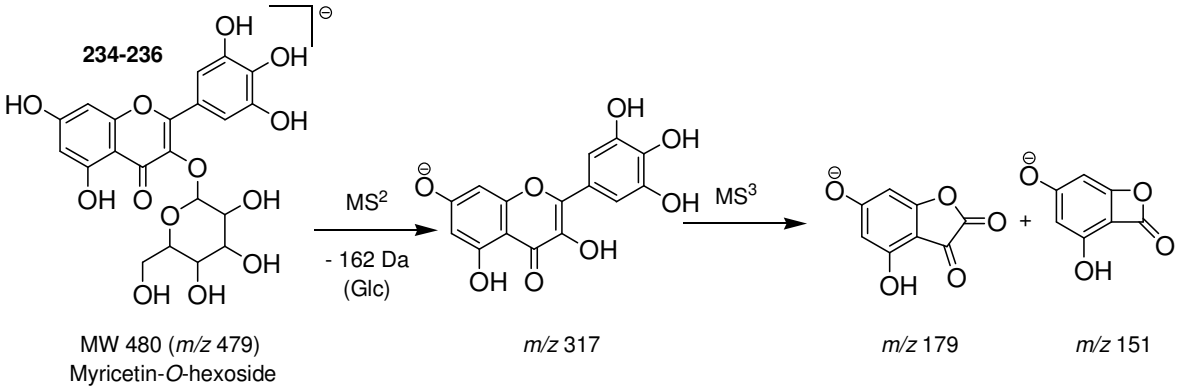

Figure 11.3: Proposed fragmentation of myricetin-*O*-hexoside

11.1.5. Characterization of myricetin-*O*-glucuronide (M_r 494)

A peak at t_R 36.5 min with *m/z* 493 and $C_{21}H_{18}O_{14}$ was assigned as myricetin-*O*-glucuronide (**237**). It produced the characteristic MS^2, MS^3 and MS^4 base peak of *m/z* 317 $[M-H-Glu]^-$, 179 and 151 respectively.

11.1.6. Characterization of myricetin-*O*-acetyl-rhamnoside (M_r 506)

A peak at t_R 37.6 min with *m/z* 505 and $C_{23}H_{22}O_{13}$ was assigned as myricetin-*O*-acetyl-rhamnoside (**238**). It produced an MS^2 base peak of *m/z* 316 and secondary peak of *m/z* 317. The fragment *m/z* 316 produced a base peak of *m/z* 271 in MS^3 and secondary peaks of *m/z* 179 and 151.

11.1.7. Characterization of myricetin-*O*-dipentoside (M_r 582)

Two isomers of myricetin-*O*-dipentoside (**239**-**240**) were identified at t_R 41.4 and 42.5 min with $C_{25}H_{26}O_{16}$ and *m/z* 581. Compound **239** produced MS^2, MS^3 and MS^4 base peaks of *m/z* 449 $[M-H-Xyl]^-$, 317 $[M-H-Xyl-Xyl]^-$ and 179 respectively. The presence of an intermediate fragment of *m/z* 449 suggested the absence of linkage between the two pentosides. Compound **240** on the other hand produced MS^2 and MS^3 base peaks of *m/z* 317 $[M-H-Xyl-Xyl]^-$ and 179 respectively and the absence of an intermediate fragment suggested the presence of linkage between the two pentosides.

11.1.8. Characterization of myricetin-*O*-benzoyl-hexoside (M_r 584)

A peak at t_R 45.7 min with *m/z* 583 and $C_{28}H_{24}O_{14}$ was assigned as myricetin-*O*-benzoyl-hexoside (**241**). It produced an MS^2 base peak of *m/z* 316 and secondary peak of *m/z* 317 $[M-H-benzoyl-Glc]^-$. The fragment *m/z* 316 produced a base peak of *m/z* 271 in MS^3 and secondary peaks of *m/z* 179 and 151.

11.1.9. Characterization of myricetin-*O*-galloyl-rhamnoside (M_r 616)

Two isomers of myricetin-*O*-galloyl-rhamnoside (**242**-**243**) were identified at t_R 38.5 and 39.2 min with $C_{28}H_{24}O_{16}$ and *m/z* 615. Both compounds produced an MS^2 base peak of *m/z* 317 $[M-H-galloyl-Rha]^-$ and secondary peak of *m/z* 463 $[M-H-galloyl]^-$. The fragment *m/z* 317 produced a

base peak of *m/z* 179 and 151 in MS^3 and MS^4 respectively. The presence of an intermediate fragment *m/z* 463 as a secondary peak suggested the presence of linkage between the galloyl group and rhamnose.

11.1.10. Characterization of myricetin-*O*-hexoside-*O*-rhamnoside (M_r 626)

Two isomers of myricetin-*O*-hexoside-*O*-rhamnoside (**244**-**245**) were identified at t_R 31.4 and 35.4 min with $C_{27}H_{30}O_{17}$ and *m/z* 625. Compound **244** produced an MS^2 base peak of *m/z* 317 $[M-H-Glc-Rha]^-$ and secondary peak of *m/z* 316. The fragment *m/z* 317 produced a base peak of *m/z* 271 and secondary peaks of *m/z* 179 and 151. The absence of an intermediate fragment suggested the presence of linkage between the rhamnose and hexose. Thus, compound **244** at t_R 31.4 min was assigned as myricetin-*O*-rutinoside. Compound **245** on the other hand produced an MS^2 base peak of *m/z* 463 $[M-H-Glc]^-$, which fragmented into 316 and 317 $[M-H-Glc-Rha]^-$ in MS^3. In MS^4, the fragment *m/z* 316 further fragmented into *m/z* 271 as the base peak and *m/z* 179 and 151 as secondary peaks. The presence of an intermediate fragment of *m/z* 463 suggested the absence of linkage between the rhamnose and hexose and that hexose was 3-*O*-glycosylated to myricetin. Thus, compound **244** at t_R 35.4 min was assigned as myricetin-3-*O*-hexoside-7-*O*-rhamnoside.

11.1.11. Characterization of myricetin-*O*-galloyl-hexose (M_r 632)

Two isomers of myricetin-*O*-galloyl-hexose (**246**-**247**) were identified at t_R 30.5 and 32.5 min with $C_{28}H_{24}O_{17}$ and *m/z* 631. Compound **246** at t_R 30.5 min produced an MS^2 base peak of *m/z* 316 and secondary peak of *m/z* 317 $[M-H-galloyl-Glc]^-$. The fragment *m/z* 316 produced a base peak of *m/z* 271 and secondary peaks of *m/z* 179 and 151. The absence of an intermediate fragment suggested the presence of linkage between the galloyl group and hexose. Compound **247** on the other hand produced an MS^2 base peak of *m/z* 479 $[M-H-galloyl]^-$, which fragmented into 316 and 317 $[M-H-galloyl-Glc]^-$ in MS^3. In MS^4, the fragment *m/z* 316 further fragmented into *m/z* 271 as the base peak and *m/z* 179 and 151 as secondary peaks. The presence of an intermediate fragment of *m/z* 479 suggested the absence of linkage between the galloyl group and hexose and that hexose was 3-*O*-glycosylated to myricetin. Thus, compound **247** at t_R 32.5 min was assigned as myricetin-7-*O*-galloyl-3-*O*-hexoside.

11.2. Quercetin and its derivatives

Quercetin derivatives were identified based on their characteristic fragmentation peaks. The aglycon of quercetin can be identified in MS^n by comparison with an authentic standard. In negative mode, quercetin at *m/z* 301 (after a loss of hydrogen) fragments to give *m/z* 300, 179 and 151.

11.2.1. Characterization of quercetin (M_r 302)

A peak at t_R 44.4 min with *m/z* 301 and $C_{15}H_{10}O_7$ was assigned as quercetin (**248**). It produced the characteristic MS^2 base peak of *m/z* 179, which produced a base peak of *m/z* 151 in MS^3.

11.2.2. Characterization of quercetin-*O*-pentoside (M_r 434)

Four isomers of quercetin-*O*-pentoside (**249**-**252**) were identified at t_R 36.6, 37.4, 39.6 and 41.2 min with $C_{20}H_{18}O_{11}$ and *m/z* 433. The compounds produced an MS^2 base peak of *m/z* 301 $[M-H-Xyl]^-$, which produced fragments of *m/z* 179 and 151.

11.2.3. Characterization of quercetin-*O*-rhamnoside (M_r 448)

A peak at t_R 38.7 min with *m/z* 447 and $C_{21}H_{20}O_{11}$ was assigned as quercetin-*O*-rhamnoside (**253**). It produced the characteristic MS^2 base peak of *m/z* 301 $[M-H-Rha]^-$, which produced a base peak of *m/z* 179 and secondary peak of *m/z* 151 in MS^3.

11.2.4. Characterization of quercetin-*O*-hexoside (M_r 464)

Three isomers of quercetin-*O*-hexoside (**254**-**256**) were identified at t_R 34.2, 35.5 and 40.7 min with $C_{21}H_{20}O_{12}$ and *m/z* 463. The compounds produced an MS^2 base peak of *m/z* 301 $[M-H-Glc]^-$, which produced fragments of *m/z* 271, 179 and 151. The EIC of *m/z* 463 in *Rhododendron concinnum* in negative mode is shown in Figure 11.4, along with the MS^n spectra of compound **254** in Figure 11.5. The proposed fragmentation of compounds **254**-**256** is shown in Figure 11.6.

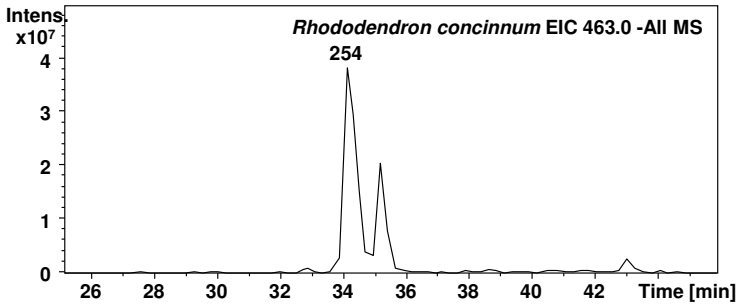

Figure 11.4: EIC of *m/z* 463 in *Rhododendron concinnum* in negative mode

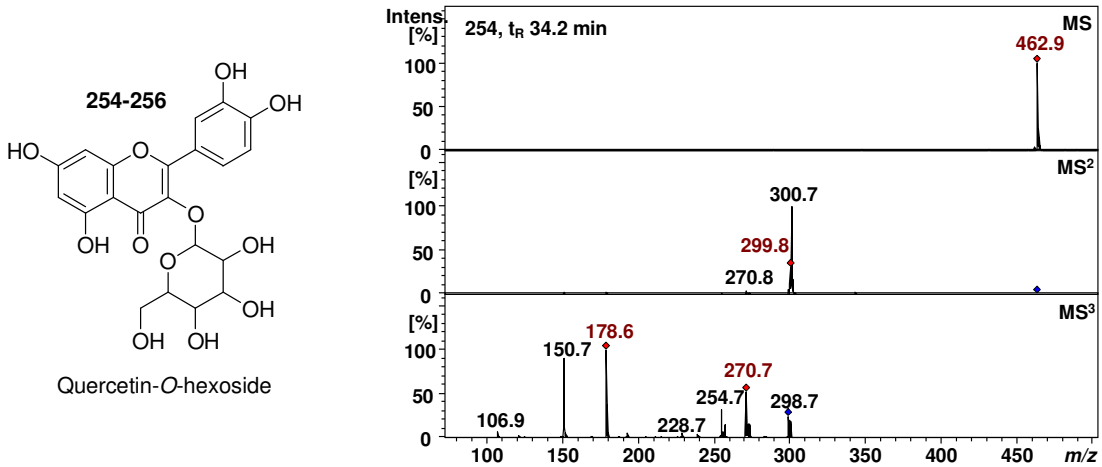

Figure 11.5: MS^n spectra of quercetin-*O*-hexoside

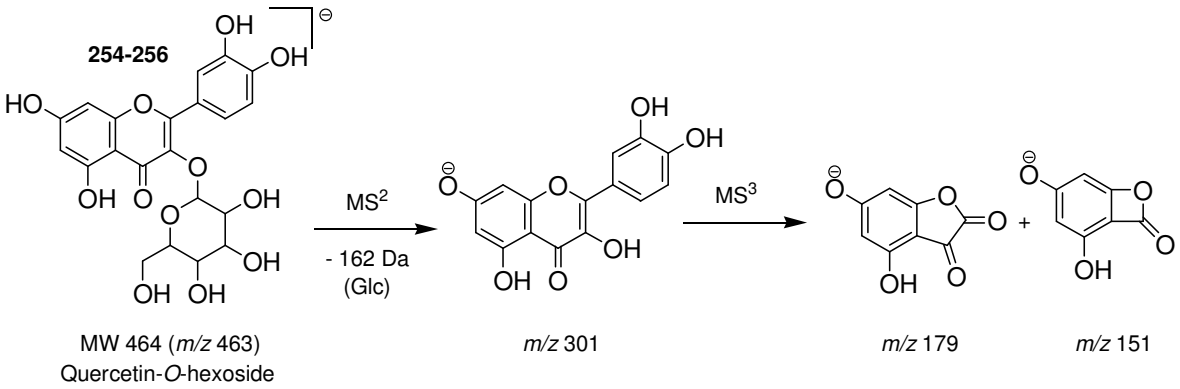

Figure 11.6: Proposed fragmentation of quercetin-*O*-hexoside

11.2.5. Characterization of quercetin-*O*-acetyl-pentoside (M_r 476)

Three isomers of quercetin-*O*-acetyl-pentoside (**257**-**259**) were identified at t_R 43.2, 45.5 and 48.0 min with $C_{22}H_{20}O_{12}$ and *m/z* 475. The compounds produced an MS^2 base peak of either *m/z* 300

or 301 [M-H-acetyl-Xyl]$^-$, which produced fragments of *m/z* 271, 179 and 151. The absence of an intermediate peak implied that there was linkage between the acetyl group and pentoside.

11.2.6. Characterization of quercetin-*O*-glucuronide (M_r 478)

A peak at t_R 40.8 min with *m/z* 477 and $C_{21}H_{18}O_{13}$ was assigned as quercetin-*O*-glucuronide (**260**). It produced an MS^2 base peak of *m/z* 301 [M-H-Glu]$^-$, which produced fragments of *m/z* 179 and 151.

11.2.7. Characterization of quercetin-*O*-acetyl-rhamnoside (M_r 490)

Three isomers of quercetin-*O*-acetyl-rhamnoside (**261**-**263**) were identified at t_R 43.5, 45.5 and 47.6 min with $C_{23}H_{22}O_{12}$ and *m/z* 489. The compounds produced an MS^2 base peak of either *m/z* 300 or 301 [M-H-acetyl-Rha]$^-$. In MS^3, the fragment *m/z* 300 further fragmented into *m/z* 271 as the base peak and *m/z* 179 and 151 as secondary peaks. The absence of an intermediate peak implied that there was linkage between the acetyl group and rhamnoside.

11.2.8. Characterization of quercetin-*O*-acetyl-hexoside (M_r 506)

Eight isomers of quercetin-*O*-acetyl-hexoside (**264**-**271**) were identified at t_R 38.0, 40.0, 42.0, 42.8, 43.4, 44.0, 45.6 and 46.5 min with $C_{23}H_{22}O_{13}$ and *m/z* 505. The compounds produced an MS^2 base peak of *m/z* 301 [M-H-acetyl-Glc]$^-$ and secondary peak of 463. In MS^3, the fragment *m/z* 301 further fragmented into *m/z* 271 as the base peak and *m/z* 179 and 151 as secondary peaks. The presence of *m/z* 301 as the base peak and *m/z* 463 as the secondary peak implied there was linkage between the acetyl group and hexoside.

11.2.9. Characterization of quercetin-*O*-diacetyl-hexoside (M_r 548)

A peak at t_R 51.5 min with *m/z* 547 and $C_{25}H_{24}O_{14}$ was assigned as quercetin-*O*-diacetyl-hexoside (**272**). It produced an MS^2 base peak of either *m/z* 300 or 301 [M-H-acetyl-acetyl-Glc]$^-$. In MS^3, the fragment *m/z* 300 further fragmented into *m/z* 271 as the base peak and *m/z* 179 and 151 as secondary peaks.

11.2.10. Characterization of quercetin-*O*-dipentoside (M_r 566)

Two isomers of quercetin-*O*-dipentoside (**273**-**274**) were identified at t_R 33.8 and 36.3 min with $C_{25}H_{26}O_{15}$ and *m/z* 565. Both compounds produced an MS^2 base peak of either *m/z* 300 or 301 $[M-H-Xyl-Xyl]^-$. The fragment 300 further fragmented in MS^3 to give a base peak of *m/z* 271 and secondary peaks of 179 and 151. The absence of an intermediate fragment suggested the presence of linkage between the two pentosides.

11.2.11. Characterization of quercetin-*O*-benzoyl-hexoside (M_r 568)

A peak at t_R 49.7 min with *m/z* 567 and $C_{28}H_{24}O_{13}$ was assigned as quercetin-*O*-benzoyl-hexoside (**275**). It produced an MS^2 base peak of *m/z* 301 $[M-H-benzoyl-Glc]^-$. The fragment *m/z* 301 further fragmented in MS^3 to give a base peak of *m/z* 271 and secondary peaks of 179 and 151. The absence of an intermediate fragment suggested the presence of linkage between the benzoyl group and hexoside.

11.2.12. Characterization of quercetin-*O*-pentoside-*O*-rhamnoside (M_r 580)

A peak at t_R 37.2 min with *m/z* 579 and $C_{26}H_{28}O_{15}$ was assigned as quercetin-*O*-pentoside-*O*-rhamnoside (**276**). It produced an MS^2 base peak of *m/z* 301 $[M-H-Xyl-Rha]^-$. In MS^3, the fragment *m/z* 301 further fragmented in MS^3 to give a base peak of *m/z* 179 and secondary peaks of 271 and 151. The absence of an intermediate fragment suggested the presence of linkage between the benzoyl group and hexoside.

11.2.13. Characterization of quercetin-*O*-(*p*-hydroxy)-benzoyl-hexoside (M_r 584)

Three isomers of quercetin-*O*-(*p*-hydroxy)-benzoyl-hexoside (**277**-**279**) were identified at t_R 41.7, 44.0 and 49.8 min with $C_{28}H_{24}O_{14}$ and *m/z* 583. All three compounds produced an MS^2, MS^3 and MS^4 base peak of *m/z* 463 $[M-H-hydroxybenzoyl]^-$, 301 $[M-H-hydroxybenzoyl-Glc]^-$ and 179 respectively and a secondary peak of 151 in MS^4. The presence of an intermediate fragment of *m/z* 463 suggested the absence of linkage between the hydroxybenzoyl group and hexoside and that hexose was 3-*O*-glycosylated to quercetin.

11.2.14. Characterization of quercetin-*O*-galloyl-pentoside (M_r 586)

Two isomers of quercetin-*O*-galloyl-pentoside (**280**-**281**) were identified at t_R 39.1 and 42.9 min with $C_{27}H_{22}O_{15}$ and *m/z* 585. Compound **280** produced MS^2, MS^3 and MS^4 base peaks of *m/z* 433 $[M-H-galloyl]^-$, 301 $[M-H-galloyl-Xyl]^-$ and 179 respectively and a secondary peak of 151 in MS^4. The presence of an intermediate fragment of *m/z* 433 suggested the absence of linkage between the galloyl group and pentoside. Compound **281** on the other hand produced MS^2 and MS^3 base peaks of *m/z* 301 $[M-H-galloyl-Xyl]^-$ and 179 respectively and a secondary peak of 151 in MS^4. The absence of an intermediate fragment suggested the presence of linkage between the galloyl group and pentoside.

11.2.15. Characterization of quercetin-3-*O*-(4"-3-hydroxy-3-methylglutaryl)-α-rhamnoside (M_r 592)

A peak at t_R 44.9 min with *m/z* 591 and $C_{27}H_{28}O_{15}$ was assigned as quercetin-3-*O*-(4"-3-hydroxy-3-methylglutaryl)-α-rhamnoside (**282**). It produced MS^2, MS^3 and MS^4 base peaks of *m/z* 301, 463 and 179 respectively.

11.2.16. Characterization of quercetin-*O*-coumaroyl-rhamnoside (M_r 594)

Two isomers of quercetin-*O*-coumaroyl-rhamnoside (**283**-**284**) were identified at t_R 52.0 and 55.1 min with $C_{30}H_{26}O_{13}$ and *m/z* 593. Both compounds produced similar fragmentation with an MS^2 base peak of *m/z* 301 $[M-H-coumaroyl-Rha]^-$ and other fragments of *m/z* 179 and 151. The absence of an intermediate fragment suggested the presence of linkage between the coumaroyl group and rhamnoside.

11.2.17. Characterization of quercetin-*O*-pentoside-*O*-hexoside (M_r 596)

Two isomers of quercetin-*O*-pentoside-*O*-hexoside (**285**-**286**) were identified at t_R 24.7 and 30.4 min with $C_{26}H_{28}O_{16}$ and *m/z* 595. Compound **285** at t_R 24.7 min produced MS^2 and MS^3 base peaks of *m/z* 463 $[M-H-Xyl]^-$ and 301 $[M-H-Xyl-Glc]^-$ respectively. The presence of an intermediate fragment of *m/z* 463 suggested the absence of linkage between the pentoside and hexoside and that hexose was 3-*O*-glycosylated to quercetin. Compound **286** at t_R 30.4 min on the other hand produced MS^2 base peaks of either *m/z* 300 and 301$[M-H-Xyl-Glc]^-$. In MS^3, the fragment *m/z* 300 further fragmented in MS^3 to give a base peak of *m/z* 271 and secondary peaks

of 179 and 151. The absence of an intermediate fragment suggested the presence of linkage between the pentoside and hexoside.

11.2.18. Characterization of quercetin-*O*-protocatechuoyl-hexoside and quercetin-*O*-galloyl-rhamnoside (M_r 600)

Two peaks were detected with $C_{28}H_{24}O_{15}$ and *m/z* 599. Compound **287** at t_R 40.6 min produced MS^2, MS^3 and MS^4 base peaks of *m/z* 463 [M-H-protocatechuoyl]$^-$, 301 [M-H-protocatechuoyl-Glc]$^-$ and 179 respectively and a secondary peak of 151 in MS^4. It was assigned as quercetin-*O*-protocatechuoyl-hexoside. Compound **288** at t_R 43.4 min on the other hand produced MS^2, MS^3 and MS^4 base peaks of *m/z* 301 [M-galloyl-Rha]$^-$, 179 and 151 respectively. The absence of an intermediate fragment suggested the presence of linkage between the galloyl group and rhamnose and thus it was assigned as quercetin-*O*-galloyl-rhamnoside.

11.2.19. Characterization of quercetin-*O*-rhamnoside-*O*-hexoside (M_r 610)

Six isomers of quercetin-*O*-rhamnoside-*O*-hexoside (**289**-**294**) were identified at t_R 25.7, 28.8, 30.3, 31.5, 34.3 and 35.0 min with $C_{27}H_{30}O_{16}$ and *m/z* 609. Compounds **289** and **292** produced an MS^2 base peak of *m/z* 447 [M-H-Glc]$^-$ and secondary peak of *m/z* 463 [M-H-Rha]$^-$. The fragment *m/z* 447 further fragmented into *m/z* 300 or 301 and 271, 179 and 151. The presence of intermediate fragments *m/z* 447 as base peak and *m/z* 463 implied that there was absence of linkage between rhamnoside and hexoside. Compounds **290**, **291**, **293** and **294** produced an MS^2 base peak of either 300 or 301 [M-H-Rha-Glc]$^-$. It further fragmented into *m/z* 271, 179 and 151 in MS^3. The absence of intermediate fragments implied that there was presence of linkage between rhamnoside and hexoside.

11.2.20. Characterization of quercetin-*O*-coumaroyl-hexoside (M_r 610)

Three isomers of quercetin-*O*-coumaroyl-hexoside (**295**-**297**) were identified at t_R 46.4, 47.8 and 49.5 min with $C_{30}H_{26}O_{14}$ and *m/z* 609. Compounds **295** and **297** at t_R 46.4 and 49.5 min produced MS^2, MS^3 and MS^4 base peaks of *m/z* 463 [M-H-coumaroyl]$^-$, 301 [M-H-coumaroyl-Glc]$^-$ and 179 respectively and a secondary peak of 151 in MS^4. The presence of an intermediate fragment *m/z* 463 implied that there was absence of linkage between the coumaroyl group and hexoside. Compound **296** at t_R 47.8 min produced an MS^2 base peak of either 301 [M-H-coumaroyl-Glc]$^-$

and a secondary peak of *m/z* 463 [M-H-coumaroyl]$^-$. In MS^3, the fragment *m/z* 301 further fragmented into *m/z* 179 as the base peak and *m/z* 151 as the secondary peak. The presence of an intermediate fragment *m/z* 463 as a secondary peak implied that there was presence of linkage between the coumaroyl group and hexoside.

11.2.21. Characterization of quercetin-*O*-galloyl-hexoside (M_r 616)

Two isomers of quercetin-*O*-galloyl-hexoside (**298**-**299**) were identified at t_R 34.5 and 35.5 min with $C_{28}H_{24}O_{16}$ and *m/z* 615. Both compounds produced MS^2, MS^3 and MS^4 base peaks of *m/z* 463 [M-H-galloyl]$^-$, 301 [M-H-galloyl-Glc]$^-$ and 179 respectively and a secondary peak of 151 in MS^4. The presence of an intermediate fragment *m/z* 463 implied that there was absence of linkage between the galloyl group and hexoside.

11.2.22. Characterization of quercetin-*O*-feruloyl-rhamnoside (M_r 624)

A peak at t_R 56.5 min with *m/z* 623 and $C_{31}H_{28}O_{14}$ was assigned as quercetin-*O*-feruloyl-rhamnoside (**300**). It produced an MS^2 base peak of *m/z* 301 [M-H-Xyl-Rha]$^-$. In MS^3, the fragment *m/z* 301 further fragmented in MS^3 to give a base peak of *m/z* 271 and secondary peaks of 179 and 151. The absence of an intermediate fragment suggested the presence of linkage between the feruloyl group and rhamnoside.

11.2.23. Characterization of cypellogin A/B or quercetin-*O*-oleuropeoyl-hexoside (M_r 630)

Three isomers of quercetin-*O*-oleuropeoyl-hexoside or commonly referred to as cypellogin A/B (**301**, **302** and **303**) were identified at t_R 48.7, 50.6 and 51.7 min with $C_{31}H_{34}O_{14}$ and *m/z* 629. Compounds **301** and **303** at t_R 48.7 and 51.7 min produced MS^2, MS^3 and MS^4 base peaks of *m/z* 463 [M-H-oleuropeoyl]$^-$, 301 [M-H-oleuropeoyl-Glc]$^-$ and 179 or 271 respectively and as secondary peak of 151 in MS^4. The presence of an intermediate fragment *m/z* 463 implied that there was no linkage between the oleuropeoyl group and hexoside. Compound **302** at t_R 50.6 min produced MS^2, MS^3 and MS^4 base peaks of *m/z* 301 [M-H-oleuropeoyl-Glc]$^-$, 179 and 151 respectively and a secondary peak of 271 in MS^3. The absence of an intermediate fragment *m/z* 463 implied that there was linkage between the oleuropeoyl group and hexoside.

11.2.24. Characterization of cypellogin C (M_r 632)

A peak at t_R 52.6 min with *m/z* 631 and $C_{31}H_{36}O_{14}$ was assigned as cypellogin C (**304**). It produced MS^2, MS^3 and MS^4 base peaks of *m/z* 301, 179 and 151 respectively and a secondary peak of 463 in MS^2.

11.2.25. Characterization of quercetin-3-(4"-*O*-acetyl)-*O*-rhamnoside-7-*O*-rhamnoside (M_r 636)

A peak at t_R 40.7 min with *m/z* 635 and $C_{29}H_{32}O_{16}$ was assigned as quercetin-3-(4"-*O*-acetyl)-*O*-rhamnoside-7-*O*-rhamnoside (**305**). It produced MS^2, MS^3 and MS^4 base peaks of *m/z* 489 [M-H-Rha]$^-$, 300 [M-H-Rha-acetyl-Rha]$^-$ and 271 respectively and a secondary peaks of 179 and 151 in MS^2. The presence of an intermediate fragment of *m/z* 489 suggested the absence of linkage between the two rhamnosides and that the acetylated rhamnoside was 3-*O*-glycosylated to quercetin.

11.2.26. Characterization of quercetin-*O*-feruloyl-hexoside (M_r 640)

Two isomers of quercetin-*O*-feruloyl-hexoside (**306-307**) were identified at t_R 47.4 and 50.9 min with $C_{31}H_{28}O_{15}$ and *m/z* 639. Both compounds produced an MS^2 base peak of *m/z* 463 [M-H-feruloyl]$^-$ and secondary peak of *m/z* 477 [M-H-Glc]$^-$. The fragment *m/z* 463 further fragmented into *m/z* 301 [M-H-feruloyl-Glc]$^-$ in MS^3 and *m/z* 179 and 151 in MS^4. The presence of an intermediate fragment of *m/z* 463 suggested the absence of linkage between the feruloyl group and hexoside and that the hexoside was 3-*O*-glycosulated to quercetin.

11.2.27. Characterization of quercetin-3-*O*-acetyl-hexoside-rhamnoside (M_r 652)

A peak at t_R 42.7 min with *m/z* 651 and $C_{29}H_{32}O_{17}$ was assigned as quercetin-3-*O*-acetyl-hexoside-rhamnoside (**308**). It produced an MS^2 base peak of *m/z* 591 and secondary peak of *m/z* 609. The fragment *m/z* 591 further fragmented into either *m/z* 300 or 301 [M-H-acetyl-Glc-Rha]$^-$ in MS^3 and *m/z* 271, 179 and 151 in MS^4.

11.2.28. Characterization of quercetin-*O*-sinapoyl-hexoside (M_r 670)

A peak at t_R 51.7 min with *m/z* 669 and $C_{32}H_{30}O_{16}$ was assigned as quercetin-*O*-sinapoyl-hexoside (**309**). It produced MS^2, MS^3 and MS^4 base peaks of *m/z* 300 or 301 [M-H-sinapoyl-

Glc]$^-$, 271 and 151 respectively and secondary peaks of 271 and 179 in MS^4. The absence of an intermediate fragment suggested that the sinapoyl group was attached to the hexoside.

11.3. Kaempferol and its derivatives

Kaempferol derivatives were identified based on their characteristic fragmentation peaks. The aglycon of kaempferol can be identified in MS^n by comparison with an authentic standard. In negative mode, kaempferol at *m/z* 285 (after a loss of hydrogen) fragments to give *m/z* 284, 257, 255 and 151.

11.3.1. Characterization of kaempferol (M_r 286)

A peak at t_R 49.5 min with *m/z* 285 and $C_{15}H_{10}O_6$ was assigned as kaempferol (**310**). It produced an MS^2 base peak of *m/z* 151 and secondary peak of 257 [M-H-CO]$^-$.

11.3.2. Characterization of kaempferol-*O*-pentoside (M_r 418)

Two isomers of kaempferol-*O*-pentoside (**311**-**312**) were identified at t_R 41.0 and 43.9 min with $C_{20}H_{18}O_{10}$ and *m/z* 417. The compounds produced an MS^2 base peak of either *m/z* 285 [M-H-Xyl]$^-$ or 284 [M-H-Xyl]$^{-\bullet}$, which further fragmented to give an MS^3 base peak of *m/z* 255 [M-H-Xyl-HCOH]$^-$.

11.3.3. Characterization of kaempferol-*O*-rhamnoside (M_r 432)

A peak at t_R 43.6 min with *m/z* 431 and $C_{21}H_{20}O_{10}$ was assigned as kaempferol-*O*-rhamnoside (**313**). It produced an MS^2 base peak of *m/z* 285 [M-H-Rha]$^-$ and secondary peak of *m/z* 284 [M-H-Rha]$^{-\bullet}$, The fragment *m/z* 285 further fragmented to give an MS^3 base peak of *m/z* 255 [M-H-Rha-HCOH]$^-$.

11.3.4. Characterization of kaempferol-*O*-hexoside (M_r 448)

Two isomers of kaempferol-*O*-hexoside (**314**-**315**) were identified at t_R 37.5 and 39.0 min with $C_{21}H_{20}O_{11}$ and *m/z* 447. The compounds produced an MS^2 base peak of either *m/z* 285 [M-H-Glc]$^-$ or 284 [M-H-Glu]$^{-\bullet}$, which further fragmented to give an MS^3 base peak of *m/z* 255 [M-H-Glc-HCOH]$^-$. The EIC of *m/z* 447 in *Rhododendron micranthum* in negative mode is shown in Figure 11.7, along with the MS^n spectra of compound **314** in Figure 11.8.

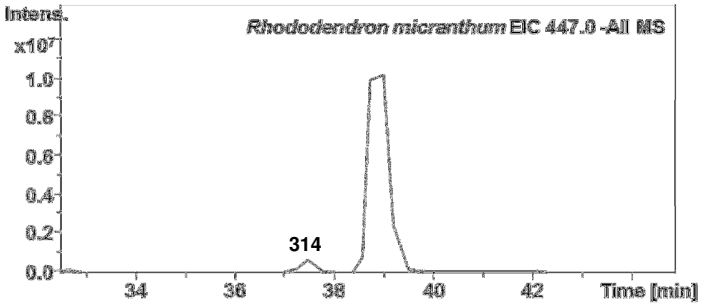

Figure 11.7: EIC of *m/z* 447 in *Rhododendron micranthum* in negative mode

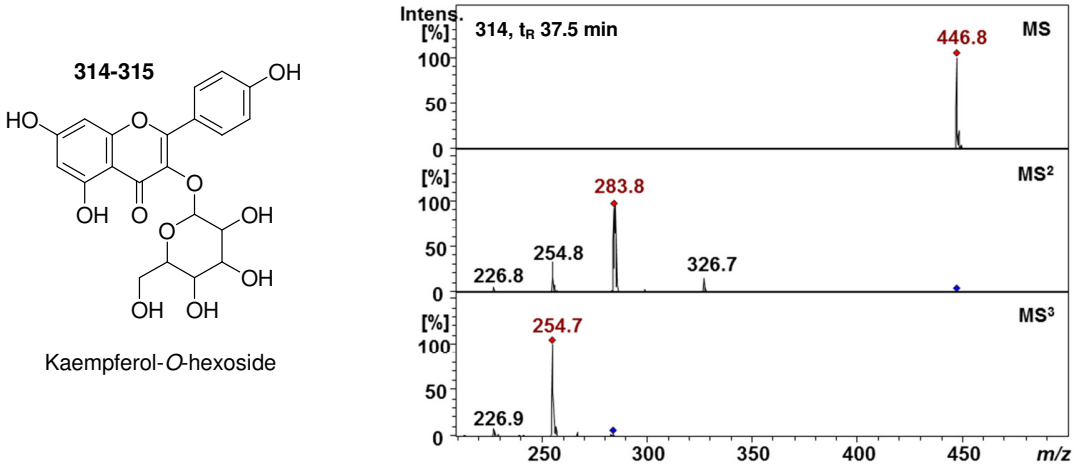

Figure 11.8: MS^n spectra of kaempferol-*O*-hexoside

11.3.5. Characterization of kaempferol-*O*-acetyl-pentoside (M_r 460)

Two isomers of kaempferol-*O*-acetyl-pentoside (**316-317**) were identified at t_R 47.6 and 50.1 min with $C_{22}H_{20}O_{11}$ and *m/z* 459. The compounds produced an MS^2 base peak of *m/z* 284 $[M\text{-}H\text{-}acetyl\text{-}Xyl]^{-\bullet}$, which further fragmented to give an MS^3 base peak of *m/z* 255 $[M\text{-}H\text{-}acetyl\text{-}Xyl\text{-}HCOH]^-$. The absence of an intermediate peak implied that there was linkage between the acetyl group and pentoside.

11.3.6. Characterization of kaempferol-*O*-glucuronide (M_r 462)

A peak at t_R 43.6 min with *m/z* 461 and $C_{21}H_{18}O_{12}$ was assigned as kaempferol-*O*-glucuronide (**318**). It produced an MS^2 base peak of *m/z* 285 $[M\text{-}H\text{-}Glu]^-$, which produced fragments of *m/z* 257 $[M\text{-}H\text{-}Glu\text{-}CO]^-$ and 151.

11.3.7. Characterization of kaempferol-*O*-acetyl-rhamnoside (M_r 474)

Two isomers of kaempferol-*O*-acetyl-rhamnoside (**319**-**320**) were identified at t_R 48.2 and 52.3 min with $C_{23}H_{22}O_{11}$ and *m/z* 473. The compounds produced an MS^2 base peak of *m/z* 285 [M-H-acetyl-Rha]$^-$, which further fragmented to give an MS^3 base peak of *m/z* 255 [M-H-acetyl-Rha-HCOH]$^-$. The absence of an intermediate peak implied that there was linkage between the acetyl group and rhamnoside.

11.3.8. Characterization of kaempferol-*O*-acetyl-hexoside (M_r 490)

Three isomers of kaempferol-*O*-acetyl-hexoside (**321**-**323**) were identified at t_R 44.5, 46.4 and 47.7 min with $C_{23}H_{22}O_{12}$ and *m/z* 489. The compounds produced an MS^2 base peak of *m/z* 285 [M-H-acetyl-Glc]$^-$, which further fragmented to give an MS^3 base peak of either *m/z* 257 [M-H-acetyl-Glc-CO]$^-$ or 255 [M-H-acetyl-Glc-HCOH]$^-$. The absence of an intermediate fragment implied there was linkage between the acetyl group and hexoside.

11.3.9. Characterization of kaempferol-*O*-diacetyl-hexoside (M_r 532)

A peak at t_R 55.0 min with *m/z* 531 and $C_{25}H_{24}O_{13}$ was assigned as kaempferol-*O*-diacetyl-hexoside (**324**). It produced an MS^2 base peak of *m/z* 285 [M-H-diacetyl-Glc]$^-$, which further fragmented to give an MS^3 base peak of *m/z* 255 [M-H-diacetyl-Glc-HCOH]$^-$. The absence of an intermediate fragment implied there was linkage between the diacetyl group and hexoside.

11.3.10. Characterization of kaempferol-*O*-rhamnoside-*O*-pentoside (M_r 564)

Three isomers of kaempferol-*O*-rhamnoside-*O*-pentoside (**325**-**327**) were identified at t_R 38.4, 41.0 and 43.4 min with $C_{26}H_{28}O_{14}$ and *m/z* 563. The compounds produced an MS^2 base peak of either *m/z* 285 [M-H-Rha-Xyl]$^-$ or 284 [M-H-Rha-Xyl]$^{-\bullet}$, which further fragmented into *m/z* 257 [M-H-Rha-Xyl-CO]$^-$ or 255 [M-H-Rha-Xyl-HCOH]$^-$. The presence of *m/z* 285 or 284 implied that there was linkage between the rhamnoside and pentoside.

11.3.11. Characterization of kaempferol-*O*-hydroxybenzoyl-hexoside (M_r 568)

A peak at t_R 45.7 min with *m/z* 567 and $C_{28}H_{24}O_{13}$ was assigned as kaempferol-*O*-hydroxybenzoyl-hexoside, which is an isomer of rugosaflavonoid C (**328**). It produced an MS^2 base peak of *m/z* 285 [M-H-hydroxybenzoyl-Glc]$^-$, which further fragmented to give an MS^3 base

peak of *m/z* 151 and secondary peak of 255 [M-H- hydroxybenzoyl-Glc-HCOH]$^-$. The absence of an intermediate fragment implied there was linkage between the hydroxybenzoyl group and hexoside.

11.3.12. Characterization of kaempferol-*O*-galloyl-pentoside (M_r 570)

A peak at t_R 47.1 min with *m/z* 569 and $C_{27}H_{22}O_{14}$ was assigned as kaempferol-*O*-galloyl-pentoside (**329**). It produced an MS^2 base peak of *m/z* 285 [M-H-galloyl-Xyl]$^-$, which further fragmented to give an MS^3 base peak of *m/z* 283 and secondary peak of *m/z* 257 [M-H-galloyl-Xyl-CO]$^-$. The absence of an intermediate fragment implied there was linkage between the galloyl group and pentoside.

11.3.13. Characterization of kaempferol-*O*-galloyl-rhamnoside (M_r 584)

A peak at t_R 47.9 min with *m/z* 583 and $C_{28}H_{24}O_{14}$ was assigned as kaempferol-*O*-galloyl-rhamnoside (**330**). It produced an MS^2 base peak of *m/z* 285 [M-H-galloyl-Rha]$^-$, which further fragmented to give an MS^3 base peak of *m/z* 257 [M-H-galloyl-Rha-CO]$^-$ and secondary peak of *m/z* 151. The absence of an intermediate fragment implied there was linkage between the galloyl group and rhamnoside.

11.3.14. Characterization of kaempferol-*O*-rhamnoside-*O*-hexoside (M_r 594)

Two isomers of kaempferol-*O*-rhamnoside-*O*-hexoside or kaempferol-*O*-rutinoside (**331**-**332**) were identified at t_R 33.5 and 38.9 min with $C_{27}H_{30}O_{15}$ and *m/z* 593. The compounds produced an MS^2 base peak of either *m/z* 285 [M-H-Rha-Glc]$^-$ or 284 [M-H-Rha-Glc]$^{-\bullet}$, which further fragmented into *m/z* 257 [M-H-Rha-Glc-CO]$^-$ or 255 [M-H-Rha-Glc-HCOH]$^-$. The presence of *m/z* 285 or 284 implied that there was linkage between the rhamnoside and hexoside.

11.3.15. Characterization of kaempferol-*O*-oleuropeoyl-hexoside or resinoside A/B (M_r 614)

A peak at t_R 51.9 min with *m/z* 613 and $C_{31}H_{34}O_{13}$ was tentatively assigned as kaempferol-*O*-oleuropeoyl-hexoside or commonly referred to as resinoside A/B (**333**). It produced an MS^2 base peak of *m/z* 285 [M-H-oleuropeoyl-Glc]$^-$, which further fragmented into *m/z* 257 [M-H-

oleuropeoyl-Glc-CO]$^-$. The absence of an intermediate fragment implied that there was linkage between the oleuropeoyl group and hexoside.

11.3.16. Characterization of kaempferol-3-*O*-(6''-acetyl-hexoside)-7-*O*-rhamnoside (M_r 636)

A peak at t_R 46.1 min with *m/z* 635 and $C_{29}H_{32}O_{16}$ was tentatively assigned as kaempferol-3-*O*-(6''-acetyl-hexoside)-7-*O*-rhamnoside (**334**). It produced MS^2, MS^3 and MS^4 base peaks of *m/z* 575, 285 [M-H-acetyl-Glc-Rha]$^-$ and 255 [M-H-acetyl-Glc-Rha-HCOH]$^-$ respectively.

11.4. Laricitrin and its derivatives

Laricitrin derivatives were identified based on their characteristic fragmentation peaks. In negative mode, the aglycon of laricitrin at *m/z* 331 (after a loss of hydrogen) fragments to give *m/z* 316, 271 and 151.

11.4.1. Characterization of laricitrin (M_r 332)

A peak at t_R 46.1 min with *m/z* 331 and $C_{16}H_{12}O_8$ was assigned as laricitrin (**335**). It produced an MS^2 base peak of *m/z* 316 [M-H-CH_3]$^-$, which fragmented into *m/z* 179 and 151.

11.4.2. Characterization of laricitrin-*O*-pentoside (M_r 464)

Three isomers of laricitrin-*O*-pentoside (**336-338**) were identified at t_R 39.7, 43.1 and 44.6 min with $C_{21}H_{20}O_{12}$ and *m/z* 463. The three isomers produced MS^2, MS^3 and MS^4 base peaks of *m/z* 331 [M-H-Xyl]$^-$, 316 [M-H-Xyl-CH_3]$^-$ and 271 respectively and secondary peaks of 179 and 151 in MS^4.

11.4.3. Characterization of laricitrin-*O*-rhamnoside (M_r 478)

A peak at t_R 40.6 min with *m/z* 477 and $C_{22}H_{22}O_{12}$ was assigned as laricitrin-*O*-rhamnoside (**339**). It produced MS^2, MS^3 and MS^4 base peaks of *m/z* 331 [M-H-Rha]$^-$, 316 [M-H-Rha-CH_3]$^-$ and 287 respectively and secondary peak of 271 in MS^4.

11.4.4. Characterization of laricitrin-*O*-hexoside (M_r 494)

Three isomers of laricitrin-*O*-hexoside (**340-342**) were identified at t_R 36.8, 40.1 and 46.2 min with $C_{22}H_{22}O_{13}$ and *m/z* 493. The compounds produced MS^2, MS^3 and MS^4 base peaks of *m/z* 331 $[M-H-Glc]^-$, 316 $[M-H-Glc-CH_3]^-$ and either 287 or 271 respectively. The EIC of *m/z* 493 in *Rhododendron annae* in negative mode is shown in Figure 11.9, along with the MS^n spectra of compound **342** in Figure 11.10.

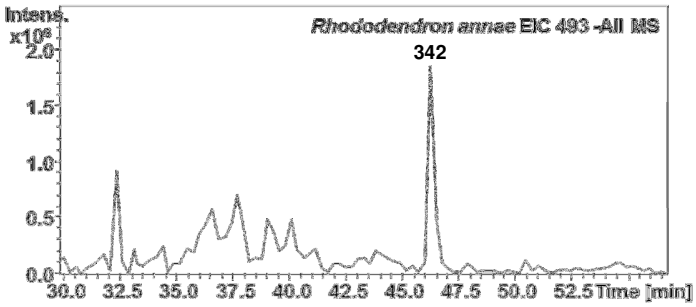

Figure 11.9: EIC of *m/z* 493 in *Rhododendron annae* in negative mode

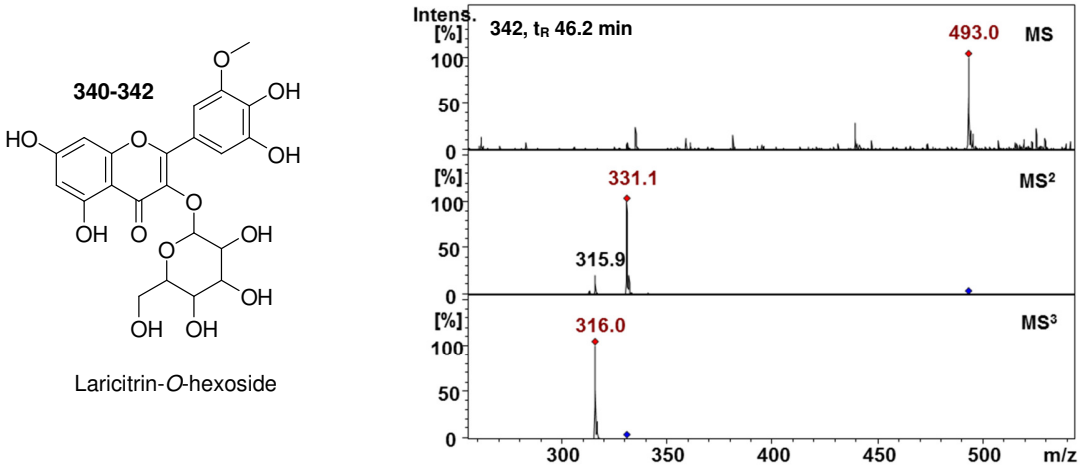

Figure 11.10: MS^n spectra of laricitrin-*O*-hexoside

11.4.5. Characterization of laricitrin-*O*-glucuronide (M_r 508)

A peak at t_R 42.7 min with *m/z* 507 and $C_{22}H_{20}O_{14}$ was assigned as laricitrin-*O*-glucuronide (**343**). It produced MS^2, MS^3 and MS^4 base peaks of *m/z* 331 $[M-H-Glu]^-$, 316 $[M-H-Glu-CH_3]^-$ and 179 respectively and secondary peaks of 271 and 151 in MS^4.

11.4.6. Characterization of laricitrin-*O*-coumaroyl-rhamnoside (M_r 624)

A peak at t_R 55.5 min with *m/z* 623 and $C_{31}H_{28}O_{14}$ was assigned as laricitrin-*O*-coumaroyl-rhamnoside (**344**). It produced MS^2, MS^3 and MS^4 base peaks of *m/z* 331 [M-H-coumaroyl-Rha]$^-$, 316 [M-H-coumaroyl-Rha-CH_3]$^-$ and 271 respectively. The absence of an intermediate fragment implied that the coumaroyl group was attached to rhamnoside.

11.4.7. Characterization of laricitrin-*O*-rhamnoside-*O*-hexoside (M_r 640)

A peak at t_R 36.8 min with *m/z* 639 and $C_{28}H_{32}O_{17}$ was assigned as laricitrin-*O*-rhamnoside-*O*-hexoside or laricitrin-*O*-rutinoside (**345**). It produced MS^2, MS^3 and MS^4 base peaks of *m/z* 331 [M-H-Rha-Glc]$^-$, 316 [M-H-Rha-Glc-CH_3]$^-$ and 271 respectively and secondary peaks of 179 and 151 in MS^3. The absence of an intermediate fragment implied that rhamnoside was linked to hexoside.

11.4.8. Characterization of laricitrin-*O*-coumaroyl-hexoside (M_r 640)

Two isomers of laricitrin-*O*-coumaroyl-hexoside (**346**-**347**) were identified at t_R 48.2 and 50.4 min with $C_{31}H_{28}O_{15}$ and *m/z* 639. Compound **346** at t_R 48.2 min produced MS^2 and MS^3 base peaks of *m/z* 331 [M-H-coumaroyl-Glc]$^-$ and 316 [M-H-coumaroyl-Glc-CH_3]$^-$ respectively and a secondary peak of 493 in MS^2. The presence of an intermediate fragment *m/z* 493 as a secondary peak implied that there was presence of linkage between the coumaroyl group and hexoside. Compound **347** at t_R 50.4 min produced MS^2, MS^3 and MS^4 base peaks of *m/z* 493 [M-H-coumaroyl]$^-$, 331 [M-H-coumaroyl-Glc]$^-$ and 316 [M-H-coumaroyl-Glc-CH_3]$^-$ respectively. The presence of an intermediate fragment *m/z* 493 implied that there was absence of linkage between the coumaroyl group and hexoside.

11.5. Isorhamnetin and its derivatives

Isorhamnetin derivatives were identified based on their characteristic fragmentation peaks. The aglycon of isorhamnetin can be identified in MS^n by comparison with an authentic standard. In negative mode, isorhamnetin at *m/z* 315 (after a loss of hydrogen) fragments to give *m/z* 300, 271 and 255.

11.5.1. Characterization of isorhamnetin-*O*-glucuronide (M_r 492)

A peak at t_R 45.2 min with *m/z* 491 and $C_{22}H_{20}O_{13}$ was assigned as isorhamnetin-*O*-glucuronide (**348**). It produced MS^2, MS^3 and MS^4 base peaks of *m/z* 315 $[M-H-Glu]^-$, 300 $[M-H-Glu-CH_3]^-$ and 271 respectively and a secondary peak of 255 in MS^4. The EIC of *m/z* 491 in *Rhododendron beesianum* in negative mode is shown in Figure 11.11, along with the MS^n spectra of compound **348** in Figure 11.12.

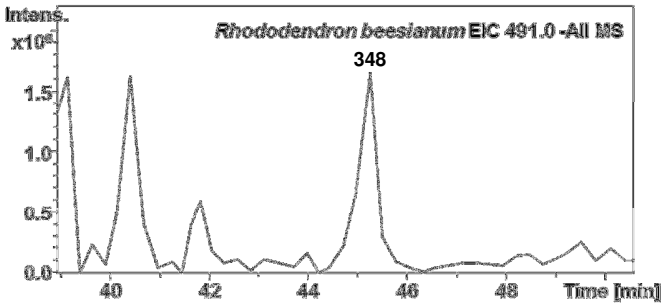

Figure 11.11: EIC of *m/z* 491 in *Rhododendron beesianum* in negative mode

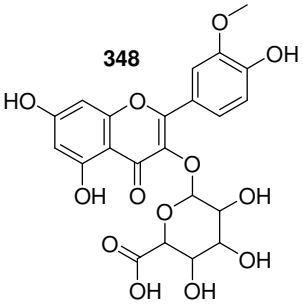

Isorhamnetin-*O*-glucuronide

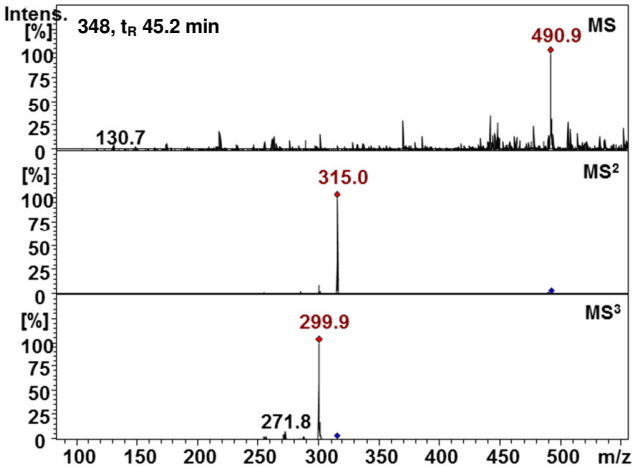

Figure 11.12 MS^n spectra of isorhamnetin-*O*-glucuronide

12. Derivatives

Some novel compounds were observed in *Rhododendron* leaves, which were not identified in literature. Since the complete assignment of the compound structures could not be determined based on MS data only, they are assigned as derivatives of specific groups and substituents.

The derivatives of quinic acid and hydroxycinnamic acids of selected *Rhododendron* species have been used in a manuscript to be submitted soon.

12.1. Quinic acid derivatives

Three derivatives of quinic acid (**349-351**) were observed. One peak was observed at *m/z* 329 ($C_{14}H_{18}O_9$ at t_R 18.9 min) and *m/z* 371 ($C_{16}H_{20}O_{10}$ at t_R 6.4 min), while two peaks were observed for *m/z* 385 ($C_{16}H_{18}O_{11}$ at t_R 10.5 and 12.3 min). All of the compounds produced a base peak of *m/z* 191 in either MS^2 or MS^3, which is characteristic for a quinic acid.

12.2. Hydroxycinnamic acid derivatives

12.2.1. Caffeic acid derivatives

Ten derivatives of caffeic acid (**352-361**) were observed. Two peaks were observed at *m/z* 299 ($C_{17}H_{16}O_5$ at t_R 47.3 and 56.9 min) and at *m/z* 461 ($C_{23}H_{26}O_{10}$ at t_R 39.2 and 47.5 min), one peak at *m/z* 475 ($C_{23}H_{24}O_{11}$ at t_R 43.2 min), *m/z* 503 ($C_{25}H_{28}O_{11}$ at t_R 55.4 min), *m/z* 515 ($C_{22}H_{28}O_{14}$ at t_R 10.0 min), two peaks at *m/z* 551 ($C_{25}H_{28}O_{14}$ at t_R 28.0 and 29.8 min) and a peak at *m/z* 593 ($C_{28}H_{34}O_{14}$ at t_R 46.2 min). The compounds produced an MS^2 or MS^3 base peak of *m/z* 179, which further fragmented into *m/z* 135. This is a typical fragmentation pattern for caffeic acid.

12.2.2. *p*-Coumaric acid derivatives

Three *p*-coumaric acid derivatives (**362-364**) were observed. One peak was observed at *m/z* 329 ($C_{18}H_{18}O_6$ at t_R 44.4 min), *m/z* 519 ($C_{25}H_{28}O_{12}$ at t_R 45.8 min) and *m/z* 663 ($C_{31}H_{36}O_{16}$ at t_R 37.7 min). They produced an MS^2 or MS^3 base peak of *m/z* 163, which further fragmented into *m/z* 119. This fragmentation pattern is observed for *p*-coumaric acid derivatives.

12.2.3. Ferulic acid derivatives

Two derivatives of ferulic acid (**365-366**) were observed. One peak was observed at *m/z* 313 ($C_{13}H_{14}O_9$ at t_R 11.5 min) and *m/z* 431 ($C_{21}H_{20}O_{10}$ at t_R 50.5 min). Both derivatives produced MS^2 and MS^3 base peak of *m/z* 193 and 149 respectively, which is usually observed in ferulic acid derivatives.

12.2.4. Dihydrocoumaric acid derivatives

Three dihydrocoumaric acid derivatives (**367-369**) were observed based on their characteristic fragmentation pattern. Three peaks were observed at *m/z* 345 with $C_{15}H_{22}O_9$ at t_R 4.4, 9.0 and 11.3 min. All three compounds produced MS^2 and MS^3 base peak of *m/z* 265 and 121 respectively.

12.3. Hydroxybenzoic acid derivatives

12.3.1. Gallic acid derivatives

Eleven derivatives of gallic acid (**370-380**) were observed. One peak was observed at *m/z* 305 ($C_{15}H_{14}O_7$ at t_R 34.4 min), *m/z* 341 ($C_{15}H_{18}O_9$ at t_R 8.5 min), *m/z* 345 ($C_{14}H_{18}O_{10}$ at t_R 10.5 min), *m/z* 419 ($C_{16}H_{20}O_{13}$ at t_R 6.8 min), two peaks at *m/z* 451 ($C_{21}H_{24}O_{11}$ at t_R 23.9 min and $C_{20}H_{20}O_{12}$ at t_R 26.6 min), and one peak at *m/z* 453 ($C_{20}H_{22}O_{12}$ at t_R 23.3 min), *m/z* 477 ($C_{21}H_{18}O_{13}$ at t_R 23.8 min), *m/z* 497 ($C_{21}H_{22}O_{14}$ at t_R 25.3 min), *m/z* 609 ($C_{30}H_{26}O_{14}$ at t_R 10.2 min) and *m/z* 619 ($C_{28}H_{28}O_{16}$ at t_R 22.1 min). All compounds produced an MS^2 or MS^3 base peak of *m/z* 169, which further fragmented into *m/z* 125. This is a fragmentation pattern observed for gallic acid derivatives.

12.3.2. Protocatechuic acid derivatives

Three protocatechuic acid derivatives (**381-383**) were observed. Two peaks were observed at *m/z* 313 ($C_{13}H_{14}O_9$ at t_R 12.0 and 15.2 min) and one peak was at *m/z* 487 ($C_{21}H_{28}O_{13}$ at t_R 46.3 min). The compounds produced an MS^2 or MS^3 base peak of *m/z* 153, which further fragmented into *m/z* 109. This fragmentation pattern is observed in protocatechuic acid derivatives.

12.3.3. Salicylic acid derivatives

Six derivatives of salicylic acid (**384-389**) were observed based on their characteristic fragmentation pattern. One peak was observed at *m/z* 301 ($C_{13}H_{18}O_8$ at t_R 6.0 min), *m/z* 343 ($C_{15}H_{20}O_9$ at t_R 12.0 min), *m/z* 345 ($C_{15}H_{22}O_9$ at t_R 8.2 min), *m/z* 391 ($C_{19}H_{20}O_9$ at t_R 31.0 min), *m/z* 419 ($C_{21}H_{24}O_9$ at t_R 37.9 min) and *m/z* 447 ($C_{21}H_{36}O_{10}$ at t_R 41.1 min). The compounds produced an MS^2 or MS^3 base peak of *m/z* 137, which further fragmented into *m/z* 93.

12.3.4. Vanillic acid derivatives

Three vanillic acid derivatives (**390-392**) were observed. One peak was observed at *m/z* 273 ($C_{15}H_{14}O_5$ at t_R 47.5 min), *m/z* 327 ($C_{14}H_{16}O_9$ at t_R 17.8 min) and *m/z* 537 ($C_{21}H_{30}O_{16}$ at t_R 6.8 min). They produced an MS^2 or MS^3 base peak of *m/z* 167, which further fragmented into either *m/z* 152, 149 or 123. This fragmentation pattern is usually observed for vanillic acid derivatives.

12.3.5. Methyl gallate derivatives

Four derivatives of methyl gallate (**393-396**) were observed. Two peaks were observed at *m/z* 467 ($C_{21}H_{24}O_{12}$ at t_R 30.2 and 31.0 min) and one peak was observed at *m/z* 471 ($C_{23}H_{20}O_{11}$ at t_R 28.4 min) and *m/z* 509 ($C_{23}H_{26}O_{13}$ at t_R 46.0 min). The compounds produced an MS^2 or MS^3 base peak of *m/z* 183, which further fragmented into *m/z* 168, 139 and 124. This fragmentation is observed in methyl gallate derivatives.

12.4. Flavan-3-ol derivatives

12.4.1. (Epi)catechin derivatives

Six (epi)catechin derivatives (**397-402**) were observed based on their fragmentation patter being similar to (epi)catechin or proanthocyanidins. Two peaks were observed at *m/z* 387 ($C_{21}H_{24}O_7$ at t_R 40.3 and 45.0 min) and one peak was observed at *m/z* 493 ($C_{23}H_{26}O_{12}$ at t_R 25.0 min), *m/z* 591 ($C_{30}H_{24}O_{13}$ at t_R 23.8 min), *m/z* 697 ($C_{37}H_{30}O_{14}$ at t_R 29.0 min) and *m/z* 879 ($C_{45}H_{36}O_{19}$ at t_R 20.3 min). Three compounds (**396-398**) produced an MS^2 base peak of *m/z* 289, which further fragmented into *m/z* 245 and 205. The other three compounds produced fragments such as *m/z* 575, 451, 407, 289 and 285, which are observed in the fragmentation of proanthocyanidins.

12.5. Flavonol derivatives

12.5.1. Quercetin derivatives

Six derivatives of quercetin (**403-408**) were observed. Two peaks were observed at *m/z* 547 ($C_{26}H_{28}O_{13}$ at t_R 46.0 and 48.2 min), one peak at *m/z* 597 ($C_{29}H_{26}O_{14}$ at t_R 50.9 min), *m/z* 629 ($C_{29}H_{26}O_{16}$ at t_R 39.5 min) and two peaks at *m/z* 643 ($C_{30}H_{28}O_{16}$ at t_R 45.0 and 46.9 min). The compounds produced an MS^2 or MS^3 base peak of either *m/z* 301 or 300, which further fragmented into *m/z* 271, 179 and 151. This fragmentation is characteristic for quercetin derivatives.

12.6. Other derivatives

A peak with *m/z* 357 was observed at 19.7 min with $C_{16}H_{22}O_9$. It was tentatively assigned as an isomer of glucoacetosyringone (**409**).

13. Polyphenol distribution in *Rhododendron*

Different classes of polyphenols were identified in the *Rhododendron* leaf extracts using LC-Ion Trap-MS and LC-TOF-MS data in negative mode. The identification was based on the molecular formula generated from their high resolution mass data, fragmentation pattern, retention time and UV absorption. Authentic standards were used to compare retention time and fragmentation pattern. The number of individual *Rhododendron* species, in which the compounds were identified, was tallied based on their subgenera in order to study the polyphenol distribution over the different subgenera of *Rhododendron* species.

The compounds identified in the *Rhododendron* species along with their molecular formula, parent ion in negative mode and retention time are shown in Table 13.1 along with the distribution among the different subgenera of *Rhododendron*. The detailed information of the compounds identified in individual *Rhododendron* species is given in the CD (Appendix: Additional Information on CD).

The twenty compounds which were found in the most number of *Rhododendron* species from the LC-Ion Trap-MS and LC-TOF-MS data were quercetin-*O*-hexoside (t_R 34.2 min), quercetin-*O*-hexoside (t_R 35.5 min), quercetin-*O*-pentoside (t_R 41.2 min), quercetin-*O*-rhamnoside (t_R 38.7 min), protocatechuic acid-*O*-hexoside (t_R 10.5 min), catechin (t_R 16.0 min), procyanidin dimer B (t_R 20.3 min), quercetin-*O*-pentoside (t_R 37.4 min), kaempferol-*O*-rhamnoside (t_R 43.6 min), procyanidin dimer B1 (t_R 13.4 min), quercetin (t_R 44.4 min), *p*-coumaric acid-*O*-hexoside (t_R 16.5 min), 3-*O*-caffeoylquinic acid (t_R 13.0 min), epicatechin (t_R 23.0 min), quercetin-*O*-pentoside (t_R 36.6 min), procyanidin dimer B (t_R 14.3 min), 5-*O*-caffeoylquinic acid (t_R 18.2 min), A-type procyanidin dimer (t_R 32.4 min), quercetin-*O*-glucuronide (t_R 40.8 min) and A-type procyanidin dimer (t_R 27.2 min).

Table 13.1: Compounds identified in different *Rhododendron* subgenera

No.	Compounds found in the six subgenera	Reference	Molecular Formula	Parent Ion $[M-H]^-$ *m/z*	RT min	Subgenus / No. of species in which the compounds were identified						Total
						Rhododendron	*Hymenanthes*	*Pentanthera*	*Azaleastrum*	*Tsutsusi*	*Mumeazalea*	
	Number of Species					**44**	**33**	**13**	**3**	**6**	**1**	**100**
	Compound											
	Hydroxycinnamic Acids											
	1. Chlorogenic Acids											
1	3-*O*-*p*-Coumaroylquinic acid	[98]	$C_{16}H_{18}O_8$	**337.0923**	18.0	22	13	4	0	4	0	43
2	*cis*-3-*O*-*p*-Coumaroylquinic acid	[98]	$C_{16}H_{18}O_8$	**337.0915**	19.4	14	8	5	0	3	0	30
3	5-*O*-*p*-Coumaroylquinic acid	[98]	$C_{16}H_{18}O_8$	**337.0923**	24.6	17	7	7	1	3	0	35
4	4-*O*-*p*-Coumaroylquinic acid	[98]	$C_{16}H_{18}O_8$	**337.0917**	26.6	8	2	4	0	2	0	16
5	*cis*-5-*O*-*p*-Coumaroylquinic acid	[98]	$C_{16}H_{18}O_8$	**337.0928**	28.4	17	8	7	0	5	0	37
6	3-*O*-Caffeoylquinic acid	[98]	$C_{16}H_{18}O_9$	**353.0876**	13.0	33	17	5	0	6	0	61
7	*cis*-3-*O*-Caffeoylquinic acid	[98]	$C_{16}H_{18}O_9$	**353.0861**	14.0	16	2	3	0	2	0	23
8	5-*O*-Caffeoylquinic acid	[98]	$C_{16}H_{18}O_9$	**353.0877**	18.2	31	11	6	1	5	0	54
9	*cis*-4-*O*-Caffeoylquinic acid	[98]	$C_{16}H_{18}O_9$	**353.0861**	20.6	9	0	3	0	0	0	12
10	4-*O*-Caffeoylquinic acid	[98]	$C_{16}H_{18}O_9$	**353.0865**	23.0	22	1	5	0	3	0	31
11	*cis*-5-*O*-Caffeoylquinic acid	[98]	$C_{16}H_{18}O_9$	**353.0862**	24.1	6	0	2	0	1	0	9

No.	Compounds found in the six subgenera	Reference	Molecular Formula	Parent Ion [M-H]⁻ *m/z*	RT min	Subgenus / No. of species in which the compounds were identified						Total
						Rhododendron	*Hymenanthes*	*Pentanthera*	*Azaleastrum*	*Tsutsusi*	*Mumeazalea*	
	Number of Species					**44**	**33**	**13**	**3**	**6**	**1**	**100**
	Compound											
12	3-*O*-Feruloylquinic acid	[98]	$C_{17}H_{20}O_9$	**367.1035**	21.7	16	4	2	0	1	0	23
13	5-*O*-Feruloylquinic acid	[98]	$C_{17}H_{20}O_9$	**367.1017**	27.5	3	0	1	0	2	0	6
14	4-*O*-Feruloylquinic acid	[98]	$C_{17}H_{20}O_9$	**367.1024**	31.6	2	0	0	0	0	0	2
15	3-*O*-hydroxydihydro-Caffeoylquinic acid	[99]	$C_{16}H_{20}O_{10}$	**371.0987**	5.9	0	0	1	0	0	0	1
16	5-*O*-hydroxydihydro-Caffeoylquinic acid	[99]	$C_{16}H_{20}O_{10}$	**371.1001**	5.4	0	0	0	0	2	0	2
17	5-*O*-hydroxydihydro-Caffeoylquinic acid	[99]	$C_{16}H_{20}O_{10}$	**371.0999**	7.0	5	0	1	0	1	0	7
18	4-*O*-hydroxydihydro-Caffeoylquinic acid	[99]	$C_{16}H_{20}O_{10}$	**371.0969**	9.8	0	0	1	0	0	0	1
19	4-*O*-hydroxydihydro-Caffeoylquinic acid	[99]	$C_{16}H_{20}O_{10}$	**371.0974**	10.8	0	0	1	0	0	0	1
	2. Caffeic acid derivatives											
20	Caffeoylthreonate	[100]	$C_{13}H_{14}O_8$	**297.0609**	15.5	7	0	2	0	3	0	12
21	Caffeoylthreonate	[100]	$C_{13}H_{14}O_8$	**297.0607**	23.7	3	0	0	0	0	0	3
22	Teucrol	[101]	$C_{17}H_{16}O_6$	**315.0861**	51.0	0	0	1	0	0	0	1
23	Caffeoylshikimic acid	[98]	$C_{16}H_{16}O_8$	**335.0756**	24.6	10	0	5	0	3	0	18
24	Caffeic acid-*O*-hexoside	[102]	$C_{15}H_{18}O_9$	**341.0878**	8.1	0	1	0	0	0	0	1
25	Caffeic acid-*O*-hexoside	[102]	$C_{15}H_{18}O_9$	**341.0862**	9.2	0	1	0	0	0	0	1
26	Caffeic acid-*O*-hexoside	[102]	$C_{15}H_{18}O_9$	**341.0866**	10.9	0	2	1	0	0	0	3

No.	Compounds found in the six subgenera	Reference	Molecular Formula	Parent Ion $[M-H]^-$ *m/z*	RT min	Subgenus / No. of species in which the compounds were identified						Total
						Rhododendron	*Hymenanthes*	*Pentanthera*	*Azaleastrum*	*Tsutsusi*	*Mumeazalea*	
	Number of Species					**44**	**33**	**13**	**3**	**6**	**1**	**100**
	Compound											
27	Caffeic acid-*O*-hexoside	[102]	$C_{15}H_{18}O_9$	**341.0863**	12.5	3	2	3	0	1	0	9
28	Caffeic acid-*O*-hexoside	[102]	$C_{15}H_{18}O_9$	**341.0866**	13.9	0	1	2	0	0	0	3
29	Caffeic acid-*O*-hexoside	[102]	$C_{15}H_{18}O_9$	**341.0895**	15.1	1	12	0	2	2	0	17
30	Caffeic acid-*O*-hexoside	[102]	$C_{15}H_{18}O_9$	**341.0861**	17.6	7	4	2	0	0	0	13
31	Caffeic acid-*O*-hexoside	[102]	$C_{15}H_{18}O_9$	**341.0866**	19.2	0	1	0	0	0	0	1
32	Teucrol-*O*-hexoside / Plantainoside	[103]	$C_{23}H_{26}O_{11}$	**477.1409**	42.0	0	0	1	0	0	0	1
	3. p-Coumaric acid derivatives											
33	*p*-Coumaric acid-*O*-shikimate	[102]	$C_{16}H_{16}O_7$	**319.0811**	30.8	0	0	1	0	0	0	1
34	*p*-Coumaric acid-*O*-hexoside	[102]	$C_{15}H_{18}O_8$	**325.0920**	15.7	1	4	0	0	0	0	5
35	*p*-Coumaric acid-*O*-hexoside	[102]	$C_{15}H_{18}O_8$	**325.0913**	16.5	26	20	10	3	5	1	65
36	*p*-Coumaric acid-*O*-hexoside	[102]	$C_{15}H_{18}O_8$	**325.0920**	24.1	1	6	1	0	0	0	8
37	*p*-Coumaric acid-*O*-hexoside	[102]	$C_{15}H_{18}O_8$	**325.0916**	26.2	0	3	0	0	0	0	3
38	*p*-Coumaric acid-*O*-glucosyl ester	[104]	$C_{15}H_{18}O_8$	**325.0922**	17.5	2	0	1	0	0	0	3
39	*p*-Coumaric acid-*O*-glucosyl ester	[104]	$C_{15}H_{18}O_8$	**325.0916**	18.7	0	0	1	0	0	0	1
40	*p*-coumaric acid-*O*-hexoside-*O*-pentoside	[105]	$C_{20}H_{26}O_{12}$	**457.1352**	17.6	0	0	0	0	0	1	1

No.	Compounds found in the six subgenera	Reference	Molecular Formula	Parent Ion $[M-H]^-$ *m/z*	RT min	Subgenus / No. of species in which the compounds were identified						Total
						Rhododendron	*Hymenanthes*	*Pentanthera*	*Azaleastrum*	*Tsutsusi*	*Mumeazalea*	
	Number of Species					**44**	**33**	**13**	**3**	**6**	**1**	**100**
	Compound											
41	*p*-coumaric acid-*O*-hexoside-*O*-pentoside	[105]	$C_{20}H_{26}O_{12}$	**457.1364**	19.2	1	0	0	0	0	0	1
42	Everlastoside M	[106]	$C_{22}H_{26}O_{12}$	**481.1362**	27.0	0	1	0	0	0	0	1
43	*p*-coumaric acid-*O*-dihexoside	[107]	$C_{21}H_{28}O_{13}$	**487.1471**	14.4	0	1	0	0	0	0	1
44	*p*-coumaric acid-*O*-dihexoside	[107]	$C_{21}H_{28}O_{13}$	**487.1481**	20.0	1	0	0	0	0	0	1
	4. Dihydro-coumaric acid derivatives											
45	Dihydrocoumaric acid-*O*-hexoside	[108]	$C_{15}H_{20}O_8$	**327.1069**	15.5	3	0	0	0	0	0	3
46	Dihydrocoumaric acid-*O*-hexoside	[108]	$C_{15}H_{20}O_8$	**327.1076**	20.4	1	3	0	0	0	0	4
	5. Ferulic acid derivatives											
47	Ferulic acid-*O*-hexoside	[102]	$C_{16}H_{20}O_9$	**355.1018**	19.0	2	1	2	0	0	0	5
48	Ferulic acid-*O*-hexoside	[102]	$C_{16}H_{20}O_9$	**355.1018**	20.4	2	1	0	0	0	0	3
49	Ferulic acid-*O*-hexoside	[102]	$C_{16}H_{20}O_9$	**355.1021**	21.2	1	3	3	0	0	0	7
50	Ferulic acid-*O*-glucosyl ester	[102]	$C_{16}H_{20}O_9$	**355.1019**	28.9	1	0	0	0	0	0	1
51	Ferulic acid-*O*-dihexoside	[109]	$C_{22}H_{30}O_{14}$	**517.1576**	17.2	0	0	0	0	1	0	1
	Hydroxybenzoic Acids											
	1. Gallic Acid derivatives											

No.	Compounds found in the six subgenera	Reference	Molecular Formula	Parent Ion $[M-H]^-$ *m/z*	RT min	Subgenus / No. of species in which the compounds were identified						Total
						Rhododendron	*Hymenanthes*	*Pentanthera*	*Azaleastrum*	*Tsutsusi*	*Mumeazalea*	
	Number of Species					**44**	**33**	**13**	**3**	**6**	**1**	**100**
	Compound											
52	Gallic acid-*O*-pentoside	[110]	$C_{12}H_{14}O_9$	**301.0570**	6.6	5	2	0	2	0	0	9
53	3-*O*-Galloylshikimic acid / 5-*O*-Galloylshikimic acid	[111]	$C_{14}H_{14}O_9$	**325.0549**	8.9	1	1	1	1	0	0	4
54	3-*O*-Galloylshikimic acid / 5-*O*-Galloylshikimic acid	[111]	$C_{14}H_{14}O_9$	**325.0557**	9.6	1	3	0	1	0	0	5
55	Gallic acid-*O*-hexoside	[112]	$C_{13}H_{16}O_{10}$	**331.0670**	4.6	10	15	3	2	0	1	31
56	Gallic acid-*O*-hexoside	[112]	$C_{13}H_{16}O_{10}$	**331.0668**	7.9	11	14	2	0	0	0	27
57	Gallic acid-*O*-glucosyl ester	[112]	$C_{13}H_{16}O_{10}$	**331.0677**	3.7	4	6	2	0	0	0	12
58	Galloylquinic acid	[113, 114]	$C_{14}H_{16}O_{10}$	**343.0664**	4.3	0	3	1	1	0	1	6
59	Galloylquinic acid	[113, 114]	$C_{14}H_{16}O_{10}$	**343.0656**	5.8	0	2	1	1	0	0	4
60	Galloylquinic acid	[113, 114]	$C_{14}H_{16}O_{10}$	**343.0687**	9.6	0	1	0	0	0	0	1
61	Gallic acid-*O*-acetyl-hexoside	[115]	$C_{15}H_{18}O_{11}$	**373.0758**	13.9	0	1	0	0	0	0	1
62	Benzyl-6'-*O*-galloyl-β-D-hexoside	[116]	$C_{20}H_{22}O_{10}$	**421.1138**	32.1	0	1	0	0	0	0	1
63	Galloylarbutin	[117]	$C_{19}H_{20}O_{11}$	**423.0926**	11.7	0	0	0	1	0	0	1
64	Galloylarbutin	[117]	$C_{19}H_{20}O_{11}$	**423.0946**	17.7	0	3	0	0	0	0	3
65	6-galloyl-1-*O*-(phloroglucinol)-hexoside	[118]	$C_{19}H_{20}O_{12}$	**439.0890**	15.0	0	1	0	0	0	0	1

No.	Compounds found in the six subgenera	Reference	Molecular Formula	Parent Ion $[M-H]^-$ *m/z*	RT min	Subgenus / No. of species in which the compounds were identified						Total
						Rhododendron	*Hymenanthes*	*Pentanthera*	*Azaleastrum*	*Tsutsusi*	*Mumeazalea*	
	Number of Species					**44**	**33**	**13**	**3**	**6**	**1**	**100**
	Compound											
66	Gallic acid-3-*O*-hexoside-4-*O*-pentoside	[119]	$C_{18}H_{24}O_{14}$	**463.1072**	7.9	1	0	0	1	0	0	2
67	*p*-hydroxyphenethyl alcohol-1-*O*-β-D-(6"-*O*-galloyl)-hexoside	[120]	$C_{21}H_{24}O_{12}$	**467.1197**	22.3	0	3	0	1	0	0	4
68	Gallic acid-*O*-galloyl-rhamnoside	[121]	$C_{20}H_{20}O_{13}$	**467.0845**	36.6	0	1	0	0	0	0	1
69	Gallic acid-*O*-rutinoside	[122]	$C_{19}H_{26}O_{14}$	**477.1267**	6.6	1	0	0	0	0	0	1
70	Gallic acid-*O*-coumaroyl-hexoside	[123]	$C_{22}H_{22}O_{12}$	**477.1041**	31.0	0	0	0	1	0	0	1
71	Gallic acid-*O*-coumaroyl-hexoside	[123]	$C_{22}H_{22}O_{12}$	**477.1057**	32.6	0	0	0	1	0	0	1
72	Gallic acid-*O*-coumaroyl-hexoside	[123]	$C_{22}H_{22}O_{12}$	**477.1039**	35.9	0	2	0	1	0	0	3
73	Querglanin	[124]	$C_{23}H_{28}O_{11}$	**479.1571**	31.9	0	3	0	0	0	0	3
74	Galloyl-*O*-vanilloyl-*O*-hexoside	[111]	$C_{21}H_{22}O_{13}$	**481.1012**	27.1	0	1	0	0	0	0	1
75	Galloyl-*O*-vanilloyl-*O*-hexoside	[111]	$C_{21}H_{22}O_{13}$	**481.1004**	30.1	1	0	0	0	0	0	1
76	Gallic acid-3-*O*-(6'-*O*-galloyl)-β-D-hexoside	[125]	$C_{20}H_{20}O_{14}$	**483.0798**	22.5	1	0	0	0	0	0	1
77	Gallic acid-*O*-dihexoside	[126]	$C_{19}H_{26}O_{15}$	**493.1223**	3.2	0	1	0	0	0	0	1
78	Gallic acid-*O*-dihexoside	[126]	$C_{19}H_{26}O_{15}$	**493.1209**	5.2	0	10	1	0	0	1	12

No.	Compounds found in the six subgenera	Reference	Molecular Formula	Parent Ion $[M-H]^-$ *m/z*	RT min	Subgenus / No. of species in which the compounds were identified						Total
						Rhododendron	*Hymenanthes*	*Pentanthera*	*Azaleastrum*	*Tsutsusi*	*Mumeazalea*	
	Number of Species					**44**	**33**	**13**	**3**	**6**	**1**	**100**
	Compound											
79	Gallic acid-*O*-dihexoside	[122]	$C_{19}H_{26}O_{15}$	**493.1202**	6.7	0	2	0	0	0	0	2
80	Gallic acid-*O*-feruloyl-hexoside	-	$C_{23}H_{24}O_{13}$	**507.1123**	36.2	0	1	0	0	0	0	1
81	Hyemaloside B / Guavinoside A	[127, 128]	$C_{26}H_{24}O_{13}$	**543.1163**	30.9	0	0	0	1	0	0	1
82	Galloylalbiflorin	[129]	$C_{30}H_{32}O_{15}$	**631.1655**	42.8	0	1	0	0	0	0	1
	2. Protocatechuic acid derivatives											
83	Protocatechuic acid-*O*-pentoside	[130]	$C_{12}H_{14}O_8$	**285.0606**	15.1	4	4	0	1	2	0	11
84	Protocatechuic acid-*O*-hexoside	[131]	$C_{13}H_{16}O_9$	**315.0707**	5.9	6	0	0	0	0	0	6
85	Protocatechuic acid-*O*-hexoside	[131]	$C_{13}H_{16}O_9$	**315.0732**	10.5	37	28	13	3	3	0	84
86	Protocatechuic acid-*O*-benzoyl-hexoside	-	$C_{20}H_{20}O_{10}$	**419.0974**	51.8	0	1	0	0	0	0	1
87	Protocatechuic acid-*O*-feruloyl-hexoside	-	$C_{23}H_{24}O_{12}$	**491.1202**	51.1	0	1	0	0	0	0	1
	3. Salicylic acid derivatives											
88	Salicylic acid-*O*-hexoside	[131]	$C_{13}H_{16}O_8$	**299.0769**	6.3	20	13	5	0	1	1	40
89	Salicylic acid-*O*-hexoside	[131]	$C_{13}H_{16}O_8$	**299.0767**	13.0	2	6	1	0	1	0	10
90	Salicylic acid-*O*-glucosyl ester	[131]	$C_{13}H_{16}O_8$	**299.0765**	8.5	4	1	1	0	1	0	7
91	Salicyloylsalicin	[132]	$C_{20}H_{22}O_9$	**405.1188**	36.6	1	0	0	0	0	0	1

No.	Compounds found in the six subgenera	Reference	Molecular Formula	Parent Ion $[M-H]^-$ *m/z*	RT min	Subgenus / No. of species in which the compounds were identified						Total
						Rhododendron	*Hymenanthes*	*Pentanthera*	*Azaleastrum*	*Tsutsusi*	*Mumeazalea*	
	Number of Species					**44**	**33**	**13**	**3**	**6**	**1**	**100**
	Compound											
92	Salicylic acid-*O*-coumaroyl-hexoside	-	$C_{22}H_{22}O_{10}$	**445.1122**	42.4	0	1	0	0	0	0	1
93	Salicylic acid-*O*-coumaroyl-hexoside	-	$C_{22}H_{22}O_{10}$	**445.1122**	46.2	1	4	0	0	0	0	5
94	Salicylic acid-*O*-dihexoside	[133]	$C_{19}H_{26}O_{13}$	**461.1318**	7.0	0	1	0	0	0	0	1
	4. Vanillic acid derivatives											
95	Vanillic acid-*O*-hexoside	[134]	$C_{14}H_{18}O_9$	**329.0869**	7.7	9	2	0	0	0	0	11
96	Vanillic acid-*O*-hexoside	[134]	$C_{14}H_{18}O_9$	**329.0864**	10.2	15	9	3	2	2	1	32
97	Vanillic acid-*O*-hexoside	[134]	$C_{14}H_{18}O_9$	**329.0865**	11.7	30	1	1	1	1	0	34
98	Vanillic acid-*O*-hexoside	[134]	$C_{14}H_{18}O_9$	**329.0863**	13.9	22	10	3	1	0	0	36
99	Amburoside B	[135]	$C_{21}H_{24}O_{10}$	**435.1289**	36.3	3	6	4	2	0	1	16
100	Vanilloyl-β-D-(2'-*O*-p-hydroxybenzoyl)-hexoside	[136]	$C_{21}H_{22}O_{11}$	**449.1093**	17.5	0	0	1	0	0	0	1
101	Vanilloyl-β-D-(2'-*O*-p-hydroxybenzoyl)-hexoside	[137]	$C_{21}H_{22}O_{11}$	**449.1096**	40.8	1	0	0	0	0	0	1
102	Vanillic acid-*O*-hexoside-*O*-pentoside	[138]	$C_{19}H_{26}O_{13}$	**461.1319**	14.9	1	0	0	0	0	0	1
103	Vanillic acid-*O*-hexoside-*O*-pentoside	[138]	$C_{19}H_{26}O_{13}$	**461.1313**	19.1	2	1	0	0	0	0	3

No.	Compounds found in the six subgenera	Reference	Molecular Formula	Parent Ion [M-H]⁻ *m/z*	RT min	Subgenus / No. of species in which the compounds were identified						Total
						Rhododendron	*Hymenanthes*	*Pentanthera*	*Azaleastrum*	*Tsutsusi*	*Mumeazalea*	
	Number of Species					**44**	**33**	**13**	**3**	**6**	**1**	**100**
	Compound											
104	Vanillic acid-*O*-rutinoside	[139]	$C_{20}H_{28}O_{13}$	**475.1477**	12.5	1	0	0	0	0	0	1
105	Vanillic acid-*O*-rutinoside	[139]	$C_{20}H_{28}O_{13}$	**475.1480**	18.9	1	0	0	0	0	0	1
106	Vanillic acid-*O*-coumaroyl-hexoside	[140]	$C_{23}H_{24}O_{11}$	**475.1258**	47.8	0	1	0	0	0	0	1
107	Vanillic acid-*O*-dihexoside / Picrorhizin	[141]	$C_{20}H_{28}O_{14}$	**491.1411**	4.6	1	0	0	0	0	0	1
108	Vanillic acid-*O*-dihexoside / Picrorhizin	[141]	$C_{20}H_{28}O_{14}$	**491.1399**	5.3	1	0	0	0	0	0	1
109	Vanillic acid-*O*-dihexoside	[142]	$C_{20}H_{28}O_{14}$	**491.1422**	8.5	1	0	0	0	0	0	1
110	Litseaefoloside A	[143]	$C_{23}H_{26}O_{12}$	**493.1340**	47.0	1	0	0	0	0	0	1
	5. Methyl gallate derivatives											
111	Methyl gallate-*O*-hexoside	[144]	$C_{14}H_{18}O_{10}$	**345.0810**	7.4	0	5	1	1	0	0	7
112	Methyl gallate-*O*-hexoside	[144]	$C_{14}H_{18}O_{10}$	**345.0818**	8.5	8	2	2	1	0	0	13
113	Methyl gallate-*O*-hexoside	[144]	$C_{14}H_{18}O_{10}$	**345.0810**	11.8	3	12	1	0	0	0	16
114	Methyl gallate-*O*-coumaroyl-hexoside	-	$C_{23}H_{24}O_{12}$	**491.1192**	42.1	0	1	0	0	0	0	1
115	Methyl gallate-*O*-dihexoside	[145]	$C_{20}H_{28}O_{15}$	**507.1375**	8.0	1	0	0	0	0	0	1
	Flavan-3-ols											
116	Catechin	[6]	$C_{15}H_{14}O_6$	**289.0709**	16.0	32	27	12	2	5	0	78
117	Epicatechin	[6]	$C_{15}H_{14}O_6$	**289.0705**	23.0	24	20	9	3	5	0	61

No.	Compounds found in the six subgenera	Reference	Molecular Formula	Parent Ion $[M-H]^-$ *m/z*	RT min	Subgenus / No. of species in which the compounds were identified						Total
						Rhododendron	*Hymenanthes*	*Pentanthera*	*Azaleastrum*	*Tsutsusi*	*Mumeazalea*	
	Number of Species					**44**	**33**	**13**	**3**	**6**	**1**	**100**
	Compound											
118	Gallocatechin	[6]	$C_{15}H_{14}O_7$	**305.0654**	8.5	6	5	4	1	0	0	16
119	Epigallocatechin	[6]	$C_{15}H_{14}O_7$	**305.0653**	15.4	4	0	1	2	0	1	8
120	(Epi)catechin-*O*-hydroxybenzoate	[146]	$C_{22}H_{18}O_8$	**409.0923**	35.8	1	1	0	0	0	1	3
121	(Epi)catechin-*O*-rhamnoside	[147]	$C_{21}H_{24}O_{10}$	**435.1293**	22.5	1	0	0	0	0	0	1
122	Malaferin B	[148]	$C_{24}H_{20}O_8$	**435.1095**	40.1	0	1	1	0	0	0	2
123	(Epi)catechin gallate	[6]	$C_{22}H_{18}O_{10}$	**441.0830**	28.1	0	8	0	0	0	0	8
124	(Epi)catechin gallate	[6]	$C_{22}H_{18}O_{10}$	**441.0829**	29.6	7	22	3	3	0	1	36
125	(Epi)catechin gallate	[6]	$C_{22}H_{18}O_{10}$	**441.0826**	31.8	2	13	0	0	0	0	15
126	(Epi)catechin gallate	[6]	$C_{22}H_{18}O_{10}$	**441.0830**	36.8	0	5	1	0	0	0	6
127	(Epi)catechin-*O*-hexoside	[149]	$C_{21}H_{24}O_{11}$	**451.1251**	10.5	10	13	4	0	3	0	30
128	(Epi)catechin-*O*-methyl-gallate	[150]	$C_{23}H_{20}O_{10}$	**455.0965**	34.4	2	4	1	0	0	0	7
129	(Epi)gallocatechin gallate	[6]	$C_{22}H_{18}O_{11}$	**457.0755**	19.8	0	0	1	0	0	0	1
130	Epigallocatechin gallate	[6]	$C_{22}H_{18}O_{11}$	**457.0776**	22.7	2	0	1	3	0	1	7
131	(Epi)gallocatechin gallate	[6]	$C_{22}H_{18}O_{11}$	**457.0757**	26.6	0	0	1	0	0	0	1
132	Malaferin C	[148]	$C_{25}H_{22}O_9$	**465.1198**	41.2	0	0	1	0	0	0	1
133	(Epi)catechin-*O*-dimethyl-gallate	[151]	$C_{24}H_{22}O_{10}$	**469.1161**	38.9	0	0	0	1	0	0	1
134	(Epi)catechin-*O*-trimethoxybenzoate	[152]	$C_{25}H_{24}O_{10}$	**483.1320**	29.5	3	2	2	0	1	0	8
135	(Epi)catechin-*O*-trimethoxybenzoate	[152]	$C_{25}H_{24}O_{10}$	**483.1300**	32.9	1	0	0	0	1	0	2

No.	Compounds found in the six subgenera	Reference	Molecular Formula	Parent Ion $[M-H]^-$ *m/z*	RT min	Subgenus / No. of species in which the compounds were identified						Total
						Rhododendron	*Hymenanthes*	*Pentanthera*	*Azaleastrum*	*Tsutsusi*	*Mumeazalea*	
	Number of Species					**44**	**33**	**13**	**3**	**6**	**1**	**100**
	Compound											
136	(Epi)catechin-(4,8/2,6)-(epi)catechin	[6]	$C_{30}H_{24}O_{12}$	**575.1206**	5.5	6	12	0	0	0	0	18
137	(Epi)catechin-(4,8/2,6)-(epi)catechin	[6]	$C_{30}H_{24}O_{12}$	**575.1216**	8.7	1	0	0	0	0	0	1
138	(Epi)catechin-(4,8/2,6)-(epi)catechin	[6]	$C_{30}H_{24}O_{12}$	**575.1216**	10.1	1	8	0	0	0	0	9
139	(Epi)catechin-(4,8/2,6)-(epi)catechin	[6]	$C_{30}H_{24}O_{12}$	**575.1194**	12.0	1	2	0	0	0	0	3
140	(Epi)catechin-(4,8/2,6)-(epi)catechin	[6]	$C_{30}H_{24}O_{12}$	**575.1190**	14.0	0	5	0	0	0	0	5
141	(Epi)catechin-(4,8/2,6)-(epi)catechin	[6]	$C_{30}H_{24}O_{12}$	**575.1190**	18.1	0	3	0	0	0	0	3
142	(Epi)catechin-(4,8/2,6)-(epi)catechin	[6]	$C_{30}H_{24}O_{12}$	**575.1211**	27.2	18	23	7	0	0	0	48
143	(Epi)catechin-(4,8/2,6)-(epi)catechin	[6]	$C_{30}H_{24}O_{12}$	**575.1190**	32.4	26	17	8	1	1	0	53
144	(Epi)catechin-(4,8/2,6)-(epi)catechin	[6]	$C_{30}H_{24}O_{12}$	**575.1184**	34.8	1	1	4	0	0	0	6
145	(Epi)catechin-(epi)catechin (Procyanidin dimer B1)	[6]	$C_{30}H_{26}O_{12}$	**577.1372**	13.4	21	25	11	1	4	0	62
146	(Epi)catechin-(epi)catechin (Procyanidin dimer B)	[6]	$C_{30}H_{26}O_{12}$	**577.1361**	14.3	17	24	7	1	2	0	51

No.	Compounds found in the six subgenera	Reference	Molecular Formula	Parent Ion $[M-H]^-$ *m/z*	RT min	Subgenus / No. of species in which the compounds were identified						Total
						Rhododendron	*Hymenanthes*	*Pentanthera*	*Azaleastrum*	*Tsutsusi*	*Mumeazalea*	
	Number of Species					**44**	**33**	**13**	**3**	**6**	**1**	**100**
	Compound											
147	(Epi)catechin-(epi)catechin (Procyanidin dimer B)	[6]	$C_{30}H_{26}O_{12}$	**577.1371**	18.6	21	20	7	1	1	0	50
148	(Epi)catechin-(epi)catechin (Procyanidin dimer B2)	[6]	$C_{30}H_{26}O_{12}$	**577.1370**	20.3	34	24	11	3	5	0	77
149	(Epi)catechin-(epi)catechin (Procyanidin dimer B)	[6]	$C_{30}H_{26}O_{12}$	**577.1374**	23.1	10	19	6	0	2	0	37
150	(Epi)catechin-(epi)catechin (Procyanidin dimer B)	[6]	$C_{30}H_{26}O_{12}$	**577.1360**	32.8	6	4	3	1	4	0	18
151	Gambiriin A/D	[153]	$C_{30}H_{28}O_{12}$	**579.1533**	19.2	0	1	0	0	0	0	1
152	(Epi)gallocatechin-(epi)catechin	[6]	$C_{30}H_{26}O_{13}$	**593.1325**	7.7	12	12	4	1	2	0	31
153	(Epi)gallocatechin-(epi)catechin	[6]	$C_{30}H_{26}O_{13}$	**593.1303**	9.7	5	11	4	0	0	0	20
154	(Epi)gallocatechin-(epi)catechin	[6]	$C_{30}H_{26}O_{13}$	**593.1321**	10.5	2	5	0	0	0	0	7
155	(Epi)gallocatechin-(epi)catechin	[6]	$C_{30}H_{26}O_{13}$	**593.1317**	12.6	3	3	3	1	0	1	11
156	(Epi)gallocatechin-(epi)catechin	[6]	$C_{30}H_{26}O_{13}$	**593.1327**	13.7	6	3	0	0	0	0	9
157	(Epi)gallocatechin-(epi)catechin	[6]	$C_{30}H_{26}O_{13}$	**593.1301**	15.2	0	0	0	1	0	1	2
158	(Epi)gallocatechin-(epi)catechin	[6]	$C_{30}H_{26}O_{13}$	**593.1310**	16.5	1	0	0	0	0	0	1
159	(Epi)gallocatechin-(epi)catechin	[6]	$C_{30}H_{26}O_{13}$	**593.1320**	18.2	1	0	0	0	0	0	1
160	(Epi)gallocatechin-(epi)gallocatechin	[6]	$C_{30}H_{26}O_{14}$	**609.1269**	4.5	3	0	0	0	0	0	3

No.	Compounds found in the six subgenera	Reference	Molecular Formula	Parent Ion $[M-H]^-$ *m/z*	RT min	Subgenus / No. of species in which the compounds were identified						Total
						Rhododendron	*Hymenanthes*	*Pentanthera*	*Azaleastrum*	*Tsutsusi*	*Mumeazalea*	
	Number of Species					**44**	**33**	**13**	**3**	**6**	**1**	**100**
	Compound											
161	(Epi)gallocatechin-(epi)gallocatechin	[6]	$C_{30}H_{26}O_{14}$	**609.1275**	6.5	5	3	2	0	0	0	10
162	(Epi)gallocatechin-(epi)gallocatechin	[6]	$C_{30}H_{26}O_{14}$	**609.1275**	7.5	1	0	2	0	0	1	4
163	(Epi)gallocatechin-(epi)gallocatechin	[6]	$C_{30}H_{26}O_{14}$	**609.1261**	10.2	5	1	1	0	0	1	8
164	(Epi)gallocatechin-(epi)gallocatechin	[6]	$C_{30}H_{26}O_{14}$	**609.1247**	13.1	1	0	2	0	0	0	3
165	(Epi)catechin-3-*O*-hexoside-7-*O*-hexoside	[154]	$C_{27}H_{34}O_{16}$	**613.1790**	9.6	0	0	2	0	0	0	2
166	(Epi)catechin-3-*O*-hexoside-7-*O*-hexoside	[154]	$C_{27}H_{34}O_{16}$	**613.1798**	11.8	0	0	1	0	0	0	1
167	(Epi)catechin-3-*O*-hexoside-7-*O*-hexoside	[154]	$C_{27}H_{34}O_{16}$	**613.1801**	13.2	0	0	1	0	0	0	1
168	3-*O*-galloyl(epi)catechin-(4,8/2,6)-(epi)catechin	[6]	$C_{37}H_{28}O_{16}$	**727.1296**	36.6	3	13	1	0	0	0	17
169	3-*O*-galloyl(epi)catechin-(4,8)-(epi)catechin	[6]	$C_{37}H_{30}O_{16}$	**729.1469**	20.3	0	11	0	0	0	0	11
170	(Epi)catechin-(4,8′)-3′-*O*-galloyl-(epi)catechin	[6]	$C_{37}H_{30}O_{16}$	**729.1484**	23.6	2	2	1	2	0	0	7
171	3-*O*-galloyl(epi)catechin-(4,8)-(epi)catechin	[6]	$C_{37}H_{30}O_{16}$	**729.1462**	27.9	0	5	0	0	0	0	5
172	(Epi)gallocatechin-(4,8′)-3′-*O*-galloyl-(epi)catechin	[6]	$C_{37}H_{30}O_{17}$	**745.1416**	20.6	1	0	2	2	0	1	6

No.	Compounds found in the six subgenera	Reference	Molecular Formula	Parent Ion [M-H]⁻ *m/z*	RT min	Subgenus / No. of species in which the compounds were identified						Total
						Rhododendron	*Hymenanthes*	*Pentanthera*	*Azaleastrum*	*Tsutsusi*	*Mumeazalea*	
	Number of Species					**44**	**33**	**13**	**3**	**6**	**1**	**100**
	Compound											
173	(Epi)gallocatechin-(4,8)-3′-*O*-galloyl(epi)gallocatechin	[6]	$C_{37}H_{30}O_{18}$	**761.1396**	13.7	1	0	2	3	0	1	7
174	(Epi)gallocatechin-(4,8)-3′-*O*-galloyl(epi)gallocatechin	[6]	$C_{37}H_{30}O_{18}$	**761.1374**	25.7	0	0	0	0	0	1	1
175	A type Procyanidin Trimer C	[155]	$C_{45}H_{36}O_{18}$	**863.1847**	22.6	15	16	4	0	4	0	39
176	A type Procyanidin Trimer C	[155]	$C_{45}H_{36}O_{18}$	**863.1836**	23.2	18	7	5	1	6	0	37
177	A type Procyanidin Trimer C	[155]	$C_{45}H_{36}O_{18}$	**863.1867**	26.7	9	5	3	0	0	0	17
178	A type Procyanidin Trimer C	[155]	$C_{45}H_{36}O_{18}$	**863.1850**	33.7	8	2	4	0	0	0	14
179	Procyanidin Trimer C	[155]	$C_{45}H_{38}O_{18}$	**865.1946**	5.6	6	14	2	0	1	0	23
180	Procyanidin Trimer C	[155]	$C_{45}H_{38}O_{18}$	**865.1959**	14.9	3	11	1	0	0	0	15
181	Procyanidin Trimer C	[155]	$C_{45}H_{38}O_{18}$	**865.1984**	15.6	1	2	1	0	1	0	5
182	Procyanidin Trimer C	[155]	$C_{45}H_{38}O_{18}$	**865.2017**	16.6	1	0	0	0	0	0	1
183	Procyanidin Trimer C	[155]	$C_{45}H_{38}O_{18}$	**865.1984**	19.2	2	4	1	0	0	0	7
184	Procyanidin Trimer C	[155]	$C_{45}H_{38}O_{18}$	**865.1966**	22.2	2	6	1	0	0	0	9
185	Procyanidin Trimer C	[155]	$C_{45}H_{38}O_{18}$	**865.2010**	25.6	14	6	6	1	4	0	31
186	(Epi)gallocatechin-(4,8′)-(epi)catechin-(4′,8″)-(epi)catechin	[156]	$C_{45}H_{38}O_{19}$	**881.1961**	11.1	1	0	0	0	0	0	1

No.	Compounds found in the six subgenera	Reference	Molecular Formula	Parent Ion [M-H]⁻ *m/z*	RT min	Subgenus / No. of species in which the compounds were identified						Total
						Rhododendron	*Hymenanthes*	*Pentanthera*	*Azaleastrum*	*Tsutsusi*	*Mumeazalea*	
	Number of Species					**44**	**33**	**13**	**3**	**6**	**1**	**100**
	Compound											
187	(Epi)catechin-(4,8′)-(epi)gallocatechin-(4′,8″)-(epi)catechin	[156]	$C_{45}H_{38}O_{19}$	**881.1938**	12.1	1	1	0	0	0	0	2
188	(Epi)gallocatechin-(4,8′)-(epi)catechin-(4′,8″)-(epi)catechin	[156]	$C_{45}H_{38}O_{19}$	**881.1969**	13.2	1	0	1	0	0	0	2
189	(Epi)gallocatechin-(4,8′/2,7′)-(epi)gallocatechin-(4′,8″)-(epi)catechin	[157]	$C_{45}H_{36}O_{20}$	**895.1767**	15.9	0	0	1	0	0	0	1
190	(Epi)gallocatechin-(4,8′)-(epi)gallocatechin-(4′,8″)-(epi)catechin	[157]	$C_{45}H_{38}O_{20}$	**897.1887**	9.1	1	0	0	0	0	0	1
191	Procyanidin trimer gallate	[156]	$C_{52}H_{42}O_{22}$	**508.1032**	13.1	0	1	0	0	0	0	1
192	Procyanidin trimer gallate	[156]	$C_{52}H_{42}O_{22}$	**508.1026**	18.3	0	1	0	0	0	0	1
193	A type procyanidin tetramer	[156]	$C_{60}H_{48}O_{24}$	**575.1217**	12.9	4	1	2	0	0	0	7
194	A type procyanidin tetramer	[156]	$C_{60}H_{48}O_{24}$	**575.1202**	19.5	2	2	1	0	2	0	7
195	A type procyanidin tetramer	[156]	$C_{60}H_{48}O_{24}$	**575.1206**	24.5	2	3	3	0	1	0	9
196	A type procyanidin tetramer	[156]	$C_{60}H_{48}O_{24}$	**575.1223**	25.9	4	1	0	0	1	0	6
197	Procyanidin tetramer	[156]	$C_{60}H_{50}O_{24}$	**576.1286**	17.7	0	1	0	0	1	0	2
198	Procyanidin tetramer	[156]	$C_{60}H_{50}O_{24}$	**576.1284**	21.3	1	2	1	0	1	0	5
199	Procyanidin tetramer	[156]	$C_{60}H_{50}O_{24}$	**576.1293**	22.2	0	1	4	0	1	0	6
200	Procyanidin tetramer	[156]	$C_{60}H_{50}O_{24}$	**576.1273**	24.5	0	1	0	0	0	0	1

No.	Compounds found in the six subgenera	Reference	Molecular Formula	Parent Ion $[M-H]^-$ *m/z*	RT min	Subgenus / No. of species in which the compounds were identified						Total
						Rhododendron	*Hymenanthes*	*Pentanthera*	*Azaleastrum*	*Tsutsusi*	*Mumeazalea*	
	Number of Species					**44**	**33**	**13**	**3**	**6**	**1**	**100**
	Compound											
201	Procyanidin tetramer	[156]	$C_{60}H_{50}O_{24}$	**576.1298**	26.2	5	2	3	0	5	0	15
202	Procyanidin tetramer	[156]	$C_{60}H_{50}O_{24}$	**576.1293**	30.5	1	0	0	0	0	0	1
	Flavanones											
	1. Naringenin											
203	(±)-Naringenin	[158]	$C_{15}H_{12}O_5$	**271.0600**	47.9	14	4	3	1	2	0	24
204	Naringenin-*O*-hexoside	[159]	$C_{21}H_{22}O_{10}$	**433.1129**	38.3	1	1	1	0	0	0	3
205	Naringenin-*O*-hexoside-*O*-pentoside	[160]	$C_{26}H_{30}O_{14}$	**565.1582**	38.0	0	0	0	0	1	0	1
	2. Taxifolin derivatives											
206	(±)-Taxifolin	[161]	$C_{15}H_{12}O_7$	**303.0500**	29.1	7	6	3	0	5	0	21
207	Taxifolin-*O*-pentoside	[6]	$C_{20}H_{20}O_{11}$	**435.0950**	27.8	14	18	2	1	4	0	39
208	Taxifolin-*O*-pentoside	[6]	$C_{20}H_{20}O_{11}$	**435.0954**	31.1	28	19	1	0	2	0	50
209	Taxifolin-*O*-pentoside	[6]	$C_{20}H_{20}O_{11}$	**435.0943**	32.4	4	6	1	0	1	0	12
210	Taxifolin-*O*-pentoside	[6]	$C_{20}H_{20}O_{11}$	**435.0933**	33.6	3	5	2	0	2	0	12
211	Taxifolin-*O*-pentoside	[6]	$C_{20}H_{20}O_{11}$	**435.0954**	35.5	12	7	0	0	1	0	20
212	Taxifolin-*O*-rhamnoside	[162]	$C_{21}H_{22}O_{11}$	**449.1109**	36.2	15	4	0	0	1	0	20
213	Taxifolin-*O*-rhamnoside	[162]	$C_{21}H_{22}O_{11}$	**449.1084**	36.6	1	0	0	0	1	0	2
214	Taxifolin-*O*-rhamnoside	[162]	$C_{21}H_{22}O_{11}$	**449.1103**	37.4	1	1	0	0	0	0	2

No.	Compounds found in the six subgenera	Reference	Molecular Formula	Parent Ion [M-H]⁻ *m/z*	RT min	Subgenus / No. of species in which the compounds were identified						Total
						Rhododendron	*Hymenanthes*	*Pentanthera*	*Azaleastrum*	*Tsutsusi*	*Mumeazalea*	
	Number of Species					**44**	**33**	**13**	**3**	**6**	**1**	**100**
	Compound											
215	Taxifolin-*O*-hexoside	[131]	$C_{21}H_{22}O_{12}$	**465.1041**	15.1	10	5	1	0	0	0	16
216	Taxifolin-*O*-hexoside	[131]	$C_{21}H_{22}O_{12}$	**465.1045**	19.3	1	2	0	0	0	0	3
217	Taxifolin-*O*-hexoside	[131]	$C_{21}H_{22}O_{12}$	**465.1032**	22.8	5	1	0	0	1	0	7
218	Taxifolin-*O*-hexoside	[131]	$C_{21}H_{22}O_{12}$	**465.1037**	24.8	9	18	2	0	2	1	32
219	Taxifolin-*O*-hexoside	[131]	$C_{21}H_{22}O_{12}$	**465.1043**	26.2	2	1	2	0	0	0	5
220	Taxifolin-*O*-hexoside	[131]	$C_{21}H_{22}O_{12}$	**465.1055**	27.9	9	4	3	0	0	0	16
221	Taxifolin-*O*-hexoside	[131]	$C_{21}H_{22}O_{12}$	**465.1052**	30.0	10	7	3	0	1	0	21
222	Taxifolin-*O*-acetyl-rhamnoside	[163]	$C_{23}H_{24}O_{12}$	**491.1219**	39.9	1	0	0	0	0	0	1
223	Taxifolin-*O*-acetyl-rhamnoside	[163]	$C_{23}H_{24}O_{12}$	**491.1214**	45.0	1	0	0	0	0	0	1
224	Taxifolin-*O*-acetyl-hexoside	[164]	$C_{23}H_{24}O_{13}$	**507.1168**	46.7	0	0	0	0	1	0	1
225	Taxifolin-*O*-acetyl-hexoside	[164]	$C_{23}H_{24}O_{13}$	**507.1165**	48.1	0	0	0	0	1	0	1
226	Taxifolin-*O*-pentoside-*O*-hexoside	[165]	$C_{26}H_{30}O_{16}$	**597.1484**	17.7	1	0	0	0	0	0	1
227	Taxifolin-*O*-rhamnoside-*O*-hexoside	[166]	$C_{27}H_{32}O_{16}$	**611.1640**	20.1	1	0	0	0	0	0	1
228	Taxifolin-*O*-rhamnoside-*O*-hexoside	[166]	$C_{27}H_{32}O_{16}$	**611.1624**	32.8	1	0	0	0	0	0	1
	Flavonols											
	1. Myricetin											

No.	Compounds found in the six subgenera	Reference	Molecular Formula	Parent Ion $[M-H]^-$ *m/z*	RT min	Subgenus / No. of species in which the compounds were identified						Total
						Rhododendron	*Hymenanthes*	*Pentanthera*	*Azaleastrum*	*Tsutsusi*	*Mumeazalea*	
	Number of Species					**44**	**33**	**13**	**3**	**6**	**1**	**100**
	Compound											
229	Myricetin	[158]	$C_{15}H_{10}O_8$	**317.0297**	38.9	5	5	0	0	0	1	11
230	Myricetin-*O*-pentoside	[6]	$C_{20}H_{18}O_{12}$	**449.0746**	32.1	10	8	3	0	0	1	22
231	Myricetin-*O*-pentoside	[6]	$C_{20}H_{18}O_{12}$	**449.0735**	37.8	7	3	1	0	0	0	11
232	Myricetin-*O*-pentoside	[6]	$C_{20}H_{18}O_{12}$	**449.0741**	39.1	12	1	0	0	0	0	13
233	Myricetin-*O*-rhamnoside	[6]	$C_{21}H_{20}O_{12}$	**463.0895**	33.0	17	9	3	3	1	1	34
234	Myricetin-*O*-hexoside	[6]	$C_{21}H_{20}O_{13}$	**479.0809**	30.8	21	11	3	2	0	1	38
235	Myricetin-*O*-hexoside	[6]	$C_{21}H_{20}O_{13}$	**479.0808**	31.2	1	2	1	2	0	0	6
236	Myricetin-*O*-hexoside	[6]	$C_{21}H_{20}O_{13}$	**479.0842**	35.3	13	3	0	0	0	0	16
237	Myricetin-*O*-glucuronide	[167]	$C_{21}H_{18}O_{14}$	**493.0630**	36.5	5	1	1	0	0	0	7
238	Myricetin-*O*-acetyl-rhamnoside	[168]	$C_{23}H_{22}O_{13}$	**505.0995**	37.6	1	0	0	0	0	0	1
239	Myricetin-*O*-dipentoside	[169]	$C_{25}H_{26}O_{16}$	**581.1144**	41.4	1	0	0	0	0	0	1
240	Myricetin-*O*-dipentoside	[169]	$C_{25}H_{26}O_{16}$	**581.1147**	42.5	1	0	0	0	0	0	1
241	Myricetin-*O*-benzoyl-hexoside	[170]	$C_{28}H_{24}O_{14}$	**583.1112**	45.7	2	0	0	1	0	0	3
242	Myricetin-*O*-galloyl-rhamnoside	[171]	$C_{28}H_{24}O_{16}$	**615.0992**	38.5	0	0	0	1	0	1	2
243	Myricetin-*O*-galloyl-rhamnoside	[171]	$C_{28}H_{24}O_{16}$	**615.1022**	39.2	0	1	0	2	0	0	3
244	Myricetin-*O*-rutinoside	[114]	$C_{27}H_{30}O_{17}$	**625.1438**	31.4	3	0	1	0	0	1	5
245	Myricetin-3-*O*-hexoside-7-*O*-rhamnoside	[114]	$C_{27}H_{30}O_{17}$	**625.1415**	35.4	0	0	0	1	0	0	1

No.	Compounds found in the six subgenera	Reference	Molecular Formula	Parent Ion $[M-H]^-$ *m/z*	RT min	Subgenus / No. of species in which the compounds were identified						Total
						Rhododendron	*Hymenanthes*	*Pentanthera*	*Azaleastrum*	*Tsutsusi*	*Mumeazalea*	
	Number of Species					**44**	**33**	**13**	**3**	**6**	**1**	**100**
	Compound											
246	Myricetin-*O*-galloyl-hexoside	[6]	$C_{28}H_{24}O_{17}$	**631.0928**	30.5	1	1	1	2	0	0	5
247	Myricetin-7-*O*-galloyl-3-*O*-hexoside	[6]	$C_{28}H_{24}O_{17}$	**631.0920**	32.5	1	0	0	2	0	0	3
	2. Quercetin derivatives											
248	Quercetin	[155]	$C_{15}H_{10}O_7$	**301.0355**	44.4	38	18	7	1	5	1	70
249	Quercetin-*O*-pentoside	[6]	$C_{20}H_{18}O_{11}$	**433.0788**	36.6	29	24	5	0	5	0	63
250	Quercetin-*O*-pentoside	[6]	$C_{20}H_{18}O_{11}$	**433.0797**	37.4	33	27	12	1	5	1	79
251	Quercetin-*O*-pentoside	[6]	$C_{20}H_{18}O_{11}$	**433.0776**	39.6	2	0	2	0	0	1	5
252	Quercetin-*O*-pentoside	[6]	$C_{20}H_{18}O_{11}$	**433.0781**	41.2	42	31	11	0	6	0	90
253	Quercetin-*O*-rhamnoside	[6]	$C_{21}H_{20}O_{11}$	**447.0952**	38.7	33	31	10	2	5	1	82
254	Quercetin-*O*-hexoside	[6]	$C_{21}H_{20}O_{12}$	**463.0898**	34.2	41	30	13	3	5	1	93
255	Quercetin-*O*-hexoside	[6]	$C_{21}H_{20}O_{12}$	**463.0880**	35.5	41	29	12	3	6	1	92
256	Quercetin-*O*-hexoside	[6]	$C_{21}H_{20}O_{12}$	**463.0896**	40.7	2	3	0	0	0	0	5
257	Quercetin-*O*-acetyl-pentoside	[114]	$C_{22}H_{20}O_{12}$	**475.0884**	43.2	2	1	3	0	1	0	7
258	Quercetin-*O*-acetyl-pentoside	[114]	$C_{22}H_{20}O_{12}$	**475.0880**	45.5	1	0	0	0	0	0	1
259	Quercetin-*O*-acetyl-pentoside	[114]	$C_{22}H_{20}O_{12}$	**475.0903**	48.0	1	0	0	0	0	0	1
260	Quercetin-*O*-glucuronide	[172]	$C_{21}H_{18}O_{13}$	**477.0694**	40.8	30	18	3	0	4	0	55

No.	Compounds found in the six subgenera	Reference	Molecular Formula	Parent Ion [M-H]⁻ *m/z*	RT min	Subgenus / No. of species in which the compounds were identified						Total
						Rhododendron	*Hymenanthes*	*Pentanthera*	*Azaleastrum*	*Tsutsusi*	*Mumeazalea*	
	Number of Species					**44**	**33**	**13**	**3**	**6**	**1**	**100**
	Compound											
261	Quercetin-*O*-acetyl-rhamnoside	[173]	$C_{23}H_{22}O_{12}$	**489.1055**	43.5	5	1	4	0	0	0	10
262	Quercetin-*O*-acetyl-rhamnoside	[173]	$C_{23}H_{22}O_{12}$	**489.1041**	45.5	4	0	1	0	0	0	5
263	Quercetin-*O*-acetyl-rhamnoside	[173]	$C_{23}H_{22}O_{12}$	**489.1057**	47.6	5	1	0	0	1	0	7
264	Quercetin-*O*-acetyl-hexoside	[174]	$C_{23}H_{22}O_{13}$	**505.0989**	38.0	1	1	0	0	0	0	2
265	Quercetin-*O*-acetyl-hexoside	[174]	$C_{23}H_{22}O_{13}$	**505.0985**	40.0	9	3	3	0	0	0	15
266	Quercetin-*O*-acetyl-hexoside	[174]	$C_{23}H_{22}O_{13}$	**505.1013**	42.0	7	0	0	0	0	0	7
267	Quercetin-*O*-acetyl-hexoside	[174]	$C_{23}H_{22}O_{13}$	**505.0995**	42.8	6	1	0	0	0	0	7
268	Quercetin-*O*-acetyl-hexoside	[174]	$C_{23}H_{22}O_{13}$	**505.1010**	43.4	9	3	1	0	0	0	13
269	Quercetin-*O*-acetyl-hexoside	[174]	$C_{23}H_{22}O_{13}$	**505.1000**	44.0	2	2	1	1	1	0	7
270	Quercetin-*O*-acetyl-hexoside	[174]	$C_{23}H_{22}O_{13}$	**505.1001**	45.6	1	0	0	0	0	0	1
271	Quercetin-*O*-acetyl-hexoside	[174]	$C_{23}H_{22}O_{13}$	**505.1004**	46.5	1	0	0	0	0	0	1
272	Quercetin-*O*-diacetyl-hexoside	[175]	$C_{25}H_{24}O_{14}$	**547.1111**	51.5	1	0	0	0	0	0	1
273	Quercetin-*O*-dipentoside	[176]	$C_{25}H_{26}O_{15}$	**565.1216**	33.8	0	1	0	0	0	0	1
274	Quercetin-*O*-dipentoside	[176]	$C_{25}H_{26}O_{15}$	**565.1219**	36.3	2	1	1	0	0	0	4
275	Quercetin-*O*-benzoyl-hexoside	[177]	$C_{28}H_{24}O_{13}$	**567.1146**	49.7	4	2	3	0	0	0	9
276	Quercetin-*O*-pentoside-*O*-rhamnoside	[155]	$C_{26}H_{28}O_{15}$	**579.1371**	37.2	0	0	1	0	0	1	2

No.	Compounds found in the six subgenera	Reference	Molecular Formula	Parent Ion $[M-H]^-$ *m/z*	RT min	Subgenus / No. of species in which the compounds were identified						Total
						Rhododendron	*Hymenanthes*	*Pentanthera*	*Azaleastrum*	*Tsutsusi*	*Mumeazalea*	
	Number of Species					**44**	**33**	**13**	**3**	**6**	**1**	**100**
	Compound											
277	Quercetin-*O*-(*p*-hydroxy)-benzoyl-hexoside	[6]	$C_{28}H_{24}O_{14}$	**583.1093**	41.7	5	4	0	0	0	0	9
278	Quercetin-*O*-(*p*-hydroxy)-benzoyl-hexoside	[6]	$C_{28}H_{24}O_{14}$	**583.1111**	44.0	15	14	2	0	2	0	33
279	Quercetin-*O*-(*p*-hydroxy)-benzoyl-hexoside	[6]	$C_{28}H_{24}O_{14}$	**583.1099**	49.8	0	5	1	0	0	0	6
280	Quercetin-*O*-galloyl-pentoside	[178]	$C_{27}H_{22}O_{15}$	**585.0886**	39.1	0	1	0	0	0	0	1
281	Quercetin-*O*-galloyl-pentoside	[178]	$C_{27}H_{22}O_{15}$	**585.0897**	42.9	2	5	0	0	0	0	7
282	Quercetin-3-*O*-(4"-3-hydroxy-3-methylglutaryl)-α-rhamnoside	[179]	$C_{27}H_{28}O_{15}$	**591.1385**	44.9	1	0	0	0	0	0	1
283	Quercetin-*O*-coumaroyl-rhamnoside	[180]	$C_{30}H_{26}O_{13}$	**593.1303**	52.0	1	4	1	0	0	0	6
284	Quercetin-*O*-coumaroyl-rhamnoside	[180]	$C_{30}H_{26}O_{13}$	**593.1304**	55.1	6	8	2	0	0	0	16
285	Quercetin-*O*-pentoside-*O*-hexoside	[6]	$C_{26}H_{28}O_{16}$	**595.1329**	24.7	0	0	1	0	0	0	1
286	Quercetin-*O*-pentoside-*O*-hexoside	[6]	$C_{26}H_{28}O_{16}$	**595.1322**	30.4	9	6	0	0	0	0	15
287	Quercetin-*O*-protocatechuoyl-hexoside	[181, 182]	$C_{28}H_{24}O_{15}$	**599.1031**	40.6	1	1	2	0	0	0	4
288	Quercetin-*O*-galloyl-rhamnoside	[181, 182]	$C_{28}H_{24}O_{15}$	**599.1048**	43.4	3	7	2	1	0	1	14

No.	Compounds found in the six subgenera	Reference	Molecular Formula	Parent Ion $[M-H]^-$ *m/z*	RT min	Subgenus / No. of species in which the compounds were identified						Total
						Rhododendron	*Hymenanthes*	*Pentanthera*	*Azaleastrum*	*Tsutsusi*	*Mumeazalea*	
	Number of Species					**44**	**33**	**13**	**3**	**6**	**1**	**100**
	Compound											
289	Quercetin-*O*-rhamnoside-*O*-hexoside	[6]	$C_{27}H_{30}O_{16}$	**609.1476**	25.7	1	0	0	0	0	0	1
290	Quercetin-*O*-rhamnoside-*O*-hexoside	[6]	$C_{27}H_{30}O_{16}$	**609.1469**	28.8	2	0	0	0	0	0	2
291	Quercetin-*O*-rhamnoside-*O*-hexoside	[6]	$C_{27}H_{30}O_{16}$	**609.1473**	30.3	2	0	0	0	0	0	2
292	Quercetin-*O*-rhamnoside-*O*-hexoside	[6]	$C_{27}H_{30}O_{16}$	**609.1470**	31.5	1	0	0	0	0	0	1
293	Quercetin-*O*-rhamnoside-*O*-hexoside	[6]	$C_{27}H_{30}O_{16}$	**609.1478**	34.3	4	2	4	0	1	0	11
294	Quercetin-*O*-rhamnoside-*O*-hexoside	[6]	$C_{27}H_{30}O_{16}$	**609.1476**	35.0	15	12	7	0	5	1	40
295	Quercetin-*O*-coumaroyl-hexoside	[183]	$C_{30}H_{26}O_{14}$	**609.1262**	46.4	3	5	3	0	1	0	12
296	Quercetin-*O*-coumaroyl-hexoside	[183]	$C_{30}H_{26}O_{14}$	**609.1258**	47.8	5	3	1	0	0	0	9
297	Quercetin-*O*-coumaroyl-hexoside	[183]	$C_{30}H_{26}O_{14}$	**609.1269**	49.5	8	17	5	1	1	0	32
298	Quercetin-*O*-galloyl-hexoside	[6]	$C_{28}H_{24}O_{16}$	**615.1006**	34.5	1	1	0	0	0	0	2
299	Quercetin-*O*-galloyl-hexoside	[6]	$C_{28}H_{24}O_{16}$	**615.1000**	35.5	6	12	2	1	0	0	21
300	Quercetin-*O*-feruloyl-rhamnoside	[180]	$C_{31}H_{28}O_{14}$	**623.1410**	56.5	1	1	0	0	0	0	2
301	Cypellogin A/B	[184]	$C_{31}H_{34}O_{14}$	**629.1899**	48.7	2	0	0	0	0	0	2

No.	Compounds found in the six subgenera	Reference	Molecular Formula	Parent Ion [M-H]⁻ *m/z*	RT min	Subgenus / No. of species in which the compounds were identified						Total
						Rhododendron	*Hymenanthes*	*Pentanthera*	*Azaleastrum*	*Tsutsusi*	*Mumeazalea*	
	Number of Species					**44**	**33**	**13**	**3**	**6**	**1**	**100**
	Compound											
302	Cypellogin A/B	[184]	$C_{31}H_{34}O_{14}$	**629.1894**	50.6	6	0	0	0	1	0	7
303	Cypellogin A/B	[184]	$C_{31}H_{34}O_{14}$	**629.1905**	51.7	0	1	0	0	0	0	1
304	Cypellogin C	[116]	$C_{31}H_{36}O_{14}$	**631.2063**	52.6	0	1	0	0	0	0	1
305	Quercetin-3-(4"-*O*-acetyl)-*O*-rhamnoside-7-*O*-rhamnoside	[185]	$C_{29}H_{32}O_{16}$	**635.1643**	40.7	0	0	1	0	0	0	1
306	Quercetin-*O*-feruloyl-hexoside	[6]	$C_{31}H_{28}O_{15}$	**639.1361**	47.4	3	7	0	0	1	0	11
307	Quercetin-*O*-feruloyl-hexoside	[6]	$C_{31}H_{28}O_{15}$	**639.1364**	50.9	11	14	3	0	1	0	29
308	Quercetin-3-*O*-acetyl-hexoside-rhamnoside	[186]	$C_{29}H_{32}O_{17}$	**651.1568**	42.7	3	0	0	0	0	0	3
309	Quercetin-*O*-sinapoyl-hexoside	[187]	$C_{32}H_{30}O_{16}$	**669.1460**	51.7	3	5	2	0	0	0	10
	3. Kaempferol derivatives											
310	Kaempferol	[155]	$C_{15}H_{10}O_6$	**285.0405**	49.5	9	1	0	0	0	1	11
311	Kaempferol-*O*-pentoside	[188]	$C_{20}H_{18}O_{10}$	**417.0808**	41.0	14	18	10	2	2	1	47
312	Kaempferol-*O*-pentoside	[188]	$C_{20}H_{18}O_{10}$	**417.0812**	43.9	32	16	2	0	1	1	52
313	Kaempferol-*O*-rhamnoside	[155]	$C_{21}H_{20}O_{10}$	**431.1003**	43.6	29	26	10	3	6	1	75
314	Kaempferol-*O*-hexoside	[155]	$C_{21}H_{20}O_{11}$	**447.0930**	37.5	17	5	3	0	0	0	25
315	Kaempferol-*O*-hexoside	[155]	$C_{21}H_{20}O_{11}$	**447.0924**	39.0	6	1	1	0	0	1	9
316	Kaempferol-*O*-acetyl-pentoside	[189]	$C_{22}H_{20}O_{11}$	**459.0941**	47.6	0	0	3	0	0	0	3
317	Kaempferol-*O*-acetyl-pentoside	[189]	$C_{22}H_{20}O_{11}$	**459.0938**	50.1	2	0	0	0	0	0	2

No.	Compounds found in the six subgenera	Reference	Molecular Formula	Parent Ion [M-H]⁻ *m/z*	RT min	Subgenus / No. of species in which the compounds were identified						Total
						Rhododendron	*Hymenanthes*	*Pentanthera*	*Azaleastrum*	*Tsutsusi*	*Mumeazalea*	
	Number of Species					**44**	**33**	**13**	**3**	**6**	**1**	**100**
	Compound											
318	Kaempferol-*O*-glucuronide	[190]	$C_{21}H_{18}O_{12}$	**461.0726**	43.6	15	8	1	0	2	0	26
319	Kaempferol-*O*-acetyl-rhamnoside	[191]	$C_{23}H_{22}O_{11}$	**473.1106**	48.2	4	0	2	0	0	0	6
320	Kaempferol-*O*-acetyl-rhamnoside	[191]	$C_{23}H_{22}O_{11}$	**473.1109**	52.3	1	0	1	0	0	0	2
321	Kaempferol-*O*-acetyl-hexoside	[174]	$C_{23}H_{22}O_{12}$	**489.1062**	44.5	9	2	0	0	0	0	11
322	Kaempferol-*O*-acetyl-hexoside	[174]	$C_{23}H_{22}O_{12}$	**489.1062**	46.4	5	0	0	0	0	1	6
323	Kaempferol-*O*-acetyl-hexoside	[174]	$C_{23}H_{22}O_{12}$	**489.1033**	47.7	6	0	0	0	0	0	6
324	Kaempferol-*O*-diacetyl-hexoside	[175]	$C_{25}H_{24}O_{13}$	**531.1156**	55.0	1	0	0	0	0	0	1
325	Kaempferol-*O*-rhamnoside-*O*-pentoside	[155]	$C_{26}H_{28}O_{14}$	**563.1391**	38.4	1	0	0	0	0	0	1
326	Kaempferol-*O*-rhamnoside-*O*-pentoside	[155]	$C_{26}H_{28}O_{14}$	**563.1425**	41.0	0	0	1	0	0	1	2
327	Kaempferol-*O*-rhamnoside-*O*-pentoside	[155]	$C_{26}H_{28}O_{14}$	**563.1425**	43.4	1	0	0	0	0	0	1
328	Kaempferol-*O*-hydroxybenzoyl-hexoside (Rugosaflavonoid C)	[192]	$C_{28}H_{24}O_{13}$	**567.1135**	45.7	7	2	0	0	0	0	9
329	Kaempferol-*O*-galloyl-pentoside	[193]	$C_{27}H_{22}O_{14}$	**569.0940**	47.1	0	0	0	0	0	1	1
330	Kaempferol-*O*-galloyl-rhamnoside	[182]	$C_{28}H_{24}O_{14}$	**583.1121**	47.9	0	2	0	1	0	1	4
331	Kaempferol-*O*-rutinoside	[155]	$C_{27}H_{30}O_{15}$	**593.1536**	33.5	3	0	0	0	0	0	3

No.	Compounds found in the six subgenera	Reference	Molecular Formula	Parent Ion [M-H]$^-$ *m/z*	RT min	Subgenus / No. of species in which the compounds were identified						Total
						Rhododendron	*Hymenanthes*	*Pentanthera*	*Azaleastrum*	*Tsutsusi*	*Mumeazalea*	
	Number of Species					**44**	**33**	**13**	**3**	**6**	**1**	**100**
	Compound											
332	Kaempferol-*O*-rutinoside	[155]	$C_{27}H_{30}O_{15}$	**593.1536**	38.9	5	2	2	0	1	1	11
333	Resinoside A/B	[116]	$C_{31}H_{34}O_{13}$	**613.1943**	51.9	1	0	0	0	0	0	1
334	Kaempferol-3-*O*-(6"-acetyl-hexoside)-7-*O*-rhamnoside	[194]	$C_{29}H_{32}O_{16}$	**635.1649**	46.1	2	0	0	0	0	0	2
	4. Laricitrin derivatives											
335	Laricitrin	[195]	$C_{16}H_{12}O_8$	**331.0470**	46.1	4	0	0	0	0	0	4
336	Laricitrin-*O*-pentoside	[196]	$C_{21}H_{20}O_{12}$	**463.0886**	39.7	2	1	0	0	0	0	3
337	Laricitrin-*O*-pentoside	[196]	$C_{21}H_{20}O_{12}$	**463.0903**	43.1	1	1	1	0	0	0	3
338	Laricitrin-*O*-pentoside	[196]	$C_{21}H_{20}O_{12}$	**463.0886**	44.6	2	2	0	0	0	0	4
339	Laricitrin-*O*-rhamnoside	[196]	$C_{22}H_{22}O_{12}$	**477.1034**	40.6	2	0	0	0	0	0	2
340	Laricitrin-*O*-hexoside	[196]	$C_{22}H_{22}O_{13}$	**493.0985**	36.8	5	0	0	0	0	0	5
341	Laricitrin-*O*-hexoside	[196]	$C_{22}H_{22}O_{13}$	**493.0993**	40.1	0	1	0	0	0	0	1
342	Laricitrin-*O*-hexoside	[196]	$C_{22}H_{22}O_{13}$	**493.0999**	46.2	0	2	0	0	0	0	2
343	Laricitrin-*O*-glucuronide	[197]	$C_{22}H_{20}O_{14}$	**507.0805**	42.7	0	1	0	0	0	0	1
344	Laricitrin-*O*-coumaroyl-rhamnoside	-	$C_{31}H_{28}O_{14}$	**623.1432**	55.5	1	0	0	0	0	0	1
345	Laricitrin-*O*-rutinoside	[196]	$C_{28}H_{32}O_{17}$	**639.1584**	36.8	1	0	0	0	0	0	1

No.	Compounds found in the six subgenera	Reference	Molecular Formula	Parent Ion $[M-H]^-$ *m/z*	RT min	Subgenus / No. of species in which the compounds were identified						Total
						Rhododendron	***Hymenanthes***	***Pentanthera***	***Azaleastrum***	***Tsutsusi***	***Mumeazalea***	
	Number of Species					**44**	**33**	**13**	**3**	**6**	**1**	**100**
	Compound											
346	Laricitrin-*O*-coumaroyl-hexoside	[198]	$C_{31}H_{28}O_{15}$	**639.1384**	48.2	1	0	0	0	0	0	1
347	Laricitrin-*O*-coumaroyl-hexoside	[198]	$C_{31}H_{28}O_{15}$	**639.1384**	50.4	0	0	1	0	0	0	1
	5. Isorhamnetin derivatives											
348	Isorhamnetin-*O*-glucuronide	[199]	$C_{22}H_{20}O_{13}$	**491.0824**	45.2	0	1	0	0	1	0	2

14. Anti-bacterial, Cytotoxic and Genetic studies

The anti-bacterial, cytotoxic and genetic studies of *Rhododendron* samples were conducted in parallel with the phytochemical studies. The highlights of these studies are included in this chapter.

14.1. Anti-bacterial studies

The *Rhododendron* leaf crude extracts were tested against 26 bacterial strains including Gram-positive (*Bacillus subtilis*) and Gram-negative bacteria (*Escherichia coli*). The anti-microbial activity was tested using the agar diffusion method. The Gram-positive bacteria were found to be more susceptible to the *Rhododendron* leaf extracts compared to the Gram-negative bacteria. *Bacillus subtilis* was used as a model organism for Gram-positive bacteria and the anti-bacterial rating of *Rhododendron* species is based on this bacterial strain. 17 species, which belong to the subgenus *Rhododendron,* were found to have significant anti-bacterial activity against Gram-positive bacteria.[2, 200] In this anti-microbial study, *Rhododendron ambiguum* (Lab no. 3) and *Rhododendron ambiguum* (Lab no. 77) were considered as one species, however they were taken from two different plants and they displayed a different phytochemical profile and are hence considered as two different species in the phytochemical studies.

14.2. Cytotoxic studies

12 *Rhododendron* leaf extracts that showed significant anti-bacterial activity were tested on model cell systems in order to determine the species, which could be used to identify possible antibiotics or lead compounds. The viability and proliferative activity of the *Rhododendron* leaf extracts were determined by using the MTT assay on cultured cells. IEC6 and HaCaT cells were used as a model for oral and dermal treatments. The leaf extracts of two species, *Rhododendron minus* and *Rhododendron racemosum* were found to be non-cytotoxic at the concentration, at which it produced a significant inhibition against *Bacillus subtilis* in the agar diffusion assay. Hence, these two crude leaf extracts show promise as antibiotics in clinical use and require further testing and development. In addition, the apoptotic effect of *Rhododendron* leaf extracts was observed.[200, 201]

14.3. Genetic studies

The diversity of the *Rhododendron* species was studied using the three genetic markers *trn*K, *trn*L-F, and ITS. The genes *trn*K and *trn*L-F are both chloroplast markers, while the gene ITS is a nuclear ribosomal marker. The DNA sequences from two nuclear DNA regions and two plastid regions of *Rhododendron* species were used to generate a (Maximum Likelihood) phylogenetic tree of *Rhododendron* (Figure 14.1). The polyploidy level of the *Rhododendron* species was also studied in order to determine their impact on the diversity.[202, 203] A few *Rhododendron* species, namely *Rhododendron campanulatum* ssp. *aeruginosum* (Lab no. 17), *Rhododendron anthopogon* ssp. *anthopogon* (Lab no. 49), *Rhododendron beesianum* (Lab no. 60), *Rhododendron tatsienense* (Lab no. 87), *Rhododendron triflorum* (Lab no. 88), *Rhododendron oldhamii* (Lab no. 102) and *Rhododendron neoglandulosum* (Lab no. 108) used in this phytochemical study were not included in the phylogenetic tree as the required experiments were not conducted.

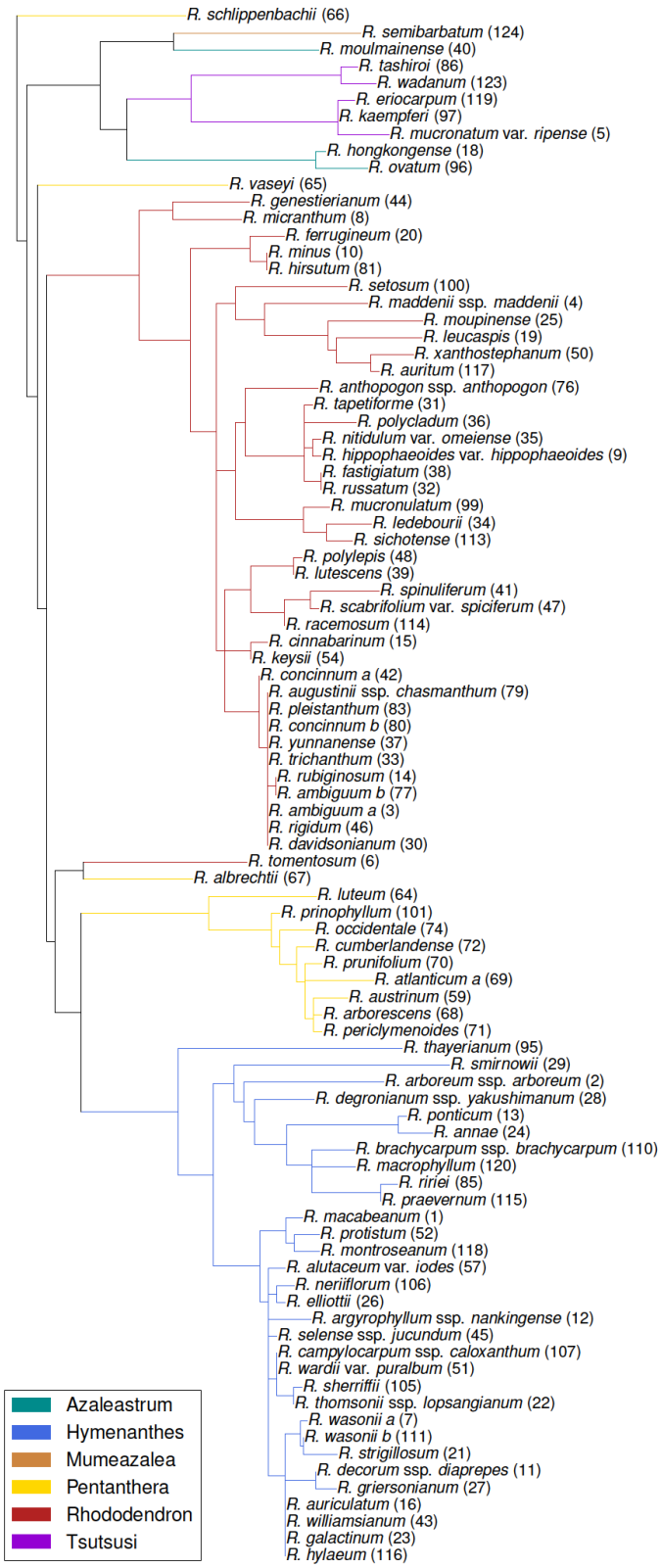

Figure 14.1: Phylogenetic tree of 100 *Rhododendron* species [202, 203]

15. Metabolomic and Statistical Studies

A wide variety of metabolites are produced by plants that perform different functions in them. The physiological functions of the plant such as growth and reproduction are managed by the primary metabolites. The other functions such as signal mechanisms to promote pollination and other defense mechanisms against microbes, viruses and herbivores are handled by the secondary metabolites. They are produced in the plant system as a reaction to external stimulus such as climate conditions. It should be noted that the actual function of *Rhododendron* secondary metabolites is largely unknown.

In this chapter, marker compounds have been identified for individual *Rhododendron* species and the six different subgenera of *Rhododendron*. The LC-TOF-MS data has been visualized using box plots, principal component analysis and hierarchical clustering analysis. Correlation studies have been performed using data generated from LC-TOF-MS and the results from anti-microbial and phylogenetic studies.

15.1. Box Plots for Subgenera

Box plots are used to present large amount of data in a simple graphical figure (Figure 15.1). In this thesis, box plots were used to display relative quantities of secondary metabolites from LC-MS data. There are five main parts of a box plot. The bottom and top lines of the rectangle represent the 1st and 3rd quartiles respectively and the difference between them is known as the interquartile range. The middle line in the rectangle represents the median or 2nd quartile. The bottom and top whiskers represent the minimum and maximum values respectively and the difference between them is known as range. The outliers are excluded in this research study.

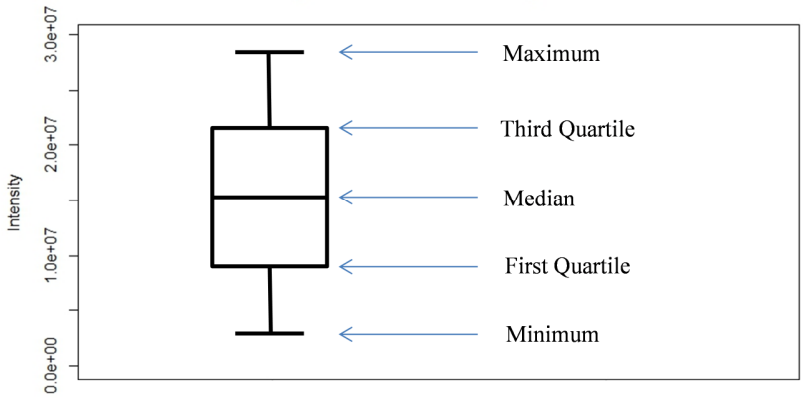

Figure 15.1: Box plot

The LC-TOF-MS data of *Rhododendron* leaf extracts were compiled together using the XCMS package in R software. The intensities as measure of relative quantities of the compounds present in the experimental data of *Rhododendron* species were stored in a csv file. This csv file was used in RStudio to generate box plots of the compounds. The following script was used to load the csv file into RStudio:

```
setwd("C:/Users/ashrestha/Desktop")
compounds<-read.csv('nameofcsvfile.csv')
```

The following function was used to generate box plots with outliers:

```
boxplot(compounds$nameofcompound~compounds$Subgenus, ylab='Intensity',
main='Comparison of nameofcompound')
```

The following function was used to generate box plots without outliers:

```
boxplot(compounds$nameofcompound~compounds$Subgenus, ylab='Intensity',
main='Comparison of nameofcompound', outline=FALSE)
```

The relative intensities could be obtained by integration versus the calibration standard. The samples were extracted and analyzed under the same conditions. The box plots were generated to achieve an overview of the intensity distribution of compounds found in different subgenus.

The box plots were generated for 128 identified compounds based on the five subgenera *Azaleastrum*, *Hymenanthes*, *Pentanthera*, *Rhododendron* and *Tsutsusi*. The subgenus *Mumeazalea* consisted of only one specie which was not enough to generate box plots. Some compounds were present only in one species and the box plots would not be useful in such a case. A few compounds, mainly glycosides of different polyphenol groups are discussed below. The complete list of box plots is given in the Appendix (Additional information on CD).

15.1.1. Hydroxycinnamic acids and their derivatives

The median of all the chlorogenic acids, namely 3-*O*-*p*-coumaroylquinic acid (**1**) (t_R 18.0 min), *cis*-3-*O*-*p*-coumaroylquinic acid (**2**) (t_R 19.4 min), 5-*O*-*p*-coumaroylquinic acid (**3**) (t_R 24.6 min), *cis*-5-*O*-*p*-coumaroylquinic acid (**5**) (t_R 28.4 min), 3-*O*-caffeoylquinic acid (**6**) (t_R 13.0 min) and 5-*O*-caffeoylquinic acid (**8**) (t_R 18.2 min) was highest in the subgenus *Tsutsusi*. For caffeoylshikimic acid (**23**) (t_R 24.6 min), it was the highest in the subgenus *Pentanthera*. The highest concentration of 3-*O*-*p*-coumaroylquinic acid (**1**), 5-*O*-*p*-coumaroylquinic acid (**3**), *cis*-5-*O*-*p*-coumaroylquinic acid (**5**) and caffeoylshikimic acid (**23**) was observed in *Pentanthera*. For *cis*-3-*O*-*p*-coumaroylquinic acid (**2**) and 5-*O*-caffeoylquinic acid (**8**), the highest concentration was observed in *Tsutsusi*. And for 3-*O*-caffeoylquinic acid (**6**), the highest concentration was observed in *Rhododendron*. The box plots of hydroxycinnamic acids of selected *Rhododendron* species have been used in a manuscript to be submitted soon.

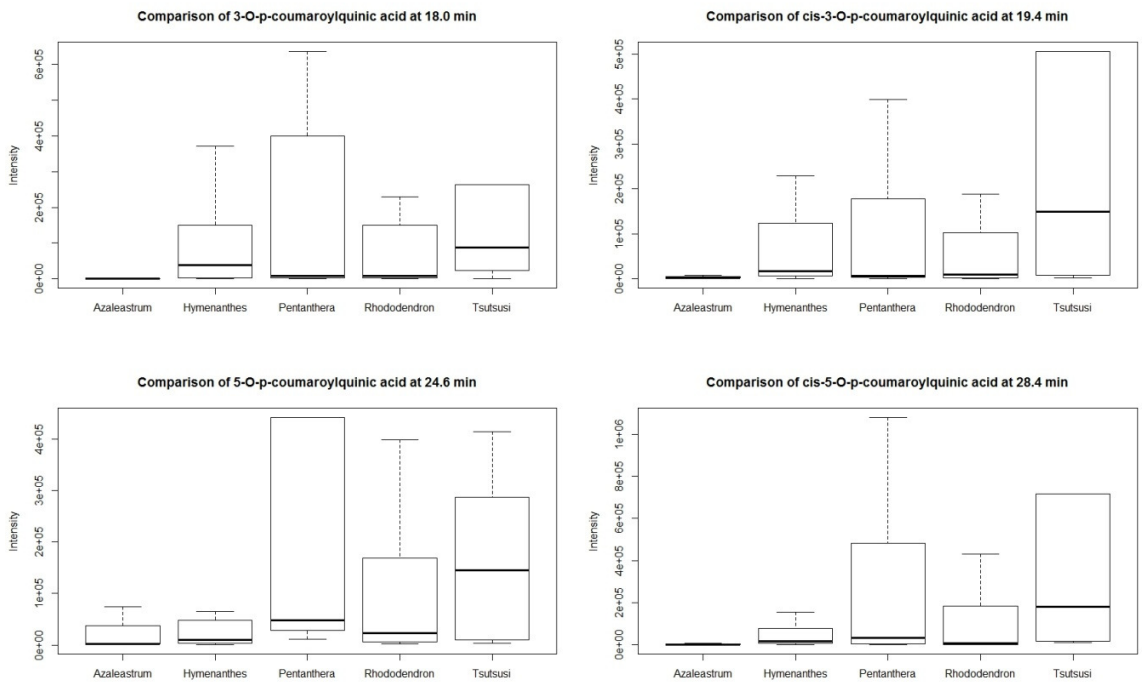

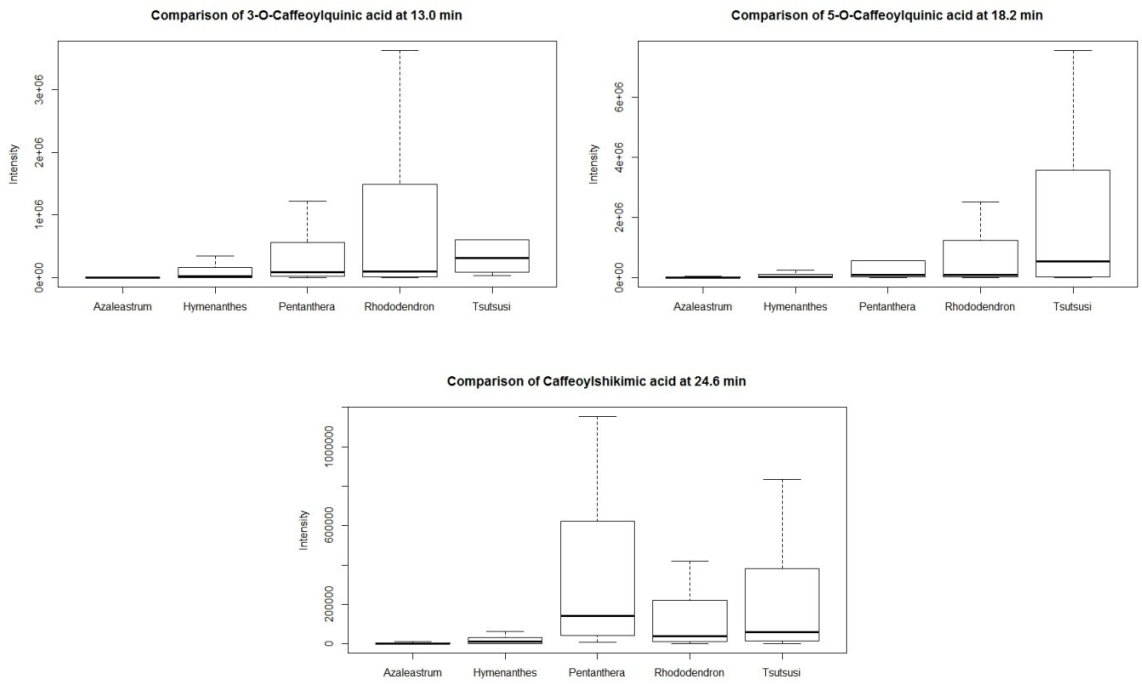

Figure 15.2: Box plots of chlorogenic acids and caffeoylshikimic acid

The highest median for the three caffeic acid-*O*-hexoside isomers (**27**, **28** and **30**) (t_R 12.5, 13.9 and 17.6 min) were found in *Azaleastrum*, *Pentanthera* and *Rhododendron* respectively. For the two *p*-coumaric acid-*O*-hexoside isomers (**35** and **36**) (t_R 16.5 and 24.1 min), the highest median was observed in *Pentanthera* and *Rhododendron* respectively. The highest median for the two ferulic acid-*O*-hexoside isomers (**47** and **48**) (t_R 19.0 and 21.2 min) were observed in *Pentanthera* and *Hymenanthes* respectively.

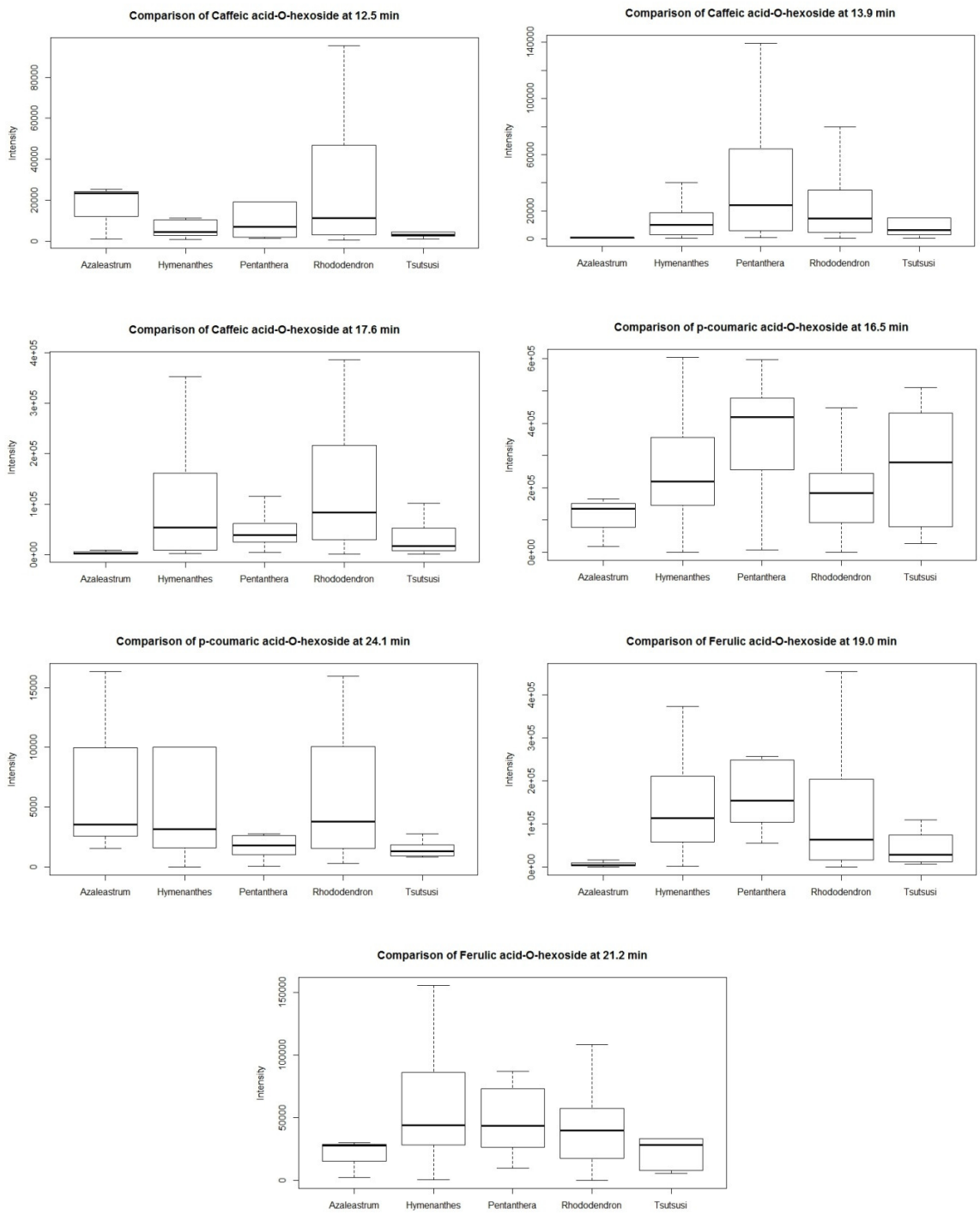

Figure 15.3: Box plots of hydroxycinnamic acid hexosides

15.1.2. Hydroxybenzoic acids and their derivatives

The highest median for both gallic acid-*O*-hexoside isomers (**55** and **56**) (t_R 4.6 and 7.9 min) was observed in *Azaleastrum*. For the two protocatechuic acid-*O*-hexoside isomers (**84** and **85**) (t_R 5.9 and 10.5 min), the highest median was observed in *Pentanthera*. Two salicylic acid-*O*-hexoside isomers (**88** and **89**) (t_R 6.3 and 13.0 min) had the highest median in *Hymenanthes* and *Azaleastrum* respectively. One vanillic acid-*O*-hexoside isomer (**96**) (t_R 10.2 min) had the highest median in *Hymenanthes* while the other three isomers (**95**, **97** and **98**) (t_R 7.7, 11.7 and 13.9 min) had the highest median in *Rhododendron*.

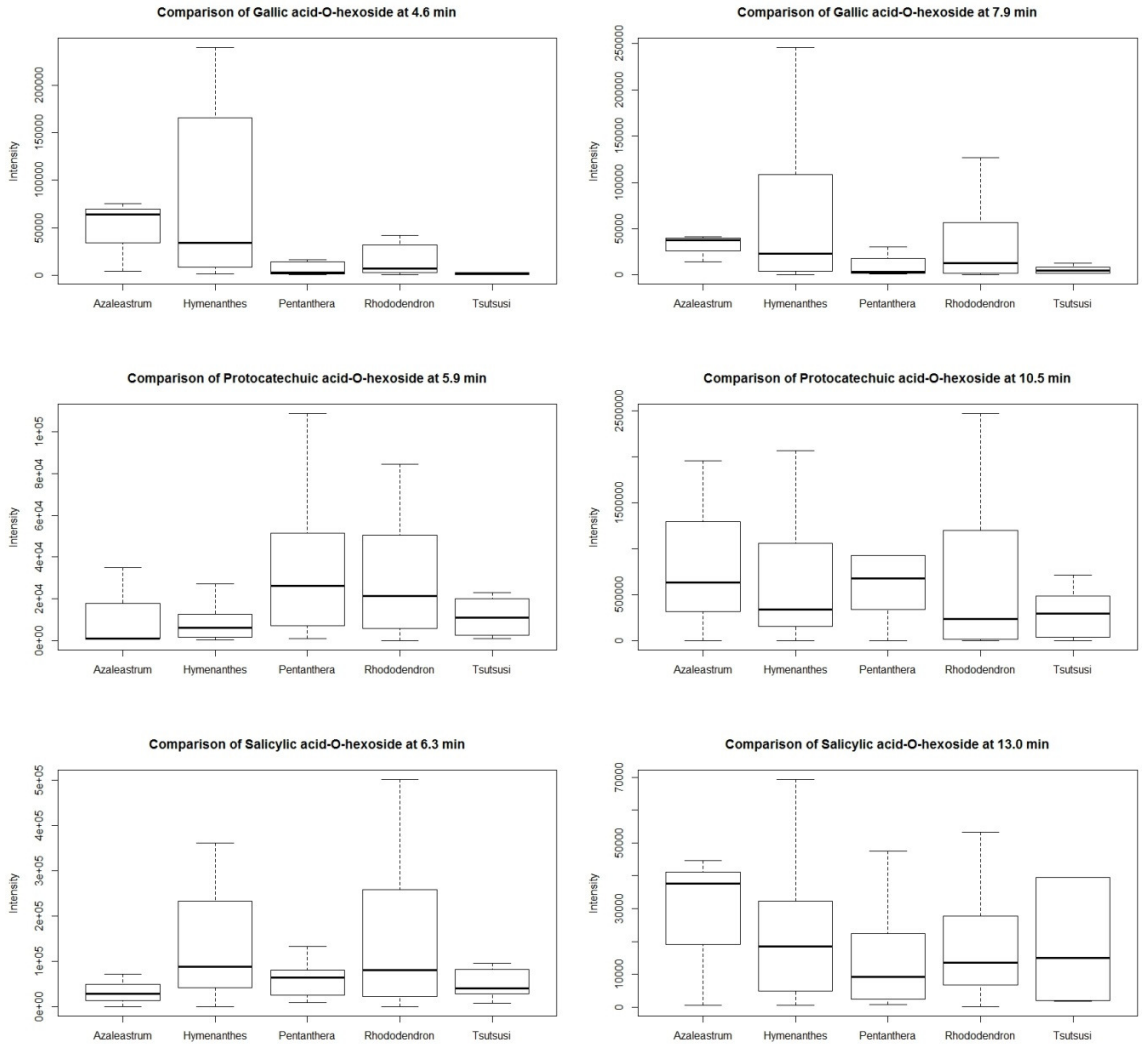

Figure 15.4: Box plots of hydroxybenzoic (gallic, protocatechuic and salicylic) acid hexosides

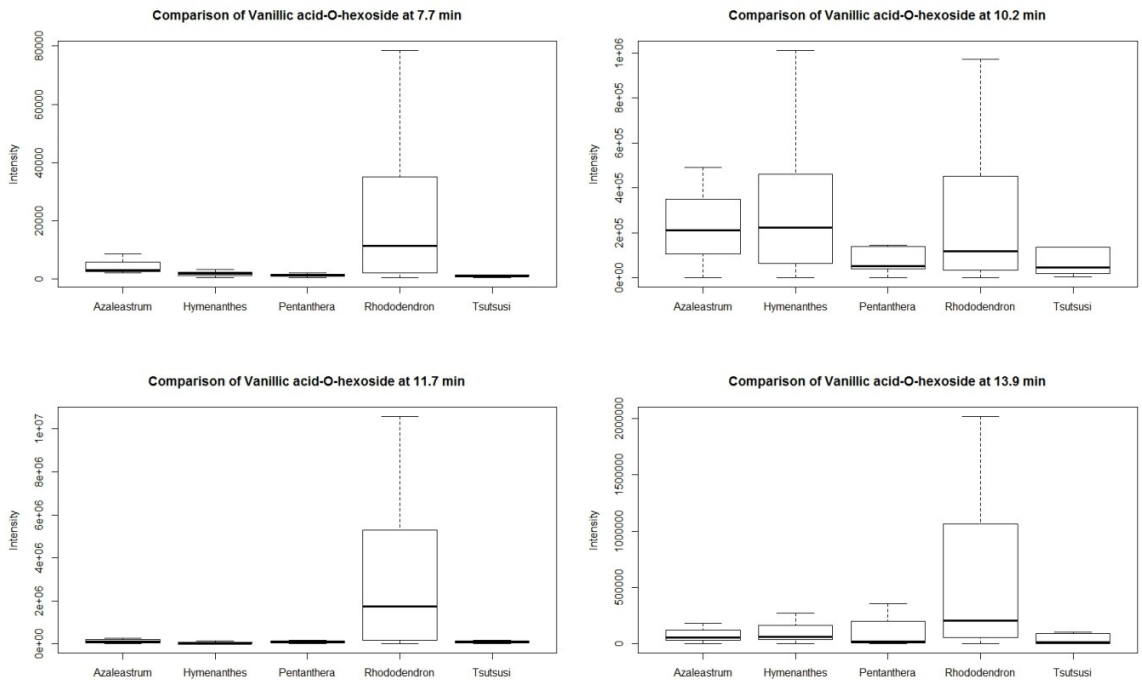

Figure 15.5: Box plots of hydroxybenzoic (vanillic) acid hexosides

15.1.3. Flavan-3-ols

The highest median for catechin (**116**) (t_R 16.0 min) and epicatechin (**117**) (t_R 23.0 min) was observed in *Hymenanthes* and *Tsutsusi* respectively. Both gallocatechin (**118**) (t_R 8.5 min) and epigallocatechin (**119**) (t_R 15.4 min) had the highest median in *Azaleastrum*. Four isomers of A-type procyanidin dimer (**136**, **138**, **140** and **142**) (t_R 5.5, 10.1, 14.0 and 27.2 min) had the highest median in *Hymenanthes* while two isomers (**143** and **144**) (t_R 32.4 and 34.8 min) had the highest median in *Pentanthera*. Four isomers of B-type procyanidin dimer (**145**, **146**, **147** and **149**) (t_R 13.4, 14.3, 18.6 and 23.1 min) had the highest median in *Hymenanthes* while two isomers (**148** and **150**) (t_R 20.3 and 32.8 min) had the highest median in *Tsutsusi*. Two isomers of A-type procyanidin trimer (**175** and **176**) (t_R 22.6 and 23.2 min) had the highest median in *Tsutsusi* while one other isomer (**177**) (t_R 26.7 min) had the highest median in *Pentanthera*. Four isomers of B-type procyanidin trimer (**179**, **180**, **181** and **184**) (t_R 5.6, 14.9, 15.6 and 22.2 min) had the highest median in *Hymenanthes* while two isomers (**183** and **185**) (t_R 19.2 and 25.6 min) had the highest median in *Tsutsusi*.

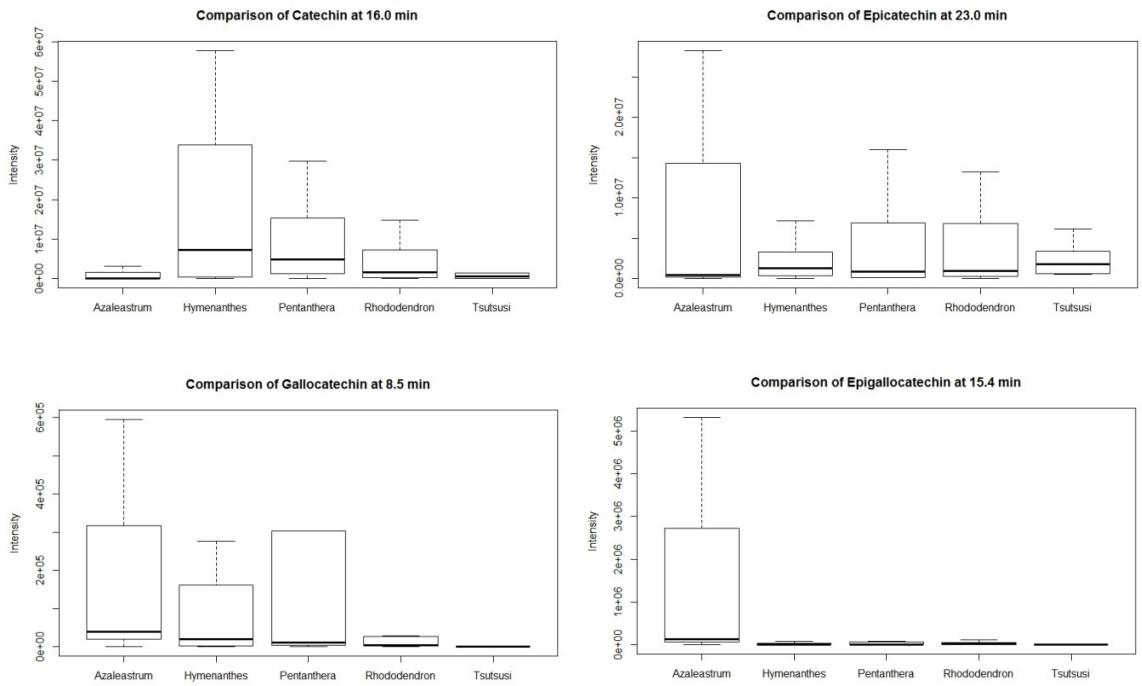

Figure 15.6: Box plots of catechin, epicatechin, gallocatechin and epigallocatechin

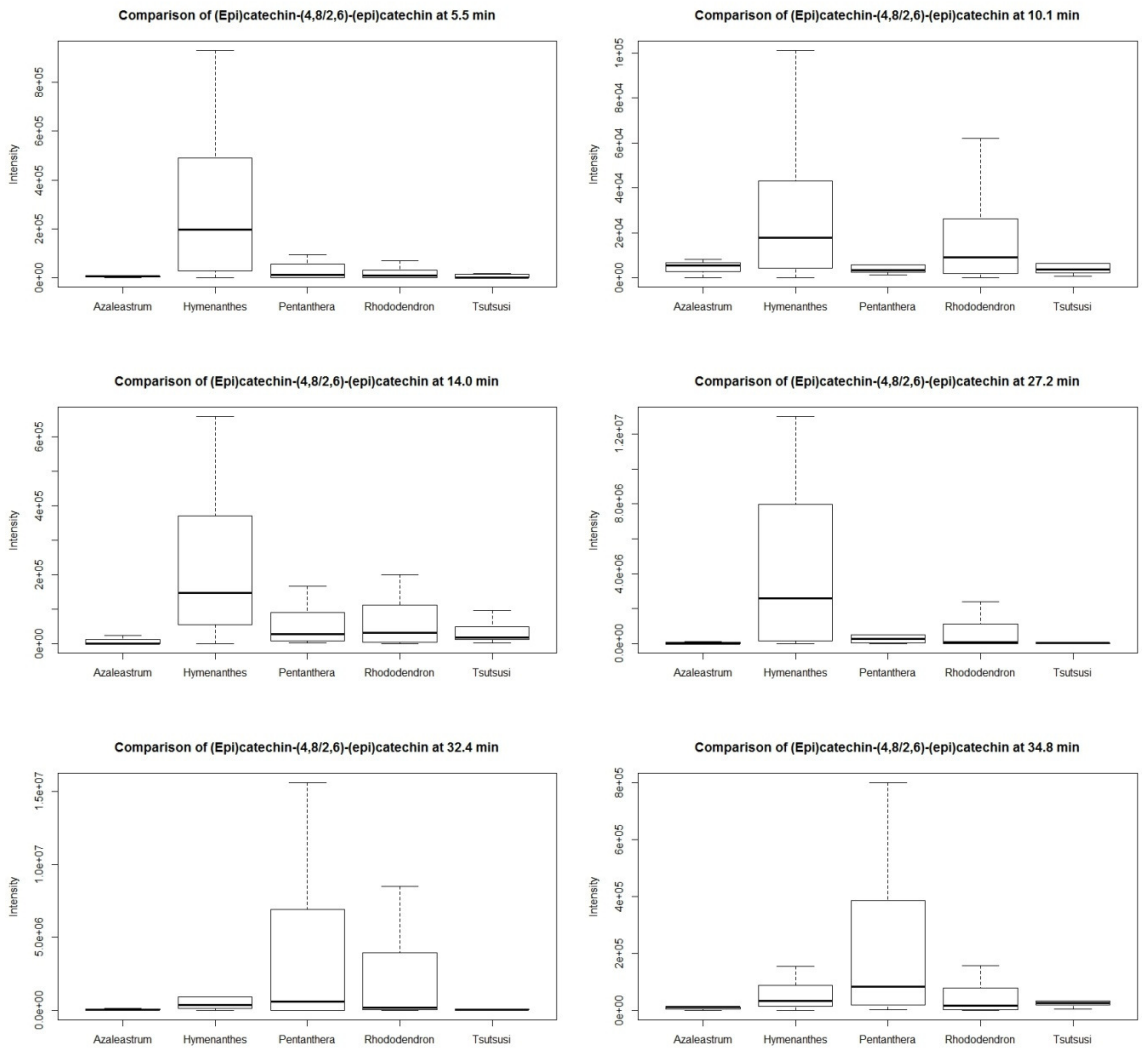

Figure 15.7: Box plots of A-type procyanidin dimers

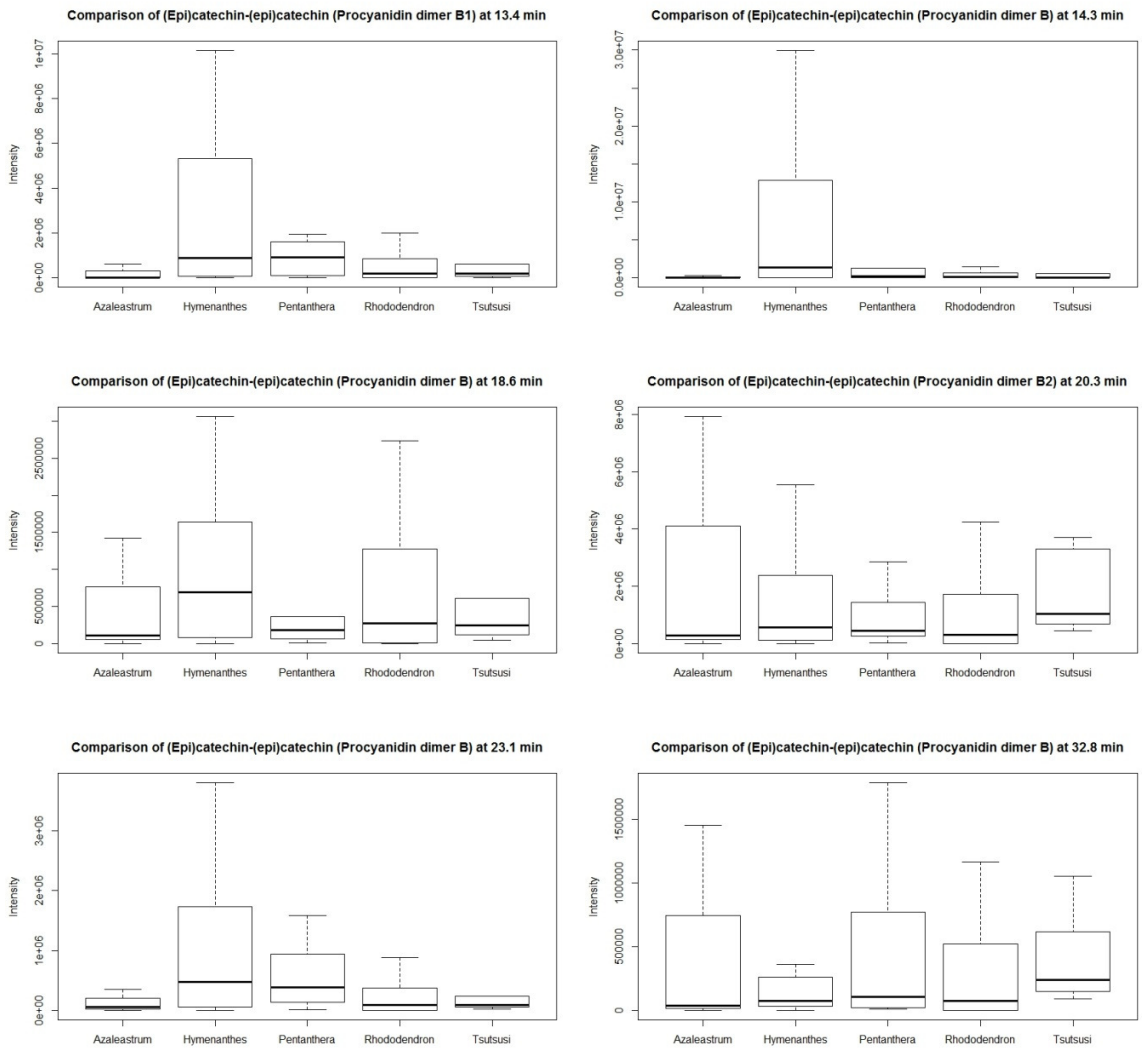

Figure 15.8: Box plots of B-type procyanidin dimers

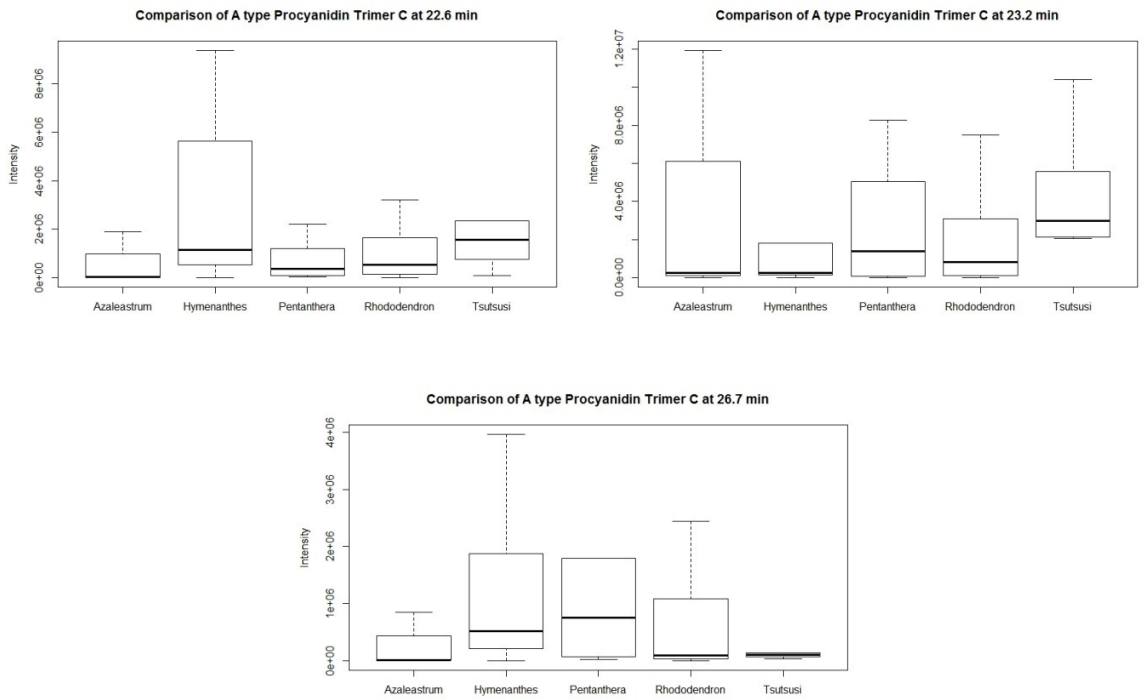

Figure 15.9: Box plots of A-type procyanidin trimers

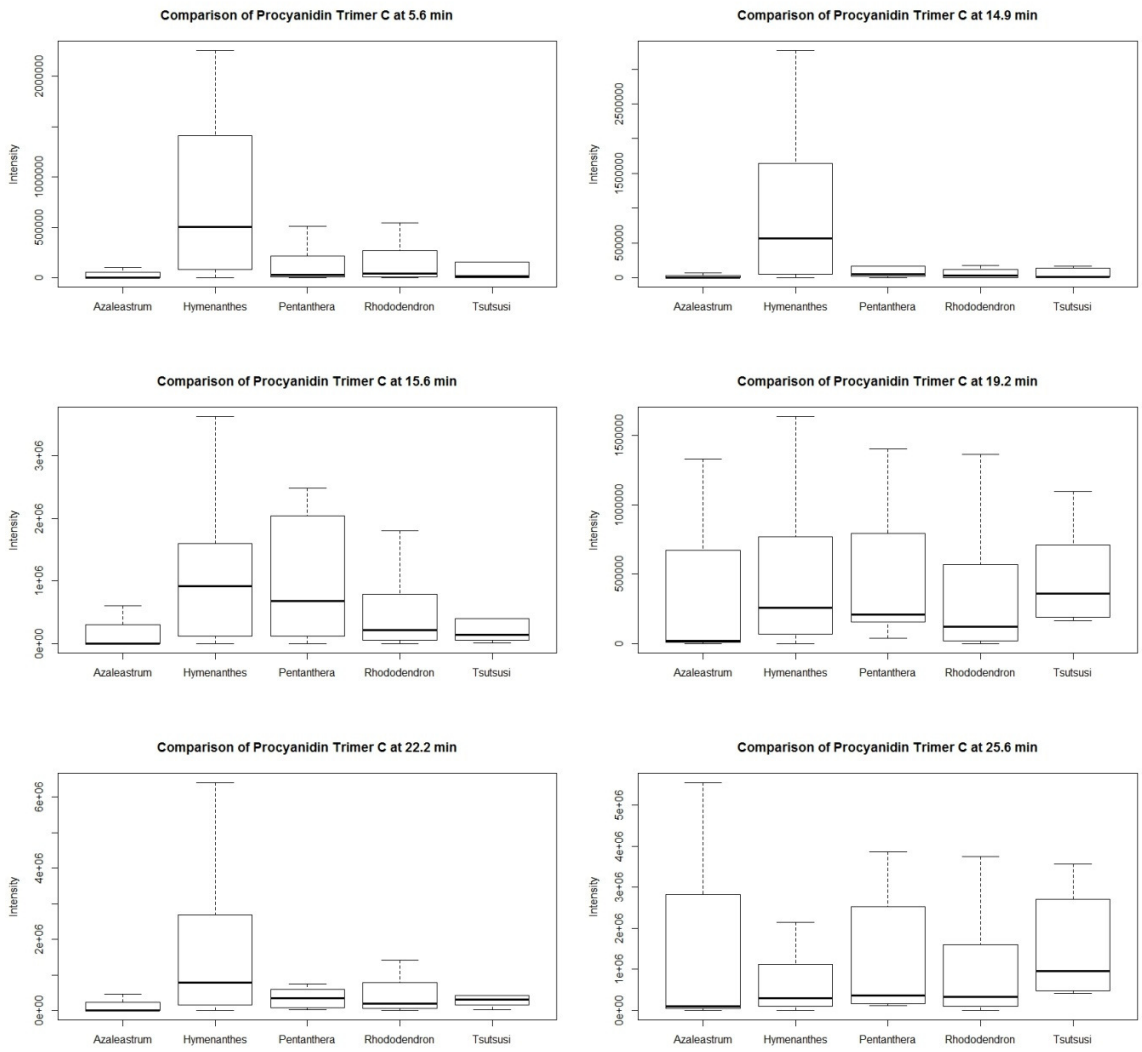

Figure 15.10: Box plots of B-type procyanidin trimers

15.1.4. Flavanones and their derivatives

Naringenin (**203**) was found to be present in the highest concentration in *Azaleastrum*. The median was found to be the highest in *Rhododendron*.

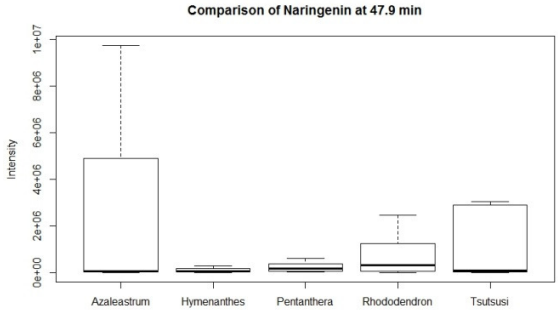

Figure 15.11: Box plot of Naringenin

15.1.5. Flavonols and their derivatives

Myricetin and its derivatives were found to have a large median in *Azaleastrum*. Myricetin (**229**) (t_R 38.9 min) had the highest concentration in *Rhododendron*. Myricetin-*O*-rhamnoside (**233**) (t_R 33.0 min) and myricetin-*O*-hexoside (**234**) (t_R 30.8 min) were found to have the highest concentration and median in *Azaleastrum*. It could be speculated that *Azaleastrum* favored the formation of some myricetin derivatives.

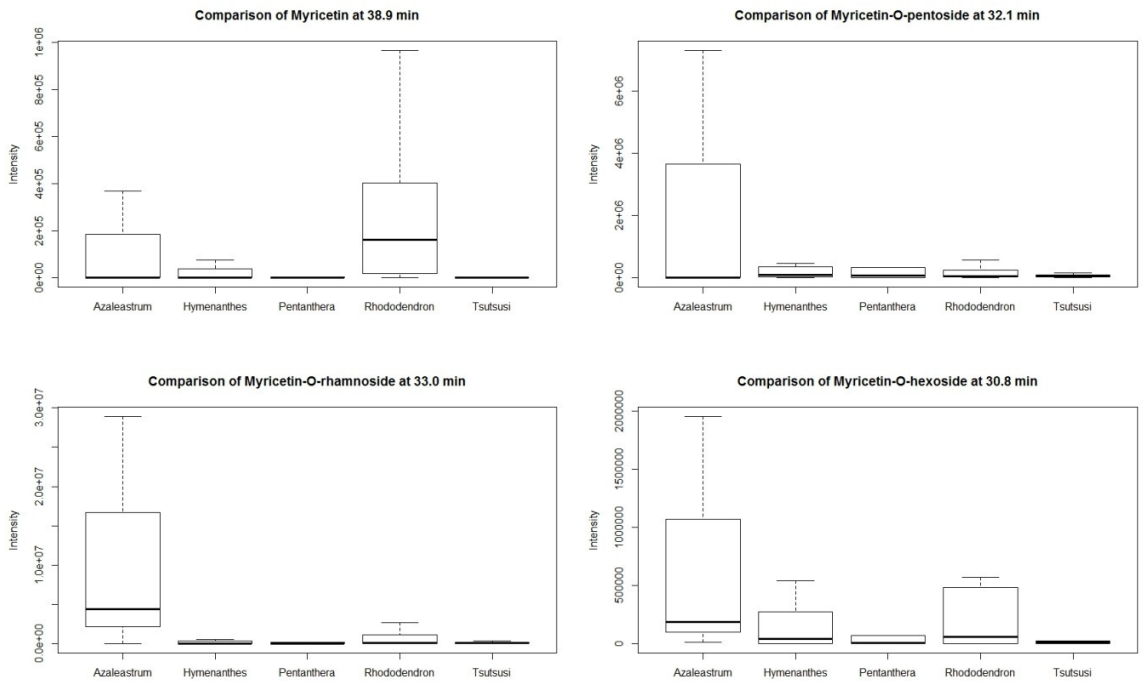

Figure 15.12: Box plots of Myricetin and its derivatives

Quercetin (**248**) (t_R 44.4 min) was found in the highest concentration with the highest median in *Rhododendron*. Two isomers of quercetin-*O*-pentoside (**249** and **252**) (t_R 36.6 and 41.2 min) were found in the highest concentration in *Rhododendron*, while the other two (**250** and **251**) (t_R 37.4 and 39.6 min) in *Hymenanthes*. The highest median for the four isomers of quercetin-*O*-pentoside (**249**, **250**, **251** and **252**) (t_R 36.6, 37.4, 39.6 and 41.2 min) were found in *Tsutsusi*, *Pentanthera*, *Tsutsusi* and *Rhododendron* respectively. Quercetin-*O*-rhamnoside (**253**) (t_R 38.7 min) was found in the highest concentration with the highest median in *Tsutsusi*. The two isomers of quercetin-*O*-hexoside (**254** and **255**) (t_R 34.2 and 35.5 min) were found in the highest concentration with the highest median in *Hymenanthes* and *Rhododendron* respectively.

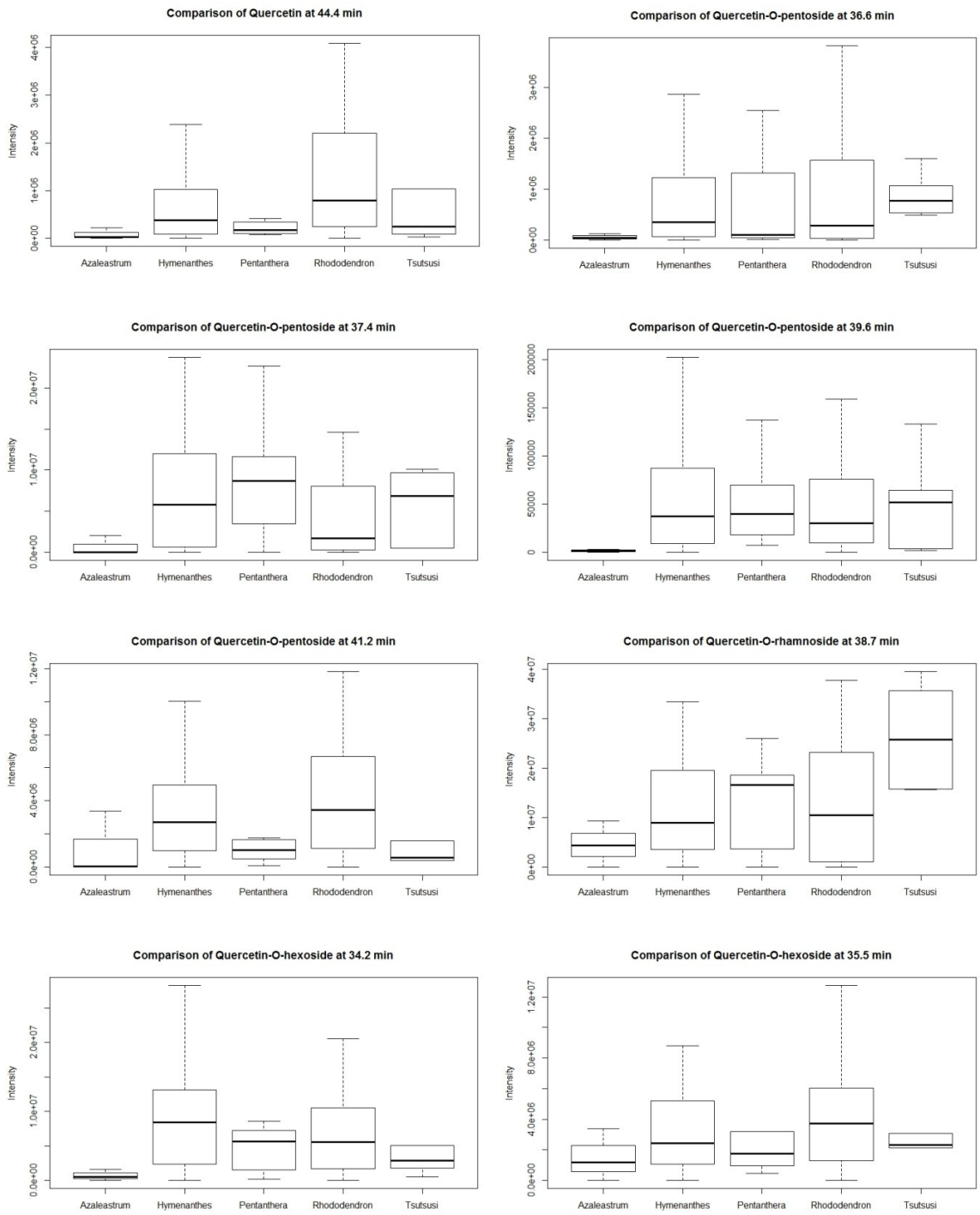

Figure 15.13: Box plots of Quercetin and its derivatives

Kaempferol (**310**) (t_R 49.5 min), kaempferol-*O*-pentoside (**312**) (t_R 43.9 min) and kaempferol-*O*-hexoside (**314**) (t_R 37.5 min) were found to have the highest median and concentration in *Rhododendron*. Kaempferol-*O*-pentoside (**311**) (t_R 41.0 min) was found in the highest median and concentration in *Pentanthera*. Kaempferol-*O*-rhamnoside (**313**) (t_R 43.6 min) on the other hand was found with the highest median in *Pentanthera* and highest concentration in *Rhododendron*.

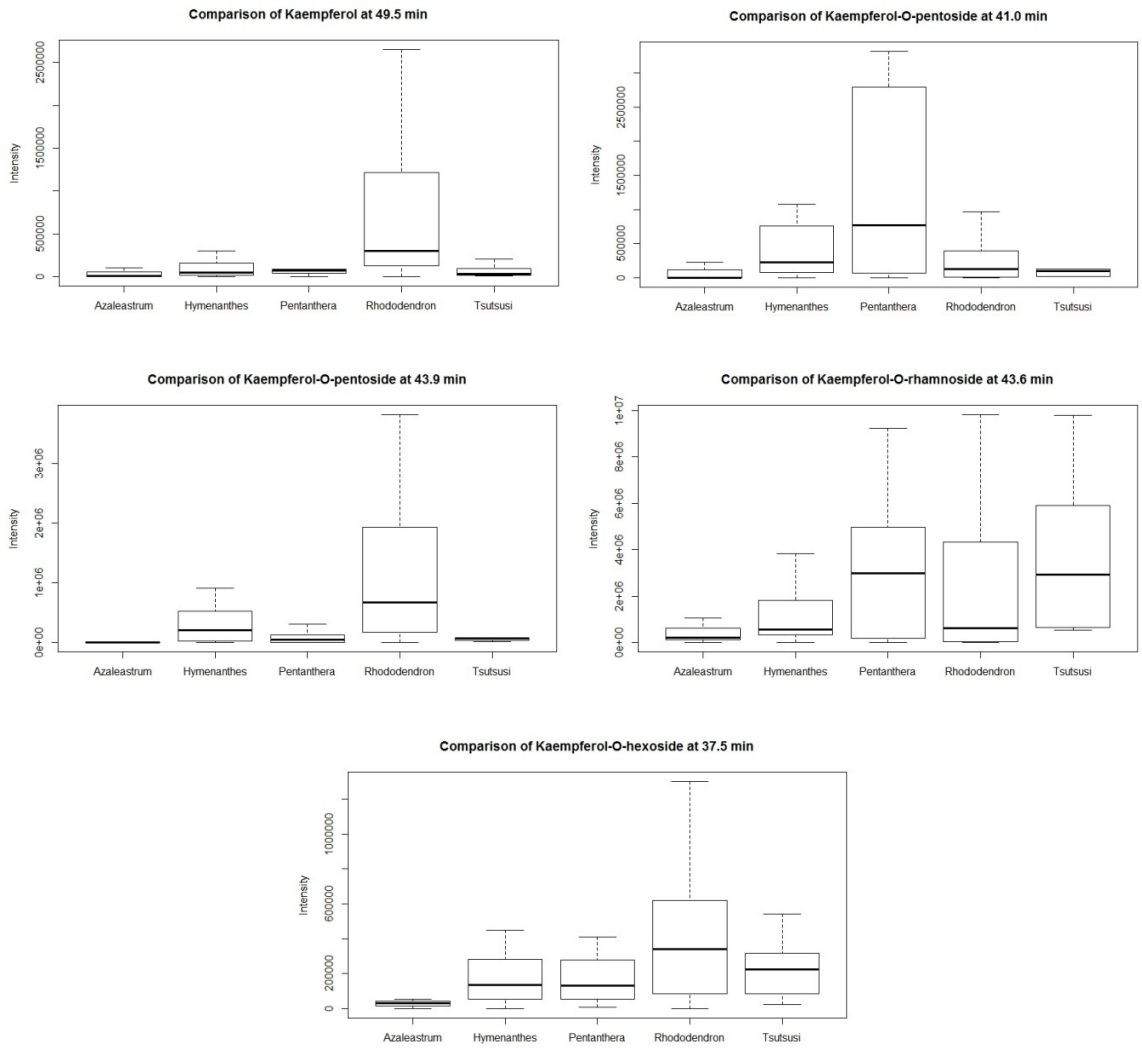

Figure 15.14: Box plots of Kaempferol and its derivatives

In the box plot studies of the five different subgenera of *Rhododendron*, the median of a few identified compounds were found to be higher in a specific subgenus (Table 15.1). It can be speculated that the *Rhododendron* species, which belong to the specific subgenus produced these compounds in a higher relative concentration compared to the other subgenera, which may be useful in the field of chemotaxonomy.

Table 15.1: Identified compounds found with highest median in five *Rhododendron* subgenera

Subgenus	Compounds
Azaleastrum	Myricetin-*O*-rhamnoside (**233**) (t_R 33.0 min), Myricetin-*O*-hexoside (**234**) (t_R 30.8 min)
Hymenanthes	A-type procyanidin dimers (**136**, **138**, **140** and **142**) (t_R 5.5, 10.1, 14.0 and 27.2 min) B-type procyanidin dimers (**145**, **146**, **147** and **149**) (t_R 13.4, 14.3, 18.6 and 23.1 min)
Pentanthera	Caffeic acid-*O*-hexoside (**28**) (t_R 13.9 min), *p*-Coumaric acid-*O*-hexoside (**35**) (t_R 16.5 min), Ferulic acid-*O*-hexoside (**47**) (t_R 19.0 min), Caffeoylshikimic acid (**23**) (t_R 24.6 min),
Rhododendron	Vanillic acid-*O*-hexosides (**95**, **97** and **98**) (t_R 7.7, 11.7 and 13.9 min)
Tsutsusi	Coumaroylquinic acids including 3-*O*-*p*-coumaroylquinic acid (**1**) (t_R 18.0 min), *cis*-3-*O*-*p*-coumaroylquinic acid (**2**) (t_R 19.4 min), 5-*O*-*p*-coumaroylquinic acid (**3**) (t_R 24.6 min), *cis*-5-*O*-*p*-coumaroylquinic acid (**5**) (t_R 28.4 min) Caffeoylquinic acids including 3-*O*-caffeoylquinic acid (**6**) (t_R 13.0 min), 5-*O*-caffeoylquinic acid (**8**) (t_R 18.2 min)

15.2. Box Plots for Isomers

In addition, some box plots were generated to compare the intensities of compounds with the same molecular weight. The following script was used to load the csv file into RStudio:

```
setwd("C:/Users/ashrestha/Desktop")
compounds<-read.csv('nameofcsvfile.csv')
```

The following function was used to generate box plots of two or more compounds without outliers:

```
a=c(compounds$Catechin)
b=c(compounds$Epicatechin)
boxplot(a, b, names=c("Catechin at 16.0 min","Epicatechin at 23.0 min"), ylab='Intensity', main='Comparison of Catechin and Epicatechin', outline=FALSE)
```

15.2.1. Hydroxycinnamic acids and their derivatives

The four isomers of coumaroylquinic acid, namely 3-*O*-*p*-coumaroylquinic acid (**1**) (t_R 18.0 min), *cis*-3-*O*-*p*-coumaroylquinic acid (**2**) (t_R 19.4 min), 5-*O*-*p*-coumaroylquinic acid (**3**) (t_R 24.6 min) and *cis*-5-*O*-*p*-coumaroylquinic acid (**5**) (t_R 28.4 min) were compared and no significant difference was observed between the compound intensities.

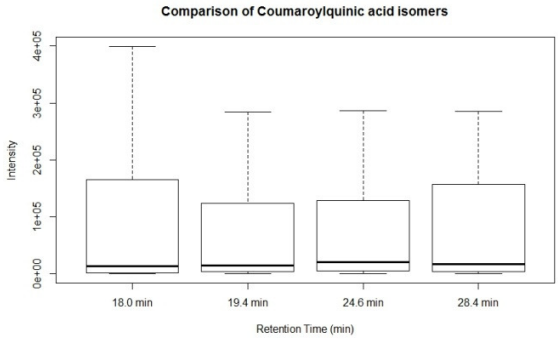

Figure 15.15: Box plots of coumaroylquinic acids

The two isomers of caffeoylquinic acid, namely 3-*O*-caffeoylquinic acid (**6**) (t_R 13.0 min) and 5-*O*-caffeoylquinic acid (**8**) (t_R 18.2 min) were compared and their intensity distribution looked similar.

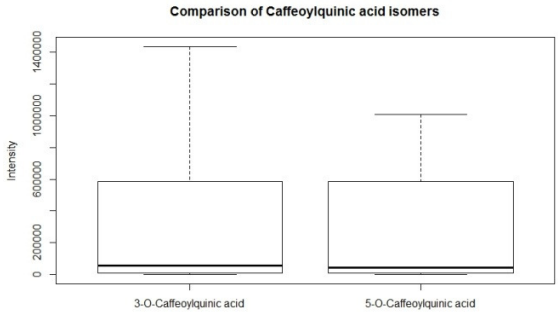

Figure 15.16: Box plots of caffeoylquinic acids

Similarly, the hexosides of caffeic acid (**27**, **28** and **30**), p-coumaric acid (**35** and **36**) and ferulic acid (**47** and **48**) were compared individually. The isomers caffeic acid-*O*-hexoside (**30**) (t_R 17.6 min), *p*-coumaric acid-*O*-hexoside (**35**) (t_R 16.5 min) and ferulic acid-*O*-hexoside (**47**) (t_R 19.0 min) were found in higher concentration in the species.

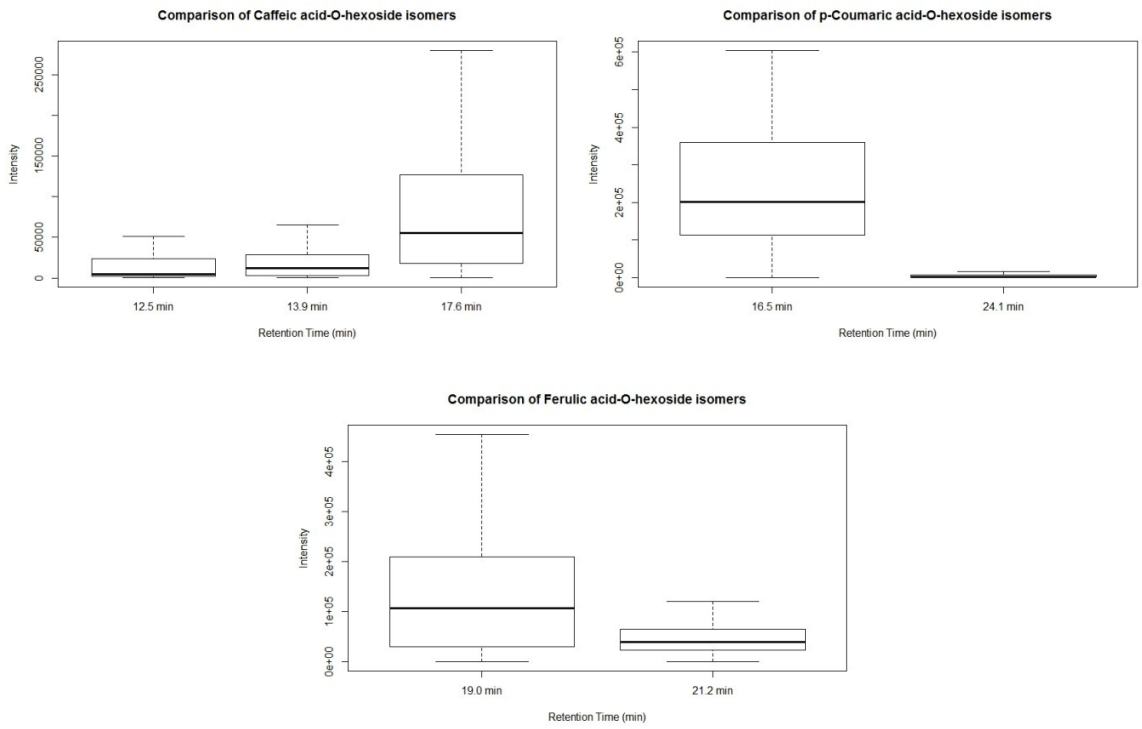

Figure 15.17: Boxplots of isomers of hexosides of caffeic, *p*-coumaric and ferulic acid

15.2.2. Hydroxybenzoic acids and their derivatives

The hexosides of gallic acid (**55** and **56**), protocatechuic acid (**84** and **85**), salicylic acid (**88** and **89**) and vanillic acid (**95**-**98**) were compared independently. The isomers protocatechuic acid-*O*-hexoside (**85**) (t_R 10.5 min) and salicylic acid-*O*-hexoside (**88**) (t_R 6.3 min) were found in higher concentration in the species. Gallic acid-*O*-hexoside isomers (**55** and **56**) were present in similar intensity range. The isomer vanillic acid-*O*-hexoside (**95**) (t_R 7.7 min) was the least abundant isomer.

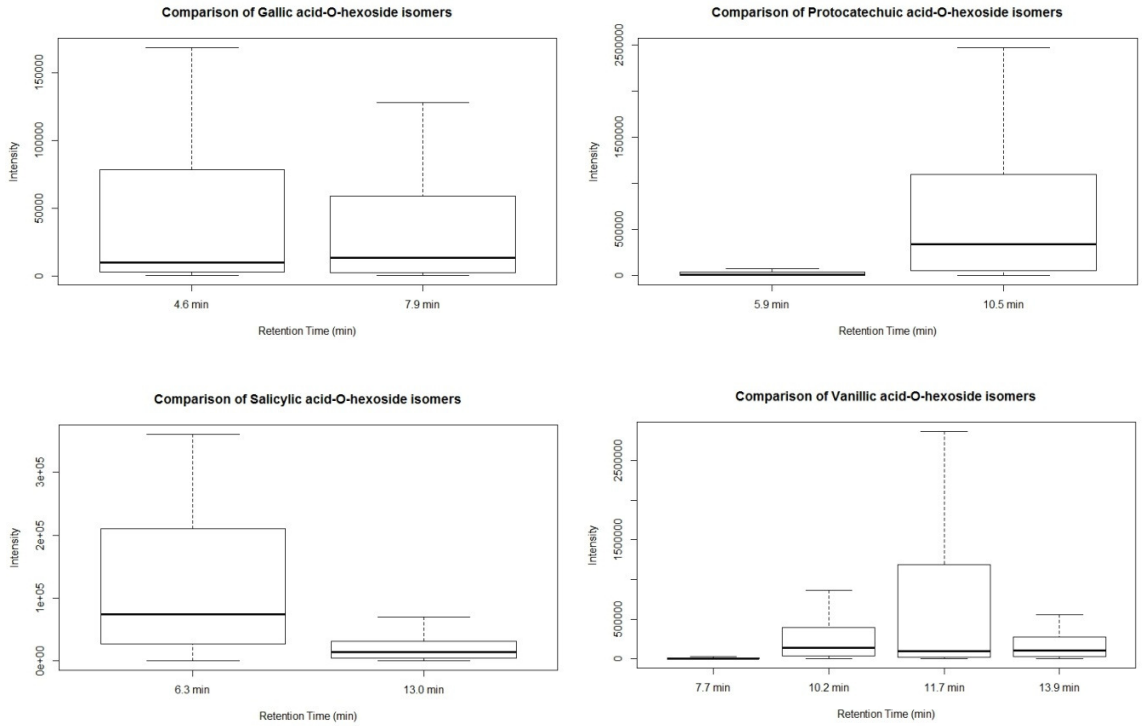

Figure 15.18: Boxplots of isomers of hexosides of gallic, protocatechuic, salicylic and vanillic acid

15.2.3. Flavan-3-ols

The box plots of catechin (**116**) and epicatechin (**117**), gallocatechin (**118**) and epigallocatechin (**119**), A-type procyanidin dimers (**136**, **138**, **140**, **142**, **143** and **144**) and trimers (**175-177**) and B-type procyanidin dimers (**145-150**) and trimers (**179-185**) were compared similarly. The median of catechin and gallocatechin were slightly higher than epicatechin and epigallocatechin respectively. The median of the A-type and B-type procyanidin dimers and trimers were similar in intensity. A few differences were observed in the highest concentration of the compounds for the dimers and trimers.

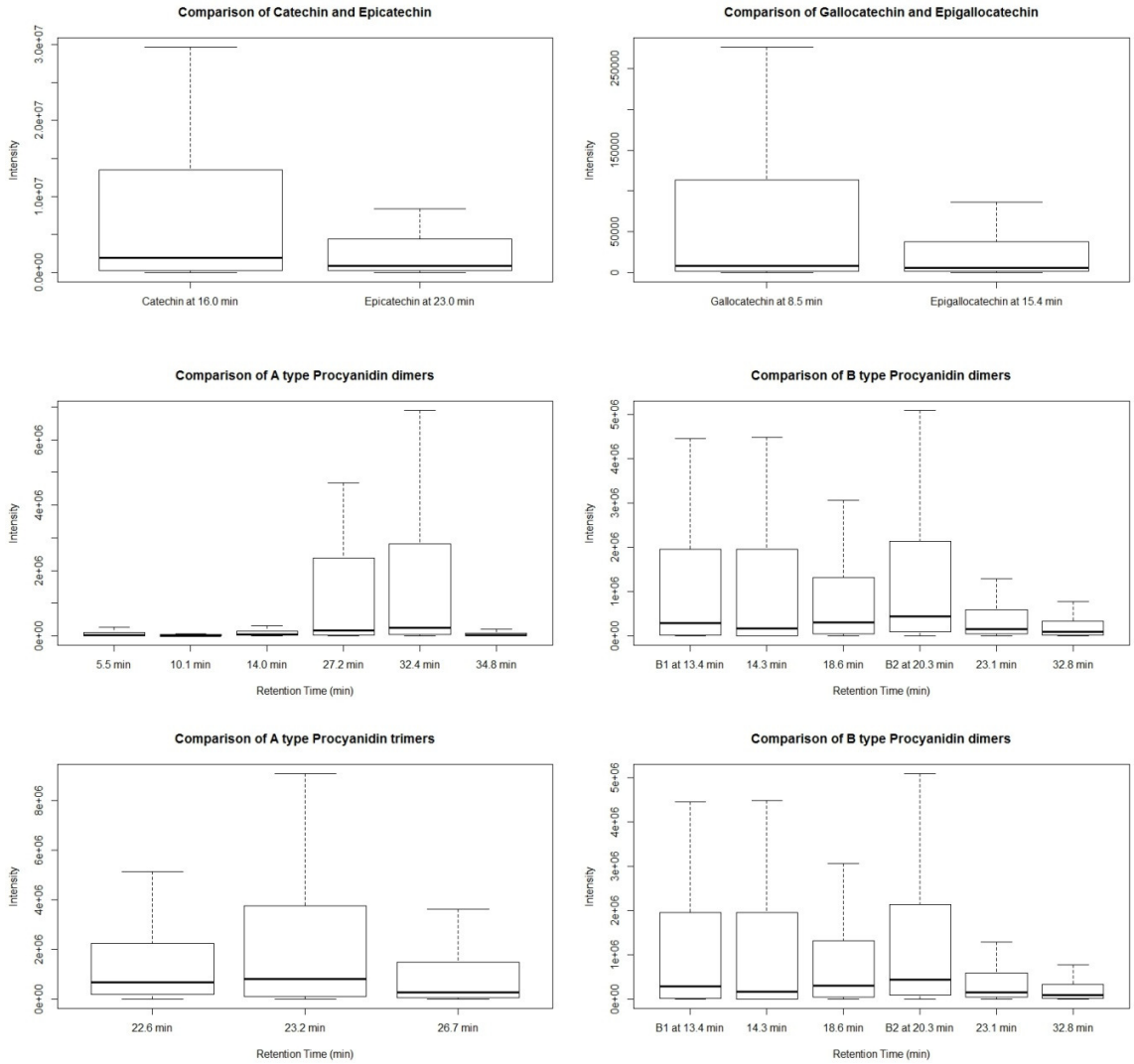

Figure 15.19: Box plots of flavan-3-ols

15.2.4. Flavonols and their derivatives

The four isomers of quercetin-*O*-pentoside (**249**-**252**) and two isomers of quercetin-*O*-hexoside (**254**-**255**) were compared separately. The isomer quercetin-*O*-pentoside (**250**) (t_R 37.4 min) and quercetin-*O*-hexoside (**254**) (t_R 34.2 min) were found in higher concentrations.

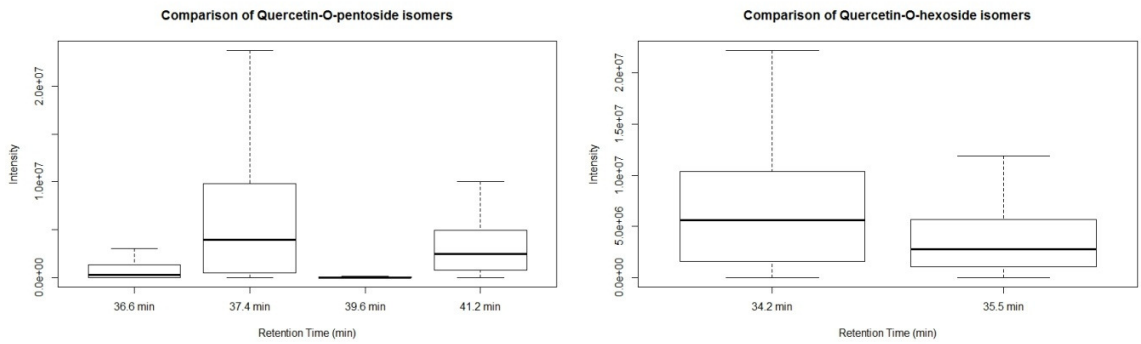

Figure 15.20: Box plots of the isomers of quercetin-*O*-pentoside and quercetin-*O*-hexoside

15.3. Marker Compounds

Marker compounds are the compound or compounds present in only one set of the samples and are thus used for chemotaxonomy and system classification. They could be present in samples, which belong in the same class for examples in the subgenus *Rhododendron* or it could be present in only one *Rhododendron* species such as *Rhododendron ambiguum*. The marker compounds could be synthesized in certain plants or groups of plants due to the presence of certain synthases, which are enzymes that plants use to form a variety of secondary metabolites. In the subgenera marker compound study, some compounds were found to be specific for a subgenus of *Rhododendron*. In the individual specie marker compound study, some *Rhododendron* species were found to have more than one marker compound.

The marker compounds for the six different subgenera of *Rhododendron* analyzed in this study are shown in Table 15.2. Some marker compounds were identified for individual species in the analyzed *Rhododendron* leaves and are shown in Table 15.3.

Table 15.2: Marker compounds of the *Rhododendron* subgenera

Subgenus	Compounds
Azaleastrum	Galloylarbutin **63** (t_R 11.7 min), Gallic acid-*O*-coumaroyl-hexoside **70** (t_R 31.0 min), Gallic acid-*O*-coumaroyl-hexoside **71** (t_R 32.6 min), Hyemaloside B / Guavinoside A **81** (t_R 30.9 min), (Epi)catechin-*O*-dimethyl-gallate **133** (t_R 38.9 min), Myricetin-3-*O*-hexoside-7-*O*-rhamnoside **245** (t_R 35.4 min)
Hymenanthes	Caffeic acid-*O*-hexoside **24** (t_R 8.1 min), Caffeic acid-*O*-hexoside **25** (t_R 9.2 min), Caffeic acid-*O*-hexoside **31** (t_R 19.2 min), Everlastoside M **42** (t_R 27.0 min), *p*-Coumaric acid-*O*-dihexoside **43** (t_R 14.4 min), Galloylquinic acid **60** (t_R 9.6 min), Gallic acid-*O*-acetyl-hexoside **61** (t_R 13.9 min), Benzyl-6'-*O*-galloyl-*β*-*D*-hexoside **62** (t_R 32.1 min), 6-galloyl-1-*O*-(phloroglucinol)-hexoside **65** (t_R 15.0 min), Gallic acid-*O*-galloyl-rhamnoside **68** (t_R 36.6 min), Galloyl-*O*-vanilloyl-*O*-hexoside **74** (t_R 27.1 min), Gallic acid-*O*-dihexoside **77** (t_R 3.2 min), Gallic acid-*O*-feruloyl-hexoside **80** (t_R 36.2 min), Galloylalbiflorin **82** (t_R 42.8 min), Protocatechuic acid-*O*-benzoyl-hexoside **86** (t_R 51.8 min),

Subgenus	Compounds
Hymenanthes	Protocatechuic acid-*O*-feruloyl-hexoside **87** (t_R 51.1 min), Salicylic acid-*O*-coumaroyl-hexoside **92** (t_R 42.4 min), Salicylic acid-*O*-dihexoside **94** (t_R 7.0 min), Vanillic acid-*O*-coumaroyl-hexoside **106** (t_R 47.8 min), Methyl gallate-*O*-coumaroyl-hexoside **114** (t_R 42.1 min), Gambiriin A/D **151** (t_R 19.2 min), Procyanidin trimer gallate **191** (t_R 13.1 min), Procyanidin trimer gallate **192** (t_R 18.3 min), Procyanidin tetramer **200** (t_R 24.5 min), Quercetin-*O*-dipentoside **273** (t_R 33.8 min), Quercetin-*O*-galloyl-pentoside **280** (t_R 39.1 min), Cypellogin A/B **303** (t_R 51.7 min), Cypellogin C **305** (t_R 52.6 min), Laricitrin-*O*-hexoside **341** (t_R 40.1 min), Laricitrin-*O*-glucuronide **343** (t_R 42.7 min)
Pentanthera	3-*O*-hydroxydihydro-Caffeoylquinic acid **15** (t_R 5.9 min), 4-*O*-hydroxydihydro-Caffeoylquinic acid **18** (t_R 9.8 min), 4-*O*-hydroxydihydro-Caffeoylquinic acid **19** (t_R 10.8 min), Teucrol **22** (t_R 51.0 min), Teucrol-*O*-hexoside **32** (t_R 42.0 min), *p*-Coumaric acid-*O*-shikimate **33** (t_R 30.8 min), *p*-Coumaric acid-*O*-glucosyl ester **39** (t_R 18.7 min), Vanilloyl-*O*-hydroxybenzoyl-hexoside **100** (t_R 17.5 min), (Epi)gallocatechin gallate **129** (t_R 19.8 min), (Epi)gallocatechin gallate **131** (t_R 26.6 min), Malaferin C **132** (t_R 41.2 min), (Epi)catechin-3-*O*-hexoside-7-*O*-hexoside **166** (t_R 11.8 min), (Epi)catechin-3-*O*-hexoside-7-*O*-hexoside **167** (t_R 13.2 min), (Epi)gallocatechin-(4,8′/2,7′)-(epi)gallocatechin-(4′,8′′)-(epi)catechin **189** (t_R 15.9 min), Quercetin-*O*-pentoside-*O*-hexoside **285** (t_R 24.7 min), Quercetin-3-(4"-*O*-acetyl)-*O*-rhamnoside-7-*O*-rhamnoside **305** (t_R 40.7 min), Laricitrin-*O*-coumaroyl-hexoside **347** (t_R 50.4 min)
Rhododendron	*p*-Coumaric acid-*O*-hexoside-*O*-pentoside **41** (t_R 19.2 min), *p*-Coumaric acid-*O*-dihexoside **44** (t_R 20.0 min), Ferulic acid-*O*-hexoside **50** (t_R 28.9 min), Gallic acid-*O*-rutinoside **69** (t_R 6.6 min), Galloyl-*O*-vanilloyl-*O*-hexoside **75** (t_R 30.1 min), Gallic acid-3-*O*-(6'-*O*-galloyl)-*β*-*D*-hexoside **76** (t_R 22.5 min), Salicyloylsalicin **91** (t_R 36.6 min), Vanilloyl-*O*-hydroxybenzoyl-hexoside **101** (t_R 40.8 min), Vanillic acid-*O*-hexoside-*O*-pentoside **102** (t_R 14.9 min), Vanillic acid-*O*-rutinoside **104** (t_R 12.5 min), Vanillic acid-*O*-rutinoside **105** (t_R 18.9 min), Vanillic acid-*O*-dihexoside **107** (t_R 4.6 min), Vanillic acid-*O*-dihexoside **108** (t_R 5.3 min), Vanillic acid-*O*-dihexoside **109** (t_R 8.5 min),

Subgenus	Compounds
Rhododendron	Litseaefoloside A **110** (t_R 47.0 min), Methyl gallate-*O*-dihexoside **115** (t_R 8.0 min), (Epi)catechin-*O*-rhamnoside **121** (t_R 22.5 min), (Epi)catechin-(4,8/2,6)-(epi)catechin **137** (t_R 8.7 min), (Epi)gallocatechin-(epi)catechin **158** (t_R 16.5 min), (Epi)gallocatechin-(epi)catechin **159** (t_R 18.2 min), Procyanidin Trimer C **182** (t_R 16.6 min), (Epi)gallocatechin-(4,8′)-(epi)gallocatechin-(4′,8″)-(epi)catechin **190** (t_R 9.1 min), Procyanidin tetramer **202** (t_R 30.5 min), Taxifolin-*O*-acetyl-rhamnoside **222** (t_R 39.9 min), Taxifolin-*O*-acetyl-rhamnoside **223** (t_R 45.0 min), Taxifolin-*O*-pentoside-*O*-hexoside **226** (t_R 17.7 min), Taxifolin-*O*-rhamnoside-*O*-hexoside **227** (t_R 20.1 min), Taxifolin-*O*-rhamnoside-*O*-hexoside **228** (t_R 32.8 min), Myricetin-*O*-acetyl-rhamnoside **238** (t_R 37.6 min), Myricetin-*O*-dipentoside **239** (t_R 41.4 min), Myricetin-*O*-dipentoside **240** (t_R 42.5 min), Quercetin-*O*-acetyl-pentoside **258** (t_R 45.5 min), Quercetin-*O*-acetyl-pentoside **259** (t_R 48.0 min), Quercetin-*O*-acetyl-hexoside **270** (t_R 45.6 min), Quercetin-*O*-acetyl-hexoside **271** (t_R 46.5 min), Quercetin-*O*-diacetyl-hexoside **272** (t_R 51.5 min), Quercetin-3-*O*-(4"-3-hydroxy-3-methylglutaryl)-*α*-rhamnoside **282** (t_R 44.9 min), Quercetin-*O*-rhamnoside-*O*-hexoside **289** (t_R 25.7 min), Kaempferol-*O*-diacetyl-hexoside **324** (t_R 55.0 min), Laricitrin-*O*-coumaroyl-rhamnoside **344** (t_R 55.5 min), Laricitrin-*O*-coumaroyl-hexoside **346** (t_R 48.2 min), Quercetin-*O*-rhamnoside-*O*-hexoside **292** (t_R 31.5 min), Kaempferol-*O*-rhamnoside-*O*-pentoside **325** (t_R 38.4 min), Kaempferol-*O*-rhamnoside-*O*-pentoside **327** (t_R 43.4 min), Resinoside A/B **333** (t_R 51.9 min), Laricitrin-*O*-rutinoside **345** (t_R 36.8 min)
Tsutsusi	Ferulic acid-*O*-dihexoside **51** (t_R 17.2 min), Naringenin-*O*-hexoside-*O*-pentoside **205** (t_R 38.0 min), Taxifolin-*O*-acetyl-hexoside **224** (t_R 46.7 min), Taxifolin-*O*-acetyl-hexoside **225** (t_R 48.1 min)
Mumeazalea	*p*-Coumaric acid-*O*-hexoside-*O*-pentoside **40** (t_R 17.6 min), (Epi)gallocatechin-(4,8)-3′-O-galloyl(epi)gallocatechin **174** (t_R 25.7 min), Kaempferol-*O*-galloyl-pentoside **329** (t_R 47.1 min)

Table 15.3: Marker compounds of individual *Rhododendron* species

Species	Lab No.	Subgenus	Compounds
Rhododendron mucronatum var. *ripense*	5	*Tsutsusi*	Taxifolin-*O*-acetyl-hexoside **224** (t_R 46.7 min), Taxifolin-*O*-acetyl-hexoside **225** (t_R 48.1 min)
Rhododendron tomentosum	6	*Rhododendron*	(Epi)catechin-(4,8/2,6)-(epi)catechin **137** (t_R 8.7 min)
Rhododendron argyrophyllum ssp. *nankingense*	12	*Hymenanthes*	Quercetin-*O*-dipentoside **273** (t_R 33.8 min)
Rhododendron ponticum	13	*Hymenanthes*	Caffeic acid-*O*-hexoside **31** (t_R 19.2 min), Galloylquinic acid **60** (t_R 9.6 min)
Rhododendron rubiginosum	14	*Rhododendron*	Vanillic acid-*O*-dihexoside **108** (t_R 5.3 min), Quercetin-*O*-diacetyl-hexoside **272** (t_R 51.5 min), Kaempferol-*O*-diacetyl-hexoside **324** (t_R 55.0 min)
Rhododendron cinnabarinum	15	*Rhododendron*	Vanillic acid-*O*-rutinoside **105** (t_R 18.9 min), Quercetin-*O*-acetyl-hexoside **270** (t_R 45.6 min), Quercetin-*O*-acetyl-hexoside **271** (t_R 46.5 min)
Rhododendron auriculatum	16	*Hymenanthes*	6-galloyl-1-*O*-(phloroglucinol)-hexoside **65** (t_R 15.0 min)
Rhododendron hongkongense	18	*Azaleastrum*	(Epi)catechin-*O*-dimethyl-gallate **133** (t_R 38.9 min)
Rhododendron leucaspis	19	*Rhododendron*	Taxifolin-*O*-acetyl-rhamnoside **222** (t_R 39.9 min), Taxifolin-*O*-acetyl-rhamnoside **223** (t_R 45.0 min)
Rhododendron ferrugineum	20	*Rhododendron*	Litseaefoloside A **110** (t_R 47.0 min)
Rhododendron strigillosum	21	*Hymenanthes*	Galloylalbiflorin **82** (t_R 42.8 min)
Rhododendron annae	24	*Hymenanthes*	Laricitrin-*O*-hexoside **341** (t_R 40.1 min)
Rhododendron elliottii	26	*Hymenanthes*	Galloyl-*O*-vanilloyl-*O*-hexoside **74** (t_R 27.1 min)
Rhododendron griersonianum	27	*Hymenanthes*	Caffeic acid-*O*-hexoside **25** (t_R 9.2 min), Salicylic acid-*O*-coumaroyl-hexoside **92** (t_R 42.4 min)
Rhododendron davidsonianum	30	*Rhododendron*	Quercetin-*O*-acetyl-pentoside **258** (t_R 45.5 min), Quercetin-*O*-acetyl-pentoside **259** (t_R 48.0 min)
Rhododendron tapetiforme	31	*Rhododendron*	Laricitrin-*O*-coumaroyl-rhamnoside **344** (t_R 55.5 min), Laricitrin-*O*-coumaroyl-hexoside **346** (t_R 48.2 min)
Rhododendron ledebourii	34	*Rhododendron*	Quercetin-*O*-rhamnoside-*O*-hexoside **289** (t_R 25.7 min)
Rhododendron polycladum	36	*Rhododendron*	Myricetin-*O*-dipentoside **239** (t_R 41.4 min)
Rhododendron lutescens	39	*Rhododendron*	Procyanidin tetramer **202** (t_R 30.5 min)

Species	Lab No.	Subgenus	Compounds
Rhododendron moulmainense	40	*Azaleastrum*	Gallic acid-*O*-coumaroyl-hexoside **70** (t_R 31.0 min), Gallic acid-*O*-coumaroyl-hexoside **71** (t_R 32.6 min)
Rhododendron spinuliferum	41	*Rhododendron*	Vanillic acid-*O*-rutinoside **104** (t_R 12.5 min)
Rhododendron williamsianum	43	*Hymenanthes*	Vanillic acid-*O*-coumaroyl-hexoside **106** (t_R 47.8 min), Cypellogin C **305** (t_R 52.6 min)
Rhododendron genestierianum	44	*Rhododendron*	Quercetin-*O*-rhamnoside-*O*-hexoside **292** (t_R 31.5 min), Kaempferol-*O*-rhamnoside-*O*-pentoside **325** (t_R 38.4 min), Kaempferol-*O*-rhamnoside-*O*-pentoside **327** (t_R 43.4 min)
Rhododendron scabrifolium var. *spiciferum*	47	*Rhododendron*	(Epi)catechin-*O*-rhamnoside **121** (t_R 22.5 min), Taxifolin-*O*-pentoside-*O*-hexoside **226** (t_R 17.7 min), Taxifolin-*O*-rhamnoside-*O*-hexoside **227** (t_R 20.1 min)
Rhododendron xanthostephanum	50	*Rhododendron*	Galloyl-*O*-vanilloyl-*O*-hexoside **75** (t_R 30.1 min), Gallic acid-3-*O*-(6'-*O*-galloyl)-*β*-*D*-hexoside **76** (t_R 22.5 min), (Epi)gallocatechin-(epi)catechin **159** (t_R 18.2 min)
Rhododendron wardii var. *puralbum*	51	*Hymenanthes*	Benzyl-6'-*O*-galloyl-*β*-*D*-hexoside **62** (t_R 32.1 min), Gallic acid-*O*-galloyl-rhamnoside **68** (t_R 36.6 min), Protocatechuic acid-*O*-benzoyl-hexoside **86** (t_R 51.8 min), Protocatechuic acid-*O*-feruloyl-hexoside **87** (t_R 51.1 min)
Rhododendron protistum	52	*Hymenanthes*	Cypellogin A/B **303** (t_R 51.7 min)
Rhododendron keysii	54	*Rhododendron*	Ferulic acid-*O*-hexoside **50** (t_R 28.9 min), Taxifolin-*O*-rhamnoside-*O*-hexoside **228** (t_R 32.8 min)
Rhododendron alutaceum var. *iodes*	57	*Hymenanthes*	Salicylic acid-*O*-dihexoside **94** (t_R 7.0 min), Laricitrin-*O*-glucuronide **343** (t_R 42.7 min)
Rhododendron austrinum	59	*Pentanthera*	Quercetin-3-(4"-*O*-acetyl)-*O*-rhamnoside-7-*O*-rhamnoside **305** (t_R 40.7 min), Laricitrin-*O*-coumaroyl-hexoside **347** (t_R 50.4 min)
Rhododendron luteum	64	*Pentanthera*	Vanilloyl-*O*-hydroxybenzoyl-hexoside **100** (t_R 17.5 min)
Rhododendron vaseyi	65	*Pentanthera*	4-*O*-hydroxydihydro-Caffeoylquinic acid **18** (t_R 9.8 min), 4-*O*-hydroxydihydro-Caffeoylquinic acid **19** (t_R 10.8 min)
Rhododendron schlippenbachii	66	*Pentanthera*	Malaferin C **132** (t_R 41.2 min)
Rhododendron albrechtii	67	*Pentanthera*	3-*O*-hydroxydihydro-Caffeoylquinic acid **15** (t_R 5.9 min), *p*-Coumaric acid-*O*-shikimate **33** (t_R 30.8 min)

Species	Lab No.	Subgenus	Compounds
Rhododendron atlanticum	69	*Pentanthera*	*p*-Coumaric acid-*O*-glucosyl ester **39** (t_R 18.7 min), (Epi)gallocatechin gallate **129** (t_R 19.8 min), (Epi)gallocatechin gallate **131** (t_R 26.6 min)
Rhododendron prunifolium	70	*Pentanthera*	Teucrol **22** (t_R 51.0 min), Teucrol-*O*-hexoside **32** (t_R 42.0 min)
Rhododendron cumberlandense	72	*Pentanthera*	(Epi)catechin-3-*O*-hexoside-7-*O*-hexoside **166** (t_R 11.8 min), (Epi)catechin-3-*O*-hexoside-7-*O*-hexoside **167** (t_R 13.2 min), Quercetin-*O*-pentoside-*O*-hexoside **285** (t_R 24.7 min)
Rhododendron occidentale	74	*Pentanthera*	(Epi)gallocatechin-(4,8′/2,7′)-(epi)gallocatechin-(4′,8″)-(epi)catechin **189** (t_R 15.9 min)
Rhododendron anthopogon ssp. *anthopogon*	76	*Rhododendron*	Myricetin-*O*-dipentoside **240** (t_R 42.5 min)
Rhododendron augustinii ssp. *chasmanthum*	79	*Rhododendron*	Myricetin-*O*-acetyl-rhamnoside **238** (t_R 37.6 min)
Rhododendron hirsutum L.	81	*Rhododendron*	Quercetin-3-*O*-(4"-3-hydroxy-3-methylglutaryl)-*α*-rhamnoside **282** (t_R 44.9 min), Laricitrin-*O*-rutinoside **345** (t_R 36.8 min)
Rhododendron ovatum	96	*Azaleastrum*	Galloylarbutin **63** (t_R 11.7 min), Hyemaloside B / Guavinoside A **81** (t_R 30.9 min), Myricetin-3-*O*-hexoside-7-*O*-rhamnoside **245** (t_R 35.4 min)
Rhododendron mucronulatum	99	*Rhododendron*	*p*-Coumaric acid-*O*-hexoside-*O*-pentoside **41** (t_R 19.2 min), Resinoside A/B **333** (t_R 51.9 min)
Rhododendron setosum	100	*Rhododendron*	Vanillic acid-*O*-dihexoside **107** (t_R 4.6 min)
Rhododendron oldhamii	102	*Tsutsusi*	Ferulic acid-*O*-dihexoside **51** (t_R 17.2 min)
Rhododendron sherriffii	105	*Hymenanthes*	Gallic acid-*O*-acetyl-hexoside **61** (t_R 13.9 min)
Rhododendron neriiflorum	106	*Hymenanthes*	Procyanidin tetramer **200** (t_R 24.5 min)
Rhododendron campylocarpum ssp. *caloxanthum*	107	*Hymenanthes*	Gambiriin A/D **151** (t_R 19.2 min), Procyanidin trimer gallate **191** (t_R 13.1 min)
Rhododendron neoglandulosum	108	*Rhododendron*	Procyanidin Trimer C **182** (t_R 16.6 min)
Rhododendron brachycarpum	110	*Hymenanthes*	Quercetin-*O*-galloyl-pentoside **280** (t_R 39.1 min)
Rhododendron wasonii	111	*Hymenanthes*	Gallic acid-*O*-dihexoside **77** (t_R 3.2 min), Gallic acid-*O*-feruloyl-hexoside **80** (t_R 36.2 min)

Species	Lab No.	Subgenus	Compounds
Rhododendron sichotense	113	*Rhododendron*	Gallic acid-*O*-rutinoside **69** (t_R 6.6 min), Vanilloyl-*O*-hydroxybenzoyl-hexoside **101** (t_R 40.8 min), Vanillic acid-*O*-hexoside-*O*-pentoside **102** (t_R 14.9 min), Vanillic acid-*O*-dihexoside **109** (t_R 8.5 min)
Rhododendron racemosum	114	*Rhododendron*	*p*-Coumaric acid-*O*-dihexoside **44** (t_R 20.0 min), Salicyloylsalicin **91** (t_R 36.6 min), Methyl gallate-*O*-dihexoside **115** (t_R 8.0 min)
Rhododendron hylaeum	116	*Hymenanthes*	Methyl gallate-*O*-coumaroyl-hexoside **114** (t_R 42.1 min)
Rhododendron auritum	117	*Rhododendron*	(Epi)gallocatechin-(epi)catechin **158** (t_R 16.5 min), (Epi)gallocatechin-(4,8′)-(epi)gallocatechin-(4′,8″)-(epi)catechin **190** (t_R 9.1 min)
Rhododendron montroseanum	118	*Hymenanthes*	Everlastoside M **42** (t_R 27.0 min), *p*-Coumaric acid-*O*-dihexoside **43** (t_R 14.4 min)
Rhododendron eriocarpum	119	*Tsutsusi*	Naringenin-*O*-hexoside-*O*-pentoside **205** (t_R 38.0 min)
Rhododendron macrophyllum	120	*Hymenanthes*	Caffeic acid-*O*-hexoside **24** (t_R 8.1 min), Procyanidin trimer gallate **192** (t_R 18.3 min)
Rhododendron semibarbatum	124	*Mumeazalea*	*p*-Coumaric acid-*O*-hexoside-*O*-pentoside **40** (t_R 17.6 min), (Epi)gallocatechin-(4,8)-3′-O-galloyl(epi)gallocatechin **174** (t_R 25.7 min), Kaempferol-*O*-galloyl-pentoside **329** (t_R 47.1 min)

15.4. Correlation, Principal Component Analysis and Hierarchical Cluster Analysis

15.4.1. Total number of compounds and correlation studies

Different types of compounds are observed in the LC-MS chromatograms of *Rhododendron* leaf extracts. These compounds can be the primary or secondary metabolites of plants, degradation products, soluble wash up impurities, fragment ions and adduct ions. The type of compounds present in samples is dependent on the solvent used for extraction, storage time of samples and other experimental conditions.

Before approaching complex statistical methods for data analysis, a simple approach of plotting the average number of compounds observed by LC-MS per subgenera was considered. For this plot, LC-TOF-MS data of the *Rhododendron* species were used. The software carried out compound peak calculation based on the assumption that it had a minimum of 0.001% intensity of the base peak and minimum signal to noise ratio of 5.

Using this method, it was observed that the highest number of peaks or compounds (288) was observed in *Rhododendron moulmainense*, which belonged to the subsection *Azaleastrum* and the lowest number of peaks (43) was observed for *Rhododendron elliottii*, which belonged to the subsection *Hymenanthes*. According to Figure 15.21, the subgenus Tsutsusi had a slightly lower mean value compared to the other subgenera. No other significant differences were observed among the different subgenera with relationship to the number of compounds. The subgenus *Mumeazalea* only had one species and thus did not have any error bars.

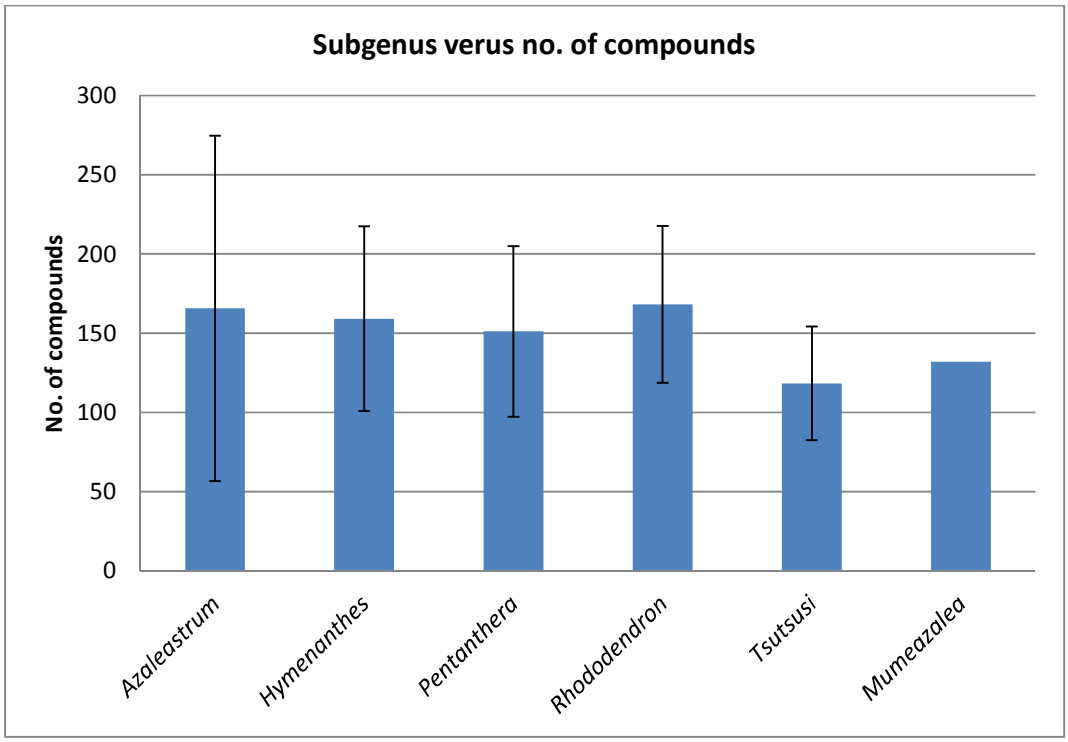

Figure 15.21: Number of compounds compared to subgenus of *Rhododendron*

The number of compounds was compared to the polyploidy level (results from Jennifer Nolzen, University of Oldenburg) (Figure 15.22).[202] From the polyploidy point of view, it was hypothesized that due to an enlarged genome size, the *Rhododendron* species could synthesize more diverse secondary metabolites. However, there was no correlation (R^2 = 0.018) observed between the polyploidy level and the number of compounds.

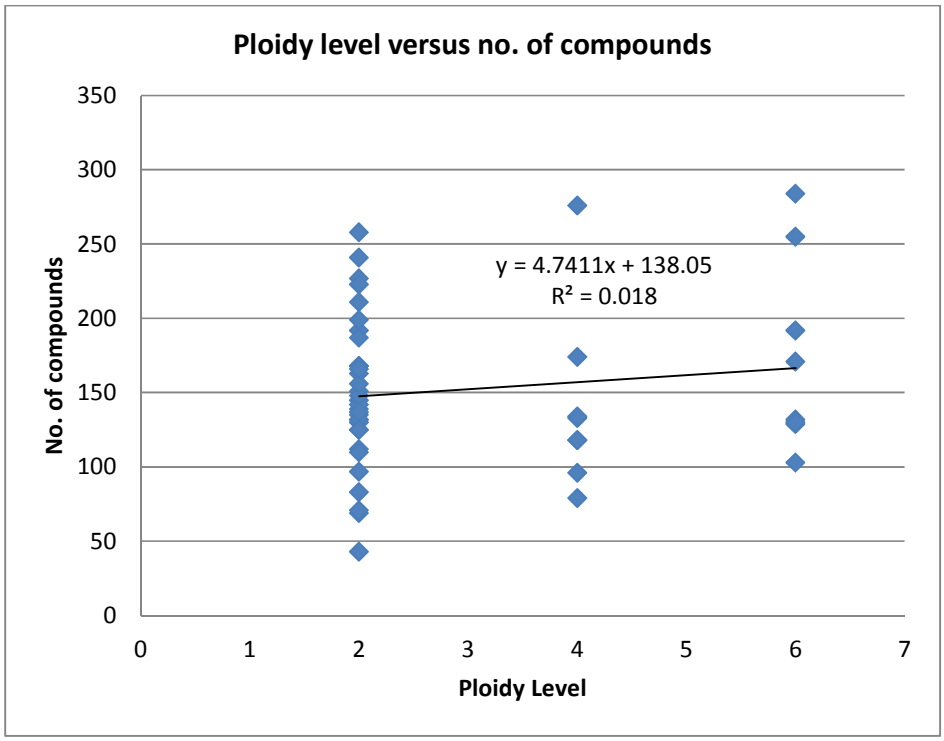

Figure 15.22: Ploidy level versus number of compounds

The number of compounds was also compared to anti-bacterial activity of the *Rhododendron* species against *Bacillus subtilis* (results from Dr. Ahmed Rezk, Jacobs University Bremen) (Figure 15.23).[2, 200] It was hypothesized that perhaps the highly active *Rhododendron* species would synthesize more compounds, which would be related to its anti-bacterial activity. For this study, the results of the agar diffusion assay using *Bacillus subtilis* were used. The *Rhododendron* species producing less than 0.4 cm radius of inhibition were considered to be inactive. The *Rhododendron* species producing activity from 0.4-0.6 cm, 0.6-0.9 cm and 0.9-1.2 cm were considered to be low, medium and high active species (Table 15.4). For PCA analysis, the inactive species were considered to be species producing activity below 0.6 cm. According to Figure 15.23, there was no correlation ($R^2 = 0.020$) observed between the number of compounds and the activity of the species.

Table 15.4: Anti-bacterial rating of *Rhododendron* species

Anti-bacterial rating	Radius of inhibition against *Bacillus subtilis* [cm]	Activity	No. of species	PCA Analysis
1	0.0 – 0.4	Inactive	61	Inactive
2	0.4 – 0.5	Low Activity	21	
3	0.5 – 0.6			
4	0.6 – 0.7	Medium Activity	10	Active
5	0.7 – 0.8			
6	0.8 – 0.9			
7	0.9 – 1.0	High Activity	8	
8	1.0 – 1.1			
9	1.1 – 1.2			

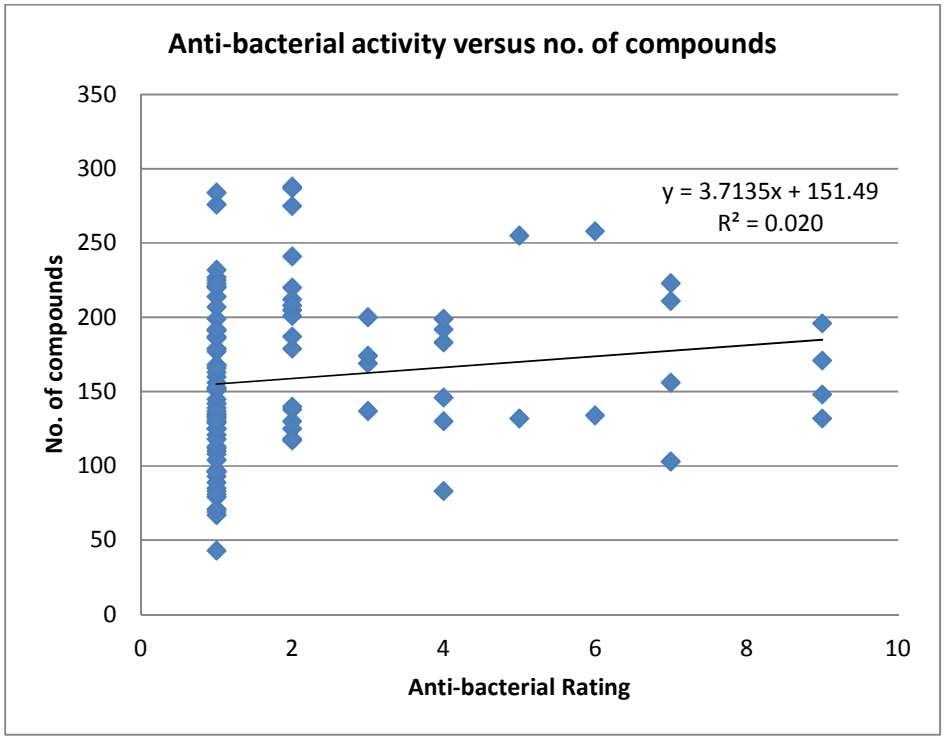

Figure 15.23: Anti-bacterial activity versus number of compounds

15.4.2. Principal Component Analysis

Principal Component Analysis was the chosen method to find out the compounds that help to differentiate the *Rhododendron* species based on subgenus or activity. The LC-TOF-MS data of the *Rhododendron* leaves were analyzed using the Bruker Profile Analysis software. The buckets for this data were generated within the range of 3-70 min. Each bucket consisted of *m/z* 1 in 1 min for the mass range *m/z* 200.5-1000.5. The kernalization of the buckets was used for every *m/z* 0.1 in 0.2 min. The normalization method of "sum of bucket values in analysis" was used along with no scaling algorithm. A few outliers were removed from the principal component analysis study.

Principal Component 1 (8.1%) and 2 (5.8%) explained a total variance of 13.9%. This low value of explained variance could be due to the diverse secondary metabolites produced by *Rhododendron* leaves. The Loadings plot (Figure 15.24) included the *m/z* values and retention times of the compounds influencing the positioning of the *Rhododendron* leaves. The most prominent peaks in the Loadings plot that were identified in the previous chapters included *m/z* 289 (Catechin), 577 (Procyanidin dimer B), 463 (Quercetin-*O*-hexoside), 447 (Quercetin-*O*-rhamnoside), 435 (Taxifolin-*O*-pentoside).

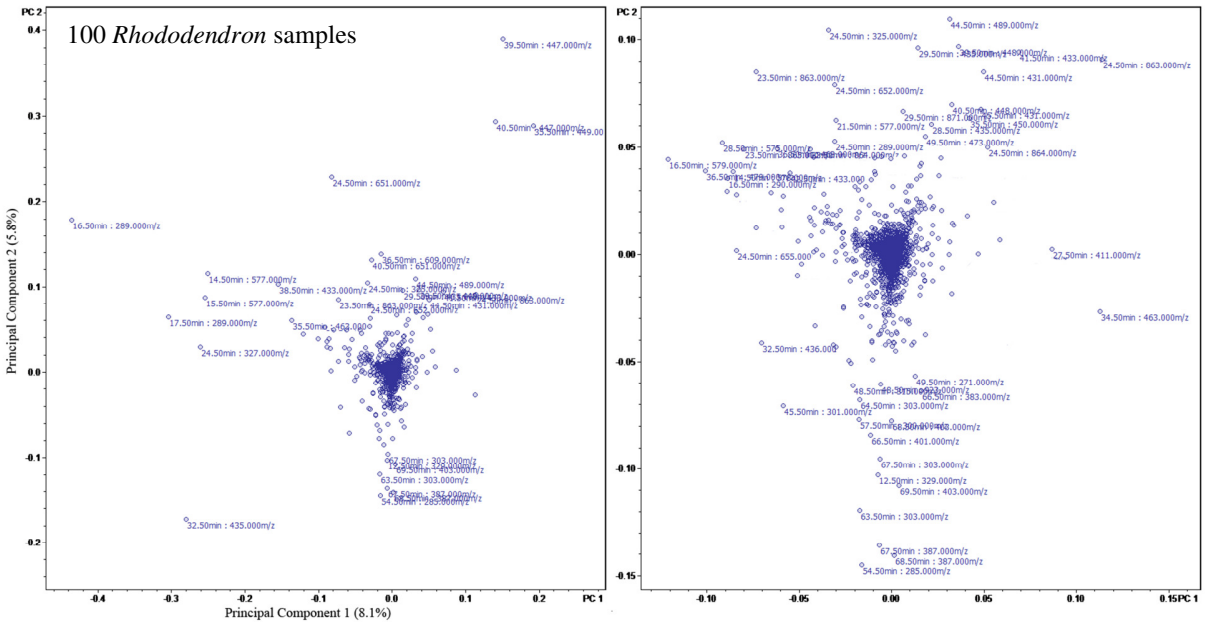

Figure 15.24: Loading plot of 100 *Rhododendron* species

The Scores plot was constructed with three different legends: subgenera (*Azaleastrum*, *Hymenanthes*, *Pentanthera*, *Rhododendron* and *Tsutsusi*) [Figure 15.25], active or inactive species [Figure 15.26] and anti-bacterial activity rating (1-9) [Figure 15.27]. In Figure 15.25, it was observed that the *Rhododendron* leaves from subgenus *Azaleastrum* formed a small cluster suggesting that the species consisted of a similar metabolomic profile. However, all the other subgenera, *Hymenanthes*, *Pentanthera*, *Rhododendron* and *Tsutsusi* were scattered throughout the plot, which suggested that genetically similar species could produce diverse secondary metabolites.

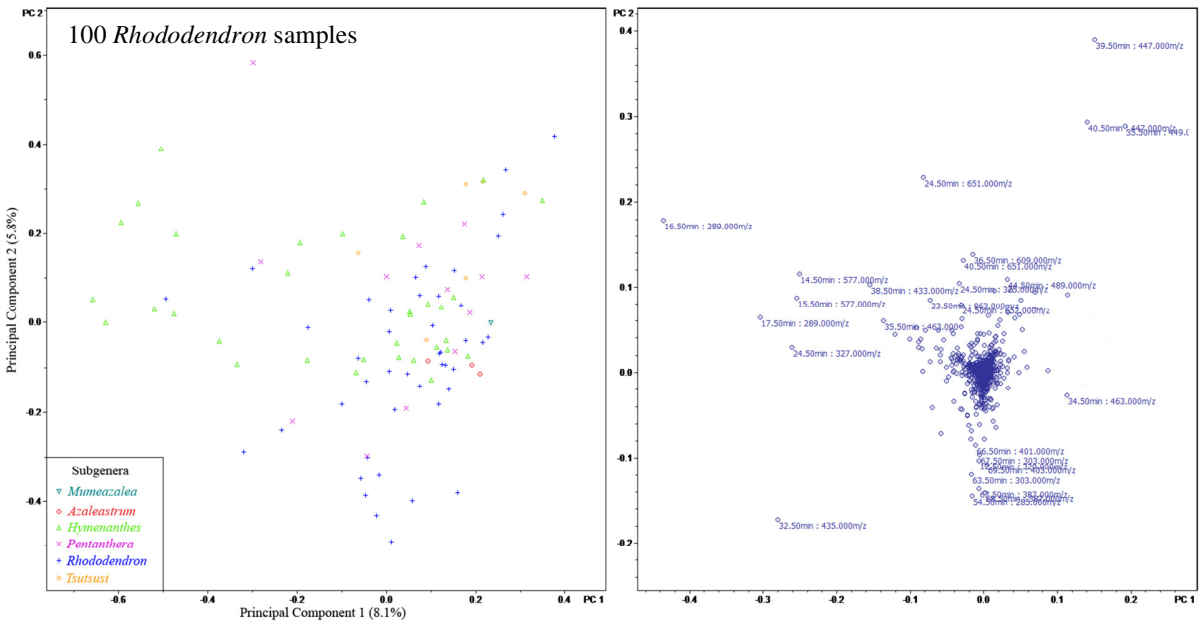

Figure 15.25: PCA score plot of 100 *Rhododendron* species based on their subgenera

The 18 active and 82 inactive species were colored in green and red respectively in Figure 15.26. The inactive species were distributed throughout the Scores plot. However, the active species were more clustered towards the center and bottom center of the plot. The loadings plot included the *m/z* values 285, 300, 301, 303, 329, 387, 401 and 403 corresponding to the part of the scores plot consisting of active species. The compounds with these *m/z* values could be considered as potential candidates responsible for their anti-bacterial activity.

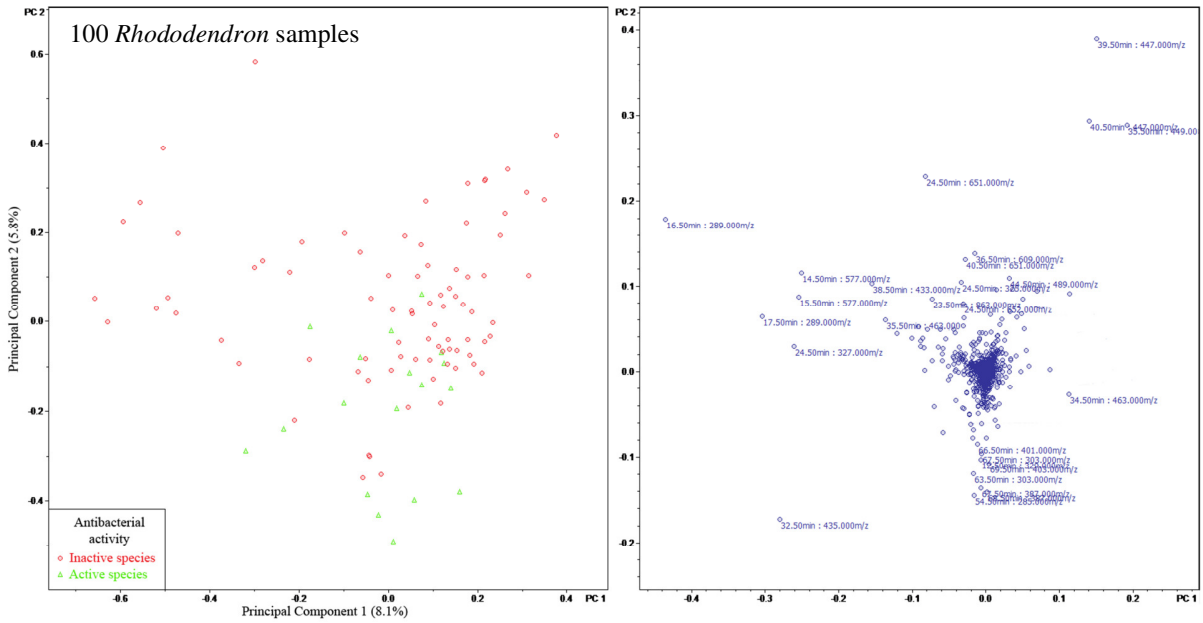

Figure 15.26: PCA score plot of (18) active and (82) inactive 100 *Rhododendron* species

To further differentiate the highly active *Rhododendron* species from the moderately active and inactive species, the Scores plot was differentiated based on the anti-bacterial rating in Figure 15.27. Four species, two varieties of *Rhododendron ambiguum*, *Rhododendron ferrugineum* and *Rhododendron anthopogon* were considered to be highly active with an anti-bacterial rating of 9. The two varieties of *Rhododendron ambiguum* were found in the center of the plot. It could be speculated that these two active species produced the most common metabolites of the *Rhododendron* species analyzed. However, *Rhododendron ferrugineum* and *Rhododendron anthopogon* were found in the bottom center of the plot suggesting that the *m/z* values of the aforementioned compounds distinguished the species and could be responsible for their anti-bacterial activity. This would require confirmation by activity guided fractionation. Clusters were not observed for the other moderately active species.

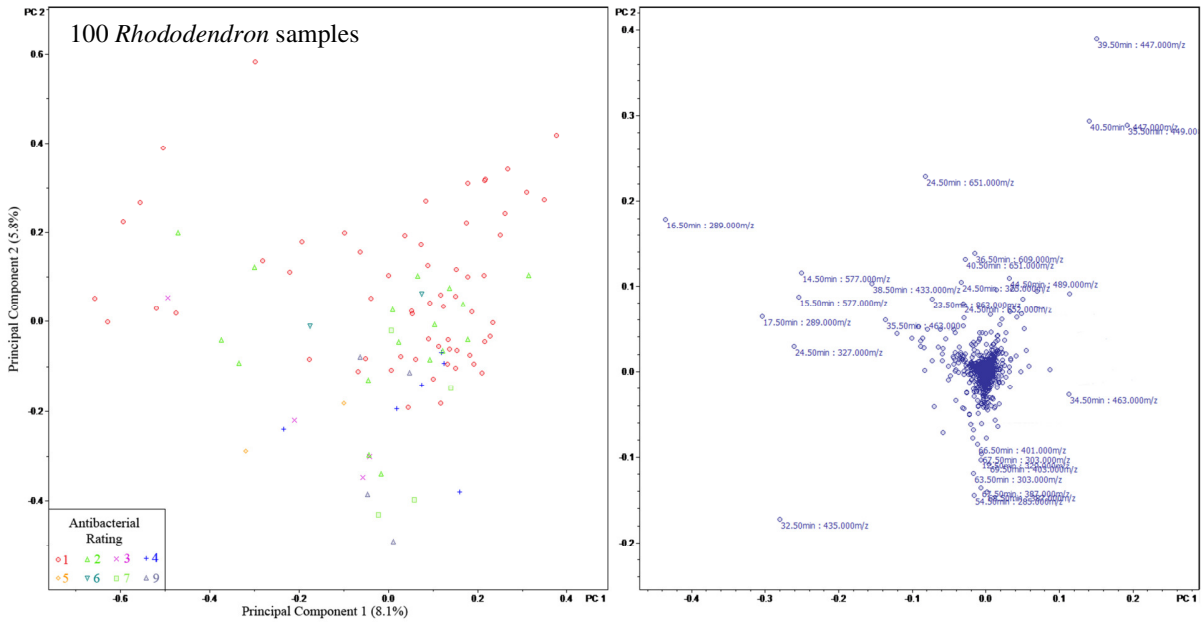

Figure 15.27: PCA score plot of 100 *Rhododendron* species based on their anti-bacterial activity rating

15.4.3. Principal Component Analysis and Hierarchical Clustering Analysis

The .csv file of the LC-TOF-MS data of 99 *Rhododendron* species was uploaded on the Metaboanalyst server through the website.[94-96] A total of 4940 variables consisting of *m/z* values were used for the analysis. *Rhododendron semibarbatum* was excluded as it was the only representative species from the subgenus *Mumeazalea* and the software required a minimum of three samples per group. A similar approach to the Bruker Profile analysis software was used.

Principal Component 1 (41.6%) and 2 (11.2%) explained a total variance of 52.8%. This variance was significantly higher compared to the one from Bruker analysis as the retention time is ignored in this analysis. It also included identified compounds with *m/z* 289 (Catechin), 577 (Procyanidin dimer B), 463 (Quercetin-*O*-hexoside), 447 (Quercetin-*O*-rhamnoside), 435 (Taxifolin-*O*-pentoside).

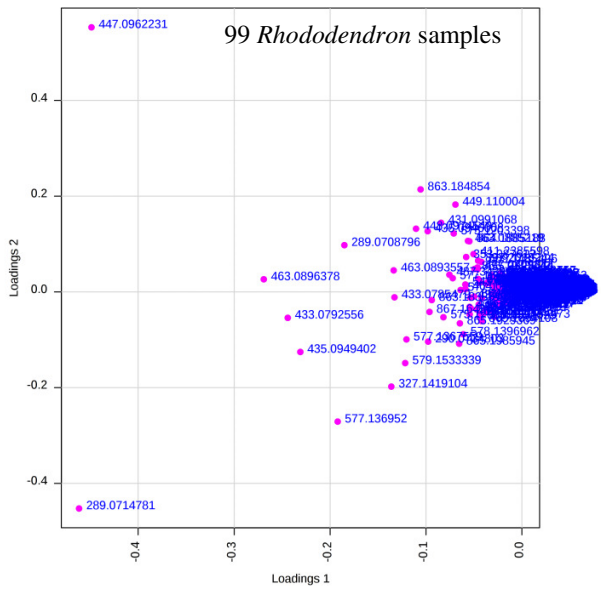

Figure 15.28: Loadings plot of 99 *Rhododendron* species

The Scores plot was constructed with three different legends: subgenera (*Azaleastrum*, *Hymenanthes*, *Pentanthera*, *Rhododendron* and *Tsutsusi*) [Figure 15.29], active or inactive species [Figure 15.30] and anti-bacterial activity rating (1-9) [Figure 15.31]. The boundary lines of the different groups were generated with a confidence level of 95%.

In Figure 15.29, it was observed that the species from *Hymenanthes* were scattered throughout the plot. It could be speculated that the species from *Hymenanthes* produce the most diverse profile of secondary metabolites. The clusters of all other subgenera were present in the center of the plot with a large overlapping area. It could be speculated that the *Rhododendron* species produced a variety of secondary metabolites irrespective of the subgenus they belong to.

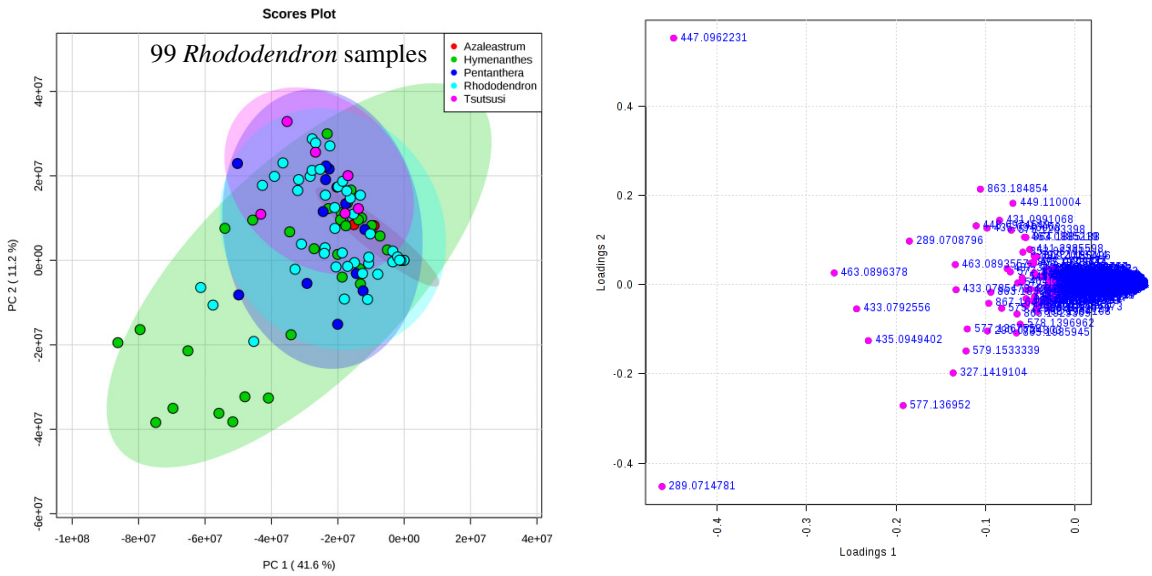

Figure 15.29: PCA score plot of 99 *Rhododendron* species based on their subgenera

The 18 active and 81 inactive species were colored in red and green respectively in Figure 15.30. The inactive species were distributed throughout the Scores plot as observed with Profile Analysis. However, the active species were more clustered towards the center of the plot. The active and inactive species could not be clearly distinguished with this plot.

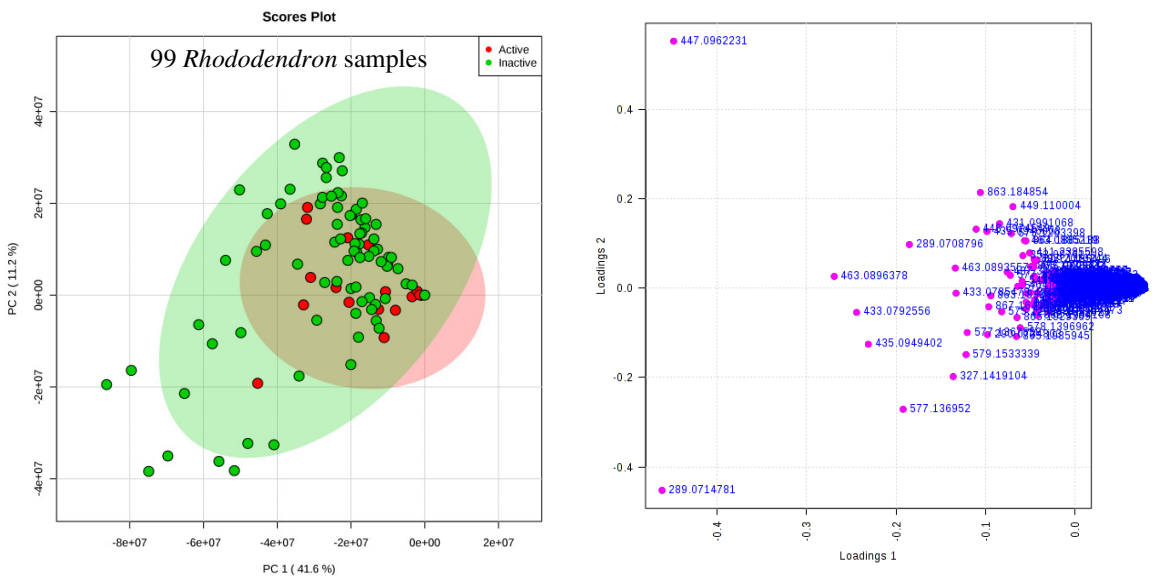

Figure 15.30: PCA score plot of (18) active and (81) inactive 99 *Rhododendron* species

To further differentiate the highly active *Rhododendron* species from the moderately active and inactive species, the Scores plot was differentiated based on the anti-bacterial rating (Figure 15.31). The species with anti-bacterial rating of 5 and 6 were merged into 6 as both consisted of 2 species each and the software required a minimum of three species per group. The inactive and moderately active species were spread across the plot. The active species with anti-bacterial rating of 7 and 9 were clustered in the center of the plot. It could be speculated that the most active species consisted of the most common metabolites found in the *Rhododendron* species.

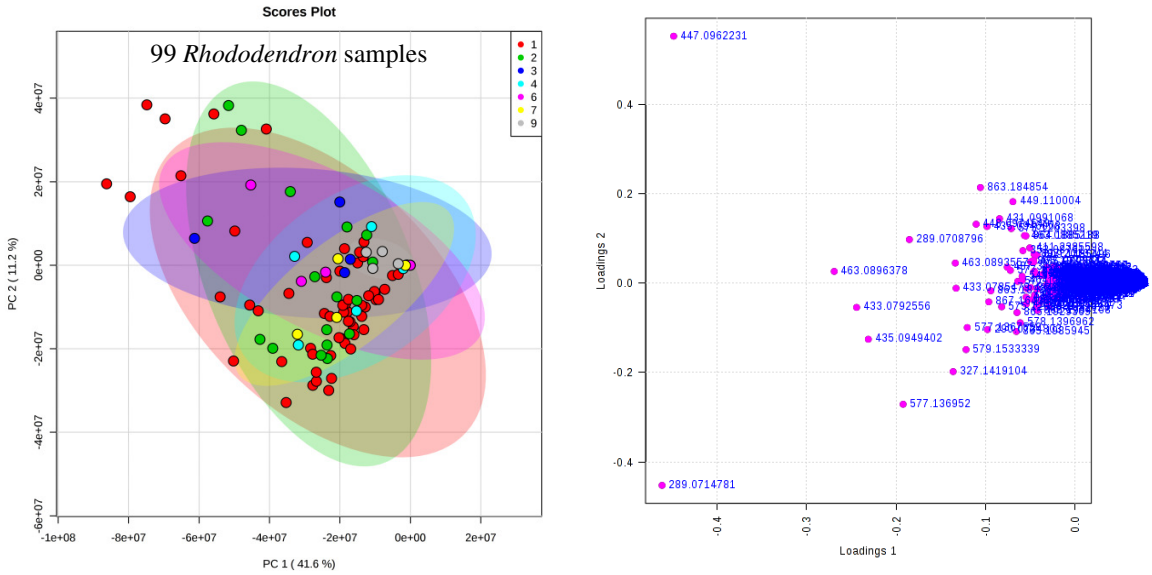

Figure 15.31: PCA score plot of 99 *Rhododendron* species based on their anti-bacterial activity rating

In addition to the Scores and Loadings plots, a hierarchical clustering (Figure 15.32) was also generated using "Spearman" for "Distance Measure" and "Complete" for "Clustering Algorithm".[94-96] The hierarchical clustering analysis groups samples based on the similarity of their metabolomic profile.

The 99 *Rhododendron* species were differentiated based on subgenus. Some clusters were observed for all the five subgenera. However, as observed with the Profile Analysis software, it was speculated that the *Rhododendron* species produced a diverse profile of secondary metabolites independent of their genetics. In other words, the *Rhododendron* species could not be differentiated genetically using their secondary metabolite profile.

Figure 15.32: Hierarchical clustering of 99 *Rhododendron* species based on their subgenera

16. Comparison of the polyphenolic profile and anti-bacterial activity of the leaves, fruits and flowers of *Rhododendron ambiguum* and *Rhododendron cinnabarinum*

Abhinandan Shrestha[1], Ahmed Rezk[1], Inamullah Hakeem Said[1], Victoria von Glasenapp[1], Rachelle Smith[1], Matthias Ullrich[1], Hartwig Schepker[2], Nikolai Kuhnert[1*]

[1] Department of Life Science & Chemistry, Jacobs University Bremen, Campus Ring 1, Bremen 28759, Germany

[2]Stiftung Bremer Rhododendronpark, Deliusweg 40, Bremen 28359, Germany

BMC Research Notes, submitted.

The compound numbers used in this chapter are used independently only for this chapter.

Authors Contribution

Abhinandan Shrestha and Ahmed Rezk designed experiments, conducted the experimental work, and prepared the manuscript; Inamullah Hakeem Said, Victoria von Glasenapp and Rachelle Smith also helped Abhinandan Shrestha to conduct the experimental work and analyze the data. Hartwig Schepker collected, identified and prepared plant materials. Nikolai Kuhnert and Matthias Ullrich organized, discussed and supervised the project and contributed to manuscript writing. All authors read and approved the final manuscript.

Abstract

Background: *Rhododendron* species have been traditionally used in countries like China, Nepal, Russia and North America for treating human diseases. These species are known to be a good source of polyphenolic plant secondary plant metabolites. They are known to have beneficial health properties for humans and have been used to treat diseases like asthma, skin diseases. In this contribution we investigate the phenolic profile and anti-bacterial activity of extracts from several plant organs including for the first time from leaves of different development stages.

Methods: In this study, the phytochemical profile of fruits, flowers and leaves of different ages of *Rhododendron ambiguum* and *Rhododendron cinnabarinum* were studied by using HPLC-MS and compounds identified based on high resolution masses and identity of tandem mass spectra, UV/VIS spectra and retention times if compared to standards.

Results: 59 different polyphenols including isomers were identified in these species by their fragmentation pattern and high resolution data. Also, the anti-bacterial activity of these parts against Gram-positive bacteria was studied.

Conclusion: The leaves and fruits contained more polyphenols than the flowers. With the exception of flowers, the fruits and leaves of both species were also determined to have a significant anti-bacterial effect against four Gram-positive bacteria.

1. Background

Polyphenols are secondary plant metabolites that are known to have different physical, chemical and biological properties. Proanthocyanidins (PAs) are a class of polyphenols, which are formed from the oligomerization and polymerization of flavan-3-ol units such as catechin and afzelechin (Figure 16.1). PAs are commonly found in fruits, vegetables and grain.[6, 204] They are known to have anti-inflammatory [205] and anti-mutagenic [206] effects and have been used in the treatment of asthma [206], skin diseases and UV radiations [207].

Rhododendron is a genus of woody plants that belong to Ericaceae family. Most of the species have attractive flowers and more than 1000 species of the genus have been described. They differ in their range of size, shape, texture, growth habit and color of blossoms.[208] The genus is

ranging from shrubs and small to large trees, having decorative flowers, which are mainly used for ornamental purposes. There is variation in the height of the plant, starting from 10 cm to 1 m (smallest species), while the example of largest specie is *R. giganteum*, which is almost 3 m tall. The leaves of most species are spirally arranged; the nature of leaves may be evergreen or deciduous.

The genus *Rhododendron* is found in almost all parts of the world except some parts in America and Africa. Species of the genus *Rhododendron* occur throughout the Northern Hemisphere and the Southern Hemisphere in South Eastern Asia and Northern Australasia. The plant is originally present in mountainous areas characterized by acidic well-drained soil, regular rainfall and cool summer temperatures.[209] On the other hand, majority of the genus prefers cooler temperature including the subgenus *Hymenanthes*. One of the subsections (*Pontica*) is indigenous to the areas outside the center of distribution and present in the areas of Japan, eastern China, Europe, North America and Russia.[210]

Rhododendron have traditionally been used in China, Nepal, North America, Russia, Korea, Austria and Romania for treating various diseases including arthritis, intestinal disorders, rheumatism, skin diseases, cough and other ailments.[5] They are known to be rich in polyphenolic compounds, namely flavonoids and their glycosides, terpenoids and essential oils.[6]

The new and exciting aspect of this study is the analysis of different plant organs where only limited data is available in the literature. In particular *Rhododendron* as an evergreen shrub grows a new generation of leaves every year offering the unique opportunity to compare the phytochemical profile of leaves of different ages and hence study the biochemical history of the plant. Such an investigation has to the best of our knowledge never been carried out. The phytochemical profile of the leaves of different age, flowers and fruits were analyzed for *R. ambiguum* and *R. cinnabarinum*. Both species belong to the subgenus *Rhododendron*, section *Rhododendron*. *R. ambiguum* and *R. cinnabarinum* belong to the subsection *Triflora* and *Cinnabarina* respectively. *R. cinnabarinum* is considered to be toxic for animals.[5, 211] It is known from our previous studies that these two species out of 17 *Rhododendron* species showed

higher activity against several Gram-positive bacteria.[2] Moreover, the high dose of both *Rhododendron* species exhibited a toxic effect in two mammalian cells and induced phenotypic changes that are characteristic for apoptosis.[201] Thus, the aim of the study was to analyze the chemical profile of *Rhododendron* crude extracts in order to contribute to our on-going investigations on the bioactivity potential of *Rhododendron*.

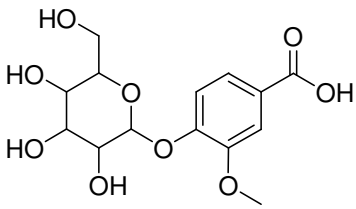

Vanillic acid-*O*-hexoside [**2**,**3**,**4**]

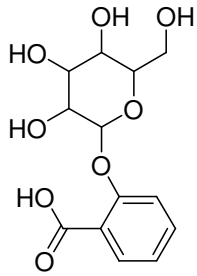

Salicylic acid-*O*-hexoside [**5**, **6**]

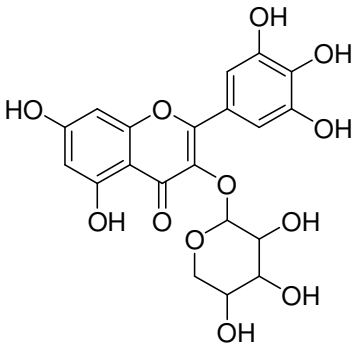

Myricetin-*O*-pentoside [**15**, **16**,**17**]

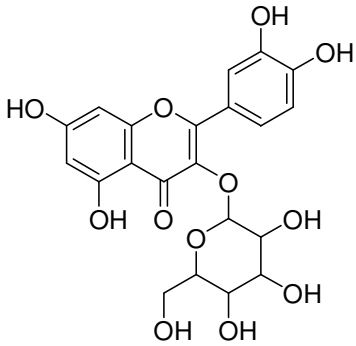

Quercetin-*O*-hexoside [**18**, **19**]

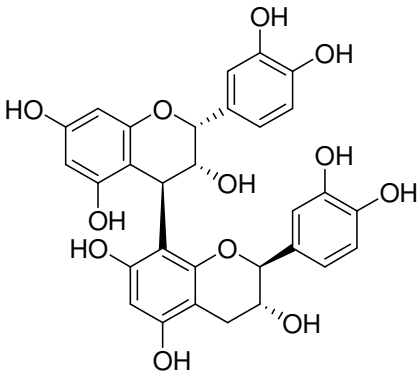

Procyanidin B1 [**39**]

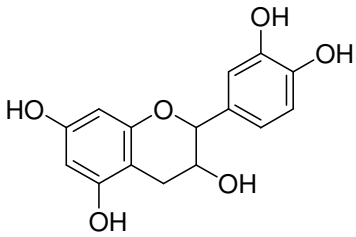

Catechin [**55**]

Figure 16.1: Representative examples of polyphenols from *Rhododendron* species

2. Methods

Plant material and chemicals

Fresh leaf material of *R. ambiguum* Hemsley and *R. cinnabarinum* Hooker were collected from plants grown in the Rhododendron-Park Bremen (www.rhododendronparkbremen.de) from spring 2013. First and second year leaves were collected for *R. ambiguum*, and first, second and third year leaves were collected for *R. cinnabarinum*. The leaves were distinguished on the basis of their morphological features. Moreover, the flowers and fruits for both *Rhododendron* species were also sampled. Each sample species was collected from three different individual plants with the help of Dr. Hartwig Schepker. The identities of all plant species have been verified according to the German Gene bank Rhododendron Database provided by the Bundessortenamt (www.bundessortenamt.de/rhodo). All chemicals (analytical grade) were purchased from Carl Roth (Karlsruhe, Germany).

Plant extraction

The *Rhododendron* leaves, fruits and flowers were freeze dried using liquid nitrogen. A mortar and pestle was used to crush the dried brittle leaves. 2 g of the powdered material were dissolved in 10 mL of 80% aqueous methanol and for 24 h at 4°C. The mixture was then sonicated for 15 min and centrifuged at 3,220 x g for 10 min. The aliquot was then separated and stored at -20°C until further analyses.

LC-ESI-TOF-MS (High resolution mass spectrometry)

The LC equipment (Agilent 1200 series, Bremen, Germany) consisted of a binary pump, an auto-sampler with 100 µL loop and a UV-Vis detector with a light-pipe flow cell. The UV detector was used at 280 nm to measure the polyphenols. The 5 µm diphenyl column having 250 x 3 mm inner diameter (Varian, Darmstadt, Germany) was used for separation. This was connected to the microTOF mass spectrometer (Bruker Daltonics, Bremen, Germany) equipped with an electrospray ionization source. The internal calibration was achieved by using 0.1 M sodium formate solution at 0.10 mL/min, which was injected through the six-port valve. The calibration was achieved by using the enhanced quadratic mode. Water/formic acid (1000:0.05 v/v) and

methanol were used as solvent A and B respectively. The flow rate of the solvents was adjusted to 500 µL/min. A linear gradient was used from 10% B to 80% B in 70 min and a further 10 min was assigned for the gradient to equilibrate from 80% B to 10% B for the next run.[93]

LC-ESI-MS^n (Tandem mass spectrometry)

The Liquid chromatography equipment (Agilent 1100 series) comprised of a binary pump, an auto sampler having a 100 µL capacity loop and a Diode Array Detector with a range from 200 to 600 nm. The detector recorded at 254, 280 and 320 nm, which is the best absorption wavelength for polyphenolic compounds. Chromatographic separation was performed using the same gradient method used in the LC-TOF-MS analyses. A 5 µm diphenyl column of 250 x 3 mm i.d. (Varian, Darmstadt, Germany) with 500 µL/min flow rate of solvent was used. The LC equipment was connected with Ion-trap mass spectrometer, which was fitted with an ESI source (Bruker Daltonics HCT Ultra, Bremen, Germany) operating in full scan auto MSn mode to obtain fragment ion *m/z*. Tandem mass spectra were acquired in Auto-MSn mode (smart fragmentation) using a ramping of the collision energy. Maximum fragmentation amplitude was fixed to 1 Volt. MS operating conditions (negative mode) had been optimized with a capillary temperature of 365 °C, a dry gas flow rate was of 10 L/min, and a nebulizer pressure of 10 psi.[93]

Bacterial strains and anti-microbial susceptibility test

Four Gram-Positive bacterial species i.e. *Bacillus subtilis* S168, *Bacillus aquimaris* MB-2011, *Bacillus thioparus*, and *Clavibacter michiganensis* were selected to compare the susceptibility of crude extracts of leaves, flower and fruit of two *Rhododendron* species i.e. *R. ambiguum* and *R. cinnabarinum* GSPB 390. Anti-microbial activity screening was conducted by the agar diffusion method.[212] Briefly, Lysogeny Broth (LB) agar plates were inoculated with 200 µL of the inoculum of the tester organism (1 x 10^7 colony forming units per mL) by evenly spreading the cell suspensions over the agar surface. Holes with diameters of 5 mm were punched into the agar plates. Subsequently, 50 µL of the plant crude extracts were filled into each well. The plates were incubated overnight at 28 ºC. Inhibition of microbial growth was determined by measuring the radius of the inhibition zone. For each bacterial strain, 80% aqueous methanol solutions were used as negative solvent controls. All experiments were performed in triplicates and the results are presented as mean values.

3. Results and discussion

The hypotheses of this study are that fruits, flowers and leaves have different phytochemical profile and that the leaves of different ages which are exposed to numerous environmental conditions might lead to the production of new compounds or variation in secondary metabolite quantities. To our knowledge, no investigation on the phytochemical profile of leaves of different ages has been carried out. The crude extracts of all parts of the two selected species *R. ambiguum* and *R. cinnabarinum* (i.e. first, second, third leaves, flowers and fruits) were extracted with 80% aqueous methanol in order to extract polyphenols. Both species were recently shown to possess promising biological activities [2] and their plants consisted of leaves of different age. These extracts were analyzed by reversed phase HPLC using a diphenyl column with a gradient using methanol and water/formic acid (1000:0.05 v/v). Negative ion mode was used to study the polyphenols using tandem mass spectrometry and high resolution mass spectrometry. The compounds were identified in the high resolution mass data by observing an absolute mass error below 5 ppm for their elemental composition. The UV spectrum at 280 nm was used to identify the PAs present in the samples. Also, the fragmentation pathway of PAs by heterocyclic ring fission (HRF) and retro-Diels-Alder (RDA) reaction described by Gu et al. were considered.[97]

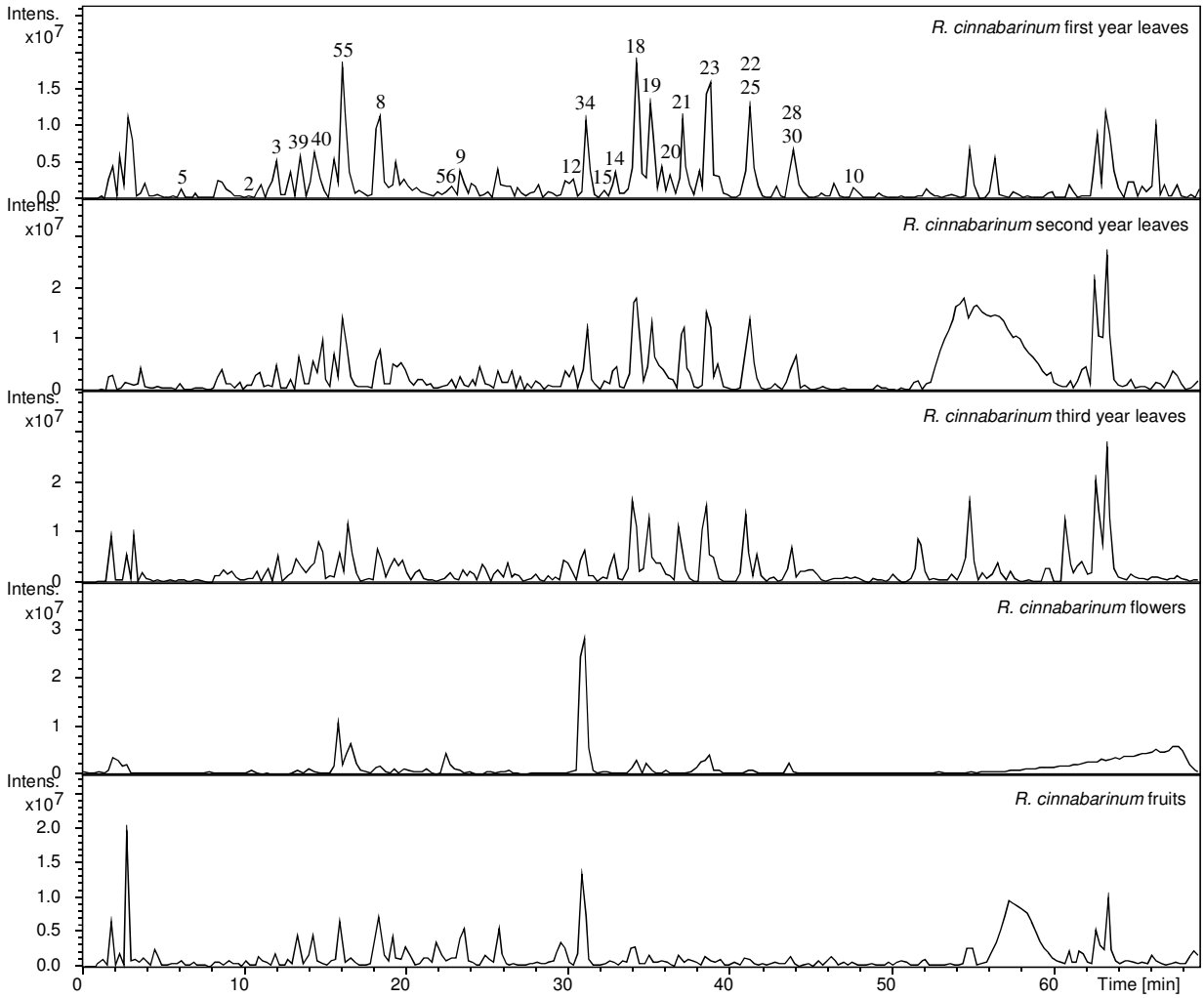

Figure 16.2: Total Ion Chromatogram of *Rhododendron cinnabarinum* leaves, flowers and fruits by LC-MS^n in negative mode

The chromatograms of *Rhododendron cinnabarinum* first year leaves, second year leaves, third year leaves, flowers and fruits were directly compared are shown in Figure 16.2. The chromatograms of the first, second and third year leaves consisted of peaks at identical retention time and comparable intensities. The chromatogram of flowers and fruits were different compared to the leaves. The chromatogram of flowers consisted of peaks with lower intensity in the region 0 – 30 min, which suggest that the hydrophilic compounds are present in lower intensity compared to the leaves. However, after 30 min, the chromatogram of the flowers was

similar to the leaves. On the other hand, the chromatogram of the fruits exhibited additional peaks not present in the leaves and flowers.

In this study, 59 polyphenolic compounds were identified from both *Rhododendron* species for the first, second third year leaves, flower and fruit (Table 16.1). The identification of reported compounds was based on their retention time, fragmentation pattern and high resolution mass data. All identified polyphenol compounds have been discovered in nature already [1, 15-26].[6, 21, 102, 131, 134, 149, 172, 188, 197, 213-216] Out of the identified compounds, 46 were already reported to be found in *Rhododendron* species.[6, 21, 214, 215] In this study, 13 new polyphenolic compounds were identified. The fruits consisted of the highest variety and concentration of PAs among the four parts of *R. ambiguum* and *R. cinnabarinum*.

Table 16.1: Polyphenols present in different year leaves, flowers and fruits of *R. ambiguum* and *R. cinnabarinum*

	Species				***R. ambiguum***				***R. cinnabarinum***				
	Part				**1st**	**2nd**	**Fl.**	**Fr.**	**1st**	**2nd**	**3rd**	**Fl.**	**Fr.**
No.	**Compound**	**Reference**	**m/z [M-H]⁻**	**RT**									
1	Methyl gallate hexoside	[217]	345.0827	11.8		Y							
2	Vanillic acid-*O*-hexoside	[134]	329.0864	10.2		Y	Y	Y	Y	Y	Y	Y	Y
3	Vanillic acid-*O*-hexoside	[134]	329.0867	11.7	Y	Y	Y	Y	Y	Y			Y
4	Vanillic acid-*O*-hexoside	[134]	329.0864	13.9					Y	Y	Y	Y	
5	Salicylic acid-*O*-hexoside	[131]	299.0761	6.3		Y			Y	Y	Y	Y	Y
6	Salicylic acid-*O*-hexoside	[131]	299.0762	8.5						Y			
7	3-*O*-Caffeoylquinic acid	[6]	353.0877	13.0	Y	Y	Y	Y			Y		
8	5-*O*-Caffeoylquinic acid	[6]	353.0873	18.2		Y	Y	Y	Y	Y	Y		Y
9	4-*O*-Caffeoylquinic acid	[6]	353.864	23.0		Y			Y	Y	Y		
10	Naringenin	[158]	271.0602	47.9	Y	Y		Y	Y			Y	Y
11	Myricetin	[158]	317.0296	38.9	Y	Y	Y	Y					Y
12	Myricetin-*O*-hexoside	[6]	479.0820	30.8			Y	Y	Y	Y	Y		Y
13	Myricetin-*O*-hexoside	[6]	479.0853	35.3	Y	Y	Y	Y					
14	Myricetin-*O*-rhamnoside	[6]	463.0899	33.0					Y	Y	Y		Y
15	Myricetin-*O*-pentoside	[6]	449.0728	32.1				Y	Y	Y	Y		Y
16	Myricetin-*O*-pentoside	[6]	449.0725	37.8				Y	Y	Y			
17	Myricetin-*O*-pentoside	[6]	449.0732	39.1	Y	Y	Y	Y					
18	Quercetin-*O*-hexoside	[6]	463.0898	34.2	Y	Y	Y	Y	Y	Y	Y	Y	Y

19	Quercetin-*O*-hexoside	[6]	463.0897	35.5	Y	Y		Y		Y	Y	Y	Y
20	Quercetin-*O*-pentoside	[6]	433.0771	36.6	Y	Y			Y	Y	Y		
21	Quercetin-*O*-pentoside	[6]	433.0795	37.4	Y	Y	Y	Y	Y	Y	Y	Y	Y
22	Quercetin-*O*-pentoside	[6]	433.0798	41.2	Y	Y	Y	Y	Y	Y	Y	Y	Y
23	Quercetin-*O*-rhamnoside	[6]	447.0921	38.7	Y	Y	Y	Y	Y	Y	Y	Y	Y
24	Quercetin-*O*-rhamnoside-*O*-hexoside	[6]	609.1442	34.3	Y	Y			Y	Y			
25	Quercetin-*O*-glucuronide	[172]	477.0676	40.8						Y	Y		Y
26	Quercetin	[6]	301.0342	44.4	Y	Y	Y	Y		Y			
27	Kaempferol	[158]	285.0414	49.5	Y	Y	Y	Y					
28	Kaempferol-3-*O*-rhamnoside	[188]	431.0982	43.6	Y	Y	Y		Y	Y	Y	Y	Y
29	Kaempferol-3-*O*-pentoside	[188]	417.0827	41.0		Y	Y	Y					
30	Kaempferol-3-*O*-pentoside	[188]	417.0833	43.9		Y	Y	Y	Y	Y	Y	Y	Y
31	Kaempferol-3-*O*-glucuronide	[197]	461.0719	43.6						Y			
32	Taxifolin	[218]	303.0507	29.1		Y	Y						
33	Taxifolin-*O*-pentoside	[6]	435.0936	27.8	Y	Y		Y					Y
34	Taxifolin-*O*-pentoside	[6]	435.0936	31.1	Y	Y	Y	Y	Y	Y	Y	Y	Y
35	Taxifolin-*O*-pentoside	[6]	435.0930	33.6		Y							
36	(Epi)gallocatechin-(epi)gallocatechin	[6]	609.1259	6.5				Y					Y
37	(Epi)gallocatechin-(epi)gallocatechin	[6]	609.1246	7.5				Y					
38	(Epi)gallocatechin-(epi)gallocatechin	[6]	609.1251	10.2				Y					
39	(Epi)catechin-(epi)catechin (Procyanidin dimer B1)	[6]	577.1372	13.4	Y	Y	Y	Y	Y	Y	Y	Y	Y
40	(Epi)catechin-(epi)catechin (Procyanidin dimer B)	[6]	577.1377	14.3	Y	Y	Y	Y	Y		Y	Y	Y
41	(Epi)catechin-(epi)catechin (Procyanidin dimer B)	[6]	577.1373	18.6			Y	Y				Y	Y
42	(Epi)catechin-(epi)catechin (Procyanidin dimer B2)	[6]	577.1367	20.3		Y	Y	Y	Y	Y	Y	Y	Y
43	(Epi)catechin-(epi)catechin (Procyanidin dimer B)	[6]	577.1358	23.1			Y	Y	Y	Y	Y		Y
44	Procyanidin Trimer C	[216]	865.1994	5.6		Y		Y	Y	Y	Y		Y
45	Procyanidin Trimer C	[216]	865.1953	25.6				Y					
46	A type Procyanidin Trimer C	[216]	863.1805	22.2					Y	Y	Y	Y	Y
47	(Epi)gallocatechin-(epi)catechin	[6]	593.1310	7.7				Y	Y	Y			Y
48	(Epi)gallocatechin-(epi)catechin	[6]	593.1309	9.7			Y	Y	Y	Y	Y		Y
49	(Epi)gallocatechin-(epi)catechin	[6]	593.1314	10.5				Y					Y
50	(Epi)gallocatechin-(epi)catechin	[6]	593.1307	12.6				Y					Y
51	(Epi)gallocatechin-(epi)catechin	[6]	593.1323	13.7			Y	Y					Y
52	(Epi)gallocatechin-(epi)catechin	[6]	593.1311	18.2				Y					
53	(Epi)catechin-(4,8/2,6)-(epi)catechin	[6]	575.1209	27.2	Y	Y	Y	Y					Y
54	(Epi)catechin-(4,8/2,6)-(epi)catechin	[6]	575.1201	32.4	Y	Y	Y	Y					Y

55	Catechin	[6]	289.0721	16.0	Y	Y	Y	Y	Y	Y	Y	Y	Y
56	Epicatechin	[6]	289.0713	23.0	Y	Y	Y	Y	Y			Y	
57	Gallocatechin	[6]	305.0656	8.5		Y	Y	Y					Y
58	Epigallocatechin	[6]	305.0660	15.4		Y	Y	Y					
59	(Epi)catechin-*O*-D-glucopyranoside	[149]	451.1258	10.5					Y	Y	Y		Y

*RT = Retention Time
1st, 2nd, 3rd = 1st, 2nd, 3rd year leaves
Fl. = Flowers
Fr. = Fruits

Characterization of Methyl gallate hexoside (1) (M_r 345)

A peak was detected at *m/z* 345 and was assigned to be methyl gallate hexoside. The peak produced the fragmentation with base peak at *m/z* 183 and secondary peaks of *m/z* 168 and 124.

Characterization of (epi)catechin-(4,8′/2,6′)-(epi)catechin (53, 54) (M_r 576)

Two peaks were detected at *m/z* 575 and were assigned as A-type dimer of (epi)catechin unit. The first peak produced an MS2 base peak of *m/z* 449 and secondary peak of *m/z* 287. The second peak produced an MS2 base peak of *m/z* 423 and secondary peak of *m/z* 285.

Characterization of catechin (55) and epicatechin (56) (M_r 290)

Two peaks were detected at *m/z* 289. The first peak was assigned as catechin and the second peak was assigned as epicatechin based on their polarity. Both peaks produced similar fragmentation, consisting of an MS2 base peak of *m/z* 245 and secondary peak of *m/z* 203.

Characterization of gallocatechin (57) and epigallocatechin (58) (M_r 306)

Two peaks were detected at *m/z* 305. The first peak was assigned as gallocatechin and the second peak was assigned as epigallocatechin based on their polarity. Both peaks produced similar fragmentation, consisting of an MS2 base peak of *m/z* 179 and secondary peak of *m/z* 164.

Characterization of (epi)catechin-(4,8′)-(epi)catechin (39, 40, 41, 42, 43) (M_r 578)

Five peaks were detected at *m/z* 577. They were assigned as the PA dimer. All the peaks produced similar fragmentation with the base peak of *m/z* 407 and secondary peaks of *m/z* 425

and 285. The standards of the dimers B1 and B2 were used to differentiate the isomers by their retention time.

Characterization of (epi)gallocatechin-(4,8′)-(epi)catechin and (epi)catechin-(4,8′)-(epi)gallocatechin (47, 48, 49, 50, 51, 52) (M_r 594)

Six peaks were detected at *m/z* 593. They were speculated to be dimeric B-type PA consisting of (epi)catechin and (epi)gallocatechin monomeric units. All the peaks produced similar fragmentation having the base peak of *m/z* 425 and secondary peak of *m/z* 407.

Characterization of (epi)gallocatechin-(4,8′)-(epi)gallocatechin (36, 37, 38) (M_r 610)

Three peaks were detected at *m/z* 609 and were speculated to be dimeric B-type PAs with (epi)gallocatechin monomeric units. The three peaks produced the fragmentation with base peak at *m/z* 423 and secondary peaks of *m/z* 441 and 283.

Characterization of Taxifolin (32) (M_r 304)

A peak was detected at *m/z* 303 and was assigned to be taxifolin. The peak produced the fragmentation with base peak at *m/z* 285 and secondary peaks of *m/z* 177 and 125.

Identification of other polyphenols

The polyphenols were identified by their specific fragmentation patterns, retention time and high resolution mass values. The other polyphenols that were identified in the leaf extracts are three vanillic acid-*O*-hexosides [134], two salicylic acid-*O*-hexosides [131, 219], three caffeoylquinic acids [6], naringenin [158], myricetin [158], two myricetin-*O*-hexosides [6], myricetin-*O*-rhamnoside [6], three myricetin-*O*-pentosides [6], two quercetin-*O*-hexosides [6], three quercetin-*O*-pentosides [6], quercetin-*O*-rhamnoside [6], quercetin-*O*-rhamnoside-*O*-hexoside [6], quercetin-*O*-glucuronide [172, 190], quercetin [6], kaempferol [158, 220], kaempferol-*O*-rhamnoside [188], two kaempferol-*O*-pentosides [188], kaempferol-*O*-glucuronide [190, 197], three taxifolin-*O*-pentosides [6, 114], two procyanidin trimers C [149, 156], one A-type procyanidin trimer C [172, 216] and (epi)catechin-O-D-glycopyranoside [149]. The tandem mass spectra of some compounds are shown in Figure 16.3.

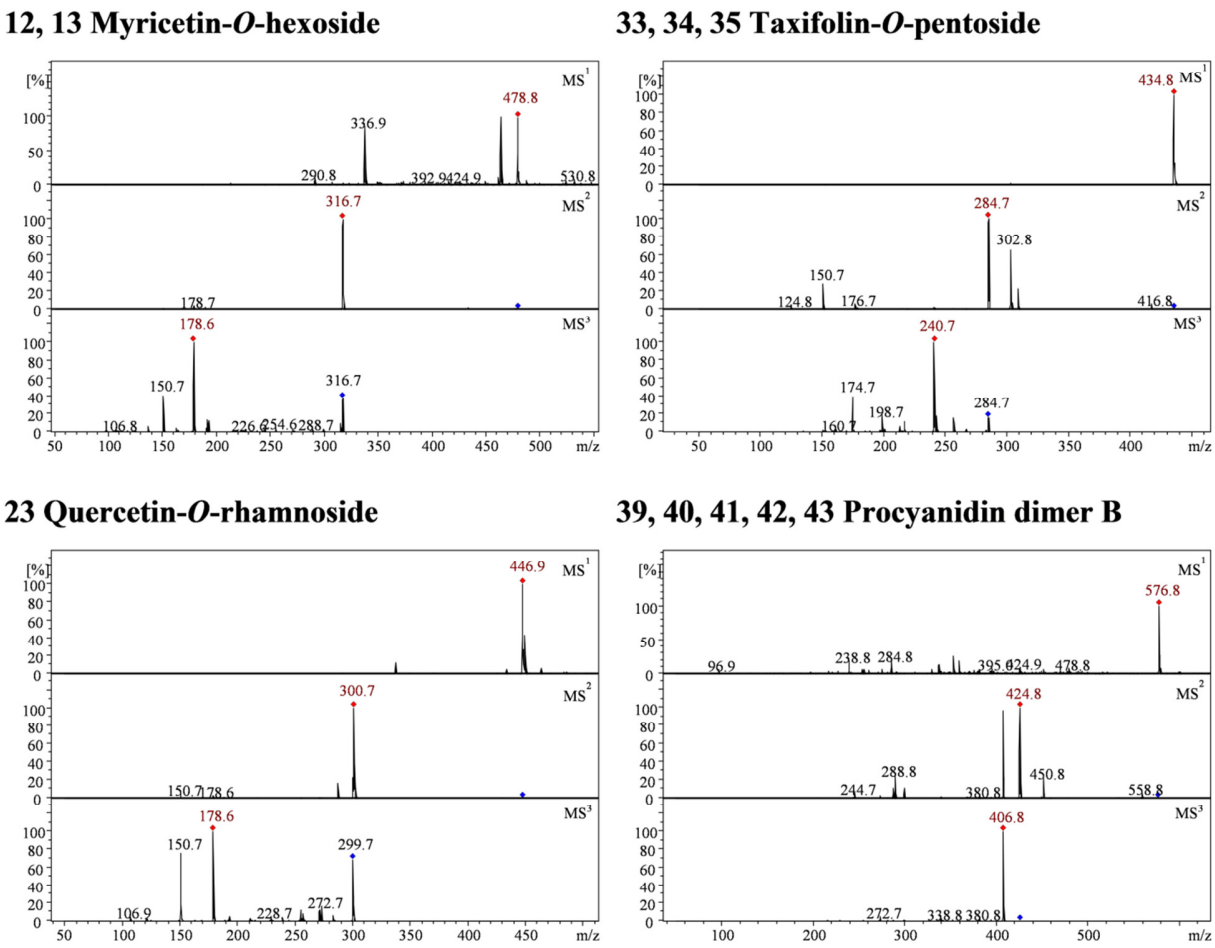

Figure 16.3: Tandem MS fragmentation of some polyphenols identified in *Rhododendron*

Anti-bacterial activity

Four Gram-positive organisms were used to compare the anti-bacterial activity of different plant parts of two species from genus *Rhododendron*. Crude extract of first, second, third year leaves in addition to flower and fruits of R. *ambiguum* and *R. cinnabarinum* were obtained using 80% methanol. The bioactivity of *R. ambiguum* ranged between 0.5-0.7 cm, while for *R. cinnabarinum* between 0.5-0.8 cm (Figure 16.4). Anti-bacterial effects of fruit and leaves extracts were in the same order of magnitude. However, there was a reduced anti-bacterial activity observed for the flowers of *R. cinnabarinum* and *R. ambiguum*. This could be due to the evolutionary aspect as flowers have a short blooming period in a year compared to the leaves and fruits. In general, *B. thioparus* was the most sensitive bacteria species towards the plant parts for both *Rhododendron*

species. These results are in agreement with our previous study, which showed a higher anti-bacterial effect of *Rhododendron* species against Gram-positive and higher effect for *R. cinnabarinum*.[2] The phytochemical analysis indicated that Taxifolin derivatives were present in high concentration in the leaves of both plant species, which could be the reason of apoptosis like phenotype observed before in other studies.[201] Moreover, this finding is also supported by other studies, which reported the effect of Taxifolin in different cancer cell lines by inducing apoptosis cell death.[221, 222]

The radius of the inhibition zones was measured in triplicates and the values are given as means ± standard deviations. The 80% aqueous methanol used as negative controls did not yield inhibition zones (data not shown).

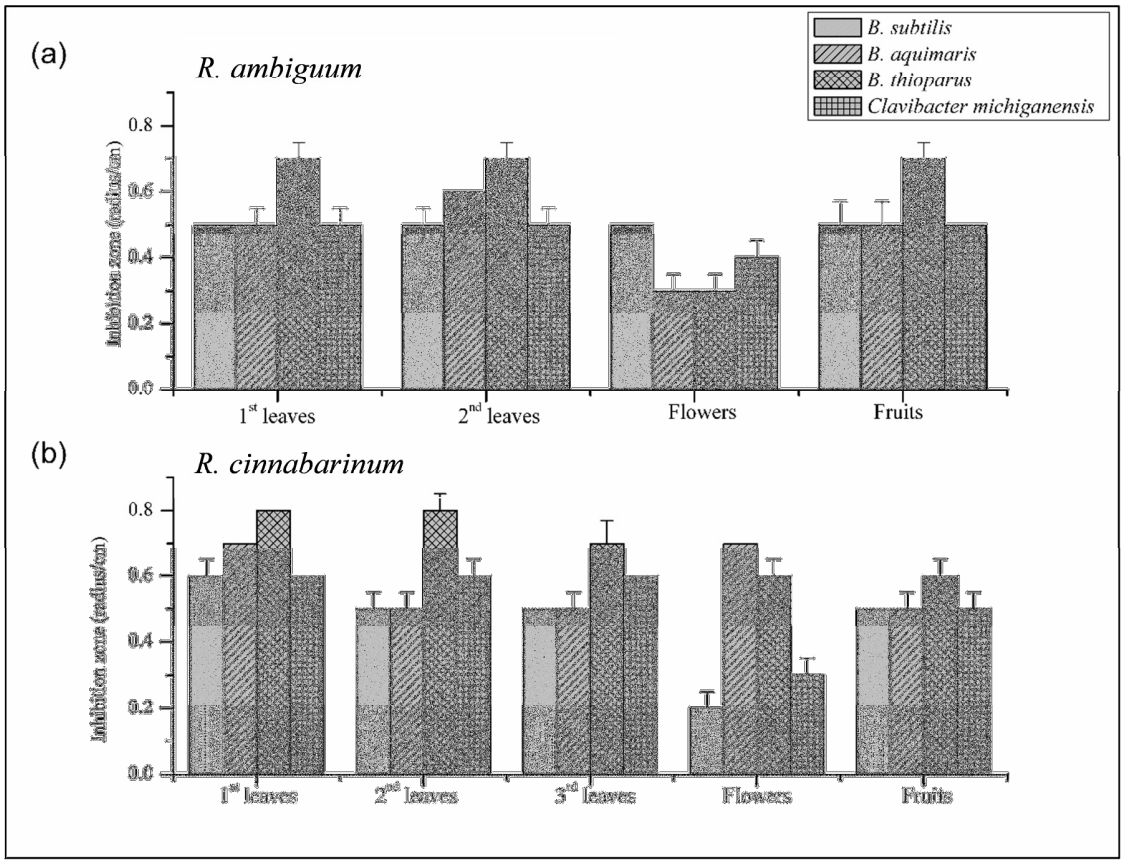

Figure 16.4: Anti-microbial activities of methanol crude extracts of different plant parts a) *R. ambiguum* and b) *R. cinnabarinum*

4. Conclusions

The different parts of the *R. ambiguum* and *R. cinnabarinum* are a rich source of polyphenols. 59 different types of polyphenols including isomers were identified in these parts based on their fragmentation pattern and high resolution mass spectra in negative ion mode. The phytochemical profile of different year leaves was found to be similar. Among all the parts, the fruits were found to contain the highest variety and concentration of polyphenols. PAs were mainly found in the fruits. However, there are many unidentified compounds present in leaves, flowers and fruits, which need to be analyzed in future. We can conclude that both *Rhododendron* species have anti-bacterial effect towards Gram-positive bacteria, while there was no significant difference between different seasonal leaves and fruits, but low effect for flowers.

Competing Interests

The authors declare that they have no competing interests.

Acknowledgements

The authors would like to thank Rhododendron Park and Jacobs University for their financial support, Ms. Anja Müller for the technical support and Dr. Hartwig Schepker for providing the material and their complete botanical information.

17. Additional Studies

17.1. Frost studies on *Rhododendron* leaves

Three *Rhododendron* species, namely *Rhododendron ambiguum* (Figure 17.1), *Rhododendron ferrugineum* (Figure 17.2) and *Rhododendron cinnabarinum* (Figure 17.3) were used for analyzing the effect of the first frost (snow) on the secondary metabolite profile of the leaves. The samples from *Rhododendron* leaves were collected a few months before winter and right after the first frost of the winter. For all three species, it was observed that the frost did not significantly affect the metabolomic profile of the *Rhododendron* leaves. The compounds were found in almost the same intensity in both cases.

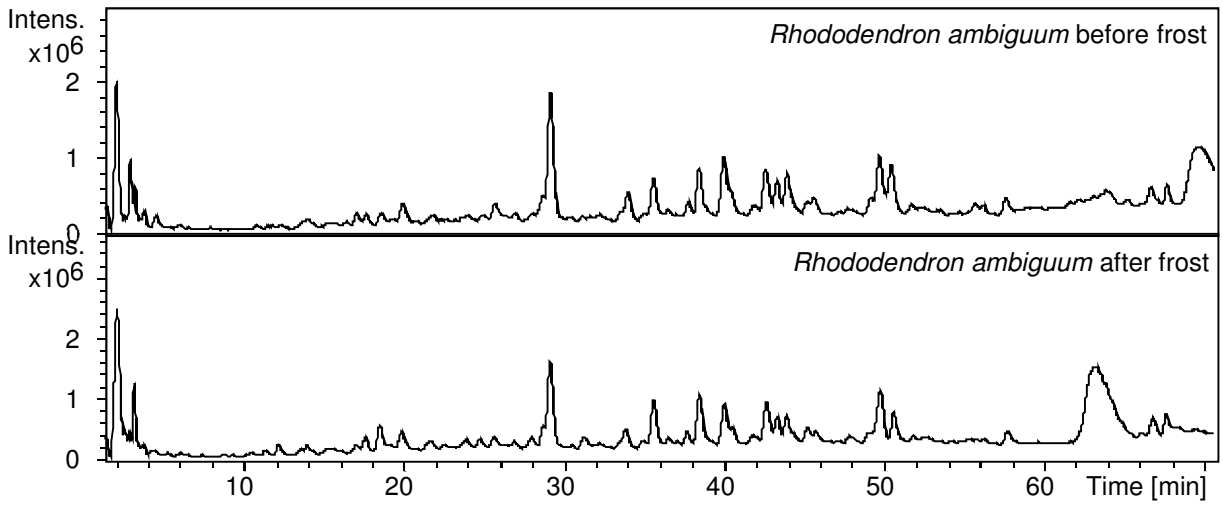

Figure 17.1: TIC of *Rhododendron ambiguum* leaves before and after first frost

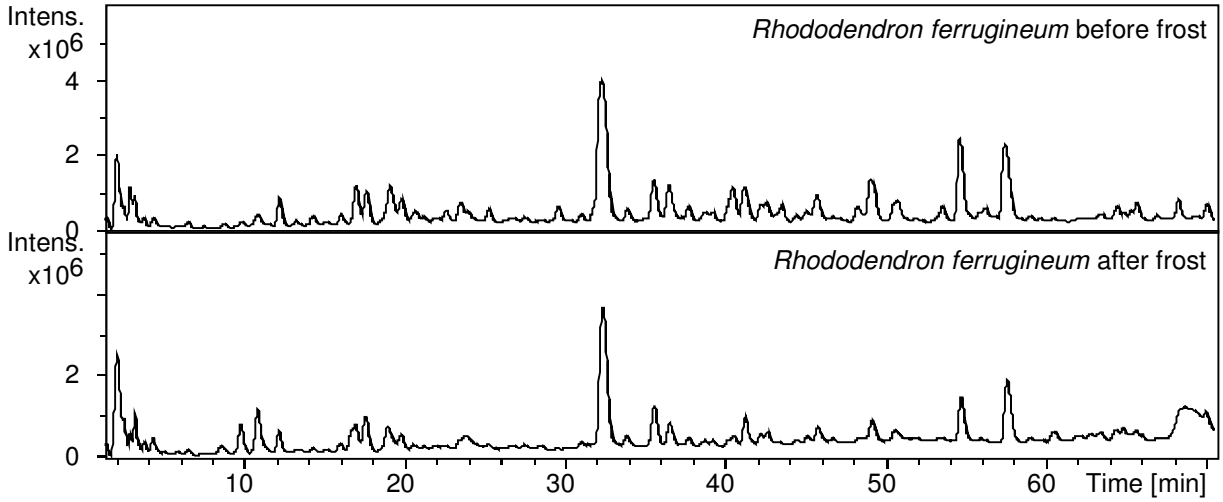

Figure 17.2: TIC of *Rhododendron ferrugineum* leaves before and after first frost

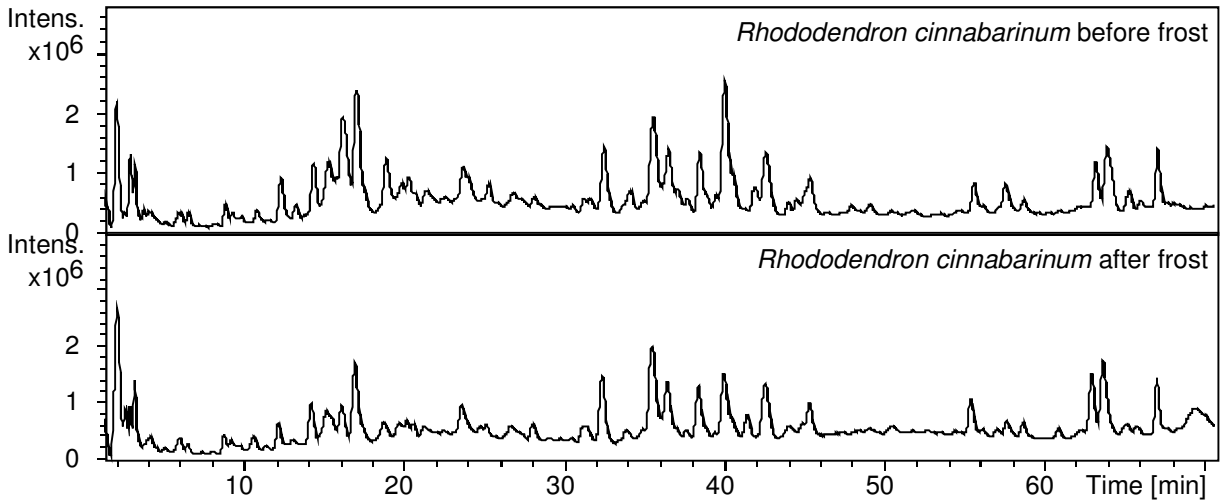

Figure 17.3: TIC of *Rhododendron cinnabarinum* leaves before and after first frost

17.2. Activity guided fractionation by Preparative HPLC of *Rhododendron ambiguum* leaf extracts

The extract of *Rhododendron ambiguum* leaves was found to have high anti-microbial activity against Gram-positive bacteria [2] and was thus chosen for activity guided fractionation in order to determine the active compound. 156 g of *Rhododendron ambiguum* leaves was extracted three times using 780 mL of aqueous methanol (80%) and left in the fridge at 0°C for 24 h. The mixture was then sonicated for 15 min and filtered using a 90 mm filter paper. The solvent was dried using a lyophilizer. 18 g of residue was obtained, which was dissolved in 180 mL methanol. This mixture was separated by using three C18 ec (15 mL, 2000 mg silica) cartridges and 5 mL solution for each. The SPE clean-up can be divided into the following five steps:

- Step 1 (Washing): The cartridge was conditioned by using 10 mL of deionized water.
- Step 2 (Sample Load): 5 mL of the sample was added.
- Step 3 (Sample Rinse): 5 mL of water was added and collected as the "Water extract"
- Step 4 (Sample Elution): 5 mL of methanol was added and collected as the "Water:MeOH extract"
- Step 5 (Sample Elution): 4 x 5 mL of methanol was added and collected as the "MeOH extract"

The five steps are clearly shown in Figure 17.4.

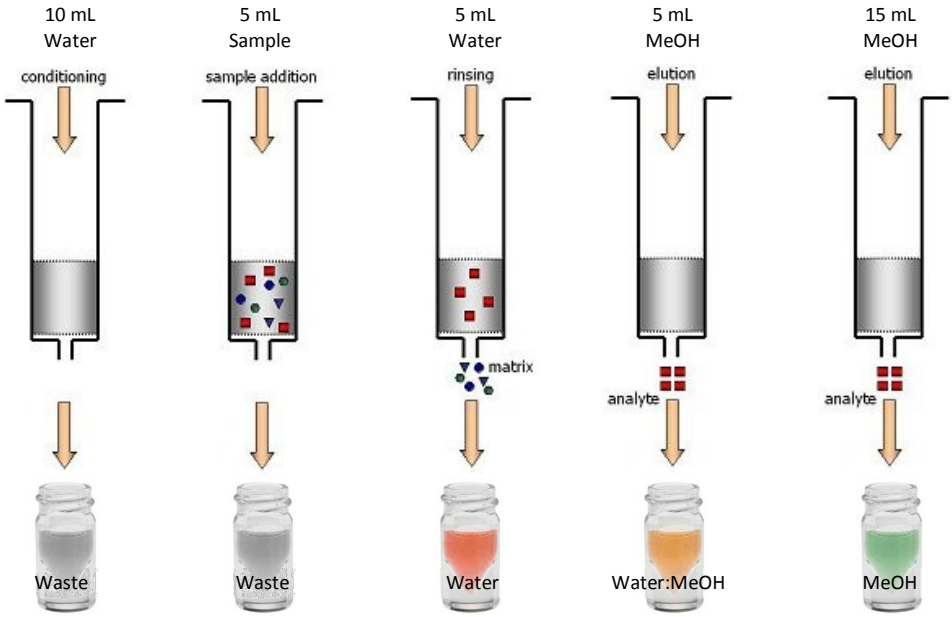

Figure 17.4: SPE Clean-Up of *Rhododendron ambiguum*

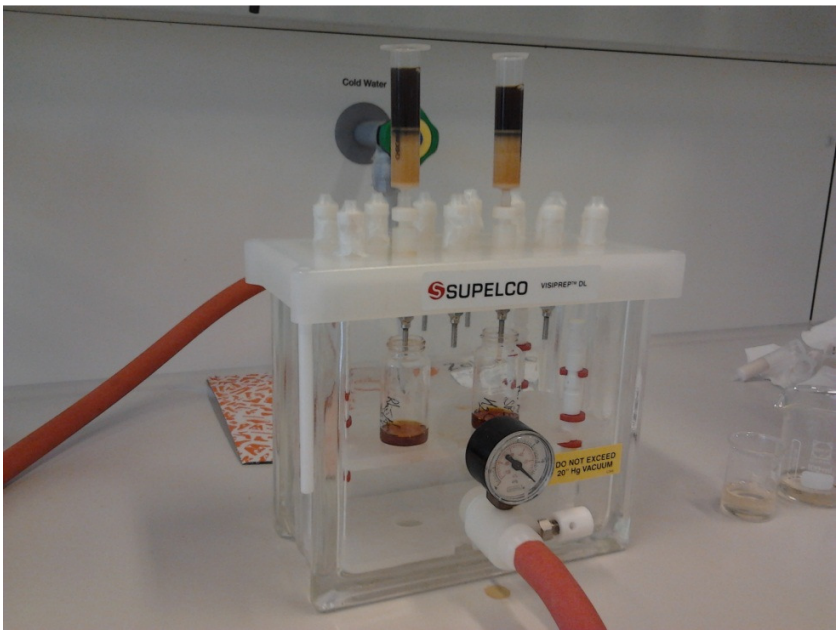

Figure 17.5: SPE setup used for *Rhododendron ambiguum*

The three extracts were analyzed by Ahmed by using the agar diffusion assay against *Bacillus subtilis*. The "MeOH" extract provided a high inhibition area as shown in Figure 17.6. The "MeOH" extract was also evaporated and the obtained 2 g of residue was dissolved in 100 mL aqueous methanol (80%). A fraction collection method was developed for this "MeOH" solution using the Prep-HPLC.

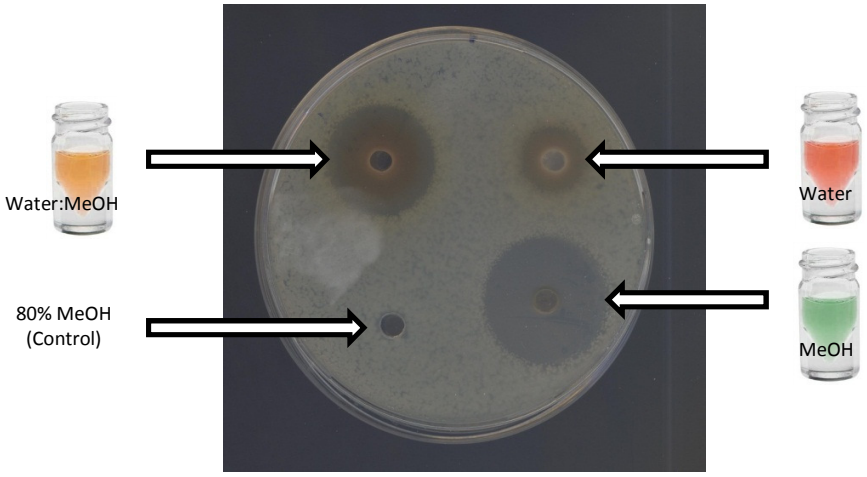

Figure 17.6: Agar diffusion assay using the three different extracts of *Rhododendron ambiguum*

The Prep-HPLC method was developed using a binary solvent system of Water (0.005% Formic acid) and acetonitrile. The diphenyl column was used for separation. The flow rate was set at 4.0 mL/min. The UV detector was set at 280 nm. 500 µL of the solution (2 g/100 mL) was injected in each run. The gradient used is given in Table 17.1:

Table 17.1: Prep-HPLC method for *Rhododendron ambiguum*

Time (min)	Percentage of ACN (%)
0	10
10	70
20	80
30	90

36 fractions were collected from the 157 prep-HPLC runs of *Rhododendron ambiguum*. The collected fractions are shown in Figure 17.7:

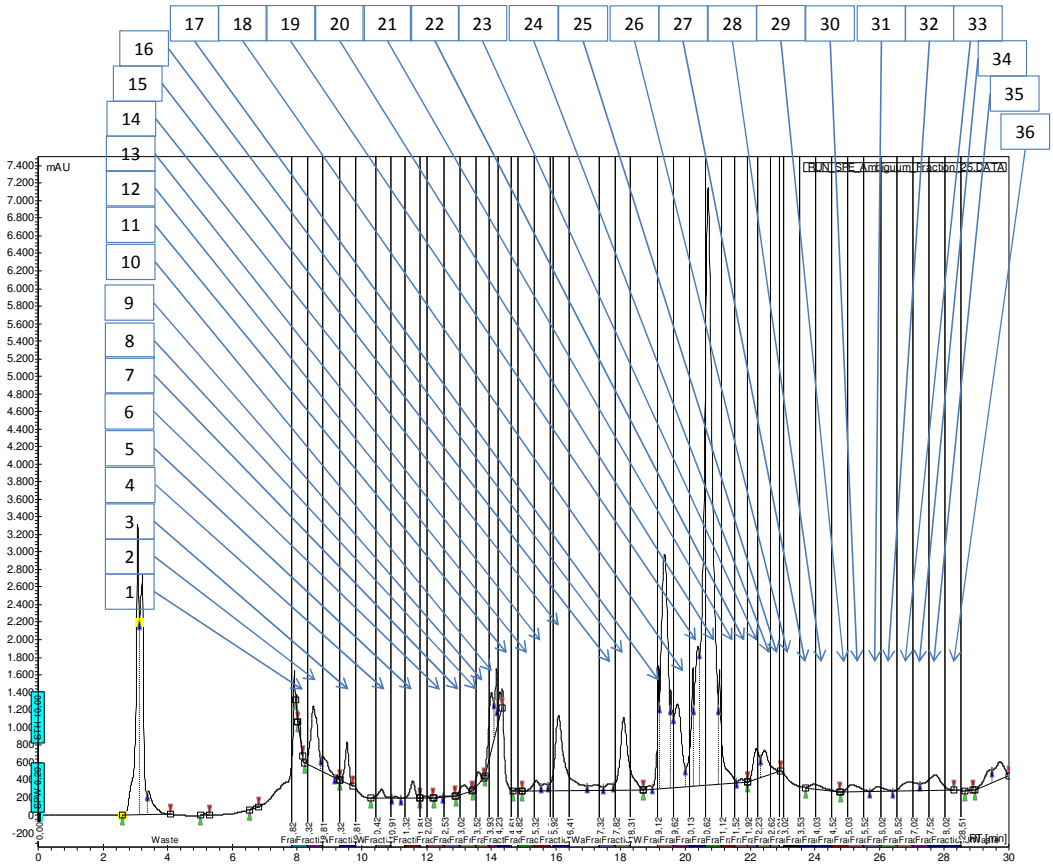

Figure 17.7: 36 fractions collected from *Rhododendron ambiguum*

The residue collected from the fractions was in the range of 2.9 to 33.3 mg. Fraction 21 produced an inhibition zone of 0.6 cm and was used for further analysis using LC-MS and NMR.

For the LC-MS^n and LC-TOF-MS analysis, a binary system of water (0.005% Formic acid) and methanol was used with a flow rate of 0.5 mL/min. The C-18 amide column was used for the separation.

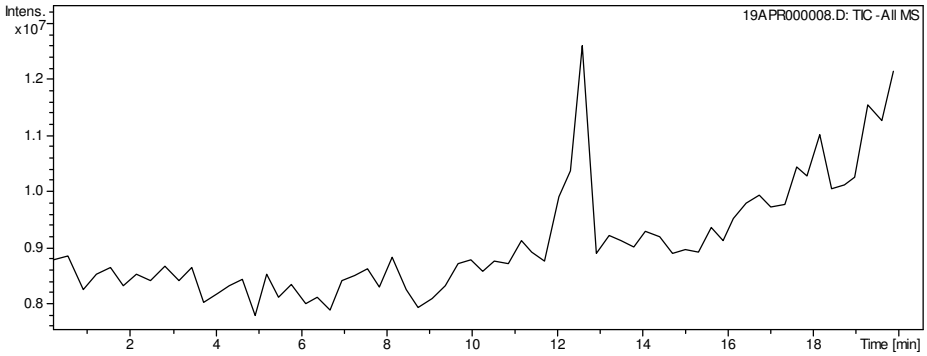

Figure 17.8: TIC of Fraction 21 using LC-Ion Trap-MS from *Rhododendron ambiguum* in negative mode

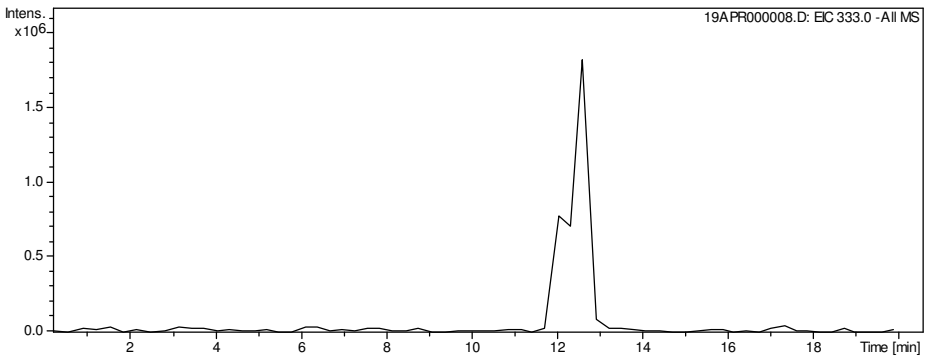

Figure 17.9: EIC at *m/z* 333 of Fraction 21 using LC-Ion Trap-MS from *Rhododendron ambiguum* in negative mode

Two isomers of *m/z* 333 were observed. The first isomer produced a base peak of *m/z* 315 and secondary peaks of *m/z* 297, 271 and 257. The second isomer produced a base peak of *m/z* 315 and secondary peaks of *m/z* 297, 271 and 244. Using high resolution data, both the isomers had the same potential molecular formula of $C_{18}H_{22}O_6$. To further study the isomers, the residue was dissolved in deuterated methanol and analyzed using NMR (^{1}H, ^{13}C, ^{13}C DEPT, COSY, NOESY,

HSQC, and HMBC). The complete structure of the isomers could not be determined as the peaks were overlapping with each other. However, a few structural parameters were determined. The active compound was speculated to be a modified diterpene, which consisted of 8 double bond equivalents, tetracyclic structure, 2 double bonds, 1 cis double bond in the ring, 1 trisubstituted double bond in the ring, 1 ester bond, 3-4 tertiary oxygen atoms and possible cyclic peroxide.

One of my colleagues, Inamullah Hakeem Said conducted a few experiments using a regular column and silica gel, which could be more efficient to collect large amount of fractions in shorter time and perform further analysis.

18. Discussion

This chapter will provide a short discussion to correlate the hypotheses of this project with its results.

From the anti-bacterial studies, 17 *Rhododendron* species were determined to have significant anti-bacterial activity against *Bacillus subtilis*.[2] One of the active species, *Rhododendron ambiguum* was used for activity guided fractionation. The structure of active compounds could only be partially identified due to the presence of impurities and insufficient residue for further studies. 12 out of 17 *Rhododendron* species were used for cytotoxic studies, out of which 2 species namely, *Rhododendron minus* and *Rhododendron racemosum* were found to be non-cytotoxic at bactericidal concentrations.[201] Hence, the hypothesis that *Rhododendron* species have significantly high anti-bacterial activity and low cytotoxicity could only be applicable for a few *Rhododendron* species.

Rhododendron ambiguum leaf extracts were used for activity guided fractionation study and the compounds present in the active fraction against *Bacillus subtilis* were analyzed using LC-MS and NMR. The molecular formula and partial structural information of the compounds were determined using the LC-MS and NMR data of the active fraction; however the structure of the compounds could not be completely elucidated. This result supported the hypothesis that the natural products from *Rhododendron* species will provide lead structures for potential antibiotics.

Principal component analysis of the LC-TOF-MS data of *Rhododendron* species did not show clear separation of the *Rhododendron* species with respect to their subgenus. In the hierarchical clustering analysis of the same set of data, several *Rhododendron* species cluster with respect to their subgenera. However, with the exception of Azaleastrum, at least two clusters were obtained for each subgenus. Further analyses are required to confirm the hypothesis that bioinformatics is a useful tool for differentiating *Rhododendron* species based on their secondary metabolite profile. The hypothesis that phylogenetically similar *Rhododendron* species have a similar secondary metabolite profile could not be confirmed as it could be only applied to some

Rhododendron species. Nevertheless, bioinformatics was useful to contextualize, compare and get an overview of the large set of data.

A few compounds that differentiated two significantly active species against *Bacillus subtilis*, namely *Rhododendron ferrugineum* and *Rhododendron anthopogon* were identified in one of the PCA analysis. The other PCA analysis consisted of the most significantly active species against *Bacillus subtilis* in the center of the plot indicating that these species contain the most common metabolites among the *Rhododendron* species. Activity guided fractionation studies are required to confirm the hypothesis that bioinformatics is useful for predicting the anti-bacterial activity of *Rhododendron* species.

A few marker compounds were identified for individual *Rhododendron* species as well as for subgenus. Some additional studies regarding secondary metabolites of more species need to be conducted in order to confirm the hypothesis that marker compounds aid in the chemotaxonomy of *Rhododendron* species or subgenera.

The number of compound peaks, calculated from the LC-TOF-MS data of *Rhododendron* species, did not have a correlation with the polyploidy level (R^2 = 0.018) and anti-bacterial activity against *Bacillus subtilis* (R^2 = 0.020) of the species. The hypothesis that the total number of compounds present in *Rhododendron* leaf extracts is dependent on the polyploidy level or influences the anti-bacterial activity was not supported by these results.

The *Rhododendron* species, which belong to the subgenus *Tsutsusi* consisted of the lowest mean among the six subgenera compared. However, with the exception of *Mumeazalea*, a high standard deviation was observed for all subgenera. Thus, the hypothesis that a specific subgenus of *Rhododendron* species produces high number of compounds compared to others was refuted.

From the box plot studies, it was observed that some compounds were found in relatively higher concentrations in certain subgenera. Some of the most common coumaroylquinic acid isomers were found in more relative abundance in the subgenus *Tsutsusi*. Three hexosides of vanillic acid were found in higher relative concentrations in the subgenus *Rhododendron*. An isomer among

the hexosides of caffeic acid, *p*-coumaric acid and ferulic acid, along with caffeoylshikimic acid was found mostly in the subgenus *Pentanthera*. The A-type and B-type procyanidin dimers were found in relatively large quantities in the subgenus *Hymenanthes*. A rhamnoside and one of the hexosides of myricetin were found in relatively higher concentration in the subgenus *Azaleastrum*. The results supported the hypothesis that some compounds are present in a higher relative quantity in certain subgenus of *Rhododendron* species.

From the frost studies of *Rhododendron* species, it was observed that the first snow of the winter did not affect the metabolomic profile of *Rhododendron* species. Thus, the hypothesis that frost influences the secondary metabolite profile of *Rhododendron* species was rejected.

From the comparison studies of the fruits, flowers and leaves of two *Rhododendron* species (*Rhododendron ambiguum* and *Rhododendron cinnabarinum*), it was observed that the different plant organs had a different phytochemical profile. The extract of fruits and leaves exhibited similar anti-bacterial activity; however the extract of flowers exhibited a relatively low anti-bacterial activity compared to them. These results supported the hypothesis that different plant organs produce different phytochemical profiles with altering bioactivity.

19. Conclusion

The polyphenolic secondary metabolite profile of the leaves of 100 *Rhododendron* species was successfully analyzed using liquid chromatography coupled to mass spectrometry. The leaves of the *Rhododendron* species were found to be a good source of polyphenols with a total of 348 polyphenolic secondary metabolites identified. A total of 51 hydroxycinnamic acid derivatives, 63 hydroxybenzoic acid derivatives, 86 flavan-3-ols, 25 flavanones and 119 flavonols were identified in them. 221 compounds identified were novel in *Rhododendron* species and 7 compounds identified were novel in nature. Numerous other compounds peaks were also present, which still remain unknown; they could be studied in the future by isolation and NMR analysis. A few polyphenolic compounds were identified in only some *Rhododendron* species, which could act like marker compounds for future distinction of the species.

The twenty most abundant compounds identified by LC-Ion Trap-MS and LC-TOF-MS were quercetin-*O*-hexoside (t_R 34.2 min), quercetin-*O*-hexoside (t_R 35.5 min), quercetin-*O*-pentoside (t_R 41.2 min), quercetin-*O*-rhamnoside (t_R 38.7 min), protocatechuic acid-*O*-hexoside (t_R 10.5 min), catechin (t_R 16.0 min), procyanidin dimer B (t_R 20.3 min), quercetin-*O*-pentoside (t_R 37.4 min), kaempferol-*O*-rhamnoside (t_R 43.6 min), procyanidin dimer B1 (t_R 13.4 min), quercetin (t_R 44.4 min), *p*-coumaric acid-*O*-hexoside (t_R 16.5 min), 3-*O*-caffeoylquinic acid (t_R 13.0 min), epicatechin (t_R 23.0 min), quercetin-*O*-pentoside (t_R 36.6 min), procyanidin dimer B (t_R 14.3 min), 5-*O*-caffeoylquinic acid (t_R 18.2 min), A-type procyanidin dimer (t_R 32.4 min), quercetin-*O*-glucuronide (t_R 40.8 min) and A-type procyanidin dimer (t_R 27.2 min).

The comprehensive analyses were not only limited to *Rhododendron* leaves, but also extended to different-aged leaves, fruits and flowers of two *Rhododendron* species (*Rhododendron ambiguum* and *Rhododendron cinnabarinum*). The phytochemical profile of the different-aged leaves was found to be similar. The fruits and flowers produced similar compounds as leaves but had different overall phytochemical profile. The fruits in particular were found to contain a high amount of proanthocyanidins and the highest diversity and concentration of polyphenols among the parts of the plant analyzed.

Several crude leaf extracts of *Rhododendron* leaves were shown to possess anti-bacterial and cytotoxic activities. Two species were shown to be anti-bacterial and non-cytotoxic and show promise for future development as anti-bacterial agents for clinical use.

In the activity guided fractionation, the active fraction of *Rhododendron ambiguum* against *Bacillus subtilis* was analyzed by LC-MS and NMR in order to determine the compound structure of the active compound. The active fraction consisted of two isomers with *m/z* 333 and potential molecular formula of $C_{18}H_{22}O_6$. However, the complete structure could not be elucidated due to the presence impurities and insufficient material for further analysis.

The relative quantities of polyphenolic compounds were successfully compared using box plots among the five subgenera of *Rhododendron*, namely *Azaleastrum*, *Hymenanthes*, *Pentanthera*, *Rhododendron* and *Tsutsusi*. Some of the compounds were found in a high intensity in a certain subgenera. It could be speculated that the species, which belong to this subgenera could favor the formation of these compounds. Similarly, some isomers were found to be more abundant compared to other isomers in the *Rhododendron* species.

The number of compound peaks of *Rhododendron* leaf extracts was compared among the 100 species. *Rhododendron moulmainense* and *Rhododendron elliottii* were found to have the highest (288) and lowest (43) number of compound peaks among the 100 species. The species of subgenus *Tsutsusi* was observed to have a slightly lower mean value compared to other subgenera. No significant differences were observed. The number of compounds was also found to have no correlation with the ploidy level or the anti-bacterial activity against *Bacillus subtilis*.

From the PCA results, it was determined that the genetically similar *Rhododendron* species produced a diverse secondary metabolite profile. In other words, the *Rhododendron* species could not be genetically differentiated based on their secondary metabolite profile. It could be speculated that the *Rhododendron* species with the highest anti-bacterial activity consisted of many common metabolites produced by other species. A few compounds that could be responsible for this activity were also identified. Some clusters were observed in the hierarchical clustering analysis for the five subgenera of *Rhododendron*; however the overall distribution was

very diverse, which further supported the genetically diverse metabolomic profile of *Rhododendron* species.

20. Reference

[1] D. Chamberlain, R. Hyam, G. Argent, G. Fairweather and K.S. Walter, '"The genus Rhododendron: its classification and synonymy.", 1996.

[2] A. Rezk, J. Nolzen, H. Schepker, D.C. Albach, K. Brix and M.S. Ullrich, '"Phylogenetic spectrum and analysis of antibacterial activities of leaf extracts from plants of the genus Rhododendron," *BMC Complement.Altern.Med.*, vol. 15, Mar 18, pp. 67-015-0596-5.

[3] D.J. Mabberley, '"Mabberley's plant-book,".

[4] P. Stevens, J. Luteyn, E. Oliver, T. Bell, E. Brown, R. Crowden, A. George, G. Jordan, P. Ladd and K. Lemson, '"Celastrales, Oxidales, Rosales, Cornales, Ericales. Ericaceae,", pp. 145-194.

[5] R. Popescu and B. Kopp, '"The genus Rhododendron: An ethnopharmacological and toxicological review," *J.Ethnopharmacol.*, vol. 147, no. 1, 5/2, pp. 42-62.

[6] R. Jaiswal, L. Jayasinghe and N. Kuhnert, '"Identification and characterization of proanthocyanidins of 16 members of the Rhododendron genus (Ericaceae) by tandem LC-MS," *J.Mass Spectrom.*, vol. 47, no. 4, APR, pp. 502-515.

[7] J.A. Duke and E.S. Ayensu, '"Medicinal plants of China,", vol. 2, 1985.

[8] Y. Fu, L. Zhang and G. Chen, '"Far infrared-assisted extraction followed by MEKC for the simultaneous determination of flavones and phenolic acids in the leaves of Rhododendron mucronulatum Turcz," *Journal of separation science*, vol. 35, no. 3, pp. 468-475.

[9] N. Iwata, N. Wang, X. Yao and S. Kitanaka, '"Structures and Histamine Release Inhibitory Effects of Prenylated Orcinol Derivatives from Rhododendron dauricum 1," *J.Nat.Prod.*, vol. 67, no. 7, pp. 1106-1109.

[10] Q. Li, L. Chen, Y. Zhu, M. Zhang, Y. Wang and M. Wang, '"Involvement of estrogen receptor-β in farrerol inhibition of rat thoracic aorta vascular smooth muscle cell proliferation," *Acta Pharmacol.Sin.*, vol. 32, no. 4, pp. 433-440.

[11] W. Zhao-yuan and L. Rong-tao, '"Chemical Constituents from the Roots of Rhododendron spiciferum." *Natural Product Research & Development*, vol. 23, no. 2.

[12] Y.H. Choi, W. Zhou, J. Oh, S. Choe, D.W. Kim, S.H. Lee and M. Na, '"Rhododendric acid A, a new ursane-type PTP1B inhibitor from the endangered plant Rhododendron brachycarpum G. Don," *Bioorg.Med.Chem.Lett.*, vol. 22, no. 19, pp. 6116-6119.

[13] L. Xue-feng, J. Hui-zi, C. Gang, Y. Shi-kai, S. Yun-heng, Y. Ming and Z. Wei-dong, "'Study Advances on Chemical Constituents and Pharmacological Activities of the Tibetan Medicine Dali." *Natural Product Research & Development*, vol. 20, no. 6.

[14] S. Guleria, V. Jaitak, R. Saini, V.K. Kaul, B. Lal, G.K. Babu, B. Singh and R. Singh, "'Comparative studies of volatile oil composition of Rhododendron anthopogon by hydrodistillation, supercritical carbon dioxide extraction and head space analysis," *Natural product research*, vol. 25, no. 13, pp. 1271-1277.

[15] R.M. Kunwar, K.P. Shrestha and R.W. Bussmann, "'Traditional herbal medicine in Far-west Nepal: a pharmacological appraisal," *Journal of Ethnobiology and Ethnomedicine*, vol. 6, no. 1, pp. 1.

[16] Y. Uprety, H. Asselin, E.K. Boon, S. Yadav and K.K. Shrestha, "'Indigenous use and bio-efficacy of medicinal plants in the Rasuwa District, Central Nepal," *Journal of Ethnobiology and Ethnomedicine*, vol. 6, no. 1, pp. 1.

[17] A. Paul, M.L. Khan and A.K. Das, "'Utilization of rhododendrons by Monpas in western Arunachal Pradesh, India," *Journal American Rhododendron Society*, vol. 64, no. 2, pp. 81-84.

[18] D. Semwal, P.P. Saradhi, C. Kala and B. Sajwan, "'Medicinal plants used by local Vaidyas in Ukhimath block, Uttarakhand," *Indian Journal of Traditional Knowledge*, vol. 9, no. 3, pp. 480-485.

[19] S. Gerlach, J. Saukel and W. Kubelka, "'Pflanzen in der österreichischen Volksmedizin-die „Volksmed-Datenbank “," *Sci Pharm*, vol. 74, no. Suppl 1, pp. S36.

[20] E. Chosson, A. Chaboud, A. Chulia and J. Raynaud, "'Dihydroflavonol glycosides from Rhododendron ferrugineum," *Phytochemistry*, vol. 49, no. 5, pp. 1431-1433.

[21] A. Louis, F. Petereit, M. Lechtenberg, A. Deters and A. Hensel, "'Phytochemical characterization of Rhododendron ferrugineum and in vitro assessment of an aqueous extract on cell toxicity," *Planta Med.*, vol. 76, no. 14, Oct, pp. 1550-1557.

[22] D. Tasdemir, B. Demirci, F. Demirci, A.A. Dönmez, K. Baser and P. Rüedia, "'Analysis of the volatile components of five Turkish Rhododendron species by headspace solid-phase microextraction and GC-MS (HS-SPME-GC-MS)," *Zeitschrift Für Naturforschung C*, vol. 58, no. 11-12, pp. 797-803.

[23] S. Alan, M. Kurkcuoglu, F. Goger, K. Baser and H. Can, "'Morphological, chemical and indumentum characteristics of Rhododendron luteum Sweet (Ericaceae)," *Pak.J.Bot.*, vol. 42, no. 6, pp. 3729-3737.

[24] N. Erdemoglu, E.K. Akkol, E. Yesilada and I. Calış, "'Bioassay-guided isolation of anti-inflammatory and antinociceptive principles from a folk remedy, Rhododendron ponticum L. leaves," *J.Ethnopharmacol.*, vol. 119, no. 1, 9/2, pp. 172-178.

[25] T. Johnson, '"Ethnobotany desk reference," *CRC Pres*, vol. 200, pp. 805-808.

[26] C. Leduc, J. Coonishish, P. Haddad and A. Cuerrier, '"Plants used by the Cree Nation of Eeyou Istchee (Quebec, Canada) for the treatment of diabetes: a novel approach in quantitative ethnobotany," *J.Ethnopharmacol.*, vol. 105, no. 1, pp. 55-63.

[27] T.W. Tam, R. Liu, J.T. Arnason, A. Krantis, W.A. Staines, P.S. Haddad and B.C. Foster, '"Actions of ethnobotanically selected Cree anti-diabetic plants on human cytochrome P450 isoforms and flavin-containing monooxygenase 3," *J.Ethnopharmacol.*, vol. 126, no. 1, pp. 119-126.

[28] C. Ratsch, '"Enzyklopadie der psychoaktiven Pflanzen: Botanik, Ethnopharmakologie und Anwendung," *Aarau: AT 941p.ISBN 3855025703 Ge Very detailed account covering c*, vol. 500.

[29] P. Sahu, C. Rao, N. Verma, A. Singh and G. Amresh, '"Anti-inflammatory and anti nociceptive activity of Rhododendron arboreum," *J Pharm Res*, vol. 3, pp. 47-57.

[30] F. Ullah, H. Hussain, J. Hussain, I.A. Bukhari, M.T.H. Khan, M.I. Choudhary, A.H. Gilani and V.U. Ahmad, '"Tyrosinase inhibitory pentacyclic triterpenes and analgesic and spasmolytic activities of methanol extracts of Rhododendron collettianum," *Phytotherapy Research*, vol. 21, no. 11, pp. 1076-1081.

[31] H.P. Chhetri, N.S. Yogol, J. Sherchan, K. Anupa, S. Mansoor and P. Thapa, '"Phytochemical and antimicrobial evaluations of some medicinal plants of Nepal," *Kathmandu university journal of science, engineering and technology*, vol. 4, no. 1, pp. 49-54.

[32] P.K. Sonar, R. Singh, S. Khan and S.K. Saraf, '"Isolation, characterization and activity of the flowers of Rhododendron arboreum (Ericaceae)," *Journal of Chemistry*, vol. 9, no. 2, pp. 631-636.

[33] C. Jin, W. Strembiski, Y. Kulchytska and Daneshtalab, Ronald G Micetich Mohsen, '"Flavonoid glycosides from *Ledum palustre* L. subsp. *decumbens* (Ait.) Hulton," *DARU Journal of Pharmaceutical Sciences*, vol. 7, no. 4, pp. 5-8.

[34] D. Tasdemir, R. Brun, R. Perozzo and A. Dönmez, '"Evaluation of antiprotozoal and plasmodial enoyl-ACP reductase inhibition potential of turkish medicinal plants," *Phytotherapy Research*, vol. 19, no. 2, pp. 162-166.

[35] M.S. Zheng, '"An experimental study of the anti-HSV-II action of 500 herbal drugs," *J.Tradit.Chin.Med.*, vol. 9, no. 2, Jun, pp. 113-116.

[36] Ö ERTÜRK, Z. DEMİRBAĞ and A.O. BELDÜZ, '"Antiviral Activity of Some Plant Extracts on the Replication of Autographa californicaNuclear Polyhedrosis Virus," *Turkish Journal of Biology*, vol. 24, no. 4, pp. 833-844.

[37] Y. Kashiwada, K. Yamazaki, Y. Ikeshiro, T. Yamagishi, T. Fujioka, K. Mihashi, K. Mizuki, L.M. Cosentino, K. Fowke, S.L. Morris-Natschke and K. Lee, "'Isolation of rhododaurichromanic acid B and the anti-HIV principles rhododaurichromanic acid A and rhododaurichromenic acid from Rhododendron dauricum," *Tetrahedron*, vol. 57, no. 8, 2/18, pp. 1559-1563.

[38] E. Kemertelidze, K. Shalashvili, B. Korsantiya, N. Nizharadze and N.S. Chipashvili, "'Therapeutic effect of phenolic compounds isolated from Rhododendron ungernii leaves," *Pharmaceutical Chemistry Journal*, vol. 41, no. 1, pp. 10-13.

[39] K. Gescher, J. Kühn, W. Hafezi, A. Louis, A. Derksen, A. Deters, E. Lorentzen and A. Hensel, "'Inhibition of viral adsorption and penetration by an aqueous extract from Rhododendron ferrugineum L. as antiviral principle against herpes simplex virus type-1," *Fitoterapia*, vol. 82, no. 3, pp. 408-413.

[40] W. WANG, Y. CAO, L. FU, H. LI, X. DENG and R. LI, "'Chemical constituents from Rhododendron spiciferum and their effects on immunocyte of mice [J]," *Chinese Traditional and Herbal Drugs*, vol. 1, pp. 006.

[41] Y.Z. Liu, Y.G. Cao, J.Q. Ye, W.G. Wang, K.J. Song, X.L. Wang, C.H. Wang, R.T. Li and X.M. Deng, "'Immunomodulatory effects of proanthocyanidin A-1 derived in vitro from Rhododendron spiciferum," *Fitoterapia*, vol. 81, no. 2, pp. 108-114.

[42] H. Takahashi, S. Hirata, H. Minami and Y. Fukuyama, "'Triterpene and flavanone glycoside from Rhododendron simsii," *Phytochemistry*, vol. 56, no. 8, pp. 875-879.

[43] S.J. Jung, D. Kim, Y. Hong, J. Lee, H. Song, Y. Rho and N. Baek, "'Flavonoids from the flower of Rhododendron yedoense var. Poukhanense and their antioxidant activities," *Arch.Pharm.Res.*, vol. 30, no. 2, pp. 146-150.

[44] N. Verma, G. Amresh, P. Sahu, C.V. Rao and A.P. Singh, "'Antihyperglycemic and antihyperlipidemic activity of ethyl acetate fraction of Rhododendron arboreum Smith flowers in streptozotocin induced diabetic rats and its role in regulating carbohydrate metabolism," *Asian Pacific journal of tropical biomedicine*, vol. 2, no. 9, pp. 696-701.

[45] T. Prakash, S.D. Fadadu, U.R. Sharma, V. Surendra, D. Goli, P. Stamina and D. Kotresha, "'Hepatoprotective activity of leaves of Rhododendron arboreum in CCl_4 induced hepatotoxicity in rats." *J. Med. Plants*, pp. 315.

[46] M.P. Mudagal, S. Karia and D. Goli, "'Preventive effect of Rhododendron arboreum on cardiac markers, lipid peroxides and antioxidants in normal and isoproterenol-induced myocardial necrosis in rats," *African Journal of Pharmacy and Pharmacology*, vol. 5, no. 6, pp. 755-763.

[47] V.U. Ahmad, F. Ullah, J. Hussain, U. Farooq, M. Zubair, M.T.H. Khan and M.I. Choudhary, "'Tyrosinase inhibitors from Rhododendron collettianum and their structure-activity relationship (SAR) studies," *Chemical and pharmaceutical bulletin*, vol. 52, no. 12, pp. 1458-1461.

[48] I. Orhan, B. Şener, M. Choudhary and A. Khalid, "'Acetylcholinesterase and butyrylcholinesterase inhibitory activity of some Turkish medicinal plants," *J.Ethnopharmacol.*, vol. 91, no. 1, pp. 57-60.

[49] S. Silici, O. Sagdic and L. Ekici, "'Total phenolic content, antiradical, antioxidant and antimicrobial activities of Rhododendron honeys," *Food Chem.*, vol. 121, no. 1, 7/1, pp. 238-243.

[50] D. Dursunoglu, S. Gur and E. Semiz, "'A case with complete atrioventricular block related to mad honey intoxication," *Ann.Emerg.Med.*, vol. 50, no. 4, pp. 484-485.

[51] A. Gunduz, S. Turedi, H. Uzun and M. Topbas, "'Mad honey poisoning," *Am.J.Emerg.Med.*, vol. 24, no. 5, pp. 595-598.

[52] D. Black, "'Rhododendron poisoning in sheep." *Vet.Rec.*, vol. 128, no. 15, pp. 363-364.

[53] S. Casteel and J. Wagstaff, "'Rhododendron macrophyllum poisoning in a group of goats and sheep," *Vet.Hum.Toxicol.*, vol. 31, no. 2, Apr, pp. 176-177.

[54] I. Hough, "'Rhododendron poisoning in a western grey kangaroo," *Aust.Vet.J.*, vol. 75, no. 3, pp. 174-175.

[55] D. Bhattacharyya, "'Rhododendron species and their uses with special reference to Himalayas–a review," *Assam University Journal of Science and Technology*, vol. 7, no. 1, pp. 161-167.

[56] Y.C. Joshi, M.P. Dobhal, B.C. Joshi and F.S. Barar, "'Chemical investigation and biological screening of the stem of Rhododendron anthopogon (D. Don.)," *Pharmazie*, vol. 36, no. 5, May, pp. 381.

[57] H. Hikino, Y. Ohizumi, C. Konno, K. Hashimoto and H. Wakasa, "'Subchronic toxicity of ericaceous toxins and Rhododendron leaves," *Chem.Pharm.Bull.(Tokyo)*, vol. 27, no. 3, Apr, pp. 874-879.

[58] P. Seephonkai, R. Popescu, M. Zehl, G. Krupitza, E. Urban and B. Kopp, "'Ferruginenes a–C from Rhododendron ferrugineum and their cytotoxic evaluation," *J.Nat.Prod.*, vol. 74, no. 4, pp. 712-717.

[59] K. Byun, Y. Lee, H. Jin, M. Lee, H. Lee, K. Lee, M. Heo, C. Yu and J. Lee, "'Genotoxicity and cytotoxicity in human cancer and normal cell lines of the extracts of Rhododendron brachycarpum D. Don leaves," *Korean Journal of Medicinal Crop Science*, vol. 13, no. 4, pp. 199-205.

[60] Y. Park and S. Kim, "'Composition and cytotoxicity of essential oil from Korean rhododendron (Rhododendon mucronulatum Turcz. var. ciliatum Nakai)," *J.Korean Soc.Appl.Biol.Chem*, vol. 51, no. 3, pp. 233-237.

[61] Y. Qiang, B. Zhou and K. Gao, "'Chemical Constituents of Plants from the Genus Rhododendron," *Chemistry & Biodiversity*, vol. 8, no. 5, pp. 792-815.

[62] C. Manach, A. Scalbert, C. Morand, C. Remesy and L. Jimenez, "'Polyphenols: food sources and bioavailability," *Am.J.Clin.Nutr.*, vol. 79, no. 5, May, pp. 727-747.

[63] R. Tsao, "'Chemistry and biochemistry of dietary polyphenols," *Nutrients*, vol. 2, no. 12, pp. 1231-1246.

[64] G. Mikutis, H. Karaköse, R. Jaiswal, A. LeGresley, T. Islam, M. Fernandez-Lahore and N. Kuhnert, "'Phenolic promiscuity in the cell nucleus–epigallocatechingallate (EGCG) and theaflavin-3, 3′-digallate from green and black tea bind to model cell nuclear structures including histone proteins, double stranded DNA and telomeric quadruplex DNA," *Food & function*, vol. 4, no. 2, pp. 328-337.

[65] R. Jaiswal, E.A. Halabi, M.G.E. Karar and N. Kuhnert, "'Identification and characterisation of the phenolics of Ilex glabra L. Gray (Aquifoliaceae) leaves by liquid chromatography tandem mass spectrometry," *Phytochemistry*, vol. 106, 10, pp. 141-155.

[66] F.A. Tomás-Barberán and M.N. Clifford, "'Dietary hydroxybenzoic acid derivatives–nature, occurrence and dietary burden," *J.Sci.Food Agric.*, vol. 80, no. 7, pp. 1024-1032.

[67] R. Jaiswal, J. Kiprotich and N. Kuhnert, "'Determination of the hydroxycinnamate profile of 12 members of the Asteraceae family," *Phytochemistry*, vol. 72, no. 8, 6, pp. 781-790.

[68] A.W. Boots, G.R. Haenen and A. Bast, "'Health effects of quercetin: from antioxidant to nutraceutical," *Eur.J.Pharmacol.*, vol. 585, no. 2, pp. 325-337.

[69] A.Y. Chen and Y.C. Chen, "'A review of the dietary flavonoid, kaempferol on human health and cancer chemoprevention," *Food Chem.*, vol. 138, no. 4, pp. 2099-2107.

[70] Y. Li and Y. Ding, "'Minireview: Therapeutic potential of myricetin in diabetes mellitus," *Food Science and Human Wellness*, vol. 1, no. 1, pp. 19-25.

[71] M. Pan, C. Lai and C. Ho, "'Anti-inflammatory activity of natural dietary flavonoids," *Food & function*, vol. 1, no. 1, pp. 15-31.

[72] P. Mak, Y. Leung, W. Tang, C. Harwood and S. Ho, "'Apigenin suppresses cancer cell growth through ERβ," *Neoplasia*, vol. 8, no. 11, pp. 896-904.

[73] S.F. Nabavi, N. Braidy, O. Gortzi, E. Sobarzo-Sanchez, M. Daglia, K. Skalicka-Woźniak and S.M. Nabavi, "'Luteolin as an anti-inflammatory and neuroprotective agent: a brief review," *Brain Res.Bull.*, vol. 119, pp. 1-11.

[74] T. Kim, G. Kim, H. Ahn, J. Cho, Y.S. Park and C. Park, "'The inhibitory effect of naringenin on atopic dermatitis induced by DNFB in NC/Nga mice," *Life Sci.*, vol. 93, no. 15, pp. 516-524.

[75] A.A. Zanwar, S.L. Badole, P.S. Shende, M.V. Hegde and S.L. Bodhankar, '"Chapter 76 - Cardiovascular Effects of Hesperidin: A Flavanone Glycoside,", pp. 989-992.

[76] M. Imen, F. Chaabane, M. Nadia, K. Soumaya, G. Kamel and C. Leila, '"Anti-melanogenesis and antigenotoxic activities of eriodictyol in murine melanoma (B16-F10) and primary human keratinocyte cells," *Life Sci.*, vol. 135, pp. 173-178.

[77] K. Manigandan, R.L. Jayaraj, K. Jagatheesh and N. Elangovan, '"Taxifolin mitigates oxidative DNA damage in vitro and protects zebrafish (Danio rerio) embryos against cadmium toxicity," *Environ.Toxicol.Pharmacol.*, vol. 39, no. 3, pp. 1252-1261.

[78] Y. Zhang, S.K. Vareed and M.G. Nair, '"Human tumor cell growth inhibition by nontoxic anthocyanidins, the pigments in fruits and vegetables," *Life Sci.*, vol. 76, no. 13, pp. 1465-1472.

[79] L.B. Davin and N.G. Lewis, '"An historical perspective on lignan biosynthesis: monolignol, allylphenol and hydroxycinnamic acid coupling and downstream metabolism," *Phytochemistry Reviews*, vol. 2, no. 3, pp. 257-288.

[80] L. Bavaresco, C. Fregoni, E. Cantu and M. Trevisan, '"Stilbene compounds: from the grapevine to wine," *Drugs Exp.Clin.Res.*, vol. 25, no. 2-3, pp. 57-63.

[81] X. Vitrac, A. Bornet, R. Vanderlinde, J. Valls, T. Richard, J. Delaunay, J. Mérillon and P. Teissédre, '"Determination of stilbenes (δ-viniferin, trans-astringin, trans-piceid, cis-and trans-resveratrol, ε-viniferin) in Brazilian wines," *J.Agric.Food Chem.*, vol. 53, no. 14, pp. 5664-5669.

[82] M. Zhu, X. Zheng, Q. Shu, H. Li, P. Zhong, H. Zhang, Y. Xu, L. Wang and L. Wang, '"Relationship between the composition of flavonoids and flower colors variation in tropical water lily (Nymphaea) cultivars," *PloS one*, vol. 7, no. 4, pp. e34335.

[83] F. Karamat, A. Olry, S. Doerper, G. Vialart, P. Ullmann, D. Werck-Reichhart, F. Bourgaud and A. Hehn, '"CYP98A22, a phenolic ester 3'-hydroxylase specialized in the synthesis of chlorogenic acid, as a new tool for enhancing the furanocoumarin concentration in Ruta graveolens," *BMC Plant.Biol.*, vol. 12, Aug 29, pp. 152-2229-12-152.

[84] D. Treutter, '"Biosynthesis of phenolic compounds and its regulation in apple," *Plant Growth Regulation*, vol. 34, no. 1, pp. 71-89.

[85] N. Sakakibara, T. Nakatsubo, S. Suzuki, D. Shibata, M. Shimada and T. Umezawa, '"Metabolic analysis of the cinnamate/monolignol pathway in Carthamus tinctorius seeds by a stable-isotope-dilution method," *Organic & biomolecular chemistry*, vol. 5, no. 5, pp. 802-815.

[86] C.D. Stalikas, '"Extraction, separation, and detection methods for phenolic acids and flavonoids," *Journal of separation science*, vol. 30, no. 18, pp. 3268-3295.

[87] T. Kind and O. Fiehn, '"Advances in structure elucidation of small molecules using mass spectrometry," *Bioanalytical reviews*, vol. 2, no. 1-4, pp. 23-60.

[88] T. Kind and O. Fiehn, '"Seven golden rules for heuristic filtering of molecular formulas obtained by accurate mass spectrometry," *BMC Bioinformatics*, vol. 8, no. 1, pp. 1.

[89] M. Wink, '"Evolution of secondary metabolites from an ecological and molecular phylogenetic perspective," *Phytochemistry*, vol. 64, no. 1, pp. 3-19.

[90] R. Hegnauer, '"Phytochemistry and plant taxonomy—An essay on the chemotaxonomy of higher plants," *Phytochemistry*, vol. 25, no. 7, pp. 1519-1535.

[91] S. Ceunen and J.M. Geuns, '"Steviol glycosides: chemical diversity, metabolism, and function," *J.Nat.Prod.*, vol. 76, no. 6, pp. 1201-1228.

[92] R. Jaiswal, M.A. Patras, P.J. Eravuchira and N. Kuhnert, '"Profile and characterization of the chlorogenic acids in green Robusta coffee beans by LC-MS n: Identification of seven new classes of compounds," *J.Agric.Food Chem.*, vol. 58, no. 15, pp. 8722-8737.

[93] R. Jaiswal and N. Kuhnert, '"Identification and characterization of the phenolic glycosides of Lagenaria siceraria Stand.(bottle gourd) fruit by liquid chromatography–tandem mass spectrometry," *J.Agric.Food Chem.*, vol. 62, no. 6, pp. 1261-1271.

[94] J. Xia, N. Psychogios, N. Young and D.S. Wishart, '"MetaboAnalyst: a web server for metabolomic data analysis and interpretation," *Nucleic Acids Res.*, vol. 37, no. Web Server issue, Jul, pp. W652-60.

[95] J. Xia, R. Mandal, I.V. Sinelnikov, D. Broadhurst and D.S. Wishart, '"MetaboAnalyst 2.0--a comprehensive server for metabolomic data analysis," *Nucleic Acids Res.*, vol. 40, no. Web Server issue, Jul, pp. W127-33.

[96] J. Xia, I.V. Sinelnikov, B. Han and D.S. Wishart, '"MetaboAnalyst 3.0--making metabolomics more meaningful," *Nucleic Acids Res.*, vol. 43, no. W1, Jul 1, pp. W251-7.

[97] L. Gu, M.A. Kelm, J.F. Hammerstone, Z. Zhang, G. Beecher, J. Holden, D. Haytowitz and R.L. Prior, '"Liquid chromatographic/electrospray ionization mass spectrometric studies of proanthocyanidins in foods," *Journal of Mass Spectrometry*, vol. 38, no. 12, pp. 1272-1280.

[98] R. Jaiswal, S. Deshpande and N. Kuhnert, '"Profiling the chlorogenic acids of Rudbeckia hirta, Helianthus tuberosus, Carlina acaulis and Symphyotrichum novae-angliae leaves by LC-MSn," *Phytochem.Anal.*, vol. 22, no. 5, SEP-OCT, pp. 432-441.

[99] M.F. Matei, R. Jaiswal and N. Kuhnert, '"Investigating the Chemical Changes of Chlorogenic Acids during Coffee Brewing: Conjugate Addition of Water to the Olefinic Moiety of Chlorogenic Acids and Their Quinides," *J.Agric.Food Chem.*, vol. 60, no. 49, 12/12, pp. 12105-12115.

[100] B. Hauck, J.A. Gallagher, S.M. Morris, D. Leemans and A.L. Winters, '"Soluble Phenolic Compounds in Fresh and Ensiled Orchard Grass (Dactylis glomerata L.), a Common Species in

Permanent Pastures with Potential as a Biomass Feedstock," *J.Agric.Food Chem.*, vol. 62, no. 2, 01/15, pp. 468-475.

[101] A.M.D. El-Mousallamy, U.W. Hawas and S.A.M. Hussein, "'Teucrol, a decarboxyrosmarinic acid and its 4′-O-triglycoside, teucroside from Teucrium pilosum," *Phytochemistry*, vol. 55, no. 8, 12, pp. 927-931.

[102] R. Jaiswal, H. Karakose, S. Ruhmann, K. Goldner, M. Neumuller, D. Treutter and N. Kuhnert, "'Identification of phenolic compounds in plum fruits (Prunus salicina L. and Prunus domestica L.) by high-performance liquid chromatography/tandem mass spectrometry and characterization of varieties by quantitative phenolic fingerprints," *J.Agric.Food Chem.*, vol. 61, no. 49, Dec 11, pp. 12020-12031.

[103] T. Miyase, M. Ishino, C. Akahori, A. Ueno, Y. Ohkawa and H. Tanizawa, "'Phenylethanoid glycosides from Plantago asiatica," *Phytochemistry*, vol. 30, no. 6, pp. 2015-2018.

[104] H. Sun, M. Liu, Z. Lin, H. Jiang, Y. Niu, H. Wang and S. Chen, "'Comprehensive identification of 125 multifarious constituents in Shuang–huang–lian powder injection by HPLC-DAD-ESI-IT-TOF-MS," *J.Pharm.Biomed.Anal.*, vol. 115, 11/10, pp. 86-106.

[105] K. Hashimoto, T. Yanagisawa, Y. Okui, Y. Ikeya, M. Maruno and T. Fujita, "'Studies on anti-allergic components in the roots of Asiasarum sieboldi," *Planta Med.*, vol. 60, no. 2, Apr, pp. 124-127.

[106] T. Morikawa, L.B. Wang, K. Ninomiya, S. Nakamura, H. Matsuda, O. Muraoka, L.J. Wu and M. Yoshikawa, "'Medicinal flowers. XXX. Eight new glycosides, everlastosides F-M, from the flowers of Helichrysum arenarium," *Chem.Pharm.Bull.(Tokyo)*, vol. 57, no. 8, Aug, pp. 853-859.

[107] R. Saito, K. Kuchitsu, Y. Ozeki and M. Nakayama, "'Spatiotemporal metabolic regulation of anthocyanin and related compounds during the development of marginal picotee petals in Petunia hybrida (Solanaceae)," *J.Plant Res.*, vol. 120, no. 4, Jul, pp. 563-568.

[108] C. Marmet, L. Actis-Goretta, M. Renouf and F. Giuffrida, "'Quantification of phenolic acids and their methylates, glucuronides, sulfates and lactones metabolites in human plasma by LC–MS/MS after oral ingestion of soluble coffee," *J.Pharm.Biomed.Anal.*, vol. 88, 1/25, pp. 617-625.

[109] V. Lozovaya, A. Ulanov, A. Lygin, D. Duncan and J. Widholm, "'Biochemical features of maize tissues with different capacities to regenerate plants," *Planta*, vol. 224, no. 6, Nov, pp. 1385-1399.

[110] J. de Jesús Ornelas-Paz, E.M. Yahia, N. Ramírez-Bustamante, J.D. Pérez-Martínez, M. del Pilar Escalante-Minakata, V. Ibarra-Junquera, C. Acosta-Muñiz, V. Guerrero-Prieto and E. Ochoa-Reyes, "'Physical attributes and chemical composition of organic strawberry fruit

(Fragaria x ananassa Duch, Cv. Albion) at six stages of ripening," *Food Chem.*, vol. 138, no. 1, pp. 372-381.

[111] Y. Huang, T. Tanaka, Y. Matsuo, I. Kouno, D. Li and G. Nonaka, '"Two new phenolic glucosides and an ellagitannin from the leaves of Castanopsis sclerophylla," *Phytochemistry Letters*, vol. 5, no. 1, pp. 158-161.

[112] C. Engels, D. Gräter, P. Esquivel, V.M. Jiménez, M.G. Gänzle and A. Schieber, '"Characterization of phenolic compounds in jocote (Spondias purpurea L.) peels by ultra high-performance liquid chromatography/electrospray ionization mass spectrometry," *Food Res.Int.*, vol. 46, no. 2, 5, pp. 557-562.

[113] C. Wu, H. Xu, J. Héritier and W. Andlauer, '"Determination of catechins and flavonol glycosides in Chinese tea varieties," *Food Chem.*, vol. 132, no. 1, 5/1, pp. 144-149.

[114] A. Ruiz, L. Bustamante, C. Vergara, D. von Baer, I. Hermosín-Gutierrez, L. Obando and C. Mardones, '"Hydroxycinnamic acids and flavonols in native edible berries of South Patagonia," *Food Chem.*, vol. 167, no. 0, 1/15, pp. 84-90.

[115] V. Ossipov, J. Loponen, S. Ossipova, E. Haukioja and K. Pihlaja, '"Gallotannins of birch Betula pubescens leaves: HLPC separation and quantification," *Biochem.Syst.Ecol.*, vol. 25, no. 6, pp. 493-504.

[116] N. Kasajima, H. Ito, T. Hatano, T. Yoshida and M. Kaneda, '"Cypellogins A, B and C, acylated flavonol glycosides from Eucalyptus cypellocarpa," *Chemical and pharmaceutical bulletin*, vol. 53, no. 10, pp. 1345-1347.

[117] P. Migas and M. Krauze-Baranowska, '"The significance of arbutin and its derivatives in therapy and cosmetics," *Phytochemistry Letters*, vol. 13, pp. 35-40.

[118] S. Lee, M. Jun, J. Choi, E. Yang, J. Hur, K. Bae, Y. Seong, T. Huh and K. Song, '"Plant phenolics as prolyl endopeptidase inhibitors," *Arch.Pharm.Res.*, vol. 30, no. 7, pp. 827-833.

[119] Z. Liang, T. Sham, G. Yang, L. Yi, H. Chen and Z. Zhao, '"Profiling of secondary metabolites in tissues from Rheum palmatum L. using laser microdissection and liquid chromatography mass spectrometry," *Analytical and bioanalytical chemistry*, vol. 405, no. 12, pp. 4199-4212.

[120] G. Nonaka, H. Nishimura and I. Nishioka, '"Tannins and related compounds. IV. Seven new phenol glucoside gallates from Quercus stenophylla Makino," *Chem.Pharm.Bull.*

[121] A. González-Sarrías, T. Yuan and N.P. Seeram, '"Cytotoxicity and structure activity relationship studies of maplexins A–I, gallotannins from red maple (Acer rubrum)," *Food and chemical toxicology*, vol. 50, no. 5, pp. 1369-1376.

[122] N. Akhtar, M. Ali and M.S. Alam, "'Gallic acid esters from the stem bark of Mimusops elengi L." *Natural product research*, vol. 24, no. 10, pp. 962-972.

[123] G. Aliotta, A. Molinaro, P. Monaco, G. Pinto and L. Previtera, "'Three biologically active phenylpropanoid glucosides from Myriophyllum verticillatum," *Phytochemistry*, vol. 31, no. 1, pp. 109-111.

[124] S. Shiow-Yunn, H. Feng-Lin and L. Yu-Chan, "'Two gallates from Quercus glauca," *Phytochemistry*, vol. 31, no. 7, pp. 2465-2468.

[125] T. Yuan, C. Wan, H. Ma and N.P. Seeram, "'New phenolics from the flowers of Punica granatum and their in vitro alpha-glucosidase inhibitory activities," *Planta Med.*, vol. 79, no. 17, Nov, pp. 1674-1679.

[126] Y. Nishida, T. Ito, M. Hosokawa, M. AONO, A. YOKOMAKU, H. KONTA, K. IIMURA, T. KATO and K. SUGIYAMA, "'Repairing effects of diglucosyl gallic acid on coloring-damaged hair," *Journal of Oleo Science*, vol. 53, no. 6, pp. 295-304.

[127] S. Xiao, K. Luo, X. Wen, X. Fan and Y. Cheng, "'A pre-classification strategy for identification of compounds in traditional Chinese medicine analogous formulas by high-performance liquid chromatography–Mass spectrometry," *J.Pharm.Biomed.Anal.*, vol. 92, pp. 82-89.

[128] K. Matsuzaki, R. Ishii, K. Kobiyama and S. Kitanaka, "'New benzophenone and quercetin galloyl glycosides from Psidium guajava L." *Journal of natural medicines*, vol. 64, no. 3, pp. 252-256.

[129] Q. Wang, Z. Liang, Y. Peng, J.L. Hou, S.L. Wei, Z.Z. Zhao and W.Q. Wang, "'Whole transverse section and specific-tissue analysis of secondary metabolites in seven different grades of root of Paeonia lactiflora using laser microdissection and liquid chromatography-quadrupole/time of flight-mass spectrometry," *J.Pharm.Biomed.Anal.*, vol. 103, pp. 7-16.

[130] C. Rodríguez-Pérez, R. Quirantes-Piné, N. Amessis-Ouchemoukh, K. Madani, A. Segura-Carretero and A. Fernández-Gutierrez, "'A metabolite-profiling approach allows the identification of new compounds from Pistacia lentiscus leaves," *J.Pharm.Biomed.Anal.*, vol. 77, pp. 167-174.

[131] I.M. Abu-Reidah, D. Arraez-Roman, A. Segura-Carretero and A. Fernandez-Gutierrez, "'Profiling of phenolic and other polar constituents from hydro-methanolic extract of watermelon (Citrullus lanatus) by means of accurate-mass spectrometry (HPLC-ESI-QTOF-MS)," *Food Res.Int.*, vol. 51, no. 1, 4, pp. 354-362.

[132] I.N. Abreu, M. Ahnlund, T. Moritz and B.R. Albrectsen, "'UHPLC-ESI/TOFMS determination of salicylate-like phenolic gycosides in Populus tremula leaves," *J.Chem.Ecol.*, vol. 37, no. 8, pp. 857-870.

[133] N. Maeda, Y. Motomura, K. Yamazaki, H. Shono and R. Otsuka, '"Preparation of novel salicylic acid derivatives as keratinocyte growth stimulators." *Jpn. Kokai Tokkyo Koho*, vol. 2013-56275; 2013-56275, no. JP2014181211, 0929; Patent Application Date: 20130319.; Priority Application Date: 20130319, pp. 9.

[134] A. Vallverdu-Queralt, O. Jauregui, G. Di Lecce, C. Andres-Lacueva and R.M. Lamuela-Raventos, '"Screening of the polyphenol content of tomato-based products through accurate-mass spectrometry (HPLC–ESI-QTOF)," *Food Chem.*, vol. 129, no. 3, 12/1, pp. 877-883.

[135] A. Zhang, Q. Ye, B. Li, H. Qi and G. Zhang, '"Phenolic and Triterpene Glycosides from the Stems of Ilex l itseaefolia," *J.Nat.Prod.*, vol. 68, no. 10, pp. 1531-1535.

[136] L. Cariello, L. Zanetti and S. De Stefano, '"Posidonia ecosystem—V. Phenolic compounds from marine phanerogames, Cymodocea Nodosa and Posidonia Oceanica," *Comparative Biochemistry and Physiology Part B: Comparative Biochemistry*, vol. 62, no. 2, pp. 159-161.

[137] E. OKUYAMA, S. FUJIMORI, M. YAMAZAKI and T. DEYAMA, '"Pharmacologically Active Components of Viticis Fructus (Vitex rotundifolia). Part 2. The Components Having Analgesic Effects." *ChemInform*, vol. 29, no. 40.

[138] I. Cesari, E.F. Queiroz, Q. Favre-Godal, L. Marcourt, G. Caccialanza, P.F. Moundipa, G. Brusotti and J. Wolfender, '"Extensive phytochemical investigation of the polar constituents of Diospyros bipindensis Gürke traditionally used by Baka pygmies," *Phytochemistry*, vol. 96, pp. 279-287.

[139] S. Katayama, F. Ohno, Y. Yamauchi, M. Kato, H. Makabe and S. Nakamura, '"Enzymatic synthesis of novel phenol acid rutinosides using rutinase and their antiviral activity in vitro," *J.Agric.Food Chem.*, vol. 61, no. 40, pp. 9617-9622.

[140] D. Liang, Z. Hao, Y. Liu, H. Luo, Y. Wang, C. Zhang, Q. Zhang, R. Chen and D. Yu, '"Bioactive carboxylic acids from Lysimachia clethroides," *J.Asian Nat.Prod.Res.*, vol. 15, no. 1, pp. 59-66.

[141] T. Wu, Y. Chan and Y. Leu, '"The constituents of the root and stem of Aristolochia heterophylla Hemsl." *Chemical and pharmaceutical bulletin*, vol. 48, no. 3, pp. 357-361.

[142] K. Takara, D. Matsui, K. Wada, T. ICHIBA and Y. NAKASONE, '"New antioxidative phenolic glycosides isolated from Kokuto non-centrifuged cane sugar," *Biosci.Biotechnol.Biochem.*, vol. 66, no. 1, pp. 29-35.

[143] Z. Wu, X. Chen, D. Fang, H. Qi, W. Ren and G. Zhang, '"Analysis of phenolic glycosides from Ilex litseaefolia using electrospray ionization quadrupole time-of-flight mass spectrometry," *Rapid Communications in Mass Spectrometry*, vol. 23, no. 23, pp. 3881-3885.

[144] J.S. Lee, H.J. Kim, H. Park and Y.S. Lee, '"New diarylheptanoids from the stems of Carpinus cordata," *J.Nat.Prod.*, vol. 65, no. 9, pp. 1367-1370.

[145] T. Koyagi and K. Matsuda, "'Hair sprays containing gallic acid derivatives." *Jpn. Kokai Tokkyo Koho*, vol. 2006-321026; 2006-321026, no. JP2008133224, 0612; Patent Application Date: 20061129.; Priority Application Date: 20061129, pp. 12.

[146] M. Watanabe and J. Ayugase, "'Chiral separation of catechins in buckwheat groats and the effects of phenolic compounds in mice subjected to restraint stress," *J.Agric.Food Chem.*, vol. 57, no. 14, pp. 6438-6442.

[147] C. Hsieh and S. Chang, "'Antioxidant activities and xanthine oxidase inhibitory effects of phenolic phytochemicals from Acacia confusa twigs and branches," *J.Agric.Food Chem.*, vol. 58, no. 3, pp. 1578-1583.

[148] X. Wu, J. Cheng, J. He, X. Zhang, L. Dong, X. Gong, L. Song, Y. Zheng, L. Peng and Q. Zhao, "'Benzophenone glycosides and epicatechin derivatives from Malania oleifera," *Fitoterapia*, vol. 83, no. 6, pp. 1068-1071.

[149] T. Zhao, J. He, X. Wang, B. Ma, X. Wang, L. Zhang, P. Li, N. Liu, J. Lu and X. Zhang, "'Rapid detection and characterization of major phenolic compounds in Radix Actinidia chinensis Planch by ultra-performance liquid chromatography tandem mass spectrometry," *J.Pharm.Biomed.Anal.*, vol. 98, no. 0, 9, pp. 311-320.

[150] Y. Zhu, J. Chen, X. Ji, X. Hu, T. Ling, Z. Zhang, G. Bao and X. Wan, "'Changes of major tea polyphenols and production of four new B-ring fission metabolites of catechins from post-fermented Jing-Wei Fu brick tea," *Food Chem.*, vol. 170, pp. 110-117.

[151] S. Aleksenko, "'Antioxidant activity and phenolic compounds of buckwheat and barley by the data of spectrophotometry and HPLC," *Journal of Analytical Chemistry*, vol. 68, no. 5, pp. 458-465.

[152] K.D. Park, S.G. Lee, S.U. Kim, S.H. Kim, W.S. Sun, S.J. Cho and D.H. Jeong, "'Anticancer activity of 3-O-acyl and alkyl-(−)-epicatechin derivatives," *Bioorg.Med.Chem.Lett.*, vol. 14, no. 20, pp. 5189-5192.

[153] S. Taniguchi, K. Kuroda, N. Yoshikado, K. Doi, M. Tanabe, T. Shibata, T. Yoshida and T. Hatano, "'New dimeric flavans from gambir, an extract of Uncaria gambir," *Heterocycles*, vol. 74, pp. 595-606.

[154] R.M. Facino, M. Carini, G. Aldini and L. De Angelis, "'A rapid screening by liquid chromatography/mass spectrometry and fast-atom bombardment tandem mass spectrometry of phenolic constituents with radical scavenging activity, from Krameria triandra roots," *Rapid communications in mass spectrometry*, vol. 11, no. 12, pp. 1303-1308.

[155] R. Jaiswal, M.G.E. Karar, H.A. Gadir and N. Kuhnert, "'Identification and Characterisation of Phenolics from Ixora coccinea L.(Rubiaceae) by Liquid Chromatography Multi-stage Mass Spectrometry," *Phytochem.Anal.*, vol. 25, no. 6, pp. 567-576.

[156] I.I. Rockenbach, E. Jungfer, C. Ritter, B. Santiago-Schubel, B. Thiele, R. Fett and R. Galensa, '"Characterization of flavan-3-ols in seeds of grape pomace by CE, HPLC-DAD-MSn and LC-ESI-FTICR-MS," *Food Res.Int.*, vol. 48, no. 2, 10, pp. 848-855.

[157] R. Jaiswal, M.G. Karar and N. Kuhnert, '"Identification and Characterization of Trimeric Proanthocyanidins of Two Members of the Rhododendron Genus (Ericaceae) by Liquid Chromatography Multi-Stage Mass Spectrometry," *Encyclopedia of Analytical Chemistry*.

[158] M. Biesaga and K. Pyrzynska, '"Liquid chromatography/tandem mass spectrometry studies of the phenolic compounds in honey," *J.Chromatogr.A*, vol. 1216, no. 38, Sep 18, pp. 6620-6626.

[159] O.R. Pereira, A.M. Peres, A.M.S. Silva, M.R.M. Domingues and S.M. Cardoso, '"Simultaneous characterization and quantification of phenolic compounds in Thymus x citriodorus using a validated HPLC–UV and ESI–MS combined method," *Food Res.Int.*, vol. 54, no. 2, 12, pp. 1773-1780.

[160] A. Morales-Soto, A.M. Gómez-Caravaca, P. García-Salas, A. Segura-Carretero and A. Fernández-Gutiérrez, '"High-performance liquid chromatography coupled to diode array and electrospray time-of-flight mass spectrometry detectors for a comprehensive characterization of phenolic and other polar compounds in three pepper (Capsicum annuum L.) samples," *Food Res.Int.*, vol. 51, no. 2, pp. 977-984.

[161] Y. Sudjaroen, R. Haubner, G. Würtele, W.E. Hull, G. Erben, B. Spiegelhalder, S. Changbumrung, H. Bartsch and R.W. Owen, '"Isolation and structure elucidation of phenolic antioxidants from Tamarind (Tamarindus indica L.) seeds and pericarp," *Food and Chemical Toxicology*, vol. 43, no. 11, 11, pp. 1673-1682.

[162] M.A. Farag, S.T. Sakna, N.M. El-fiky, M.M. Shabana and L.A. Wessjohann, '"Phytochemical, antioxidant and antidiabetic evaluation of eight Bauhinia L. species from Egypt using UHPLC–PDA–qTOF-MS and chemometrics," *Phytochemistry*, vol. 119, pp. 41-50.

[163] B. Wungsintaweekul, K. Umehara, T. Miyase and H. Noguchi, '"Estrogenic and anti-estrogenic compounds from the Thai medicinal plant, Smilax corbularia (Smilacaceae)," *Phytochemistry*, vol. 72, no. 6, pp. 495-502.

[164] A. Muhammad, P.S. Haddad, T. Durst and J.T. Arnason, '"Phytochemical constituents of Sarracenia purpurea L.(pitcher plant)," *Phytochemistry*, vol. 94, pp. 238-242.

[165] H. Yamashita, '"Processing agent for silver halide photographic material and processing of the material." *Jpn. Kokai Tokkyo Koho*, vol. 1997-223556; 1997-223556, no. JP11065041, 0305; Patent Application Date: 19970820.; Priority Application Date: 19970820, pp. 26.

[166] S. El Sawi, D. Moawad and S. El Alfy, '"Activity of Chorisia insignis HBK. against larynx carcinoma and chemical investigation of its polar extracts," *J Appl Sci Res*, vol. 8, no. 11, pp. 5564-5571.

[167] M.T. Barcia, P.B. Pertuzatti, S. Gómez-Alonso, H.T. Godoy and I. Hermosín-Gutiérrez, '"Phenolic composition of grape and winemaking by-products of Brazilian hybrid cultivars BRS Violeta and BRS Lorena," *Food Chem.*, vol. 159, no. 0, 9/15, pp. 95-105.

[168] L. Tian, M. Xu, D. Wang, H. Zhu, C. Yang and Y. Zhang, '"Phenolic constituents from the leaves of Syzygium forrestii Merr. and Perry," *Biochem.Syst.Ecol.*, vol. 39, no. 2, pp. 156-158.

[169] B.A. Bohm and C.K. Wilkins, '"Chemosystematic studies in the Saxifragaceae sensu lato. 8. The flavonoids of Elmera racemosa (Watson) Rydberg," *Brittonia*, vol. 30, no. 3, pp. 327-333.

[170] L.C. Lin and C.J. Chou, '"Flavonoids and phenolics from Limonium sinense," *Planta Med.*, vol. 66, no. 4, May, pp. 382-383.

[171] T. Lee, F. Qiu, G.R. Waller and C. Chou, '"Three new flavonol galloylglycosides from leaves of Acacia confusa," *J.Nat.Prod.*, vol. 63, no. 5, pp. 710-712.

[172] Y. Ma, A. Kosinska-Cagnazzo, W.L. Kerr, R. Amarowicz, R.B. Swanson and R.B. Pegg, '"Separation and characterization of phenolic compounds from dry-blanched peanut skins by liquid chromatography-electrospray ionization mass spectrometry," *Journal of Chromatography A*, vol. 1356, no. 0, 8/22, pp. 64-81.

[173] T. Fossen, Å Larsen, B.T. Kiremire and ØM. Andersen, '"Flavonoids from blue flowers of Nymphaea caerulea," *Phytochemistry*, vol. 51, no. 8, pp. 1133-1137.

[174] C. Carazzone, D. Mascherpa, G. Gazzani and A. Papetti, '"Identification of phenolic constituents in red chicory salads (Cichorium intybus) by high-performance liquid chromatography with diode array detection and electrospray ionisation tandem mass spectrometry," *Food Chem.*, vol. 138, no. 2–3, 6/1, pp. 1062-1071.

[175] D. Olennikov and N. Kashchenko, '"New isorhamnetin glycosides and other phenolic compounds from Calendula officinalis," *Chemistry of natural compounds*, vol. 49, no. 5, pp. 833-840.

[176] M.C. Bomfim-Patrício, A. Salatino, ÂB. Martins, M.L. Salatino and J.J. Wurdack, '"Flavonoids of Lavoisiera, Microlicia and Trembleya (Melastomataceae) and their taxonomic meaning," *Biochem.Syst.Ecol.*, vol. 29, no. 7, pp. 711-726.

[177] B.L. White, L.R. Howard and R.L. Prior, '"Polyphenolic composition and antioxidant capacity of extruded cranberry Pomace," *J.Agric.Food Chem.*, vol. 58, no. 7, pp. 4037-4042.

[178] E. Al-Sayed, A. Singab, N. Ayoub, O. Martiskainen, J. Sinkkonen and K. Pihlaja, '"HPLC–PDA–ESI–MS/MS profiling and chemopreventive potential of Eucalyptus gomphocephala DC," *Food Chem.*, vol. 133, no. 3, pp. 1017-1024.

[179] J. Hokkanen, S. Mattila, L. Jaakola, A.M. Pirttilä and A. Tolonen, '"Identification of phenolic compounds from lingonberry (Vaccinium vitis-idaea L.), bilberry (Vaccinium myrtillus

L.) and hybrid bilberry (Vaccinium x intermedium Ruthe L.) leaves," *J.Agric.Food Chem.*, vol. 57, no. 20, pp. 9437-9447.

[180] T. Yahagi, A. Daikonya and S. Kitanaka, "'Flavonol acylglycosides from flower of Albizia julibrissin and their inhibitory effects on lipid accumulation in 3T3-L1 cells," *Chemical and Pharmaceutical Bulletin*, vol. 60, no. 1, pp. 129-136.

[181] I.M. Abu-Reidah, M.S. Ali-Shtayeh, R.M. Jamous, D. Arráez-Román and A. Segura-Carretero, "'HPLC–DAD–ESI-MS/MS screening of bioactive components from Rhus coriaria L.(Sumac) fruits," *Food Chem.*, vol. 166, pp. 179-191.

[182] E.W.L. Chan, A.I. Gray, J.O. Igoli, S.M. Lee and J.K. Goh, "'Galloylated flavonol rhamnosides from the leaves of Calliandra tergemina with antibacterial activity against methicillin-resistant Staphylococcus aureus (MRSA)," *Phytochemistry*, vol. 107, pp. 148-154.

[183] A. Wojdyło, M. Teleszko and J. Oszmiański, "'Antioxidant property and storage stability of quince juice phenolic compounds," *Food Chem.*, vol. 152, pp. 261-270.

[184] L. Tian, Y. Zhang, C. Qu, Y. Wang and C. Yang, "'Phloroglucinol glycosides from the fresh fruits of Eucalyptus maideni," *J.Nat.Prod.*, vol. 73, no. 2, pp. 160-163.

[185] L. Pistelli, C. Noccioli, M. Martera, L. Giamperi, A. Bucchini, D. Fraternale and D. Ricci, "'Antioxidant flavonol glycosides from Dorycnium hirsutum," *Chemistry of natural compounds*, vol. 42, no. 3, pp. 281-284.

[186] M. Yoshikawa, T. Murakami, T. Ishiwada, T. Morikawa, M. Kagawa, Y. Higashi and H. Matsuda, "'New Flavonol Oligoglycosides and Polyacylated Sucroses with Inhibitory Effects on Aldose Reductase and Platelet Aggregation from the Flowers of Prunus mume 1," *J.Nat.Prod.*, vol. 65, no. 8, pp. 1151-1155.

[187] C. Zhang, J. Chen, L. Zhao, D. Zhang, M. Zhang and Z. Wang, "'Three new flavonoids from the active extract of Fallopia convolvulus," *J.Asian Nat.Prod.Res.*, vol. 13, no. 02, pp. 136-142.

[188] A. Lhuillier, N. Fabre, F. Moyano, N. Martins, C. Claparols, I. Fouraste and C. Moulis, "'Comparison of flavonoid profiles of Agauria salicifolia (Ericaceae) by liquid chromatography-UV diode array detection-electrospray ionisation mass spectrometry," *Journal of Chromatography A*, vol. 1160, no. 1-2, 8/10, pp. 13-20.

[189] Y. Chin and J. Kim, "'Three new flavonol glycosides from the aerial parts of Rodgersia podophylla," *Chemical and pharmaceutical bulletin*, vol. 54, no. 2, pp. 234-236.

[190] H. Zhou, J. Liang, D. Lv, Y. Hu, Y. Zhu, J. Si and S. Wu, "'Characterization of phenolics of Sarcandra glabra by non-targeted high-performance liquid chromatography fingerprinting and following targeted electrospray ionisation tandem mass spectrometry/time-of-flight mass spectrometry analyses," *Food Chem.*, vol. 138, no. 4, 6/15, pp. 2390-2398.

[191] S. Ruslay, F. Abas, K. Shaari, Z. Zainal, H. Sirat, D.A. Israf and N.H. Lajis, '"Characterization of the components present in the active fractions of health gingers (Curcuma xanthorrhiza and Zingiber zerumbet) by HPLC–DAD–ESIMS," *Food Chem.*, vol. 104, no. 3, pp. 1183-1191.

[192] Q. Hu, B. Zhou, J. Huang, Z. Jiang, X. Huang, L. Yang, X. Gao, G. Yang and C. Che, '"Cytotoxic oxepinochromenone and flavonoids from the flower buds of Rosa rugosa," *J.Nat.Prod.*, vol. 76, no. 10, pp. 1866-1871.

[193] F. Ferreres, A. Gil-Izquierdo, J. Vinholes, S.T. Silva, P. Valentão and P.B. Andrade, '"Bauhinia forficata Link authenticity using flavonoids profile: Relation with their biological properties," *Food Chem.*, vol. 134, no. 2, pp. 894-904.

[194] J. Oszmianski, J. Kolniak-Ostek and A. Wojdyło, '"Characterization and content of flavonol derivatives of Allium ursinum L. plant," *J.Agric.Food Chem.*, vol. 61, no. 1, pp. 176-184.

[195] N. Briz-Cid, M. Figueiredo-González, R. Rial-Otero, B. Cancho-Grande and J. Simal-Gándara, '"The measure and control of effects of botryticides on phenolic profile and color quality of red wines," *Food Control*, vol. 50, pp. 942-948.

[196] M. Mikulic-Petkovsek, A. Slatnar, F. Stampar and R. Veberic, '"HPLC–MSn identification and quantification of flavonol glycosides in 28 wild and cultivated berry species," *Food Chem.*, vol. 135, no. 4, pp. 2138-2146.

[197] M. De Rosso, L. Tonidandel, R. Larcher, G. Nicolini, A. Dalla Vedova, F. De Marchi, M. Gardiman, M. Giust and R. Flamini, '"Identification of new flavonols in hybrid grapes by combined liquid chromatography–mass spectrometry approaches," *Food Chem.*, vol. 163, no. 0, 11/15, pp. 244-251.

[198] G.J. Niemann, '"Phenolics from Larix Needles. XV. High-Performance Liquid Chromatography of L. gmelinii Flavonoids," *Zeitschrift für Naturforschung C*, vol. 35, no. 5-6, pp. 514-515.

[199] S. Granica, M.E. Czerwińska, B. Żyżyńska-Granica and A.K. Kiss, '"Antioxidant and anti-inflammatory flavonol glucuronides from Polygonum aviculare L." *Fitoterapia*, vol. 91, pp. 180-188.

[200] A. Rezk, '"From Ethnomedicine to Application: Biological Activities and Cytotoxicity of Leaf Extracts from Plants of the Genus *Rhododendron*,".

[201] A. Rezk, A. Al-Hashimi, W. John, H. Schepker, M.S. Ullrich and K. Brix, '"Assessment of cytotoxicity exerted by leaf extracts from plants of the genus Rhododendron towards epidermal keratinocytes and intestine epithelial cells," *BMC complementary and alternative medicine*, vol. 15, no. 1, pp. 1.

[202] J. Nolzen, '"Unpublished thesis,".

[203] A. Grimbs, A. Shrestha, A. Rezk, J. Nolzen, S. Grimbs, I.H. Said, H. Schepker, M. Hütt, D.C. Albach, K. Brix, N. Kuhnert and M.S. Ullrich, '"Bioactivity in Rhododendron: A systemic analysis of antimicrobial and cytotoxic activities and their phylogenetic and phytochemical origins," *In preparation*.

[204] N. Kuhnert, H. Karakoese and R. Jaiswal, '"Analysis of Chlorogenic Acids and Other Hydroxycinnamates in Food, Plants, and Pharmacokinetic Studies," *Handbook of Analysis of Active Compounds in Functional Foods*, 01/18; 2015/05, pp. 461-510.

[205] M.J. Kruger, N. Davies, K.H. Myburgh and S. Lecour, '"Proanthocyanidins, anthocyanins and cardiovascular diseases," *Food Res.Int.*, vol. 59, no. 0, 5, pp. 41-52.

[206] D.Y. Zhou, Q. Du, R.R. Li, M. Huang, Q. Zhang and G.Z. Wei, '"Grape seed proanthocyanidin extract attenuates airway inflammation and hyperresponsiveness in a murine model of asthma by downregulating inducible nitric oxide synthase," *Planta Med.*, vol. 77, no. 14, Sep, pp. 1575-1581.

[207] A. Deters, A. Dauer, E. Schnetz, M. Fartasch and A. Hensel, '"High molecular compounds (polysaccharides and proanthocyanidins) from Hamamelis virginiana bark: influence on human skin keratinocyte proliferation and differentiation and influence on irritated skin," *Phytochemistry*, vol. 58, no. 6, Nov, pp. 949-958.

[208] M.A. Dirr, '"*Manual of Woody Landscape Plants: Their Identification, Ornamental Characteristics, Culture, Propagation and Uses*,", ed. 6th, 2009.

[209] C.N. Horn, '"Distribution and Ecological Preference of Rhododendron eastmanii Kron & Creel (May-White Azalea) in South Carolina," *Castanea*, vol. 70, no. 1, Mar., pp. 1-12.

[210] D.F. Chamberlain and M. Tian-Lu, '"The distribution of Rhododendron subgenus Hymenanthes with special reference to Yunnan (W China)," *Notes RBG Edinburgh*, vol. 43, no. 1, pp. 7-13.

[211] Anonymous '"Rhododendron cinnabarinum Hook." *Indian Medicinal Plants*, 01/01, pp. 1-1.

[212] P. Nathan, E.J. Law, D.F. Murphy and B.G. MacMillan, '"A laboratory method for selection of topical antimicrobial agents to treat infected burn wounds," *Burns*, vol. 4, no. 3, 3, pp. 177-187.

[213] T. Cserhati, E. Forgacs, M.H. Morais and T. Mota, '"Liquid chromatography of natural pigments," *Biomed.Chromatogr.*, vol. 14, no. 5, Aug, pp. 281-286.

[214] A. Swiderski, P. Muras and H. Koloczek, '"Flavonoid composition in frost-resistant Rhododendron cultivars grown in Poland," *Scientia Horticulturae*, vol. 100, no. 14, 3/19, pp. 139-151.

[215] Y. Cao, Q. Chu and J. Ye, '"Chromatographic and electrophoretic methods for pharmaceutically active compounds in Rhododendron dauricum," *Journal of Chromatography B*, vol. 812, no. 12, 12/5, pp. 231-240.

[216] S. Li, J. Xiao, L. Chen, C. Hu, P. Chen, B. Xie and Z. Sun, '"Identification of A-series oligomeric procyanidins from pericarp of Litchi chinensis by FT-ICR-MS and LC-MS," *Food Chem.*, vol. 135, no. 1, 11/1, pp. 31-38.

[217] Z. He and W. Xia, '"Analysis of phenolic compounds in Chinese olive (Canarium album L.) fruit by RPHPLC-DAD-ESI-MS," *Food Chem.*, vol. 105, no. 3, pp. 1307-1311.

[218] R. Perestrelo, Y. Lu, S.A.O. Santos, A.J.D. Silvestre, C.P. Neto, J.S. Câmara and S.M. Rocha, '"Phenolic profile of Sercial and Tinta Negra Vitis vinifera L. grape skins by HPLC–DAD–ESI-MSn: Novel phenolic compounds in Vitis vinifera L. grape," *Food Chem.*, vol. 135, no. 1, 11/1, pp. 94-104.

[219] L. Torras-Claveria, O. Jáuregui, C. Codina, A.F. Tiburcio, J. Bastida and F. Viladomat, '"Analysis of phenolic compounds by high-performance liquid chromatography coupled to electrospray ionization tandem mass spectrometry in senescent and water-stressed tobacco," *Plant Science*, vol. 182, no. 0, 1, pp. 71-78.

[220] Y. Sapozhnikova, '"Development of liquid chromatography-tandem mass spectrometry method for analysis of polyphenolic compounds in liquid samples of grape juice, green tea and coffee," *Food Chem.*, vol. 150, no. 0, 5/1, pp. 87-93.

[221] Z.R. Zhang, M. Al Zaharna, M.M. Wong, S.K. Chiu and H.Y. Cheung, '"Taxifolin enhances andrographolide-induced mitotic arrest and apoptosis in human prostate cancer cells via spindle assembly checkpoint activation," *PLoS One*, vol. 8, no. 1, pp. e54577.

[222] W. Watjen, G. Michels, B. Steffan, P. Niering, Y. Chovolou, A. Kampkotter, Q.H. Tran-Thi, P. Proksch and R. Kahl, '"Low concentrations of flavonoids are protective in rat H4IIE cells whereas high concentrations cause DNA damage and apoptosis," *J.Nutr.*, vol. 135, no. 3, Mar, pp. 525-531.

21. Appendix

21.1. Phylogenetic tree and intensity of compounds

The results from the genetic studies were coupled with the results from the phytochemical studies by combining the phylogenetic tree with the intensity of compounds from the LC-TOF-MS data. Selected compounds from the five different polyphenol groups (hydroxycinnamic acid derivatives, hydroxybenzoic acid derivatives, flavan-3-ols, flavanones and flavonols) identified in the *Rhododendron* species were used. The intensity of the compounds is defined by the gradient from white (low intensity) to green (high intensity).

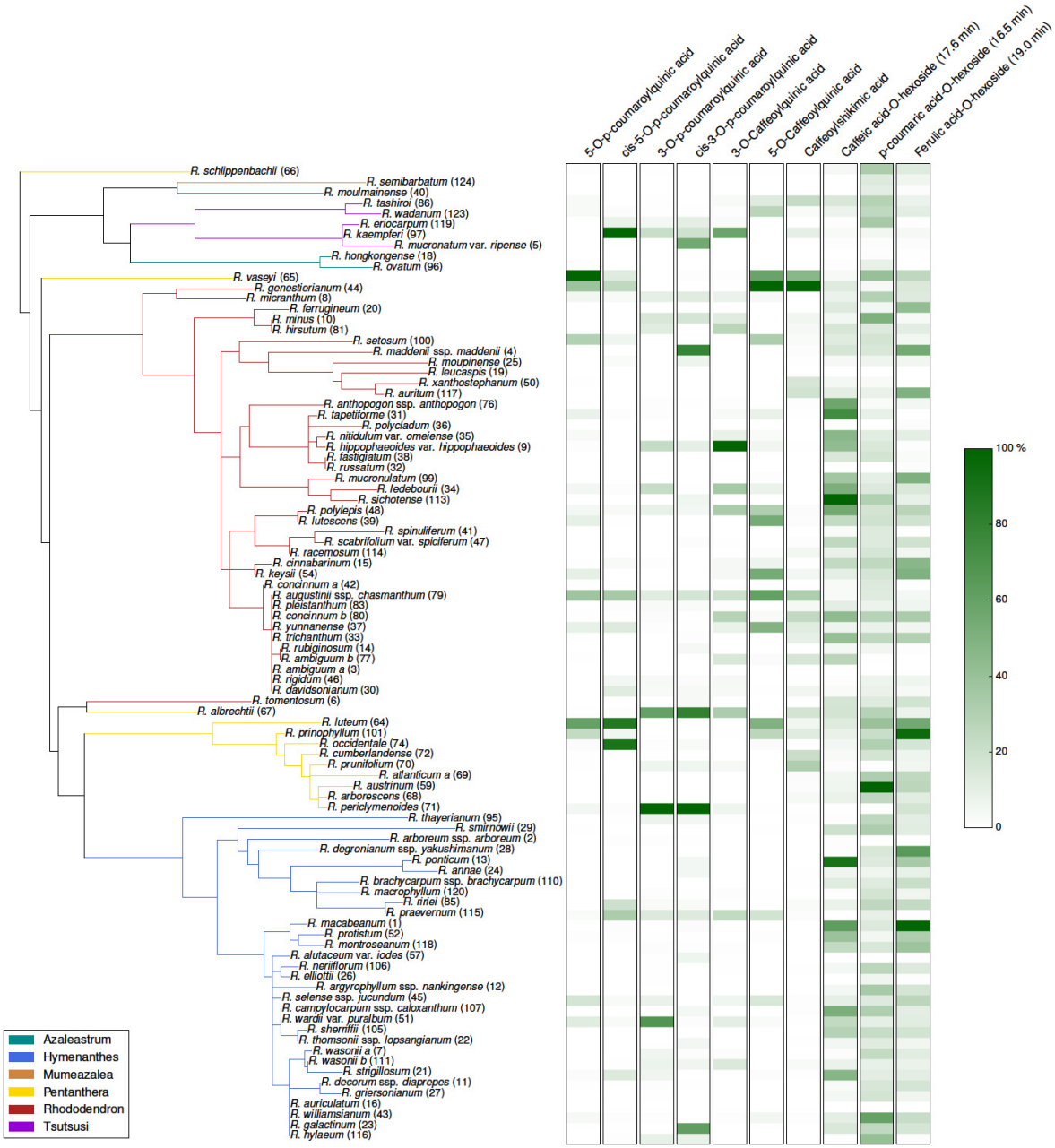

Figure 21.1: Phylogenetic tree of *Rhododendron* species and hydroxycinnamic acid derivatives

(Phylogenetic tree was obtained from Ms. J. Nolzen, University of Oldenburg)

Figure 21.2: Phylogenetic tree of *Rhododendron* species and hydroxybenzoic acid derivatives

(Phylogenetic tree was obtained from Ms. J. Nolzen, University of Oldenburg)

Figure 21.3: Phylogenetic tree of *Rhododendron* species and flavan-3-ols

(Phylogenetic tree was obtained from Ms. J. Nolzen, University of Oldenburg)

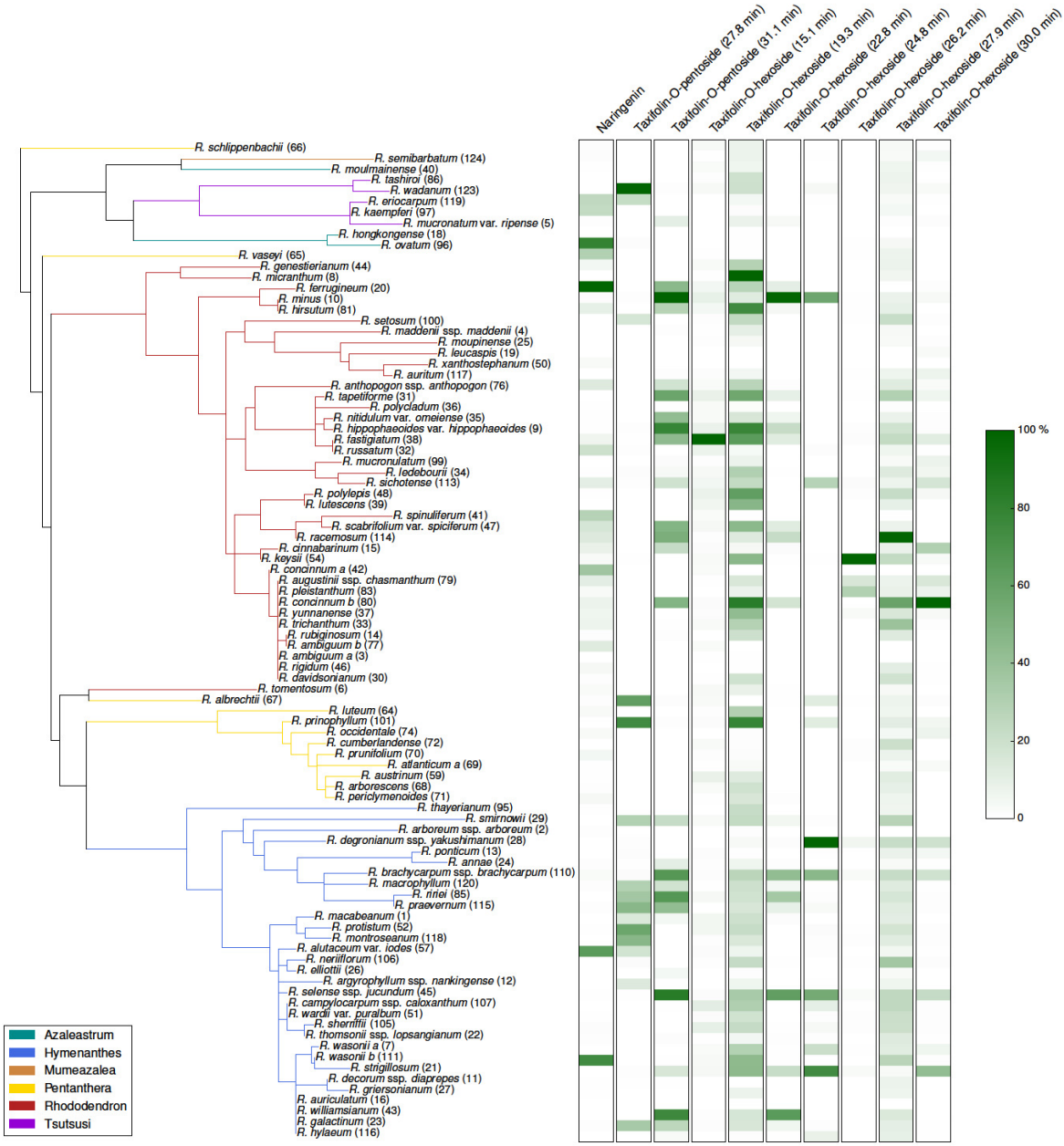

Figure 21.4: Phylogenetic tree of *Rhododendron* species and flavanones

(Phylogenetic tree was obtained from Ms. J. Nolzen, University of Oldenburg)

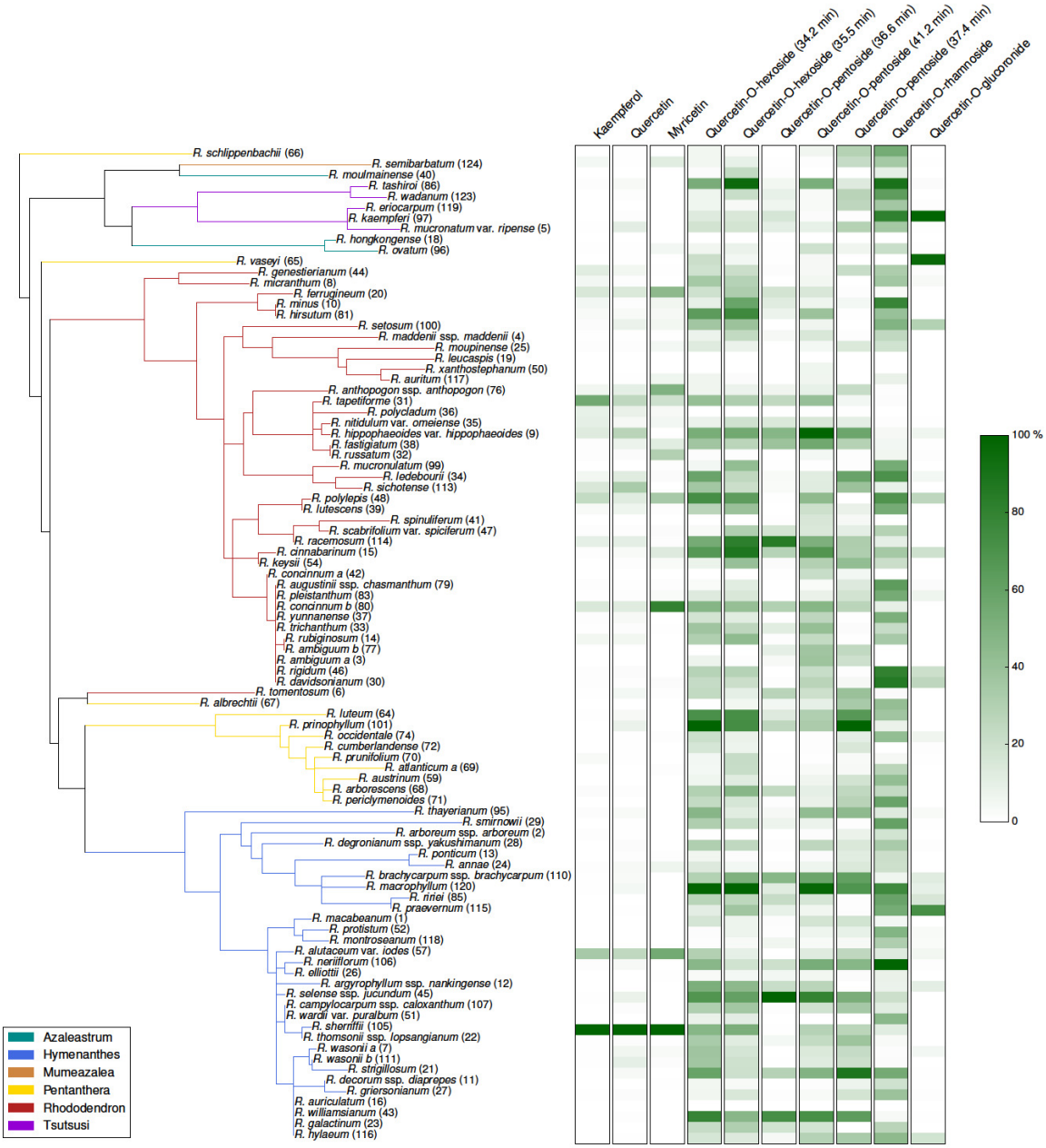

Figure 21.5: Phylogenetic tree of *Rhododendron* species and flavonols

(Phylogenetic tree was obtained from Ms. J. Nolzen, University of Oldenburg)

21.2. Standards

Authentic standards were analyzed using the LC-Ion Trap-MS in order to compare the retention time of compounds and similar fragmentation observed in other compounds found in *Rhododendron* leaves. The standards were run with the same gradient used for the *Rhododendron* samples in order to have comparable retention time. The conditions included using a diphenyl column with a binary solvent system of water (0.005% formic acid) and methanol. The standards used along with their retention time and fragmentation pattern in negative mode are shown in Table 21.1.

Table 21.1: Standards and their retention time and fragmentation pattern

Standard	**[M-H$^-$]**	**Retention Time [min]**	**Fragmentation**
Quercetin-3-*O*-galactoside	463	34.9	MS^2 → 301 (100); MS^3 → 179 (100), 271 (59), 255 (38), 151 (99); MS^4 → 151 (100)
Quercetin-3-*O*-arabinopyranoside	433	41.8	MS^2 → 301 (100); MS^3 → 271 (100), 255 (71), 179 (60), 151 (52)
Quercetin	301	43.9	MS^2 → 179 (100), 151 (99); MS^3 → 151 (100); MS^4 → 107 (100)
Rutin	609	35.0	MS^2 → 301 (100); MS^3 → 179 (100), 271 (46), 255 (24), 151 (99); MS^4 → 151 (100)
Kaempferol	285	49.9	MS^2 → 151 (100), 257 (25); MS^3 → 107 (100); MS^4 → 63 (100)
Dihydrokaempferol	287	37.1	MS^2 → 259 (100); MS^3 → 125 (100), 215 (90), 173 (53)
Robinin (Kaempferol-3-*O*-gal-rham-7-*O*-rham, Kaempferol-3-*O*-robinoside-7-*O*-rhamnoside, Kaempferol robinoside)	739	34.1	MS^2 → 593 (100); MS^3 → 285 (100); MS^4 → 255 (100), 151 (13)
Kaempferol-3-*O*-rutinoside	593	39.4	MS^2 → 285 (100); MS^3 → 257 (100); MS^4 → 255 (100)
Kaempferol-3-*O*-glucuronide	461	42.0	MS^2 → 285 (100); MS^3 → 257 (100);

			MS^4 → 255 (100)
Rebaudoside A (Steviol glycoside)	965	57.5	MS^2 → 803 (100); MS^3 → 641 (100), 479 (18), 317 (11); MS^4 → 479 (100), 317 (26)
Luteolin-7-*O*-glucoside	447	35.6	MS^2 → 285 (100); MS^3 → 241 (100), 218 (64), 199 (56), 175 (61)
Luteolin	285	47.0	MS^2 → 241 (100), 175 (28), 151 (36); MS^3 → 199 (100)
Luteolin-8-*C*-glucoside	447	29.0	MS^2 → 327 (100), 357 (42); MS^3 → 299 (100), 284 (19), 255 (3)
Resveratrol	227	38.3	MS^2 → 185 (100), 159 (46), 143 (15); MS^3 → 143 (100)
Epicatechin	289	23.6	MS^2 → 245 (100), 205 (35); MS^3 → 203 (100); MS^4 → 175 (100)
Epigallocatechin gallate	457	23.2	MS^2 → 169 (100), 331 (57), 305 (29); MS^3 → 125 (100); MS^4 → (100)
Gallocatechin	305	9.2	MS^2 → 179 (100), 219 (99); MS^3 → 164 (100), 151 (50), 135 (47)
Procyanidin B1	577	13.8	MS^2 → 425 (100), 451 (31), 407 (76), 289 (31); MS^3 → 407 (100); MS^4 → 285 (100)
Procyanidin B2	577	20.7	MS^2 → 425 (100), 451 (26), 407 (83), 289 (34); MS^3 → 407 (100); MS^4 → 285 (100)
5-CQA	353	17.5	MS^2 → 191 (100); MS^3 → 173 (100), 127 (99), 85 (89)
3, 4-diCQA	515	38.5	MS^2 → 353 (100); MS^3 → 173 (100), 191 (39); MS^4 → 93 (100)
3, 5-diCQA	515	37.2	MS^2 → 353 (100); MS^3 → 191 (100), 179 (52), 135 (7); MS^4 → 127 (100), 173 (81)
4, 5-diCQA	515	40.6	MS^2 → 353 (100); MS^3 → 173 (100), 191 (23); MS^4 → 93 (100), 111 (65)
p-Coumaric acid	163	24.8	MS^2 → 119 (100)
Gallic acid	169	4.7	MS^2 → 125 (100)
Quinic acid	191	2.1	MS^2 → 127 (100), 111 (31); MS^3 → 109 (100), 83 (50);
Malic acid	133	2.4	MS^2 → 115 (100); MS^3 → 71 (100)
Shikimic acid	173	2.5	MS^2 → 155 (100), 111 (68), 93 (62);

			MS^3 → 111 (100); MS^4 → 83 (100)
Glucuronic acid	193	2.7	MS^2 → 131 (100); MS^3 → 113 (100); MS^4 → 85 (100)
Neochlorogenic acid	353	11.9	MS^2 → 191 (100), 179 (46), 135 (11); MS^3 → 127 (100), 173 (57), 111 (52), 93 (42), 85 (73); MS^4 → 109 (100), 85 (29)
Tartaric acid	149	2.1	MS^2 → 103 (100), 131 (99), 87 (83); MS^3 → 59 (100)
Sinapic acid	223	32.0	MS^2 → 208 (100), 179 (51), 164 (41); MS^3 → 164 (100), 149 (26); MS^4 → 149 (100), 135 (24)
Ascorbic acid	175	2.5	MS^2 → 115 (100); MS^3 → 87 (100); MS^4 → 60 (100)
Trans-cinnamic acid	147	36.6	MS^2 → 103 (100), 119 (10); MS^3 → 60 (100)
2, 3-Dihydroxybenzoic acid	153	11.9	MS^2 → 109 (100)
2, 5-Dihydroxybenzoic acid	153	9.3	MS^2 → 109 (100);
Ferulic acid	193	28.9	MS^2 → 149 (100), 178 (47), 134 (43); MS^3 → 134 (100)
3, 4, 5 –Trimethoxy transcinnamic acid	237	41.9	MS^2 → 133 (100), 193 (53), 179 (19); MS^3 → 103 (100)
3-hydroxy-4-methoxy cinnamic acid	193	31.3	MS^2 → 178 (100), 149 (3), 134 (12); MS^3 → 134 (100)
Isorhamnetin rutinoside	623	41.1	MS^2 → 315 (100); MS^3 → 300 (100); MS^4 → 271 (100), 255 (59)
Caffeic acid	179	17.2	MS^2 → 135 (100)
Cryptochlorogenic acid	353	21.2	MS^2 → 173 (100), 179 (54), 191 (9); MS^3 → 93 (100), 111 (39), 71 (29)

21.3. Compound Structures

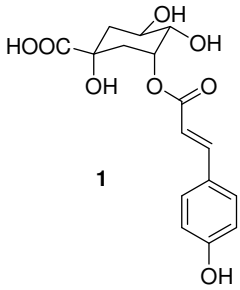

3-*O*-*p*-Coumaroylquinic acid

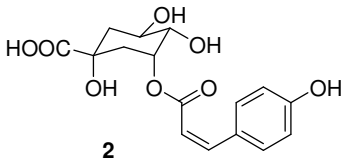

cis-3-*O*-*p*-Coumaroylquinic acid

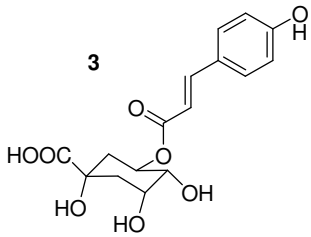

5-*O*-*p*-Coumaroylquinic acid

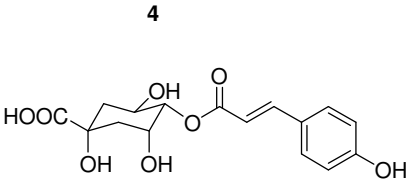

4-*O*-*p*-Coumaroylquinic acid

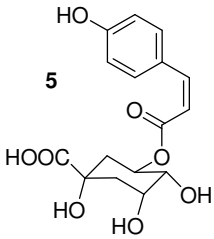

cis-5-*O*-*p*-Coumaroylquinic acid

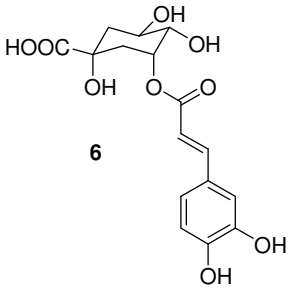

3-*O*-Caffeoylquinic acid

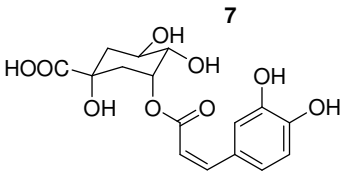

cis-3-*O*-Caffeoylquinic acid

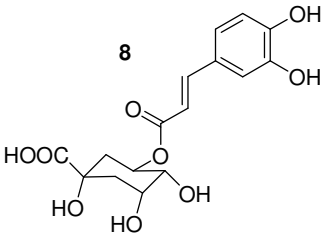

5-*O*-Caffeoylquinic acid

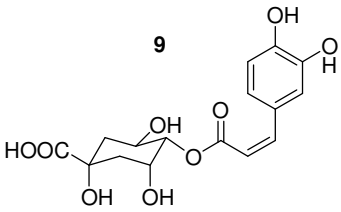

cis-4-*O*-Caffeoylquinic acid

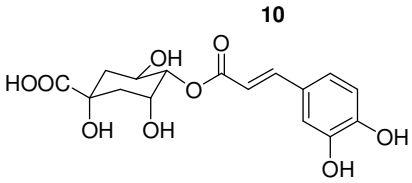

4-*O*-Caffeoylquinic acid

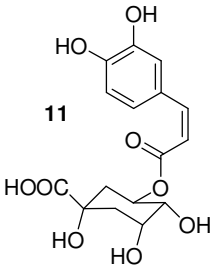

cis-5-*O*-Caffeoylquinic acid

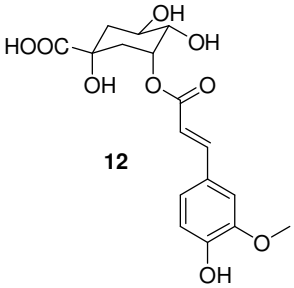

3-*O*-Feruloylquinic acid

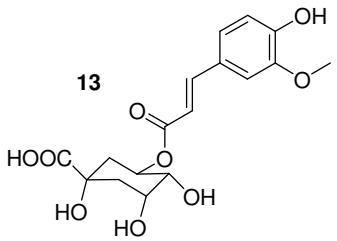

5-*O*-Feruloylquinic acid

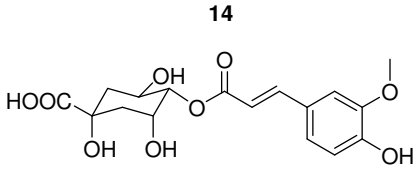

4-*O*-Feruloylquinic acid

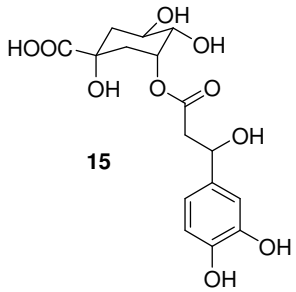

3-*O*-hydroxy-Caffeoylquinic acid

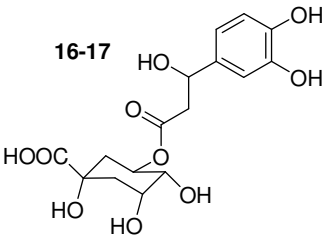

5-*O*-hydroxy-Caffeoylquinic acid

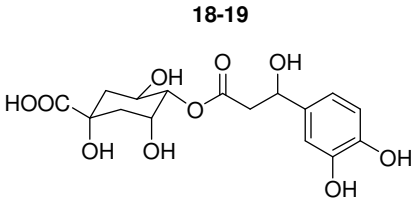

4-*O*-hydroxy-Caffeoylquinic acid

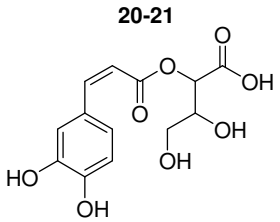

Caffeoylthreonate

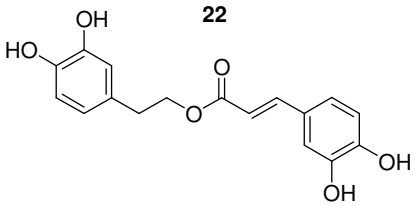

Teucrol

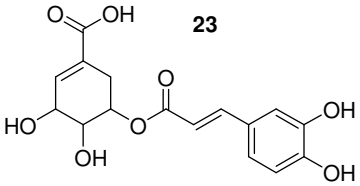

Caffeoylshikimic acid

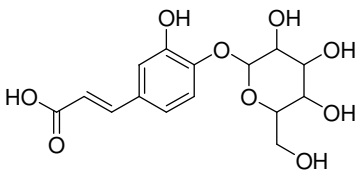

Caffeic acid-*O*-hexoside

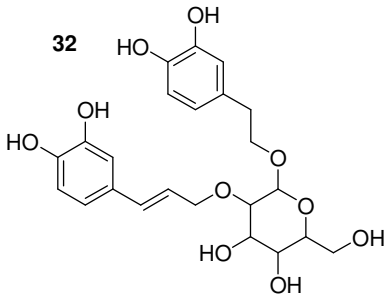

Plantainoside

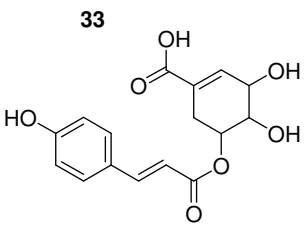

p-Coumaric acid-*O*-shikimate

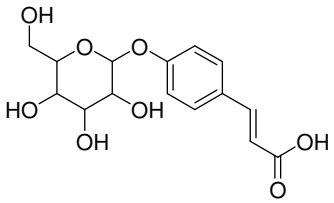

p-Coumaric acid-*O*-hexoside

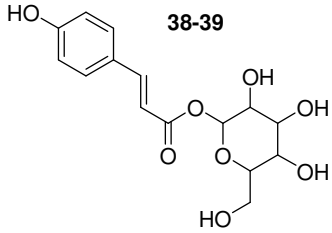

p-Coumaric acid-*O*-glucosyl ester

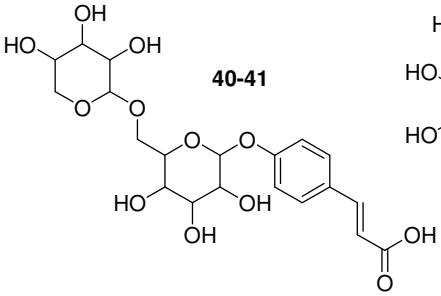

p-Coumaric acid-*O*-hexoside-*O*-pentoside

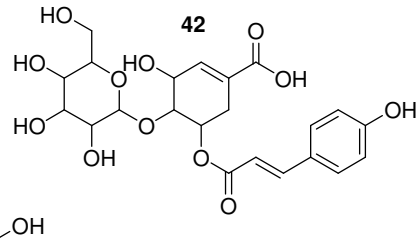

Everlastoside M

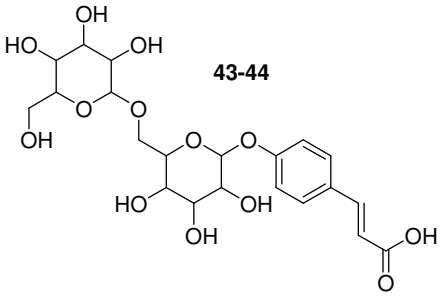

p-Coumaric acid-*O*-dihexoside

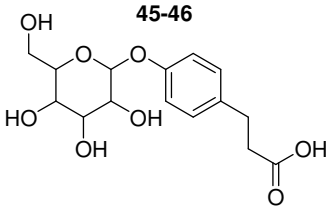

Dihydrocoumaric acid-*O*-hexoside

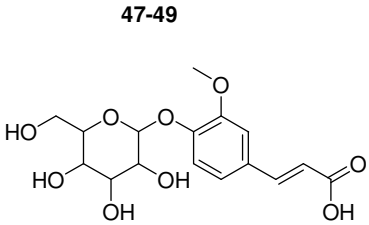

Ferulic acid-*O*-hexoside

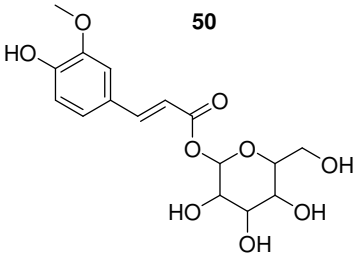

Ferulic acid-*O*-glucosyl ester

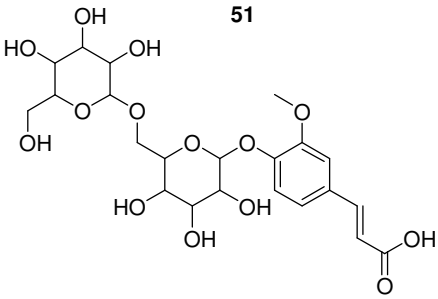

Ferulic acid-*O*-dihexoside

52

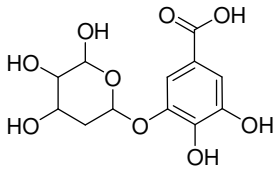

Gallic acid-*O*-pentoside

53-54

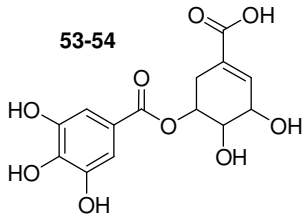

Galloylshikimic acid

55-56

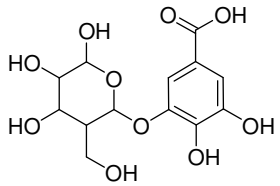

Gallic acid-*O*-hexoside

57

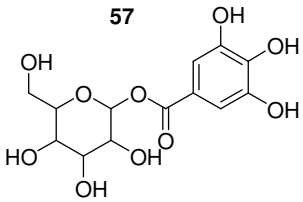

Gallic acid-*O*-glucosyl ester

58-60

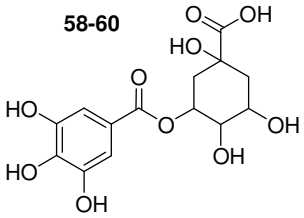

Galloylquinic acid

61

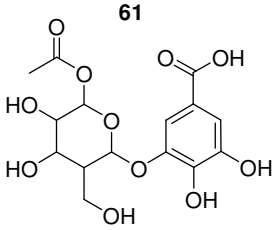

Gallic acid-*O*-acetyl-hexoside

62

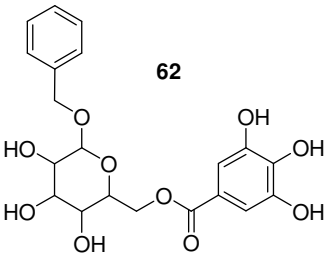

Benzyl-6'-*O*-galloyl-*ß*-*D*-hexoside

63-64

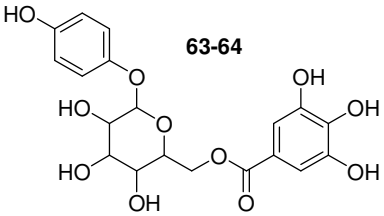

Galloylarbutin

65

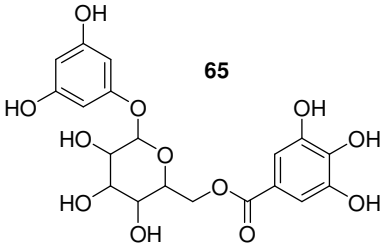

6-galloyl-1-*O*-(phloroglucinol)-hexoside

66

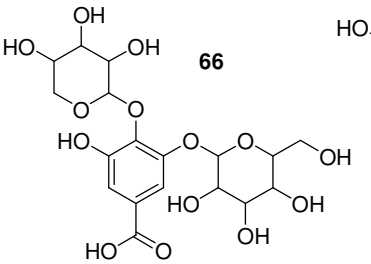

Gallic acid-3-*O*-hexoside-4-*O*-pentoside

67

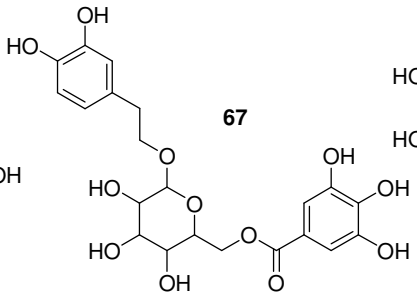

p-hydroxyphenethyl alcohol-1-*O*-*ß*-*D*-(6"-*O*-galloyl)-hexoside

68

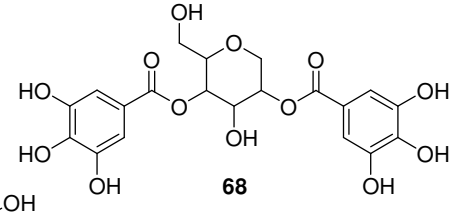

Gallic acid-*O*-galloyl-rhamnoside

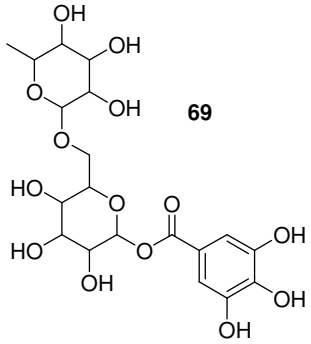

69

Gallic acid-*O*-rutinoside

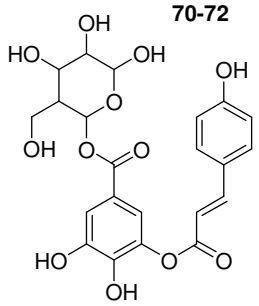

70-72

Gallic acid-*O*-coumaroyl-hexoside

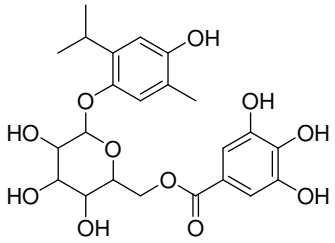

73

Querglanin

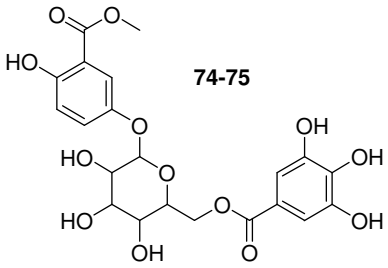

74-75

Galloyl-*O*-vanilloyl-*O*-hexoside

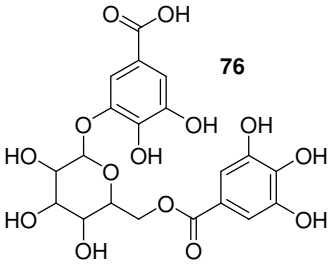

76

Gallic acid-3-*O*-(6'-*O*-galloyl)-*ß*-*D*-hexoside

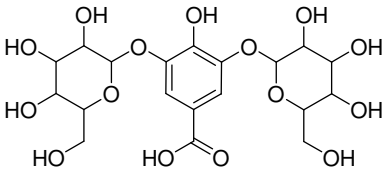

77-78

Gallic acid-*O*-dihexoside

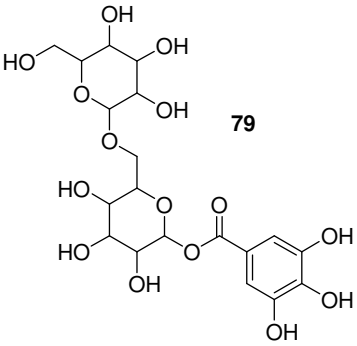

79

Gallic acid-*O*-dihexoside

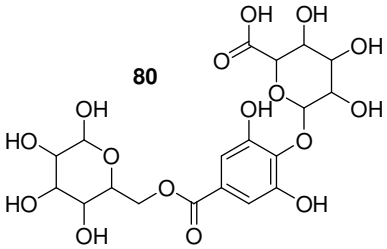

80

Gallic acid-*O*-feruloyl-hexoside

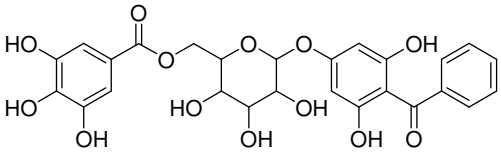

81

Guavinoside A

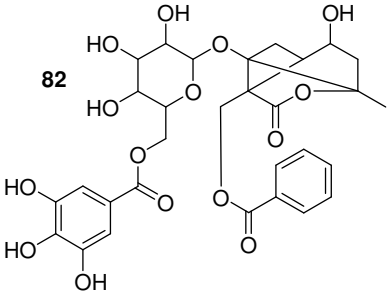

82

Galloylalbiflorin

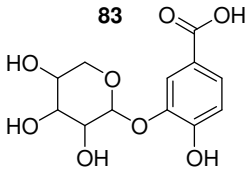

Protocatechuic acid-*O*-pentoside

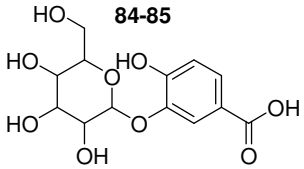

Protocatechuic acid-*O*-hexoside

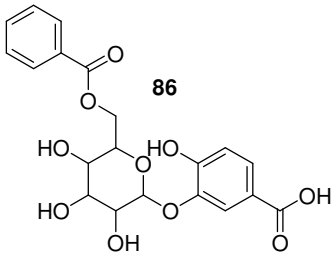

Protocatechuic acid-*O*-benzoyl-hexoside

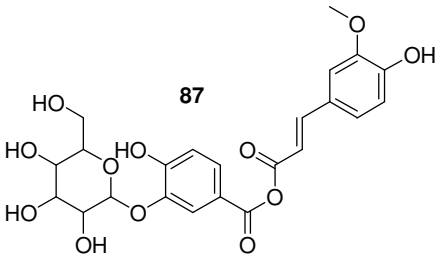

Protocatechuic acid-*O*-feruloyl-hexoside

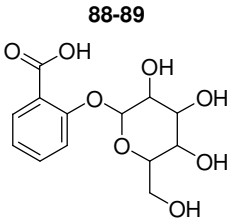

Salicylic acid-*O*-hexoside

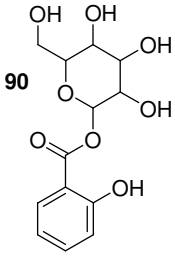

Salicylic acid-*O*-glucosyl ester

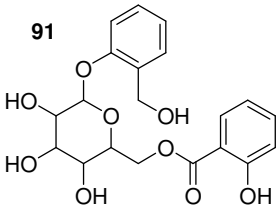

Salicyloylsalicin

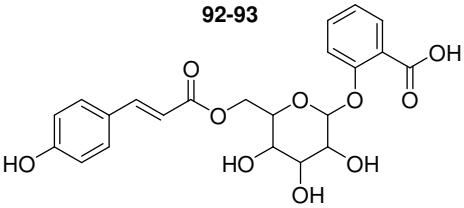

Salicylic acid-*O*-coumaroyl-hexoside

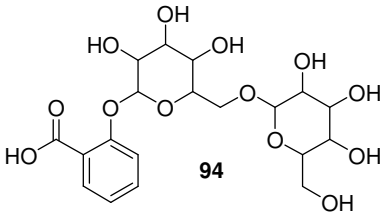

Salicylic acid-*O*-dihexoside

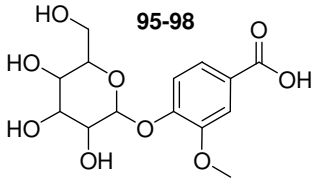

Vanillic acid-*O*-hexoside

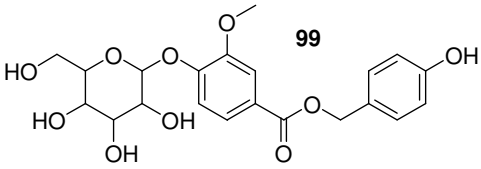

Amburoside B

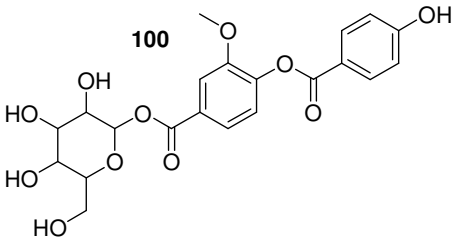

Vanilloyl-*O*-hydroxybenzoyl-hexoside

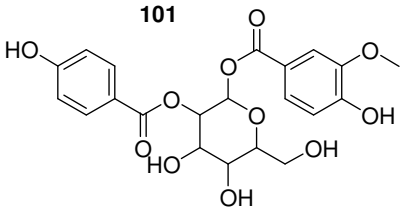

Vanilloyl-*O*-hydroxybenzoyl-hexoside

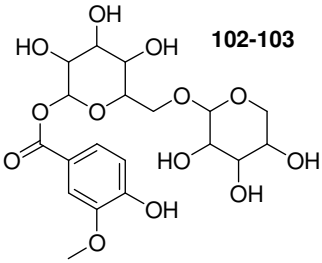

Vanillic acid-*O*-hexoside-*O*-pentoside

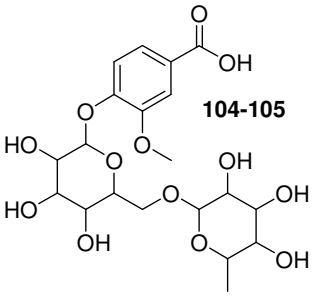

Vanillic acid-*O*-rutinoside

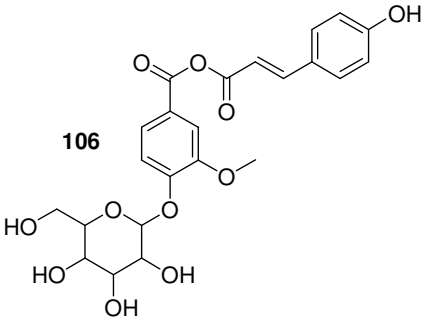

Vanillic acid-*O*-coumaroyl-hexoside

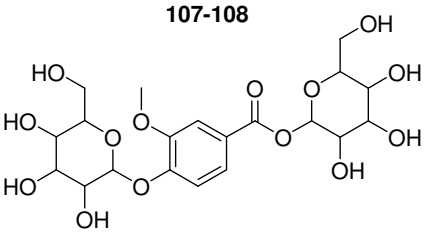

Vanillic acid-*O*-dihexoside

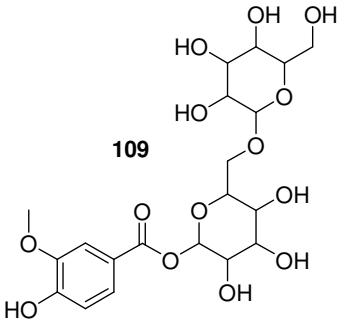

Vanillic acid-*O*-dihexoside

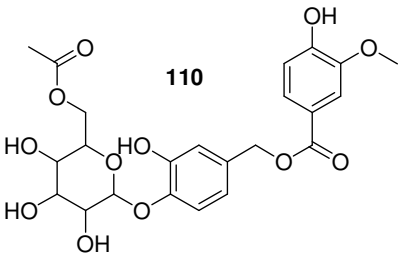

Litseaefoloside A

111-113

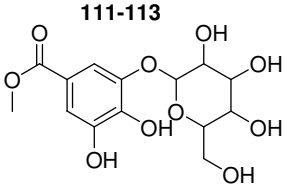

Methyl gallate-*O*-hexoside

114

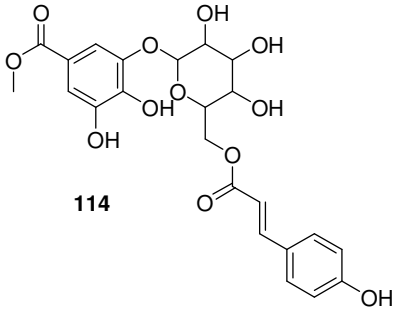

Methyl gallate-*O*-coumaroyl-hexoside

115

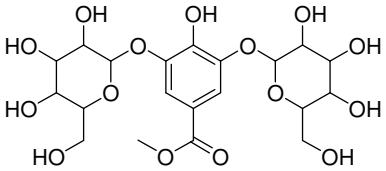

Methyl gallate-*O*-dihexoside

116

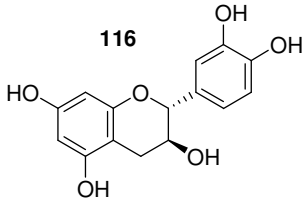

Catechin

117

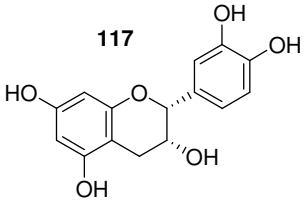

Epicatechin

118

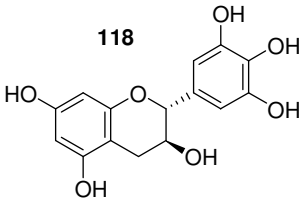

Gallocatechin

119

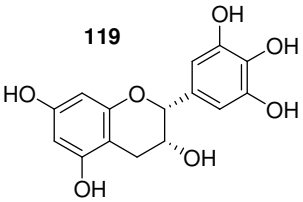

Epigallocatechin

120

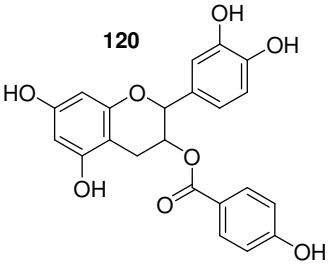

(Epi)catechin-*O*-hydroxybenzoate

121

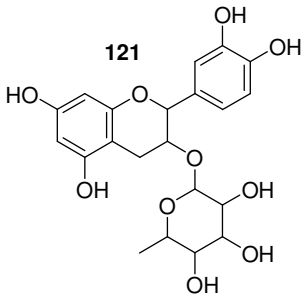

(Epi)catechin-*O*-rhamnoside

122

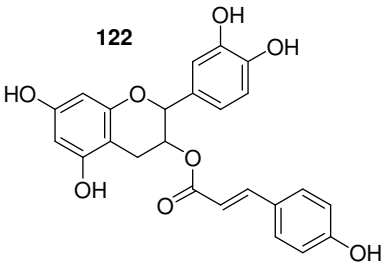

Malaferin B

123-126

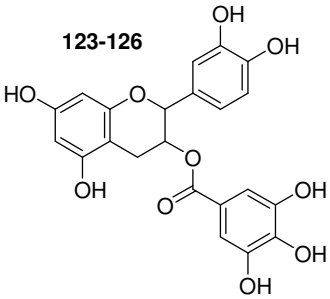

(Epi)catechin gallate

127

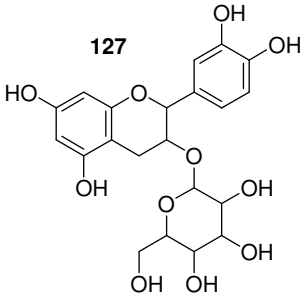

(Epi)catechin-*O*-hexoside

128

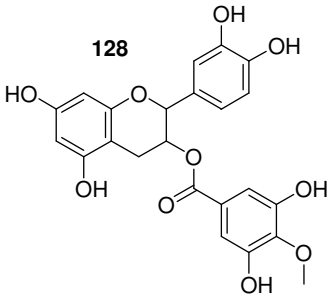

(Epi)catechin-*O*-methyl-gallate

129-131

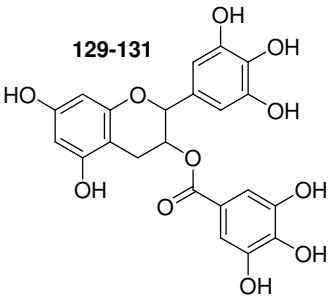

(Epi)gallocatechin gallate

132

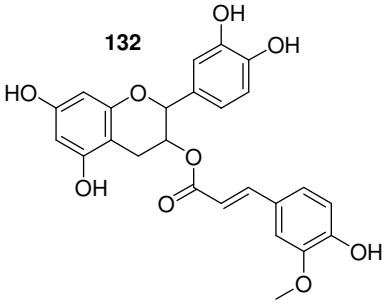

Malaferin C

133

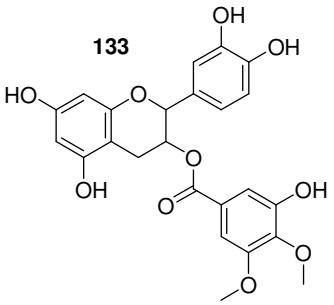

(Epi)catechin-*O*-dimethyl-gallate

134-135

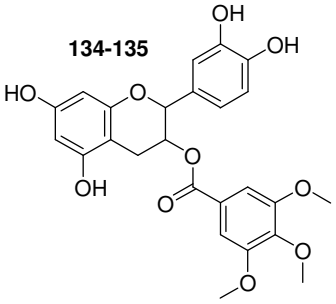

(Epi)catechin-*O*-dimethyl-gallate

136-144

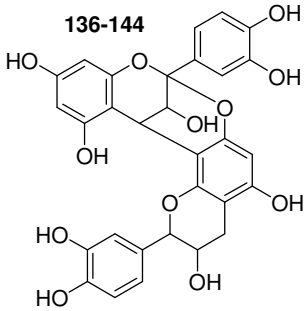

(Epi)catechin-(4,8/2,6)-(epi)catechin

145-150

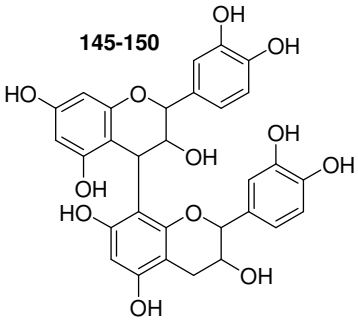

(Epi)catechin-(epi)catechin
(Procyanidin dimer B)

151

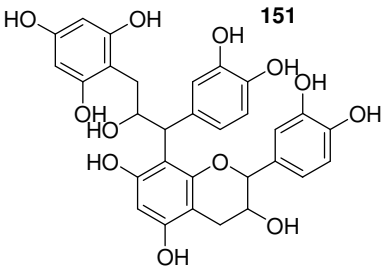

Gambiriin A

152-159

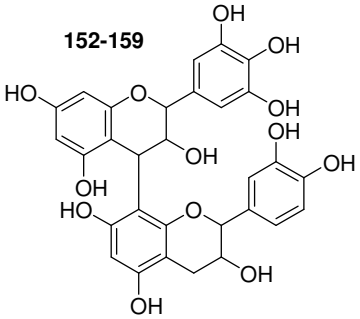

(Epi)gallocatechin-(epi)catechin

160-164

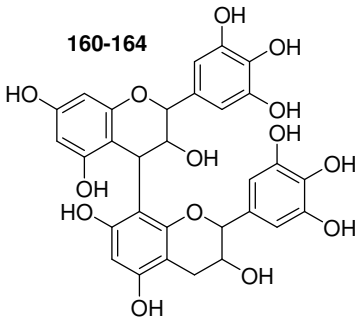

(Epi)gallocatechin-(epi)gallocatechin

165-167

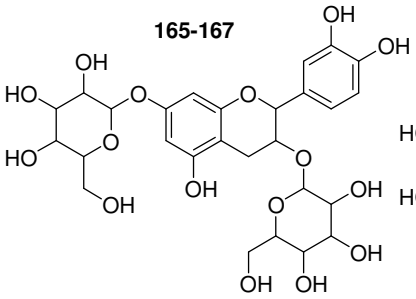

(Epi)catechin-3-*O*-hexoside-7-*O*-hexoside

168

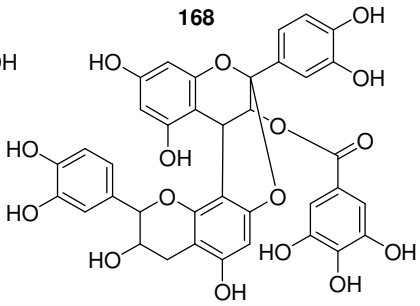

3-*O*-galloyl(epi)catechin-
(4,8/2,6)-(epi)catechin

169, 171

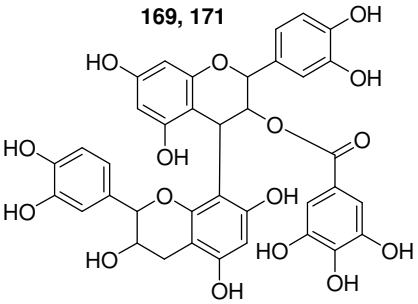

3-*O*-galloyl(epi)catechin-(4,8)-(epi)catechin

170

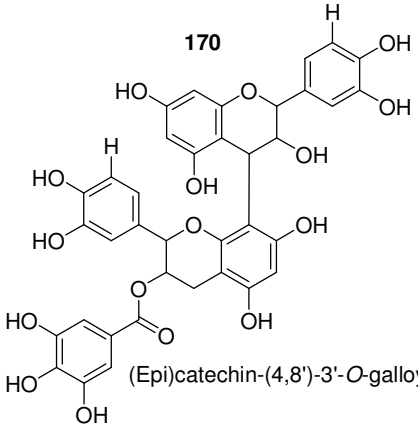

(Epi)catechin-(4,8')-3'-*O*-galloyl-(epi)catechin

172

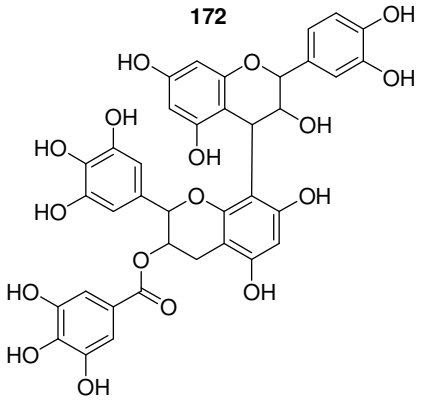

(Epi)gallocatechin-(4,8')-3'-*O*-galloyl-(epi)catechin

173-174

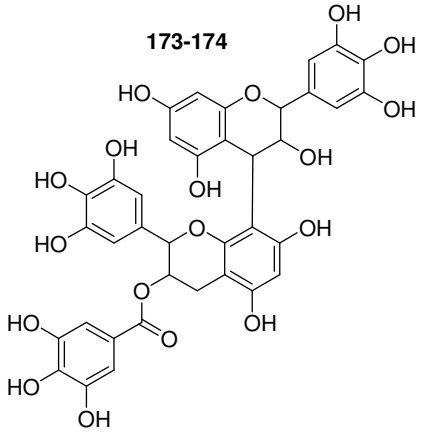

(Epi)gallotcatechin-(4,8)-3'-*O*-galloyl(epi)gallocatechin

175-176

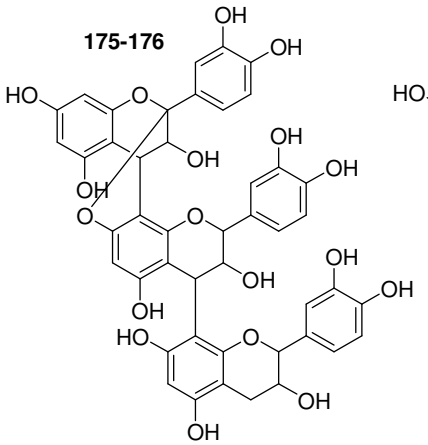

(Epi)catechin-(4,8'/2,7')-(epi)catechin-(4',8'')-(epi)catechin

177-178

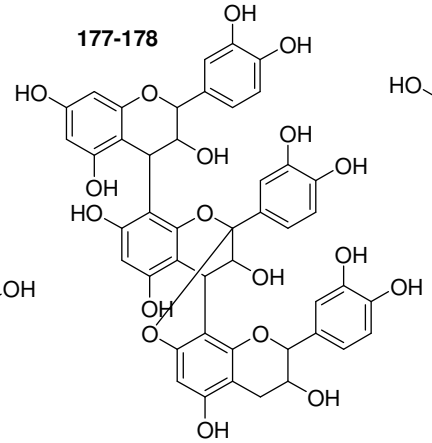

(Epi)catechin-(4',8')-(epi)catechin-(4,8''/2',7'')-(epi)catechin

179-185

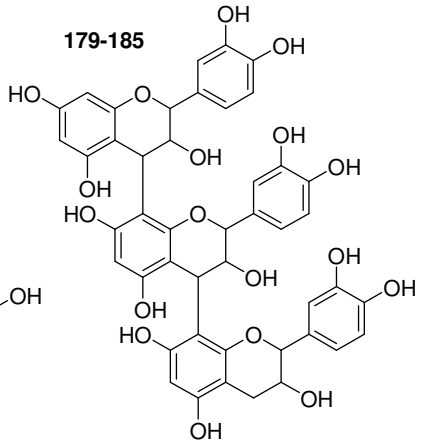

(Epi)catechin-(4,8')-(epi)catechin-(4',8'')-(epi)catechin

186, 188

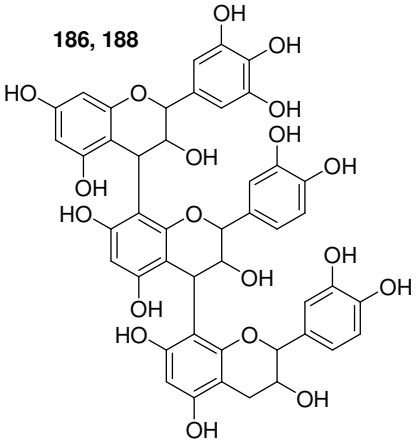

(Epi)gallocatechin-(4,8')-(epi)catechin-(4',8'')-(epi)catechin

187

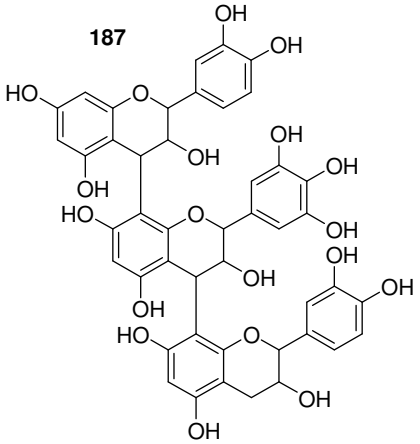

(Epi)catechin-(4,8')-(epi)gallocatechin-(4',8'')-(epi)catechin

189

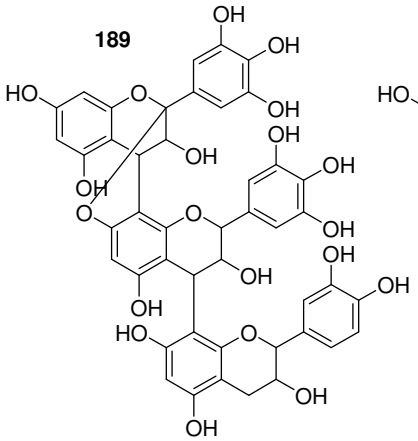

(Epi)gallocatechin-(4,8'/2,7')-(epi)gallocatechin-(4',8'')-(epi)catechin

190

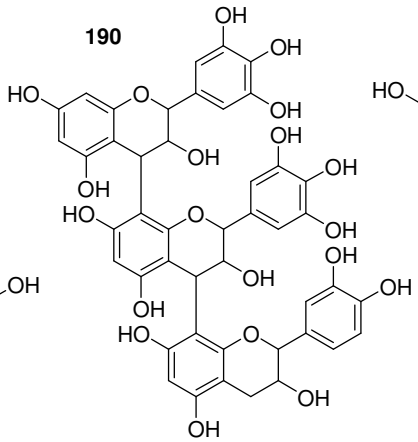

(Epi)gallocatechin-(4,8')-(epi)gallocatechin-(4',8'')-(epi)catechin

191-192

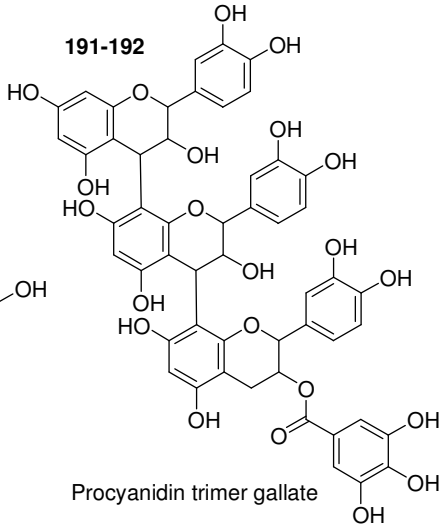

Procyanidin trimer gallate

193-196

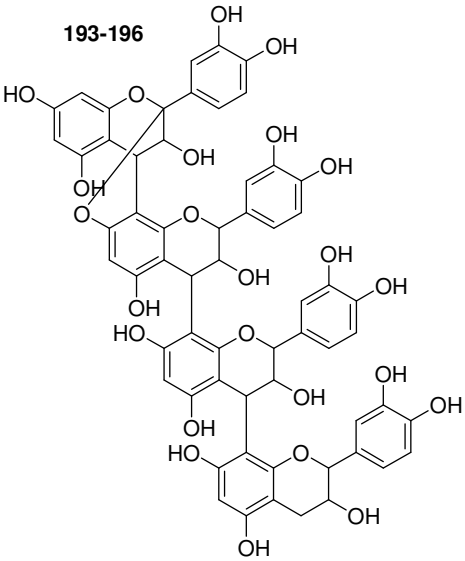

A type procyanidin tetramer

197-202

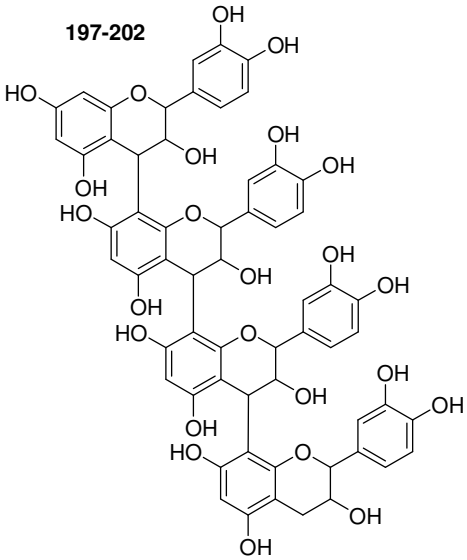

Procyanidin tetramer D

203

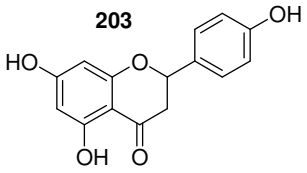

Naringenin

204

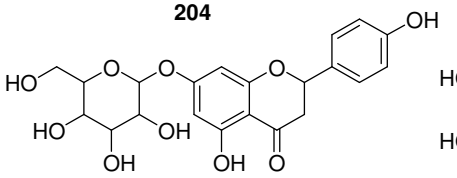

Naringenin-*O*-hexoside

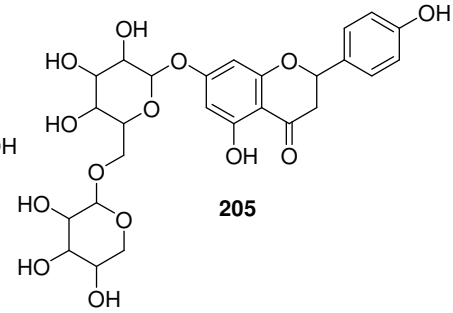

205

Naringenin-*O*-hexoside-*O*-pentoside

206

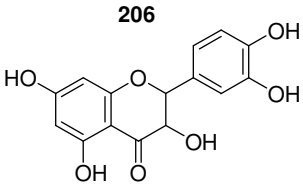

Taxifolin

207-211

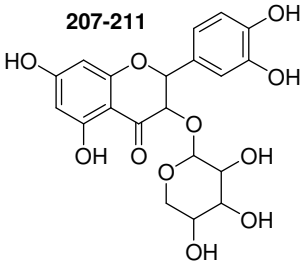

Taxifolin-*O*-pentoside

212-214

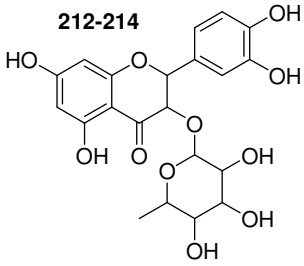

Taxifolin-*O*-rhamnoside

215-221

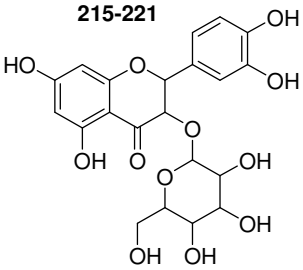

Taxifolin-*O*-hexoside

222-223

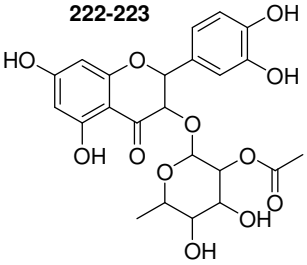

Taxifolin-*O*-acetyl-rhamnoside

224-225

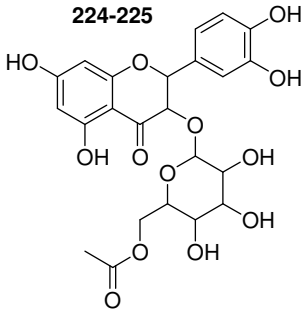

Taxifolin-*O*-acetyl-hexoside

226

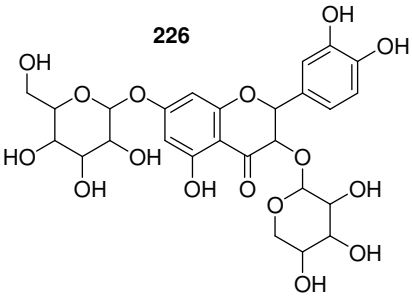

Taxifolin-*O*-pentoside-*O*-hexoside

227-228

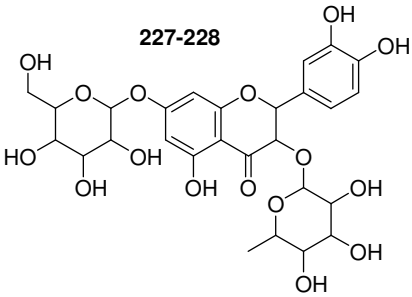

Taxifolin-*O*-rhamnoside-*O*-hexoside

229

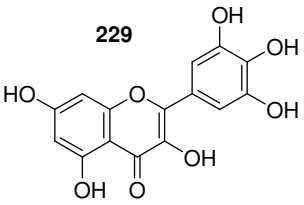

Myricetin

230-232

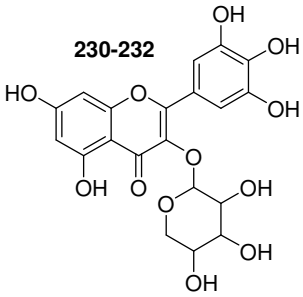

Myricetin-*O*-pentoside

233

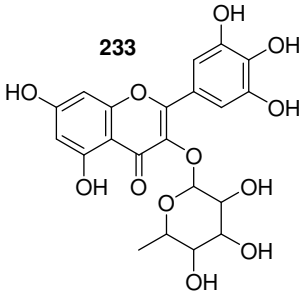

Myricetin-*O*-rhamnoside

234-236

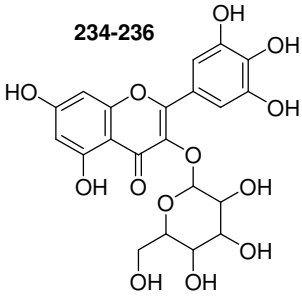

Myricetin-*O*-hexoside

237

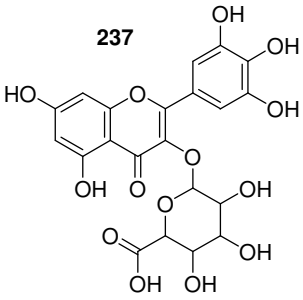

Myricetin-*O*-glucuronide

238

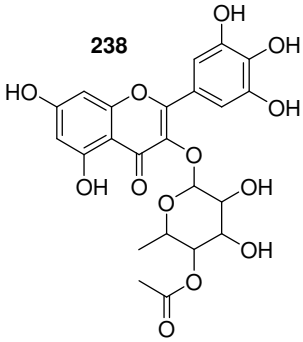

Myricetin-*O*-acetyl-rhamnoside

239

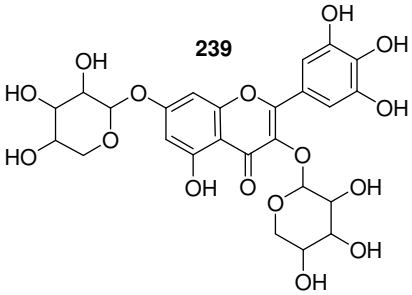

Myricetin-*O*-dipentoside

240

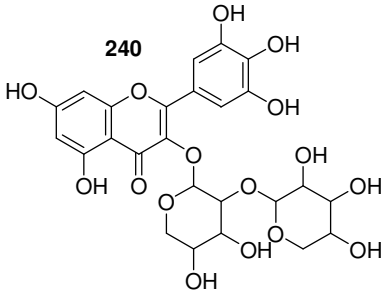

Myricetin-*O*-dipentoside

241

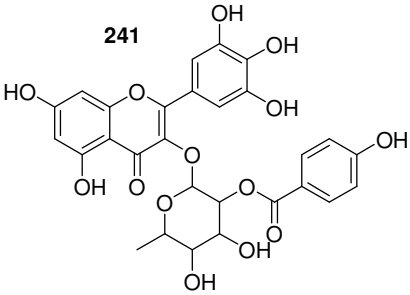

Myricetin-*O*-benzoyl-hexoside

242-243

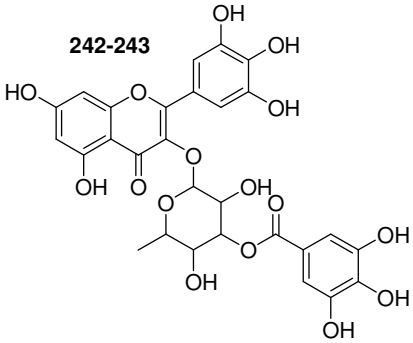

Myricetin-*O*-galloyl-rhamnoside

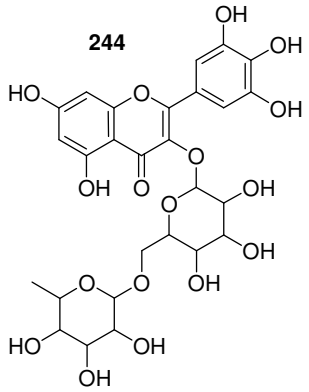

Myricetin-*O*-rutinoside

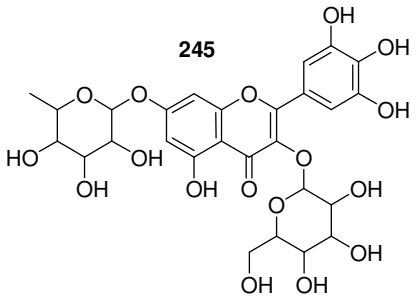

Myricetin-3-*O*-hexoside-7-*O*-rhamnoside

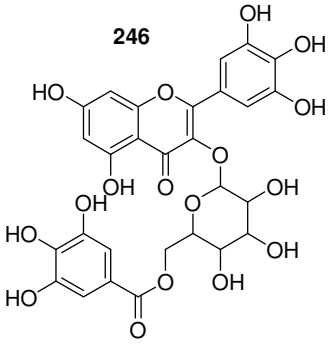

Myricetin-*O*-galloyl-hexoside

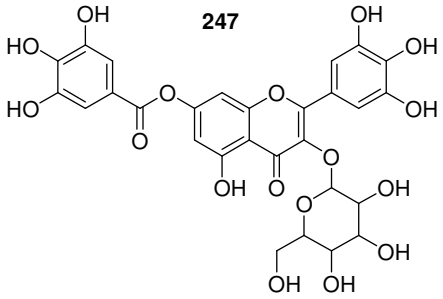

Myricetin-7-*O*-galloyl-3-*O*-hexoside

248

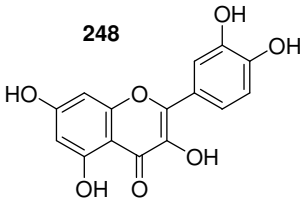

Quercetin

249-252

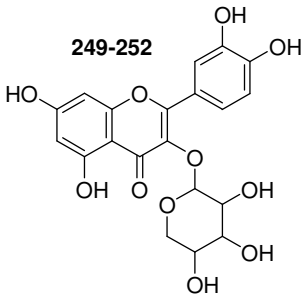

Quercetin-*O*-pentoside

253

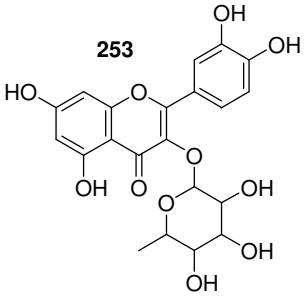

Quercetin-*O*-rhamnoside

254-256

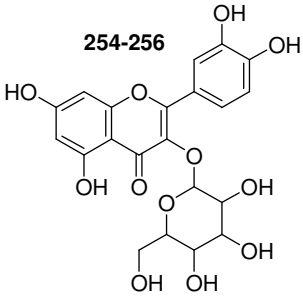

Quercetin-*O*-hexoside

257-259

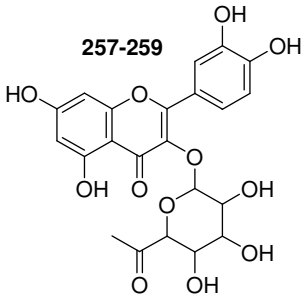

Quercetin-*O*-acetyl-pentoside

260

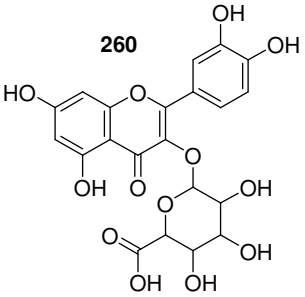

Quercetin-*O*-glucuronide

261-263

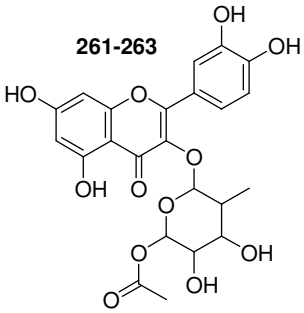

Quercetin-*O*-acetyl-rhamnoside

264-271

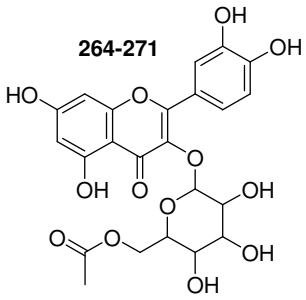

Quercetin-*O*-acetyl-hexoside

272

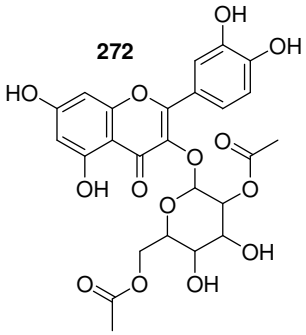

Quercetin-*O*-diacetyl-hexoside

273-274

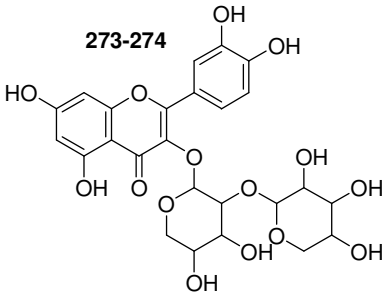

Quercetin-*O*-dipentoside

275

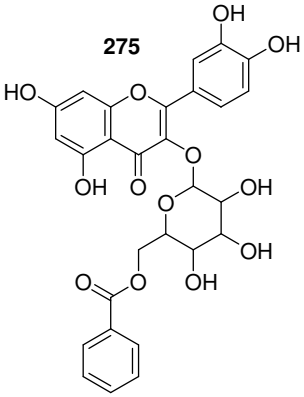

Quercetin-*O*-benzoyl-hexoside

276

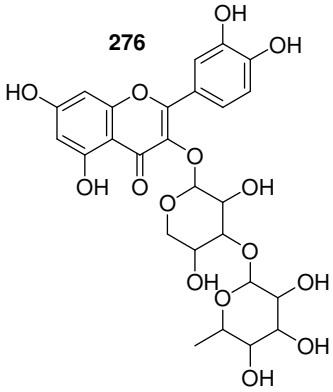

Quercetin-*O*-pentoside-*O*-rhamnoside

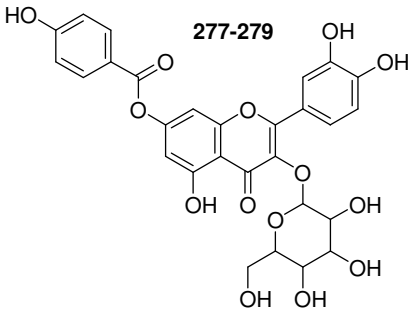

Quercetin-*O*-(*p*-hydroxy)-benzoyl-hexoside

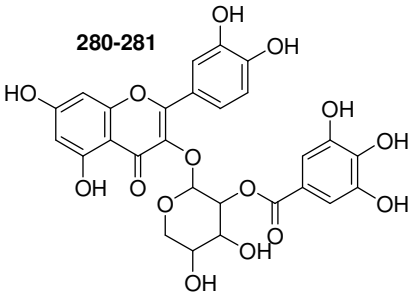

Quercetin-*O*-galloyl-pentoside

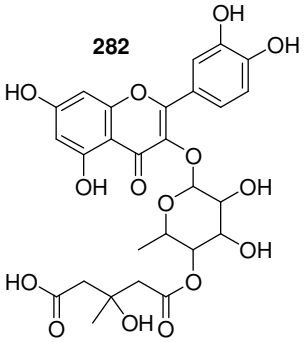

Quercetin-3-O-(4"-3-hydroxy-3-methylglutaryl)-a-rhamnoside

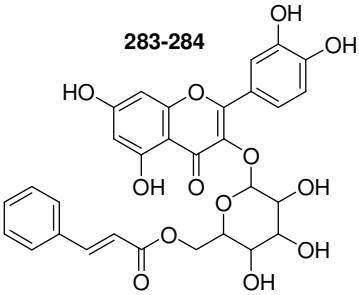

Quercetin-*O*-coumaroyl-rhamnoside

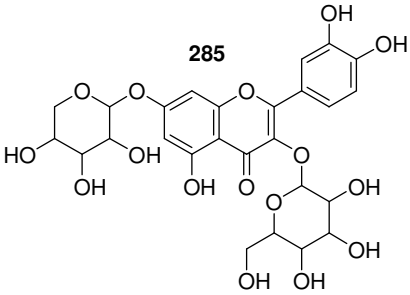

Quercetin-*O*-pentoside-*O*-hexoside

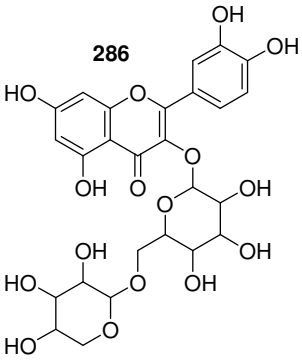

Quercetin-*O*-pentoside-*O*-hexoside

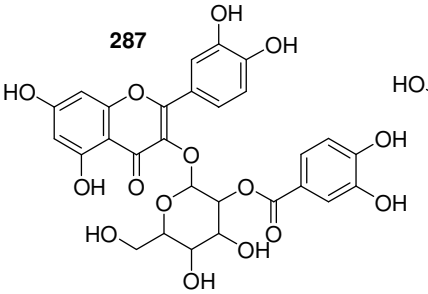

Quercetin-*O*-protocatechuoyl-hexoside

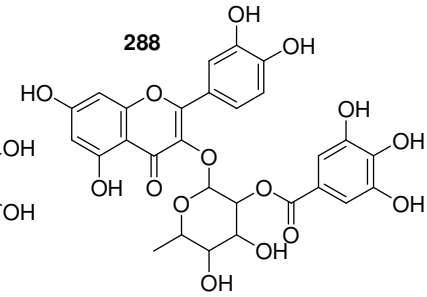

Quercetin-*O*-galloyl-rhamnoside

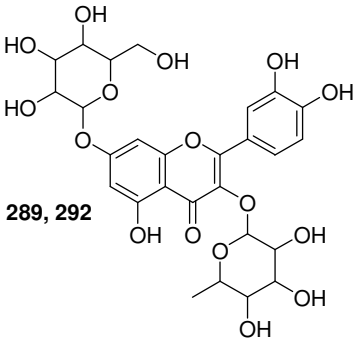

Quercetin-*O*-rhamnoside-*O*-hexoside

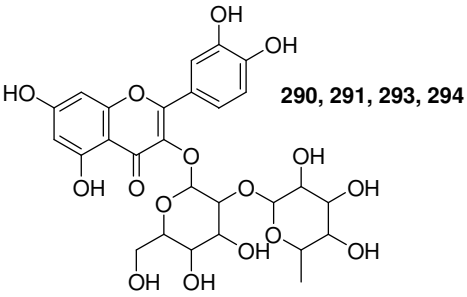

Quercetin-*O*-rhamnoside-*O*-hexoside

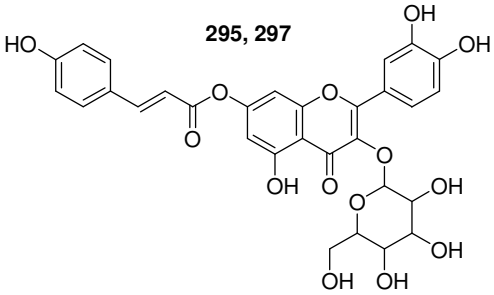

Quercetin-*O*-coumaroyl-hexoside

296

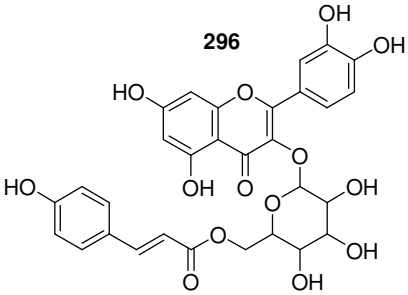

Quercetin-*O*-coumaroyl-hexoside

298-299

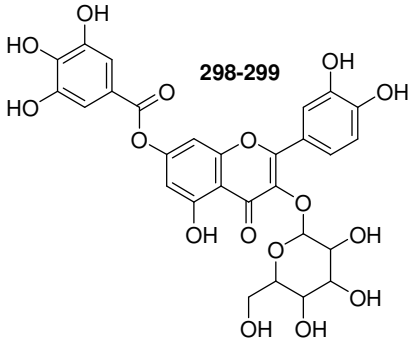

Quercetin-O-galloyl-hexoside

300

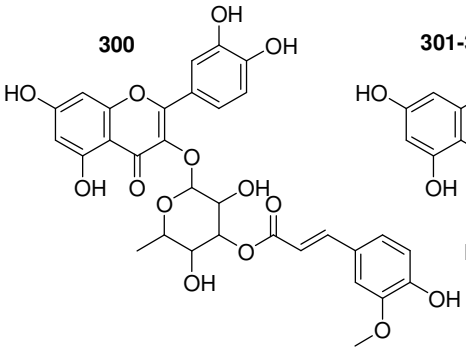

Quercetin-O-feruloyl-rhamnoside

301-303

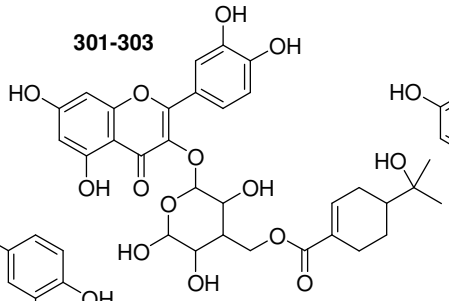

Cypellogin A/B

304

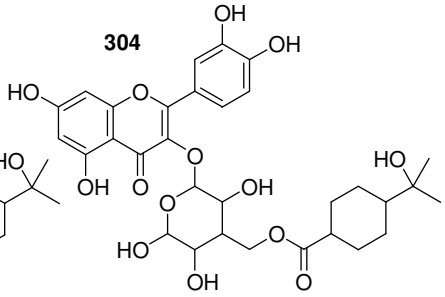

Cypellogin C

305

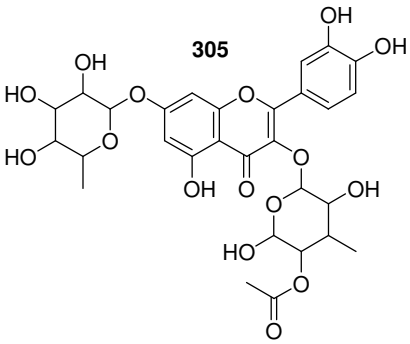

Quercetin-3-(4"-O-acetyl)-O-rhamnoside-7-O-rhamnoside

306-307

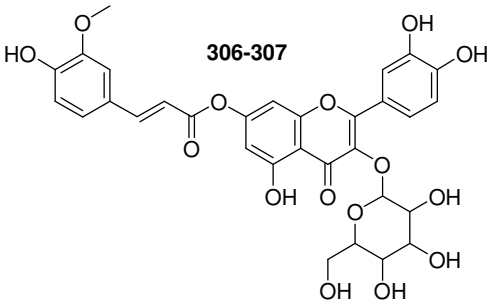

Quercetin-O-feruloyl-hexoside

308

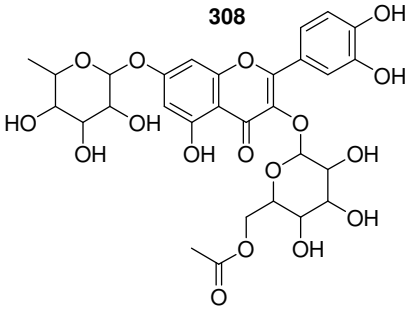

Quercetin-3-O-acetyl-hexoside-rhamnoside

309

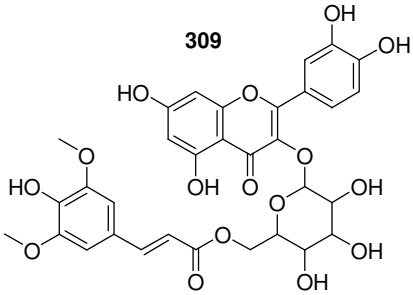

Quercetin-O-sinapoyl-hexoside

310

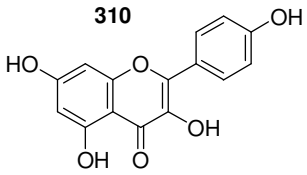

Kaempferol

311-312

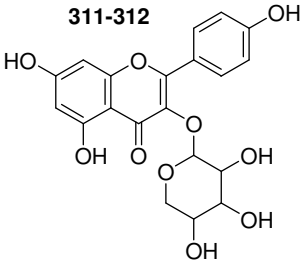

Kaempferol-*O*-pentoside

313

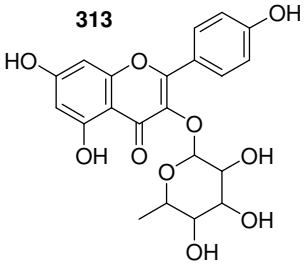

Kaempferol-*O*-rhamnoside

314-315

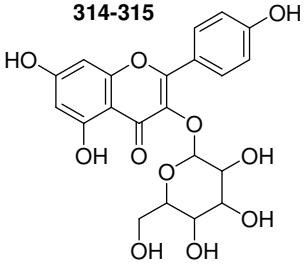

Kaempferol-*O*-hexoside

316-317

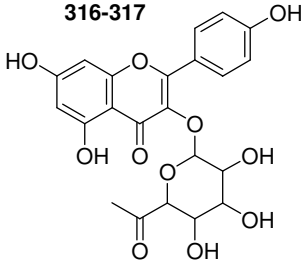

Kaempferol-*O*-acetyl-pentoside

318

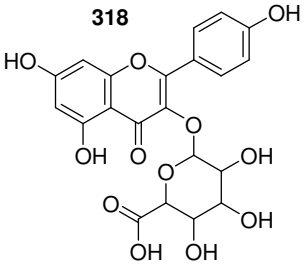

Kaempferol-*O*-glucuronide

319-320

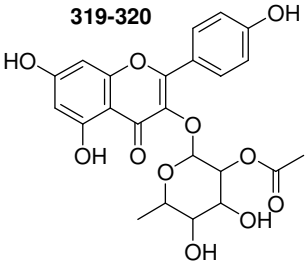

Kaempferol-O-acetyl-rhamnoside

321-323

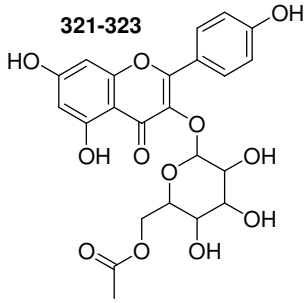

Kaempferol-*O*-acetyl-hexoside

324

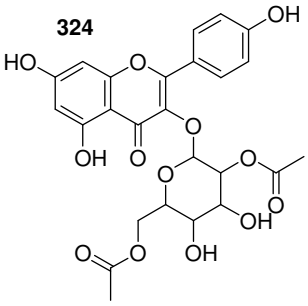

Kaempferol-*O*-diacetyl-hexoside

325-327

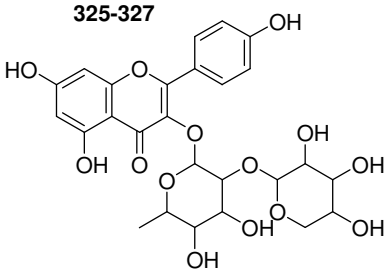

Kaempferol-*O*-rhamnoside-O-pentoside

328

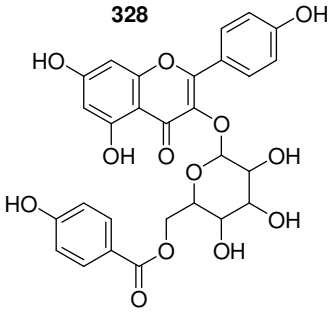

Kaempferol-*O*-hydroxybenzoyl-hexoside

329

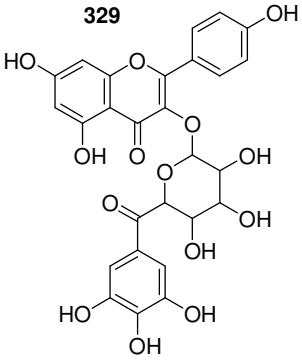

Kaempferol-O-galloyl-pentoside

330

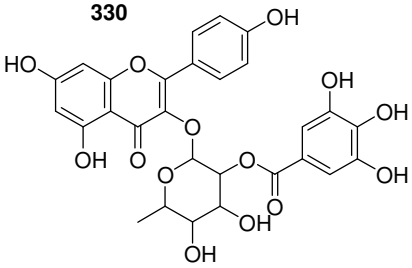

Kaempferol-O-galloyl-rhamnoside

331-332

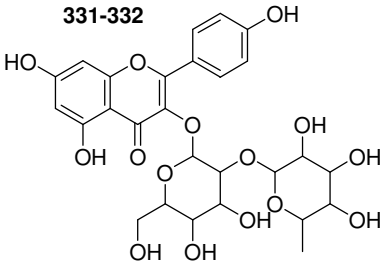

Kaempferol-O-rutinoside

333

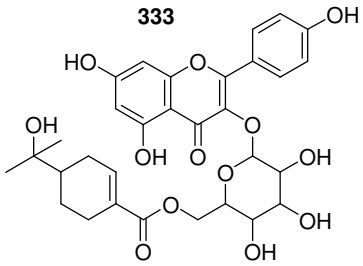

Resinoside A/B

334

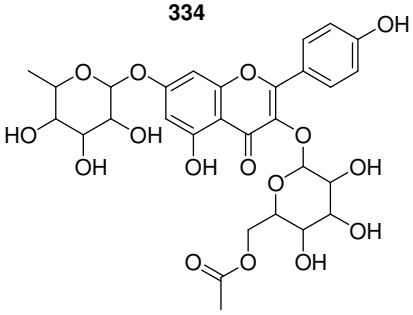

Kaempferol-3-O-(6''-acetyl-hexoside)-7-O-rhamnoside

335

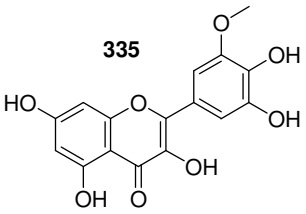

Laricitrin

336-338

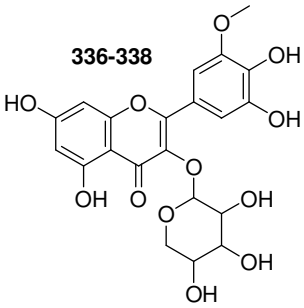

Laricitrin-*O*-pentoside

339

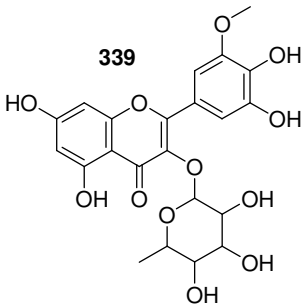

Laricitrin-*O*-rhamnoside

340-342

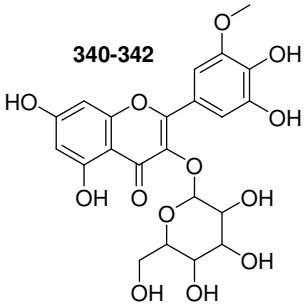

Laricitrin-*O*-hexoside

343

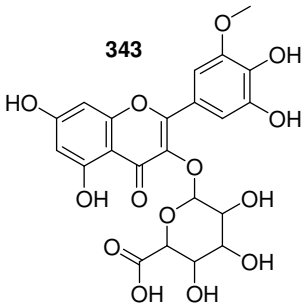

Laricitrin-*O*-glucuronide

344

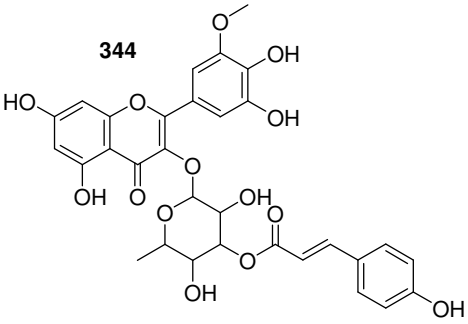

Laricitrin-*O*-coumaroyl-rhamnoside

345

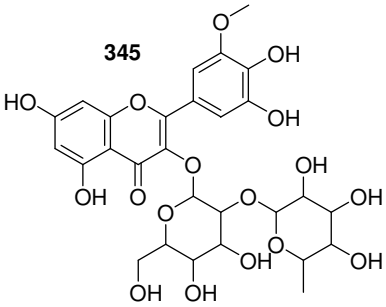

Laricitrin-*O*-rutinoside

346

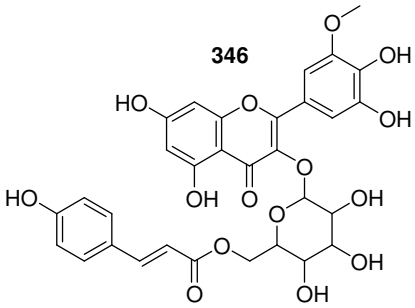

Laricitrin-*O*-coumaroyl-hexoside

347

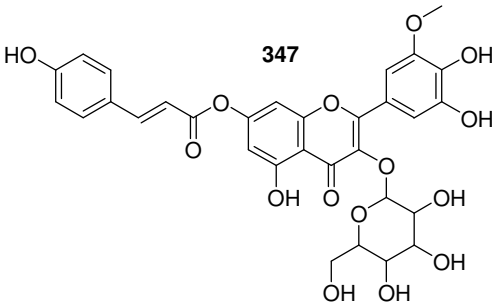

Laricitrin-*O*-coumaroyl-hexoside

348

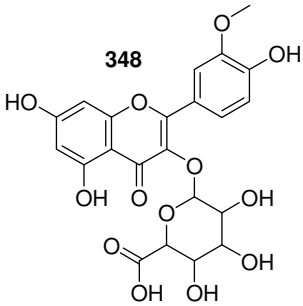

Isorhamnetin-*O*-glucuronide

21.4. Fragmentation Pattern of identified compounds

The fragmentation pattern of the identified compounds along with their theoretical *m/z* value, error in experimental *m/z* value, retention time, *m/z* value and molecular formula are shown in Table 21.2.

Table 21.2: Fragmentation pattern of identified compounds in *Rhododendron* species

No.	Compound	Molecular Formula	Experimental Molecular Weight *m/z* $[M-H]^-$	Theoretical Molecular Weight *m/z* $[M-H]^-$	Error (ppm)	RT (min)	Fragmentation
	Hydroxycinnamic Acids						
	1. Chlorogenic Acids						
1	3-*O*-*p*-Coumaroylquinic acid	$C_{16}H_{18}O_8$	337.0923	337.0929	1.8	18.0	MS^2 → 163 (100), 191 (7), 173 (5); MS^3 → 119 (100)
2	*cis*-3-*O*-*p*-Coumaroylquinic acid	$C_{16}H_{18}O_8$	337.0915	337.0929	4.1	19.4	MS^2 → 163 (100), 191 (6), 173 (3); MS^3 → 119 (100)
3	5-*O*-*p*-Coumaroylquinic acid	$C_{16}H_{18}O_8$	337.0923	337.0929	1.8	24.6	MS^2 → 191 (100), 163 (5)
4	4-*O*-*p*-Coumaroylquinic acid	$C_{16}H_{18}O_8$	337.0917	337.0929	3.5	26.6	MS^2 → 173 (100), 163 (9); MS^3 → 93 (100)
5	*cis*-5-*O*-*p*-Coumaroylquinic acid	$C_{16}H_{18}O_8$	337.0928	337.0929	0.3	28.4	MS^2 → 191 (100), 173 (12), 163 (6)
6	3-*O*-Caffeoylquinic acid	$C_{16}H_{18}O_9$	353.0876	353.0878	0.6	13.0	MS^2 → 191 (100), 179 (33)
7	*cis*-3-*O*-Caffeoylquinic acid	$C_{16}H_{18}O_9$	353.0861	353.0878	4.8	14.0	MS^2 → 191 (100), 179 (50)
8	5-*O*-Caffeoylquinic acid	$C_{16}H_{18}O_9$	353.0877	353.0878	0.3	18.2	MS^2 → 191 (100)
9	*cis*-4-*O*-Caffeoylquinic acid	$C_{16}H_{18}O_9$	353.0861	353.0878	4.8	20.6	MS^2 → 173 (100), 179 (57), 193 (29), 191 (12)
10	4-*O*-Caffeoylquinic acid	$C_{16}H_{18}O_9$	353.0865	353.0878	3.7	23.0	MS^2 → 173 (100), 179 (57), 191 (15)
11	*cis*-5-*O*-Caffeoylquinic acid	$C_{16}H_{18}O_9$	353.0862	353.0878	4.5	24.1	MS^2 → 191 (100)
12	3-*O*-Feruloylquinic acid	$C_{17}H_{20}O_9$	367.1035	367.1035	0.0	21.7	MS^2 → 193 (100); MS^3 → 134 (100), 149 (25)
13	5-*O*-Feruloylquinic acid	$C_{17}H_{20}O_9$	367.1017	367.1035	4.8	27.5	MS^2 → 191 (100); MS^3 → 127 (100), 173 (58)

No.	Compound	Molecular Formula	Experimental Molecular Weight *m/z* [M-H]$^-$	Theoretical Molecular Weight *m/z* [M-H]$^-$	Error (ppm)	RT (min)	Fragmentation
14	4-*O*-Feruloylquinic acid	$C_{17}H_{20}O_9$	367.1024	367.1035	2.9	31.6	MS^2 → 173 (100), 193 (12); MS^3 → 93 (100), 111 (71), 155 (46)
15	3-*O*-hydroxydihydro-Caffeoylquinic acid	$C_{16}H_{20}O_{10}$	371.0987	371.0984	0.9	5.9	MS^2 → 353 (100), 233 (2); MS^3 → 191 (100), 179 (31), 173 (11)
16	5-*O*-hydroxydihydro-Caffeoylquinic acid	$C_{16}H_{20}O_{10}$	371.1001	371.0984	4.7	5.4	MS^2 → 191 (100), 233 (0.1)
17	5-*O*-hydroxydihydro-Caffeoylquinic acid	$C_{16}H_{20}O_{10}$	371.0999	371.0984	4.1	7.0	MS^2 → 191 (100), 353 (70), 233 (0.3)
18	4-*O*-hydroxydihydro-Caffeoylquinic acid	$C_{16}H_{20}O_{10}$	371.0969	371.0984	4.0	9.8	MS^2 → 173 (100), 191 (42), 233 (6) ; MS^3 → 93 (100)
19	4-*O*-hydroxydihydro-Caffeoylquinic acid	$C_{16}H_{20}O_{10}$	371.0974	371.0984	2.6	10.8	MS^2 → 173 (100), 191 (38), 233 (0.1); MS^3 → 93 (100)
	2. Caffeic acid derivatives						
20	Caffeoylthreonate	$C_{13}H_{14}O_8$	297.0609	297.0616	2.3	15.5	MS^2 → 135 (100), 179 (22); MS^3 → 117 (100), 89 (56)
21	Caffeoylthreonate	$C_{13}H_{14}O_8$	297.0607	297.0616	3.0	23.7	MS^2 → 135 (100), 179 (27); MS^3 → 117 (100), 89 (53)
22	Teucrol	$C_{17}H_{16}O_6$	315.0861	315.0874	4.2	51.0	MS^2 → 179 (100); MS^3 → 135 (100)
23	Caffeoylshikimic acid	$C_{16}H_{16}O_8$	335.0756	335.0772	4.9	24.6	MS^2 → 179 (100); MS^3 → 135 (100)
24	Caffeic acid-*O*-hexoside	$C_{15}H_{18}O_9$	341.0878	341.0878	0.0	8.1	MS^2 → 135 (100), 169 (31), 179 (5); MS^3 → 107 (100)
25	Caffeic acid-*O*-hexoside	$C_{15}H_{18}O_9$	341.0862	341.0878	4.7	9.2	MS^2 → 135 (100), 161 (3), 179 (6); MS^3 → 107 (100)
26	Caffeic acid-*O*-hexoside	$C_{15}H_{18}O_9$	341.0866	341.0878	3.5	10.9	MS^2 → 179 (100); MS^3 → 135 (100)
27	Caffeic acid-*O*-hexoside	$C_{15}H_{18}O_9$	341.0863	341.0878	4.4	12.5	MS^2 → 179 (100), 161(44); MS^3 → 135 (100)
28	Caffeic acid-*O*-hexoside	$C_{15}H_{18}O_9$	341.0866	341.0878	3.5	13.9	MS^2 → 179 (100); MS^3 → 135 (100)

No.	Compound	Molecular Formula	Experimental Molecular Weight *m/z* [M-H]$^-$	Theoretical Molecular Weight *m/z* [M-H]$^-$	Error (ppm)	RT (min)	Fragmentation
29	Caffeic acid-*O*-hexoside	$C_{15}H_{18}O_9$	341.0895	341.0878	5.0	15.1	MS^2 → 135 (100), 179 (79); MS^3 → 107 (100)
30	Caffeic acid-*O*-hexoside	$C_{15}H_{18}O_9$	341.0861	341.0878	5.0	17.6	MS^2 → 179 (100); MS^3 → 135 (100)
31	Caffeic acid-*O*-hexoside	$C_{15}H_{18}O_9$	341.0866	341.0878	3.5	19.2	MS^2 → 179 (100); MS^3 → 135 (100)
32	Teucrol-*O*-hexoside / Plantainoside	$C_{23}H_{26}O_{11}$	477.1409	477.1402	1.4	42.0	MS^2 → 315 (100); MS^3 → 179 (100); MS4 → 135 (100)
	3. p-Coumaric acid derivatives						
33	*p*-Coumaric acid-*O*-shikimate	$C_{16}H_{16}O_7$	319.0811	319.0823	3.8	30.8	MS^2 → 163 (100); MS^3 → 119 (100)
34	*p*-Coumaric acid-*O*-hexoside	$C_{15}H_{18}O_8$	325.0920	325.0929	2.7	15.7	MS^2 → 163 (100); MS^3 → 119 (100)
35	*p*-Coumaric acid-*O*-hexoside	$C_{15}H_{18}O_8$	325.0913	325.0929	4.9	16.5	MS^2 → 163 (100); MS^3 → 119 (100)
36	*p*-Coumaric acid-*O*-hexoside	$C_{15}H_{18}O_8$	325.0920	325.0929	2.7	24.1	MS^2 → 163 (100); MS^3 → 119 (100)
37	*p*-Coumaric acid-*O*-hexoside	$C_{15}H_{18}O_8$	325.0916	325.0929	4.0	26.2	MS^2 → 163 (100), 119 (59)
38	*p*-Coumaric acid-*O*-glucosyl ester	$C_{15}H_{18}O_8$	325.0922	325.0929	2.1	17.5	MS^2 → 163 (100), 265 (19), 235 (8), 205 (13), 145 (97); MS^3 → 119 (100)
39	*p*-Coumaric acid-*O*-glucosyl ester	$C_{15}H_{18}O_8$	325.0916	325.0929	4.0	18.7	MS^2 → 163 (100), 265 (17), 235 (10), 205 (11), 145 (88); MS^3 → 119 (100)
40	*p*-Coumaric acid-*O*-hexoside-*O*-pentoside	$C_{20}H_{26}O_{12}$	457.1352	457.1352	0.0	17.6	MS^2 → 163 (100); MS^3 → 119 (100)
41	*p*-Coumaric acid-*O*-hexoside-*O*-pentoside	$C_{20}H_{26}O_{12}$	457.1364	457.1352	2.7	19.2	MS^2 → 163 (100); MS^3 → 119 (100)
42	Everlastoside M	$C_{22}H_{26}O_{12}$	481.1362	481.1352	2.2	27.0	MS^2 → 367 (100), 307 (30); MS^3 → 163 (100); MS4 → 119 (100)
43	*p*-Coumaric acid-*O*-dihexoside	$C_{21}H_{28}O_{13}$	487.1471	487.1457	2.8	14.4	MS^2 → 163 (100), 325 (75); MS^3 → 119 (100)

No.	Compound	Molecular Formula	Experimental Molecular Weight *m/z* [M-H]$^-$	Theoretical Molecular Weight *m/z* [M-H]$^-$	Error (ppm)	RT (min)	Fragmentation
44	*p*-Coumaric acid-*O*-dihexoside	$C_{21}H_{28}O_{13}$	487.1481	487.1457	4.9	20.0	MS^2 → 163 (100), 325 (37); MS^3 → 119 (100)
	4. Dihydrocoumaric acid derivatives						
45	Dihydrocoumaric acid-*O*-hexoside	$C_{15}H_{20}O_8$	327.1069	327.1085	5.0	15.5	MS^2 → 165 (100); MS^3 → 121 (100)
46	Dihydrocoumaric acid-*O*-hexoside	$C_{15}H_{20}O_8$	327.1076	327.1085	2.9	20.4	MS^2 → 165 (100); MS^3 → 121 (100)
	5. Ferulic acid derivatives						
47	Ferulic acid-*O*-hexoside	$C_{16}H_{20}O_9$	355.1018	355.1035	4.7	19.0	MS^2 → 193 (100); MS^3 → 149 (100), 178 (64), 134 (39)
48	Ferulic acid-*O*-hexoside	$C_{16}H_{20}O_9$	355.1021	355.1035	3.8	21.2	MS^2 → 193 (100); MS^3 → 149 (100), 178 (71), 134 (85)
49	Ferulic acid-*O*-hexoside	$C_{16}H_{20}O_9$	355.1019	355.1035	4.4	28.9	MS^2 → 193 (100); MS^3 → 149 (100), 134 (6)
50	Ferulic acid-*O*-glucosyl ester	$C_{16}H_{20}O_9$	355.1018	355.1035	4.7	20.4	MS^2 → 193 (100), 295 (6), 265 (4), 235 (10); MS^3 → 134 (100), 178 (17), 149 (31)
51	Ferulic acid-*O*-dihexoside	$C_{22}H_{30}O_{14}$	517.1576	517.1563	2.6	17.2	MS^2 → 175 (100), 193 (80); MS^3 of 175 → 160 (100); MS^3 of 193 → 149 (100), 178 (77), 134 (77)
	Hydroxybenzoic Acids						
	1. Gallic Acid						
52	Gallic acid-*O*-pentoside	$C_{12}H_{14}O_9$	301.0570	301.0565	1.6	6.6	MS^2 → 169 (100); MS^3 → 125 (100)
53	3-*O*-Galloylshikimic acid / 5-*O*-Galloylshikimic acid	$C_{14}H_{14}O_9$	325.0549	325.0565	4.9	8.9	MS^2 → 169 (100); MS^3 → 125 (100)
54	3-*O*-Galloylshikimic acid / 5-*O*-Galloylshikimic acid	$C_{14}H_{14}O_9$	325.0557	325.0565	2.6	9.6	MS^2 → 169 (100); MS^3 → 125 (100)

No.	Compound	Molecular Formula	Experimental Molecular Weight *m/z* [M-H]$^-$	Theoretical Molecular Weight *m/z* [M-H]$^-$	Error (ppm)	RT (min)	Fragmentation
55	Gallic acid-*O*-hexoside	$C_{13}H_{16}O_{10}$	331.0670	331.0671	0.2	4.6	MS^2 → 169 (100), 271 (11); MS^3 → 125 (100)
56	Gallic acid-*O*-hexoside	$C_{13}H_{16}O_{10}$	331.0668	331.0671	0.8	7.9	MS^2 → 169 (100), 271 (5); MS^3 → 125 (100)
57	Gallic acid-*O*-glucosyl ester	$C_{13}H_{16}O_{10}$	331.0677	331.0671	1.9	3.7	MS^2 → 169 (100), 271 (67), 241 (5), 211 (27); MS^3 → 125 (100)
58	Galloylquinic acid	$C_{14}H_{16}O_{10}$	343.0664	343.0671	2.0	4.3	MS^2 → 169 (100), 191 (71); MS^3 → 125 (100)
59	Galloylquinic acid	$C_{14}H_{16}O_{10}$	343.0656	343.0671	4.3	5.8	MS^2 → 191 (100), 169 (7), 125 (1)
60	Galloylquinic acid	$C_{14}H_{16}O_{10}$	343.0687	343.0671	4.8	9.6	MS^2 → 169 (100); MS^3 → 125 (100)
61	Gallic acid-*O*-acetyl-hexoside	$C_{15}H_{18}O_{11}$	373.0758	373.0776	4.9	13.9	MS^2 → 169 (100); MS^3 → 125 (100)
62	Benzyl-6'-*O*-galloyl-β-D-hexoside	$C_{20}H_{22}O_{10}$	421.1138	421.1140	0.5	32.1	MS^2 → 169 (100), 313 (63); MS^3 → 125 (100)
63	Galloylarbutin	$C_{19}H_{20}O_{11}$	423.0926	423.0933	1.6	11.7	MS^2 → 313 (100); MS^3 → 169 (100); MS^4 → 125 (100)
64	Galloylarbutin	$C_{19}H_{20}O_{11}$	423.0946	423.0933	3.1	17.7	MS^2 → 313 (100); MS^3 → 169 (100); MS^4 → 125 (100)
65	6-galloyl-1-*O*-(phloroglucinol)-hexoside	$C_{19}H_{20}O_{12}$	439.0890	439.0882	1.8	15.0	MS^2 → 313 (100), 271 (16), 211 (14); MS^3 → 169 (100); MS^4 → 125 (100)
66	Gallic acid-3-*O*-hexoside-4-*O*-pentoside	$C_{18}H_{24}O_{14}$	463.1072	463.1093	4.5	7.9	MS^2 → 301 (100); MS^3 → 169 (100); MS^4 → 125 (100)
67	*p*-hydroxyphenethyl alcohol-1-*O*-β-D-(6"-*O*-galloyl)-hexoside	$C_{21}H_{24}O_{12}$	467.1197	467.1195	0.3	22.3	MS^2 → 313 (100); MS^3 → 169 (100); MS^4 → 125 (100)
68	Gallic acid-*O*-galloyl-rhamnoside	$C_{20}H_{20}O_{13}$	467.0845	467.0831	2.9	36.6	MS^2 → 423 (100); MS^3 → 313 (100); MS^4 → 169 (100), 125 (18)
69	Gallic acid-*O*-rutinoside	$C_{19}H_{26}O_{14}$	477.1267	477.1250	3.7	6.6	MS^2 → 169 (100); MS^3 → 125 (100)
70	Gallic acid-*O*-coumaroyl-hexoside (diff sides)	$C_{22}H_{22}O_{12}$	477.1041	477.1039	0.5	31.0	MS^2 → 313 (100); MS^3 → 169 (100); MS^4 → 125 (100)

No.	Compound	Molecular Formula	Experimental Molecular Weight *m/z* [M-H]$^-$	Theoretical Molecular Weight *m/z* [M-H]$^-$	Error (ppm)	RT (min)	Fragmentation
71	Gallic acid-*O*-coumaroyl-hexoside (diff sides)	$C_{22}H_{22}O_{12}$	477.1057	477.1039	3.9	32.6	MS^2 → 313 (100); MS^3 → 169 (100); MS^4 → 125 (100)
72	Gallic acid-*O*-coumaroyl-hexoside (diff sides)	$C_{22}H_{22}O_{12}$	477.1039	477.1039	0.1	35.9	MS^2 → 313 (100); MS^3 → 169 (100); MS^4 → 125 (100)
73	Querglanin	$C_{23}H_{28}O_{11}$	479.1571	479.1559	2.5	31.9	MS^2 → 169 (100), 313 (59); MS^3 → 125 (100)
74	Galloyl-*O*-vanilloyl-*O*-hexoside	$C_{21}H_{22}O_{13}$	481.1012	481.0988	5.0	27.1	MS^2 → 313 (100); MS^3 → 169 (100); MS^4 → 125 (100)
75	Galloyl-*O*-vanilloyl-*O*-hexoside	$C_{21}H_{22}O_{13}$	481.1004	481.0988	3.4	30.1	MS^2 → 437 (100); MS^3 → 313 (100); MS^4 → 169 (100), 125 (18)
76	Gallic acid-3-*O*-(6'-*O*-galloyl)-β-D-hexoside	$C_{20}H_{20}O_{14}$	483.0798	483.0780	3.7	22.5	MS^2 → 439 (100); MS^3 → 287 (100), 313 (85), 169 (7); MS^4 → 125 (100)
77	Gallic acid-*O*-dihexoside (diff sides)	$C_{19}H_{26}O_{15}$	493.1223	493.1199	4.9	3.2	MS^2 → 331 (100); MS^3 → 169 (100); MS^4 → 125 (100)
78	Gallic acid-*O*-dihexoside (diff sides)	$C_{19}H_{26}O_{15}$	493.1209	493.1199	2.0	5.2	MS^2 → 331 (100); MS^3 → 169 (100); MS^4 → 125 (100)
79	Gallic acid-*O*-dihexoside (same side)	$C_{19}H_{26}O_{15}$	493.1202	493.1199	0.6	6.7	MS^2 → 169 (100); MS^3 → 125 (100)
80	Gallic acid-*O*-feruloyl-hexoside	$C_{23}H_{24}O_{13}$	507.1123	507.1144	4.2	36.2	MS^2 → 331 (100); MS^3 → 169 (100); MS^4 → 125 (100)
81	Hyemaloside B / Guavinoside A	$C_{26}H_{24}O_{13}$	543.1163	543.1144	3.5	30.9	MS^2 → 169 (100), 405 (84); MS^3 → 125 (100)
82	Galloylalbiflorin	$C_{30}H_{32}O_{15}$	631.1655	631.1668	2.1	42.8	MS^2 → 479 (100); MS^3 → 169 (100); MS^4 → 125 (100)
	2. Protocatechuic acid						
83	Protocatechuic acid-*O*-pentoside	$C_{12}H_{14}O_8$	285.0606	285.0616	3.5	15.1	MS^2 → 153 (100); MS^3 → 109 (100)
84	Protocatechuic acid-*O*-hexoside	$C_{13}H_{16}O_9$	315.0707	315.0722	4.6	5.9	MS^2 → 153 (100); MS^3 → 109 (100)

No.	Compound	Molecular Formula	Experimental Molecular Weight *m/z* [M-H]$^-$	Theoretical Molecular Weight *m/z* [M-H]$^-$	Error (ppm)	RT (min)	Fragmentation
85	Protocatechuic acid-*O*-hexoside	$C_{13}H_{16}O_9$	315.0732	315.0722	3.3	10.5	MS^2 → 153 (100); MS^3 → 109 (100)
86	Protocatechuic acid-*O*-benzoyl-hexoside	$C_{20}H_{20}O_{10}$	419.0974	419.0984	2.3	51.8	MS^2 → 153 (100); MS^3 → 109 (100)
87	Protocatechuic acid-*O*-feruloyl-hexoside	$C_{23}H_{24}O_{12}$	491.1202	491.1195	1.4	51.1	MS^2 → 315 (100); MS^3 → 153 (100); MS^4 → 109 (100)
	3. Salicylic acid						
88	Salicylic acid-*O*-hexoside	$C_{13}H_{16}O_8$	299.0769	299.0772	1.1	6.3	MS^2 → 137 (100); MS^3 → 93 (100)
89	Salicylic acid-*O*-hexoside	$C_{13}H_{16}O_8$	299.0767	299.0772	1.8	13.0	MS^2 → 137 (100); MS^3 → 93 (100)
90	Salicylic acid-*O*-glucosyl ester	$C_{13}H_{16}O_8$	299.0765	299.0772	2.5	8.5	MS^2 → 137 (100), 239 (91), 209 (26), 179 (94); MS^3 → 93 (100)
91	Salicyloylsalicin	$C_{20}H_{22}O_9$	405.1188	405.1191	0.8	36.6	MS^2 → 281 (100); MS^3 → 137 (100); MS^4 → 93 (100)
92	Salicylic acid-*O*-coumaroyl-hexoside	$C_{22}H_{22}O_{10}$	445.1122	445.1140	4.1	42.4	MS^2 → 281 (100); MS^3 → 137 (100); MS^4 → 93 (100)
93	Salicylic acid-*O*-coumaroyl-hexoside	$C_{22}H_{22}O_{10}$	445.1122	445.1140	4.1	46.2	MS^2 → 281 (100); MS^3 → 137 (100); MS^4 → 93 (100)
94	Salicylic acid-*O*-dihexoside (Same side)	$C_{19}H_{26}O_{13}$	461.1318	461.1301	3.8	7.0	MS^2 → 137 (100); MS^3 → 93 (100)
	4. Vanillic acid						
95	Vanillic acid-*O*-hexoside	$C_{14}H_{18}O_9$	329.0869	329.0878	2.8	7.7	MS^2 → 167 (100); MS^3 → 123 (100)
96	Vanillic acid-*O*-hexoside	$C_{14}H_{18}O_9$	329.0864	329.0878	4.3	10.2	MS^2 → 167 (100); MS^3 → 152 (100), 123 (53), 108 (38)
97	Vanillic acid-*O*-hexoside	$C_{14}H_{18}O_9$	329.0865	329.0878	4.0	11.7	MS^2 → 167 (100); MS^3 → 149 (100), 123 (6)
98	Vanillic acid-*O*-hexoside	$C_{14}H_{18}O_9$	329.0863	329.0878	4.6	13.9	MS^2 → 167 (100); MS^3 → 123 (100)

No.	Compound	Molecular Formula	Experimental Molecular Weight *m/z* [M-H]$^-$	Theoretical Molecular Weight *m/z* [M-H]$^-$	Error (ppm)	RT (min)	Fragmentation
99	Amburoside B	$C_{21}H_{24}O_{10}$	435.1289	435.1297	1.8	36.3	MS^2 → 273 (100); MS^3 → 167 (100); MS^4 → 123 (100)
100	Vanilloyl-*O*-hydroxybenzoyl-hexoside (Diff sides)	$C_{21}H_{22}O_{11}$	449.1093	449.1089	0.8	17.5	MS^2 → 329 (100), 359 (36); MS^3 → 301 (100); MS^4 → 167 (100), 123 (4)
101	Vanilloyl-*O*-hydroxybenzoyl-hexoside (Same side)	$C_{21}H_{22}O_{11}$	449.1096	449.1089	1.5	40.8	MS^2 → 167 (100), 281 (39); MS^3 → 123 (100)
102	Vanillic acid-*O*-hexoside-*O*-pentoside (Same side)	$C_{19}H_{26}O_{13}$	461.1319	461.1301	4.0	14.9	MS^2 → 167 (100); MS^3 → 123 (100)
103	Vanillic acid-*O*-hexoside-*O*-pentoside (Same side)	$C_{19}H_{26}O_{13}$	461.1313	461.1301	2.7	19.1	MS^2 → 167 (100), 191 (72); MS^3 → 123 (100)
104	Vanillic acid-*O*-rutinoside (Same side)	$C_{20}H_{28}O_{13}$	475.1477	475.1457	4.2	12.5	MS^2 → 167 (100); MS^3 → 123 (100), 152 (48)
105	Vanillic acid-*O*-rutinoside (Same side)	$C_{20}H_{28}O_{13}$	475.1480	475.1457	4.8	18.9	MS^2 → 167 (100), 191 (86); MS^3 → 123 (100)
106	Vanillic acid-*O*-coumaroyl-hexoside (Diff sides) ref is on same side	$C_{23}H_{24}O_{11}$	475.1258	475.1246	2.6	47.8	MS^2 → 311 (100); MS^3 → 167 (100); MS^4 → 123 (100)
107	Vanillic acid-*O*-dihexoside (diff sides) Picrorhizin	$C_{20}H_{28}O_{14}$	491.1411	491.1406	1.0	4.6	MS^2 → 329 (100); MS^3 → 167 (100), 149 (55), 123 (4)
108	Vanillic acid-*O*-dihexoside (diff sides) Picrorhizin	$C_{20}H_{28}O_{14}$	491.1399	491.1406	1.5	5.3	MS^2 → 329 (100); MS^3 → 167 (100); MS^4 → 149 (100), 123 (26)
109	Vanillic acid-*O*-dihexoside (same side) β-D-fructfuranosyl-α-D-(6-vanilloyl)-glucopyranoside	$C_{20}H_{28}O_{14}$	491.1422	491.1406	3.2	8.5	MS^2 → 167 (100); MS^3 → 123 (26)
110	Litseaefoloside A	$C_{23}H_{26}O_{12}$	493.1340	493.1352	2.3	47.0	MS^2 → 167 (100); MS^3 → 152 (100), 123 (48)
	5. Methyl gallate						

No.	Compound	Molecular Formula	Experimental Molecular Weight *m/z* $[M-H]^-$	Theoretical Molecular Weight *m/z* $[M-H]^-$	Error (ppm)	RT (min)	Fragmentation
111	Methyl gallate-*O*-hexoside	$C_{14}H_{18}O_{10}$	345.0810	345.0827	5.0	7.4	MS^2 → 183 (100); MS^3 → 168 (100); MS^4 → 124 (100)
112	Methyl gallate-*O*-hexoside	$C_{14}H_{18}O_{10}$	345.0818	345.0827	2.7	8.5	MS^2 → 183 (100); MS^3 → 168 (100); MS^4 → 124 (100)
113	Methyl gallate-*O*-hexoside	$C_{14}H_{18}O_{10}$	345.0810	345.0827	5.0	11.8	MS^2 → 183 (100); MS^3 → 168 (100); MS^4 → 124 (100)
114	Methyl gallate-*O*-coumaroyl-hexoside	$C_{23}H_{24}O_{12}$	491.1192	491.1195	0.6	42.1	MS^2 → 327 (100); MS^3 → 183 (100); MS^4 → 168 (100), 139 (5), 124 (8)
115	Methyl gallate-*O*-dihexoside (Diff sides)	$C_{20}H_{28}O_{15}$	507.1375	507.1355	3.9	8.0	MS^2 → 345 (100); MS^3 → 183 (100); MS^4 → 168 (100), 139 (97), 123 (24)
	Flavan-3-ols						
116	Catechin	$C_{15}H_{14}O_6$	289.0709	289.0718	3.0	16.0	MS^2 → 245 (100), 205 (28), 179 (18); MS^3 → 203 (100), 227 (31), 187 (16), 161 (20)
117	Epicatechin	$C_{15}H_{14}O_6$	289.0705	289.0718	4.4	23.0	MS^2 → 245 (100), 205 (31), 179 (15); MS^3 → 203 (100), 227 (28), 187 (15), 161 (22)
118	Gallocatechin	$C_{15}H_{14}O_7$	305.0654	305.0667	4.2	8.5	MS^2 → 179 (100), 221 (64), 261 (14); MS^3 → 164 (100), 151 (94), 135 (19)
119	Epigallocatechin	$C_{15}H_{14}O_7$	305.0653	305.0667	4.5	15.4	MS^2 → 179 (100), 221 (64), 261 (29); MS^3 → 164 (100), 151 (27), 135 (25)
120	2-(3,4-dihydroxyphenyl)-5,7-dihydroxychroman-3-yl-4-hydroxybenzoate / (Epi)catechin-*O*-hydroxybenzoate	$C_{22}H_{18}O_8$	409.0923	409.0929	1.4	35.8	MS^2 → 289 (100); MS^3 → 245 (100), 205 (34)
121	(Epi)catechin-*O*-rhamnoside	$C_{21}H_{24}O_{10}$	435.1293	435.1297	0.9	22.5	MS^2 → 289 (100); MS^3 → 245 (100), 205 (31)

No.	Compound	Molecular Formula	Experimental Molecular Weight *m/z* [M-H]$^-$	Theoretical Molecular Weight *m/z* [M-H]$^-$	Error (ppm)	RT (min)	Fragmentation
122	Malaferin B	$C_{24}H_{20}O_8$	435.1095	435.1085	2.2	40.1	MS^2 → 289 (100); MS^3 → 245 (100), 205 (31)
123	(Epi)catechin gallate	$C_{22}H_{18}O_{10}$	441.0830	441.0827	0.6	28.1	MS^2 → 289 (100); MS^3 → 245 (100), 205 (34)
124	(Epi)catechin gallate	$C_{22}H_{18}O_{10}$	441.0829	441.0827	0.4	29.6	MS^2 → 289 (100); MS^3 → 245 (100), 205 (32)
125	(Epi)catechin gallate	$C_{22}H_{18}O_{10}$	441.0826	441.0827	0.3	31.8	MS^2 → 289 (100); MS^3 → 245 (100), 205 (34)
126	(Epi)catechin gallate	$C_{22}H_{18}O_{10}$	441.0830	441.0827	0.6	36.8	MS^2 → 289 (100); MS^3 → 245 (100), 205 (38)
127	(Epi)catechin-*O*-hexoside	$C_{21}H_{24}O_{11}$	451.1251	451.1246	1.1	10.5	MS^2 → 289 (100); MS^3 → 245 (100), 205 (25)
128	(Epi)catechin-*O*-methyl-gallate	$C_{23}H_{20}O_{10}$	455.0965	455.0984	4.1	34.4	MS^2 → 289 (100); MS^3 → 245 (100), 205 (34)
129	(Epi)gallocatechin gallate	$C_{22}H_{18}O_{11}$	457.0755	457.0776	4.7	19.8	MS^2 → 305 (100); MS^3 → 179 (100), 125 (21)
130	Epigallocatechin gallate	$C_{22}H_{18}O_{11}$	457.0776	457.0776	0.0	22.7	MS^2 → 169 (100), 305 (19); MS^3 → 125 (100)
131	(Epi)gallocatechin gallate	$C_{22}H_{18}O_{11}$	457.0757	457.0776	4.2	26.6	MS^2 → 169 (100), 305 (24); MS^3 → 125 (100)
132	Malaferin C	$C_{25}H_{22}O_9$	465.1198	465.1191	1.5	41.2	MS^2 → 289 (100); MS^3 → 245 (100), 205 (34)
133	(Epi)catechin-*O*-dimethyl-gallate	$C_{24}H_{22}O_{10}$	469.1161	469.1140	4.4	38.9	MS^2 → 289 (100); MS^3 → 245 (100), 205 (37)
134	(Epi)catechin-*O*-trimethoxybenzoate	$C_{25}H_{24}O_{10}$	483.1320	483.1297	4.8	29.5	MS^2 → 289 (100); MS^3 → 245 (100), 205 (35)
135	(Epi)catechin-*O*-trimethoxybenzoate	$C_{25}H_{24}O_{10}$	483.1300	483.1297	0.7	32.9	MS^2 → 289 (100); MS^3 → 245 (100), 205 (37)
136	(Epi)catechin-(4,8/2,6)-(epi)catechin	$C_{30}H_{24}O_{12}$	575.1206	575.1195	1.9	5.5	MS^2 → 423 (100), 449 (72), 407 (77)
137	(Epi)catechin-(4,8/2,6)-(epi)catechin	$C_{30}H_{24}O_{12}$	575.1216	575.1195	3.7	8.7	MS^2 → 423 (100), 449 (17), 407 (33)
138	(Epi)catechin-(4,8/2,6)-(epi)catechin	$C_{30}H_{24}O_{12}$	575.1216	575.1195	3.7	10.1	MS^2 → 423 (100), 449 (10), 407 (85)
139	(Epi)catechin-(4,8/2,6)-(epi)catechin	$C_{30}H_{24}O_{12}$	575.1194	575.1195	0.2	12.0	MS^2 → 423 (100), 449 (9), 407 (32)
140	(Epi)catechin-(4,8/2,6)-(epi)catechin	$C_{30}H_{24}O_{12}$	575.1190	575.1195	0.9	14.0	MS^2 → 423 (100), 449 (6), 407 (42)

No.	Compound	Molecular Formula	Experimental Molecular Weight *m/z* [M-H]$^-$	Theoretical Molecular Weight *m/z* [M-H]$^-$	Error (ppm)	RT (min)	Fragmentation
141	(Epi)catechin-(4,8/2,6)-(epi)catechin	$C_{30}H_{24}O_{12}$	575.1190	575.1195	0.9	18.1	MS^2 → 407 (100), 449 (88), 423 (67)
142	(Epi)catechin-(4,8/2,6)-(epi)catechin	$C_{30}H_{24}O_{12}$	575.1211	575.1195	2.8	27.2	MS^2 → 449 (100), 539 (36), 423 (19), 407 (32), 289 (53), 285 (39); MS^3 → 287 (100), 313 (26), 245 (13)
143	(Epi)catechin-(4,8/2,6)-(epi)catechin	$C_{30}H_{24}O_{12}$	575.1190	575.1195	0.9	32.4	MS^2 → 423 (100), 449 (100), 539 (17), 407 (13) 289 (27), 285 (31); MS^3 → 285 (100), 313 (18)
144	(Epi)catechin-(4,8/2,6)-(epi)catechin	$C_{30}H_{24}O_{12}$	575.1184	575.1195	1.9	34.8	MS^2 → 423 (100), 449 (94), 407 (27); MS^3 → 285 (100)
145	(Epi)catechin-(epi)catechin (Procyanidin dimer B1)	$C_{30}H_{26}O_{12}$	577.1372	577.1352	3.6	13.4	MS^2 → 407 (100), 425 (93), 451 (21), 289 (27); MS^3 → 285 (100), 283 (20)
146	(Epi)catechin-(epi)catechin (Procyanidin dimer B)	$C_{30}H_{26}O_{12}$	577.1361	577.1352	1.6	14.3	MS^2 → 425 (100), 407 (92), 451 (24), 289 (19); MS^3 → 285 (100), 283 (40)
147	(Epi)catechin-(epi)catechin (Procyanidin dimer B)	$C_{30}H_{26}O_{12}$	577.1371	577.1352	3.4	18.6	MS^2 → 407 (100), 425 (74), 451 (26), 289 (28); MS^3 → 285 (100), 283 (33)
148	(Epi)catechin-(epi)catechin (Procyanidin dimer B2)	$C_{30}H_{26}O_{12}$	577.1370	577.1352	3.2	20.3	MS^2 → 425 (100), 407 (89), 451 (24), 289 (22); MS^3 → 407 (100); MS^4 → 285 (100), 283 (29)
149	(Epi)catechin-(epi)catechin (Procyanidin dimer B)	$C_{30}H_{26}O_{12}$	577.1374	577.1352	3.9	23.1	MS^2 → 425 (100), 407 (76), 451 (12), 289 (16); MS^3 → 407 (100); MS^4 → 285 (100), 283 (18)
150	(Epi)catechin-(epi)catechin (Procyanidin dimer B)	$C_{30}H_{26}O_{12}$	577.1360	577.1352	1.5	32.8	MS^2 → 425 (100), 407 (90), 451 (19), 289 (21); MS^3 → 407 (100); MS^4 → 285 (100), 283 (33)
151	Gambiriin A/D	$C_{30}H_{28}O_{12}$	579.1533	579.1508	4.3	19.2	MS^2 → 289 (100), 425 (30); MS^3 → 245 (100), 205 (42)

No.	Compound	Molecular Formula	Experimental Molecular Weight *m/z* [M-H]$^-$	Theoretical Molecular Weight *m/z* [M-H]$^-$	Error (ppm)	RT (min)	Fragmentation
152	(Epi)gallocatechin-(epi)catechin	$C_{30}H_{26}O_{13}$	593.1325	593.1301	4.1	7.7	MS^2 → 425 (100), 407 (94), 289 (29); MS^3 → 407 (100); MS^4 → 285 (100), 283 (25)
153	(Epi)gallocatechin-(epi)catechin	$C_{30}H_{26}O_{13}$	593.1303	593.1301	0.4	9.7	MS^2 → 425 (100), 407 (74), 289 (19); MS^3 → 407 (100); MS^4 → 285 (100), 283 (35)
154	(Epi)gallocatechin-(epi)catechin	$C_{30}H_{26}O_{13}$	593.1321	593.1301	3.4	10.5	MS^2 → 423 (100), 441 (48), 467 (32), 305 (41); MS^3 → 283 (100), 297 (78)
155	(Epi)gallocatechin-(epi)catechin	$C_{30}H_{26}O_{13}$	593.1317	593.1301	2.8	12.6	MS^2 → 425 (100), 407 (65), 289 (15); MS^3 → 407 (100); MS^4 → 285 (100), 283 (38)
156	(Epi)gallocatechin-(epi)catechin	$C_{30}H_{26}O_{13}$	593.1327	593.1301	4.4	13.7	MS^2 → 425 (100), 407 (70), 289 (22); MS^3 → 407 (100); MS^4 → 285 (100), 283 (30)
157	(Epi)gallocatechin-(epi)catechin	$C_{30}H_{26}O_{13}$	593.1301	593.1301	0.1	15.2	MS^2 → 423 (100), 575 (24), 441 (36), 305 (39); MS^3 → 297 (100), 283 (96)
158	(Epi)gallocatechin-(epi)catechin	$C_{30}H_{26}O_{13}$	593.1310	593.1301	1.6	16.5	MS^2 → 423 (100), 575 (16), 441 (52), 305 (33); MS^3 → 297 (100), 283 (99)
159	(Epi)gallocatechin-(epi)catechin	$C_{30}H_{26}O_{13}$	593.1320	593.1301	3.3	18.2	MS^2 → 425 (100), 407 (85), 289 (20); MS^3 → 407 (100); MS^4 → 285 (100), 283 (41)
160	(Epi)gallocatechin-(epi)gallocatechin	$C_{30}H_{26}O_{14}$	609.1269	609.1250	3.2	4.5	MS^2 → 423 (100), 441 (49), 305 (30); MS^3 → 297 (100), 283 (89), 255 (33)
161	(Epi)gallocatechin-(epi)gallocatechin	$C_{30}H_{26}O_{14}$	609.1275	609.1250	4.1	6.5	MS^2 → 423 (100), 441 (62), 305 (24); MS^3 → 283 (100), 297 (90), 255 (41)
162	(Epi)gallocatechin-(epi)gallocatechin	$C_{30}H_{26}O_{14}$	609.1275	609.1250	4.1	7.5	MS^2 → 423 (100), 441 (37), 305 (29); MS^3 → 283 (100), 297 (78), 255 (16)

No.	Compound	Molecular Formula	Experimental Molecular Weight *m/z* [M-H]$^-$	Theoretical Molecular Weight *m/z* [M-H]$^-$	Error (ppm)	RT (min)	Fragmentation
163	(Epi)gallocatechin-(epi)gallocatechin	$C_{30}H_{26}O_{14}$	609.1261	609.1250	1.8	10.2	MS^2 → 423 (100), 441 (41), 305 (26); MS^3 → 297 (100), 283 (66), 255 (30)
164	(Epi)gallocatechin-(epi)gallocatechin	$C_{30}H_{26}O_{14}$	609.1247	609.1250	0.5	13.1	MS^2 → 423 (100), 441 (58), 305 (23); MS^3 → 297 (100), 283 (90), 255 (18)
165	(Epi)catechin-3-*O*-hexoside-7-*O*-hexoside	$C_{27}H_{34}O_{16}$	613.1790	613.1774	2.6	9.6	MS^2 → 451 (100); MS^3 → 289 (100); MS^4 → 245 (100), 205 (20)
166	(Epi)catechin-3-*O*-hexoside-7-*O*-hexoside	$C_{27}H_{34}O_{16}$	613.1798	613.1774	3.9	11.8	MS^2 → 451 (100); MS^3 → 289 (100); MS^4 → 245 (100), 205 (45)
167	(Epi)catechin-3-*O*-hexoside-7-*O*-hexoside	$C_{27}H_{34}O_{16}$	613.1801	613.1774	4.4	13.2	MS^2 → 451 (100); MS^3 → 289 (100); MS^4 → 245 (100), 205 (34)
168	3-*O*-galloyl(epi)catechin-(4,8/2,6)-(epi)catechin	$C_{37}H_{28}O_{16}$	727.1296	727.1305	1.2	36.6	MS^2 → 575 (100), 559 (35), 449 (11), 423 (32); MS^3 → 449 (100), 289 (59)
169	3-*O*-galloyl(epi)catechin-(4,8)-(epi)catechin	$C_{37}H_{30}O_{16}$	729.1469	729.1461	1.1	20.3	MS^2 → 577 (100), 451 (20), 425 (24), 407 (51), 289 (14); MS^3 → 407 (100), 451 (69), 425 (23), 289 (43)
170	(Epi)catechin-(4,8′)-3′-*O*-galloyl-(epi)catechin	$C_{37}H_{30}O_{16}$	729.1484	729.1461	3.1	23.6	MS^2 → 407 (100), 711 (7), 577 (33), 559 (38), 451 (27), 441 (22), 289 (19); MS^3 → 285 (100)
171	3-*O*-galloyl(epi)catechin-(4,8)-(epi)catechin	$C_{37}H_{30}O_{16}$	729.1462	729.1461	0.1	27.9	MS^2 → 577 (100), 559 (34), 451 (20), 425 (30), 407 (69); MS^3 → 407 (100), 451 (44), 425 (34), 289 (32)
172	(Epi)gallocatechin-(4,8′)-3′-*O*-galloyl-(epi)catechin	$C_{37}H_{30}O_{17}$	745.1416	745.1410	0.8	20.6	MS^2 → 407 (100), 727 (12), 593 (25), 441 (23), 289 (42); MS^3 → 285 (100)
173	(Epi)gallocatechin-(4,8)-3′-*O*-galloyl(epi)gallocatechin	$C_{37}H_{30}O_{18}$	761.1396	761.1359	4.8	13.7	MS^2 → 423 (100), 609 (47), 575 (31), 305 (26); MS^3 → 283 (100)

No.	Compound	Molecular Formula	Experimental Molecular Weight *m/z* [M-H]$^-$	Theoretical Molecular Weight *m/z* [M-H]$^-$	Error (ppm)	RT (min)	Fragmentation
174	(Epi)gallocatechin-(4,8)-3′-*O*-galloyl(epi)gallocatechin	$C_{37}H_{30}O_{18}$	761.1374	761.1359	1.9	25.7	MS^2 → 423 (100), 609 (17), 575 (23), 305 (11); MS^3 → 283 (100)
175	(Epi)catechin-(4,8′/2,7′)-(epi)catechin-(4′,8″)-(epi)catechin	$C_{45}H_{36}O_{18}$	863.1847	863.1829	2.1	22.6	MS^2 → 711 (100), 693 (65), 559 (36), 541 (17), 451 (28), 411 (39), 289 (15); MS^3 → 693 (100), 559 (54), 541 (30), 407 (24)
176	(Epi)catechin-(4,8′/2,7′)-(epi)catechin-(4′,8″)-(epi)catechin	$C_{45}H_{36}O_{18}$	863.1836	863.1829	0.8	23.2	MS^2 → 711 (100), 693 (43), 559 (39), 541 (12), 451 (23), 411 (52), 289 (11); MS^3 → 693 (100), 559 (97), 541 (53), 407 (40)
177	(Epi)catechin-(4,8′)-(epi)catechin-(4′,8″/2′,7″)-(epi)catechin	$C_{45}H_{36}O_{18}$	863.1867	863.1829	4.4	26.7	MS^2 → 575 (100), 711 (77), 693 (64), 559 (44); MS^3 → 449 (100), 539 (32), 289 (20)
178	(Epi)catechin-(4,8′)-(epi)catechin-(4′,8″/2′,7″)-(epi)catechin	$C_{45}H_{36}O_{18}$	863.1850	863.1829	2.4	33.7	MS^2 → 693 (100), 575 (99), 449 (26); MS^3 → 657 (100), 541 (20), 449 (9), 403 (60)
179	Procyanidin Trimer C	$C_{45}H_{38}O_{18}$	865.1946	865.1985	4.6	5.6	MS^2 → 695 (100), 577 (25), 575 (21), 543 (24), 451 (14), 425 (13), 407 (36), 287 (20); MS^3 → 243 (100), 543 (73), 525 (68), 451 (68), 405 (99), 289 (38)
180	Procyanidin Trimer C	$C_{45}H_{38}O_{18}$	865.1959	865.1985	3.0	14.9	MS^2 → 745 (100), 695 (14), 577 (13), 575 (5), 451 (11), 407 (20)
181	Procyanidin Trimer C	$C_{45}H_{38}O_{18}$	865.1984	865.1985	0.2	15.6	MS^2 → 695 (100), 577 (75), 575 (21), 543 (29), 451 (29), 425 (27), 407 (64), 287 (29); MS^3 → 243 (100), 543 (99), 525 (92), 451 (46), 405 (34), 289 (39)

No.	Compound	Molecular Formula	Experimental Molecular Weight *m/z* [M-H]$^-$	Theoretical Molecular Weight *m/z* [M-H]$^-$	Error (ppm)	RT (min)	Fragmentation
182	Procyanidin Trimer C	$C_{45}H_{38}O_{18}$	865.2017	865.1985	3.7	16.6	MS^2 → 695 (100), 577 (52), 575 (34), 543 (36), 451 (27), 425 (29), 407 (65), 287 (30); MS^3 → 543 (100), 525 (71), 451 (32), 405 (26), 289 (20), 243 (43)
183	Procyanidin Trimer C	$C_{45}H_{38}O_{18}$	865.1984	865.1985	0.2	19.2	MS^2 → 695 (100), 577 (58), 575 (47), 543 (30), 451 (28), 425 (20), 407 (70), 287 (60); MS^3 → 543 (100), 525 (14), 451 (23), 405 (20), 289 (1), 243 (27)
184	Procyanidin Trimer C	$C_{45}H_{38}O_{18}$	865.1966	865.1985	2.2	22.2	MS^2 → 711 (100), 695 (63), 577 (15), 575 (15), 543 (18), 451 (28), 425 (13), 407 (34), 287 (16); MS^3 → 693 (100), 559 (55), 541 (37), 407 (28), 285 (4)
185	Procyanidin Trimer C	$C_{45}H_{38}O_{18}$	865.2010	865.1985	2.8	25.6	MS^2 → 695 (100), 577 (65), 575 (31), 543 (26), 451 (20), 425 (24), 407 (62), 287 (26); MS^3 → 543 (100), 525 (38), 451 (19), 405 (21), 289 (15), 283 (13), 243 (41)
186	(Epi)gallocatechin-(4,8′)-(epi)catechin-(4′,8″)-(epi)catechin	$C_{45}H_{38}O_{19}$	881.1961	881.1935	3.0	11.1	MS^2 → 695 (100), 755 (24), 577 (27), 451 (17), 407 (23), 303 (6); MS^3 → 243 (100), 543 (98), 525 (72), 451 (69), 289 (27)
187	(Epi)catechin-(4,8′)-(epi)gallocatechin-(4′,8″)-(epi)catechin	$C_{45}H_{38}O_{19}$	881.1938	881.1935	0.4	12.1	MS^2 → 711 (100), 695 (31), 593 (56), 543 (59), 425 (39), 407 (68), 289 (42); MS^3 → 543 (100), 525 (60), 407 (28), 289 (32)
188	(Epi)gallocatechin-(4,8′)-(epi)catechin-(4′,8″)-(epi)catechin	$C_{45}H_{38}O_{19}$	881.1969	881.1935	3.9	13.2	MS^2 → 695 (100), 755 (21), 577 (19), 451 (18), 407 (14), 303 (7); MS^3 → 543 (100), 525 (50), 451 (50), 289 (11), 243 (37)

No.	Compound	Molecular Formula	Experimental Molecular Weight *m/z* [M-H]$^-$	Theoretical Molecular Weight *m/z* [M-H]$^-$	Error (ppm)	RT (min)	Fragmentation
189	(Epi)gallocatechin-(4,8′/2,7′)-(epi)gallocatechin-(4′,8″)-(epi)catechin	$C_{45}H_{36}O_{20}$	895.1767	895.1727	4.4	15.9	MS^2 → 727 (100), 709 (17), 575 (12), 467 (3), 427 (20), 289 (6); MS^3 → 575 (100), 525 (22), 407 (58)
190	(Epi)gallocatechin-(4,8′)-(epi)gallocatechin-(4′,8″)-(epi)catechin	$C_{45}H_{38}O_{20}$	897.1887	897.1884	0.4	9.1	MS^2 → 711 (100), 771 (23), 543 (52), 467 (14), 423 (26), 407 (26), 289 (9); MS^3 → 283 (100), 297 (73), 243 (58)
191	Procyanidin trimer gallate	$C_{52}H_{42}O_{22}$	508.1032	508.1011	4.1	13.1	MS^2 → 695 (100), 727 (35), 577 (37), 303 (99), 289 (55); MS^3 → 525 (100), 451 (60), 289 (28), 243 (25)
192	Procyanidin trimer gallate	$C_{52}H_{42}O_{22}$	508.1026	508.1011	2.9	18.3	MS^2 → 423 (100), 727 (40), 695 (12), 303 (37), 289 (55); MS^3 → 243 (100), 289 (71)
193	A type procyanidin tetramer	$C_{60}H_{48}O_{24}$	575.1217	575.1195	3.8	12.9	MS^2 → 863 (100), 711 (18), 499 (32), 490 (45), 451 (20), 289 (21), 245 (14); MS^3 → 411 (100), 711 (83), 693 (46), 573 (45), 559 (65), 451 (43), 289 (25)
194	A type procyanidin tetramer	$C_{60}H_{48}O_{24}$	575.1202	575.1195	1.2	19.5	MS^2 → 861 (100), 739 (16), 559 (7), 499 (9), 491 (7), 451 (11), 411 (47), 407 (13), 289 (71), 245 (11); MS^3 → 411 (100), 691 (85), 449 (40), 287 (73), 243 (9)
195	A type procyanidin tetramer	$C_{60}H_{48}O_{24}$	575.1206	575.1195	1.9	24.5	MS^2 → 861 (100), 739 (14), 547 (8), 499 (12), 490 (8), 451 (18), 411 (59), 289 (66), 245 (9); MS^3 → 411 (100), 691 (50), 573 (86), 547 (84), 529 (47), 449 (40), 287 (69)

No.	Compound	Molecular Formula	Experimental Molecular Weight *m/z* [M-H]$^-$	Theoretical Molecular Weight *m/z* [M-H]$^-$	Error (ppm)	RT (min)	Fragmentation
196	A type procyanidin tetramer	$C_{60}H_{48}O_{24}$	575.1223	575.1195	4.9	25.9	MS^2 → 863 (100), 739 (10), 693 (9), 491 (37), 451 (27), 423 (17), 407 (33), 289 (99), 245 (11); MS^3 → 575 (100), 449 (38), 287 (73), 245 (18)
197	Procyanidin tetramer	$C_{60}H_{50}O_{24}$	576.1286	576.1273	2.2	17.7	MS^2 → 865 (100), 739 (25), 693 (14), 491 (50), 451 (38), 407 (55), 289 (74), 287 (71), 245 (24); MS^3 → 695 (100), 543 (67), 451 (40), 245 (45)
198	Procyanidin tetramer	$C_{60}H_{50}O_{24}$	576.1284	576.1273	1.9	21.3	MS^2 → 863 (100), 739 (15), 693 (11), 491 (72), 451 (33), 425 (73), 407 (57), 289 (91), 287 (48), 245 (11); MS^3 → 695 (100), 575 (46), 449 (47), 243 (18)
199	Procyanidin tetramer	$C_{60}H_{50}O_{24}$	576.1293	576.1273	3.4	22.2	MS^2 → 863 (100), 739 (22), 693 (12), 491 (58), 451 (32), 425 (28), 407 (55), 289 (96), 287 (36), 245 (16); MS^3 → 575 (100), 693 (29), 449 (78), 243 (66)
200	Procyanidin tetramer	$C_{60}H_{50}O_{24}$	576.1273	576.1273	0.0	24.5	MS^2 → 407 (100), 863 (99), 739 (14), 693 (6), 491 (44), 451 (44), 425 (55), 289 (91), 287 (59), 245 (20); MS^3 → 285 (100), 243 (46)
201	Procyanidin tetramer	$C_{60}H_{50}O_{24}$	576.1298	576.1273	4.3	26.2	MS^2 → 863 (100), 739 (8), 693 (6), 491 (30), 451 (13), 425 (14), 407 (25), 289 (99), 287 (39), 245 (13); MS^3 → 575 (100), 693 (32), 449 (57), 245 (19)

No.	Compound	Molecular Formula	Experimental Molecular Weight *m/z* [M-H]$^-$	Theoretical Molecular Weight *m/z* [M-H]$^-$	Error (ppm)	RT (min)	Fragmentation
202	Procyanidin tetramer	$C_{60}H_{50}O_{24}$	576.1293	576.1273	3.4	30.5	MS^2 → 863 (100), 739 (14), 693 (4), 491 (26), 451 (17), 425 (24), 407 (33), 289 (82), 287 (35), 243 (17); MS^3 → 413 (100), 693 (4), 575 (62), 287 (67)
	Flavanone and Flavanone Glycosides						
	1. Naringenin						
203	(±)-Naringenin	$C_{15}H_{12}O_5$	271.0600	271.0612	4.4	47.9	MS^2 → 151 (100), 177 (24); MS^3 → 107 (100)
204	Naringenin-*O*-hexoside	$C_{21}H_{22}O_{10}$	433.1129	433.1140	2.6	38.3	MS^2 → 271 (100); MS^3 → 151 (100), 177 (10); MS^4 → 107 (100)
205	Naringenin-*O*-hexoside-*O*-pentoside	$C_{26}H_{30}O_{14}$	565.1582	565.1563	3.4	38.0	MS^2 → 271 (100); MS^3 → 151 (100)
	2. Taxifolin						
206	(±)-Taxifolin	$C_{15}H_{12}O_7$	303.0500	303.0510	3.4	29.1	MS^2 → 285 (100), 177 (10), 125 (9); MS^3 → 241 (100)
207	Taxifolin-*O*-pentoside	$C_{20}H_{20}O_{11}$	435.0950	435.0933	3.9	27.8	MS^2 → 285 (100), 303 (53); MS^3 → 241 (100), 175 (50)
208	Taxifolin-*O*-pentoside	$C_{20}H_{20}O_{11}$	435.0954	435.0933	4.9	31.1	MS^2 → 285 (100), 303 (12); MS^3 → 241 (100), 175 (38)
209	Taxifolin-*O*-pentoside	$C_{20}H_{20}O_{11}$	435.0943	435.0933	2.3	32.4	MS^2 → 285 (100), 303 (12); MS^3 → 241 (100), 175 (33)
210	Taxifolin-*O*-pentoside	$C_{20}H_{20}O_{11}$	435.0933	435.0933	0.0	33.6	MS^2 → 303 (100), 285 (97); MS^3 → 241 (100), 175 (64)
211	Taxifolin-*O*-pentoside	$C_{20}H_{20}O_{11}$	435.0954	435.0933	4.9	35.5	MS^2 → 285 (100), 303 (7); MS^3 → 241 (100), 175 (39)

No.	Compound	Molecular Formula	Experimental Molecular Weight *m/z* [M-H]$^-$	Theoretical Molecular Weight *m/z* [M-H]$^-$	Error (ppm)	RT (min)	Fragmentation
212	Taxifolin-*O*-rhamnoside	$C_{21}H_{22}O_{11}$	449.1109	449.1089	4.4	36.2	MS^2 → 285 (100), 303 (54); MS^3 → 241 (100)
213	Taxifolin-*O*-rhamnoside	$C_{21}H_{22}O_{11}$	449.1084	449.1089	1.2	36.6	MS^2 → 285 (100), 303 (51); MS^3 → 241 (100)
214	Taxifolin-*O*-rhamnoside	$C_{21}H_{22}O_{11}$	449.1103	449.1089	3.0	37.4	MS^2 → 285 (100), 303 (59); MS^3 → 241 (100)
215	Taxifolin-*O*-hexoside	$C_{21}H_{22}O_{12}$	465.1041	465.1039	0.5	15.1	MS^2 → 303 (100); MS^3 → 285 (100); MS^4 → 241 (100), 175 (48)
216	Taxifolin-*O*-hexoside	$C_{21}H_{22}O_{12}$	465.1045	465.1039	1.4	19.3	MS^2 → 303 (100); MS^3 → 285 (100); MS^4 → 241 (100), 175 (73)
217	Taxifolin-*O*-hexoside	$C_{21}H_{22}O_{12}$	465.1032	465.1039	1.4	22.8	MS^2 → 285 (100), 303 (11); MS^3 → 241 (100), 175 (33)
218	Taxifolin-*O*-hexoside	$C_{21}H_{22}O_{12}$	465.1037	465.1039	0.3	24.8	MS^2 → 285 (100), 303 (7); MS^3 → 241 (100), 175 (36)
219	Taxifolin-*O*-hexoside	$C_{21}H_{22}O_{12}$	465.1043	465.1039	1.0	26.2	MS^2 → 285 (100), 303 (30); MS^3 → 241 (100), 175 (41)
220	Taxifolin-*O*-hexoside	$C_{21}H_{22}O_{12}$	465.1055	465.1039	3.5	27.9	MS^2 → 285 (100), 303 (25); MS^3 → 241 (100), 175 (37)
221	Taxifolin-*O*-hexoside	$C_{21}H_{22}O_{12}$	465.1052	465.1039	2.9	30.0	MS^2 → 303 (100), 285 (6); MS^3 → 151 (100)
222	Taxifolin-*O*-acetyl-rhamnoside	$C_{23}H_{24}O_{12}$	491.1219	491.1195	4.9	39.9	MS^2 → 285 (100), 303 (7); MS^3 → 241 (100)
223	Taxifolin-*O*-acetyl-rhamnoside	$C_{23}H_{24}O_{12}$	491.1214	491.1195	3.9	45.0	MS^2 → 285 (100), 303 (2); MS^3 → 241 (100)
224	Taxifolin-*O*-acetyl-hexoside	$C_{23}H_{24}O_{13}$	507.1168	507.1144	4.7	46.7	MS^2 → 285 (100), 303 (8); MS^3 → 241 (100), 175 (50), 151 (13)
225	Taxifolin-*O*-acetyl-hexoside	$C_{23}H_{24}O_{13}$	507.1165	507.1144	4.1	48.1	MS^2 → 285 (100), 303 (2); MS^3 → 241 (100), 175 (17), 151 (17)
226	Taxifolin-*O*-pentoside-*O*-hexoside (diff side)	$C_{26}H_{30}O_{16}$	597.1484	597.1461	3.8	17.7	MS^2 → 435 (100); MS^3 → 285 (100), 303 (5); MS^4 → 241 (100)

No.	Compound	Molecular Formula	Experimental Molecular Weight *m/z* $[M-H]^-$	Theoretical Molecular Weight *m/z* $[M-H]^-$	Error (ppm)	RT (min)	Fragmentation
227	Taxifolin-*O*-rhamnoside-*O*-hexoside	$C_{27}H_{32}O_{16}$	611.1640	611.1618	3.7	20.1	MS^2 → 449 (100); MS^3 → 285 (100), 303 (46); MS^4 → 241 (100)
228	Taxifolin-*O*-rhamnoside-*O*-hexoside	$C_{27}H_{32}O_{16}$	611.1624	611.1618	1.0	32.8	MS^2 → 449 (100); MS^3 → 285 (100), 303 (33); MS^4 → 241 (100)
	Flavonol and Flavonol Glycosides						
	1. Myricetin						
229	Myricetin	$C_{15}H_{10}O_8$	317.0297	317.0303	1.9	38.9	MS^2 → 179 (100); MS^3 → 151 (100)
230	Myricetin-*O*-pentoside	$C_{20}H_{18}O_{12}$	449.0746	449.0726	4.6	32.1	MS^2 → 317 (100), 316 (77); MS^3 → 271 (100), 179 (94) 151 (35)
231	Myricetin-*O*-pentoside	$C_{20}H_{18}O_{12}$	449.0735	449.0726	2.1	37.8	MS^2 → 316 (100), 317 (44); MS^3 → 271 (100), 179 (15), 151 (8)
232	Myricetin-*O*-pentoside	$C_{20}H_{18}O_{12}$	449.0741	449.0726	3.5	39.1	MS^2 → 317 (100); MS^3 → 179 (100); MS^4 → 151 (100)
233	Myricetin-*O*-rhamnoside	$C_{21}H_{20}O_{12}$	463.0895	463.0882	2.8	33.0	MS^2 → 316 (100), 317 (68); MS^3 → 271 (100), 179 (53), 151 (18)
234	Myricetin-*O*-hexoside	$C_{21}H_{20}O_{13}$	479.0809	479.0831	4.6	30.8	MS^2 → 316 (100), 317 (89); MS^3 → 271 (100), 179 (53) 151 (19)
235	Myricetin-*O*-hexoside	$C_{21}H_{20}O_{13}$	479.0808	479.0831	4.8	31.2	MS^2 → 316 (100), 317 (99); MS^3 → 271 (100), 179 (56) 151 (31)
236	Myricetin-*O*-hexoside	$C_{21}H_{20}O_{13}$	479.0842	479.0831	2.3	35.3	MS^2 → 317 (100); MS^3 → 179 (100); MS^4 → 151 (100)
237	Myricetin-*O*-glucuronide	$C_{21}H_{18}O_{14}$	493.0630	493.0624	1.3	36.5	MS^2 → 317 (100); MS^3 → 179 (100); MS^4 → 151 (100)
238	Myricetin-*O*-acetyl-rhamnoside	$C_{23}H_{22}O_{13}$	505.0995	505.0988	1.5	37.6	MS^2 → 316 (100), 317 (36); MS^3 → 271 (100), 179 (10), 151 (8)

No.	Compound	Molecular Formula	Experimental Molecular Weight *m/z* [M-H]$^-$	Theoretical Molecular Weight *m/z* [M-H]$^-$	Error (ppm)	RT (min)	Fragmentation
239	Myricetin-*O*-dipentoside (diff side)	$C_{25}H_{26}O_{16}$	581.1144	581.1148	0.7	41.4	MS^2 → 449 (100); MS^3 → 317 (100); MS^4 → 179 (100), 271 (27), 151 (30)
240	Myricetin-*O*-dipentoside (same side)	$C_{25}H_{26}O_{16}$	581.1147	581.1148	0.2	42.5	MS^2 → 317 (100); MS^3 → 179 (100), 271 (36); MS^4 → 151 (100)
241	Myricetin-*O*-benzoyl-hexoside	$C_{28}H_{24}O_{14}$	583.1112	583.1093	3.2	45.7	MS^2 → 316 (100), 317 (66); MS^3 → 271 (100), 179 (56), 151 (28)
242	Myricetin-*O*-galloyl-rhamnoside	$C_{28}H_{24}O_{16}$	615.0992	615.0992	0.0	38.5	MS^2 → 317 (100), 463 (36); MS^3 → 179 (100); MS^4 → 151 (100)
243	Myricetin-*O*-galloyl-rhamnoside	$C_{28}H_{24}O_{16}$	615.1022	615.0992	4.9	39.2	MS^2 → 317 (100), 463 (24); MS^3 → 179 (100); MS^4 → 151 (100)
244	Myricetin-*O*-rutinoside	$C_{27}H_{30}O_{17}$	625.1438	625.1410	4.4	31.4	MS^2 → 317 (100), 316 (92); MS^3 → 271 (100), 179 (52), 151 (18)
245	Myricetin-3-*O*-hexoside-7-*O*-rhamnoside	$C_{27}H_{30}O_{17}$	625.1415	625.1410	0.8	35.4	MS^2 → 463 (100); MS^3 → 316 (100), 317 (72); MS^4 → 271 (100), 179 (44), 151 (37)
246	Myricetin-*O*-galloyl-hexoside	$C_{28}H_{24}O_{17}$	631.0928	631.0941	2.0	30.5	MS^2 → 316 (100), 317 (73); MS^3 → 271 (100), 179 (60), 151 (19)
247	Myricetin-7-*O*-galloyl-3-*O*-hexoside	$C_{28}H_{24}O_{17}$	631.0920	631.0941	3.3	32.5	MS^2 → 479 (100); MS^3 → 316 (100), 317 (75); MS^4 → 271 (100), 179 (75), 151 (26)
	2. Quercetin						
248	Quercetin	$C_{15}H_{10}O_7$	301.0355	301.0354	0.4	44.4	MS^2 → 179 (100); MS^3 → 151 (100)
249	Quercetin-*O*-pentoside	$C_{20}H_{18}O_{11}$	433.0788	433.0776	2.7	36.6	MS^2 → 301 (100); MS^3 → 179 (100), 151 (87)
250	Quercetin-*O*-pentoside	$C_{20}H_{18}O_{11}$	433.0797	433.0776	4.8	37.4	MS^2 → 301 (100); MS^3 → 179 (100), 151 (82)
251	Quercetin-*O*-pentoside	$C_{20}H_{18}O_{11}$	433.0776	433.0776	0.0	39.6	MS^2 → 301 (100); MS^3 → 151 (100), 179 (89)

No.	Compound	Molecular Formula	Experimental Molecular Weight *m/z* [M-H]$^-$	Theoretical Molecular Weight *m/z* [M-H]$^-$	Error (ppm)	RT (min)	Fragmentation
252	Quercetin-*O*-pentoside	$C_{20}H_{18}O_{11}$	433.0781	433.0776	1.1	41.2	MS^2 → 301 (100); MS^3 → 271 (100), 179 (44), 151 (32)
253	Quercetin-*O*-rhamnoside	$C_{21}H_{20}O_{11}$	447.0952	447.0933	4.3	38.7	MS^2 → 301 (100); MS^3 → 179 (100), 151 (87)
254	Quercetin-*O*-hexoside	$C_{21}H_{20}O_{12}$	463.0898	463.0882	3.5	34.2	MS^2 → 301 (100); MS^3 → 179 (100), 151 (90)
255	Quercetin-*O*-hexoside	$C_{21}H_{20}O_{12}$	463.0880	463.0882	0.4	35.5	MS^2 → 301 (100); MS^3 → 179 (100), 151 (87)
256	Quercetin-*O*-hexoside	$C_{21}H_{20}O_{12}$	463.0896	463.0882	3.0	40.7	MS^2 → 301 (100); MS^3 → 179 (100), 151 (88)
257	Quercetin-*O*-acetyl-pentoside	$C_{22}H_{20}O_{12}$	475.0884	475.0882	0.4	43.2	MS^2 → 300 (100), 301 (25); MS^3 → 271 (100), 179 (2), 151 (2)
258	Quercetin-*O*-acetyl-pentoside	$C_{22}H_{20}O_{12}$	475.0880	475.0882	0.4	45.5	MS^2 → 300 (100), 301 (56); MS^3 → 271 (100), 179 (16), 151 (15)
259	Quercetin-*O*-acetyl-pentoside	$C_{22}H_{20}O_{12}$	475.0903	475.0882	4.4	48.0	MS^2 → 300 (100), 301 (61); MS^3 → 271 (100), 255 (70), 179 (24), 151 (17)
260	Quercetin-*O*-glucuronide	$C_{21}H_{18}O_{13}$	477.0694	477.0675	4.1	40.8	MS^2 → 301 (100); MS^3 → 179 (100), 151 (78)
261	Quercetin-*O*-acetyl-rhamnoside	$C_{23}H_{22}O_{12}$	489.1055	489.1039	3.4	43.5	MS^2 → 300 (100), 301 (75); MS^3 → 271 (100), 179 (37), 151 (32)
262	Quercetin-*O*-acetyl-rhamnoside	$C_{23}H_{22}O_{12}$	489.1041	489.1039	0.5	45.5	MS^2 → 301 (100); MS^3 → 271 (100), 179 (61), 151 (58)
263	Quercetin-*O*-acetyl-rhamnoside	$C_{23}H_{22}O_{12}$	489.1057	489.1039	3.8	47.6	MS^2 → 300 (100), 301 (40); MS^3 → 271 (100), 179 (12), 151 (11)
264	Quercetin-*O*-acetyl-hexoside	$C_{23}H_{22}O_{13}$	505.0989	505.0988	0.3	38.0	MS^2 → 301 (100), 463 (59); MS^3 → 271 (100), 179 (96), 151 (83)
265	Quercetin-*O*-acetyl-hexoside	$C_{23}H_{22}O_{13}$	505.0985	505.0988	0.5	40.0	MS^2 → 301 (100), 463 (27); MS^3 → 271 (100), 179 (97), 151 (66)
266	Quercetin-*O*-acetyl-hexoside	$C_{23}H_{22}O_{13}$	505.1013	505.0988	5.0	42.0	MS^2 → 301 (100), 463 (42); MS^3 → 271 (100), 179 (58), 151 (46)

No.	Compound	Molecular Formula	Experimental Molecular Weight *m/z* [M-H]$^-$	Theoretical Molecular Weight *m/z* [M-H]$^-$	Error (ppm)	RT (min)	Fragmentation
267	Quercetin-*O*-acetyl-hexoside	$C_{23}H_{22}O_{13}$	505.0995	505.0988	1.5	42.8	MS^2 → 301 (100), 463 (16); MS^3 → 271 (100), 179 (44), 151 (41)
268	Quercetin-*O*-acetyl-hexoside	$C_{23}H_{22}O_{13}$	505.1010	505.0988	4.4	43.4	MS^2 → 301 (100), 463 (43); MS^3 → 271 (100), 179 (62), 151 (58)
269	Quercetin-*O*-acetyl-hexoside	$C_{23}H_{22}O_{13}$	505.1000	505.0988	2.4	44.0	MS^2 → 301 (100), 463 (56); MS^3 → 300 (100), 271 (61), 179 (65), 151 (57)
270	Quercetin-*O*-acetyl-hexoside	$C_{23}H_{22}O_{13}$	505.1001	505.0988	2.6	45.6	MS^2 → 301 (100), 463 (15); MS^3 → 179 (100), 271 (72), 151 (79)
271	Quercetin-*O*-acetyl-hexoside	$C_{23}H_{22}O_{13}$	505.1004	505.0988	3.2	46.5	MS^2 → 301 (100), 463 (52); MS^3 → 271 (100), 179 (54), 151 (53)
272	Quercetin-*O*-diacetyl-hexoside	$C_{25}H_{24}O_{14}$	547.1111	547.1093	3.2	51.5	MS^2 → 300 (100), 301 (66); MS^3 → 271 (100), 179 (27), 151 (25)
273	Quercetin-*O*-dipentoside (same side)	$C_{25}H_{26}O_{15}$	565.1216	565.1199	3.0	33.8	MS^2 → 300 (100), 301 (46); MS^3 → 271 (100), 255 (54), 179 (8), 151 (10)
274	Quercetin-*O*-dipentoside (same side)	$C_{25}H_{26}O_{15}$	565.1219	565.1199	3.6	36.3	MS^2 → 300 (100), 301 (58); MS^3 → 271 (100), 255 (46), 179 (40), 151 (21)
275	Quercetin-*O*-benzoyl-hexoside	$C_{28}H_{24}O_{13}$	567.1146	567.1144	0.3	49.7	MS^2 → 301 (100); MS^3 → 271 (100), 255 (61), 179 (94), 151 (78)
276	Quercetin-*O*-pentoside-*O*-rhamnoside (same side)	$C_{26}H_{28}O_{15}$	579.1371	579.1355	2.7	37.2	MS^2 → 301 (100); MS^3 → 179 (100), 271 (43), 151 (93)
277	Quercetin-*O*-(*p*-hydroxy)-benzoyl-hexoside	$C_{28}H_{24}O_{14}$	583.1093	583.1093	0.0	41.7	MS^2 → 463 (100); MS^3 → 301 (100); MS^4 → 179 (100), 151 (49)
278	Quercetin-*O*-(*p*-hydroxy)-benzoyl-hexoside	$C_{28}H_{24}O_{14}$	583.1111	583.1093	3.0	44.0	MS^2 → 463 (100); MS^3 → 301 (100); MS^4 → 179 (100), 151 (96)
279	Quercetin-*O*-(*p*-hydroxy)-benzoyl-hexoside	$C_{28}H_{24}O_{14}$	583.1099	583.1093	1.0	49.8	MS^2 → 463 (100); MS^3 → 301 (100); MS^4 → 179 (100), 151 (90)

No.	Compound	Molecular Formula	Experimental Molecular Weight *m/z* [M-H]$^-$	Theoretical Molecular Weight *m/z* [M-H]$^-$	Error (ppm)	RT (min)	Fragmentation
280	Quercetin-*O*-galloyl-pentoside	$C_{27}H_{22}O_{15}$	585.0886	585.0886	0.0	39.1	MS^2 → 433 (100); MS^3 → 301 (100); MS^4 → 179 (100), 151 (52)
281	Quercetin-*O*-galloyl-pentoside	$C_{27}H_{22}O_{15}$	585.0897	585.0886	1.9	42.9	MS^2 → 301 (100), 429 (40); MS^3 → 179 (100), 151 (86)
282	Quercetin-3-*O*-(4"-3-hydroxy-3-methylglutaryl)-α-rhamnoside	$C_{27}H_{28}O_{15}$	591.1385	591.1355	5.0	44.9	MS^2 → 301 (100), 463 (17); MS^3 → 179 (100); MS^4 → 151 (100)
283	Quercetin-*O*-coumaroyl-rhamnoside	$C_{30}H_{26}O_{13}$	593.1303	593.1301	0.4	52.0	MS^2 → 301 (100), 445 (18); MS^3 → 179 (100); MS^4 → 151 (100)
284	Quercetin-*O*-coumaroyl-rhamnoside	$C_{30}H_{26}O_{13}$	593.1304	593.1301	0.6	55.1	MS^2 → 301 (100), 445 (12); MS^3 → 271 (100), 179 (72), 151 (80)
285	Quercetin-*O*-pentoside-*O*-hexoside (diff side)	$C_{26}H_{28}O_{16}$	595.1329	595.1305	4.1	24.7	MS^2 → 463 (100), 433 (32); MS^3 → 301 (100)
286	Quercetin-*O*-pentoside-*O*-hexoside (same side)	$C_{26}H_{28}O_{16}$	595.1322	595.1305	2.9	30.4	MS^2 → 300 (100), 301 (57); MS^3 → 271 (100), 255 (74), 179 (34), 151 (19)
287	Quercetin-*O*-protocatechuoyl-hexoside	$C_{28}H_{24}O_{15}$	599.1031	599.1042	1.9	40.6	MS^2 → 463 (100); MS^3 → 301 (100); MS^4 → 179 (100), 271 (65), 151 (70)
288	Quercetin-*O*-galloyl-rhamnoside	$C_{28}H_{24}O_{15}$	599.1048	599.1042	0.9	43.4	MS^2 → 301 (100); MS^3 → 179 (100); MS^4 → 151 (100)
289	Quercetin-*O*-rhamnoside-*O*-hexoside	$C_{27}H_{30}O_{16}$	609.1476	609.1461	2.4	25.7	MS^2 → 447 (100), 463 (91); MS^3 → 300 (100), 301 (63); MS^4 → 271 (100)
290	Quercetin-*O*-rhamnoside-*O*-hexoside	$C_{27}H_{30}O_{16}$	609.1469	609.1461	1.3	28.8	MS^2 → 300 (100), 301 (66); MS^3 → 271 (100), 179 (12), 151 (19)
291	Quercetin-*O*-rhamnoside-*O*-hexoside	$C_{27}H_{30}O_{16}$	609.1473	609.1461	2.0	30.3	MS^2 → 300 (100), 301 (44); MS^3 → 271 (100), 179 (11), 151 (14)
292	Quercetin-*O*-rhamnoside-*O*-hexoside	$C_{27}H_{30}O_{16}$	609.1470	609.1461	1.5	31.5	MS^2 → 447 (100), 463 (57); MS^3 → 301 (100), 179 (1), 151 (1)

No.	Compound	Molecular Formula	Experimental Molecular Weight *m/z* [M-H]$^-$	Theoretical Molecular Weight *m/z* [M-H]$^-$	Error (ppm)	RT (min)	Fragmentation
293	Quercetin-*O*-rhamnoside-*O*-hexoside (Rutin)	$C_{27}H_{30}O_{16}$	609.1478	609.1461	2.8	34.3	MS^2 → 301 (100); MS^3 → 179 (100), 271 (88), 151 (78)
294	Quercetin-*O*-rhamnoside-*O*-hexoside (Rutin)	$C_{27}H_{30}O_{16}$	609.1476	609.1461	2.4	35.0	MS^2 → 301 (100); MS^3 → 179 (100), 151 (74)
295	Quercetin-*O*-coumaroyl-hexoside	$C_{30}H_{26}O_{14}$	609.1262	609.1250	2.0	46.4	MS^2 → 463 (100); MS^3 → 301 (100); MS^4 → 179 (100), 151 (86)
296	Quercetin-*O*-coumaroyl-hexoside	$C_{30}H_{26}O_{14}$	609.1258	609.1250	1.3	47.8	MS^2 → 301 (100), 463 (48); MS^3 → 179 (100), 151 (57)
297	Quercetin-*O*-coumaroyl-hexoside	$C_{30}H_{26}O_{14}$	609.1269	609.1250	3.2	49.5	MS^2 → 463 (100); MS^3 → 301 (100); MS^4 → 179 (100), 151 (82)
298	Quercetin-*O*-galloyl-hexoside	$C_{28}H_{24}O_{16}$	615.1006	615.0992	2.3	34.5	MS^2 → 463 (100); MS^3 → 301 (100); MS^4 → 179 (100), 151 (84)
299	Quercetin-*O*-galloyl-hexoside	$C_{28}H_{24}O_{16}$	615.1000	615.0992	1.4	35.5	MS^2 → 463 (100); MS^3 → 301 (100); MS^4 → 179 (100), 151 (96)
300	Quercetin-*O*-feruloyl-rhamnoside	$C_{31}H_{28}O_{14}$	623.1410	623.1406	0.6	56.5	MS^2 → 301 (100); MS^3 → 271 (100), 179 (59), 151 (53)
301	Cypellogin A/B	$C_{31}H_{34}O_{14}$	629.1899	629.1876	3.7	48.7	MS^2 → 463 (100); MS^3 → 301 (100); MS^4 → 179 (100), 151 (75)
302	Cypellogin A/B	$C_{31}H_{34}O_{14}$	629.1894	629.1876	2.9	50.6	MS^2 → 301 (100); MS^3 → 179 (100), 271 (71); MS^4 → 151 (100)
303	Cypellogin A/B	$C_{31}H_{34}O_{14}$	629.1905	629.1876	4.6	51.7	MS^2 → 463 (100); MS^3 → 301 (100); MS^4 → 271 (100), 179 (98)
304	Cypellogin C	$C_{31}H_{36}O_{14}$	631.2063	631.2032	4.9	52.6	MS^2 → 301 (100), 463 (64); MS^3 → 179 (100), 271 (60); MS^4 → 151 (100)
305	Quercetin-3-(4"-*O*-acetyl)-*O*-rhamnoside-7-*O*-rhamnoside	$C_{29}H_{32}O_{16}$	635.1643	635.1618	4.0	40.7	MS^2 → 489 (100); MS^3 → 300 (100); MS^4 → 271 (100), 179 (8), 151 (10)

No.	Compound	Molecular Formula	Experimental Molecular Weight *m/z* $[M-H]^-$	Theoretical Molecular Weight *m/z* $[M-H]^-$	Error (ppm)	RT (min)	Fragmentation
306	Quercetin-*O*-feruloyl-hexoside	$C_{31}H_{28}O_{15}$	639.1361	639.1355	0.9	47.4	MS^2 → 463 (100), 477 (29); MS^3 → 301 (100); MS^4 → 179 (100), 151 (38)
307	Quercetin-*O*-feruloyl-hexoside	$C_{31}H_{28}O_{15}$	639.1364	639.1355	1.3	50.9	MS^2 → 463 (100), 477 (28); MS^3 → 301 (100); MS^4 → 179 (100), 151 (78)
308	Quercetin-3-*O*-acetyl-hexoside-rhamnoside	$C_{29}H_{32}O_{17}$	651.1568	651.1567	0.2	42.7	MS^2 → 591 (100), 609 (44); MS^3 → 300 (100), 301 (60); MS^4 → 271 (100), 179 (9), 151 (14)
309	Quercetin-*O*-sinapoyl-hexoside	$C_{32}H_{30}O_{16}$	669.1460	669.1461	0.2	51.7	MS^2 → 463 (100); MS^3 → 301 (100); MS^4 → 151 (100), 271 (63), 179 (96)
	3. Kaempferol						
310	Kaempferol	$C_{15}H_{10}O_6$	285.0405	285.0405	0.0	49.5	MS^2 → 151 (100), 257 (11); MS^3 → 107 (100)
311	Kaempferol-*O*-pentoside	$C_{20}H_{18}O_{10}$	417.0808	417.0827	4.6	41.0	MS^2 → 284 (100), 285 (91); MS^3 → 255 (100), 151 (1)
312	Kaempferol-*O*-pentoside	$C_{20}H_{18}O_{10}$	417.0812	417.0827	3.6	43.9	MS^2 → 285 (100), 284 (28); MS^3 → 255 (100), 151 (1)
313	Kaempferol-*O*-rhamnoside	$C_{21}H_{20}O_{10}$	431.1003	431.0984	4.5	43.6	MS^2 → 285 (100), 284 (22); MS^3 → 255 (100), 151 (1)
314	Kaempferol-*O*-hexoside	$C_{21}H_{20}O_{11}$	447.0930	447.0933	0.6	37.5	MS^2 → 284 (100), 285 (79); MS^3 → 255 (100), 151 (2)
315	Kaempferol-*O*-hexoside	$C_{21}H_{20}O_{11}$	447.0924	447.0933	2.0	39.0	MS^2 → 285 (100), 284 (93); MS^3 → 255 (100), 151 (1)
316	Kaempferol-*O*-acetyl-pentoside	$C_{22}H_{20}O_{11}$	459.0941	459.0933	1.8	47.6	MS^2 → 284 (100); MS^3 → 255 (100)
317	Kaempferol-*O*-acetyl-pentoside	$C_{22}H_{20}O_{11}$	459.0938	459.0933	1.1	50.1	MS^2 → 284 (100); MS^3 → 255 (100)
318	Kaempferol-*O*-glucuronide	$C_{21}H_{18}O_{12}$	461.0726	461.0726	0.0	43.6	MS^2 → 285 (100); MS^3 → 257 (100), 151 (11)

No.	Compound	Molecular Formula	Experimental Molecular Weight *m/z* [M-H]$^-$	Theoretical Molecular Weight *m/z* [M-H]$^-$	Error (ppm)	RT (min)	Fragmentation
319	Kaempferol-*O*-acetyl-rhamnoside	$C_{23}H_{22}O_{11}$	473.1106	473.1089	3.5	48.2	MS^2 → 285 (100); MS^3 → 255 (100)
320	Kaempferol-*O*-acetyl-rhamnoside	$C_{23}H_{22}O_{11}$	473.1109	473.1089	4.2	52.3	MS^2 → 285 (100), 413 (45); MS^3 → 255 (100)
321	Kaempferol-*O*-acetyl-hexoside	$C_{23}H_{22}O_{12}$	489.1062	489.1039	4.8	44.5	MS^2 → 285 (100); MS^3 → 255 (100), 151 (1)
322	Kaempferol-*O*-acetyl-hexoside	$C_{23}H_{22}O_{12}$	489.1062	489.1039	4.8	46.4	MS^2 → 285 (100); MS^3 → 257 (100), 255 (55), 151 (1)
323	Kaempferol-*O*-acetyl-hexoside	$C_{23}H_{22}O_{12}$	489.1033	489.1039	1.1	47.7	MS^2 → 285 (100); MS^3 → 257 (100), 255 (24)
324	Kaempferol-*O*-diacetyl-hexoside	$C_{25}H_{24}O_{13}$	531.1156	531.1144	2.2	55.0	MS^2 → 285 (100); MS^3 → 255 (100)
325	Kaempferol-*O*-rhamnoside-*O*-pentoside	$C_{26}H_{28}O_{14}$	563.1391	563.1406	2.7	38.4	MS^2 → 285 (100), 431 (95); MS^3 → 257 (100)
326	Kaempferol-*O*-rhamnoside-*O*-pentoside	$C_{26}H_{28}O_{14}$	563.1425	563.1406	3.3	41.0	MS^2 → 285 (100); MS^3 → 257 (100)
327	Kaempferol-*O*-rhamnoside-*O*-pentoside	$C_{26}H_{28}O_{14}$	563.1425	563.1406	3.3	43.4	MS^2 → 284 (100); MS^3 → 255 (100)
328	Kaempferol-*O*-hydroxybenzoyl-hexoside (Rugosaflavonoid C)	$C_{28}H_{24}O_{13}$	567.1135	567.1144	1.6	45.7	MS^2 → 285 (100); MS^3 → 151 (100), 257 (76)
329	Kaempferol-*O*-galloyl-pentoside	$C_{27}H_{22}O_{14}$	569.0940	569.0937	0.6	47.1	MS^2 → 285 (100); MS^3 → 283 (100), 257 (73)
330	Kaempferol-*O*-galloyl-rhamnoside	$C_{28}H_{24}O_{14}$	583.1121	583.1093	4.8	47.9	MS^2 → 285 (100); MS^3 → 257 (100), 151 (67)
331	Kaempferol-*O*-rutinoside	$C_{27}H_{30}O_{15}$	593.1536	593.1512	4.1	33.5	MS^2 → 284 (100), 285 (60); MS^3 → 255 (100), 151 (7)
332	Kaempferol-*O*-rutinoside	$C_{27}H_{30}O_{15}$	593.1536	593.1512	4.1	38.9	MS^2 → 285 (100); MS^3 → 257 (100), 151 (11)
333	Resinoside A/B	$C_{31}H_{34}O_{13}$	613.1943	613.1927	2.7	51.9	MS^2 → 285 (100); MS^3 → 257 (100)
334	Kaempferol-3-*O*-(6''-acetyl-hexoside)-7-*O*-rhamnoside	$C_{29}H_{32}O_{16}$	635.1649	635.1618	4.9	46.1	MS^2 → 575 (100); MS^2 → 285 (100); MS^3 → 255 (100), 151 (6)

No.	Compound	Molecular Formula	Experimental Molecular Weight *m/z* [M-H]$^-$	Theoretical Molecular Weight *m/z* [M-H]$^-$	Error (ppm)	RT (min)	Fragmentation
	4. Laricitrin						
335	Laricitrin	$C_{16}H_{12}O_8$	331.0470	331.0459	3.2	46.1	MS^2 → 316 (100); MS^3 → 316 (100), 179 (64), 164 (73), 151 (35)
336	Laricitrin-*O*-pentoside	$C_{21}H_{20}O_{12}$	463.0886	463.0882	0.9	39.7	MS^2 → 331 (100); MS^3 → 316 (100); MS^4 → 271 (100), 179 (73), 151 (12)
337	Laricitrin-*O*-pentoside	$C_{21}H_{20}O_{12}$	463.0903	463.0882	4.5	43.1	MS^2 → 331 (100); MS^3 → 316 (100); MS^4 → 271 (100), 179 (7), 151 (1)
338	Laricitrin-*O*-pentoside	$C_{21}H_{20}O_{12}$	463.0886	463.0882	0.9	44.6	MS^2 → 331 (100); MS^3 → 316 (100); MS^4 → 179 (100), 271 (25), 151 (6)
339	Laricitrin-*O*-rhamnoside	$C_{22}H_{22}O_{12}$	477.1034	477.1039	0.9	40.6	MS^2 → 331 (100); MS^3 → 316 (100); MS^4 → 287 (100), 271 (94)
340	Laricitrin-*O*-hexoside	$C_{22}H_{22}O_{13}$	493.0985	493.0988	0.5	36.8	MS^2 → 331 (100); MS^3 → 316 (100); MS^4 → 287 (100), 271 (90)
341	Laricitrin-*O*-hexoside	$C_{22}H_{22}O_{13}$	493.0993	493.0988	1.1	40.1	MS^2 → 331 (100); MS^3 → 316 (100); MS^4 → 271 (100)
342	Laricitrin-*O*-hexoside	$C_{22}H_{22}O_{13}$	493.0999	493.0988	2.3	46.2	MS^2 → 331 (100); MS^3 → 316 (100); MS^4 → 271 (100)
343	Laricitrin-*O*-glucuronide	$C_{22}H_{20}O_{14}$	507.0805	507.0780	4.9	42.7	MS^2 → 331 (100); MS^3 → 316 (100); MS^4 → 179 (100), 271 (71), 151 (25)
344	Laricitrin-*O*-coumaroyl-rhamnoside	$C_{31}H_{28}O_{14}$	623.1432	623.1406	4.1	55.5	MS^2 → 331 (100); MS^3 → 316 (100); MS^4 → 271 (100)
345	Laricitrin-*O*-rutinoside	$C_{28}H_{32}O_{17}$	639.1584	639.1567	2.7	36.8	MS^2 → 331 (100); MS^3 → 316 (100), 179 (24), 151 (6); MS^4 → 271 (100)
346	Laricitrin-*O*-coumaroyl-hexoside (same side)	$C_{31}H_{28}O_{15}$	639.1384	639.1355	4.5	48.2	MS^2 → 331 (100), 493 (45); MS^3 → 316 (100)
347	Laricitrin-*O*-coumaroyl-hexoside (diff sides)	$C_{31}H_{28}O_{15}$	639.1384	639.1355	4.5	50.4	MS^2 → 493 (100); MS^3 → 331 (100); MS^4 → 316 (100)

No.	Compound	Molecular Formula	Experimental Molecular Weight *m/z* $[M-H]^-$	Theoretical Molecular Weight *m/z* $[M-H]^-$	Error (ppm)	RT (min)	Fragmentation
	5. Isorhamnetin						
348	Isorhamnetin-*O*-glucuronide	$C_{22}H_{20}O_{13}$	491.0824	491.0831	1.5	45.2	MS^2 → 315 (100); MS^3 → 300 (100); MS^4 → 271 (100), 255 (81)

21.5. Fragmentation Pattern of derivatives

The fragmentation pattern of the derivatives along with their theoretical *m/z* value, error in experimental *m/z* value, retention time, *m/z* value and molecular formula are shown in Table 21.3

Table 21.3: Fragmentation pattern of derivatives in *Rhododendron* species

No.	Compound	Molecular Formula	Experimental Molecular Weight *m/z* $[M-H]^-$	Theoretical Molecular Weight *m/z* $[M-H]^-$	Error (ppm)	RT (min)	Fragmentation
	Quinic acid novel compounds						
349	Quinic acid derivative 1	$C_{14}H_{18}O_9$	329.0873	329.0878	1.5	18.9	MS^2 → 191 (100), 167 (38), 147 (31)
350	Quinic acid derivative 3	$C_{16}H_{18}O_{11}$	385.0761	385.0776	4.0	10.5	MS^2 → 191 (100)
351	Quinic acid derivative 4	$C_{16}H_{18}O_{11}$	385.0764	385.0776	3.2	12.3	MS^2 → 191 (100)
	Hydroxycinnamic Acids						
	Caffeic acid novel compounds						
352	Caffeic acid derivative 1	$C_{17}H_{16}O_5$	299.0916	299.0925	3.0	47.3	MS^2 → 179 (100), 205 (23); MS^3 → 135 (100)
353	Caffeic acid derivative 2	$C_{17}H_{16}O_5$	299.0919	299.0925	2.0	56.9	MS^2 → 179 (100), 205 (43); MS^3 → 135 (100)
354	Caffeic acid derivative 3	$C_{23}H_{26}O_{10}$	461.1471	461.1453	3.9	39.2	MS^2 → 299 (100); MS^3 → 179 (100), 205 (30), 193 (21); MS^4 → 135 (100)
355	Caffeic acid derivative 4	$C_{23}H_{26}O_{10}$	461.1466	461.1453	2.8	47.5	MS^2 → 299 (100); MS^3 → 179 (100), 205 (29), 193 (9); MS^4 → 135 (100)
356	Caffeic acid derivative 5	$C_{23}H_{24}O_{11}$	475.1269	475.1246	4.9	43.2	MS^2 → 179 (100); MS^3 → 135 (100)
357	Caffeic acid derivative 6	$C_{25}H_{28}O_{11}$	503.1581	503.1559	4.4	55.4	MS^2 → 299 (100); MS^3 → 179 (100); MS^4 → 135 (100)
358	Caffeic acid derivative 7	$C_{22}H_{28}O_{14}$	515.1423	515.1406	3.2	10.0	MS^2 → 179 (100), 353 (31), 341 (23); MS^3 → 135 (100)

No.	Compound	Molecular Formula	Experimental Molecular Weight *m/z* [M-H]$^-$	Theoretical Molecular Weight *m/z* [M-H]$^-$	Error (ppm)	RT (min)	Fragmentation
359	Caffeic acid derivative 8	$C_{25}H_{28}O_{14}$	551.1428	551.1406	3.9	28.0	MS^2 → 179 (100), MS^3 → 135 (100)
360	Caffeic acid derivative 9	$C_{25}H_{28}O_{14}$	551.1401	551.1406	1.0	29.8	MS^2 → 179 (100), MS^3 → 135 (100)
361	Caffeic acid derivative 10	$C_{28}H_{34}O_{14}$	593.1903	593.1876	4.6	46.2	MS^2 → 299 (100); MS^3 → 179 (100); MS^4 → 135 (100)
	***p*-coumaric acid novel compounds**						
362	*p*-coumaric acid derivative 1	$C_{18}H_{18}O_6$	329.1034	329.1031	1.0	44.4	MS^2 → 163 (100); MS^3 → 119 (100)
363	*p*-coumaric acid derivative 2	$C_{25}H_{28}O_{12}$	519.1515	519.1508	1.3	45.8	MS^2 → 313 (100); MS^3 → 163 (100); MS^4 → 119 (100)
364	*p*-coumaric acid derivative 3	$C_{31}H_{36}O_{16}$	663.1933	663.1931	0.4	37.7	MS^2 → 487 (100), 307 (91); MS^3 → 163 (100); MS^4 → 119 (100)
	Ferulic acid novel compounds						
365	Ferulic acid derivative 1	$C_{13}H_{14}O_9$	313.0555	313.0565	3.2	11.5	MS^2 → 193 (100); MS^3 → 149 (100), 105 (33)
366	Ferulic acid derivative 2	$C_{21}H_{20}O_{10}$	431.0991	431.0984	1.7	50.5	MS^2 → 193 (100); MS^3 → 149 (100), 178 (32); MS^4 → 134 (100)
	Dihydrocoumaric acid novel compounds						
367	Dihydrocoumaric acid derivative 1	$C_{15}H_{22}O_9$	345.1174	345.1191	4.9	4.4	MS^2 → 165 (100); MS^3 → 121 (100)
368	Dihydrocoumaric acid derivative 2	$C_{15}H_{22}O_9$	345.1174	345.1191	4.9	9.0	MS^2 → 165 (100); MS^3 → 121 (100)
369	Dihydrocoumaric acid derivative 3	$C_{15}H_{22}O_9$	345.1191	345.1191	0.0	11.3	MS^2 → 165 (100); MS^3 → 121 (100)
	Hydroxybenzoic Acids						

No.	Compound	Molecular Formula	Experimental Molecular Weight *m/z* $[M-H]^-$	Theoretical Molecular Weight *m/z* $[M-H]^-$	Error (ppm)	RT (min)	Fragmentation
	Derivatives of GA						
370	Gallic acid derivative 1	$C_{15}H_{14}O_7$	305.0657	305.0667	3.2	34.4	MS^2 → 169 (100); MS^3 → 125 (100)
371	Gallic acid derivative 2	$C_{15}H_{18}O_9$	341.0889	341.0878	3.2	8.5	MS^2 → 135 (100), 169 (31), 125 (3); MS^3 of 135→ 107 (100); MS^3 of 169 → 125 (100)
372	Gallic acid derivative 3	$C_{14}H_{18}O_{10}$	345.0811	345.0827	4.7	10.5	MS^2 → 169 (100); MS^3 → 125 (100)
373	Gallic acid derivative 4	$C_{16}H_{20}O_{13}$	419.0835	419.0831	0.9	6.8	MS^2 → 169 (100); MS^3 → 125 (100)
374	Gallic acid derivative 5	$C_{21}H_{24}O_{11}$	451.1246	451.1246	0.0	23.9	MS^2 → 313 (100); MS^3 → 169 (100); MS^4 → 125 (100)
375	Gallic acid derivative 6	$C_{20}H_{20}O_{12}$	451.0892	451.0882	2.2	26.6	MS^2 → 313 (100), 271 (27); MS^3 → 169 (100); MS^4 → 125 (100)
376	Gallic acid derivative 7	$C_{20}H_{22}O_{12}$	453.1028	453.1039	2.3	23.3	MS^2 → 313 (100); MS^3 → 169 (100); MS^4 → 125 (100)
377	Gallic acid derivative 8	$C_{21}H_{18}O_{13}$	477.0680	477.0675	1.1	23.8	MS^2 → 169 (100), 325 (72); MS^3 → 125 (100)
378	Gallic acid derivative 9	$C_{21}H_{22}O_{14}$	497.0958	497.0937	4.3	25.3	MS^2 → 313 (100), 271 (80); MS^3 → 169 (100); MS^4 → 125 (100)
379	Gallic acid derivative 10	$C_{30}H_{26}O_{14}$	609.1275	609.1250	4.1	10.2	MS^2 → 331 (100); MS^3 → 169 (100); MS^4 → 125 (100)
380	Gallic acid derivative 11	$C_{28}H_{28}O_{16}$	619.1314	619.1305	1.5	22.1	MS^2 → 331 (100); MS^3 → 169 (100); MS^4 → 125 (100)
	Derivatives of PCA						
381	Protocatechuic acid derivative 1	$C_{13}H_{14}O_9$	313.0565	313.0565	0.0	12.0	MS^2 → 153 (100); MS^3 → 109 (100)
382	Protocatechuic acid derivative 2	$C_{13}H_{14}O_9$	313.0558	313.0565	2.4	15.2	MS^2 → 153 (100); MS^3 → 109 (100)
383	Protocatechuic acid derivative 3	$C_{21}H_{28}O_{13}$	487.1448	487.1457	1.9	46.3	MS^2 → 357 (100); MS^3 → 153 (100); MS^4 → 109 (100)

No.	Compound	Molecular Formula	Experimental Molecular Weight *m/z* [M-H]$^-$	Theoretical Molecular Weight *m/z* [M-H]$^-$	Error (ppm)	RT (min)	Fragmentation
	Derivatives of SA						
384	Salicylic acid derivative 1	$C_{13}H_{18}O_8$	301.0924	301.0929	1.6	6.0	MS^2 → 137 (100), 161 (62); MS^3 → 93 (100)
385	Salicylic acid derivative 2	$C_{15}H_{20}O_9$	343.1022	343.1035	3.7	12.0	MS^2 →181 (100); MS^3 → 137 (100), 163 (35); MS^4 → 93 (100)
386	Salicylic acid derivative 3	$C_{15}H_{22}O_9$	345.1198	345.1191	2.0	8.2	MS^2 → 299 (100); MS^3 → 137 (100), 161 (47)
387	Salicylic acid derivative 4	$C_{19}H_{20}O_9$	391.1048	391.1035	3.4	31.0	MS^2 → 281 (100); MS^3 → 137 (100); MS^4 → 93 (100)
388	Salicylic acid derivative 5	$C_{21}H_{24}O_9$	419.1334	419.1348	3.2	37.9	MS^2 → 137 (100), 179 (56), 209 (29), 239 (97); MS^3 → 93 (100)
389	Salicylic acid derivative 6	$C_{21}H_{36}O_{10}$	447.2244	447.2236	1.9	41.1	MS^2 → 137 (100), 327 (21), 301 (14); MS^3 → 93 (100)
	Derivatives of VA						
390	Vanillic acid derivative 1	$C_{15}H_{14}O_5$	273.0759	273.0769	3.5	47.5	MS^2 → 167 (100); MS^3 → 123 (100)
391	Vanillic acid derivative 2	$C_{14}H_{16}O_9$	327.0712	327.0722	2.9	17.8	MS^2 → 167 (100); MS^3 → 149 (100), 123 (66); MS^4 → 105 (100)
392	Vanillic acid derivative 3	$C_{21}H_{30}O_{16}$	537.1474	537.1461	2.4	6.8	MS^2 → 329 (100); MS^3 → 167 (100); MS^4 → 152 (100), 123 (26), 108 (37)
	Derivatives of MG						
393	Methyl gallate derivative 1	$C_{21}H_{24}O_{12}$	467.1184	467.1195	2.4	30.2	MS^2 → 327 (100); MS^3 → 183 (100); MS^4 → 124 (100), 168 (55), 139 (97)
394	Methyl gallate derivative 2	$C_{21}H_{24}O_{12}$	467.1195	467.1195	0.0	31.0	MS^2 → 327 (100); MS^3 → 183 (100); MS^4 → 139 (100), 168 (53), 124 (26)
395	Methyl gallate derivative 3	$C_{23}H_{20}O_{11}$	471.0943	471.0933	2.2	28.4	MS^2 → 183 (100); MS^3 → 168 (100), 139 (6), 124 (39)

No.	Compound	Molecular Formula	Experimental Molecular Weight *m/z* [M-H]$^-$	Theoretical Molecular Weight *m/z* [M-H]$^-$	Error (ppm)	RT (min)	Fragmentation
396	Methyl gallate derivative 4	$C_{23}H_{26}O_{13}$	509.1309	509.1301	1.6	46.0	MS^2 → 327 (100), 465 (51); MS^3 → 183 (100); MS^4 → 139 (100), 168 (86), 124 (37)
	Flavan-3-ols						
397	(Epi)catechin derivative 1	$C_{21}H_{24}O_7$	387.1438	387.1449	2.9	40.3	MS^2 → 289 (100); MS^3 → 245 (100), 205 (38)
398	(Epi)catechin derivative 2	$C_{21}H_{24}O_7$	387.1431	387.1449	4.7	45.0	MS^2 → 289 (100); MS^3 → 245 (100), 205 (44)
399	(Epi)catechin derivative 3	$C_{23}H_{26}O_{12}$	493.1351	493.1352	0.1	25.0	MS^2 → 289 (100); MS^3 → 245 (100), 205 (48)
400	(Epi)catechin derivative 4	$C_{30}H_{24}O_{13}$	591.1159	591.1144	2.5	23.8	MS^2 → 407 (100); MS^3 → 285 (100); MS^4 → 257 (100)
401	(Epi)catechin derivative 5	$C_{37}H_{30}O_{14}$	697.1561	697.1563	0.3	29.0	MS^2 → 545 (100), 451 (30), 289 (13); MS^3 → 407 (100)
402	(Epi)catechin derivative 6	$C_{45}H_{36}O_{19}$	879.1791	879.1778	1.5	20.3	MS^2 → 727 (100), 589 (28), 575 (23), 451 (18); MS^3 → 709 (100)
	Flavonol and Flavonol Glycosides						
403	Quercetin derivative 1	$C_{26}H_{28}O_{13}$	547.1478	547.1457	3.9	46.0	MS^2 → 301 (100); MS^3 → 271 (100), 179 (77), 151 (75)
404	Quercetin derivative 2	$C_{26}H_{28}O_{13}$	547.1472	547.1457	2.7	48.2	MS^2 → 300 (100), 301 (66); MS^3 → 271 (100), 179 (27), 151 (25)
405	Quercetin derivative 3	$C_{29}H_{26}O_{14}$	597.1256	597.1250	1.0	50.9	MS^2 → 301 (100), 445 (8); MS^3 → 271 (100), 179 (47), 151 (41)
406	Quercetin derivative 4	$C_{29}H_{26}O_{16}$	629.1135	629.1148	2.1	39.5	MS^2 → 463 (100); MS^3 → 301 (100); MS^4 → 151 (100), 179 (70)
407	Quercetin derivative 5	$C_{30}H_{28}O_{16}$	643.1317	643.1305	1.9	45.0	MS^2 → 301 (100), 477 (36); MS^3 → 271 (100), 179 (41), 151 (25)

No.	Compound	Molecular Formula	Experimental Molecular Weight *m/z* $[M-H]^-$	Theoretical Molecular Weight *m/z* $[M-H]^-$	Error (ppm)	RT (min)	Fragmentation
408	Quercetin derivative 6	$C_{30}H_{28}O_{16}$	643.1318	643.1305	2.1	46.9	MS^2 → 301 (100), 477 (51); MS^3 → 271 (100), 179 (65), 151 (52)
	Other Derivatives						
409	Glucoacetosyringone isomer	$C_{16}H_{22}O_9$	357.1178	357.1191	3.7	19.7	MS^2 → 195 (100); MS^3 → 136 (100), 151 (81), 123 (8)

21.6. Additional Information on CD

The description of the files present on the CD is given in the table below:

Name	Content
Box plots - Isomers.docx	Box plots for comparison of isomers
Box plots - Subgenus.docx	Box plots for comparison of compounds in the five different subgenera
EIC and Tandem MS of 348 compounds.docx	Extract Ion Chromatogram and Tandem Mass Spectra of 348 identified compounds
Heatmap - Additional Flavan-3-ols.pdf	Heatmap of additional flavan-3-ols (based on intensity) along with the phylogenetic tree
Heatmap - Additional Flavonols.pdf	Heatmap of additional flavonols (based on intensity) along with the phylogenetic tree
Heatmap - All compounds.jpg	Heatmap of 348 identified compounds (present or absent) in *Rhododendron* species
Protocols.docx	Protocols of instruments in the labs
Rhododendron Results.xlsx	Table of *Rhododendron* species, lab number, gene bank number, herbarium number, compounds identified in different species
Rhododendron Species.accdb	List of *Rhododendron* species received from Rhododendron Park Bremen

The additional CD is attached here.